

Herbal medicines for gastrointestinal and hepatic diseases - novel pharmacological and toxicological approaches, volume I, 2nd Edition

Edited by

Muhammad Hasnat, Mirza Muhammad Faran Ashraf Baig,
Mohammad Saleem, Aftab Ullah, Muhammad Faisal Nadeem,
Alessandra Durazzo and Massimo Lucarini

Published in

Frontiers in Pharmacology



FRONTIERS EBOOK COPYRIGHT STATEMENT

The copyright in the text of individual articles in this ebook is the property of their respective authors or their respective institutions or funders. The copyright in graphics and images within each article may be subject to copyright of other parties. In both cases this is subject to a license granted to Frontiers.

The compilation of articles constituting this ebook is the property of Frontiers.

Each article within this ebook, and the ebook itself, are published under the most recent version of the Creative Commons CC-BY licence. The version current at the date of publication of this ebook is CC-BY 4.0. If the CC-BY licence is updated, the licence granted by Frontiers is automatically updated to the new version.

When exercising any right under the CC-BY licence, Frontiers must be attributed as the original publisher of the article or ebook, as applicable.

Authors have the responsibility of ensuring that any graphics or other materials which are the property of others may be included in the CC-BY licence, but this should be checked before relying on the CC-BY licence to reproduce those materials. Any copyright notices relating to those materials must be complied with.

Copyright and source acknowledgement notices may not be removed and must be displayed in any copy, derivative work or partial copy which includes the elements in question.

All copyright, and all rights therein, are protected by national and international copyright laws. The above represents a summary only. For further information please read Frontiers' Conditions for Website Use and Copyright Statement, and the applicable CC-BY licence.

ISSN 1664-8714
ISBN 978-2-8325-3111-2
DOI 10.3389/978-2-8325-3111-2

About Frontiers

Frontiers is more than just an open access publisher of scholarly articles: it is a pioneering approach to the world of academia, radically improving the way scholarly research is managed. The grand vision of Frontiers is a world where all people have an equal opportunity to seek, share and generate knowledge. Frontiers provides immediate and permanent online open access to all its publications, but this alone is not enough to realize our grand goals.

Frontiers journal series

The Frontiers journal series is a multi-tier and interdisciplinary set of open-access, online journals, promising a paradigm shift from the current review, selection and dissemination processes in academic publishing. All Frontiers journals are driven by researchers for researchers; therefore, they constitute a service to the scholarly community. At the same time, the *Frontiers journal series* operates on a revolutionary invention, the tiered publishing system, initially addressing specific communities of scholars, and gradually climbing up to broader public understanding, thus serving the interests of the lay society, too.

Dedication to quality

Each Frontiers article is a landmark of the highest quality, thanks to genuinely collaborative interactions between authors and review editors, who include some of the world's best academicians. Research must be certified by peers before entering a stream of knowledge that may eventually reach the public - and shape society; therefore, Frontiers only applies the most rigorous and unbiased reviews. Frontiers revolutionizes research publishing by freely delivering the most outstanding research, evaluated with no bias from both the academic and social point of view. By applying the most advanced information technologies, Frontiers is catapulting scholarly publishing into a new generation.

What are Frontiers Research Topics?

Frontiers Research Topics are very popular trademarks of the *Frontiers journals series*: they are collections of at least ten articles, all centered on a particular subject. With their unique mix of varied contributions from Original Research to Review Articles, Frontiers Research Topics unify the most influential researchers, the latest key findings and historical advances in a hot research area.

Find out more on how to host your own Frontiers Research Topic or contribute to one as an author by contacting the Frontiers editorial office: frontiersin.org/about/contact

Herbal medicines for gastrointestinal and hepatic diseases - novel pharmacological and toxicological approaches, volume I, 2nd Edition

Topic editors

Muhammad Hasnat — University of Veterinary and Animal Sciences, Pakistan

Mirza Muhammad Faran Ashraf Baig — The University of Hong Kong, Hong Kong, SAR China

Mohammad Saleem — University of the Punjab, Pakistan

Aftab Ullah — Jiangsu University, China

Muhammad Faisal Nadeem — University of Veterinary and Animal Sciences, Pakistan

Alessandra Durazzo — Research Centre for Food and Nutrition, Council for Agricultural Research and Economics, Italy

Massimo Lucarini — Research Centre for Food and Nutrition, Council for Agricultural Research and Economics, Italy

Citation

Hasnat, M., Baig, M. M. F. A., Saleem, M., Ullah, A., Nadeem, M. F., Durazzo, A., Lucarini, M., eds. (2023). *Herbal medicines for gastrointestinal and hepatic diseases - novel pharmacological and toxicological approaches, volume I, 2nd Edition*. Lausanne: Frontiers Media SA.
doi: 10.3389/978-2-8325-3111-2

Publisher's note: In this 2nd edition, the following article has been updated:

Hasnat M, Baig MMFA, Saleem M, Ullah A, Nadeem MF, Durazzo A and Lucarini M (2023)

Editorial: Herbal medicines for gastrointestinal and hepatic diseases - novel pharmacological and toxicological approaches, Volume I. *Front. Pharmacol.* 14:1157229. doi: 10.3389/fphar.2023.1157229

Table of contents

- 05 **Editorial: Herbal medicines for gastrointestinal and hepatic diseases - novel pharmacological and toxicological approaches, Volume I**
Muhammad Hasnat, Mirza Muhammad Faran Ashraf Baig, Mohammad Saleem, Aftab Ullah, Muhammad Faisal Nadeem, Alessandra Durazzo and Massimo Lucarini
- 08 **Qingluo Tongbi Formula Alleviates Hepatotoxicity Induced by *Tripterygium wilfordii* Hook. F. by Regulating Excessive Mitophagy Through the PERK-ATF4 Pathway**
Linluo Zhang, Jie Zhou, Zhe Feng, Baoping Jiang, Changqing Li, Lingling Zhou and Xueping Zhou
- 21 **The Effect of Lithocholic Acid on the Gut-Liver Axis**
Wei Sheng, Guang Ji and Li Zhang
- 33 **Huangkui lianchang decoction attenuates experimental colitis by inhibiting the NF- κ B pathway and autophagy**
Xudong Cheng, Jun Du, Qing Zhou, Bensheng Wu, Haodong Wang, Zhizhong Xu, Shuguang Zhen, Jieyu Jiang, Xiaopeng Wang and Zongqi He
- 50 **Chinese herbal medicine combined with oxaliplatin-based chemotherapy for advanced gastric cancer: A systematic review and meta-analysis of contributions of specific medicinal materials to tumor response**
Ying Tan, Heping Wang, Bowen Xu, Xiaoxiao Zhang, Guanghui Zhu, Yuansha Ge, Taicheng Lu, Ruike Gao and Jie Li
- 80 **CGX, a standardized herbal syrup, inhibits colon-liver metastasis by regulating the hepatic microenvironments in a splenic injection mouse model**
Sung-Bae Lee, Seung-Ju Hwang and Chang-Gue Son
- 92 **The Antigastric Cancer Effect of Triptolide is Associated With H19/NF- κ B/FLIP Axis**
Weiwei Yuan, Jinxi Huang, Shanshan Hou, Huahua Li, Liangyu Bie, Beibei Chen, Gaofeng Li, Yang Zhou and Xiaobing Chen
- 107 **Flavonoids-Rich Plant Extracts Against *Helicobacter pylori* Infection as Prevention to Gastric Cancer**
Renaly Ivyna de Araújo Rêgo, Geovana Ferreira Guedes Silvestre, Demis Ferreira de Melo, Sonaly Lima Albino, Marcela Monteiro Pimentel, Sara Brito Silva Costa Cruz, Sabrina Daniela Silva Wurzba, Wellington Francisco Rodrigues, Bolívar Ponciano Goulart de Lima Damasceno and Lúcio Roberto Cançado Castellano
- 127 **Gastroprotective mechanism of modified Ivdou gancao decoction on ethanol-induced gastric lesions in mice: Involvement of Nrf-2/HO-1/NF- κ B signaling pathway**
Lei Xie, Minyi Luo, Junlin Li, Wenguan Huang, Guangjun Tian, Xiuyun Chen, Ying Ai, Yan Zhang, Haolan He and Jinyang He

- 147 **β 1-Integrin plays a major role in resveratrol-mediated anti-invasion effects in the CRC microenvironment**
Aranka Brockmueller, Anna-Lena Mueller, Parviz Shayan and Mehdi Shakibaei
- 165 **Traditional Chinese medicine prescription Shenling BaiZhu powder to treat ulcerative colitis: Clinical evidence and potential mechanisms**
Jing Chen, Bixin Shen and Zhengli Jiang
- 192 **Chrysophanol-8-O-glucoside protects mice against acute liver injury by inhibiting autophagy in hepatic stellate cells and inflammatory response in liver-resident macrophages**
Tao Wang, Zhuo Lu, Xin-Hui Qu, Zi-Ying Xiong, Ya-Ting Wu, Yong Luo, Zi-Yu Zhang, Xiao-Jian Han and Cai-Feng Xie
- 206 **Herbal therapies in gastrointestinal and hepatic disorders: An evidence-based clinical review**
Yongfang Yao, Murad Habib, Hajra Fazeelat Bajwa, Anina Qureshi, Rameesha Fareed, Reem Altaf, Umair Ilyas, Yongtao Duan and Muhammad Abbas
- 213 **Immunostimulatory activity and structure-activity relationship of epimedin B from *Epimedium brevicornu* Maxim.**
Yuan Gao, Wei Shi, Can Tu, Peng Li, Guanyu Zhao, Xiaohe Xiao, Jiabo Wang and Zhaofang Bai
- 228 **Efficacy and safety of traditional Chinese medicine external washing in the treatment of postoperative wound of diabetes complicated with anal fistula: Study protocol of a randomized, double-blind, placebo-controlled, multi-center clinical trial**
Jian Kang, Ya Liu, Sihan Peng, Xiao Tang, Lu Liu, Ziyang Xie, Yuchi He and Xiyu Zhang



OPEN ACCESS

EDITED BY

Javier Echeverria,
University of Santiago, Chile

REVIEWED BY

Hari Prasad Devkota,
Kumamoto University, Japan

*CORRESPONDENCE

Muhammad Hasnat,
✉ muhammad.hasnat@uvas.edu.pk

RECEIVED 02 February 2023

ACCEPTED 22 June 2023

PUBLISHED 07 July 2023

CITATION

Hasnat M, Baig MMFA, Saleem M, Ullah A, Nadeem MF, Durazzo A and Lucarini M (2023), Editorial: Herbal medicines for gastrointestinal and hepatic diseases - novel pharmacological and toxicological approaches, Volume I. *Front. Pharmacol.* 14:1157229. doi: 10.3389/fphar.2023.1157229

COPYRIGHT

© 2023 Hasnat, Baig, Saleem, Ullah, Nadeem, Durazzo and Lucarini. This is an open-access article distributed under the terms of the [Creative Commons Attribution License \(CC BY\)](#). The use, distribution or reproduction in other forums is permitted, provided the original author(s) and the copyright owner(s) are credited and that the original publication in this journal is cited, in accordance with accepted academic practice. No use, distribution or reproduction is permitted which does not comply with these terms.

Editorial: Herbal medicines for gastrointestinal and hepatic diseases - novel pharmacological and toxicological approaches, Volume I

Muhammad Hasnat^{1*}, Mirza Muhammad Faran Ashraf Baig², Mohammad Saleem³, Aftab Ullah⁴, Muhammad Faisal Nadeem⁵, Alessandra Durazzo⁶ and Massimo Lucarini⁶

¹Institute of Pharmaceutical Sciences, University of Veterinary and Animal Sciences, Lahore, Pakistan, ²The Hong Kong University of Science and Technology, Hong Kong, Hong Kong SAR, China, ³University of the Punjab Lahore, Lahore, Pakistan, ⁴Jiangsu University, Zhenjiang, China, ⁵University of Veterinary and Animal Sciences, Lahore, Pakistan, ⁶CREA-Research Centre for Food and Nutrition, Rome, Italy

KEYWORDS

herbal medicines, traditional medicines, active ingredients from herbal medicines, GIT, liver, toxicology

Editorial on the Research Topic

Herbal medicines for gastrointestinal and hepatic diseases - novel pharmacological and toxicological approaches, Volume I

After respiratory tract diseases, acute gastrointestinal infections are the second most common infections among infants and children and are responsible for morbidity and mortality (Ferguson et al., 2020). These infections are caused by a variety of microorganisms with the most common species are *Helicobacter pylori*, *Salmonella species*, *Clostridium difficile*, *Shigella species*, *Giardia lamblia* and *Escherichia coli* (Shariati et al., 2019). Gastrointestinal system is also associated with the hepatic complications including NAFLD and gastrointestinal malignancies, i.e., HCC (Younossi et al., 2018). Worldwide, liver cancer causes second most cancer related deaths (Jemal et al., 2011). For the management of hepatic and gastrointestinal diseases, long-term strategies are required from government and international bodies because hepatitis B virus and hepatitis C virus infected subjects are 370 million and 130 million, respectively (Alter, 2006). Traditional and complementary medicines (TCMs) are clinical practices that are used in the diagnosis, treatment and prevention of diseases. They are not completely merged into the healthcare system, however they are affordable, accessible and culturally accepted by the people. Herbal products are one of the major part of TCM. It is reported that market share of natural preparations is up to several billions of dollars in developing and developed nations, showing the trust of people on these products (Hitl et al., 2019). Herbal medicines treat gastrointestinal diseases by affecting intestinal barrier, microbial composition and metabolites, and inflammation (Wang et al., 2023).

In the Research Topic of papers under the Research Topic “Herbal Medicines for Gastrointestinal and Hepatic Diseases - Novel Pharmacological and Toxicological approaches - Volume I”, 15 papers were published., mainly focusing the herbal medicines for gastrointestinal and hepatic diseases.

This Research Topic includes the following dimensions: Pre-clinical and clinical studies of herbal products and their biologically active metabolites in the management of GIT and liver diseases. Novel *in vitro* assays for the identification of potentially biologically active compounds for the treatment of gastric and hepatic cancer. Novel cellular and molecular mechanisms that describe the therapeutic effects as well as toxic effects of herbal medicines and their active metabolites on the GIT and liver. The role of the GI-microbiome in preventing and treating gastrointestinal and hepatic diseases.

The papers within this Research Topic carry out interesting themes in the area of research. As instance, [Lee et al.](#) found that treatment with Chunggan syrup (CGX) reduced tumor nodules in normal and HFD fed mice. Molecular biology studies explained that CGX antitumor effect was associated with the activation of E-Cadherin and reduction in the expression of VE-Cadherin in liver under MC38 free condition. CGX also reduced liver steatosis *via* modulating AMPK and PPAR α . [Yuan et al.](#) showed that triptolide (TP), one of the fat-soluble components extracted from the Chinese medicinal herb *Tripterygium wilfordii* Hook F. (TWHF), induced cell death in TNF α -pretreated MKN45 cells and AGS cells. Both TP and TNF α , in combination promoted the gastric cancer cell death through influencing H19/miR-204-5p/NF- κ B/FLIP axis.

[Ivyna de Araújo Rêgo et al.](#) reported the role of flavonoids in the prevention of gastric cancer by treating *H. pylori* infection and explored that flavonoid rich extracts had anti-*H. pylori* action by inhibiting urease, distortion of genetic material, decreasing protein synthesis and adhesion of microorganism to host cells. [Tan et al.](#) published a systematic review and meta-analysis on Chinese herbal medicine with oxaliplatin and showed that these agents improve the tumor response in advance gastric cancer. [Brockmueller et al.](#) showed for the first time that β 1 integrin partly suppressed the inhibitory effects of resveratrol on the metastasis of colorectal cancer (CRC) cells. Resveratrol inhibited TME induced phosphorylation and nuclear shift of NF- κ B which is associated with CXCR-4, MMP-9, FAK and caspase-3. However, β 1 integrin inhibited the anti-invasive and anti-metastatic effects of resveratrol.

Several studies have focused the autophagy pathway like, [Zhang et al.](#) expressed that Qingluo Tongbi Formula (QTF), a Chinese herbal formula, reduced TWHF-induced hepatotoxicity. TWHF caused an increase in endoplasmic reticulum stress (ERS) that regulated the mitochondrial autophagy through PERK-ATF4 pathway. QTF reduced the TW-induced ERS and mitophagy. [Wang et al.](#) concluded that chrysophanol-8-O-glucoside (CPOG) protected mice from LPS/D-galactosamine-induced acute liver damage by decreasing inflammation, oxidative stress and autophagy. CPOG inhibited the levels of p-I κ B, p-p65, TNF- α and IL-1 β upregulated by LPS. CPOG also reduced the levels of LC3B, P62, ATG5 and Beclin 1 by reducing reactive oxygen species and MAPK pathway. [Cheng et al.](#) reported that Huangkui lianchang decoction (HLD), a Chinese herbal preparation, treated colitis by

blocking NF- κ B pathway and autophagy markers. HLD showed anti-inflammatory effects by increasing the level of IL-10 and decreasing the level of pro-inflammatory cytokines. HLD also reduced the levels of LC3II/I and Beclin 1.

Couple of studies reported ethanol-induced gastric complications, i.e., [Ke et al.](#) first time reported that LDOP-1 had protective effect against ethanol-induced gastric mucosal damage by controlling AMPK/mTOR pathway. [Xie et al.](#) performed a study on ethanol-induced gastric lesions and showed that MLG could enhance defensive mechanism through NF- κ B/Nrf2/HO-1 pathway and had protective effect against Ethanol-induced gastric lesions. This study reported that MLG increased the levels of antioxidant enzymes and reduced the levels of TNF- α and IL-1 β . MLG increased the expressions of Nrf-2 and HO-1 and decreased the expressions of COX-2 and NF- κ B.

Other studies on herbal medicines treating gastrointestinal and liver diseases have also significant findings. [Chen et al.](#) published a clinical evidence base study and expressed that SLBZP had capacity to treat ulcerative colitis. [Kang et al.](#) reported the randomized, double-blind, placebo-controlled, multi-center clinical trial study for the assessment of the efficacy and safety of traditional Chinese medicine external washing for treating the postoperative wounds in diabetic patients with anal fistula. [Yao et al.](#) proposed the general guidelines about the use of herbal preparations in the treatment of gastrointestinal and liver complications. [Sheng et al.](#) showed that lithocholic acid had significant protective activities on the intestinal environment, including the maintenance of tight junctions, anti-bacterial and anti-inflammatory responses. [Gao et al.](#) showed that epimedin B caused the Epimedium Folium (EF)-induced Idiosyncratic drug-induced liver injury (IDILI) and the glycogen concentration in EF is not dependent on NLRP3 inflammasome activity. They studied that epimedin B increased the secretion of IL-1 β , played a role in the maturation of caspase-1 and activated the NLRP3 inflammasome by increasing the level of ROS.

In conclusion, this Research Topic provided recent advances in the scientific knowledge on the gastrointestinal system.

Author contributions

All authors listed have made a substantial, direct, and intellectual contribution to the work and approved it for publication.

Acknowledgments

We would like to acknowledge the authors for their valuable publications in this Research Topic.

Conflict of interest

The authors declare that the research was conducted in the absence of any commercial or financial relationships that could be construed as a potential conflict of interest.

Publisher's note

All claims expressed in this article are solely those of the authors and do not necessarily represent those of their affiliated

organizations, or those of the publisher, the editors and the reviewers. Any product that may be evaluated in this article, or claim that may be made by its manufacturer, is not guaranteed or endorsed by the publisher.

References

- Alter, M. J. (2006). Epidemiology of viral hepatitis and HIV co-infection. *J. Hepatology* 44, S6–S9. doi:10.1016/j.jhep.2005.11.004
- Ferguson, N., Laydon, D., Nedjati-Gilani, G., Imai, N., Ainslie, K., and Baguelin, M. (2020). *Report 9: Impact of non-pharmaceutical interventions (NPIs) to reduce COVID19 mortality and healthcare demand [Internet]*. London, UK: Imperial College COVID-19 Response Team, Imperial College London. [cited at 2021 Oct 15]. Available from: [CrossRef][Google Scholar] 2020.
- Hitl, M., Gavarić, N., Kladar, N., Brkić, S., Samojlik, I., Dragović, G., et al. (2019). Herbal preparations use in prevention and treatment of gastrointestinal and hepatic disorders—data from vojvodina, Serbia. *Complementary Ther. Med.* 43, 265–270. doi:10.1016/j.ctim.2019.02.018
- Jemal, A., Bray, F., Center, M. M., Ferlay, J., Ward, E., and Forman, D. (2011). Global cancer statistics. *CA a cancer J. Clin.* 61, 69–90. doi:10.3322/caac.20107
- Shariati, A., Fallah, F., Pormohammad, A., Taghipour, A., Safari, H., Chirani, A. S., et al. (2019). The possible role of bacteria, viruses, and parasites in initiation and exacerbation of irritable bowel syndrome. *J. Cell. physiology* 234, 8550–8569. doi:10.1002/jcp.27828
- Wang, L., Gou, X., Ding, Y., Liu, J., Wang, Y., Wang, Y., et al. (2023). The interplay between herbal medicines and gut microbiota in metabolic diseases. *Front. Pharmacol.* 14, 1105405. doi:10.3389/fphar.2023.1105405
- Younossi, Z., Anstee, Q. M., Marietti, M., Hardy, T., Henry, L., Eslam, M., et al. (2018). Global burden of NAFLD and NASH: Trends, predictions, risk factors and prevention. *Nat. Rev. Gastroenterology hepatology* 15, 11–20. doi:10.1038/nrgastro.2017.109



Qingluo Tongbi Formula Alleviates Hepatotoxicity Induced by *Tripterygium wilfordii* Hook. F. by Regulating Excessive Mitophagy Through the PERK-ATF4 Pathway

Linluo Zhang¹, Jie Zhou¹, Zhe Feng¹, Baoping Jiang², Changqing Li¹, Lingling Zhou^{2*} and Xueping Zhou^{1*}

¹The First Clinical Medical College, Nanjing University of Chinese Medicine, Nanjing, China, ²Jiangsu Provincial Key Laboratory of Pharmacology and Safety Evaluation of Material Medical, School of Pharmacy, Nanjing University of Chinese Medicine, Nanjing, China

OPEN ACCESS

Edited by:

Mirza Muhammad Faran Ashraf Baig,
The University of Hong Kong, Hong
Kong SAR, China

Reviewed by:

Sun Lixin,
China Pharmaceutical University,
China
Meng Xing,
Shanghai University of Traditional
Chinese Medicine, China

*Correspondence:

Lingling Zhou
zhoulingling@njucm.edu.cn
Xueping Zhou
xzp@njucm.edu.cn

Specialty section:

This article was submitted to
Ethnopharmacology,
a section of the journal
Frontiers in Pharmacology

Received: 12 April 2022

Accepted: 17 June 2022

Published: 07 July 2022

Citation:

Zhang L, Zhou J, Feng Z, Jiang B, Li C,
Zhou L and Zhou X (2022) Qingluo
Tongbi Formula Alleviates
Hepatotoxicity Induced by
Tripterygium wilfordii Hook. F. by
Regulating Excessive Mitophagy
Through the PERK-ATF4 Pathway.
Front. Pharmacol. 13:918466.
doi: 10.3389/fphar.2022.918466

Qingluo Tongbi Formula (QTF) is an empirical formula of Chinese medicine master Zhongying Zhou for the treatment of rheumatoid arthritis. Although including *Tripterygium wilfordii* Hook. F. (TW), it has not shown liver toxicity in clinical application for many years. Our previous studies have shown that QTF can significantly reduce TW-caused hepatotoxicity, but the mechanism is still unclear. This study aimed to explore the important roles of mitophagy and endoplasmic reticulum stress (ERS) and the relationship between them in QTF in alleviating TW-induced hepatotoxicity. *In vivo*, C57BL/6J female mice were used to build a model of TW-induced liver toxicity; Then mice were randomly divided into control, TW, TW + RG, TW + PN, TW + SA, TW + BM, and QTF groups. After intragastric administration for 7 days, the levels of alanine aminotransferase (ALT), aspartate aminotransferase (AST) and lactate dehydrogenase (LDH) in serum were detected; H and E staining, Oil Red O staining, transmission electron microscopy, Western blotting, and RT-qPCR were used to detect the pathological changes in liver tissue, the levels of ERS and mitophagy related proteins and genes, including GRP78, PERK, DRP1, LC3, etc., *In vitro*, triptolide (TP), catalpol (CAT), and panax notoginseng saponins (PNS), the main active ingredients of QTF, were selected. The mitophagy inhibitor, ERS inhibitor, and PERK inhibitor were used to further study the relationship between TW-induced ERS and mitophagy in HepaRG cells. The results showed that, QTF reduced excessive mitophagy and ERS in TW-induced hepatotoxicity in C57BL/6J mice, and the attenuating effects of RG and PN in QTF were most obvious, and they also significantly restrained the TW-induced ERS and mitophagy by the PERK-ATF4 pathway.

Abbreviations: ALT, Alanine aminotransferase; AST, Aspartate aminotransferase; ATF4, Activating transcription factor 4; BM, *Bombyx mori* L; CAT, Catalpol; CCK8, Cell Counting Kit-8; DRP1, Dynamin-related protein 1; ERS, Endoplasmic reticulum; FIS1, Fission 1; GRP78, Glucose-regulated protein 78; H and E, Hematoxylin-Eosin staining; LC3, Microtubule-associated protein 1A/1B-light chain 3; LDH, Lactate dehydrogenase; Mdivi-1, Mitochondrial division inhibitor 1; MFN1, Mitofusin-1; PERK, PKR-like endoplasmic reticulum kinase; PN, *Panax notoginseng* (Burkill) F.H.Chen; PNS, Panax notoginseng saponins; QTF, Qingluotongbi formula; RA, Rheumatoid arthritis; RG, *Rehmannia glutinosa* (Gaertn.) DC; TW, *Tripterygium wilfordii* Hook. F; TCM, traditional Chinese medicine; TP, Triptolide; UPR, Unfolded protein response; 4-PBA, 4-Phenylbutyric acid;

Furthermore, PNS was superior to CAT in inhibiting the expression levels of GRP78, PERK, and ATF4, while CAT was superior to PNS in reversing the expression levels of DRP1, P62, and LC3. The combination of CAT and PNS had the best attenuating effect and the most significant regulation on ERS and mitophagy. In conclusion, QTF can alleviate TW-induced hepatotoxicity by differentially downregulating the PERK-ATF4 pathway and excessive mitophagy by different components.

Keywords: *Tripterygium wilfordii* hook. f., hepatotoxicity, qingluo tongbi formula, mitophagy, ERS, PERK

1 INTRODUCTION

Tripterygium Wilfordii Hook. F. (TW) is commonly used in traditional Chinese medicine (TCM) to treat rheumatoid arthritis (RA), systemic lupus erythematosus (SLE), and various tumor diseases, because of its significant immunomodulatory, anti-inflammatory, and anti-tumor effects (Lv et al., 2019). However, the potential side effects of TW, such as hepatotoxicity and so on, seriously limit its further clinical application (Zhang et al., 2018). It is one of the current research hotspots to clarify the mechanism of the TW-induced hepatotoxicity and to reduce or/and eliminate its hepatotoxicity while ensuring the efficacy.

The application of TW in TCM has a long history, and the compound compatibility of TCM is one of the important methods to enhance the efficacy or/and reduce its liver toxicity. QTF is composed of TW, *Rehmannia glutinosa* (Gaertn.) DC. (RG), *Panax notoginseng* (Burkill) F. H. Chen (PN), *Sinomenium acutum* (Thunb.) Rehder and E. H. Wilson (SA), and *Bombyx mori* L. (BM). As an empirical prescription from Chinese medicine master Prof. Zhongying Zhou in the clinical treatment of RA with Yin Deficiency and Collateral Heat (Yinxu Luore) Syndrome, no liver toxicity of QTF was found after many years of application (Liu et al., 2015; Yang et al., 2020). Our team previous research has proved that QTF can reduce and eliminate the TW-induced liver toxicity in SD rats and HepaRG cells (Yu et al., 2022), but the specific molecular biological mechanism in QTF alleviating TW-induced hepatotoxicity is not yet very clear.

Mitochondria is a key organelle for aerobic respiration and energy metabolism, so its normal number and function are very important. Mitochondrial autophagy (also known as mitophagy) maintains the homeostasis and balance of mitochondria by removing damaged mitochondria to regulate cell fate. At the same time, the endoplasmic reticulum (ER) and mitochondria are closely connected and interact by the mitochondrial-related endoplasmic reticulum membranes (MAMs), coordinately regulating autophagy and apoptosis. Our previous study showed that ER stress (ERS) and excessive autophagy, which are the important mechanisms of TP-induced hepatocyte injury in HepaRG cells (Yu et al., 2022; Zhang et al., 2022). However, the role that mitophagy plays in reducing the TW-induced hepatotoxicity by QTF and the relationship between ERS and mitophagy are not very clear and need to be further studied.

This study focused on investigating the role of mitophagy in QTF in alleviating TW-induced liver injury, and the relationship between ERS and mitophagy, to elucidate the specific mechanism in alleviating the TW-induced hepatotoxicity by QTF.

2 MATERIALS AND METHODS

2.1 In vivo Study

2.1.1 Preparation of Qingluo Tongbi Formula

The Chinese herbal medicines of QTF were purchased from the Bozhou Medicinal Material Center (batch number: 190816, Anhui, China), and were identified by the School of Pharmacy at Nanjing University of CM (NJUCM, 20180922-20180926, Nanjing, China). The QTF is composed of TW, RG, PN, SA, and BM by the ratio of 15:15:3:15:10. The formulas were decocted with 11 times pure water for 1.5 h, and then decocted with 7 times pure water for 1.5 h, and the two were mixed, concentrated, and filtered. The crude drug contents of TW, TW + RG (the ratio is 1:1), TW + PN (the ratio is 5:1), TW + SA (the ratio is 1:1), TW + BM (the ratio is 3:2), and QTF were 1.95, 3.90, 2.34, 3.90, 3.25, and 7.54 g/ml, respectively.

In order to ensure the consistency and reproducibility of QTF extracts, the content of the main active components was analyzed by the HPLC method. Samples were separated on the Agilent ZORBAX SB-C18 column (4.6 × 250 mm, 5 μm), maintained at 30°C. The mobile phase consisted of acetonitrile (A), 0.1% phosphoric acid and 0.05% triethylamine (B) in a gradient elution: 5% A (0–2 min), 5%–10% A (2–10 min), 10% A (10–12 min), 10%–12% A (12–15 min), 12%–30% A (15–35 min), and 30% A (35–40 min). The flow rate was 0.8 ml/min, the injection volume was 10 μl, and the detection wavelength was set at 203 nm. The HPLC chromatogram and quantitative data of the main chemical components are used as supplementary material (Supplementary Figure S1).

2.1.2 Animals and Treatment

C57BL/6J female mice (6–8 weeks old, 18–22 g) were purchased from Hangzhou Medical College [Animal license number: SCXK (Zhe)2019-0002], and were treated in the Animal Center of Nanjing University of CM with the temperature of 23 ± 2°C, humidity 40%–60%, and a standard 12 h light/12 h dark cycle, fed standard pelleted diet and provided free drinking water.

First, different doses of TW decoction (containing 0.4875, 0.975, and 1.95 g/ml of TW, respectively) were administered orally to establish an ideal mouse model of liver injury. Then, mice were divided into 7 groups, with 8 mice in each group to study the attenuation mechanism, namely: control, TW, TW + RG, TW + PN, TW + SA, TW + BM, and QTF groups. The mice were sacrificed after 7 days of oral administration at a dose of 0.02 ml/g body weight, and the serum was extracted to detect alanine aminotransferase (ALT), aspartate aminotransferase (AST) and lactate dehydrogenase (LDH). The liver tissue was detected by H and E and Oil Red O staining, and the protein and RNA were extracted for Western blotting and RT-qPCR. All animal experiments were approved by the Laboratory Animal Center of Nanjing University of CM and carried out in accordance with the Principles of Animal Use and Guidelines for the Care and Use of Laboratory Animals.

2.1.3 Hematoxylin-Eosin Staining of Liver Tissue

The fresh liver tissue was fixed in 4% paraformaldehyde solution, paraffin-embedded, sectioned, and then stained with H and E. Histopathological scores were scored as previously described (Brunt 2000; Ramos et al., 2015).

2.1.4 Oil Red O Staining of Liver Tissue

The fresh liver tissue was fixed with 4% paraformaldehyde, stained with Oil Red O working solution for 10 min, and then destained with 60% isopropanol. Rinse three times with distilled water, observe and photograph under the microscope. Oil Red O quantitative statistical analysis was performed using Image-Pro Plus 6.0 software (Media Cybernetics, Inc., Rockville, MD, United States).

$$\text{Fat percentage (\%)} = \text{fat area/tissue area} \times 100\%$$

2.1.5 Transmission Electron Microscope Observation of Liver Tissue

Fresh mouse liver tissue was fixed in TEM fixative, dehydrated, infiltrated, embedded, sliced, photographed and analyzed under TEM.

2.1.6 Detection of Liver Functions

After mice were treated, blood was collected from the orbit, left at room temperature for 4 h, centrifuged at 3,000 rpm/min at 4°C for 10 min, the supernatant was taken, and the levels of ALT, AST, and LDH were detected according to the kit instructions.

2.1.7 Real-Time Quantitative PCR

20 mg of liver tissue was weighed, and then RNA isolater Total RNA Extraction Reagent was added. Perform reverse transcription and amplification according to the instructions of the RT-qPCR reverse transcription and amplification kit. Among them, the mRNAs of *GRP78*, *PERK*, *DPR1*, and *LC3*

were detected, and the housekeeping gene *GAPDH* was used as a control. Data were analyzed using the $2^{-\Delta\Delta Ct}$ method. The sequences of the gene primers in mice are shown as supplementary material (**Supplementary Figure S2**).

2.2 In vitro Study

2.2.1 Cell Culture

The HepaRG cell line, an ideal cell model for hepatotoxicity studies (Wu et al., 2016), was purchased from Beina Chuanglian Biotechnology Company (BNCC340037, Beijing, China), cells were cultured in RPMI 1640 medium containing 10% fetal bovine serum (FBS) and 1% antibiotics, and then cells were cultured in 5% carbon dioxide incubate at 37°C.

2.2.2 Detection of Cell Viability

Cell proliferation was detected by the CCK8 assay. To test the cytotoxicity of TP, HepaRG cells (5×10^4 cells/mL) were placed in 96-well plates for 24 h, then treated with different doses of TP for 12, 24, 36, and 48 h, respectively. After incubation with 10 μ l of CCK8 solution for 3 h, the optical density values were determined using a microplate reader (TECAN, Switzerland) at an excitation wavelength of 450 nm.

2.2.3 Detection of Autophagosomes

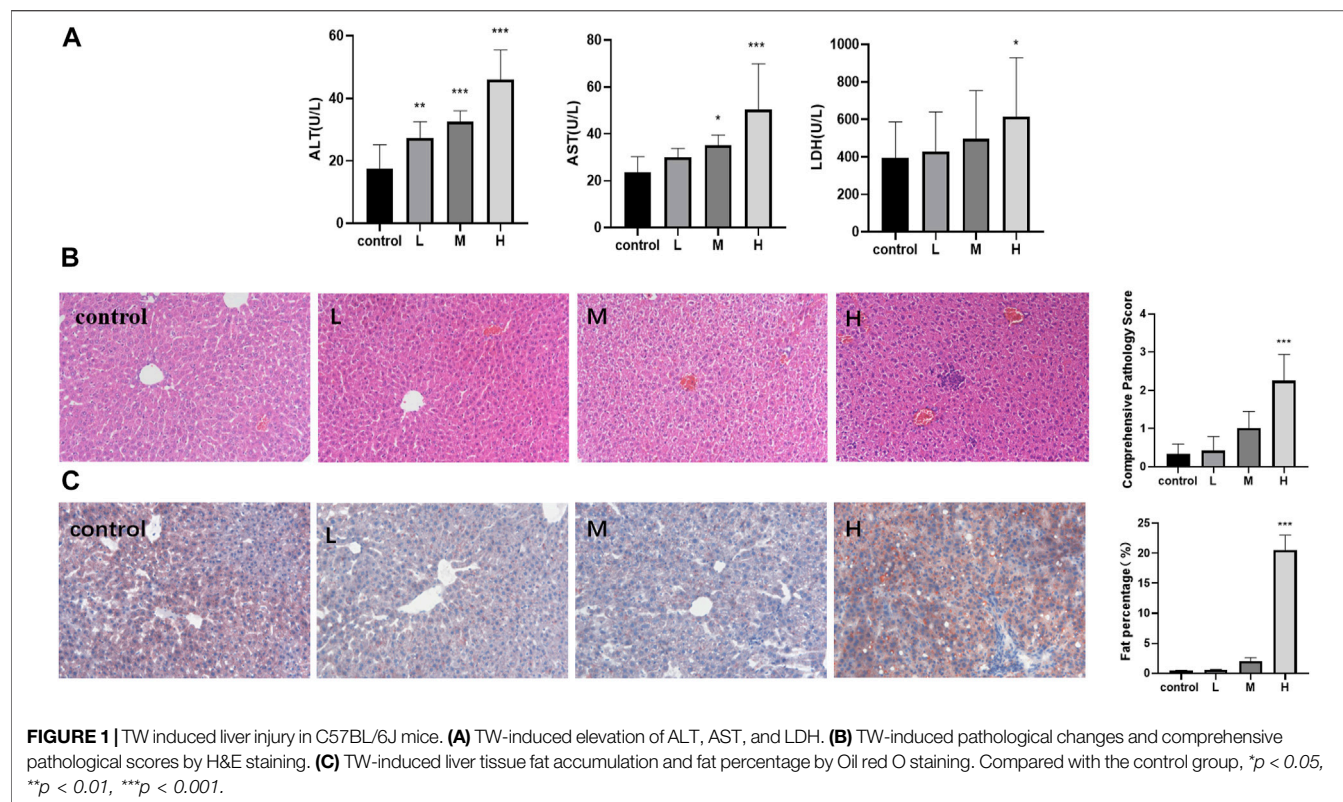
Acidic autophagic vacuoles were detected by monodansidine cadaverine (MDC) staining using an autophagy detection kit (KeyGEN, Nanjing, China) (Veeran et al., 2017). Cells (1×10^5 cells/mL) were placed in 12-well plates and incubated with different concentrations of TP at 37°C for 24 h. Cells were processed according to the kit instructions and observed and photographed using a fluorescence microscope (Zeiss, Thuringia, Germany) at an excitation wavelength of 355 nm.

2.3 Western Blotting

30 mg of mouse liver tissue was weighed or different groups of HepaRG cells were collected, and then 1 ml of lysis buffer was added to disrupt and homogenize, and lysed on ice for 30 min. BCA kit was used for protein concentration detection. 30 μ g of protein samples were taken for protein electrophoresis in 10% SDS-PAGE gel. Transfer membrane (300 v, 400 mA/h, 1 h) and block (5% BSA), incubate with primary antibody overnight at 4°C. After washing, the secondary antibody was incubated at room temperature for 1 h. After 3 additional washes, exposure was performed using an ECL system (Bio-Rad, California, United States).

2.4 Statistics

The data is presented as mean \pm standard deviation (*SD*), and statistical analysis was performed using GraphPad Prism 8.0.2. One-way ANOVA followed by Dunnett's post-hoc test and *t*-test were used to compare mean differences between multiple groups or two groups. Differences were considered significant when $p < 0.05$.



3 RESULTS

3.1 Qingluo Tongbi Formula Alleviated *T. wilfordii*-Induced Hepatotoxicity in C57BL/6J Mice

TW increased the levels of ALT, AST, and LDH in a dose-dependent manner in mice, and the three indexes were most significantly elevated in the high-dose TW group (Figure 1A). The pathological results indicated that with the increase of the dose of TW, the liver cells showed different degrees of steatosis, edema degeneration, and inflammatory cell infiltration by H and E staining, and the comprehensive pathological score increased in a dose-dependent manner (Figure 1B). The results by Oil Red O staining indicated that, after administration of TW, the liver cells accumulated fat and the fat percentage of the high-dose TW group was significantly higher than the control (Figure 1C). It can be seen that TW-induced liver damage in mice is dose-dependent. Since the high-dose TW induced the most obvious liver damage, the high dose of TW was used in the subsequent attenuation experiments.

While QTF markedly reduced the elevations of ALT, AST, and LDH caused by TW. Among QTF, RG, and PN significantly reduced the elevation of ALT, AST, and LDH, and BM reduced the TW-induced elevation of ALT; And QTF had the most obvious improvement in the ALT, AST, and LDH caused by TW (Figure 2A). RG, PN, and QTF improved the

TW-induced pathological damage of liver cell steatosis, edema degeneration, and inflammatory cell degeneration, and reduced the TW-induced pathological score. And QTF had the most obvious improvement in TW-induced pathological injury and comprehensive pathological score (Figure 2B). Simultaneously, PN and QTF significantly improved the fat accumulation and significantly reduced the fat percentage induced by TW (Figure 2C).

These results showed that QTF reduced the TW-caused hepatotoxicity of mice, and among the drug compatibility of QTF, RG, and PN had the best attenuating effect.

3.2 Qingluo Tongbi Formula Attenuated *T. wilfordii*-Induced Excessive Mitophagy and Endoplasmic Reticulum Stress in C57BL/6J Mice

The results of TEM showed that, TW caused mitochondrial outer membrane and cristae rupture and an increase in autophagosomes and autophagolysosomes in hepatocytes, accompanied by abnormal ER morphology. And the higher the dose of TW was administered, the more severe the damage of mitochondria and ER was shown, and the more autophagosomes and autophagolysosomes were generated (Figure 3A). TW increased the expression levels of mitophagy proteins DRP1 and LC3, and decreased the expression level of P62, while the expression level of MFN1 and FIS1 had no significant changes. It suggested that TW-

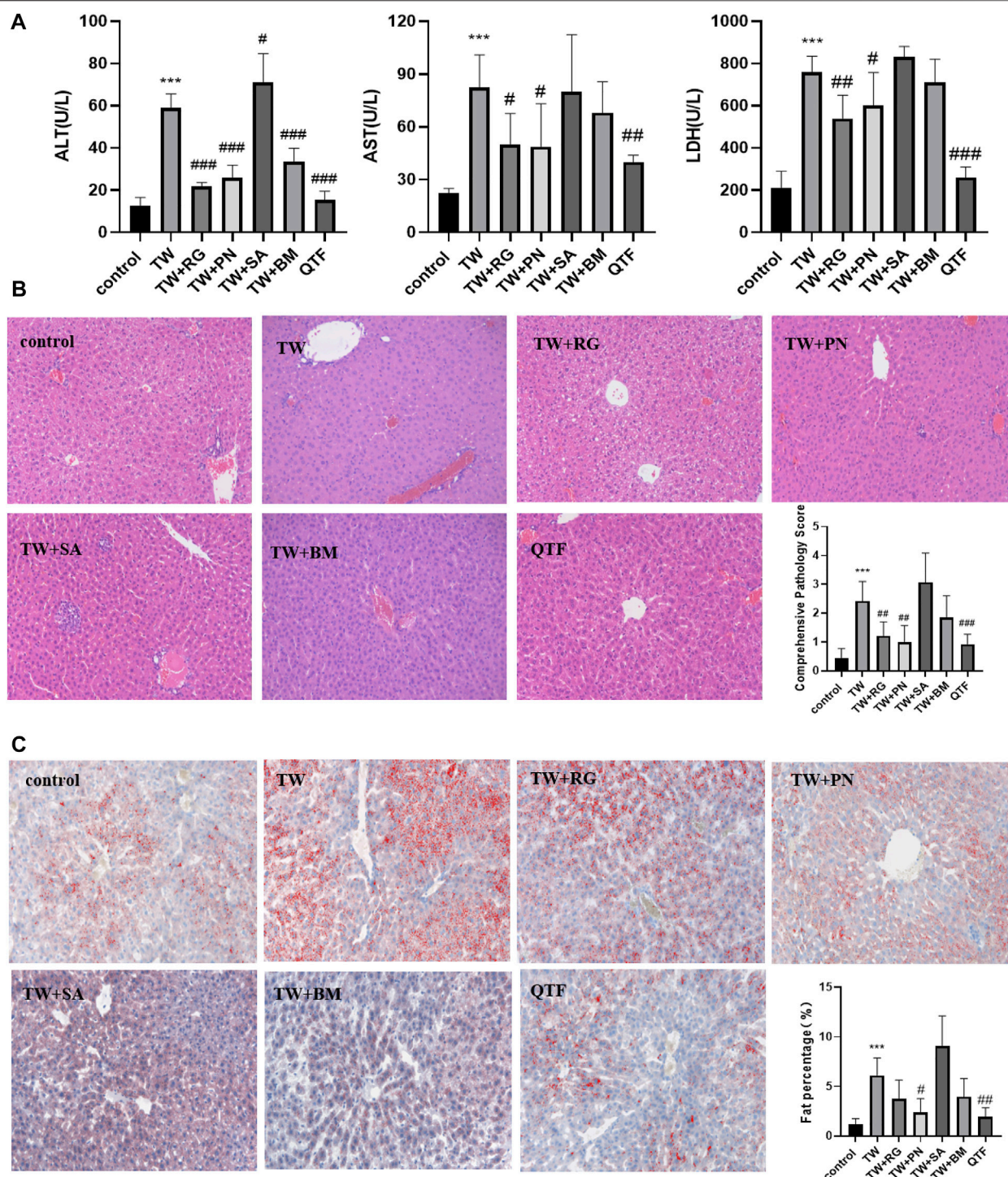


FIGURE 2 | QTF alleviated TW-induced hepatotoxicity in C57BL/6J mice. **(A)** QTF reduced the levels of ALT, AST and LDH caused by TW. **(B)** QTF reduced TW-induced pathological damage and comprehensive pathological score by H&E staining. **(C)** QTF reduced the fat accumulation and fat percentage by Oil red O staining. Compared with the control group, * $p < 0.05$, ** $p < 0.01$, *** $p < 0.001$; compared with the TW group, # $p < 0.05$, ## $p < 0.01$, ### $p < 0.001$.

induced mitophagy was characterized by elevated DRP1. Simultaneously, the expressions of ERS marker protein GRP78 and PERK, and ATF4 were upregulated, indicating

that TW induced ERS by activating the PERK-ATF4 pathway in a dose-dependent manner (**Figure 3B**). And TW simultaneously increased the mRNA levels of GRP78, PERK,

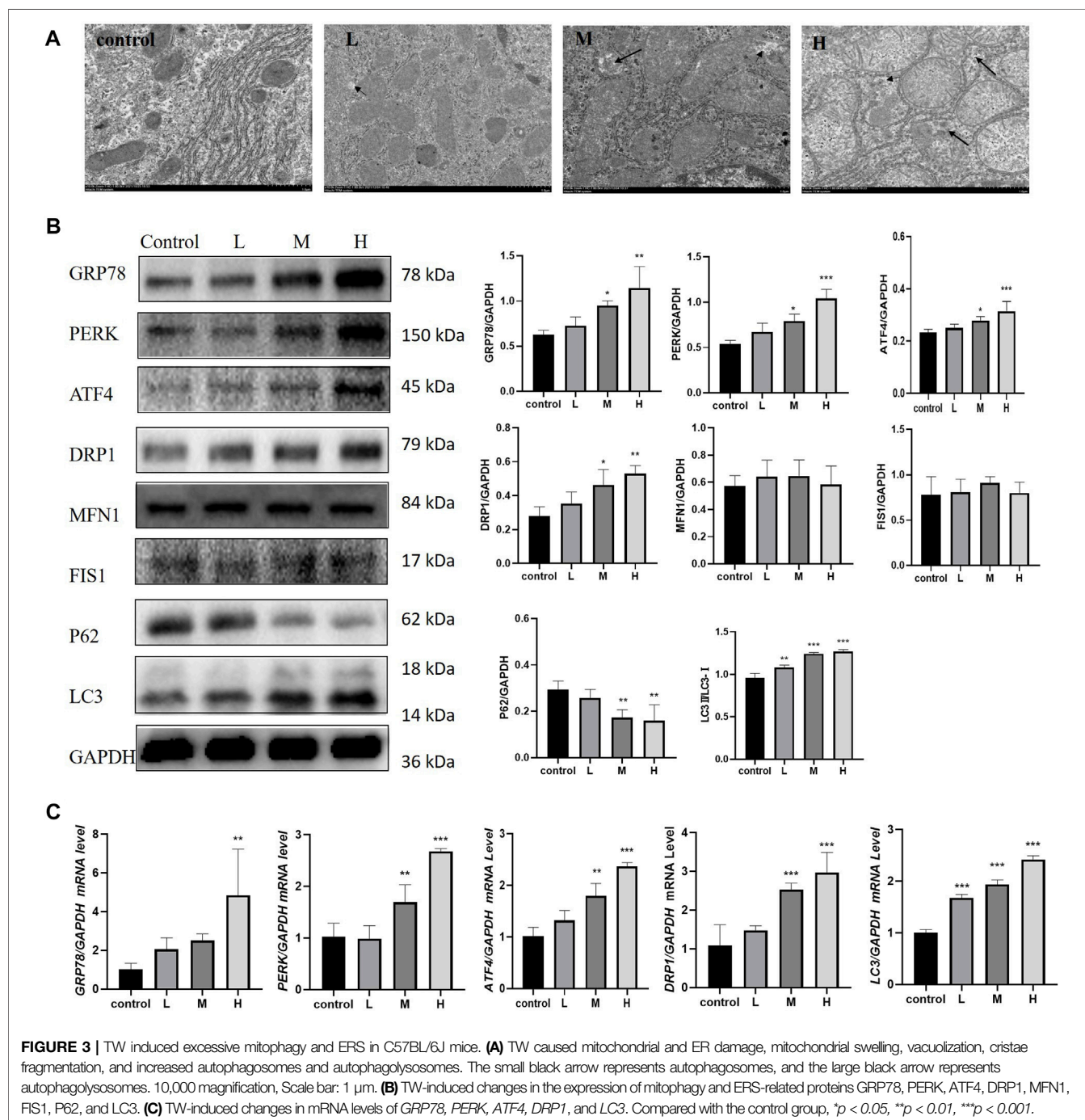
ATF4, *DRP1*, and *LC3* (**Figure 3C**). The results indicated that TW induced upregulation of mitophagy and ERS in hepatotoxicity.

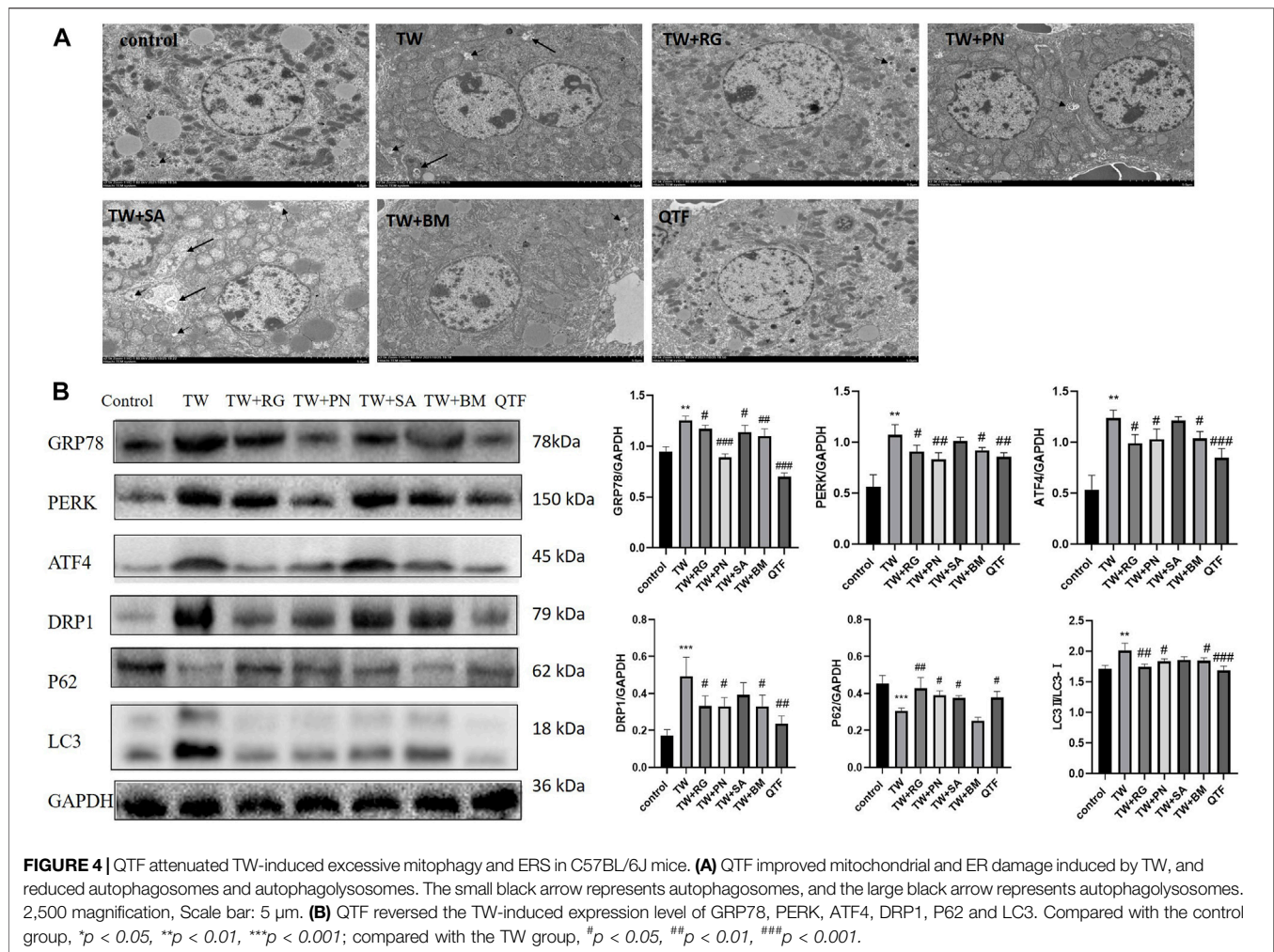
While RG, PN, BM, and QTF improved the TW-induced damage to mitochondria and ER in mice, and reduced autophagosomes and autophagolysosomes (**Figure 4A**). Simultaneously, RG, PN, BM, and QTF reversed the expression of *DRP1*, *LC3*, *P62*, *GRP78*, *PERK*, and *ATF4* induced by TW. And among them, QTF improved the most significantly (**Figure 4B**).

These results indicated that QTF reversed the mitophagy and down-regulated the ERS induced by TW.

3.3 Inhibition of Mitophagy and Endoplasmic Reticulum Stress Attenuated Triptolide-Induced Cytotoxicity in HepaRG Cells

In order to further verify the mitophagy and ERS are important mechanisms of TW-induced hepatotoxicity, triptolide (TP), the





main active component and also the main toxic component of TW, was used in HepaRG cells.

4–64 μ g/L TP resulted in HepaRG cell viability decreased in a time- and dose-dependent manner by CCK8 (Figure 5A). And 4–64 μ g/L TP led to an increase in ALT, AST, and LDH indexes in the cell supernatant (Figure 5B). Immunofluorescence results showed that the production of autophagosomes increased after TP treatment for 24 h in a dose-dependent manner in HepaRG cells (Figure 5C). Simultaneously, TP led to the up-regulation of DRP1, LC3, GRP78, PERK, and ATF4 (P62 down-regulated) (Figure 5D). The results indicated that TP induced HepaRG cell damage, causing excessive mitophagy and ERS. Since TP at a dose of 16 μ g/L induced moderate damage to HepaRG cells, 16 μ g/L TP was set for subsequent experiments.

To explore the role of mitophagy in TW-induced hepatotoxicity, we used Mdivi-1 (Deng et al., 2021), a specific inhibitor of mitophagy. When the cells were treated with Mdivi-1, compared to the TP group, the expression levels of DRP1 and LC3 were significantly decreased (that of P62 was significantly increased), suggesting that TP-induced mitophagy was effectively inhibited (Figure 5E). After inhibiting mitophagy, the cell viability was increased (Figure 5F); At the same time, the

elevations of ALT, AST, and LDH indexes in the cell supernatant were reduced (Figure 5G).

Likewise, to verify the role of ERS in TW-induced live damage, we applied 4-PBA (Pao et al., 2021), the specific inhibitor of ERS. When HepaRG cells were treated with 4-PBA, the expression level of GRP78 was significantly decreased, suggesting that TP-induced ERS was effectively inhibited (Figure 5H). After inhibiting ERS by 4-PBA, the cell viability induced by TP was increased (Figure 5I); Simultaneously, the elevation of ALT, AST, and LDH indexes in the cell supernatant was decreased (Figure 5J).

These results suggested that excessive mitophagy and ERS were important mechanisms of TW-induced cytotoxicity.

3.4 Inhibition of Endoplasmic Reticulum Stress Attenuated TP-Induced Excessive Mitophagy in HepaRG Cells

To further explore the relationship between ERS and mitophagy in TW-induced hepatotoxicity, 4-PBA was used. When ERS was inhibited by 4-PBA in HepaRG cells, the expression level of GRP78 was down-regulated, and the expression levels of DRP1 and LC3 were also decreased

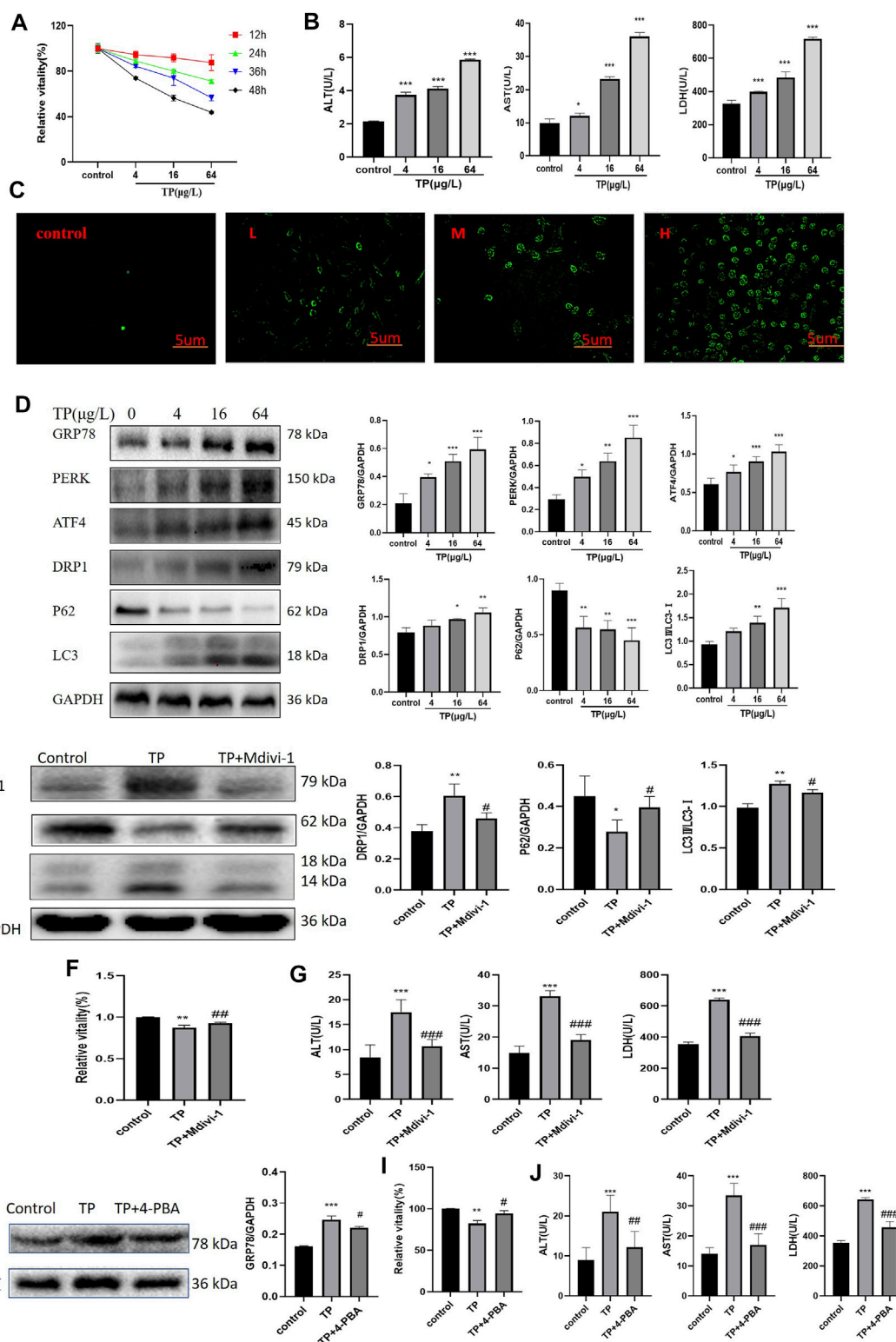
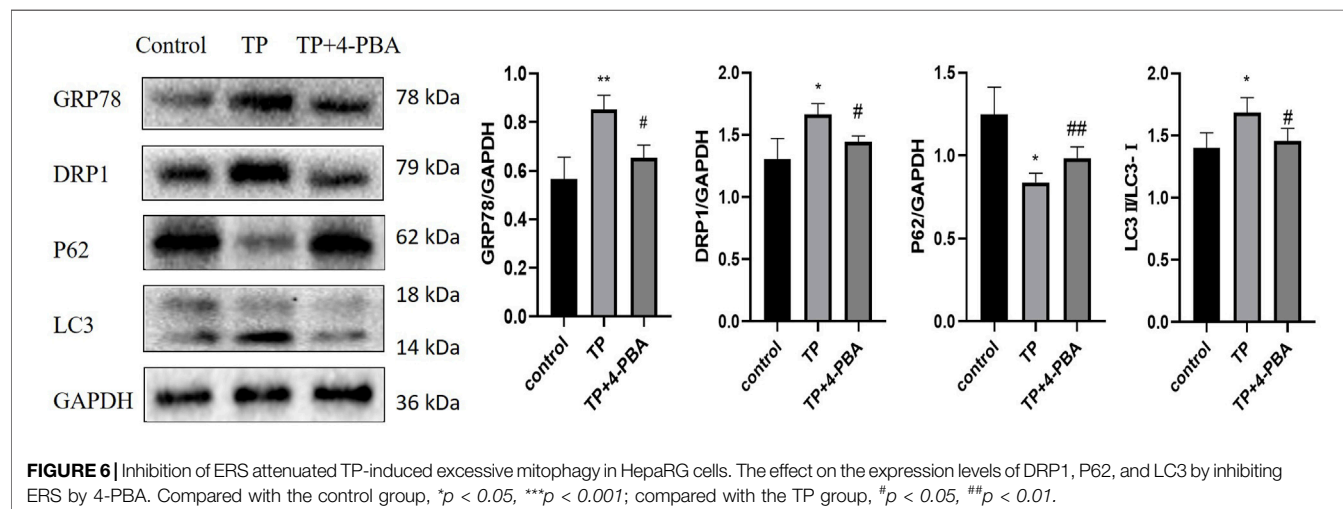


FIGURE 5 | Inhibition of mitophagy and ERS attenuated TP-induced cytotoxicity in HepaRG cells. **(A)** The effect of 4–64 $\mu\text{g/L}$ TP on the viability of HepaRG cells for 12, 24, 36, and 48 h, respectively. **(B)** 4–64 $\mu\text{g/L}$ TP led to the increase of ALT, AST, and LDH indexes in the supernatant of HepaRG cells. **(C)** 4–64 $\mu\text{g/L}$ TP caused the increase of autophagosome production in HepaRG cells. Green fluorescence represented autophagosome. 200 magnification, Scale bar: 5 μm . **(D)** The effect of 4–64 $\mu\text{g/L}$ TP on the expression of GRP78, PERK, ATF4, DRP1, P62, and LC3 in HepaRG cells. **(E)** The effect on the expression levels of DRP1, P62, and LC3 in cells by inhibiting mitophagy by Mdivi-1. **(F)** The effect on cell viability by inhibiting mitophagy by Mdivi-1. **(G)** The effect on ALT, AST, and LDH indexes in the supernatant (Continued)

FIGURE 5 | of HepaRG cells by inhibiting mitophagy by Midivi-1. **(H)** The effect of 4-PBA on the expression of GRP78 in cells. **(I)** The effect on HepaRG cell viability by inhibiting ERS by 4-PBA. **(J)** The effect on ALT, AST, and LDH indexes in cell supernatant by inhibiting ERS by 4-PBA. Compared with the control group, * $p < 0.05$, ** $p < 0.01$, *** $p < 0.001$; compared with the TP group, # $p < 0.05$, ## $p < 0.01$, ### $p < 0.001$.



(that of P62 was increased), indicating that ERS regulated mitophagy (Figure 6).

3.5 Inhibition of the PERK-ATF4 Pathway Downregulated TP-Induced Excessive Mitophagy in HepaRG Cells

To further verify the relationship between the PERK-ATF4 pathway and mitophagy, we applied GSK2656157 (Axten et al., 2013), the specific inhibitor of PERK. When the expression level of PERK was down-regulated by GSK2656157, the expression of ATF4, a key protein downstream of PERK, was down-regulated, and simultaneously, the expression levels of DRP1 and LC3 were decreased (that of P62 was increased) (Figure 7), indicating that the PERK-ATF4 pathway regulates mitophagy in TP-induced cell damage.

3.6 The Pharmacodynamics Combination of Qingluo Tongbi Formula Reduced TP-Induced Damage by DownRegulating Excessive Mitophagy Through the PERK-ATF4 Pathway in HepaRG Cells

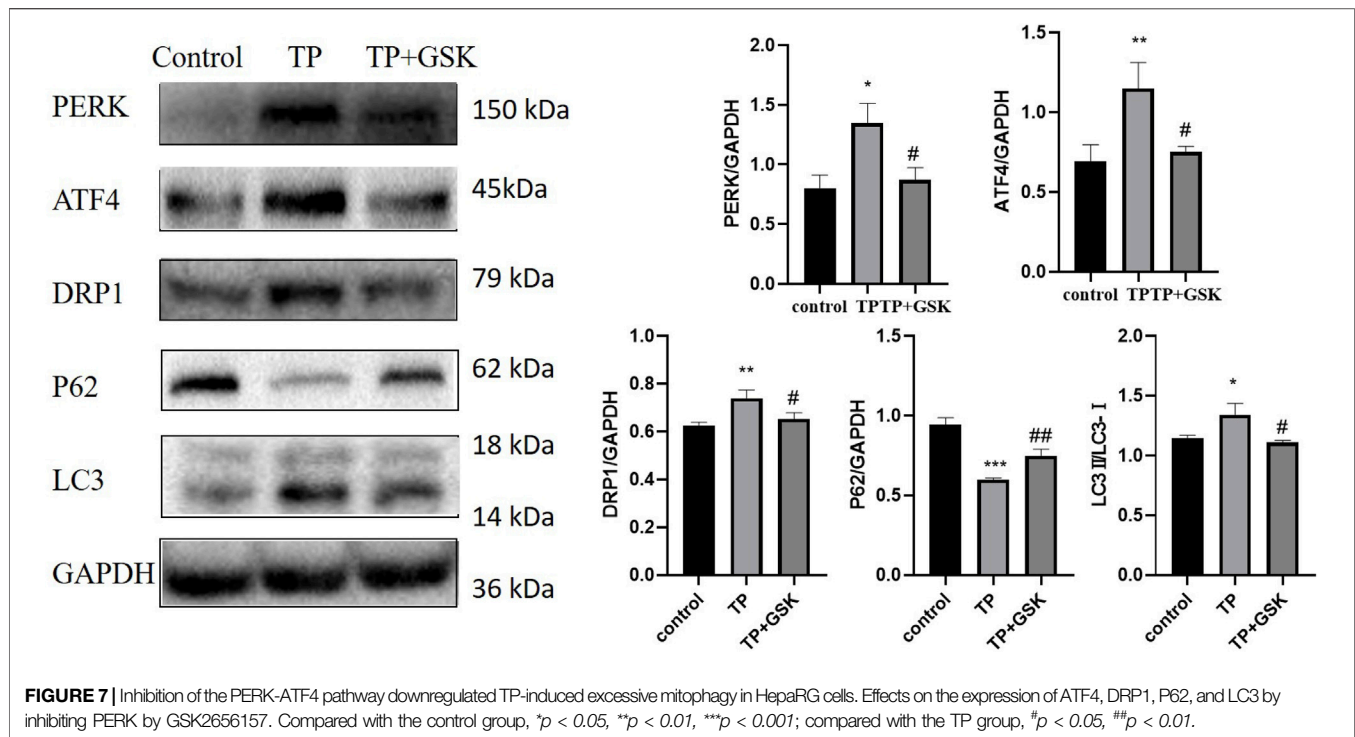
To further verify that QTF reduces TW-caused hepatotoxicity by inhibiting ERS by the PERK-ATF4 pathway and then downregulating excessive mitophagy, we used TP, catalpol (CAT, the main active ingredient of RG), and panax notoginseng saponins (PNS, the main active ingredient of PN), which are the main active ingredients of QTF.

Firstly, the safe dosage of CAT and PNS was screened in HepaRG cells by CCK8, respectively. Then we screened the respective optimal protective doses of CAT and PNS, and

found that when CAT was 80 $\mu\text{g/l}$ and PNS was 10 $\mu\text{g/l}$, their respective protective effect was the most obvious (Supplementary Figure S3). The combination of CAT and PNS improved the viability of HepaRG cells induced by TP (Figure 8A); Simultaneously, they significantly reduced the ALT, AST, and LDH in the supernatant of HepaRG cells induced by TP (Figure 8B). CAT and PNS also significantly ameliorated TP-induced cell morphological damage and death (Figure 8C); Meanwhile, they also reduced TP-induced autophagosomes in HepaRG cells (Figure 8D). PNS was superior to CAT in inhibiting the expression levels of GRP78, PERK, and ATF4 (Figure 8E), while CAT was superior to PNS in reversing the expression levels of DRP1, P62, and LC3 (Figure 8F). The combination of CAT and PNS had the most obvious regulatory effect on the PERK-ATF4 pathway and mitophagy.

4 DISCUSSION

Mitochondria is the “energy reservoir” of cells, providing the necessary energy for various cellular activities through oxidative phosphorylation (Annesley & Fisher 2019). Studies have shown that mitochondrial damage and dysfunction play a causative role in drug-induced liver injury (Fromenty & Pessayre 1995; Pessayre et al., 1999; Lin et al., 2019). Mitophagy, as an important type of selective autophagy, is the main way to remove damaged mitochondria and determines the normal performance of mitochondrial quantity and function (Ashrafi & Schwarz 2013). However, excessive mitophagy induced by drugs and other stimuli results in abnormal mitochondrial number and energy metabolism, causing apoptosis or autophagic death. Mitochondria is an organelle that constantly undergoes



division and fusion. The balance between mitochondrial division and fusion maintains its normal shape and function and is an important basis for ensuring the normal progress of various physiological activities of cells (Yoo & Jung 2018). Mitochondrial fragmentation resulting from an imbalance of mitochondrial fission and fusion is a prerequisite for mitophagy (Chen et al., 2016). Some research has shown that, mitochondrial fission-related factors and degradation of mitochondrial fusion-related factors are required for mitophagy (Shirihai et al., 2015). In mammals, the main proteins that regulate mitochondrial fission are dynamin-related protein 1 (DRP1), mitochondrial fission 1 (FIS1), etc., The proteins that regulate mitochondrial fusion mainly include mitochondrial fusion (MFN, which has two isoforms, MFN1 and MFN2), optic atrophy 1 (OPA1) (Chan 2006). DRP1 is mainly located in the cytoplasm and is a member of the protein dynein superfamily, also known as dynein 1 (Dynamin 1, DNM1L). Some studies suggest that DRP1 is required for mitochondrial fission (Fonseca et al., 2019) and is also the key marker of mitophagy in TP-induced hepatotoxicity (Hasnat et al., 2019). Our study proved that in mice treated with TW, the expression of mitophagy-related proteins was abnormal, which was characterized by the increased expression level of DRP1, while the expression levels of MFN1 and FIS1 did not change significantly. QTF could significantly reverse TW-induced expression levels of mitophagy proteins DRP1, P62, and LC3-II. And QTF could intuitively improve TW-induced mitochondrial morphological damage and reduce autophagosomes and autophagolysosomes by TEM. To further study the important role of mitophagy in the TW-induced hepatotoxicity, we used, TP, CAT, and PNS to verify the

mechanism with the mitophagy inhibitor Midivi-1 in HepaRG cells. The results showed that, when mitophagy was inhibited by Midivi-1, the expression levels of DRP1, LC3-II were down-regulated (that of P62 was up-regulated), and cell viability and liver function indicators ALT, AST, and LDH were improved, suggesting that excessive mitophagy was an important mechanism of TW-induced hepatotoxicity.

Furthermore, TW-caused hepatotoxicity was also accompanied by morphological damage of the ER and the protein and gene levels of Glucose-regulated protein 78 (GRP78) and protein kinase R-like endoplasmic reticulum kinase (PERK) increased, while QTF significantly improved the TW-induced morphological damage of ER and reduced the expression level of GRP78 and PERK. When physical, chemical, and other factors stimulate the body, too many unfolded/misfolded proteins accumulate in the ER, causing ERS and triggering unfolded protein response (UPR) (Ron & Walter 2007); If UPR fails to maintain balance, the cell survival mechanism will turn to the death mechanism (Hetz 2012; Kraskiewicz & FitzGerald 2012). When cells initiate the UPR, GRP78 expression is upregulated, depolymerized and activated to further correct the protein folding of erroneous proteins while activating mechanisms such as autophagy and apoptosis (Lu et al., 2020). In *in vitro* experiments, we used 4-PBA for mechanistic studies to further clarify the role of ERS in TW-induced hepatotoxicity. When ERS was inhibited by 4-PBA, the cell viability and the levels of ALT, AST, and LDH improved, indicating that ERS was also an important mechanism of TW-induced hepatotoxicity, while QTF inhibited the TW-caused ERS.

A cell is an organic whole, like the human body. As the largest membranous organelle in cells, the ER is an important site for protein synthesis, processing and modification (Wang & Kaufman

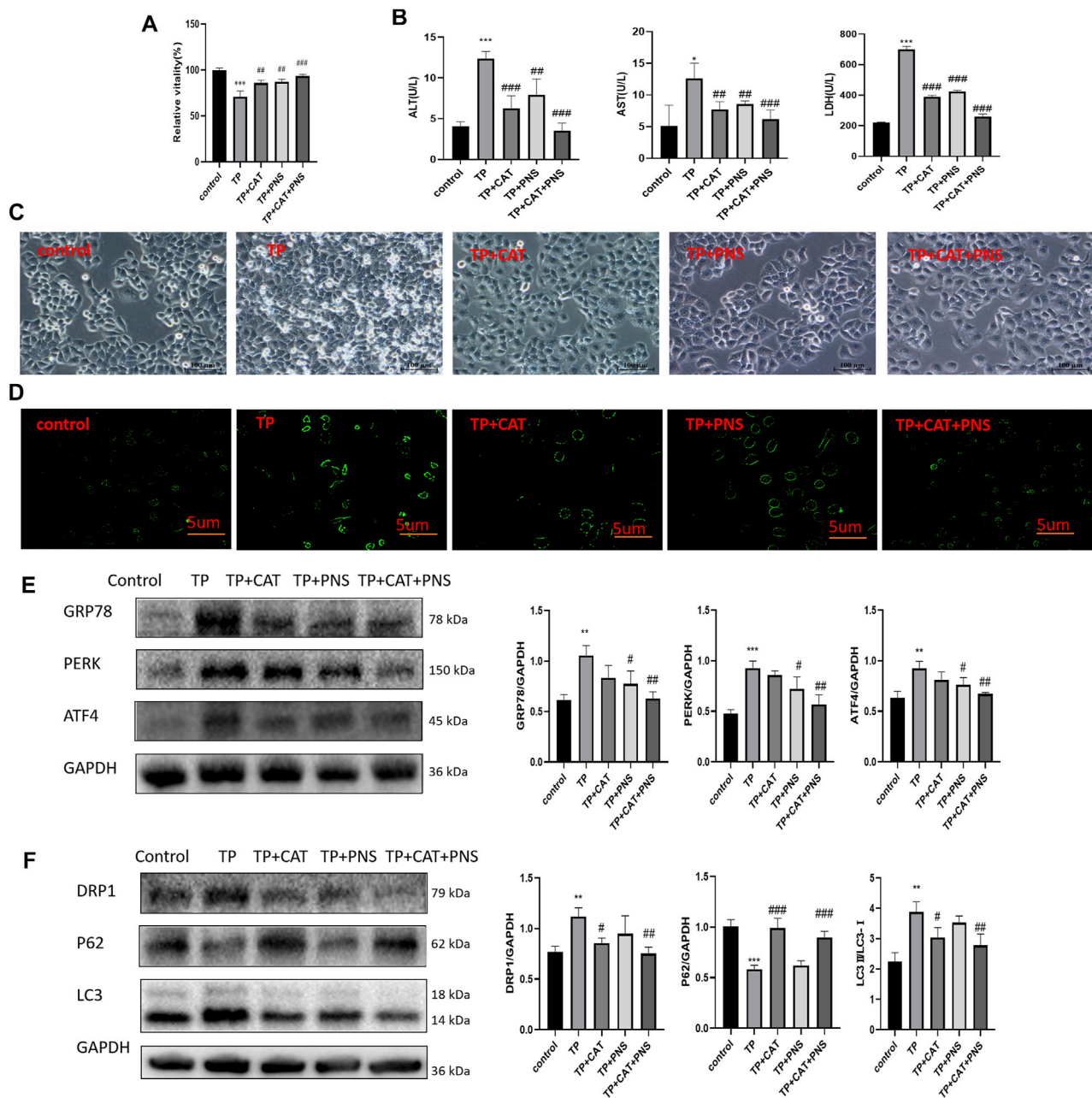


FIGURE 8 | The pharmacodynamic combination of QTF reduced TP-induced damage by down-regulating excessive mitophagy by the PERK-ATF4 pathway in HepaRG cells. **(A)** CAT and PNS improved the TP-induced reduction of HepaRG cell viability. **(B)** CAT and PNS improved the levels of ALT, AST, and LDH in the supernatant of HepaRG cells induced by TP. **(C)** CAT and PNS improved the TP-induced morphological damage to HepaRG cells. 200 magnification, Scale bar: 10 μ m. **(D)** CAT and PNS reduced the TP-induced increase of autophagosomes in HepaRG cells. The green fluorescence represents autophagosomes. 200 magnification, Scale bar: 5 μ m. **(E)** CAT and PNS reduced the expression level of GRP78, PERK, and ATF4 in HepaRG cells induced by TP. **(F)** CAT and PNS reversed the expression level of DRP1, P62, and LC3 in HepaRG cells induced by TP. Compared with the control group, * $p < 0.05$, ** $p < 0.01$, *** $p < 0.001$; compared with the TP group, # $p < 0.05$, ## $p < 0.01$.

2016). It can coordinately regulate physiological activities such as autophagy with mitochondria through MAMs. However, it is not clear that how ERS affects mitophagy and whether QTF reduces the hepatotoxicity of TW is related to ERS and mitophagy. We inhibited ERS by 4-PBA to investigate the link between ERS and mitophagy in TW-induced hepatotoxicity; When ERS was inhibited by 4-PBA, the

expression levels of DRP1 and LC3-II were downregulated (that of P62 was upregulated), demonstrating that ERS regulates mitophagy. It is known that under ERS, cells mainly initiate UPR through three pathways: PERK, inositol-requiring enzyme 1 (IRE1), and activated transcription factor 6 (ATF6). The PERK pathway is the preferred activation pathway induced by ERS (Fung et al., 2015). PERK is a

transmembrane protein located in the ER. When ERS occurs, PERK dissociates from GRP78 and is activated by autophosphorylation, and further activates Activating Transcription Factor 4 (ATF4) by phosphorylating eukaryotic initiation factor 2 α (eIF2 α) (Krishnamoorthy et al., 2014). ATF4, located downstream of the PERK pathway, can regulate the expression of multiple autophagy-related genes, including *LC3B*, *ATG5*, *ATG7*, and *Beclin1*, and plays an extremely important role in regulating autophagy (Rzymiski et al., 2009). Simultaneously, under persistent ERS, ATF4 also induces apoptosis by degrading XIAP and cooperating with C/EBP-homologous protein (CHOP) (B'Chir et al., 2013). The results of our study demonstrated that the PERK-ATF4 pathway was activated in TW-induced hepatotoxicity. To further verify that ERS regulates mitophagy by the PERK-ATF4 pathway, we applied GSK2656157. When the PERK-ATF4 pathway was inhibited by GSK2656157, the expression levels of DRP1 and LC3-II decreased (that of P62 increased), suggesting the PERK-ATF4 pathway was an important pathway for ERS to regulate mitophagy.

The detoxification effects of RG and PN in QTF were the most obvious. *In vitro* studies showed that CAT, the main active ingredient of RG, significantly inhibited the expression of mitophagy proteins DRP1 and LC3-II induced by TP (down-regulated the expression of P62), while PNS, the main active ingredient of PN, significantly inhibited the expression of GRP78, PERK and ATF4 induced by TP. CAT is superior to PNS in regulating mitophagy, and PNS is superior to CAT in regulating ERS.

However, how does DRP1 regulate mitophagy in TW-induced hepatotoxicity? And whether QTF alleviates TW-induced hepatotoxicity by regulating mitophagy by the PINK1-Parkin pathway? These are not quite clear yet and our team will conduct further research in the future.

5 CONCLUSION

Our study shows that, TW-induced hepatotoxicity is associated with excessive mitophagy and ERS, and ERS regulates mitophagy by the PERK-ATF4 pathway; QTF downregulates excessive mitophagy to reduce the TW-induced hepatotoxicity by inhibiting ERS by the PERK-ATF4 pathway. QTF differentially regulates different sites of the PERK-ATF4 pathway and mitophagy through different components to exert the attenuation effect.

REFERENCES

- Annesley, S. J., and Fisher, P. R. (2019). Mitochondria in Health and Disease. *Cells* 8, 680. doi:10.3390/cells8070680
- Ashrafi, G., and Schwarz, T. L. (2013). The Pathways of Mitophagy for Quality Control and Clearance of Mitochondria. *Cell. Death Differ.* 20, 31–42. doi:10.1038/cdd.2012.81
- Axten, J. M., Romeril, S. P., Shu, A., Ralph, J., Medina, J. R., Feng, Y., et al. (2013). Discovery of GSK2656157: An Optimized PERK Inhibitor Selected for Preclinical Development. *ACS Med. Chem. Lett.* 4, 964–968. doi:10.1021/ml400228e
- B'Chir, W., Maurin, A. C., Carraro, V., Averous, J., Jousse, C., Muranishi, Y., et al. (2013). The eIF2 α /ATF4 Pathway Is Essential for Stress-Induced

DATA AVAILABILITY STATEMENT

The raw data supporting the conclusion of this article will be made available by the authors, without undue reservation.

ETHICS STATEMENT

The animal study was reviewed and approved by the Laboratory Animal Center at Nanjing University of Chinese medicine.

AUTHOR CONTRIBUTIONS

LZ conceived and designed the experiments, performed the experiments, prepared figures, authored draft of the paper. JZ, ZF, BJ, and CL helped to perform the experiments, process and analyze data, and review the manuscript. LZ and XZ designed the study and critically reviewed the manuscript. All authors reviewed and approved the final manuscript.

FUNDING

This work was supported by the National Natural Science Foundation of China (NO. 81973741) and the Postgraduate Research and Practice Innovation Program of Jiangsu Province (NO. KYCX21-1673).

ACKNOWLEDGMENTS

We would like to acknowledge the reviewers for their constructive feedback on this manuscript. We would also like to thank the National Natural Science Foundation of China for the financial support.

SUPPLEMENTARY MATERIAL

The Supplementary Material for this article can be found online at: <https://www.frontiersin.org/articles/10.3389/fphar.2022.918466/full#supplementary-material>

Autophagy Gene Expression. *Nucleic Acids Res.* 41, 7683–7699. doi:10.1093/nar/gkt563

- Brunt, E. M. (2000). Grading and Staging the Histopathological Lesions of Chronic Hepatitis: the Knodell Histology Activity Index and beyond. *Hepatology* 31, 241–246. doi:10.1002/hep.510310136
- Chan, D. C. (2006). Mitochondria: Dynamic Organelles in Disease, Aging, and Development. *Cell* 125, 1241–1252. doi:10.1016/j.cell.2006.06.010
- Chen, M., Chen, Z., Wang, Y., Tan, Z., Zhu, C., Li, Y., et al. (2016). Mitophagy Receptor FUNDC1 Regulates Mitochondrial Dynamics and Mitophagy. *Autophagy* 12, 689–702. doi:10.1080/15548627.2016.1151580
- Deng, Y., Li, S., Chen, Z., Wang, W., Geng, B., and Cai, J. (2021). Mdivi-1, a Mitochondrial Fission Inhibitor, Reduces Angiotensin-II- Induced Hypertension by Mediating VSMC Phenotypic Switch. *Biomed. Pharmacother.* 140, 111689. doi:10.1016/j.biopha.2021.111689

- Fonseca, T. B., Sánchez-Guerrero, Á., Milosevic, I., and Raimundo, N. (2019). Mitochondrial Fission Requires DRP1 but Not Dynamins. *Nature* 570, E34–e42. doi:10.1038/s41586-019-1296-y
- Fromenty, B., and Pessayre, D. (1995). Inhibition of Mitochondrial Beta-Oxidation as a Mechanism of Hepatotoxicity. *Pharmacol. Ther.* 67, 101–154. doi:10.1016/0163-7258(95)00012-6
- Fung, T. S., Torres, J., and Liu, D. X. (2015). The Emerging Roles of Viroporins in ER Stress Response and Autophagy Induction during Virus Infection. *Viruses* 7, 2834–2857. doi:10.3390/v7062749
- Hasnat, M., Yuan, Z., Naveed, M., Khan, A., Raza, F., Xu, D., et al. (2019). Drp1-associated Mitochondrial Dysfunction and Mitochondrial Autophagy: a Novel Mechanism in Triptolide-Induced Hepatotoxicity. *Cell. Biol. Toxicol.* 35, 267–280. doi:10.1007/s10565-018-9447-8
- Hetz, C. (2012). The Unfolded Protein Response: Controlling Cell Fate Decisions under ER Stress and beyond. *Nat. Rev. Mol. Cell. Biol.* 13, 89–102. doi:10.1038/nrm3270
- Kraskiewicz, H., and FitzGerald, U. (2012). InterfERing with Endoplasmic Reticulum Stress. *Trends Pharmacol. Sci.* 33, 53–63. doi:10.1016/j.tips.2011.10.002
- Krishnamoorthy, J., Rajesh, K., Mirzajani, F., Kesoglidou, P., Papadakis, A. I., and Koromilas, A. E. (2014). Evidence for eIF2 α Phosphorylation-independent Effects of GSK2656157, a Novel Catalytic Inhibitor of PERK with Clinical Implications. *Cell. Cycle* 13, 801–806. doi:10.4161/cc.27726
- Lin, L., Liu, Y., Fu, S., Qu, C., Li, H., and Ni, J. (2019). Inhibition of Mitochondrial Complex Function-The Hepatotoxicity Mechanism of Emodin Based on Quantitative Proteomic Analyses. *Cells* 8, 263. doi:10.3390/cells8030263
- Liu, T. Y., Zhou, L. L., Zhou, C., Liu, Z. P., Chen, C., Feng, Z., et al. (2015). Inhibition Mechanism of Qingluo Tongbi Granule () on Osteoclast Differentiation Induced by Synovial Fibroblast and Monocytes Co-culture in Adjuvant-Induced Arthritic Rats. *Chin. J. Integr. Med.* 21, 291–298. doi:10.1007/s11655-014-1839-x
- Lu, G., Luo, H., and Zhu, X. (2020). Targeting the GRP78 Pathway for Cancer Therapy. *Front. Med. (Lausanne)* 7, 351. doi:10.3389/fmed.2020.00351
- Lv, H., Jiang, L., Zhu, M., Li, Y., Luo, M., Jiang, P., et al. (2019). The Genus Tripterygium: A Phytochemistry and Pharmacological Review. *Fitoterapia* 137, 104190. doi:10.1016/j.fitote.2019.104190
- Pao, H. P., Liao, W. I., Tang, S. E., Wu, S. Y., Huang, K. L., and Chu, S. J. (2021). Suppression of Endoplasmic Reticulum Stress by 4-PBA Protects Against Hyperoxia-Induced Acute Lung Injury via Up-Regulating Claudin-4 Expression. *Front. Immunol.* 12, 674316. doi:10.3389/fimmu.2021.674316
- Pessayre, D., Mansouri, A., Haouzi, D., and Fromenty, B. (1999). Hepatotoxicity Due to Mitochondrial Dysfunction. *Cell. Biol. Toxicol.* 15, 367–373. doi:10.1023/a:1007649815992
- Ramos, M. I., Karpus, O. N., Broekstra, P., Aarass, S., Jacobsen, S. E., Tak, P. P., et al. (2015). Absence of Fms-like Tyrosine Kinase 3 Ligand (Flt3L) Signalling Protects against Collagen-Induced Arthritis. *Ann. Rheum. Dis.* 74, 211–219. doi:10.1136/annrheumdis-2013-203371
- Ron, D., and Walter, P. (2007). Signal Integration in the Endoplasmic Reticulum Unfolded Protein Response. *Nat. Rev. Mol. Cell. Biol.* 8, 519–529. doi:10.1038/nrm2199
- Rzymiski, T., Milani, M., Singleton, D. C., and Harris, A. L. (2009). Role of ATF4 in Regulation of Autophagy and Resistance to Drugs and Hypoxia. *Cell. Cycle* 8, 3838–3847. doi:10.4161/cc.8.23.10086
- Shirihai, O. S., Song, M., and Dorn, G. W., 2nd (2015). How Mitochondrial Dynamism Orchestrates Mitophagy. *Circ. Res.* 116, 1835–1849. doi:10.1161/circresaha.116.306374
- Veeran, S., Shu, B., Cui, G., Fu, S., and Zhong, G. (2017). Curcumin Induces Autophagic Cell Death in Spodoptera Frugiperda Cells. *Pestic. Biochem. Physiol.* 139, 79–86. doi:10.1016/j.pestbp.2017.05.004
- Wang, M., and Kaufman, R. J. (2016). Protein Misfolding in the Endoplasmic Reticulum as a Conduit to Human Disease. *Nature* 529, 326–335. doi:10.1038/nature17041
- Wu, Y., Geng, X. C., Wang, J. F., Miao, Y. F., Lu, Y. L., and Li, B. (2016). The HepaRG Cell Line, a Superior *In Vitro* Model to L-02, HepG2 and hiHeps Cell Lines for Assessing Drug-Induced Liver Injury. *Cell. Biol. Toxicol.* 32, 37–59. doi:10.1007/s10565-016-9316-2
- Yang, P., Qian, F., Zhang, M., Xu, A. L., Wang, X., Jiang, B., et al. (2020). Zishen Tongluo Formula Ameliorates Collagen-Induced Arthritis in Mice by Modulation of Th17/Treg Balance. *J. Ethnopharmacol.* 250, 112428. doi:10.1016/j.jep.2019.112428
- Yoo, S. M., and Jung, Y. K. (2018). A Molecular Approach to Mitophagy and Mitochondrial Dynamics. *Mol. Cells* 41, 18–26. doi:10.14348/molcells.2018.2277
- Yu, Z., Feng, Z., Fu, L., Wang, J., Li, C., Zhu, H., et al. (2022). Qingluotongbi Formula Regulates the LXRA-ERS-SREBP-1c Pathway in Hepatocytes to Alleviate the Liver Injury Caused by Tripterygium Wilfordii Hook. F. *J. Ethnopharmacol.* 287, 114952. doi:10.1016/j.jep.2021.114952
- Zhang, L., Li, C., Fu, L., Yu, Z., Xu, G., Zhou, J., et al. (2022). Protection of Catalpol against Triptolide-Induced Hepatotoxicity by Inhibiting Excessive Autophagy via the PERK-ATF4-CHOP Pathway. *PeerJ* 10, e12759. doi:10.7717/peerj.12759
- Zhang, Q., Li, Y., Liu, M., Duan, J., Zhou, X., and Zhu, H. (2018). Compatibility with Panax Notoginseng and Rehmannia Glutinosa Alleviates the Hepatotoxicity and Nephrotoxicity of Tripterygium Wilfordii via Modulating the Pharmacokinetics of Triptolide. *Int. J. Mol. Sci.* 19, 10305. doi:10.3390/ijms19010305

Conflict of Interest: The authors declare that the research was conducted in the absence of any commercial or financial relationships that could be construed as a potential conflict of interest.

Publisher's Note: All claims expressed in this article are solely those of the authors and do not necessarily represent those of their affiliated organizations, or those of the publisher, the editors and the reviewers. Any product that may be evaluated in this article, or claim that may be made by its manufacturer, is not guaranteed or endorsed by the publisher.

Copyright © 2022 Zhang, Zhou, Feng, Jiang, Li, Zhou and Zhou. This is an open-access article distributed under the terms of the Creative Commons Attribution License (CC BY). The use, distribution or reproduction in other forums is permitted, provided the original author(s) and the copyright owner(s) are credited and that the original publication in this journal is cited, in accordance with accepted academic practice. No use, distribution or reproduction is permitted which does not comply with these terms.



The Effect of Lithocholic Acid on the Gut-Liver Axis

Wei Sheng, Guang Ji and Li Zhang*

Institute of Digestive Diseases, Longhua Hospital, Shanghai University of Traditional Chinese Medicine, Shanghai, China

Lithocholic acid (LCA) is a monohydroxy bile acid produced by intestinal flora, which has been found to be associated with a variety of hepatic and intestinal diseases. LCA is previously considered to be toxic, however, recent studies revealed that LCA and its derivatives may exert anti-inflammatory and anti-tumor effects under certain conditions. LCA goes through enterohepatic circulation along with other bile acids, here, we mainly discuss the effects of LCA on the gut-liver axis, including the regulation of gut microbiota, intestinal barrier, and relevant nuclear receptors (VDR, PXR) and G protein-coupled receptor five in related diseases. In addition, we also find that some natural ingredients are involved in regulating the detoxification and excretion of LCA, and the interaction with LCA also mediates its own biological activity.

Keywords: lithocholic acid, natural products, intestinal barrier, gut microbiota, bile acid receptors

OPEN ACCESS

Edited by:

Massimo Lucarini,
Council for Agricultural Research and
Economics, Italy

Reviewed by:

Jianye Dai,
Lanzhou University, China
Waddah Alrefai,
University of Illinois at Chicago,
United States

*Correspondence:

Li Zhang
zhangli.hl@163.com

Specialty section:

This article was submitted to
Ethnopharmacology,
a section of the journal
Frontiers in Pharmacology

Received: 01 April 2022

Accepted: 16 June 2022

Published: 07 July 2022

Citation:

Sheng W, Ji G and Zhang L (2022) The
Effect of Lithocholic Acid on the Gut-
Liver Axis.
Front. Pharmacol. 13:910493.
doi: 10.3389/fphar.2022.910493

INTRODUCTION

Bile acids (BAs) have been shown to play an irreplaceable role in many diseases (Fuchs and Trauner, 2022). The size and composition of the BA pool is the target for the treatment of a series of hepatointestinal diseases including inflammatory bowel disease (IBD), primary biliary cholangitis (PBC) and non-alcoholic steatohepatitis (NASH) (Ridlon et al., 2006; Kim et al., 2019). Lithocholic acid (LCA), also known as 3 α -hydroxy-5 β -cholan-24-oic acid, is a monohydroxy BA produced from chenodeoxycholic acid (CDCA) or ursodeoxycholic acid (UDCA) by the action of intestinal bacteria (Fiorucci et al., 2018; Marion et al., 2019). LCA acts as a detergent to solubilize fat for absorption in intestine, but is considered to be toxic for hepatocytes (Hofmann, 2004; Doden et al., 2021). Particularly, LCA has also been considered to be a carcinogen, high concentrations of LCA induce oxidative stress and DNA damage, and promote tumor development by inhibiting the action of DNA repair enzymes and promoting the proliferation of cells (Bernstein et al., 2005; Ridlon et al., 2016b; Nguyen et al., 2021). Contrary to the previous reports, recent studies revealed that LCA might be a protector in restraining hepatic and intestinal inflammation (Hamilton et al., 2007; Ward et al., 2017; Sinha et al., 2020). Some other studies have found that LCA also potentiates anti-aging and anti-tumor effects (Burstein et al., 2012; Arlia-Ciommo et al., 2014; Arlia-Ciommo et al., 2018). For example, galactosylated poly (ethyleneglycol)-LCA, a nanoparticle formulation can selectively induce apoptosis in hepatocellular carcinoma cells without adverse effects on normal liver cells (Gankhuyag et al., 2015).

Many natural extracts from plants or animals can regulate intestinal microbiota, BA metabolism and related signaling pathways (Han et al., 2017; Hu et al., 2021). Recent studies have shown that natural components are involved in the regulation of LCA production, detoxification and related signaling pathways. For example, grape seed proanthocyanidin and polyphenol extracts from pomegranate are reported to promote the production of LCA (Yang et al., 2018; Wu et al., 2021). Glycyrrhizin and oleanolic are found to accelerate LCA detoxification by up-regulating the expression of detoxification enzymes (Wang et al., 2012; Chai et al., 2015). Kaki-tannin increases

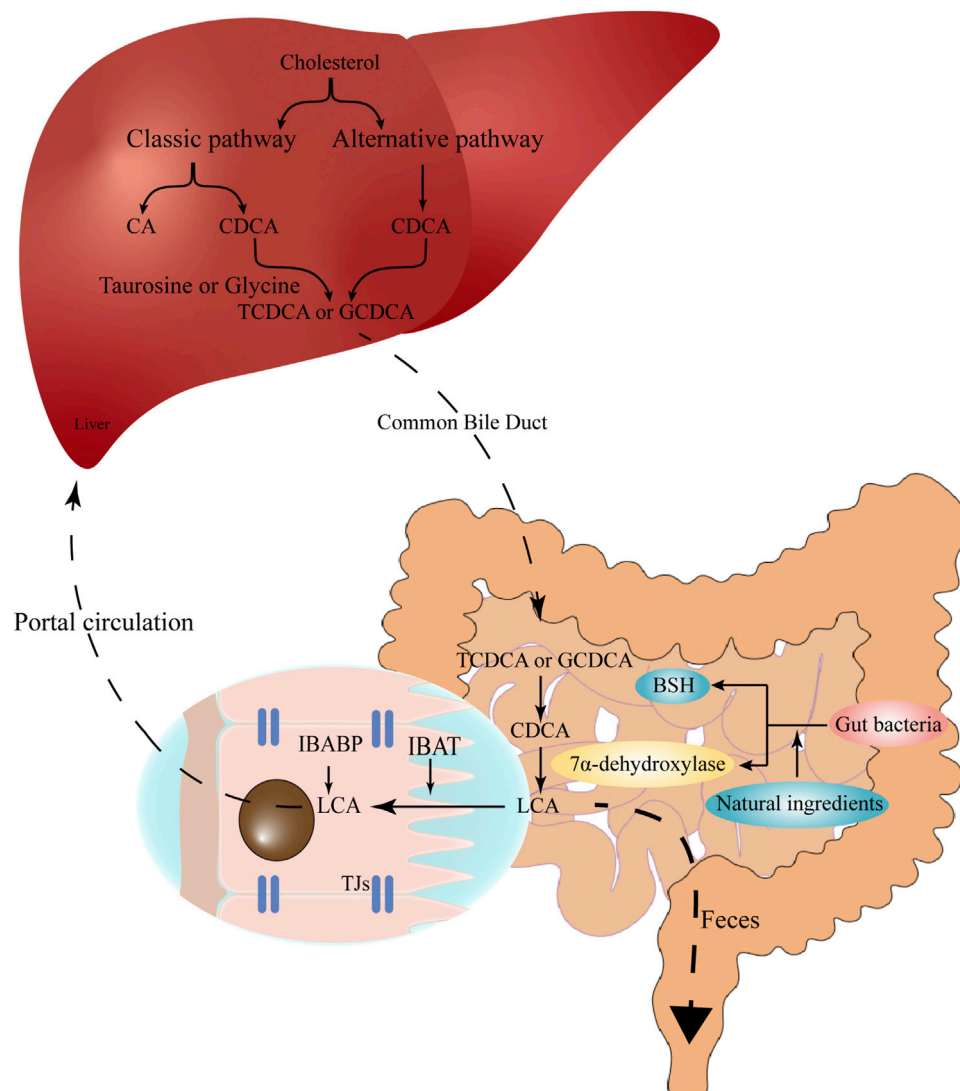


FIGURE 1 | The synthesis and enterohepatic circulation of LCA. Cholesterol is converted into primary BAs (CA and CDCA) under the action of CYP7A1, CYP27A1, CYP8B1 and related enzymes in hepatocytes. Primary BAs conjugate with taurine or glycine, temporarily store in the gallbladder, and then are excreted into the gut upon food intake. In the gut, the conjugated BAs are subsequently uncoupled by gut bacteria and converted to secondary BAs (e.g., LCA) via 7 α -dehydroxylation. The high-affinity IBAT actively transports conjugated and unconjugated LCA from the intestinal lumen to the ileocytes, where they are bound to IBABP and eventually exported across the basement membrane to the portal circulation and back to the liver. Natural ingredients can up-regulate the expression of bile salt hydrolase and 7 α -dehydroxylase, therefore promote the production of LCA. LCA, lithocholic acid; BAs, bile acids; CA, cholic acid; CDCA, chenodeoxycholic acid; CYP7A1, cholesterol 7 α -hydroxylase; CYP27A1, sterol 27-hydroxylase; CYP8B1, 24-hydroxycholesterol-7 α -hydroxylase; IBAT, intestinal bile acid transporter; IBABP, ileal bile acid binding protein.

the fecal excretion of LCA (Nishida et al., 2021). Bufalin enhances the activation of vitamin D receptor (VDR) via LCA binding (Nakano et al., 2005). Furthermore, natural ingredients modified by LCA can enhance their albumin affinity and stability, thus continuously exhibiting effective concentrations and better therapeutic effects (Han et al., 2018; Sreekanth et al., 2021).

Collectively, LCA undergoes enterohepatic circulation along with other BA species, and affects the gut-liver axis and the development of related diseases. A series of natural ingredients are involved in the regulation of LCA metabolism. Therefore, this review will discuss the new understanding and update the

progression of the functions of LCA, and how natural ingredients modulate LCA metabolism.

THE SYNTHESIS OF LCA

BAs are synthesized from cholesterol in the liver via both the classic pathway and the alternative pathway. Currently, 14 essential enzymes are identified in converting cholesterol to primary BAs in the liver (Ridlon et al., 2006). In the classic pathway, the rate-limiting enzyme cholesterol 7 α -hydroxylase

(CYP7A1) is mainly responsible for the cholic acid (CA) and CDCA synthesis. As far as the alternative pathway, the main rate-limiting enzyme is sterol 27-hydrolase (CYP27A1), which responds to CDCA production (Fuchs and Trauner, 2022). It is reported that extracts from some natural products can promote LCA production via activating intestinal farnesoid X receptor (FXR) signaling and increasing the gene expression of BA alternative pathway synthetases CYP7B1 and CYP27A1 (Wu et al., 2021). Polyphenol extracts from pomegranates also increase the expression of CYP7A1 and CYP7B1, and increase the expression levels of some hepatic genes involved in fatty acid β -oxidation (Yang et al., 2018).

These primary BAs (CA and CDCA) are then conjugated with taurine or glycine to form conjugated BAs in the liver, the conjugation can reduce the pK_a and increase the solubility of BAs (Ridlon et al., 2006). Conjugated primary BAs are then temporarily stored in the gallbladder and transported into the gut upon food intake for emulsifying dietary lipids and fat-soluble vitamins (Doden et al., 2021). In the gut, the conjugated primary BAs are subsequently uncoupled by intestinal bacteria via the action of bile salt hydrolase (BSH) (Ridlon et al., 2016a), and then converted to secondary BAs via 7 α -dehydroxylation (Dawson and Karpen, 2015). The production of LCA is mainly attributed to 7 α -dehydroxylase-producing bacteria such as *Clostridium* and *Eubacterium* in human, while in rodents, LCA can also be produced by UDCA through 7 β -dehydroxylase (Fiorucci et al., 2018). Furthermore, a Chinese medicinal herb, vinegar frankincense is reported to activate the BSH activity and LCA production, thus promote the conjugation of BAs in the liver (Peng et al., 2022) (Figure 1). Therefore, the cellular cholesterol, primary BA excretion, as well as the structure of gut microbiota conjointly determine the production of LCA in the gut.

THE ENTEROHEPATIC CIRCULATION AND EXCRETION OF LCA

The size of the BA pool, under physiological conditions, is defined as the total amount of BAs in the enterohepatic circulation (Sarathy et al., 2017). Secondary BAs such as deoxycholic acid (DCA), LCA and their derivatives are important components of the circulating BA pool (Arab et al., 2017), accounting for more than 90% of the BA pool in the intestine and more than 25% in the gallbladder (Ridlon et al., 2006). The total BA pool is about 1,300–3,650 mg, while the physiological concentration of LCA is about 50–150 mg (Sarathy et al., 2017). In the enterohepatic circulation, LCA is mainly detected in the portal vein as conjugates, such as glyco-LCA (GLCA) and tauro-LCA (TLCA) (Bansal and Lau, 2019), the free form of LCA can reach 0.5 μ M in the peripheral circulation (Steiner et al., 2011). During the enterohepatic circulation, the high-affinity intestinal bile acid transporter (IBAT) actively transports conjugated and unconjugated BAs from the intestinal lumen to the ileocytes, where they are bound to ileal bile acid-binding protein (IBABP), exported across the basement membrane to the portal circulation, and eventually back to the liver (Dawson and Karpen, 2015; Ridlon et al., 2016b). When

LCA reenters the liver via the enterohepatic circulation, it is mainly converted to taurine and glycosylated conjugates, and conjugated LCA is then converted to 3-sulfate and 3-glucosylate LCA via sulfotransferase (SULT) and UDP-glucuronosyltransferase (Stiehl, 1974; Dionne et al., 1994).

About 2 g of the BAs undergo continuous enterohepatic circulation 8–10 times per day, while 95% BAs can be re-absorbed in each cycle, about 600–800 mg of BAs directly enter the large intestine and are excreted via the feces (Fiorucci et al., 2018; Doden et al., 2021). The fecal-dependent excretion is mainly attributed to the conjugation of LCA. Although the free form of LCA is insoluble in water and effectively precipitated in the acidic environment of the colon, the conjugated LCAs are soluble in acidic pH solutions and are resistant to precipitation (Hofmann and Roda, 1984). In addition, binding to VDR leads to enzymatic sulfidation of LCA, which increases LCA hydrophilicity and inhibits the passive absorption by the colonic epithelium (Huang et al., 2010; Ridlon et al., 2016b). Supplementation of natural products may also affect the excretion of LCA. Kaki-tannin (an extract from persimmon) preferentially binds to monohydroxy LCA and promotes its excretion (Nishida et al., 2021). Ethanolic extract of *Fructus schisandrae* enhances the excretion of BAs to the intestine and feces and restores the structure of intestinal flora that is destroyed by excess LCA (Li et al., 2020).

DETOXIFICATION OF LCA

The liver is the primary place for drug metabolism and elimination, including processes such as drug uptake, phase I and II reactions, and excretion (Ruiz et al., 2013). The biotransformation can effectively reduce the toxicity of various endogenous and exogenous toxins. After reabsorption to the liver, LCA initially undergoes a phase I metabolic reaction catalyzed by cytochrome P450 (CYP450) enzymes in hepatocytes and a subsequent phase II reaction in which the 3 α -hydroxyl site is conjugated to sulfate (Kitada et al., 2003; Hartley et al., 2004). CYP450-mediated hydroxylation is considered to be an effective detoxification mechanism in rodents and monkeys, whereas human LCA is detoxified mainly through sulfated conjugation (Hartley et al., 2004). In addition, studies on Caco-2 cells (human colon cancer cell line) showed that LCA is rapidly metabolized to the less toxic metabolites by sulfation during its first pass through the human liver, whereas other BA species lack such an efficient sulfation ability (Gadacz et al., 1976; Hofmann, 2004).

However, recent studies have shown that SULT2A1-catalyzed LCA sulfation is also a predominant detoxification pathway in mouse liver, whereas CYP3A is only involved in the formation of 6 α - and 6 β -hydroxylation of LCA microsomes as an alternative pathway (Kitada et al., 2003). In Caco-2 cells, LCA is mainly detoxified in the sulfonation reaction catalyzed by SULT2A1 to form LCA-S (Huang et al., 2010; Kurogi et al., 2011), while GLCA and TLCA undergoes sulfonation to form glycolithocholic acid sulfate (GLCA-S) and tauroolithocholic acid sulfate (TLCA-S), respectively (Chen and Segel, 1985). In rat liver, LCA is mainly transformed into murideoxycholic acid (MDCA) under the

action of 6 β -hydroxylation of CYP2C, CYP3A and CYP2D1 (Zimniak et al., 1989; Dionne et al., 1994; Deo and Bandiera, 2008). In addition, the most predominant subfamily of CYP450 enzymes is CYP2C in rat liver, whereas in the human liver, CYP3A is the predominant enzyme for the formation of LCA metabolites, such as LCA 6 α - and 6 β -hydroxylation (Araya and Wikvall, 1999; Xie et al., 2001; Deo and Bandiera, 2008). LCA can be sulfated in Caco-2 cells, this sulfation appeared to be an important mechanism for blocking LCA-induced malignant epithelial phenotype, as LCA alone induces a tumor-invasive phenotype in Caco-2 cell, whereas its sulfate counterpart LCA-S does not (Halvorsen et al., 2000). Once the sulfation is impaired, excessive accumulation of LCA may lead to associated adverse effects (e.g., cholestasis) (Bansal and Lau, 2019).

Many natural components can participate in the process of LCA detoxification and reduce LCA-induced liver damage. For example, glycyrrhizin, the main component of licorice, can promote the detoxification process of LCA by accelerating CYP3A catalyzation (Wang et al., 2012). Both juniperus procera extract and artemisinin treatment prevent hepatotoxicity and cholestasis caused by LCA exposure (Alkhedaide, 2018; Alkhedaide et al., 2018). Lysimachia christinae Hance also improves LCA-induced cholecystitis (Yang et al., 2011). Oleanolic acid isolated from swede has also been shown to promote the expression of detoxification enzymes CYP3A, UGT2b, and SULT2A1, and significantly reduce the serum BA levels (Chai et al., 2015).

LCA AND THE INTESTINAL ENVIRONMENT

LCA and Intestinal Flora

BA is steroid molecules that modulate the host and the microorganisms that they carry, and their antimicrobial properties inhibit the overgrowth of intestinal bacteria (Zhou and Hylemon, 2014). Similarly, as the second “genome”, the microbiome content and their genetic structure also influence the composition of the BA pool (Begley et al., 2005; Ridlon et al., 2016b). BAs undergo different biotransformation, in the liver, predominant BAs are conjugative and oxidative, whereas they are prone to be hydrolytic and reductive in the gut by the action of microbiota (Ridlon et al., 2016b). Secondary BAs are the most concentrated bacterial-derived intestinal metabolites (Sinha et al., 2020). Clostridium and Eubacterium expressing 7 α -dehydroxylase is known to promote LCA synthesis (do Nascimento et al., 2015). The enrichment of 7 α -dehydroxylase producing-bacteria might be a key rate-limiting enzyme in the formation of LCA (Wells et al., 2000). The abundance of Clostridium and Eubacterium in the colon is relatively low, whereas the amount of primary BAs to be treated is large (Ridlon et al., 2006). Many natural ingredients have been reported to up-regulate the expressing 7 α -dehydroxylase producing gut microbiota and promote LCA production. For example, capsaicin significantly increases the abundance of Bacteroides genera, which is associated with LCA production (Hui et al., 2020a). Curcumin increases the relative abundance of Lactobacillus, the prominent BSH-producing bacteria (Han et al.,

2021). In mice with dextran sulfate sodium-induced colitis, dihydromyricetin also significantly increases the ratio of Lactobacillus and Akkermansia genera, thus increasing the intestinal LCA species (Dong et al., 2021).

BAs can cause non-specific damage to the cytoplasmic membrane of bacteria due to their lipophilicity and decontamination ability (Gonzalez et al., 2020). It should be noted that among these amphiphilic molecules, LCA is the most lipophilic and hydrophobic BA (Goldberg et al., 2010; Ward et al., 2017). Moreover, LCA also exhibits specific antibacterial effects against certain bacteria. LCA at 32 mg/L rapidly destroyed Helicobacter pylori and prevented its growth, more importantly, LCA even shows synergistic effects with clarithromycin or levofloxacin (Gonzalez et al., 2020). Furthermore, in the evaluation of the function of LCA and its metabolites, Nascimento et al. found that these metabolites not only show significant antibacterial activity against Escherichia coli, Staphylococcus aureus, Bacillus cereus, and Pseudomonas aeruginosa, certain LCA metabolites could even synergistically enhance the function of antibiotics (do Nascimento et al., 2015).

The enrichment of bacteria that promote secondary BA production is reported to be reduced in patients with ulcerative colitis, while secondary BAs supplementation could alleviate intestinal inflammation (Sinha et al., 2020). In addition, dihydromyricetin supplementation also restores the relevant dysbiosis and increases the gastrointestinal levels of CDCA and LCA, thereby improving the metabolism of BAs and alleviating the colitis in mice (Dong et al., 2021). Furthermore, compared to healthy children, the abundance of BSH and 7 α -dehydroxylase-producing bacteria Eubacterium and Ruminococcus in children with NAFLD is significantly decreased, which is in correlation with the concentration of fecal LCA (Yu et al., 2021). In addition, Ruminococcus is also significantly reduced in patients with irritable bowel syndrome with diarrhea (IBS-D), which may cause an increase in primary BAs (CA and CDCA) and a decrease in secondary BAs (LCA and UDCA) in feces (Wei et al., 2020). The clinical significance of these findings lies in the fact that we can reduce the intestinal inflammatory response in IBD by specifically restoring the original levels of secondary BAs, either through direct BA supplementation or indirectly bacteria modulation (Sinha et al., 2020).

Diet is another critical modulator of gut microbiota and BAs (Ridlon et al., 2014). A hydrolysable protein diet is found to diminish chronic enteropathy (e.g., Crohn's disease), possibly through inhibiting the growth of pathogenic bacteria such as Escherichia coli and Clostridium perfringens, and promoting secondary BA production (Wang et al., 2019). High-fat diet or high-animal protein diet may stimulate BA excretion into the intestine, increase BSH-producing bacteria, and lead to LCA accumulation (David et al., 2014; O'Keefe et al., 2015; Ridlon et al., 2016b). Consuming excessive animal protein or fat potentiate risks for CRC, which may be associated with a high concentration of LCA in the gut (Durko and Malecka-Panas, 2014). Another study pointed out that a high-fat and high-sugar diet-induced dysbiosis subsequently initiates BA alteration and liver injury in mice (Iwamoto et al., 2021). Therefore, there is a

dynamic balance between the diet, gut microbiome and the size or composition of the BA pool.

LCA and Intestinal Barrier

The intestinal barrier is mainly composed of a biological barrier, mechanical barrier, immune barrier and chemical barrier. Among them, the mechanical barrier is the most important line of defense in the intestinal epithelial barrier. The mechanical barrier is composed of mucosal epithelial cells, lateral tight junction proteins (TJs) and a basement membrane, which can protect against microorganisms, pathogens and potentially toxic substances. Intestinal mucosal barrier dysfunction can lead to increased permeability and inflammatory-related diseases, including IBD, necrotizing enterocolitis, and NASH (Wang et al., 2015; Holmberg et al., 2018). TJs, also known as interepithelial cell junctions, are located in the most apical region of cell-cell contacts, and are composed of a group of transmembrane proteins (e.g., Occludin and Claudin-1), as well as peripheral membrane proteins (e.g., Zonula occludens-1, E-cadherin) (Sanchez de Medina et al., 2014; Chen et al., 2015; Otani and Furuse, 2020). Studies have shown that altered expression and localization of TJs are associated with impairment of intestinal epithelial barrier induced by proinflammatory cytokines (PiC) (Suzuki et al., 2011).

Under physiological conditions, conjugated BAs are completely ionized and impermeable to epithelial cell membranes such as hepatocyte membranes and bile duct cell membranes (Ridlon et al., 2016b). Once the intestinal barrier is damaged, various toxic substances (e.g., endotoxins, BAs, bacterial debris) can enter the circulation, thus causing intestinal and systematic inflammation. Overwhelm BAs are usually assumed to be toxic to the physiological intestinal structure. Surprisingly, CDCA and its 7 α -deoxy derivative LCA may have exactly the opposite effect on the epithelial integrity of human colonic cells (Sarathy et al., 2017). CDCA stimulates the secretion of Cl⁻ (Dharmasathaphorn et al., 1989; Ao et al., 2013), whereas physiological concentration (0.005–0.05 mmol/L) of LCA inhibits Cl⁻ secretion in the colon (Ao et al., 2016). This finding suggests that a low dose of LCA has potential in the treatment of diarrhoeal diseases. Conversely, high concentrations of LCA may contribute to the development of constipation. This is also evidenced by the improvement in constipation observed in rats with constipation treated with rhubarb, because rhubarb treatment reduced intestinal LCA levels (Yang et al., 2022).

In TNF- α stressed Caco-2 cells, LCA partially reversed the decrease in transepithelial electrical resistance (TEER) and the increase in FITC-Dextran flux, and increased the expression of TJs (Yao et al., 2019). LCA alone had no effect either on TEER or paracellular permeability, however, LCA significantly attenuated ($\geq 80\%$) the effect of PiC on intestinal barrier permeability (Sarathy et al., 2017). Further research has shown that LCA also attenuated intestinal barrier permeability induced by CDCA combined with PiC (Sarathy et al., 2017). LCA significantly improves TEER of co-cultured Caco-2 and HT29-MTX-E12 cells, and increases the expression of TJs (van der Lugt et al., 2022). Our recent work revealed that Traditional Chinese

medicine prescription Jiangzhi Granule attenuates NASH through secondary BAs (e.g., LCA and keto-LCA) mediated VDR activation (Cao et al., 2022). Paradoxically, another Caco-2 cell assay showed that a higher concentration of LCA (100–200 μ M) down-regulates the expression of genes encoding TJs and up-regulates epidermal growth factor receptor (EGFR) as well as Src protein. Inhibition of EGFR and Src expression eliminates LCA-induced Zonula occludens-1 downregulation, suggesting that LCA impairs intestinal barrier function by enhancing EGFR-SRC pathway (Pi et al., 2020). However, a recent study showed that piperine can inhibit EGFR and Src and block LCA-stimulated IL-8 expression (Li et al., 2022). Furthermore, direct exposure to secondary BAs rather than sulfating secondary BAs resulted in reduced PiC production, suggesting that sulfation of secondary BAs might diminish their anti-inflammatory effects (van der Lugt et al., 2022). Therefore, under certain conditions, LCA may play a protective role in maintaining the stability of intestinal TJs and intestinal barrier permeability. Studies related to LCA and intestinal barrier are summarized in Table 1.

RECEPTORS FOR LCA

LCA mediates its functions through corresponding receptors, including VDR, G protein-coupled receptor 5 (TGR5), FXR and pregnane X receptor (PXR) (Lajczak-McGinley et al., 2020).

LCA and VDR

VDR is a member of the nuclear receptor superfamily that primarily mediates the biological activity of 1 α ,25-dihydroxyvitamin D₃ (1,25(OH)₂D₃), and plays an important role in the regulation of calcium homeostasis, cell growth, immune response and cardiovascular functions (Nishida et al., 2020). In 2008, it is firstly reported that LCA could conduct some of the functions that are associated with vitamin D in a vitamin D deficiency rat model (Matsubara et al., 2008). Initially, LCA was found to be a selective VDR agonist (Makishima et al., 2002). However, in contrast to 1,25(OH)₂D₃, which acts mainly in the upper intestine, LCA acts mainly in the lower intestine, especially the ileum (Makishima et al., 2002; Ishizawa et al., 2018). VDR shows a high affinity for LCA in most animal species, but the ability of LCA to act as a VDR ligand appears to be present only in higher vertebrates such as birds and mammals (Kollitz et al., 2016). Interestingly, studies have found that bufalin (an active ingredient in toad venom) does not directly activate VDR, but regulates LCA and enhances LCA-mediated VDR activation (Nakano et al., 2005).

The binding of LCA to the VDR activates a signaling cascade that leads to VDR-dependent sulfation, and the sensitivity of the LCA and its metabolites to VDR is at least one magnitude higher than that of other nuclear receptors (Makishima et al., 2002). The sulfation that occurs in the intestinal epithelium also contributes to the detoxification of LCA. Intestinal VDR deficiency increased LCA-induced hepatic necrosis and inflammation (Cheng et al., 2014). Notably, Makishima (Makishima et al., 2002) and Cheng (Cheng et al., 2014), further demonstrated that activation of VDR

TABLE 1 | Effects of LCA on intestinal barrier in different models.

Models	Effects of LCA on Intestinal Barrier	Refs
Human colonic T84 cells	Inhibition of Cl ⁻ secretion	Ao et al. (2016)
TNF- α -stressed Caco-2 cells	Alleviation of the decrease in TEER and the increase in FITC-Dextran flux	Yao et al. (2019)
	Expression of TJs increase	
Human colonic T84 cells	No effect either on TEER or paracellular permeability	Sarathy et al. (2017)
	Attenuation the effect of PIC on intestinal barrier permeability	
Co-cultured Caco-2 and HT29-MTX-E12 cells	Improvement of TEER	van der Lugt et al. (2022)
	Expression of TJs increase	
Caco-2 cells	VDR activation and expression of TJs increase	Cao et al. (2022)
Caco-2 cells	Down-regulation of TJs expression	Pi et al. (2020)
	Up-regulation of EGFR and Src protein	

TEER, transepithelial electrical resistance; EGFR, epidermal growth factor receptor.

by LCA or vitamin D subsequently increases the expression of CYP3A, which detoxifies LCA in the liver and intestine.

The combination of LCA and VDR not only mediates its own detoxification, but also shows biological activities such as anti-inflammation and immune regulation. In Caco-2 cells, LCA inhibits TNF- α -mediated downregulation of silent information regulator 1 (SIRT1), nuclear factor erythroid 2-related factor 2 (Nrf2), and heme oxygenase 1 (HO 1), as well as the increase of NF- κ B p-p65 and p-I κ B- α (Yao et al., 2019). In CRC cells, LCA activates VDR to block NF- κ B inflammatory signaling, and significantly reduces IL-1 β -induced IL-8 secretion (Sun et al., 2008). LCA also regulates adaptive immunity and inhibits Th1 cell activation through VDR signaling (Pols et al., 2017). Although the concentration of free-form LCA in the peripheral circulation is only 0.5 μ M (Steiner et al., 2011), it is sufficient to suppress the inflammatory response to Th1 cells (Pols et al., 2017). The free-form of LCA impede the activation of Th1 cells mainly in three ways: 1) inhibits the production of Th1 cytokines IFN- γ and TNF- α ; 2) inhibits the expression of Th1 regulatory genes such as T-box protein (T-bet), Stat-1 and Stat-4 expressed in T cells; and 3) inhibits the phosphorylation of STAT1 α / β (Pols et al., 2017) (Figure 2). Although the exact mechanisms are unknown, it recently has been found that LCA at physiological concentration inhibits ERK-1/2 phosphorylation and increases the basal phosphorylation level of p38 in Jurkat T cells (Pols et al., 2017). And phosphorylation of p38 signaling in T cells has been reported to induce T cell apoptosis, thereby suppressing chronic inflammation (Lanna et al., 2014). Unfortunately, the exact mechanisms by which LCA inhibits ERK phosphorylation and promotes P38 phosphorylation are still unknown.

LCA and TGR5

As a member of the G protein-coupled receptor family, TGR5 is a cell membrane receptor of LCA. TGR5 expression is widely distributed in endocrine glands, adipocytes, muscles, immune organs, gallbladder and enteric nervous system (Marki, 1966). It has been reported that LCA and its analogue TLCA are the most potent endogenous ligands for TGR5 due to their hydrophobicity (Kawamata et al., 2003; Nguyen and

Bouscarel, 2008; Sato et al., 2008). The EC₅₀ value of LCA on TRG5 is reported to be 0.58 μ M (Sato et al., 2008). Activation of TGR5 leads to receptor internalization, increased levels of cyclic adenosine monophosphate (cAMP), protein kinase A (PKA) activation, and increased levels of phosphorylation of target proteins (Li et al., 2018). The LCA induced TGR5 activation is broad and cell-specific, including the anti-inflammatory effects on macrophages, increased energy expenditure in brown adipose tissue (BAT), improved glucose metabolism and insulin sensitivity, gallbladder relaxation, and promotion of intestinal motility (Watanabe et al., 2006; Thomas et al., 2009).

In C57Bl/6J mice, LCA treatment significantly reduces body weight (Ward et al., 2017), which might be related to the effect of LCA on energy expenditure and fat metabolism. LCA binds to TGR5 on intestinal epithelial cells to activate the cAMP-D2 signaling pathway and promote energy expenditure (Watanabe et al., 2006). Enhancing the expression of TGR5 downstream thermogenic genes in BAT reduces the uptake of free fatty acid (FFA) in the liver (Fan et al., 2022). More surprisingly, the most potent TGR5 agonist developed by Yu et al., 23(S)-methyl-LCA (23(S)-m-LCA), was three times more active than LCA at a concentration of 5 μ M, but glucagon-like peptide-1 (GLP-1) transcripts in the mouse intestine increased nearly 26-fold (Yu et al., 2015). These results suggest that LCA is involved in mediating energy expenditure and GLP-1 secretion via TGR5 signaling.

Some natural components are also involved in the regulation of glucose metabolism by LCA and TGR5. As previously mentioned, natural ingredients can alter the structure of the gut microbiota and promote LCA production. Resveratrol can increase the LCA level, which activates TGR5 and up-regulate uncoupling protein one expression, thus accelerating energy expenditure (Chevalier et al., 2015; Hui et al., 2020b). Curcumin and capsaicin also rely on the reshaping of intestinal flora to promote LCA production, and the subsequent activation of TGR5 mediated cAMP/PKA signaling in maintaining glucose homeostasis (Hui et al., 2020a; Han et al., 2021). It is important to note that the beneficial effects of these natural ingredients on glucose intolerance are partially eliminated by the application of antibiotics, probably due to the inhibition of LCA-producing bacteria (Figure 2).

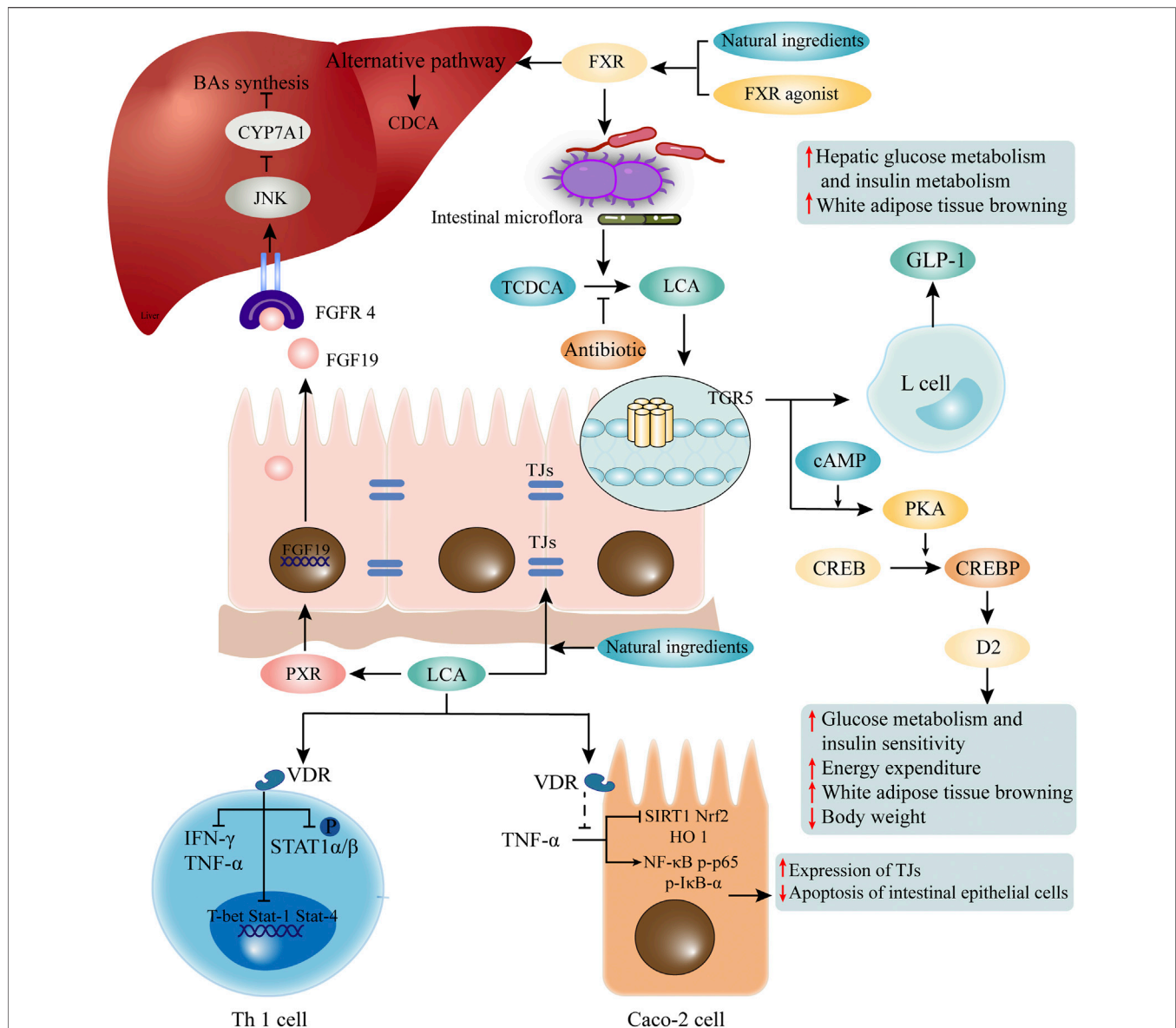


FIGURE 2 | LCA mediated receptors and pathways. LCA mediates its functions through corresponding receptors. LCA activates VDR, and is involved in maintaining the function of TJs of intestinal epithelial cells and inhibition of Th1 cells. Natural ingredients can enhance VDR activation through LCA. Elevated LCA can activate TGR5, which promotes the secretion of GLP1 by intestinal epithelial cells, and participates in glucose metabolism and fat metabolism. The binding of LCA and PXR activates the transcription of FGF19. After recognition of FGFR4 on hepatocytes, it initiates the c-Jun N-terminal kinase (JNK) signaling pathway, which inhibits CYP7A1 and BA synthesis. In addition, activation of FXR induced by FXR agonist or some natural ingredients may change the composition of intestinal flora and promote the production of LCA. LCA, lithocholic acid; VDR, vitamin D receptor; TJs, tight junctions; TGR5, G protein-coupled receptor five; GLP1, glucagon-like peptide-1; PXR, pregnane X receptor; FGF19, fibroblast growth factor 19; FGFR4, FGF receptor four; CYP7A1, cholesterol 7 α -hydroxylase.

An *in vitro* assay has demonstrated that LCA can inhibit the production of PiC in macrophages through activation of TGR5 (Yoneno et al., 2013). As mentioned previously, the anti-inflammatory effects of LCA on intestinal inflammation in ulcerative colitis patients are also partially dependent on the TGR5 signaling (Sinha et al., 2020). More importantly, the anti-cancer effect of LCA has been linked to TGR5 in studies of cancer cells from different tissues (Arnould et al., 2002; Astanehe et al., 2008; Arlia-Ciommo et al., 2014).

LCA and FXR, PXR

Dysregulation of lipid metabolism has been linked to cancer, as cancer cells often exhibit a larger lipid requirement to meet their uncontrolled proliferation and metastasis (Luu et al., 2018). Moreover, the proliferation and metastasis of cancer cells are associated with increased exogenous lipid uptake, as well as the endogenous synthesis of lipids (Beloribi-Djefalia et al., 2016). FXR activation is important in the regulation of lipid metabolism and glucose metabolism (Ding et al., 2015). Unlike TGR5, FXR

inhibits GLP-1 transcriptional activity by promoting miR-33 expression and repressing its downstream targets glucagon (GCG) and CREBP1 (Li et al., 2019). While the LCA derivative 7-ethylidene-lithocholic acid effectively inhibits FXR-induced gene expression in hepatocytes and activates TGR5 to stimulate GLP-1 secretion from enteroendocrine cells, synergistical effects are achieved in maintaining glucose homeostasis (Stefela et al., 2021).

Activation of intestinal FXR by fexaramine (an intestine-restricted FXR agonist) can shape the intestinal microbiota to induce the conversion of TCDCA to LCA by *Acetatifactor* and *Bacteroides*, and the elevation of LCA then activates intestinal TGR5, which then stimulates intestinal "L" cells to secrete GLP-1 (Trabelsi et al., 2015), thereby modulates glucose metabolism and white adipose tissue browning. However, antibiotic treatment reverses the beneficial metabolic effects of fexaramine in obese and diabetic mice (Pathak et al., 2018). In addition, as mentioned above, natural ingredients can also promote LCA production by activating FXR or altering the gut microbiome. However, different from current FXR agonists, natural ingredients (e.g. grape seed proanthocyanidin) activate the gut FXR signaling and increase gene expression of BA synthetases of alternative pathway, contributing to the increased LCA production rather than modulation of the gut microbiome (Wu et al., 2021) (Figure 2). It has also been reported that activation of intestinal FXR signaling by LCA facilitates the reduction of inflammatory cytokines such as TNF- α , IL-1 β and IL-6 in the ileum and serum, and protects the intestine against inflammation (Wu et al., 2021).

PXR has been shown to play an important role in the induction of phase I-III genes that are involved in the metabolism, transport and excretion of a variety of metabolites (Xing et al., 2020). PXR can only be activated by LCA and its derivative 3-keto-LCA, but does not respond to CDCA, DCA, or CA. The binding of LCA and PXR induces activation of the fibroblast growth factor 19 (FGF19) promoter (Wistuba et al., 2007). Intestinally secreted FGF19 binds to FGF receptor 4 (FGFR4) on hepatocytes and initiates the c-jun N-terminal kinase (JNK) signaling, which inhibits CYP7A1 and BA synthesis (Wistuba et al., 2007). Recent studies have reported that intestinal PXR regulates the expression of NF- κ B and may be protect the mice from IBD (Okamura et al., 2020), but it remains to be determined whether LCA or 3-keto-LCA is involved in activation of hepatic and intestinal PXR.

The processing of Chinese medicinal herbs is believed to promote the absorption of the active ingredients (Chen et al., 2018). A recent study found that frankincense made with vinegar increases LCA level, activates constitutional androstane receptor

and PXR, and upregulates the expression of drug absorption-associated protein in the liver, such as multidrug resistance-associated protein 2 (MRP2) and organic anion transporting polypeptide 1B3 (OATP1B3). Meanwhile, LCA activates PXR expression in the colon, which also promotes the expression of MRP2 and OATP1B3, thus facilitating drug absorption (Peng et al., 2022).

CONCLUSION AND PERSPECTIVES

In summary, LCA shows considerable protective effects on the intestinal environment, including maintaining the stability of TJs, and anti-bacterial and anti-inflammatory effects. Moreover, LCA can up-regulate the expression of absorption-related proteins, promote the absorption of herbs, and mediate the biological functions of these herbs in regulating glucose metabolism, lipid metabolism, and energy homeostasis. The utilization of the beneficial effects of LCA is an attractive topic.

Focusing on the molecular mechanisms of the anti-apoptotic and anti-inflammatory effects of LCA, the proper dosage as well as the intestinal environment should be taken into consideration for drug development. In addition, the significant differences in the composition of intestinal microorganisms and BA composition between humans and mice may also affect the validity of the conclusions obtained so far in the relevant studies. Gut microbiota is crucial for LCA transformation, while diet and some natural products can also affect the transformation. Therefore, a healthy microbial ecology is critical for maintaining BA homeostasis. The composition of the microbiota, changes in BA composition, and the interaction between LCA and related nuclear receptors and TGR5 signaling appear to be highly promising for the treatment of intestinal and hepatic diseases, as well as certain metabolic-related disorders.

AUTHOR CONTRIBUTIONS

LZ conceptualized the manuscript, WS collected the literature and drafted the manuscript, LZ and GJ revised the manuscript. All authors edited, revised, and approved the final version of this review.

FUNDING

This work was supported by grants from the National Natural Science Foundation of China (No. 82174250).

REFERENCES

- Alkhedaide, A. Q., Ismail, T. A., Alotaibi, S. H., Nassan, M. A., and Shehri, Z. S. A. (2018). Preventive Effect of Artemisinin Extract against Cholestasis Induced via Lithocholic Acid Exposure. *Biosci. Rep.* 38 (6), BSR20181011. doi:10.1042/bsr20181011
- Alkhedaide, A. Q. (2018). Preventive Effect of Juniperus Procera Extract on Liver Injury Induced by Lithocholic Acid. *Cell Mol. Biol. (Noisy-le-grand)* 64 (13), 63–68. doi:10.14715/cmb/2018.64.13.12
- Ao, M., Sarathy, J., Domingue, J., Alrefai, W. A., and Rao, M. C. (2013). Chenodeoxycholic Acid Stimulates Cl(-) Secretion via cAMP Signaling and Increases Cystic Fibrosis Transmembrane Conductance Regulator Phosphorylation in T84 Cells. *Am. J. Physiol. Cell Physiol.* 305 (4), C447–C456. doi:10.1152/ajpcell.00416.2012

- Ao, M., Domingue, J. C., Khan, N., Javed, F., Osmani, K., Sarathy, J., et al. (2016). Lithocholic Acid Attenuates cAMP-dependent Cl⁻ Secretion in Human Colonic Epithelial T84 Cells. *Am. J. Physiol. Cell Physiol.* 310 (11), C1010–C1023. doi:10.1152/ajpcell.00350.2015
- Arab, J. P., Karpen, S. J., Dawson, P. A., Arrese, M., and Trauner, M. (2017). Bile Acids and Nonalcoholic Fatty Liver Disease: Molecular Insights and Therapeutic Perspectives. *Hepatology* 65 (1), 350–362. doi:10.1002/hep.28709
- Araya, Z., and Wikvall, K. (1999). 6 α -hydroxylation of Taurochenodeoxycholic Acid and Lithocholic Acid by CYP3A4 in Human Liver Microsomes. *Biochim. Biophys. Acta* 1438 (1), 47–54. doi:10.1016/s1388-1981(99)00031-1
- Arlia-Ciommo, A., Piano, A., Svistkova, V., Mohtashami, S., and Titorenko, V. I. (2014). Mechanisms Underlying the Anti-aging and Anti-tumor Effects of Lithocholic Bile Acid. *Int. J. Mol. Sci.* 15 (9), 16522–16543. doi:10.3390/ijms150916522
- Arlia-Ciommo, A., Leonov, A., Mohammad, K., Beach, A., Richard, V. R., Bourque, S. D., et al. (2018). Mechanisms through Which Lithocholic Acid Delays Yeast Chronological Aging under Caloric Restriction Conditions. *Oncotarget* 9 (79), 34945–34971. doi:10.18632/oncotarget.26188
- Arnould, T., Vankoningsloo, S., Renard, P., Houbion, A., Ninane, N., Demazy, C., et al. (2002). CREB Activation Induced by Mitochondrial Dysfunction is a New Signaling Pathway that Impairs Cell Proliferation. *EMBO J.* 21 (1–2), 53–63. doi:10.1093/emboj/21.1.53
- Astanehe, A., Arenillas, D., Wasserman, W. W., Leung, P. C., Dunn, S. E., Davies, B. R., et al. (2008). Mechanisms Underlying P53 Regulation of PIK3CA Transcription in Ovarian Surface Epithelium and in Ovarian Cancer. *J. Cell Sci.* 121 (Pt 5), 664–674. doi:10.1242/jcs.013029
- Bansal, S., and Lau, A. J. (2019). Inhibition of Human Sulfotransferase 2A1-Catalyzed Sulfonation of Lithocholic Acid, Glycolithocholic Acid, and Tauroolithocholic Acid by Selective Estrogen Receptor Modulators and Various Analogs and Metabolites. *J. Pharmacol. Exp. Ther.* 369 (3), 389–405. doi:10.1124/jpet.119.256255
- Begley, M., Gahan, C. G., and Hill, C. (2005). The Interaction between Bacteria and Bile. *FEMS Microbiol. Rev.* 29 (4), 625–651. doi:10.1016/j.femsre.2004.09.003
- Beloribi-Djefafalia, S., Vasseur, S., and Guillaumond, F. (2016). Lipid Metabolic Reprogramming in Cancer Cells. *Oncogenesis* 5, e189. doi:10.1038/oncsis.2015.49
- Bernstein, H., Bernstein, C., Payne, C. M., Dvorakova, K., and Garewal, H. (2005). Bile Acids as Carcinogens in Human Gastrointestinal Cancers. *Mutat. Res.* 589 (1), 47–65. doi:10.1016/j.mrrrev.2004.08.001
- Burstein, M. T., Kyryakov, P., Beach, A., Richard, V. R., Koupaki, O., Gomez-Perez, A., et al. (2012). Lithocholic Acid Extends Longevity of Chronologically Aging Yeast Only if Added at Certain Critical Periods of Their Lifespan. *Cell Cycle* 11 (18), 3443–3462. doi:10.4161/cc.21754
- Cao, Y., Shu, X., Li, M., Yu, S., Li, C., Ji, G., et al. (2022). Jiangzhi Granule Attenuates Non-alcoholic Steatohepatitis through Modulating Bile Acid in Mice Fed High-Fat Vitamin D Deficiency Diet. *Biomed. Pharmacother.* 149, 112825. doi:10.1016/j.biopha.2022.112825
- Chai, J., Du, X., Chen, S., Feng, X., Cheng, Y., Zhang, L., et al. (2015). Oral Administration of Oleanolic Acid, Isolated from *Swertia Musstii* Franch, Attenuates Liver Injury, Inflammation, and Cholestasis in Bile Duct-Ligated Rats. *Int. J. Clin. Exp. Med.* 8 (2), 1691–1702.
- Chen, L. J., and Segel, I. H. (1985). Purification and Characterization of Bile Salt Sulfotransferase from Human Liver. *Arch. Biochem. Biophys.* 241 (2), 371–379. doi:10.1016/0003-9861(85)90559-4
- Chen, P., Bakke, D., Kolodziej, L., Lodolce, J., Weber, C. R., Boone, D. L., et al. (2015). Antrum Mucosal Protein-18 Peptide Targets Tight Junctions to Protect and Heal Barrier Structure and Function in Models of Inflammatory Bowel Disease. *Inflamm. Bowel Dis.* 21 (10), 2393–2402. doi:10.1097/MIB.0000000000000499
- Chen, L. L., Verpoorte, R., Yen, H. R., Peng, W. H., Cheng, Y. C., Chao, J., et al. (2018). Effects of Processing Adjuvants on Traditional Chinese Herbs. *J. Food Drug Anal.* 26 (2S), S96–S114. doi:10.1016/j.jfda.2018.02.004
- Cheng, J., Fang, Z. Z., Kim, J. H., Krausz, K. W., Tanaka, N., Chiang, J. Y., et al. (2014). Intestinal CYP3A4 Protects against Lithocholic Acid-Induced Hepatotoxicity in Intestine-specific VDR-Deficient Mice. *J. Lipid Res.* 55 (3), 455–465. doi:10.1194/jlr.M044420
- Chevalier, C., Stojanović, O., Colin, D. J., Suarez-Zamorano, N., Tarallo, V., Veyrat-Durebex, C., et al. (2015). Gut Microbiota Orchestrates Energy Homeostasis during Cold. *Cell* 163 (6), 1360–1374. doi:10.1016/j.cell.2015.11.004
- David, L. A., Maurice, C. F., Carmody, R. N., Gootenberg, D. B., Button, J. E., Wolfe, B. E., et al. (2014). Diet Rapidly and Reproducibly Alters the Human Gut Microbiome. *Nature* 505 (7484), 559–563. doi:10.1038/nature12820
- Dawson, P. A., and Karpen, S. J. (2015). Intestinal Transport and Metabolism of Bile Acids. *J. Lipid Res.* 56 (6), 1085–1099. doi:10.1194/jlr.R054114
- Deo, A. K., and Bandiera, S. M. (2008). Biotransformation of Lithocholic Acid by Rat Hepatic Microsomes: Metabolite Analysis by Liquid Chromatography/mass Spectrometry. *Drug Metab. Dispos.* 36 (2), 442–451. doi:10.1124/dmd.107.017533
- Dharmasathaphorn, K., Huott, P. A., Vongkavit, P., Beuerlein, G., Pandol, S. J., and Ammon, H. V. (1989). Cl⁻ Secretion Induced by Bile Salts. A Study of the Mechanism of Action Based on a Cultured Colonic Epithelial Cell Line. *J. Clin. Invest.* 84 (3), 945–953. doi:10.1172/JCI114257
- Ding, L., Yang, L., Wang, Z., and Huang, W. (2015). Bile Acid Nuclear Receptor FXR and Digestive System Diseases. *Acta Pharm. Sin. B* 5 (2), 135–144. doi:10.1016/j.apsb.2015.01.004
- Dionne, S., Tuchweber, B., Plaa, G. L., and Yousef, I. M. (1994). Phase I and Phase II Metabolism of Lithocholic Acid in Hepatic Acinar Zone 3 Necrosis. Evaluation in Rats by Combined Radiochromatography and Gas-Liquid Chromatography-Mass Spectrometry. *Biochem. Pharmacol.* 48 (6), 1187–1197. doi:10.1016/0006-2952(94)90156-2
- do Nascimento, P. G., Lemos, T. L., Almeida, M. C., de Souza, J. M., Bizerra, A. M., Santiago, G. M., et al. (2015). Lithocholic Acid and Derivatives: Antibacterial Activity. *Steroids* 104, 8–15. doi:10.1016/j.steroids.2015.07.007
- Doden, H. L., Wolf, P. G., Gaskins, H. R., Anantharaman, K., Alves, J. M. P., and Ridlon, J. M. (2021). Completion of the Gut Microbial Epi-bile Acid Pathway. *Gut Microbes* 13 (1), 1–20. doi:10.1080/19490976.2021.1907271
- Dong, S., Zhu, M., Wang, K., Zhao, X., Hu, L., Jing, W., et al. (2021). Dihydromyricetin Improves DSS-Induced Colitis in Mice via Modulation of Fecal-Bacteria-Related Bile Acid Metabolism. *Pharmacol. Res.* 171, 105767. doi:10.1016/j.phrs.2021.105767
- Durko, L., and Malecka-Panas, E. (2014). Lifestyle Modifications and Colorectal Cancer. *Curr. Colorectal Cancer Rep.* 10, 45–54. doi:10.1007/s11888-013-0203-4
- Fan, M., Wang, Y., Jin, L., Fang, Z., Peng, J., Tu, J., et al. (2022). Bile Acid-Mediated Activation of Brown Fat Protects From Alcohol-Induced Steatosis and Liver Injury in Mice. *Cell Mol. Gastroenterol. Hepatol.* 13 (3), 809–826. doi:10.1016/j.jcmgh.2021.12.001
- Fiorucci, S., Biagioli, M., Zampella, A., and Distrutti, E. (2018). Bile Acids Activated Receptors Regulate Innate Immunity. *Front. Immunol.* 9, 1853. doi:10.3389/fimmu.2018.01853
- Fuchs, C. D., and Trauner, M. (2022). Role of Bile Acids and Their Receptors in Gastrointestinal and Hepatic Pathophysiology. *Nat. Rev. Gastroenterol. Hepatol.* 1–19. doi:10.1038/s41575-021-00566-7
- Gadacz, T. R., Allan, R. N., Mack, E., and Hofmann, A. F. (1976). Impaired Lithocholate Sulfation in the Rhesus Monkey: A Possible Mechanism for Chenodeoxycholate Toxicity. *Gastroenterology* 70 (6), 1125–1129. doi:10.1016/s0016-5085(76)80324-1
- Gankhuyag, N., Singh, B., Maharjan, S., Choi, Y. J., Cho, C. S., and Cho, M. H. (2015). Galactosylated Poly(Ethylene glycol)-Lithocholic Acid Selectively Kills Hepatoma Cells, While Sparing Normal Liver Cells. *Macromol. Biosci.* 15 (6), 777–787. doi:10.1002/mabi.201400475
- Goldberg, A. A., Richard, V. R., Kyryakov, P., Bourque, S. D., Beach, A., Burstein, M. T., et al. (2010). Chemical Genetic Screen Identifies Lithocholic Acid as an Anti-Aging Compound that Extends Yeast Chronological Life Span in a TOR-Independent Manner, by Modulating Housekeeping Longevity Assurance Processes. *Aging (Albany NY)* 2 (7), 393–414. doi:10.18632/aging.100168
- Gonzalez, A., Casado, J., Chueca, E., Salillas, S., Velázquez-Campoy, A., Sancho, J., et al. (2020). Small Molecule Inhibitors of the Response Regulator ArsR Exhibit Bactericidal Activity against *Helicobacter pylori*. *Microorganisms* 8 (4), 503. doi:10.3390/microorganisms8040503
- Halvorsen, B., Staff, A. C., Ligaarden, S., Prydz, K., and Kolset, S. O. (2000). Lithocholic Acid and Sulphated Lithocholic Acid Differ in the Ability to Promote Matrix Metalloproteinase Secretion in the Human Colon Cancer

- Cell Line CaCo-2. *Biochem. J.* 349 (Pt 1), 189–193. doi:10.1042/0264-6021:3490189
- Hamilton, J. P., Xie, G., Raufman, J. P., Hogan, S., Griffin, T. L., Packard, C. A., et al. (2007). Human Cecal Bile Acids: Concentration and Spectrum. *Am. J. Physiol. Gastrointest. Liver Physiol.* 293 (1), G256–G263. doi:10.1152/ajpgi.00027.2007
- Han, K., Bose, S., Wang, J. H., Lim, S. K., Chin, Y. W., Kim, Y. M., et al. (2017). *In Vivo* Therapeutic Effect of Combination Treatment with Metformin and *Scutellaria Baicalensis* on Maintaining Bile Acid Homeostasis. *PLoS One* 12 (9), e0182467. doi:10.1371/journal.pone.0182467
- Han, J., Chen, X., Zhao, L., Fu, J., Sun, L., Zhang, Y., et al. (2018). Lithocholic Acid-Based Peptide Delivery System for an Enhanced Pharmacological and Pharmacokinetic Profile of Xenopus GLP-1 Analogs. *Mol. Pharm.* 15 (7), 2840–2856. doi:10.1021/acs.molpharmaceut.8b00336
- Han, Z., Yao, L., Zhong, Y., Xiao, Y., Gao, J., Zheng, Z., et al. (2021). Gut Microbiota Mediates the Effects of Curcumin on Enhancing Ucp1-Dependent Thermogenesis and Improving High-Fat Diet-Induced Obesity. *Food Funct.* 12 (14), 6558–6575. doi:10.1039/d1fo00671a
- Hartley, D. P., Dai, X., He, Y. D., Carlini, E. J., Wang, B., Huskey, S. E., et al. (2004). Activators of the Rat Pregnane X Receptor Differentially Modulate Hepatic and Intestinal Gene Expression. *Mol. Pharmacol.* 65 (5), 1159–1171. doi:10.1124/mol.65.5.1159
- Hofmann, A. F., and Roda, A. (1984). Physicochemical Properties of Bile Acids and Their Relationship to Biological Properties: An Overview of the Problem. *J. Lipid Res.* 25 (13), 1477–1489. doi:10.1016/s0022-2275(20)34421-7
- Hofmann, A. F. (2004). Detoxification of Lithocholic Acid, A Toxic Bile Acid: Relevance to Drug Hepatotoxicity. *Drug Metab. Rev.* 36 (3–4), 703–722. doi:10.1081/dmr-200033475
- Holmberg, F. E. O., Pedersen, J., Jørgensen, P., Soendergaard, C., Jensen, K. B., and Nielsen, O. H. (2018). Intestinal Barrier Integrity and Inflammatory Bowel Disease: Stem Cell-Based Approaches to Regenerate the Barrier. *J. Tissue Eng. Regen. Med.* 12 (4), 923–935. doi:10.1002/term.2506
- Hu, Q., Zhang, W., Wu, Z., Tian, X., Xiang, J., Li, L., et al. (2021). Baicalin and the Liver-Gut System: Pharmacological Bases Explaining its Therapeutic Effects. *Pharmacol. Res.* 165, 105444. doi:10.1016/j.phrs.2021.105444
- Huang, J., Bathena, S. P., Tong, J., Roth, M., Hagenbuch, B., and Alnouti, Y. (2010). Kinetic Analysis of Bile Acid Sulfation by Stably Expressed Human Sulfotransferase 2A1 (SULT2A1). *Xenobiotica* 40 (3), 184–194. doi:10.3109/00498250903514607
- Hui, S., Huang, L., Wang, X., Zhu, X., Zhou, M., Chen, M., et al. (2020a). Capsaicin Improves Glucose Homeostasis by Enhancing Glucagon-Like Peptide-1 Secretion Through the Regulation of Bile Acid Metabolism via the Remodeling of the Gut Microbiota in Male Mice. *FASEB J.* 34 (6), 8558–8573. doi:10.1096/fj.201902618RR
- Hui, S., Liu, Y., Huang, L., Zheng, L., Zhou, M., Lang, H., et al. (2020b). Resveratrol Enhances Brown Adipose Tissue Activity and White Adipose Tissue Browning in Part by Regulating Bile Acid Metabolism via Gut Microbiota Remodeling. *Int. J. Obes. (Lond)* 44 (8), 1678–1690. doi:10.1038/s41366-020-0566-y
- Ishizawa, M., Akagi, D., and Makishima, M. (2018). Lithocholic Acid is a Vitamin D Receptor Ligand That Acts Preferentially in the Ileum. *Int. J. Mol. Sci.* 19 (7), 1975. doi:10.3390/ijms19071975
- Iwamoto, J., Honda, A., Miyazaki, T., Monma, T., Ueda, H., Morishita, Y., et al. (2021). Western Diet Changes Gut Microbiota and Ameliorates Liver Injury in a Mouse Model with Human-Like Bile Acid Composition. *Hepatol. Commun.* 5 (12), 2052–2067. doi:10.1002/hep4.1778
- Kawamata, Y., Fujii, R., Hosoya, M., Harada, M., Yoshida, H., Miwa, M., et al. (2003). A G Protein-Coupled Receptor Responsive to Bile Acids. *J. Biol. Chem.* 278 (11), 9435–9440. doi:10.1074/jbc.M209706200
- Kim, H. N., Joo, E. J., Cheong, H. S., Kim, Y., Kim, H. L., Shin, H., et al. (2019). Gut Microbiota and Risk of Persistent Nonalcoholic Fatty Liver Diseases. *J. Clin. Med.* 8 (8), 1089. doi:10.3390/jcm8081089
- Kitada, H., Miyata, M., Nakamura, T., Tozawa, A., Honma, W., Shimada, M., et al. (2003). Protective Role of Hydroxysteroid Sulfotransferase in Lithocholic Acid-Induced Liver Toxicity. *J. Biol. Chem.* 278 (20), 17838–17844. doi:10.1074/jbc.M210634200
- Kollitz, E. M., Zhang, G., Hawkins, M. B., Whitfield, G. K., Reif, D. M., and Kullman, S. W. (2016). Evolutionary and Functional Diversification of the Vitamin D Receptor-Lithocholic Acid Partnership. *PLoS One* 11 (12), e0168278. doi:10.1371/journal.pone.0168278
- Kurogi, K., Krasowski, M. D., Injeti, E., Liu, M. Y., Williams, F. E., Sakakibara, Y., et al. (2011). A Comparative Study of the Sulfation of Bile Acids and a Bile Alcohol by the Zebra Danio (*Danio rerio*) and Human Cytosolic Sulfotransferases (SULTs). *J. Steroid Biochem. Mol. Biol.* 127 (3–5), 307–314. doi:10.1016/j.jsbmb.2011.07.011
- Lajczak-McGinley, N. K., Porru, E., Fallon, C. M., Smyth, J., Curley, C., McCarron, P. A., et al. (2020). The Secondary Bile Acids, Ursodeoxycholic Acid and Lithocholic Acid, Protect against Intestinal Inflammation by Inhibition of Epithelial Apoptosis. *Physiol. Rep.* 8 (12), e14456. doi:10.14814/phy2.14456
- Lanna, A., Henson, S. M., Escors, D., and Akbar, A. N. (2014). The Kinase p38 Activated by the Metabolic Regulator AMPK and Scaffold TAB1 Drives the Senescence of Human T Cells. *Nat. Immunol.* 15 (10), 965–972. doi:10.1038/ni.2981
- Li, P., Zhu, L., Yang, X., Li, W., Sun, X., Yi, B., et al. (2018). Farnesoid X Receptor (FXR) Interacts with Camp Response Element Binding Protein (CREB) to Modulate Glucagon-Like Peptide-1 (7–36) Amide (GLP-1) Secretion by Intestinal L Cell. *Cell Physiol. Biochem.* 47 (4), 1442–1452. doi:10.1159/000490836
- Li, P., Gao, X., Sun, X., Li, W., Yi, B., and Zhu, L. (2019). A Novel Epigenetic Mechanism of FXR Inhibiting GLP-1 Secretion via miR-33 and its Downstream Targets. *Biochem. Biophys. Res. Commun.* 517 (4), 629–635. doi:10.1016/j.bbrc.2019.07.079
- Li, D. S., Huang, Q. F., Guan, L. H., Zhang, H. Z., Li, X., Fu, K. L., et al. (2020). Targeted Bile Acids and Gut Microbiome Profiles Reveal the Hepato-Protective Effect of WZ Tablet (*Schisandra Sphenanthera* Extract) against LCA-Induced Cholestasis. *Chin. J. Nat. Med.* 18 (3), 211–218. doi:10.1016/S1875-5364(20)30023-6
- Li, S., Nguyen, T. T., Ung, T. T., Sah, D. K., Park, S. Y., Lakshmanan, V.-K., et al. (2022). Piperine Attenuates Lithocholic Acid-Stimulated Interleukin-8 by Suppressing Src/EGFR and Reactive Oxygen Species in Human Colorectal Cancer Cells. *Antioxidants* 11 (3), 530. doi:10.3390/antiox11030530
- Luu, T. H., Bard, J. M., Carbonnelle, D., Chaillou, C., Huvelin, J. M., Bobin-Dubigeon, C., et al. (2018). Lithocholic Bile Acid Inhibits Lipogenesis and Induces Apoptosis in Breast Cancer Cells. *Cell Oncol. (Dordr)* 41 (1), 13–24. doi:10.1007/s13402-017-0353-5
- Makishima, M., Lu, T. T., Xie, W., Whitfield, G. K., Domoto, H., Evans, R. M., et al. (2002). Vitamin D receptor as an Intestinal Bile Acid Sensor. *Science* 296 (5571), 1313–1316. doi:10.1126/science.1070477
- Marion, S., Studer, N., Desharnais, L., Menin, L., Escrig, S., Meibom, A., et al. (2019). *In Vitro* and *In Vivo* Characterization of Clostridium Scindens Bile Acid Transformations. *Gut Microbes* 10 (4), 481–503. doi:10.1080/19490976.2018.1549420
- Marki, H. H. (1966). Medical Chemical Laboratory Tests for the Practice. *Praxis* 55 (6), 158–163.
- Matsubara, T., Yoshinari, K., Aoyama, K., Sugawara, M., Sekiya, Y., Nagata, K., et al. (2008). Role of Vitamin D Receptor in the Lithocholic Acid-Mediated CYP3A Induction *In Vitro* and *In Vivo*. *Drug Metab. Dispos.* 36 (10), 2058–2063. doi:10.1124/dmd.108.021501
- Nakano, H., Matsunawa, M., Yasui, A., Adachi, R., Kawana, K., Shimomura, I., et al. (2005). Enhancement of Ligand-Dependent Vitamin D Receptor Transactivation by the Cardiotonic Steroid Bufalin. *Biochem. Pharmacol.* 70 (10), 1479–1486. doi:10.1016/j.bcp.2005.08.012
- Nguyen, A., and Bouscarel, B. (2008). Bile Acids and Signal Transduction: Role in Glucose Homeostasis. *Cell Signal* 20 (12), 2180–2197. doi:10.1016/j.cellsig.2008.06.014
- Nguyen, T.-T., Ung, T.-T., Li, S., Sah, D. K., Park, S.-Y., Lian, S., et al. (2021). Lithocholic Acid Induces miR21, Promoting PTEN Inhibition via STAT3 and ERK-1/2 Signaling in Colorectal Cancer Cells. *Int. J. Mol. Sci.* 22 (19), 10209. doi:10.3390/ijms221910209
- Nishida, S., Ishizawa, M., Kato, S., and Makishima, M. (2020). Vitamin D Receptor Deletion Changes Bile Acid Composition in Mice Orally Administered Chenodeoxycholic Acid. *J. Nutr. Sci. Vitaminol. (Tokyo)* 66 (4), 370–374. doi:10.3177/jnsv.66.370
- Nishida, S., Katsumi, N., and Matsumoto, K. (2021). Prevention of the Rise in Plasma Cholesterol and Glucose Levels by Kaki-Tannin and Characterization of its Bile Acid Binding Capacity. *J. Sci. Food Agric.* 101 (5), 2117–2124. doi:10.1002/jsfa.10834

- Okamura, M., Shizu, R., Abe, T., Kodama, S., Hosaka, T., Sasaki, T., et al. (2020). PXR Functionally Interacts with NF- κ B and AP-1 to Downregulate the Inflammation-Induced Expression of Chemokine CXCL2 in Mice. *Cells* 9 (10), 2296. doi:10.3390/cells9102296
- O'Keefe, S. J., Li, J. V., Lahti, L., Ou, J., Carbonero, F., Mohammed, K., et al. (2015). Fat, Fibre and Cancer Risk in African Americans and Rural Africans. *Nat. Commun.* 6, 6342. doi:10.1038/ncomms7342
- Otani, T., and Furuse, M. (2020). Tight Junction Structure and Function Revisited. *Trends Cell Biol.* 30 (10), 805–817. doi:10.1016/j.tcb.2020.08.004
- Pathak, P., Xie, C., Nichols, R. G., Ferrell, J. M., Boehme, S., Krausz, K. W., et al. (2018). Intestine Farnesoid X Receptor agonist and the Gut Microbiota Activate G-Protein Bile Acid Receptor-1 Signaling to Improve Metabolism. *Hepatology* 68 (4), 1574–1588. doi:10.1002/hep.29857
- Peng, S., Song, Z., Wang, C., Liang, D., Wan, X., Liu, Z., et al. (2022). Frankincense Vinegar-Processing Improves the Absorption of Boswellic Acids by Regulating Bile Acid Metabolism. *Phytomedicine* 98, 153931. doi:10.1016/j.phymed.2022.153931
- Pi, Y., Mu, C., Gao, K., Liu, Z., Peng, Y., and Zhu, W. (2020). Increasing the Hindgut Carbohydrate/Protein Ratio by Cecal Infusion of Corn Starch or Casein Hydrolysate Drives Gut Microbiota-Related Bile Acid Metabolism To Stimulate Colonic Barrier Function. *mSystems* 5 (3), e00176. doi:10.1128/mSystems.00176-20
- Polis, T. W. H., Puchner, T., Korkmaz, H. I., Vos, M., Soeters, M. R., and de Vries, C. J. M. (2017). Lithocholic Acid Controls Adaptive Immune Responses by Inhibition of Th1 Activation Through the Vitamin D Receptor. *PLoS One* 12 (5), e0176715. doi:10.1371/journal.pone.0176715
- Ridlon, J. M., Kang, D. J., and Hylemon, P. B. (2006). Bile Salt Biotransformations by Human Intestinal Bacteria. *J. Lipid Res.* 47 (2), 241–259. doi:10.1194/jlr.R500013-JLR200
- Ridlon, J. M., Kang, D. J., Hylemon, P. B., and Bajaj, J. S. (2014). Bile Acids and the Gut Microbiome. *Curr. Opin. Gastroenterol.* 30 (3), 332–338. doi:10.1097/MOG.0000000000000057
- Ridlon, J. M., Harris, S. C., Bhowmik, S., Kang, D. J., and Hylemon, P. B. (2016a). Consequences of Bile Salt Biotransformations by Intestinal Bacteria. *Gut Microbes* 7 (1), 22–39. doi:10.1080/19490976.2015.1127483
- Ridlon, J. M., Wolf, P. G., and Gaskins, H. R. (2016b). Taurocholic Acid Metabolism by Gut Microbes and Colon Cancer. *Gut microbes* 7 (3), 201–215. doi:10.1080/19490976.2016.1150414
- Ruiz, M. L., Mottino, A. D., Catania, V. A., and Vore, M. (2013). Hormonal Regulation of Hepatic Drug Biotransformation and Transport Systems. *Compr. Physiol.* 3 (4), 1721–1740. doi:10.1002/cphy.c130018
- Sánchez de Medina, F., Romero-Calvo, I., Mascaraque, C., and Martínez-Augustín, O. (2014). Intestinal Inflammation and Mucosal Barrier Function. *Inflamm. Bowel Dis.* 20 (12), 2394–2404. doi:10.1097/MIB.0000000000000204
- Sarathy, J., Detloff, S. J., Ao, M., Khan, N., French, S., Sirajuddin, H., et al. (2017). The Yin and Yang of Bile Acid Action on Tight Junctions in a Model Colonic Epithelium. *Physiol. Rep.* 5 (10), e13294. doi:10.14814/phy2.13294
- Sato, H., Macchiarulo, A., Thomas, C., Gioiello, A., Une, M., Hofmann, A. F., et al. (2008). Novel Potent and Selective Bile Acid Derivatives as TGR5 Agonists: Biological Screening, Structure-Activity Relationships, and Molecular Modeling Studies. *J. Med. Chem.* 51 (6), 1831–1841. doi:10.1021/jm7015864
- Sinha, S. R., Haileselassie, Y., Nguyen, L. P., Tropini, C., Wang, M., Becker, L. S., et al. (2020). Dysbiosis-Induced Secondary Bile Acid Deficiency Promotes Intestinal Inflammation. *Cell Host Microbe* 27 (4), 659. doi:10.1016/j.chom.2020.01.021
- Sreekanth, V., Kar, A., Kumar, S., Pal, S., Yadav, P., Sharma, Y., et al. (2021). Bile Acid Tethered Docetaxel-Based Nanomicelles Mitigate Tumor Progression through Epigenetic Changes. *Angew. Chem. Int. Ed. Engl.* 60 (10), 5394–5399. doi:10.1002/anie.202015173
- Stefela, A., Kaspar, M., Drastik, M., Kronenberger, T., Micuda, S., Dracinsky, M., et al. (2021). (E)-7-Ethylidene-lithocholic Acid (7-ELCA) Is a Potent Dual Farnesoid X Receptor (FXR) Antagonist and GPBAR1 Agonist Inhibiting FXR-Induced Gene Expression in Hepatocytes and Stimulating Glucagon-like Peptide-1 Secretion from Enterendocrine Cells. *Front. Pharmacol.* 12, 713149. doi:10.3389/fphar.2021.713149
- Steiner, C., Othman, A., Saelly, C. H., Rein, P., Drexel, H., von Eckardstein, A., et al. (2011). Bile Acid Metabolites in Serum: Intraindividual Variation and Associations with Coronary Heart Disease, Metabolic Syndrome and Diabetes Mellitus. *PLoS One* 6 (11), e25006. doi:10.1371/journal.pone.0025006
- Stiehl, A. (1974). Bile Salt Sulphates in Cholestasis. *Eur. J. Clin. Invest.* 4 (1), 59–63. doi:10.1111/j.1365-2362.1974.tb00373.x
- Sun, J., Mustafi, R., Cerda, S., Chumsangsri, A., Xia, Y. R., Li, Y. C., et al. (2008). Lithocholic Acid Down-Regulation of NF- κ B Activity Through Vitamin D Receptor in Colonic Cancer Cells. *J. Steroid Biochem. Mol. Biol.* 111 (1–2), 37–40. doi:10.1016/j.jsbmb.2008.01.003
- Suzuki, T., Yoshinaga, N., and Tanabe, S. (2011). Interleukin-6 (IL-6) Regulates Claudin-2 Expression and Tight Junction Permeability in Intestinal Epithelium. *J. Biol. Chem.* 286 (36), 31263–31271. doi:10.1074/jbc.M111.238147
- Thomas, C., Gioiello, A., Noriega, L., Strehle, A., Oury, J., Rizzo, G., et al. (2009). TGR5-Mediated Bile Acid Sensing Controls Glucose Homeostasis. *Cell Metab.* 10 (3), 167–177. doi:10.1016/j.cmet.2009.08.001
- Trabelsi, M. S., Daoudi, M., Prawitt, J., Ducastel, S., Touche, V., Sayin, S. I., et al. (2015). Farnesoid X Receptor Inhibits Glucagon-Like Peptide-1 Production by Enterendocrine L Cells. *Nat. Commun.* 6, 7629. doi:10.1038/ncomms8629
- van der Lugt, B., Vos, M. C. P., Grootte Bromhaar, M., Jssennagger, N., Vrieling, F., Meijerink, J., et al. (2022). The Effects of Sulfated Secondary Bile Acids on Intestinal Barrier Function and Immune Response in an Inflammatory *in Vitro* Human Intestinal Model. *Heliyon* 8 (2), e08883. doi:10.1016/j.heliyon.2022.e08883
- Wang, Y. G., Zhou, J. M., Ma, Z. C., Li, H., Liang, Q. D., Tan, H. L., et al. (2012). Pregnane X Receptor Mediated-Transcription Regulation Of CYP3A by Glycyrrhizin: A Possible Mechanism for its Hepatoprotective Property against Lithocholic Acid-Induced Injury. *Chem. Biol. Interact.* 200 (1), 11–20. doi:10.1016/j.cbi.2012.08.023
- Wang, B., Wu, G., Zhou, Z., Dai, Z., Sun, Y., Ji, Y., et al. (2015). Glutamine and Intestinal Barrier Function. *Amino Acids* 47 (10), 2143–2154. doi:10.1007/s00726-014-1773-4
- Wang, S., Martins, R., Sullivan, M. C., Friedman, E. S., Misis, A. M., El-Fahmawi, A., et al. (2019). Diet-induced Remission in Chronic Enteropathy is Associated with Altered Microbial Community Structure and Synthesis of Secondary Bile Acids. *Microbiome* 7 (1), 126. doi:10.1186/s40168-019-0740-4
- Ward, J. B. J., Lajczak, N. K., Kelly, O. B., O'Dwyer, A. M., Giddam, A. K., Ní Gabhann, J., et al. (2017). Ursodeoxycholic Acid and Lithocholic Acid Exert Anti-Inflammatory Actions in the Colon. *Am. J. Physiol. Gastrointest. Liver Physiol.* 312 (6), G550–G558. doi:10.1152/ajpgi.00256.2016
- Watanabe, M., Houten, S. M., Matak, C., Christoffolete, M. A., Kim, B. W., Sato, H., et al. (2006). Bile Acids Induce Energy Expenditure by Promoting Intracellular Thyroid Hormone Activation. *Nature* 439 (7075), 484–489. doi:10.1038/nature04330
- Wei, W., Wang, H. F., Zhang, Y., Zhang, Y. L., Niu, B. Y., and Yao, S. K. (2020). Altered Metabolism of Bile Acids Correlates with Clinical Parameters and the Gut Microbiota in Patients with Diarrhea-Predominant Irritable Bowel Syndrome. *World J. Gastroenterol.* 26 (45), 7153–7172. doi:10.3748/wjg.v26.i45.7153
- Wells, J. E., Berr, F., Thomas, L. A., Dowling, R. H., and Hylemon, P. B. (2000). Isolation and Characterization of Cholic Acid 7 α -Dehydroxylating Fecal Bacteria from Cholesterol Gallstone Patients. *J. Hepatol.* 32 (1), 4–10. doi:10.1016/s0168-8278(00)80183-x
- Wistuba, W., Gnewuch, C., Liebisch, G., Schmitz, G., and Langmann, T. (2007). Lithocholic Acid Induction of the FGF19 Promoter in Intestinal Cells is Mediated by PXR. *World J. Gastroenterol.* 13 (31), 4230–4235. doi:10.3748/wjg.v13.i31.4230
- Wu, Y., Mo, R., Zhang, M., Zhou, W., and Li, D. (2021). Grape Seed Proanthocyanidin Alleviates Intestinal Inflammation Through Gut Microbiota-Bile Acid Crosstalk in Mice. *Front. Nutr.* 8, 786682. doi:10.3389/fnut.2021.786682
- Xie, W., Radominska-Pandya, A., Shi, Y., Simon, C. M., Nelson, M. C., Ong, E. S., et al. (2001). An Essential Role for Nuclear Receptors SXR/PXR in Detoxification of Cholestatic Bile Acids. *Proc. Natl. Acad. Sci. U. S. A.* 98 (6), 3375–3380. doi:10.1073/pnas.051014398
- Xing, Y., Yan, J., and Niu, Y. (2020). PXR: A Center of Transcriptional Regulation in Cancer. *Acta Pharm. Sin. B* 10 (2), 197–206. doi:10.1016/j.apsb.2019.06.012
- Yang, X., Wang, B. C., Zhang, X., Liu, W. Q., Qian, J. Z., Li, W., et al. (2011). Evaluation of Lysimachia Christinae Hance Extracts as Anticholestyitis and

- Cholagogic Agents in Animals. *J. Ethnopharmacol.* 137 (1), 57–63. doi:10.1016/j.jep.2011.04.029
- Yang, J., Zhang, S., Henning, S. M., Lee, R., Hsu, M., Grojean, E., et al. (2018). Cholesterol-lowering Effects of Dietary Pomegranate Extract and Inulin in Mice Fed an Obesogenic Diet. *J. Nutr. Biochem.* 52, 62–69. doi:10.1016/j.jnutbio.2017.10.003
- Yang, L., Wan, Y., Li, W., Liu, C., Li, H. F., Dong, Z., et al. (2022). Targeting Intestinal Flora and its Metabolism to Explore the Laxative Effects of Rhubarb. *Appl. Microbiol. Biotechnol.* 106 (4), 1615–1631. doi:10.1007/s00253-022-11813-5
- Yao, B., He, J., Yin, X., Shi, Y., Wan, J., and Tian, Z. (2019). The Protective Effect of Lithocholic Acid on the Intestinal Epithelial Barrier is Mediated by the Vitamin D Receptor via a SIRT1/Nrf2 and NF- κ B Dependent Mechanism in Caco-2 Cells. *Toxicol. Lett.* 316, 109–118. doi:10.1016/j.toxlet.2019.08.024
- Yoneno, K., Hisamatsu, T., Shimamura, K., Kamada, N., Ichikawa, R., Kitazume, M. T., et al. (2013). TGR5 Signalling Inhibits the Production of Pro-Inflammatory Cytokines by *In Vitro* Differentiated Inflammatory and Intestinal Macrophages in Crohn's Disease. *Immunology* 139 (1), 19–29. doi:10.1111/imm.12045
- Yu, D. D., Sousa, K. M., Mattern, D. L., Wagner, J., Fu, X., Vaidehi, N., et al. (2015). Stereoselective Synthesis, Biological Evaluation, and Modeling of Novel Bile Acid-derived G-Protein Coupled Bile Acid Receptor 1 (GP-BAR1, TGR5) Agonists. *Bioorg Med. Chem.* 23 (7), 1613–1628. doi:10.1016/j.bmc.2015.01.048
- Yu, J., Zhang, H., Chen, L., Ruan, Y., Chen, Y., and Liu, Q. (2021). Disease-Associated Gut Microbiota Reduces the Profile of Secondary Bile Acids in Pediatric Nonalcoholic Fatty Liver Disease. *Front. Cell Infect. Microbiol.* 11, 698852. doi:10.3389/fcimb.2021.698852
- Zhou, H., and Hylemon, P. B. (2014). Bile Acids are Nutrient Signaling Hormones. *Steroids* 86, 62–68. doi:10.1016/j.steroids.2014.04.016
- Zimniak, P., Holsztynska, R., Lester, A., Waxman, D. J., and Radomska, A. (1989). Detoxification of Lithocholic Acid. Elucidation of the Pathways of Oxidative Metabolism in Rat Liver Microsomes. *J. Lipid Res.* 30 (6), 907–918. doi:10.1016/s0022-2275(20)38317-6

Conflict of Interest: The authors declare that the research was conducted in the absence of any commercial or financial relationships that could be construed as a potential conflict of interest.

Publisher's Note: All claims expressed in this article are solely those of the authors and do not necessarily represent those of their affiliated organizations, or those of the publisher, the editors and the reviewers. Any product that may be evaluated in this article, or claim that may be made by its manufacturer, is not guaranteed or endorsed by the publisher.

Copyright © 2022 Sheng, Ji and Zhang. This is an open-access article distributed under the terms of the Creative Commons Attribution License (CC BY). The use, distribution or reproduction in other forums is permitted, provided the original author(s) and the copyright owner(s) are credited and that the original publication in this journal is cited, in accordance with accepted academic practice. No use, distribution or reproduction is permitted which does not comply with these terms.



OPEN ACCESS

EDITED BY

Alessandra Durazzo,
Council for Agricultural Research and
Economics, Italy

REVIEWED BY

Bing Ding,
Zhejiang Chinese Medical University,
China
Xun Wang,
Sichuan Agricultural University, China

*CORRESPONDENCE

Xiaopeng Wang,
wxpeng2004@163.com
Zongqi He,
hzq_009@163.com

[†]These authors have contributed equally
to this work

SPECIALTY SECTION

This article was submitted to
Ethnopharmacology,
a section of the journal
Frontiers in Pharmacology

RECEIVED 24 May 2022

ACCEPTED 05 July 2022

PUBLISHED 22 August 2022

CITATION

Cheng X, Du J, Zhou Q, Wu B, Wang H,
Xu Z, Zhen S, Jiang J, Wang X and He Z
(2022), Huangkui lianchang decoction
attenuates experimental colitis by
inhibiting the NF- κ B pathway
and autophagy.
Front. Pharmacol. 13:951558.
doi: 10.3389/fphar.2022.951558

COPYRIGHT

© 2022 Cheng, Du, Zhou, Wu, Wang, Xu,
Zhen, Jiang, Wang and He. This is an
open-access article distributed under
the terms of the [Creative Commons
Attribution License \(CC BY\)](#). The use,
distribution or reproduction in other
forums is permitted, provided the
original author(s) and the copyright
owner(s) are credited and that the
original publication in this journal is
cited, in accordance with accepted
academic practice. No use, distribution
or reproduction is permitted which does
not comply with these terms.

Huangkui lianchang decoction attenuates experimental colitis by inhibiting the NF- κ B pathway and autophagy

Xudong Cheng^{1†}, Jun Du^{1†}, Qing Zhou², Bensheng Wu¹,
Haodong Wang³, Zhizhong Xu¹, Shuguang Zhen¹, Jieyu Jiang⁴,
Xiaopeng Wang^{1*} and Zongqi He^{1*}

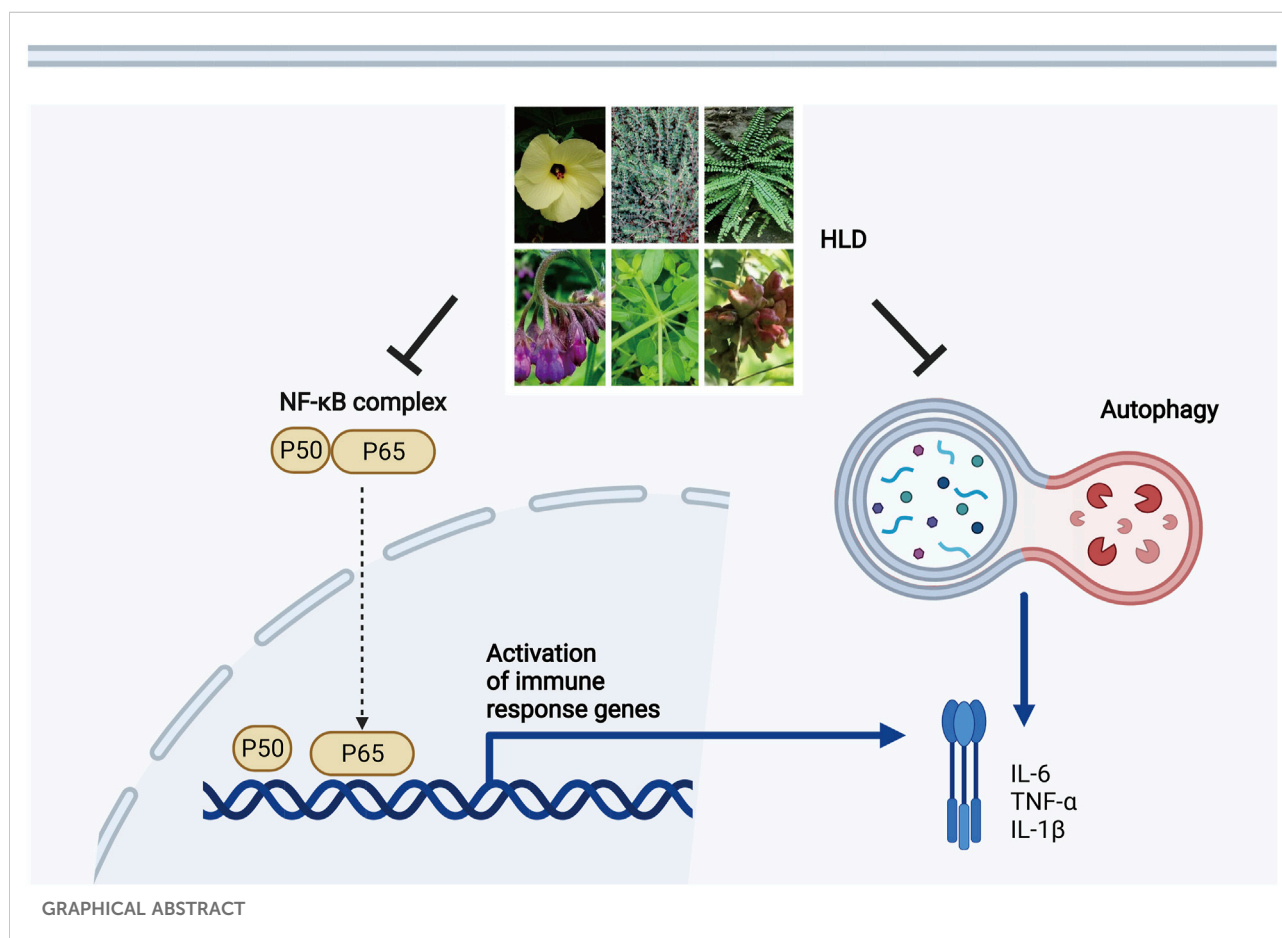
¹Suzhou TCM Hospital Affiliated to Nanjing University of Chinese Medicine, Suzhou, China, ²Affiliated Hospital of Nanjing University of Chinese Medicine, Nanjing, China, ³Jingren Medical Laboratory, Nanjing, China, ⁴Suzhou Foreign Language School, Suzhou, China

Ulcerative colitis (UC) is a chronic inflammatory colorectal disease characterized by excessive mucosal immune response activation and dysfunction of autophagy in intestinal epithelial cells. Traditional herbal preparations, including the Huangkui lianchang decoction (HLD), are effective in UC clinical treatment in East Asia, but the underlying mechanism is unclear. This study evaluated the therapeutic effects and associated molecular mechanisms of HLD in UC *in vivo* and *in vitro*. A C57BL/6 UC mouse model was established using 2.5% dextran sulfate sodium. The effects of HLD on the colonic structure and inflammation in mice were evaluated using mesalazine as the control. The anti-inflammatory effects of HLD were assessed using disease activity index (DAI) scores, histological scores, enzyme-linked immunosorbent assay, immunohistochemistry, immunofluorescence, and western blotting. HLD displayed a protective effect in UC mice by reducing the DAI and colonic histological scores, as well as levels of inflammatory cytokines and NF- κ B p65 in colonic tissues. NCM460 lipopolysaccharide-induced cells were administered drug serum-containing HLD (HLD-DS) to evaluate the protective effect against UC and the effect on autophagy. HLD-DS exhibited anti-inflammatory effects in NCM460 cells by reducing the levels of inflammatory cytokines and increasing interleukin 10 levels. HLD-DS reduced p-NF- κ B p65, LC3II/I, and Beclin 1 expression, which suggested that HLD alleviated colitis by inhibiting the NF- κ B pathway and autophagy. However, there was no crosstalk between the NF- κ B pathway and autophagy. These findings confirmed that HLD was an effective herbal preparation for the treatment of UC.

Abbreviations: CRP, C-reactive protein; DAB, diaminobenzidine; DAI, Disease activity index; DSS, Dextran sulfate sodium; ESR, erythrocyte sedimentation rate; HE, hematoxylin-eosin; HLD, Huangkui lianchang decoction; HLD-DS, Drug serum-containing HLD; IBD, Inflammatory bowel disease; IKK, I κ B kinase; LPS, Lipopolysaccharide; 3-MA, 3-Methyladenine; NCM, Normal colon mucosa; PDTC, Pyrrolidine dithiocarbamate; PVDF, polyvinylidene fluoride; RAPA, Rapamycin; SD, standard deviation; UC, Ulcerative colitis; UHPLC-MS/MS, ultra-high performance liquid chromatography-tandem mass spectrometry.

KEYWORDS

ulcerative colitis, Huangkui lianchang decoction, mesalazine enema, NF- κ B pathway, autophagy



Introduction

Ulcerative colitis (UC) is a chronic, recurrent, inflammatory intestinal disease of unknown etiology with a prolonged and recurrent course and can involve any colon part (Raine et al., 2022). Recently, UC incidence has been on the rise worldwide, seriously endangering the lives and health of people and increasing medical expenses (Wei et al., 2021).

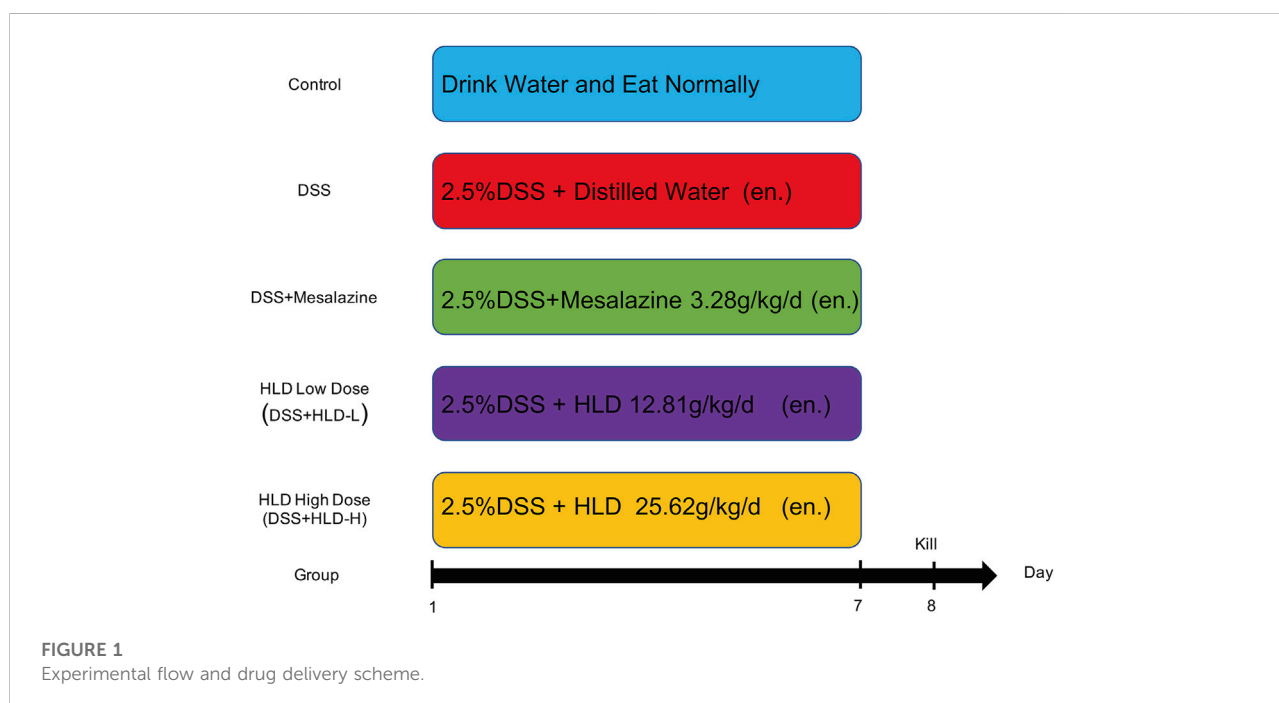
The primary goal of UC treatment is to prevent disability and avoid colectomy and colorectal cancer by maintaining remission (Turner et al., 2021; Raine et al., 2022). Currently, the primary medicines used to treat UC include corticosteroids, 5-aminosalicylic acid, immunosuppressants, and biologics. Although these drugs have reduced the UC recurrence rate, they generally have disadvantages such as side effects, high price, reduced quality of life and patient satisfaction, and increased medical burden with long-term use (Raine et al., 2022). Therefore, it is necessary to find an alternative

treatment that is safe, effective, and well-tolerated. Studies have found that a variety of herbs have excellent anti-inflammatory activities and can be used to alleviate intestinal inflammation.

Autophagy is essential for maintaining intestinal mucosal immunity, intestinal epithelial barrier integrity, and microbial defenses (Wu et al., 2019). Autophagy dysfunction can disrupt the intestinal mucosal barrier and consequently lead to the development of inflammatory bowel disease (IBD) (Lassen and Xavier, 2018; Trentesaux et al., 2020). Therefore, targeting autophagy to repair the intestinal mucosal barrier has become a fundamental approach to treating IBD. Studies have confirmed that the NF- κ B signaling pathway and autophagy are mutually regulated, and that activation of the NF- κ B signaling pathway can further activate autophagy and trigger inflammation (Cadwell, 2016; Piao et al., 2017). Therefore, inhibiting autophagy via NF- κ B pathway inhibition is a potential therapeutic approach for treating IBD.

TABLE 1 Plant names and used parts of herbs included in the HLD.

Herb id	Chinese name	English name	Latin name	Plant name	Used parts
HERB 002574	HUANG SHU KUI HUA	Setose Abolmoschus	Abolmoschus manihot	Abolmoschus manihot (L.) Medik	flower
HERB 001254	DI JIN CAO	all - grass of Humifuse Euphorbia	Herba Euphorbiae humifusae	Euphorbia humifusa Willd	whole herb
HERB 001713	FENG WEI CAO	all - grass of Chinese brake	Herba Pteridis multifidae	Pteris multifida Poir	whole herb or rhizome
HERB 007160	ZI CAO	Arnebia root Gromwell root	Radix Arnebiae seu Lithospermi	Arnebia euchroma (Royle) I.M. Johnst	root
HERB 004446	QIAN CAO	Tali Madder root	Radix rubiae	Rubia cordifolia L	root
HERB 005692	WU BEI ZI	Chinese gall	Galla Chinensis	Rhus chinensis Mill	gall



Huangkui lianchang decoction (HLD) is a traditional herbal formula consisting of six common herbs, *Huang Shu Kui Hua*, *Di Jin Cao*, *Feng Wei Cao*, *Zi Cao*, *Qian Cao*, and *Wu Bei Zi*. In our previous clinical observation, we found that HLD enema reduced the erythrocyte sedimentation rate (ESR) and C-reactive protein (CRP) expression in patients with UC, showing an excellent anti-inflammatory effect. Further studies showed that HLD alleviates intestinal inflammation in UC mice by inhibiting the NF- κ B signaling pathway (He et al., 2019); however, the effects of HLD on autophagy and the crosstalk between NF- κ B and autophagy are unknown.

Here, we hypothesized that HLD exerts anti-UC effects by regulating autophagy via NF- κ B pathway inhibition *in vitro* and

in vivo. We evaluated the anti-inflammatory effect of HLD using a UC mouse model and verified its anti-UC effect exerted through autophagy and NF- κ B pathway inhibition in intestinal epithelial cells. This study provides a scientific basis for preventing and treating UC using HLD.

Materials and methods

Main reagents and drugs

Mesalazine enemas (Salofalk, 60 g; 4 g, manufactured by Vifor AG Zweigniederlassung Medichemie Ettingen, Switzerland;

TABLE 2 DAI scores in mice.

Score	Weight loss (%)	Stool consistency	Occult/gross bleeding
0	None	Normal	None
1	1–5	Soft, shaped	Between the two
2	6–10	dilute stool	Fecal Occult Blood
3	11–15	Between the two	Between the two
4	>15	Diarrhea	Blood in the stool

DAI = (combined score of weight loss, stool consistency, and bleeding)/3, 5% body weight loss was scored as 1. On the modeling day, the body weight was used as the basal body weight.

import drug license number: H20150127) were purchased from Shenzhen Kangzhe Pharmaceutical Co. Dextran sodium sulfate (DSS), NF- κ B p65, Beclin 1, p-NF- κ B p65, LC3II, LC3I, and β -actin antibodies were purchased from Cell Signaling Technology (CST). Antibodies against 3-Methyladenine (3-MA), rapamycin (RAPA), and pyrrolidine dithiocarbamate (PDTC) were purchased from Malone Pharma Consulting.

HLD preparation and quality control

Abelmoschus manihot (produced in Sichuan Province, China; lot No. 181015006), *Herba Euphorbiae humifusae* (produced in Jiangsu Province, China; lot No. 180801010), *Herba Pteridis multifidae* (produced in Jiangsu Province, China; lot No. 181004015), *Radix Arnebiae seu Lithospermi* (produced in Xinjiang Province, China; lot No. 180703), *Radix Rubiae* (produced in Shaanxi Province, China; lot No. 180617), and *Galla Chinensis* (produced in Guizhou Province, China; lot No. 180504005) were purchased from Suzhou Tianling Chinese Herbal Medicine Co., Ltd. All drugs were identified by the Suzhou Hospital of TCM pharmacist per Chinese Pharmacopoeia standards. Their corresponding English names, Latin names, plant names, and herb IDs were retrieved from <http://herb.ac.cn> and are listed in Table 1. Plant names were verified at <http://www.theplantlist.org>.

The drugs were washed with water and soaked in distilled water equivalent to eight times the number of herbs for 60 min, boiled for 40 min, and extracted twice; the extracts were centrifuged at 3000 r/min for 30 min, concentrated to 2.5 g/ml liquid, sterilized with flow-through steam at 100°C for 30 min, and stored at 4°C.

UHPLC- MS analysis

HLD was separated on an EXIONLC System (Sciex Technologies, United States) ultra-performance liquid chromatography using a Waters Acquity HSS T3 column (1.8 μ m 2.1 \times 100 mm) at a flow rate of 0.4 ml/min. Mobile phases A and B were aqueous solutions containing 0.1% formic acid and acetonitrile, respectively. Gradient elution was performed as follows: 0–0.5 min, 2% B; 0.5–10 min, 2–50% B; 10–11 min,

50–95% B; 11–13 min, 95% B; 13–13.1 min, 95–2% B; 13.1–15 min, 2% B. The column temperature was 40°C. The autosampler temperature was 4°C, and the injection volume was 2 μ l.

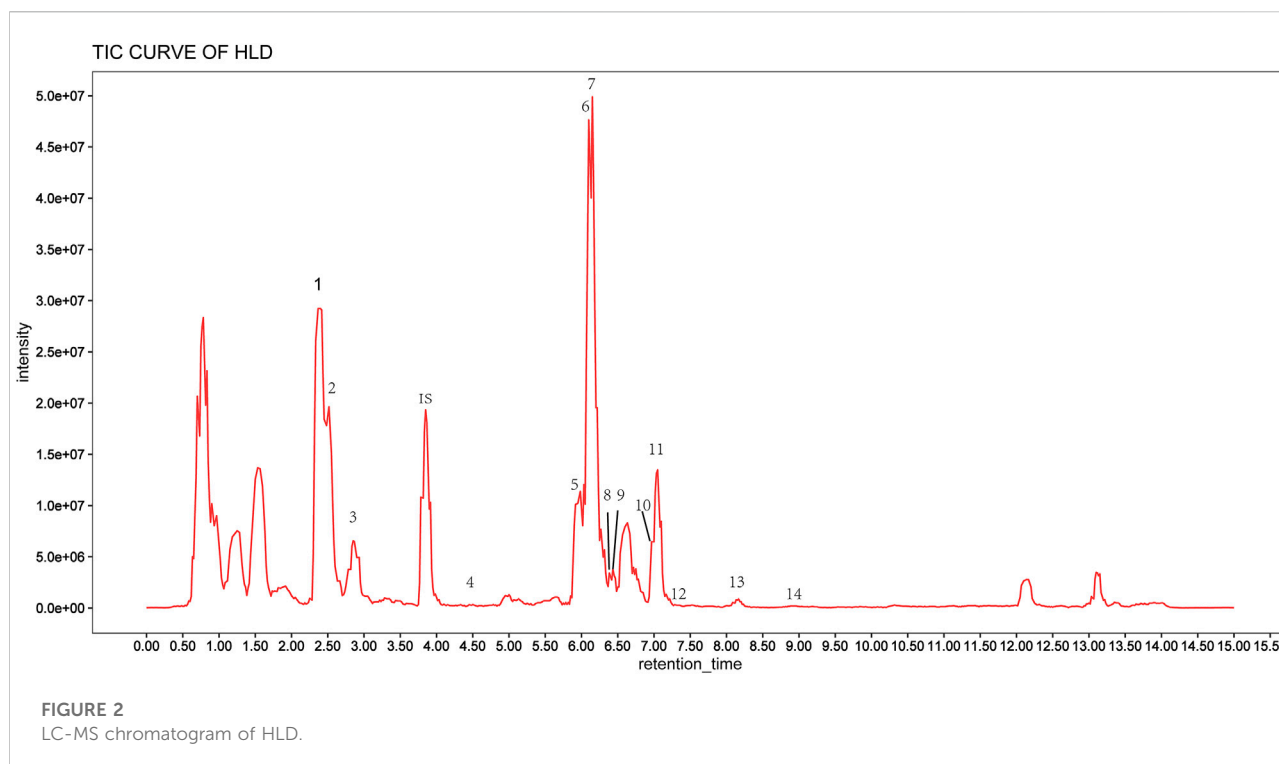
Sciex Q Trap 6500+ (Sciex Technologies) was used for the assay development. Typical ion source parameters were: ion spray voltage: +5500 V, curtain gas: 35 psi, temperature: 400°C, ion source gas 1: 60 psi, ion source gas 2: 60 psi, DP: \pm 100 V. The SCIEX Analyst Work Station Software (Version 1.6.3) was employed for multiple reaction monitoring data acquisition and processing.

Model preparation and drug delivery

Fifty 8-week-old C57BL/6 male mice were purchased from Charles River Laboratories (Beijing, China). Mice were acclimatized and housed for 1 week on a 12 h light/12 h dark cycle. The mouse UC model was established referring to previous literature (Murano et al., 2000; Wang et al., 2018; Peng et al., 2020). In brief, DSS was dissolved in sterile water to form a 2.5% DSS (36,000–50,000 Da) solution, and mice drank continuously for 7 days. The control group was administered saline. Mice were divided into five groups (10 mice in each group) by the random number table method as follows: Control group, DSS group, Mesalazine group (DSS+Mesalazine), HLD low-dose group (DSS+HLD-L), and HLD high-dose group (DSS+HLD-H). The modeling protocol and procedure are shown in Figure 1. The study was approved by the Medical Ethics Committee of Suzhou Hospital of TCM (Grant No. 2020 Ethical Animal Approval 002) before implementation. The research was conducted per the Directive 2020/63/EU to protect the laboratory animals. The study followed the ARRIVE guidelines 2.0 for the design, analysis, and reporting. The experimental operators were aware of the group distribution, experiment conduct, and outcome assessment during group allocations. Data analysts were not aware of group allocations.

Anesthesia and enema method

According to the manufacturer's instructions, mice were anesthetized with isoflurane, an inhalational anesthetic, using



an ABS-type small animal anesthesia machine. Anesthetized mice were placed in the prone position. The drug was injected slowly into the intestinal lumen with a 1 ml syringe and a 20G cannula needle (lubricated with Vaseline), the top of which was approximately 4 cm from the anus. The abdomen was gently rubbed for 1 min and then placed restraining the mouse head down, and the body was tilted by 45° for 10 min, once a day.

Disease activity index (DAI) score

The disease activity index (DAI) was determined as described previously (Murano et al., 2000; Wang et al., 2018; Peng et al., 2020). Body weight loss, stool haemoccult positivity or gross bleeding, and stool consistency were evaluated according to Table 2. DAI was calculated with the following formula: DAI = (combined score of weight loss, stool consistency, and bleeding)/3.

Histological scoring

On day eight of the experiment, the mice were euthanized, and blood and colonic tissue specimens were collected according to standard operating procedures. Distal colon tissues with significant inflammation/ulcer were fixed in a 4% paraformaldehyde solution, embedded in paraffin, serially sectioned at 4 μm, and stained with hematoxylin-eosin (HE). The inflammatory infiltration and colonic mucosal damage degree were observed using CaseViewer, a digital

microscopy application, and histological scores were obtained. Histological scoring was performed according to the following criteria: epithelium: 0, normal form; 1, loss of cup cells; 2, significant loss of cup cells; 3, loss of crypt; 4, significant loss of crypt and inflammatory infiltration: 0, no infiltration; 1, infiltration at the base of the crypt; 2, infiltration into the mucosal muscular layer; 3, extensive infiltration into the mucosal muscular layer with mucosal thickening and edema; 4, infiltration into the submucosal layer. The total histological score included the sum of the epithelial and inflammatory infiltration scores.

ELISA

According to the standard experimental procedure, ELISA kits were used to detect NF-κB and TGF-β concentrations in mouse serum and TNF-α, IL-1β, IL-6, and IL-10 concentrations in mouse serum and cell supernatants.

Immunohistochemistry

The preserved paraffin sections were analyzed *via* microscopy following the dewaxing, rehydration, fire extinguishing, closure, secondary antibody labeling, incubation, diaminobenzidine (DAB) color development, and hematoxylin re-staining and sealing process. Five high-magnification fields (1000×) were selected for each section

TABLE 3 HLD bioactive components.

Number	Components	Rt (min)	Formula	MS	MS ²
1	2-Phenylacetamide	2.52	C ₈ H ₉ NO	135.0684	119
2	Inosine	2.60	C ₁₀ H ₁₂ N ₄ O ₅	268.0807	137
3	L-Phenylalanine	2.82	C ₉ H ₁₁ NO ₂	165.0789	120.1
4	Cianidanol	4.50	C ₁₅ H ₁₄ O ₆	290.0790	165
5	Rutin	5.85	C ₂₇ H ₃₀ O ₁₆	610.1534	465
6	Cynaroside	6.10	C ₂₁ H ₂₀ O ₁₁	448.1005	286.9
7	Isoquercitrin	6.22	C ₂₁ H ₂₀ O ₁₂	464.0954	303
8	Gossypetin	6.46	C ₁₅ H ₁₀ O ₈	318.0375	109
9	Rhoifolin	6.50	C ₂₇ H ₃₀ O ₁₄	578.1636	433
10	Hyperoside	6.99	C ₂₁ H ₂₀ O ₁₂	464.0955	302.8
11	Myricetin	7.05	C ₁₅ H ₁₀ O ₈	318.0376	272.9
12	Alizarin 2-methyl ether	7.38	C ₁₅ H ₁₀ O ₄	254.2245	237.15
13	Quercetin	8.07	C ₁₅ H ₁₀ O ₇	302.0426	153
14	Lucidin	8.89	C ₁₅ H ₁₀ O ₅	270.0528	253.1

and analyzed after quantitative grayscale scanning using the image analysis system. NF- κ B p65 expression and localization in the cytoplasm and nucleus and autophagy-related protein (LC3 and Beclin 1) expression in colon tissue sections were detected using immunohistochemistry.

Immunofluorescence

After deparaffinization and rehydration, distal colon sections were microwaved in citric acid (pH 6.0). After washing with phosphate-buffered saline containing Tween-20 (pH 7.4), the sections were incubated in a 3% H₂O₂ solution and blocked with 3% bovine serum albumin for 20 min at room temperature (Zhao et al., 2020). The sections were then incubated with NF- κ B p65 (1:100; CST, Danvers, MA, United States), LC3 (1:200; CST, Danvers, MA, United States), and Beclin 1 (1:150; CST, Danvers, MA, United States) primary antibodies at 4°C overnight. The blots were incubated with horseradish peroxidase (HRP)-conjugated secondary antibody (1:200; Servicebio, China) for 30 min at room temperature, followed by DAB solution (Servicebio, China). The sections were counterstained with hematoxylin, dehydrated, and mounted. Sections were observed using Caseviewer and Leica LAS image acquisition systems. Positive DAB staining areas were quantified using the NIH ImageJ software (National Institutes of Health, Bethesda, MD, United States).

HLD-DS preparation

Sprague Dawley rats were administered HLD 1.5 ml/time (five times the adult equivalent dose) twice a day for three consecutive days. One hour after the last administration, the

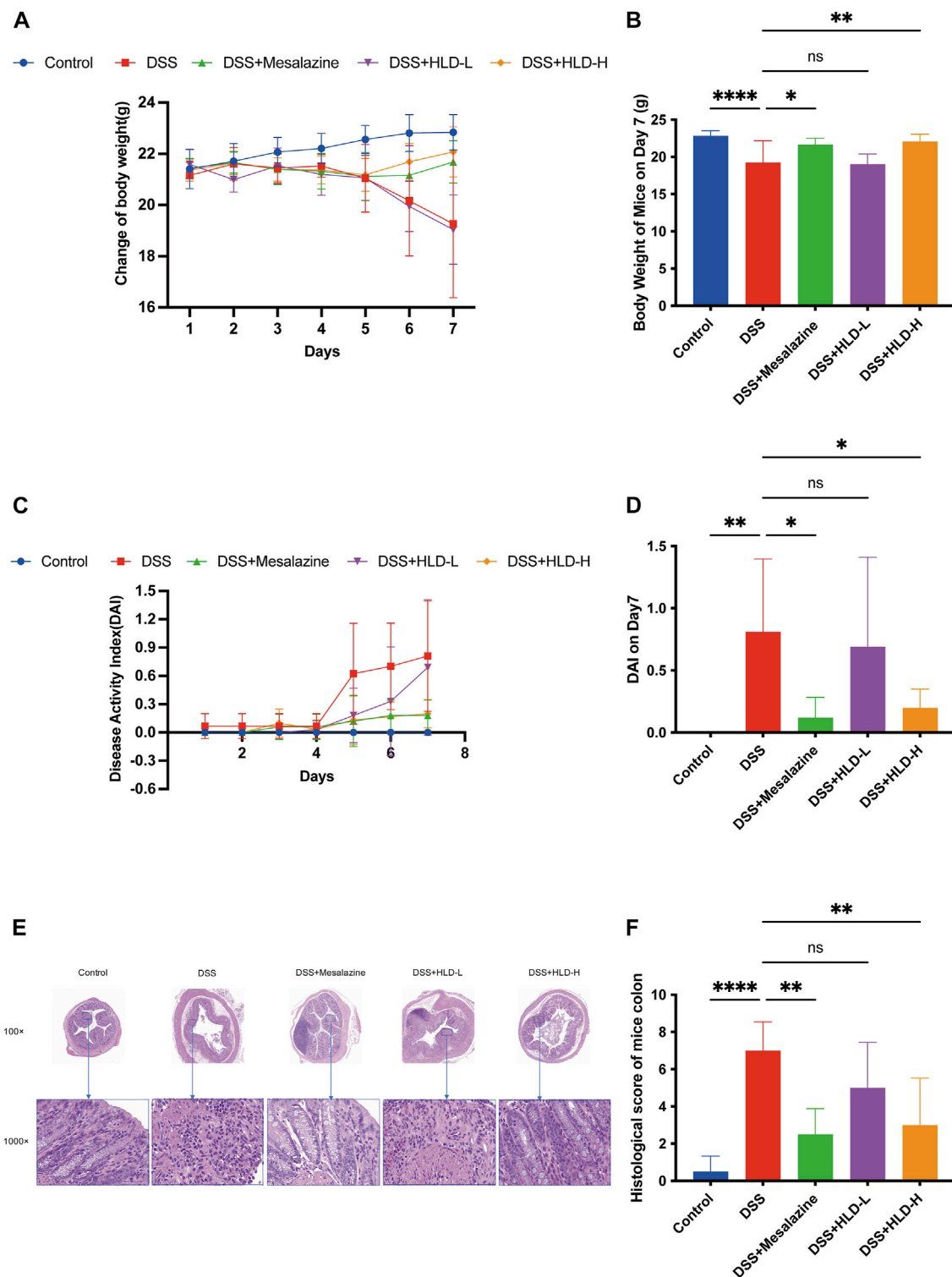
rats were sacrificed by carbon dioxide asphyxiation, and blood was drawn from the abdominal aorta. The serum was aseptically separated by centrifugation at 2500 rpm for 10 min, inactivated at 56°C for 30 min, and filtered through a 0.22 μ m microporous membrane to remove bacteria. Blood was stored at -80°C.

Cellular experiments

NCM460 human colonic epithelial cells were purchased from Shanghai Meiwang Biotechnology Co., Ltd and grown in RPMI medium containing penicillin (100 U/ml)-streptomycin (100 U/ml) (Invitrogen, Carlsbad, CA, United States) and 10% fetal bovine serum (Hyclone, Logan, UT, United States) (Zhou et al., 2018). Lipopolysaccharide (LPS, 10 ng/ml) was used to induce inflammation and autophagy in NCM460 cells (Zeng et al., 2018; Ba et al., 2021; Guo et al., 2021; Shang et al., 2021). The groups were divided into control, LPS, LPS+HLD-DS, LPS+HLD-DS+3-MA, LPS+HLD-DS+RAPA, LPS+HLD-DS+PDTC, LPS+HLD-DS+PDTC+RAPA, and LPS+HLD-DS+PDTC+3-MA. The concentrations of 3-MA, RAPA, and PDTC were 100 nmol/L, 3 mmol/L, and 50 μ mol/L, respectively.

Cell counting kit-8 (CCK-8) assay

According to the manufacturer's protocol, the effect of different HLD-DS concentrations on cell proliferation was examined using CCK-8. NCM460 cell suspension with a density of 1×10^4 cells/ml was inoculated into a 96-well plate (100 μ l per well) and incubated at 37°C for 4 h. Cells were treated with 10 μ l of CCK-8 and incubated for 4 h. The OD value at 450 nm was measured, and the measurement of each sample was repeated six times.

**FIGURE 3**

HLD improved DAI and alleviated the UC mice's pathology. (A,B) The trend of body weight changes in mice and a comparison of body weight on day 7 were presented. (C,D) The trend of DAI changes in mice and a comparison of DAI on day 7 were presented. (E,F) The comparison of hematoxylin & eosin (HE) staining results and histological scores of mice colonic tissues. All data are expressed as the mean \pm SD. ($n = 3$). * $p < 0.05$, ** $p < 0.01$, **** $p < 0.0001$.

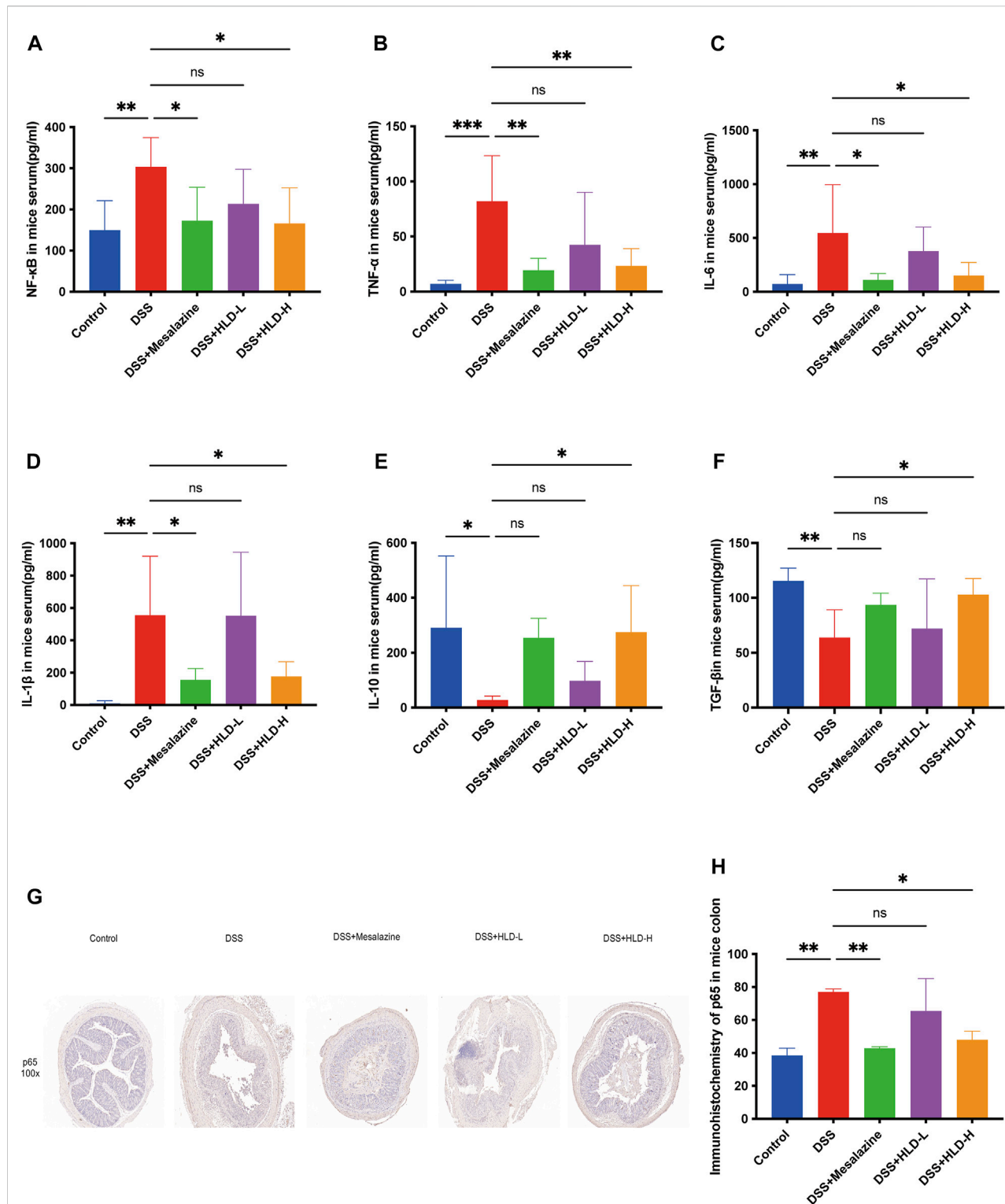
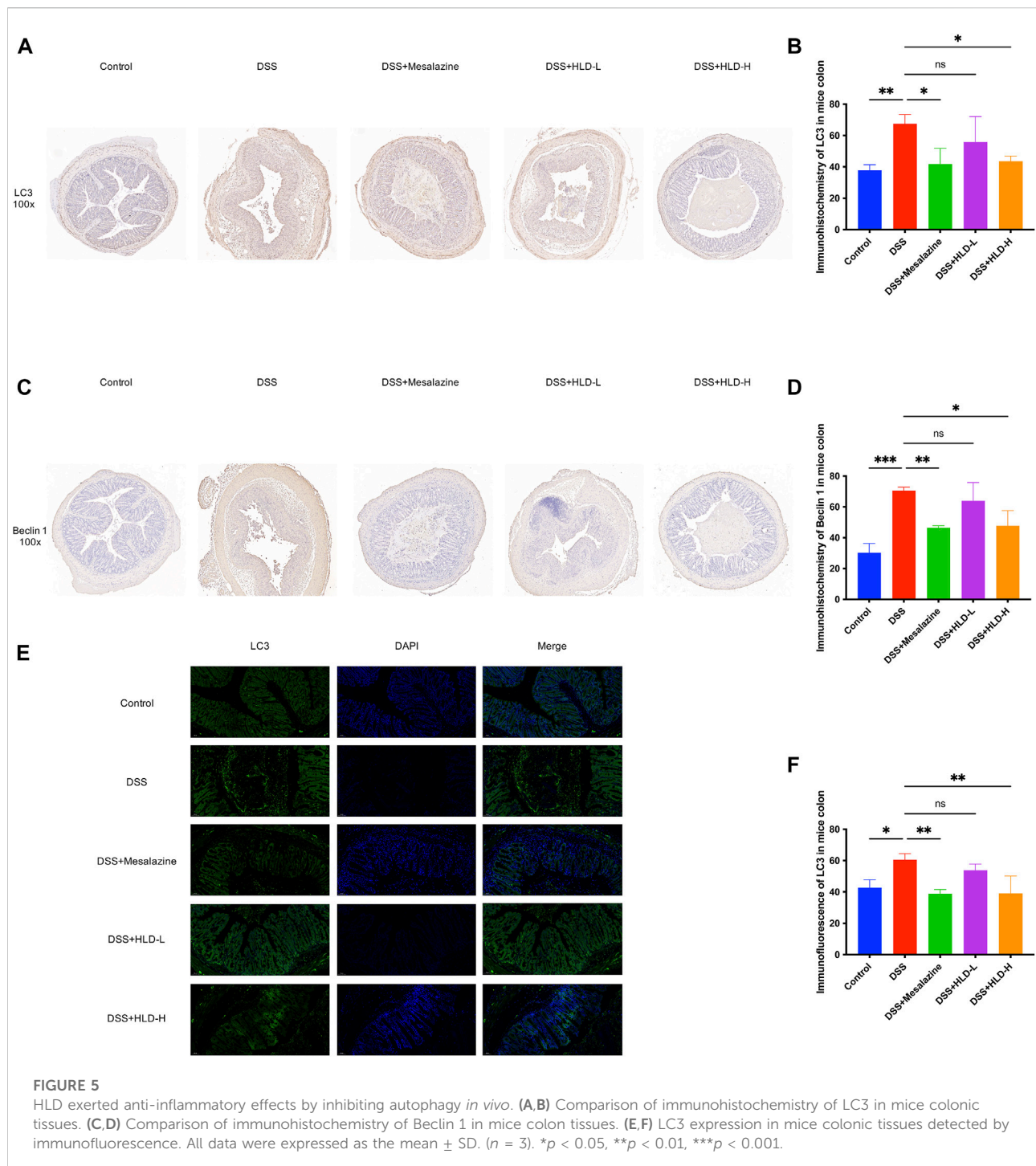


FIGURE 4

HLD exerted anti-inflammatory effects by inhibiting NF-κB *in vivo*. (A–F) The levels of pro-inflammatory cytokines such as NF-κB, TNF-α, IL-6, IL-1β and anti-inflammatory factors such as TGF-β and IL-10 were detected by ELISA in response to the anti-inflammatory activities of HLD. (*n* = 6). (G,H) Immunohistochemical sections and data comparison of NF-κB p65 in mice colonic tissues. All data were expressed as the mean ± SD. (*n* = 3).

p* < 0.05, *p* < 0.01, ****p* < 0.001.



Western blotting

Total cellular proteins were extracted using a Radio Immunoprecipitation Assay buffer, and protein concentrations were determined using the bicinchoninic acid (BCA) method. Equal amounts of proteins were electrophoresed on 10% sodium dodecyl sulfate-polyacrylamide gels by electrophoresis, followed

by immunoblotting to transfer the proteins to polyvinylidene fluoride (PVDF) membranes. PVDF membranes were blocked with skim milk for 2 h at room temperature and incubated with LC3II and LC3I (1:1000; #12741s, CST), Beclin1 (1:1000; #4122, CST), NF- κ B p65 (1:1000; #6956s, CST), p-NF- κ B p65 (1:1000; #3033, CST), and β -actin (1:1000; #3700, CST) antibodies overnight at 4°C. After incubation with HRP-conjugated

secondary antibodies, proteins were detected by electrochemiluminescence (ECL) using the ChemiDoc CRS imaging system and analyzed using Quantity One analysis software (Bio-Rad Laboratories, San Francisco, CA, United States).

Data analysis and graphing

All data are presented as mean \pm standard deviation (SD) from a minimum of three replicates. Differences between the groups were evaluated using GraphPad Prism version 9.0.0 (GraphPad Software, San Diego, California, United States) with Student's *t*-test when comparing only two groups or assessed by one-way ANOVA when more than two groups were compared. Differences were considered statistically significant at $p < 0.05$.

Results

Chemical characteristics of HLD

An ultra-high performance liquid chromatography-tandem mass spectrometry (UHPLC-MS/MS) method was developed to characterize 14 compounds in HLD. The base peak chromatograms of HLD are shown in Figure 2. The compounds were identified by literature comparison and mass spectrometry, and the results are presented in Table 3. The results indicated that HLD mainly contained flavonoids, such as rutin, isoquercitrin, gossypetin, and quercetin. These flavonoids were present in more than one herb.

HLD improved the DAI and alleviated the pathology of UC mice

DSS-induced UC mice exhibited persistent weight loss from day 4, accompanied by diarrhea and fecal occult blood (Figure 3A). By day 7, the weights of the DSS group mice were significantly lower than those of the control mice ($p < 0.0001$) (Figure 3B) and were accompanied by fecal blood. The weights of the mesalazine and DSS+HLD-H groups decreased slightly and then gradually increased. On the seventh day, the body weights of the mesalazine and DSS+HLD-H groups were significantly different from those of the DSS group (Figure 3B). One mouse in each of the DSS and HLD-H groups died during the experiment, and five mice died in the Mesalazine group. No death was observed in the remaining groups.

The DAI scores of the DSS group mice were significantly higher than those of the control group ($p < 0.01$) (Figure 3D). The DAI scores of the mesalazine and DSS+HLD-H groups were significantly lower than those of the DSS group ($p < 0.05$). In

contrast, the DAI score of the DSS+HLD-L group was not significantly different from that of the DSS group (Figure 3D).

As shown in Figure 3E, the control group showed a clear colonic tissue structure in all layers, intact mucosal epithelium, tightly arranged crypts, regular muscle fibers arrangement in the muscular layer, and no apparent inflammatory reaction. The DSS group showed extensive ulcer formation. Many inflammatory cells infiltrated the mucosal and submucosal layers. Dilated intestinal glands and a few acidophilic or basophilic masses in the glandular lumen were observed, suggesting successful modeling. The inflammatory reaction, ulceration, submucosal edema, and plasma membrane layer inflammation were less severe in the mesalazine and HLD-H groups compared with the DSS group. The HLD-L group showed intestinal mucosa ulceration, numerous inflammatory cells in the mucosal and submucosal layers, and bleeding in the intestinal lumen in some samples. There was a significant difference in histological scores between the mesalazine and HLD-H groups compared with the DSS but not the HLD-L group (Figure 3F).

HLD exerts anti-inflammatory effects by inhibiting NF- κ B *in vivo*

As shown in Figure 4 A-F, TGF- β and IL-10 levels were significantly reduced in the DSS group compared to the control group, and NF- κ B, TNF- α , IL-6, and IL-1 β levels were significantly increased in the DSS group. The HLD-H group showed significantly increased TGF- β and IL-10 levels and reduced NF- κ B, TNF- α , IL-6, and IL-1 β levels compared to the DSS group ($p < 0.05$).

Furthermore, NF- κ B p65 was deeply stained in the nucleus during the apparent colonic tissue inflammation in the DSS group (Figure 4G). NF- κ B p65 expression decreased in the colon tissues of the HLD-H and mesalazine groups, suggesting that HLD exerted an anti-inflammatory effect by inhibiting NF- κ B (Figure 4H).

HLD exerts anti-inflammatory effects by inhibiting autophagy *in vivo*

On comparing LC3 immunohistochemical sections and immunofluorescence staining pictures of colonic mouse tissues, LC3 expression was significantly higher in the DSS group than that in the control group, with a statistically significant difference. This suggested that autophagic activity was significantly higher when colonic inflammation was active (Figures 5A,B,E,F). Compared with the DSS group, LC3 was significantly lower in the mesalazine and HLD-H groups, suggesting a decrease in autophagic activity (Figures 5A,B,E,F). A comparison of Beclin 1 immunohistochemical sections yielded results consistent with LC3 (Figures 5C,D).

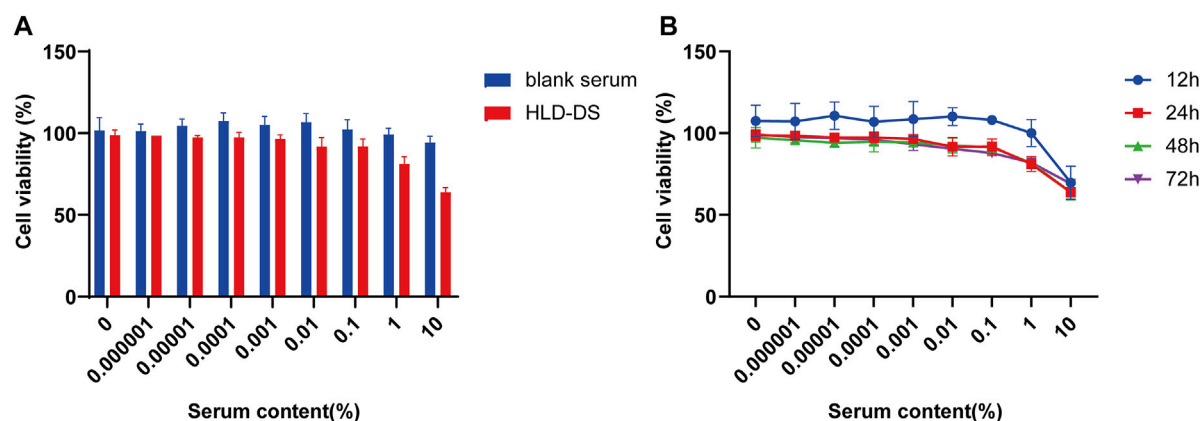


FIGURE 6

HLD-DS CCK-8 experiment. The cytotoxicity of NCM460 cells treated by HLD-DS was investigated by the CCK-8 assay. (A) Effects of serial concentrations of HLD-DS on cell viability. (B) The effect of 1% HLD-DS on cell viability at 12, 24, 48, and 72 h. All data are presented as mean \pm SD. ($n = 6$).

HLD-DS CCK-8 experiment

NCM 460 cells are immortalized cells isolated from normal human tissues and are a common cell model for studying various biological colon functions. As shown in Figure 6, there was no significant difference in cell survival at a concentration of 1% HLD-DS upon exposure for 24 h when compared with the same concentration of blank serum. There was a significant difference in cell viability with up to 10% HLD-DS concentration. Therefore, 1% HLD-DS was chosen as the optimal concentration.

HLD-DS alleviates LPS-induced inflammation in NCM460 cells by inhibiting the NF- κ B pathway and autophagy

ELISA results showed that the inflammatory response was evident after being induced by LPS in the NCM460 cells (Figure 7). Compared to that in the control group, TNF- α , IL-1 β , and IL-6 expressions were elevated in the cell culture medium, and IL-10 expression was significantly reduced when induced by LPS. The difference was statistically significant, suggesting that the cells were modeled successfully. Compared with the LPS group, the levels of TNF- α , IL-1 β and IL-6 were significantly decreased in the LPS + HLD-DS group, and the level of IL-10 was significantly increased. This indicated that HLD-DS could inhibit inflammation in UC significantly. It was also observed that TNF- α , IL-1 β , and IL-6 were significantly decreased, and IL-10 was significantly increased when LPS-induced NCM460 cells were exposed to HLD-DS with 3-MA or PDTC simultaneously. However, RAPA reduced the effect of HLD-DS on reducing TNF- α , IL-1 β , and IL-6 and increasing IL-

10. These results suggested that HLD-DS protected against LPS-induced inflammation in NCM460 cells by inhibiting the NF- κ B pathway and autophagy.

HLD-DS inhibited autophagy induced by LPS in NCM460 cells

Immunofluorescence results showed that LC3 expression was significantly enhanced after induction by LPS in NCM460 cells (Figure 8). Compared with the LPS group, the LC3 level in the LPS+HLD-DS group was significantly decreased, indicating that HLD-DS could significantly inhibit autophagy. When LPS-induced NCM460 cells received HLD-DS and 3-MA or PDTC, LC3 expression was significantly reduced. Conversely, RAPA can increase LC3 expression. These results suggested that HLD-DS could inhibit LPS-induced autophagy in NCM460 cells.

HLD inhibited the NF- κ B pathway and autophagy in LPS-induced NCM460 cells

Western blotting showed that p-NF- κ B p65 expression was significantly higher in the LPS group than that in the control group (Figure 9). Compared to LPS expression, p-NF- κ B p65 expression was significantly reduced in the LPS+HLD-DS and LPS+HLD-DS+PDTC groups. The LPS+HLD-DS+PDTC group was superior to the LPS+HLD-DS group ($p < 0.05$). These results suggest that HLD-DS protects against LPS-induced NCM460 cells by inhibiting the NF- κ B pathway. LC3II/I and Beclin 1 protein expressions were significantly higher in the LPS group than in the control group. Compared to that in the LPS group, LC3II/I and Beclin 1 protein expression in the LPS+HLD-

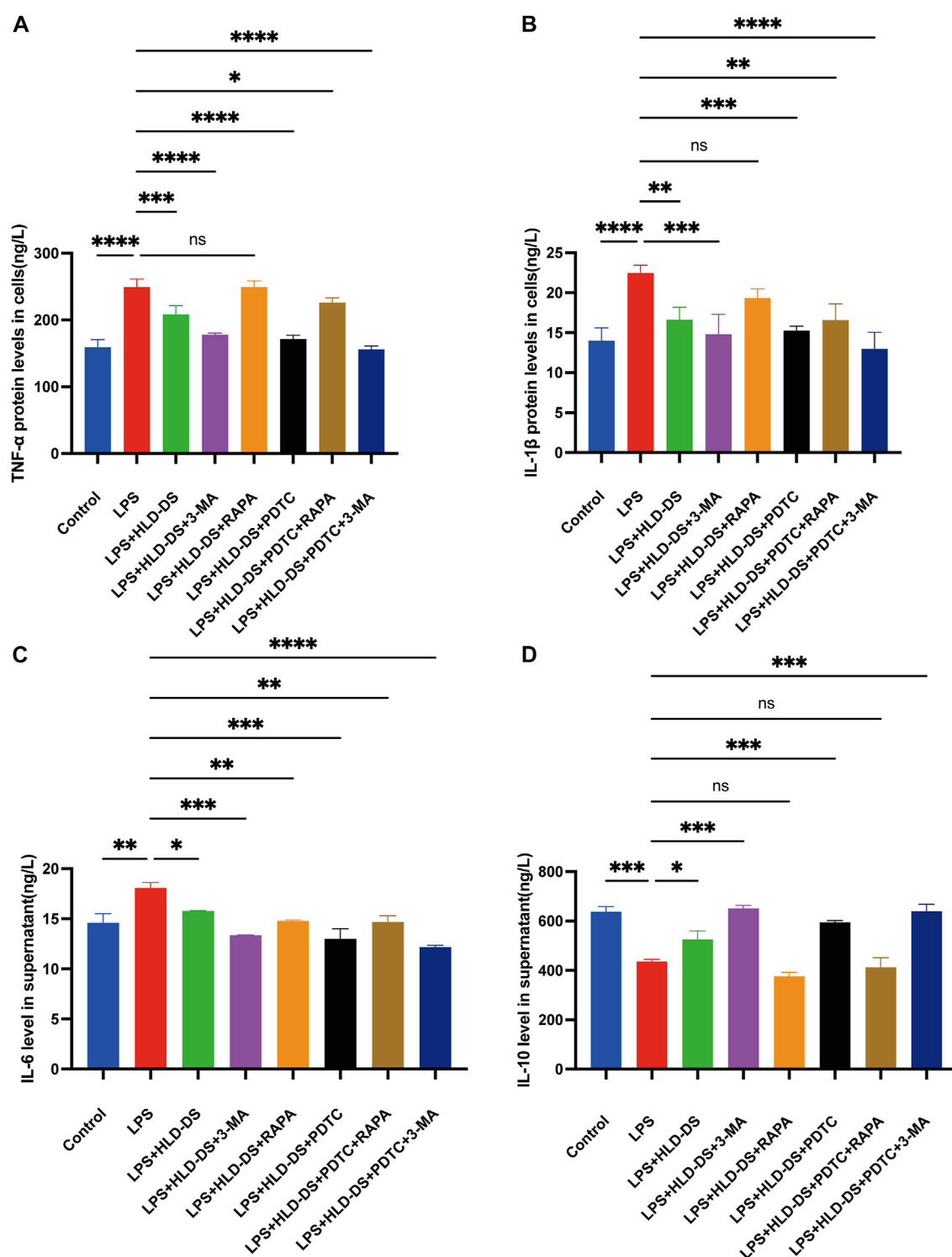


FIGURE 7

HLD alleviated LPS-induced inflammation in NCM460 cells by inhibiting the NF- κ B pathway and autophagy. (A–D) TNF- α , IL-6, IL-1 β , and IL-10 levels in the cell supernatant were detected by Elisa. All data are expressed as the mean \pm SD. ($n = 3$). * $p < 0.05$, ** $p < 0.01$, *** $p < 0.001$, **** $p < 0.0001$.

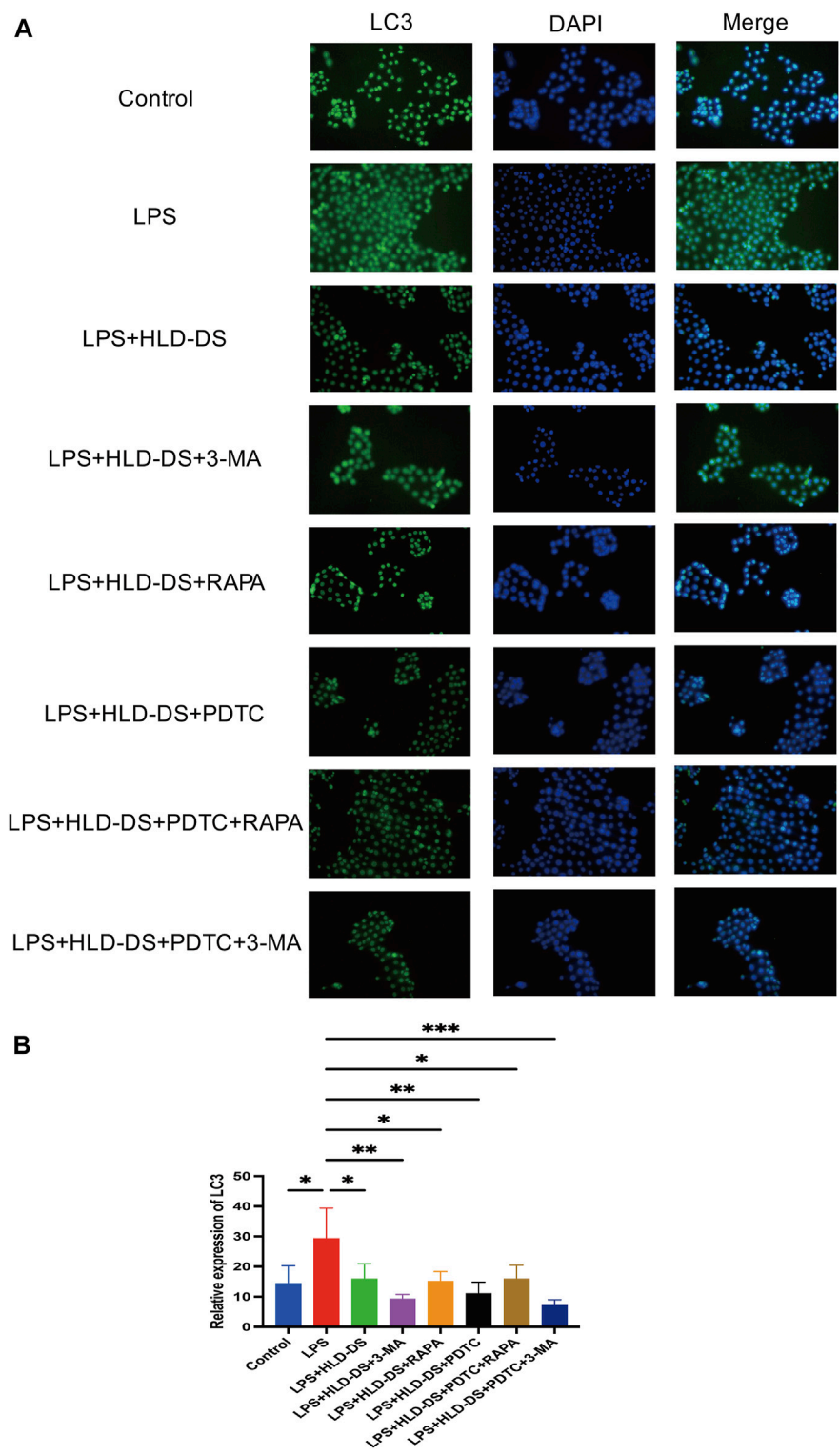


FIGURE 8
HLD-DS inhibited expression of LC3 in cells detected by immunofluorescence. **(A)** LC3 expression was detected by immunofluorescence in LPS-induced NCM-460 cells. **(B)** Quantitative results of LC3 protein expression in LPS-induced NCM460 cells. All data are expressed as the mean \pm SD. ($n = 3$). * $p < 0.05$, ** $p < 0.01$, *** $p < 0.001$.

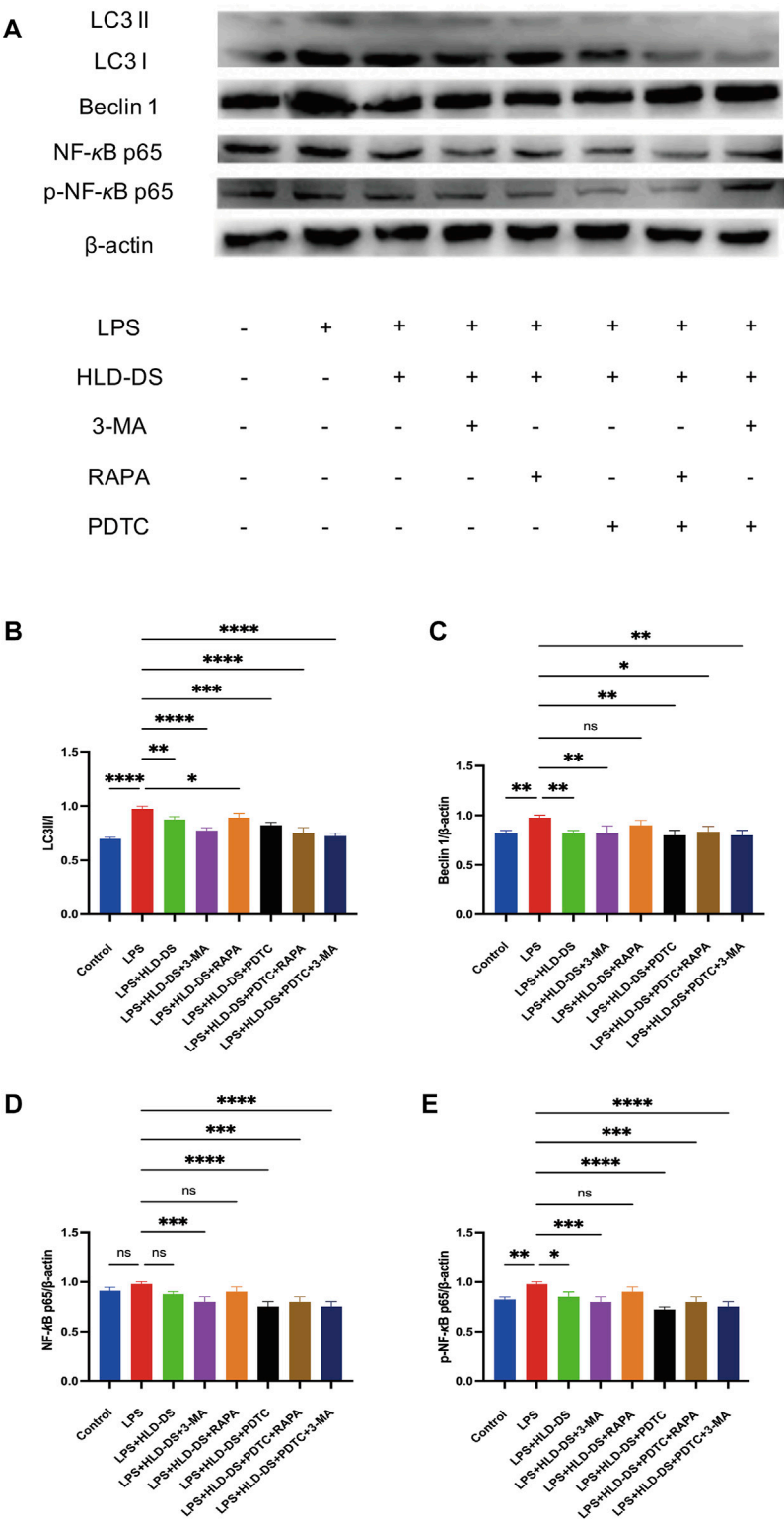


FIGURE 9
HLD-DS affected protein expressions related to the NF-κB pathway and autophagy. **(A)** Western blots of LC3I, LC3II, Beclin 1, NF-κB p65, and p-NF-κB p65 in LPS-induced NCM-460 cells. **(B)** Quantitative results of LC3II/LC3I protein expression in LPS-induced NCM460 cells. **(C)** Quantitative results of Beclin I protein expression in LPS-induced NCM460 cells. **(D,E)** Quantitative results of NF-κB p65 and p-NF-κB p65 protein expression in LPS-induced NCM460 cells. All data are expressed as the mean ± SD. (*n* = 3). **p* < 0.05, ***p* < 0.01, ****p* < 0.001, *****p* < 0.0001.

DS group decreased. The changes in LC3II/I and Beclin 1 protein expression in the LPS+HLD-DS+PDTC group were not apparent after the addition of the NF- κ B pathway inhibitor, PDTC, compared to the LPS+HLD-DS group.

These results suggested that HLD-DS inhibited LPS-induced inflammation in NCM460 cells. The underlying mechanisms were found as the NF- κ B pathway and autophagy. However, there was no obvious crosstalk between the NF- κ B pathway and autophagy.

Discussion

The NF- κ B pathway is essential for IBD development and progression. HLD has been used clinically for several years to treat mild-to-moderate UC with good efficacy. HLD is a traditional Chinese medicine preparation with clinical efficacy for UC treatment. This study verified for the first time that HLD could simultaneously inhibit autophagy and the NF- κ B pathway to alleviate DSS-induced colitis in mice, although with no apparent crosstalk between autophagy and the NF- κ B pathway.

The synergistic effects of multiple components are a characteristic of herbal medicines (Rao et al., 2022; Yu et al., 2022). HLD complexity was demonstrated by characterizing 14 major compounds, including flavonoids, phenols, and alkaloids, using UHPLC-MS/MS. *Abelmoschus manihot* is the main HLD drug. The results showed that it contains a variety of flavonoids such as isoquercitrin, hyperin, myricetin, and quercetin. Recent data have suggested that flavonoids have significant efficacy in UC treatment. Pepper extract consisting of rutin, quercetin, and isoquercitrin attenuated colonic length shortening and pathological injury in a DSS-induced UC model. In addition, ZBE inhibited TNF- α , IL-1 β , and IL-12 by regulating the TLR4 and TLR4-related pathways in mice and LPS-induced cellular inflammation in DSS-induced experimental colitis (Zhang et al., 2016). Flos *Lonicerae* flavonoids (mainly hyperin, lonicerflavone, and luteolin) attenuated TBNS-induced UC by inhibiting the NF- κ B pathway (Liu et al., 2020). Myricetin improved the severity of acute UC, increased IL-10 and TGF- β levels, and increased regulatory T cell proportion (Qu et al., 2020). *Alhagi pseudalhagi* extract containing hyperin, rutin, kaempferol, and isorhamnetin may protect against intestinal inflammation in UC by affecting the TLR 4-dependent NF- κ B signaling pathway (Xu et al., 2021). Therefore, the synergistic effect of multiple components may be responsible for the therapeutic effect of HLD in UC.

This study found that high-dose HLD protected mice colonic tissues with DSS-induced colitis, as evidenced by reduced DAI and colonic histological scores, reduced NF- κ B pathway-related inflammatory cytokines in mouse serum, and reduced NF- κ B p65 levels in colonic tissues. More importantly, increased p-NF- κ B p65 protein expression was observed in the LPS-induced cell models, and HLD-DS treatment reduced p-NF- κ B

p65 expression. These results further confirmed that HLD protects against DSS-induced colitis in mice and LPS-induced inflammation in NCM460 cells by inhibiting the NF- κ B pathway. NF- κ B pathway-related pro-inflammatory cytokines such as TNF- α , IL-1 β , and IL-6 have long been identified as targets for anti-inflammatory strategies in UC. The expression of these pro-inflammatory cytokines was significantly elevated in the DSS-induced mice colitis and was significantly decreased after *Anneslea fragrans* Wall. and SYD interventions, followed by remission of colitis (Deng et al., 2021; Wei et al., 2021). These were consistent with the results of this study. The present study revealed that HLD protects against LPS-induced inflammation in NCM460 cells by inhibiting autophagy. We observed that autophagy-related LC3 and Beclin 1 protein expression was significantly increased *in vitro*; HLD-DS reversed this phenomenon, and the effect was more evident after adding the autophagy inhibitor 3-MA. Proteins LC3 and Beclin 1 were the most commonly used assays in autophagy-related studies (Haq et al., 2019). Herbal prescription Jianpi Qingchang Decoction significantly reduced LC3 and Beclin 1 protein expression and improved colitis in DSS-induced UC mice (Dai et al., 2017).

The regulation of autophagy and the NF- κ B pathway has been demonstrated in malignant tumors, cardiovascular diseases, and bone and joint diseases (Feng et al., 2016; He et al., 2017; Qi et al., 2020; Wang and Gao, 2021). The related roles of autophagy and NF- κ B pathway in HLD anti-UC were explored in this study. However, there revealed no clear regulatory relationship between the NF- κ B pathway and autophagy. NF- κ B transactivates many autophagy-related genes (eg, Beclin 1); thus, NF- κ B-related inflammatory response signaling pathways overlap with those of autophagy. Normally, NF- κ B in the cytoplasm binds to its inhibitor I κ B, and when activated by the I κ B kinase (IKK) complex, the displaced I κ B is degraded by the proteasome. This activated NF- κ B translocated into the nucleus to activate the inflammatory response. However, TGF- β -activating kinase 1 (TAK1) and its cofactors TAB2 and TAB3 were required for IKK activation. Because TAB2/TAB3 could also form a complex with Beclin 1, NF- κ B activation could only result from changes in these balances and occurs concurrently with the autophagic response (Simon et al., 2017). This study confirmed that HLD exerted anti-UC effects by inhibiting autophagy and NF- κ B pathways with non-crosstalk in UC. It was also shown that NF- κ B couldn't be involved in the induction of autophagy in the canonical NF- κ B pathway. It was IKK α activity rather than NF- κ B that controlled the basal expression of the autophagy gene LC3. Starvation induces the expression of LC3, ATG5, and Beclin-1 in an IKK-dependent manner (Comb et al., 2011).

In addition to the classical NF- κ B pathway, the non-classical NF- κ B signaling pathway plays a key role in various

biological functions, including chronic inflammation and tumorigenesis (Sun, 2017). The activation of non-classical NF- κ B signaling is mainly dependent on the abundance of NF- κ B family members p100/p52. The transcription factor p100 inhibited the pathway in the resting state. Upon activation of this pathway, p100 was processed as a precursor to transcriptionally active p52 via the proteasome pathway, which in turn activated the non-classical NF- κ B pathway. p100/p52 was further activated by IKK α activation, and eventually, p52 entered the nucleus leading to inflammatory activation. The substrate receptor p62 in selective autophagy inhibited the non-classical NF- κ B signaling pathway by recognizing the K63 ubiquitinated chain at the N-terminal end of p52/p100, which in turn induced autophagic degradation of p52/p100 (Chen et al., 2020).

A limitation of this study was that there was no evidence of crosstalk between the NF- κ B pathway and autophagy in HLD-relieved UC. Further studies should be conducted to explore the roles and mechanisms of non-canonical NF- κ B pathway genes such as IKK α and p52/p100 and autophagy in HLD treatment of UC.

Conclusion

The study findings suggested that HLD protected against DSS-induced colitis in mice. In addition, HLD protected against LPS-induced inflammation in NCM460 cells by inhibiting autophagy and the NF- κ B pathway. There was no crosstalk between autophagy and the NF- κ B pathway, which may have synergistic anti-inflammatory effects.

Data availability statement

The raw data supporting the conclusion of this article will be made available by the authors, without undue reservation.

References

- Ba, H., Jiang, R., Zhang, M., Yin, B., Wang, J., Li, Z., et al. (2021). Suppression of transmembrane tumor necrosis factor alpha processing by a specific antibody protects against colitis-associated cancer. *Front. Immunol.* 12, 687874. doi:10.3389/fimmu.2021.687874
- Cadwell, K. (2016). Crosstalk between autophagy and inflammatory signalling pathways: balancing defence and homeostasis. *Nat. Rev. Immunol.* 16, 661–675. doi:10.1038/nri.2016.100
- Chen, M., Zhao, Z., Meng, Q., Liang, P., Su, Z., Wu, Y., et al. (2020). TRIM14 promotes noncanonical NF- κ B activation by modulating p100/p52 stability via selective autophagy. *Adv. Sci.* 7, 1901261. doi:10.1002/advs.201901261
- Comb, W. C., Cogswell, P., Sitcheran, R., and Baldwin, A. S. (2011). IKK-dependent, NF- κ B-independent control of autophagic gene expression. *Oncogene* 30, 1727–1732. doi:10.1038/onc.2010.553
- Dai, Y. C., Zheng, L., Zhang, Y. L., Chen, X., Chen, D. L., Wang, L. J., et al. (2017). Jianpi Qingchang decoction regulates intestinal motility of dextran sulfate sodium-

Ethics statement

The animal study was reviewed and approved by Medical Ethics Committee of Suzhou Hospital of TCM.

Author contributions

XC: Investigation, Visualization, Writing-Review, and Editing. JD: Writing- Original draft preparation. QZ, BW, SZ: Software, Formal analysis, Data curation. HW, ZX: Methodology, Validation. JJ: Writing-Review and Editing. XW: Supervision, Writing-Review, and Editing. ZH: Funding acquisition, Project administration, Conceptualization, Writing-Original draft preparation.

Funding

This study was supported by the Natural Science Foundation of Jiangsu Province (Grant No. BK20200212) and Suzhou Science and Technology Program Project (Grant No. SYS2020185).

Conflict of interest

The authors declare that the research was conducted in the absence of any commercial or financial relationships that could be construed as a potential conflict of interest.

Publisher's note

All claims expressed in this article are solely those of the authors and do not necessarily represent those of their affiliated organizations, or those of the publisher, the editors and the reviewers. Any product that may be evaluated in this article, or claim that may be made by its manufacturer, is not guaranteed or endorsed by the publisher.

induced colitis through reducing autophagy of interstitial cells of Cajal. *World J. Gastroenterol.* 23, 4724–4734. doi:10.3748/wjg.v23.i26.4724

Deng, X., Wang, Y., Tian, L., Yang, M., He, S., Liu, Y., et al. (2021). Anneslea fragrans Wall. ameliorates ulcerative colitis via inhibiting NF- κ B and MAPK activation and mediating intestinal barrier integrity. *J. Ethnopharmacol.* 278, 114304. doi:10.1016/j.jep.2021.114304

Feng, Y., Cui, Y., Gao, J. L., Li, M. H., Li, R., Jiang, X. H., et al. (2016). Resveratrol attenuates neuronal autophagy and inflammatory injury by inhibiting the TLR4/NF- κ B signaling pathway in experimental traumatic brain injury. *Int. J. Mol. Med.* 37, 921–930. doi:10.3892/ijmm.2016.2495

Guo, C., Guo, D., Fang, L., Sang, T., Wu, J., Guo, C., et al. (2021). Ganoderma lucidum polysaccharide modulates gut microbiota and immune cell function to inhibit inflammation and tumorigenesis in colon. *Carbohydr. Polym.* 267, 118231. doi:10.1016/j.carbpol.2021.118231

- Haq, S., Grondin, J., Banskota, S., and Khan, W. I. (2019). Autophagy: roles in intestinal mucosal homeostasis and inflammation. *J. Biomed. Sci.* 26, 19. doi:10.1186/s12929-019-0512-2
- He, Z. J., Zhu, F. Y., Li, S. S., Zhong, L., Tan, H. Y., Wang, K., et al. (2017). Inhibiting ROS-NF- κ B-dependent autophagy enhanced brazilin-induced apoptosis in head and neck squamous cell carcinoma. *Food Chem. Toxicol.* 101, 55–66. doi:10.1016/j.fct.2017.01.002
- He, Z., Zhou, Q., Wen, K., Wu, B., Sun, X., Wang, X., et al. (2019). Huangkui Lianchang decoction ameliorates DSS-induced ulcerative colitis in mice by inhibiting the NF- κ B signaling pathway. *Evid. Based. Complement. Altern. Med.* 2019, 1040847. doi:10.1155/2019/1040847
- Lassen, K. G., and Xavier, R. J. (2018). Mechanisms and function of autophagy in intestinal disease. *Autophagy* 14, 216–220. doi:10.1080/15548627.2017.1389358
- Liu, D., Yu, X., Sun, H., Zhang, W., Liu, G., Zhu, L., et al. (2020). Flos Ionicerae flavonoids attenuate experimental ulcerative colitis in rats via suppression of NF- κ B signaling pathway. *Naunyn. Schmiedeberg. Arch. Pharmacol.* 393, 2481–2494. doi:10.1007/s00210-020-01814-4
- Murano, M., Maemura, K., Hirata, I., Toshina, K., Nishikawa, T., Hamamoto, N., et al. (2000). Therapeutic effect of intracolonic administration of nuclear factor κ B (p65) antisense oligonucleotide on mouse dextran sulphate sodium (DSS)-induced colitis. *Clin. Exp. Immunol.* 120, 51–58. doi:10.1046/j.1365-2249.2000.01183.x
- Peng, L., Gao, X., Nie, L., Xie, J., Dai, T., Shi, C., et al. (2020). Astragalus attenuates dextran sulfate sodium (DSS)-induced acute experimental colitis by alleviating gut microbiota dysbiosis and inhibiting NF- κ B activation in mice. *Front. Immunol.* 11, 2058. doi:10.3389/fimmu.2020.02058
- Piao, X., Liu, B., Guo, L., Meng, F., and Gao, L. (2017). Picriside II shows protective functions for severe acute pancreatitis in rats by preventing NF- κ B-dependent autophagy. *Oxid. Med. Cell. Longev.* 2017, 7085709. doi:10.1155/2017/7085709
- Qi, H., Ren, J., Ba, L., Song, C., Zhang, Q., Cao, Y., et al. (2020). MSTN attenuates cardiac hypertrophy through inhibition of excessive cardiac autophagy by blocking AMPK/mTOR and miR-128/PPAR γ /NF- κ B. *Mol. Ther. Nucleic Acids* 19, 507–522. doi:10.1016/j.omtn.2019.12.003
- Qu, X., Li, Q., Song, Y., Xue, A., Liu, Y., Qi, D., et al. (2020). Potential of myricetin to restore the immune balance in dextran sulfate sodium-induced acute murine ulcerative colitis. *J. Pharm. Pharmacol.* 72, 92–100. doi:10.1111/jphp.13197
- Raine, T., Bonovas, S., Burisch, J., Kucharzik, T., Adamina, M., Annesse, V., et al. (2022). ECCO guidelines on therapeutics in ulcerative colitis: medical treatment. *J. Crohns Colitis* 16, 2–17. doi:10.1093/ecco-jcc/jjab178
- Rao, Z., Zeng, J., Li, X., Peng, L., Wang, B., Luan, F., et al. (2022). JFNE-A isolated from Jing-Fang n-butanol extract attenuates lipopolysaccharide-induced acute lung injury by inhibiting oxidative stress and the NF- κ B signaling pathway via promotion of autophagy. *Phytomedicine* 96, 153891. doi:10.1016/j.phymed.2021.153891
- Shang, L., Liu, Y., Li, J., Pan, G., Zhou, F., Yang, S., et al. (2021). Emodin protects sepsis associated damage to the intestinal mucosal barrier through the VDR/Nrf2/HO-1 pathway. *Front. Pharmacol.* 12, 724511. doi:10.3389/fphar.2021.724511
- Simon, H. U., Friis, R., Tait, S. W. G., and Ryan, K. M. (2017). Retrograde signaling from autophagy modulates stress responses. *Sci. Signal.* 10, eaag2791. doi:10.1126/scisignal.aag2791
- Sun, S. C. (2017). The non-canonical NF- κ B pathway in immunity and inflammation. *Nat. Rev. Immunol.* 17, 545–558. doi:10.1038/nri.2017.52
- Trentesaux, C., Fraudeau, M., Pitasi, C. L., Lemarchand, J., Jacques, S., Duche, A., et al. (2020). Essential role for autophagy protein ATG7 in the maintenance of intestinal stem cell integrity. *Proc. Natl. Acad. Sci. U. S. A.* 117, 11136–11146. doi:10.1073/pnas.1917174117
- Turner, D., Ricciotti, A., Lewis, A., D'Amico, F., Dhaliwal, J., Griffiths, A. M., et al. (2021). STRIDE-II: An update on the selecting therapeutic targets in inflammatory bowel disease (STRIDE) initiative of the international organization for the study of IBD (IOIBD): determining therapeutic goals for treat-to-target strategies in IBD. *Gastroenterology* 160, 1570–1583. doi:10.1053/j.gastro.2020.12.031
- Wang, K., Li, Y., Lv, Q., Li, X., Dai, Y., Wei, Z., et al. (2018). Bergenin, acting as an agonist of PPAR γ , ameliorates experimental colitis in mice through improving expression of SIRT1, and therefore inhibiting NF- κ B-Mediated macrophage activation. *Front. Pharmacol.* 8, 981. doi:10.3389/fphar.2017.00981
- Wang, Y., and Gao, W. (2021). Effects of TNF- α on autophagy of rheumatoid arthritis fibroblast-like synoviocytes and regulation of the NF- κ B signaling pathway. *Immunobiology* 226, 152059. doi:10.1016/j.imbio.2021.152059
- Wei, S. C., Sollano, J., Hui, Y. T., Yu, W., Santos Estrella, P. V., Llamado, L. J. Q., et al. (2021). Epidemiology, burden of disease, and unmet needs in the treatment of ulcerative colitis in asia. *Expert Rev. Gastroenterol. Hepatol.* 15, 275–289. doi:10.1080/17474124.2021.1840976
- Wei, Y. Y., Fan, Y. M., Ga, Y., Zhang, Y. N., Han, J. C., Hao, Z. H., et al. (2021). Shaoyao decoction attenuates DSS-induced ulcerative colitis, macrophage and NLRP3 inflammasome activation through the MKP1/NF- κ B pathway. *Phytomedicine* 92, 153743. doi:10.1016/j.phymed.2021.153743
- Wu, Y., Tang, L., Wang, B., Sun, Q., Zhao, P., Li, W., et al. (2019). The role of autophagy in maintaining intestinal mucosal barrier. *J. Cell. Physiol.* 234, 19406–19419. doi:10.1002/jcp.28722
- Xu, X., Zhang, J., Chen, L., Sun, Y., Qing, D., Xin, X., et al. (2021). Alhagi pseudalhagi extract exerts protective effects against intestinal inflammation in ulcerative colitis by affecting TLR4-dependent NF- κ B signaling pathways. *Front. Pharmacol.* 12, 764602. doi:10.3389/fphar.2021.764602
- Yu, W., Wang, G., Lu, C., Liu, C., Jiang, L., Jiang, Z., et al. (2022). Pharmacological mechanism of Shenlingbaizhu formula against experimental colitis. *Phytomedicine* 98, 153961. doi:10.1016/j.phymed.2022.153961
- Zeng, L., Li, K., Wei, H., Hu, J., Jiao, L., Yu, S., et al. (2018). A novel EphA2 inhibitor exerts beneficial effects in PI-IBS in vivo and in vitro models via Nrf2 and NF- κ B signaling pathways. *Front. Pharmacol.* 9, 272. doi:10.3389/fphar.2018.00272
- Zhang, Z., Liu, J., Shen, P., Cao, Y., Lu, X., Gao, X., et al. (2016). Zanthoxylum bungeanum pericarp extract prevents dextran sulfate sodium-induced experimental colitis in mice via the regulation of TLR4 and TLR4-related signaling pathways. *Int. Immunopharmacol.* 41, 127–135. doi:10.1016/j.intimp.2016.10.021
- Zhao, J., Wang, H., Yang, H., Zhou, Y., and Tang, L. (2020). Autophagy induction by rapamycin ameliorates experimental colitis and improves intestinal epithelial barrier function in IL-10 knockout mice. *Int. Immunopharmacol.* 81, 105977. doi:10.1016/j.intimp.2019.105977
- Zhou, K., Cheng, R., Liu, B., Wang, L., Xie, H., Zhang, C., et al. (2018). Eupatilin ameliorates dextran sulphate sodium-induced colitis in mice partly through promoting AMPK activation. *Phytomedicine* 46, 46–56. doi:10.1016/j.phymed.2018.04.033



OPEN ACCESS

EDITED BY
Aftab Ullah,
Jiangsu University, China

REVIEWED BY
Shuntai Chen,
Beijing University of Chinese Medicine,
China
Huanli Xu,
Capital Medical University, China

*CORRESPONDENCE
Jie Li,
qfm2020jieli@yeah.net

[†]These authors have contributed equally
to this work

SPECIALTY SECTION
This article was submitted to
Ethnopharmacology,
a section of the journal
Frontiers in Pharmacology

RECEIVED 24 June 2022
ACCEPTED 22 July 2022
PUBLISHED 25 August 2022

CITATION
Tan Y, Wang H, Xu B, Zhang X, Zhu G,
Ge Y, Lu T, Gao R and Li J (2022),
Chinese herbal medicine combined
with oxaliplatin-based chemotherapy
for advanced gastric cancer: A
systematic review and meta-analysis of
contributions of specific medicinal
materials to tumor response.
Front. Pharmacol. 13:977708.
doi: 10.3389/fphar.2022.977708

COPYRIGHT
© 2022 Tan, Wang, Xu, Zhang, Zhu, Ge,
Lu, Gao and Li. This is an open-access
article distributed under the terms of the
[Creative Commons Attribution License](https://creativecommons.org/licenses/by/4.0/)
(CC BY). The use, distribution or
reproduction in other forums is
permitted, provided the original
author(s) and the copyright owner(s) are
credited and that the original
publication in this journal is cited, in
accordance with accepted academic
practice. No use, distribution or
reproduction is permitted which does
not comply with these terms.

Chinese herbal medicine combined with oxaliplatin-based chemotherapy for advanced gastric cancer: A systematic review and meta-analysis of contributions of specific medicinal materials to tumor response

Ying Tan^{1†}, Heping Wang^{1†}, Bowen Xu^{1,2†}, Xiaoxiao Zhang¹,
Guanghui Zhu^{1,2}, Yuansha Ge^{1,2}, Taicheng Lu^{1,2}, Ruike Gao¹ and
Jie Li^{1*}

¹Department of Oncology, Guang'anmen Hospital, China Academy of Chinese Medical Sciences, Beijing, China, ²Graduate School, Beijing University of Chinese Medicine, Beijing, China

Introduction: The incidence and mortality of gastric cancer ranks among the highest, and the 5-year survival rate of advanced gastric cancer (AGC) is less than 10%. Currently, chemotherapy is the main treatment for AGC, and oxaliplatin is an important part of the commonly used chemotherapy regimen for AGC. A large number of RCTs have shown that Chinese herbal medicine (CHM) combined with oxaliplatin-based chemotherapy can improve objective response rate (ORR) and disease control rate (DCR), reduce the toxic and side effects of chemotherapy. There is currently a lack of systematic evaluation of the evidence to account for the efficacy and safety of CHM combined with oxaliplatin-based chemotherapy in AGC. Therefore, we carried out this study and conducted the sensitivity analysis on the herbal composition to explore the potential anti-tumor efficacy.

Methods: Databases of PubMed, EMBASE, CENTRAL, Web of Science, the Chinese Biomedical Literature Database, the China National Knowledge Infrastructure, the Wanfang database, and the Chinese Scientific Journals Database were searched from their inception to April 2022. RCTs evaluating the efficacy of CHM combined with oxaliplatin-based chemotherapy on AGC were included. Stata 16 was used for data synthesis, RoB 2 for quality evaluation of included RCTs, and GRADE for quality of synthesized evidence. Additional sensitivity analysis was performed to explore the potential anti-tumor effects of single herbs and combination of herbs.

Results: Forty trials involving 3,029 participants were included. Most included RCTs were assessed as "Some concerns" of risk of bias. Meta-analyses showed that compare to oxaliplatin-based chemotherapy alone, that CHM combined

with oxaliplatin-based chemotherapy could increase the objective response rate (ORR) by 35% [risk ratio (RR) = 1.35, 95% confidence intervals (CI) (1.25, 1.45)], and disease control rate (DCR) by 12% [RR = 1.12, 95% CI (1.08, 1.16)]. Subgroup analysis showed that compared to SOX, FOLFOX, and XELOX regimens alone, CHM plus SOX, CHM plus FOLFOX, and CHM plus XELOX could significantly increase the ORR and DCR. Sensitivity analysis identified seven herbs of Astragalus, Liquorice, Poria, Largehead Atractylodes, Chinese Angelica, Codonopsis, and Tangerine Peel with potentials to improve tumor response of oxaliplatin-based chemotherapy in AGC.

Conclusion: Synthesized evidence showed moderate certainty that CHM plus oxaliplatin-based chemotherapy may promote improvement in tumor response in AGC. CHM treatment is safe for AGC. Due to the poor quality of included RCTs and small samplesizes, the quality of synthesized evidence was not high. Specific combinations of herbs appeared to produce higher contributions to ORR than the herb individually. Each of these seven above mentioned herbs has been shown in experimental studies to potentially contribute to the improvement of tumor response. To support this conclusion, these seven herbs are worthy of further clinical research.

Systematic Review Registration: [http://www.crd.york.ac.uk/PROSPERO/display_record.php?RecordID=262595], identifier [CRD42022262595].

KEYWORDS

advanced gastric cancer, Chinese herbal medicine, oxaliplatin, meta-analysis, efficacy, tumor response, synergistic action

1 Introduction

According to Global Cancer Statistics 2020, there were 1,089,000 new cases and 769,000 mortality cases of gastric cancer (GC) globally, ranked second of incidence and mortality rate of all malignant tumors of digestive system (Sung et al., 2021). The number of GC cases in China accounts for 43.9% of the global total. About 50% of GC patients were in advanced stage at the initial diagnosis. Advanced gastric cancer (AGC) has a poor prognosis, with a median overall survival (OS) of 10–12 months (Digkila et al., 2016), and the 5-year survival rate is no more than 10% (Song et al., 2017). AGC generally have distant metastasis and local infiltration, and 50% of recurrent patients were local lymph node positive (Peng et al., 2010). It is reported that the OS of patients with metastatic GC after palliative chemotherapy is only 7–15 months, and the 5-year survival rate is only 2% (Leong, 2005; Ajani et al., 2007). In recent years, the incidence and death of GC are on the rise. Therefore, AGC has become one of the main diseases endangering human life and health (Johnston et al., 2019).

Chemotherapy is the standard first-line treatment for AGC patients, and palliative chemotherapy has a statistically significant advantage over best supportive care in improving survival in AGC patients (Wagner et al., 2006). The NCCN guidelines recommend that combined chemotherapy containing platinum and fluorouracil is preferred for AGC patients (Ajani

et al., 2022). Oxaliplatin is a third-generation platinum-type anticancer drug. Clinical studies have proved that it has a significant inhibitory effect on locally AGC or AGC, and its efficacy is no less than that of cisplatin (Ajani et al., 2016; Smyth et al., 2016; Yoshino et al., 2018). The median progression-free survival (mPFS) of first-line chemotherapy is 4–6 months and median overall survival (mOS) is 10–15 months (Van Cutsem et al., 2006; Cunningham et al., 2008; Koizumi et al., 2008; Kang et al., 2009). Moreover, oxaliplatin is better tolerated than cisplatin and has a better synergistic effect with fluorouracil (Al-Batran et al., 2008). Based on the above advantages, oxaliplatin has become the main platinum drug in AGC chemotherapy, which is used to form SOX, XELOX and FOLFOX regimens. However, peripheral neurotoxicity is the main side effect of oxaliplatin, which incidence of peripheral neurotoxicity is higher than that of cisplatin (63% vs. 22%), especially grade 3 or 4 neuropathy (Al-Batran et al., 2008; Cunningham et al., 2008). The targeted drugs approved for the treatment of AGC are mainly anti-angiogenic drugs, including trastuzumab and ramucirumab. The mOS of trastuzumab in the treatment of AGC patients with positive HER-2 is 7.9 months, but the incidence of anemia and visceral bleeding, two kinds of serious adverse events (AEs), is about 19% (Thuss-Patience et al., 2017). In addition, HER-2 overexpression only accounts for 15%–20% of AGC (Joshi et al., 2021), and the benefit in OS of other drugs is unclear, and the selection of targeted drugs is limited. There is no evidence supporting

survival benefit of immunotherapy alone in patients with AGC (Shitara et al., 2018; Bang et al., 2019; Van Cutsem et al., 2021). Therefore, despite the variety of treatment options for AGC, chemotherapy is still the best choice for AGC, and chemotherapy drugs are constantly updated and iterated. However, obstacles such as serious AEs of chemotherapy, poor quality of life (QoL) and short survival of patients with AGC have not been well solved, and the treatment of AGC is still a major challenge.

CHM has been widely used in east Asia to fight against tumors for a long time. In particular, CHM combined with chemotherapy has advantages of synergistic efficacy and toxicity reduction, improving QoL and enhancing immune function (Cheng et al., 2021). A meta-analysis of 2,670 patients with AGC found that patients with astragalus-containing Chinese medicine combined with platinum-containing chemotherapy had better objective response rate (ORR) [risk ratio (RR) = 1.24, 95% confidence interval (CI): 1.15–1.34] and disease control rate (DCR) (RR = 1.10, 95% CI: 1.06–1.14), the AEs caused by chemotherapy were significantly reduced, and the QoL was significantly improved (Cheng et al., 2021). There was no previous meta-analysis of oxaliplatin-based chemotherapy regimen plus CHM, but some high quality clinical studies have demonstrated the important role of CHM combined with oxaliplatin. Yiqi Huoxue Jiedu formula combined with XELOX regimen could improve DCR (60.78% vs. 41.67%) (Hu, 2011). Shenlian capsules combined with SOX chemotherapy intervention in 157 patients with AGC, the ORR and DCR of the treatment group were 78.1% and 92.7%, respectively, while those of the control group were 66.4% and 79.9%, besides, which significantly reduced the incidence of neurotoxicity and other toxic and side effects (52.2% vs. 94.6%) and prolonged OS about 2.7 months (Diao et al., 2018). The ORR and DCR in the treatment group of Weifu formula combined with FOLFOX6 were significantly improved (ORR, 70.0% vs. 26.7%; DCR, 83.3% vs. 56.7%), and the KPS score was also improved (83.3% vs. 60.0%) (Fan et al., 2015). However, these individual studies are not enough to explain the clinical role of traditional Chinese medicine (TCM) in AGC. Evidence-based medicine should be used to comprehensively analyze existing clinical studies and to evaluate available evidence. Due to the complexity and diversity of Chinese medicine prescriptions, it is impossible to determine which CHM herbs play an important role to synergistic action with chemotherapy.

With the further development of basic research, the role and mechanism of TCM in inhibiting the division and proliferation of tumor cells, promoting the apoptosis of tumor cells, inhibiting the metastasis of tumor cells, and enhancing the curative effect with chemotherapy have been gradually revealed, laying a foundation for the effective application of anti-tumor (Zhou et al., 2016; Liu et al., 2020; Ren et al., 2020; Xiang et al., 2020; Zhang L. et al., 2021). Available experimental studies indicate that TCM compounds do have anti-tumor activity,

but the more appropriate and accurate drug selection is still unknown. Therefore, future research will focus on finding individual herbs with special contributions to chemotherapy efficacy of AGC, and to improve survival benefit of AGC and precise selection of TCM.

There are several RCTs evaluated the efficacy and safety of CHM in AGC, but these clinical evidence were not systematically evaluated. Furthermore, whether CHM have a synergistic effect with oxaliplatin-based chemotherapy, the key component of the first-line treatment of AGC, also need further evaluation. The objective of this study was to systematically evaluate the available evidence of tumor response and safety of CHM combined with oxaliplatin-based chemotherapy in AGC. Furthermore, we performed sensitivity analysis of single herb and combination of herbs, to explore the potential anti-tumor effects of these herbs.

2 Methods

This study was performed by the guidance of the Preferred Reporting Items for Systematic Reviews and Meta-Analyses (PRISMA) statement and checklist (Moher et al., 2009), PRISMA checklist is available in [Supplementary Material S1](#). This study was registered on PROSPERO (No. CRD42022262595).

2.1 Eligibility criteria

2.1.1 Type of studies

This study included RCTs with or without the blinded method, observational studies and quasi-RCTs were excluded. Trials did not describe the randomization process in details were considered as non-RCTs, and were excluded. Animal studies were also excluded.

2.1.2 Types of participants

RCTs which participants diagnosed with AGC through cytological or pathological tests were included.

2.1.3 Types of intervention and control

The intervention of CHM combined with oxaliplatin-based chemotherapy, and control of oxaliplatin-based chemotherapy were included in this study. We only included CHM formulas or oral patented drugs as the treatment of intervention, Chinese medicine injections and plant extracts were excluded.

2.1.4 Types of outcomes

RCTs reporting outcomes of tumor response and safety of CHM in GC treatment were included in this study. Trials reported other efficacy outcomes were excluded. Given the strong correlation between the two anti-tumor treatment

response evaluation criteria, WHO criteria, and RECIST criteria, the outcomes reported by these two criteria were considered homogeneous (Aras et al., 2016).

2.2 Search strategy

We searched PubMed, EMBASE, CENTRAL, Web of Science, the Chinese Biomedical Literature Database (CBM), the China National Knowledge Infrastructure (CNKI), the Wanfang database, and the Chinese Scientific Journals Database (VIP database). Searches were performed from the databases initiation to April 2022. The language restriction was English and Chinese. The search strategy was based on the combination of controlled vocabulary (MeSH terms and Emtree terms) and free-text terms. The terms of “Stomach Neoplasms,” “Oxaliplatin,” “Antineoplastic Combined Chemotherapy Protocols,” “Herbal Medicine,” “Medicine, Chinese Traditional,” and “Drugs, Chinese Herbal” were used to develop the search strategy for PubMed, which is shown in [Supplementary Material S2](#). Modifications to the search strategy were used with other databases.

2.3 Screening and selection

Search results were imported to EndNote 20. The titles and abstracts of retrievals were screened after duplicates removal, then full articles of potential trials were assessed for their eligibility. Screening and selection were independently and in duplicate performed by the review authors (YT and HW). RCTs that met the inclusion criteria were included. The process was summarized using a PRISMA flow diagram.

2.4 Data extraction

The following data were extracted from the included studies: 1) identification information (first author, year of publication); 2) general information (study setting, sample size, and duration of follow-up); 3) participants (clinical stage, age, and sex); 4) intervention details (name of CHM intervention, compositions, and duration); 5) comparison details (chemotherapy regimen, dose, frequency, and duration of treatment), and 6) outcomes details.

2.5 Quality assessment

The Risk of Bias 2 (RoB-2) tool was used to assess the methodological quality of included studies (Sterne et al., 2019). We evaluated included studies of quality of the randomization process, deviation from intended intervention,

missing outcome data, outcome measurement, and selection of the reported result. The overall quality of RCTs were evaluated as low, some concerns or high RoB.

2.6 Evidence synthesis for RCTs

Stata 16 was used in data synthesis to perform a meta-analysis. The RR for dichotomous data with 95% CIs were evaluated. The random-effects model was used when synthesizing data for the meta-analysis. As for the outcomes reported with zero event, the Mantel-Haenszel methods were adopted. We quantified inconsistency by applying the I^2 statistic; a value of $I^2 > 40\%$ was considered important heterogeneity, and $I^2 > 75\%$ was considerable heterogeneity (Higgins et al., 2019). Subgroup analysis were performed according to the different regimens of chemotherapy that patients received, and to explore the source of heterogeneity if substantial heterogeneity existed. Publication bias of the cumulative evidence among individual studies was evaluated using a graphical method of funnel plot (Egger et al., 1997).

2.7 Sensitivity analysis

We performed sensitivity analysis to investigate the potential contributions of specific herbs to tumor response. Previous studies proposed that if a particular herb possessed anti-tumor effects, they would be reflected in the pooled effect estimates of the studies which interventions containing this herb (Chen et al., 2016a; Chen et al., 2016b). Sensitivity analysis of ORR will be performed for studies on herbs used in AGC, herbs, or combinations of herbs presented in two or more studies, and the following principles will be applied:

- 1) Studies containing the same herb or combination of herbs will be treated as one, and the pooled RR (95% CI) and I^2 will be calculated;
- 2) herbs or combinations of herbs will be excluded if there is no significant effect in the pooled results (95% CIs of RR overlap 1.0) and/or important heterogeneity exists between studies ($I^2 \geq 40\%$);
- 3) the RR results will be listed in ascending order with 95% CI, the number of studies and I^2 values;
- 4) the combination of herbs will be excluded when they have lower RRs than herbs alone;
- and 5) when herb combinations have higher RRs than herbs alone, they will be identified as potential examples of synergistic effects.

2.8 Quality of evidence

The quality of the cumulative evidence was evaluated using the Grading of Recommendations Assessment,

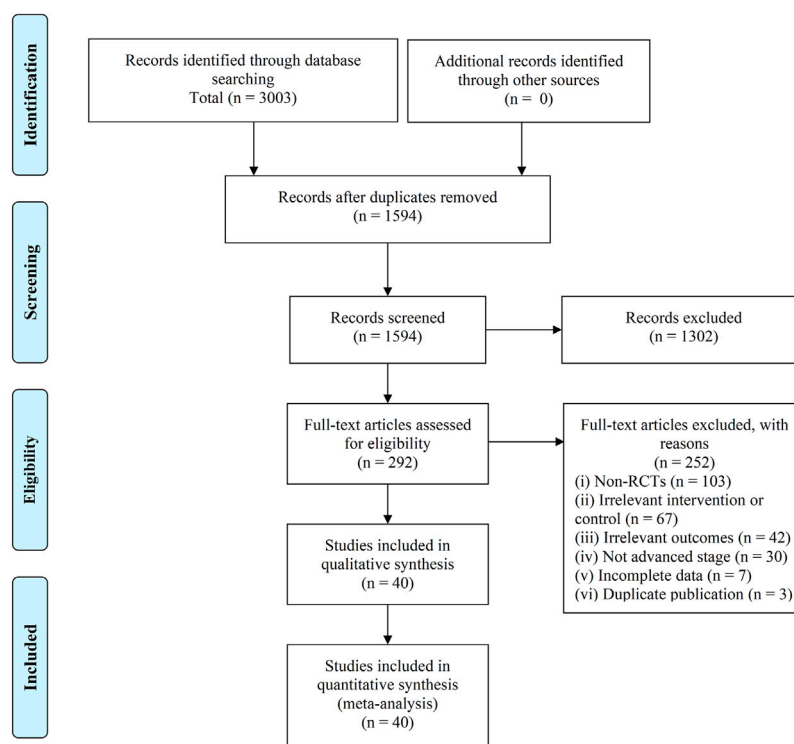


FIGURE 1
Flowchart of records screening and selection.

Development, and Evaluation (GRADE) system. Study limitations, inconsistency, indirectness, imprecision, and publication bias were evaluated. Quality of evidence was classified as high, moderate, low, or very low quality (Guyatt et al., 2008). We presented our findings in a Summary of Finding table.

3 Results

There were 3,003 retrievals exported from databases searches, and after the selection process, 40 trials involving 3,029 participants were included in this SR (Chen et al., 2007; Chi et al., 2010; Hu, 2011; Yuan, 2011; Zhao, 2011; Zhu et al., 2011; Qin, 2012; Guo, 2014; Huang, 2014; Liu et al., 2015; Li et al., 2016; Zhao et al., 2016; Chu et al., 2017; Feng, 2017; Huang et al., 2017; Wang N. et al., 2018; Yang et al., 2018; Yuan, 2018; Cai et al., 2019; Gu et al., 2019; Jiao, 2019; Liu et al., 2019; Xie, 2019; Yu et al., 2019; Zhai, 2019; Zhang, 2019; Zhong et al., 2019; Bao, 2020; Gong, 2020; Li D. H. et al., 2020; Sun et al., 2020; Zhang et al., 2020; Zhang, 2021a; Zhang, 2021b; Feng et al., 2021; Jiang et al., 2021; Long, 2021; Zhang H. O. et al., 2021; Zhao, 2021; Zhong et al., 2021). The selection process was summarized as a flowchart shown in Figure 1.

3.1 Details of included trials

All these 40 trials are non-blinded RCTs that conducted in single-center. The sample sizes of included trials ranged from 50 to 124. Among these included trials, one published in an English journal (Li Y. et al., 2020), and other 39 trials were published in Chinese (Chen et al., 2007; Chi et al., 2010; Hu, 2011; Yuan, 2011; Zhao, 2011; Zhu et al., 2011; Qin, 2012; Guo, 2014; Huang, 2014; Liu et al., 2015; Li et al., 2016; Zhao et al., 2016; Chu et al., 2017; Feng, 2017; Huang et al., 2017; Wang Y. et al., 2018; Yang et al., 2018; Yuan, 2018; Cai et al., 2019; Gu et al., 2019; Jiao, 2019; Liu et al., 2019; Xie, 2019; Yu et al., 2019; Zhai, 2019; Zhang, 2019; Zhong et al., 2019; Bao, 2020; Gong, 2020; Sun et al., 2020; Zhang et al., 2020; Zhang, 2021a; Zhang, 2021b; Feng et al., 2021; Jiang et al., 2021; Long, 2021; Zhang L. et al., 2021; Zhao, 2021; Zhong et al., 2021). The characteristics of included RCTs were shown in Table 1.

3.1.1 Intervention details

Among these 40 trials, three trials adopted TCM syndrome differentiation treatment, and patients in these three trials received more than one core prescription, other 37 trials used single formula as core prescription. As for the chemotherapy, SOX was the most frequent regimen that adopted by 16 trials

TABLE 1 Study characteristics of included RCTs.

Study	Study Design	Sample Size		Age		Sex (Male/Female)		Stage		Outcomes
		T	C	T	C	T	C	T	C	
Bao (2020)	Single center	34	34	44–86 (66.42 ± 7.48)	45–87 (65.73 ± 7.21)	21/13	22/12	III-IV	III-IV	①②③
Cai et al. (2019)	Single center	60	60	42–74 (61.5 ± 7.9)	41–73 (61.2 ± 7.6)	35/25	38/22	III-IV	III-IV	①②③
Chen et al. (2007)	Single center	27	23	34–78 (median: 58)		32/18		IV	IV	①③
Chi et al. (2010)	Single center	30	30	40–70 (median: 57)		38/22		IV	IV	①②③
Chu et al. (2017)	Single center	30	30	42–68 (56.3 ± 4.2)	40–75 (55.6 ± 4.5)	20/10	22/8	IIIb-IV	IIIb-IV	①②③
Feng et al. (2021)	Single center	41	41	35–67 (52.29 ± 4.71)	34–69 (53.84 ± 4.91)	23/18	21/20	III-IV	III-IV	①③
Feng (2017)	Single center	30	30	>60: 19, ≤60: 11	>60: 21, ≤60: 9	18/12	22/8	III-IV	III-IV	①②③
Gong (2020)	Single center	32	32	66.08 ± 9.52	(65.56 ± 7.65	19/13	17/15	III-IV	III-IV	①③
Gu et al. (2019)	Single center	35	35	27–76 (48.3 ± 5.2)	28–77 (47.5 ± 4.8)	19/16	21/14	III-IV	III-IV	①
Guo (2014)	Single center	30	30	57.10 ± 6.65	56.26 ± 7.51	22/8	21/9	IIIb-IV	IIIb-IV	①②③
Hu et al. (2012)	Single center	51	48	35–74 (57.65 ± 9.42)	32–75 (59.09 ± 10.62)	35/16	34/14	IV	IV	①②③
Huang et al. (2017)	Single center	34	34	41–70 (57.9 ± 61.2)	40–69 (58.9 ± 6.6)	19/15	20/14	III-IV	III-IV	①②③
Huang (2014)	Single center	32	32	55.13 ± 10.676	53.97 ± 10.304	17/15	16/16	IV	IV	①②③
Jiang et al. (2021)	Single center	51	51	55.78 ± 6.85	55.92 ± 6.49	32/19	30/21	III-IV	III-IV	①③
Jiao (2019)	Single center	52	52	32–68 (54.23 ± 8.67)	33–70 (56.32 ± 8.40)	27/25	29/23	IV	IV	①
Li et al. (2016)	Single center	34	34	46.35 ± 6.21	46.97 ± 6.31	20/14	22/12	T3-T4	T3-T4	①②③
Li D. H. et al. (2020)	Single center	29	28	45–73 (57.36 ± 8.87)	44–75 (58.25 ± 9.64)	17/12	16/12	IIIb-IV	IIIb-IV	①②③
Liu et al. (2015)	Single center	62	62	61.8 ± 11.6	60.5 ± 10.8	43/19	46/16	IIIb-IV	IIIb-IV	①②③
Liu et al. (2019)	Single center	48	48	54.37 ± 8.10	55.09 ± 8.05	26/22	25/23	IV	IV	①②③
Long (2021)	Single center	32	32	59.03 ± 8.32	57.81 ± 7.49	23/19	20/12	IV	IV	②③
Qin (2012)	Single center	27	26	59.04 ± 8.716	57.73 ± 10.724	19/8	20/6	III-IV	III-IV	①②③
Sun et al. (2020)	Single center	40	40	35–74 (63.1 ± 8.6)	32–75 (2.7 ± 8.9)	27/13	26/14	III-IV	III-IV	①②③
Wang N. et al. (2018)	Single center	60	60	55–78 (64.16 ± 1.17)	61–79 (68/58 ± 1.25)	34/26	31/29	III-IV	III-IV	①②③
Xie (2019)	Single center	33	31	62.73 ± 8.769	59.52 ± 9.095	18/15	15/10	III-IV	III-IV	①②③
Yang et al. (2018)	Single center	40	40	59.41 ± 13.59	59.41 ± 13.59	21/19	23/17	III-IV	III-IV	①②③
Yu et al. (2019)	Single center	41	41	42–78 (55.17 ± 5.86)	43–79 (56.30 ± 6.28)	23/18	25/16	IIIb-IV	IIIb-IV	①②③
Yuan (2011)	Single center	26	25	18–75	18–75	18/8	20/5	IV	IV	①②③
Yuan (2018)	Single center	30	30	58.93 ± 7.056	61.43 ± 7.142	23/7	20/10	IIIb-IV	IIIb-IV	①②③
Zhai (2019)	Single center	32	32	18–70	18–70	24/8	20/12	IIIb	IIIb	①②③
Zhang H. O. et al. (2021)	Single center	30	30	66.66 ± 5.912	67.21 ± 6.425	21/9	21/9	IIIb-IV	IIIb-IV	①②③
Zhang H. O. et al. (2021)	Single center	30	30	62.16 ± 9.53	64.30 ± 8.92	13/17	11/19	III-IV	III-IV	①②③
Zhang L. et al. (2021)	Single center	28	27	65.57 ± 6.06	66.56 ± 5.57	20/8	18/9	IIIb-IV	IIIb-IV	①②③
Zhang et al. (2020)	Single center	43	43	33–80 (50.41 ± 8.16)	35–78 (49.06 ± 7.34)	24/19	26/17	III-IV	III-IV	①③
Zhang (2019)	Single center	50	50	65.24 ± 5.27	68.46 ± 5.94	30/16	26/11	III-IV	III-IV	①②③
Zhao (2011)	Single center	30	24	57.60 ± 11.34	57.47 ± 12.06	19/11	11/7	IIIb-IV	IIIb-IV	①②③
Zhao et al. (2016)	Single center	39	39	38–70 (57.03 ± 9.47)	41–69 (58.31 ± 10.23)	28/11	26/13	III-IV	III-IV	①②③
Zhao (2021)	Single center	49	49	48–77 (57.21 ± 4.58)	47–76 (56.87 ± 4.62)	26/23	25/24	IIIb-IV	IIIb-IV	①③
Zhong et al. (2021)	Single center	41	41	36.70 (58.8 ± 9.2)	35.70 (58.3 ± 9.5)	24/17	22/19	IIIb-IV	IIIb-IV	①③
Zhong et al. (2019)	Single center	41	41	33–76 (54.86 ± 3.77)	32–78 (55.04 ± 3.14)	22/19	20/21	IV	IV	①②③
Zhu et al. (2011)	Single center	40	40	35–86 (54.5 ± 4.5)		51/29		III-IV	III-IV	①②

T Treatment group, C Control group.
Outcomes: ①Tumor Response, ②Quality of Life, ③Adverse Events.

TABLE 2 Intervention details of included RCTs.

Study	Treatment in intervention group	Treatment in intervention group
Bao (2020)	Yiqi Huoxue Formula combined with SOX regimen chemotherapy. Formula composition: Acraginuous turmeric, Chinese angelica, Finger citron, Villous amomum, Sanchi, Codonopsis, Astragalus	SOX regimen for 4 cycles: S-1 Capsules 40 mg, twice daily, taking it for 14 days, stopping for 7 days; Oxaliplatin injection 130 mg/m ² intra venous drip for 3 h on day 1, one cycle for 21 days
Cai et al. (2019)	Jianpi Yiqi Formula combined with XELOX regimen chemotherapy. Formula composition: Codonopsis, Poria, Largehead atractylodes, Perilla frutescens leaf, Coxi seed, Pinellia, Inula, Ruddle, Villous amomum, Liquorice	XELOX regimen for 3 cycles: Capetabine 1,000 mg/m ² , twice daily, taking it for 14 days, stopping for 7 days; Oxaliplatin injection 130 mg/m ² intra venous drip on day 1, one cycle for 21 days
Chen et al. (2007)	TCM syndrome differentiation treatment combined with FOLFOX regimen chemotherapy	FOLFOX regimen chemotherapy: Oxaliplatin injection 130 mg/m ² intra venous drip on day 1; CF 200 mg intra venous drip on day 1–3; 5-Fu 400 mg/m ² on day 1, and a infusion (2,000 mg/m ²) for 70 consecutive hours, one cycle for 21 days
Chi et al. (2010)	Yiqi Huoxue Formula combined with FOLFOX regimen chemotherapy. Formula composition: Astragalus, Pseudostellaria, Suberect spatholobus, Largehead atractylodes, Poria, Wolfberry, Ligustrum, Cuscuta, Red paeony, Coxi seed, Actinidia root	FOLFOX4 regimen chemotherapy: Oxaliplatin injection 85 mg/m ² intra venous drip on day 1; CF 200 mg/m ² intra venous drip on day 1–2; 5-Fu 400 mg/m ² on day 1–2, and a 20-h infusion (600 mg/m ² /d) for 2 consecutive days, one cycle for 21 days
Chu et al. (2017)	Zhangshi Yiwei Decoction combined with FOLFOX regimen chemotherapy. Formula composition: Largehead atractylodes, Poria, Codonopsis, Coptis, Tangerine peel, Thunberg fritillary, Aucklandia, Pinellia, Villous amomum, Dandelion, Silktree bark, Bletilla, Liquorice	FOLFOX4 regimen chemotherapy: Oxaliplatin injection 130 mg/m ² intra venous drip on day 1; CF 100 mg/m ² intra venous drip on day 1–5; 5-Fu 300 mg/m ² on day 1–5, one cycle for 21 days
Feng et al. (2021)	Xuezheng Decoction combined with XELOX regimen chemotherapy. Formula composition: Acraginuous turmeric, Hedyotis diffusa, Smilax, Chinese angelica, Red paeony, Sparganii, Cassia twig, Frankincense, Myrrh	XELOX regimen for 2 cycles: Capetabine 1,000 mg/m ² , twice daily, once after breakfast and dinner respectively, taking it for 14 days, stopping for 7 days; Oxaliplatin injection 85 mg/m ² intra venous drip on day 1, one cycle for 21 days
Feng (2017)	Gancao Xiexin Decoction combined with SOX regimen chemotherapy. Formula composition: Liquorice, Scutellaria, Coptis, Pinellia, Dried ginger, Ginseng, Red date	SOX regimen: S-1 Capsules 40–60 mg, twice daily, once after breakfast and dinner respectively, taking it for 14 days, stopping for 7 days; Oxaliplatin injection 130 mg/m ² intra venous drip for 3 h on day 1, one cycle for 21 days
Gong (2020)	Wenyang Sanjie Decoction combined with SOX regimen chemotherapy. Formula composition: Astragalus, Yam, Chinese clematis, Coxi seed, Scutellaria barbata, White paeony, Ruddle, Largehead atractylodes, Psoralea, Cuscuta, Barley sprout, Dandelion, Wolfberry, Acraginuous turmeric, Membrane of chickens gizzard, Inula, Pinellia, Gekko, Cassia twig, Tangerine peel, Dried ginger	SOX regimen: S-1 Capsules 40–60 mg, twice daily, once after breakfast and dinner respectively, taking it for 14 days, stopping for 7 days; Oxaliplatin injection 130 mg/m ² intra venous drip for 3 h on day 1, one cycle for 21 days
Gu et al. (2019)	Jianwei Yiai Powder combined with FOLFOX regimen chemotherapy. Formula composition: Nightshade, Vietnamese sophora root, Scutellaria barbata, Hedyotis diffusa, Scolopendra, Pinellia, Arcae concha, Aucklandia, Poria, Suberect spatholobus, Codonopsis, Largehead atractylodes, Liquorice	FOLFOX4 regimen chemotherapy: Oxaliplatin injection 85 mg/m ² intra venous drip on day 1; CF 200 mg/m ² intra venous drip on day 1–2; 5-Fu 400 mg/m ² on day 1, and a 22-h infusion (600 mg/m ² /d) for 2 consecutive days, one cycle for 21 days
Guo (2014)	Wenyang Sanjie Decoction combined with SOX regimen chemotherapy. Formula composition: Codonopsis, Astragalus, Largehead atractylodes, Poria, Ligustrum, Pinellia, Hedyotis diffusa, Cremastra, Tangerine peel, Actinidia root, Membrane of chickens gizzard, Liquorice	SOX regimen: S-1 Capsules 40 mg, twice daily, once after breakfast and dinner respectively, taking it for 14 days, stopping for 7 days; Oxaliplatin injection 130 mg/m ² intra venous drip for 3 h on day 1, one cycle for 21 days
Hu (2011)	Yiqi Huoxue Jiedu Formula combined with XELOX regimen chemotherapy. Formula composition: Astragalus, Codonopsis, Pseudostellaria, Largehead atractylodes, Poria, Wolfberry, Ligustrum Cuscuta, Suberect spatholobus, Red paeony, Acraginuous turmeric, Paris polyphylla, Hedyotis diffusa, Actinidia root	XELOX regimen for 3 cycles: Capetabine 1,000 mg/m ² , twice daily, once after breakfast and dinner respectively, taking it for 14 days, stopping for 7 days; Oxaliplatin injection 85 mg/m ² intra venous drip on day 1, one cycle for 21 days
Huang (2017)	Jianpi Yangwei Formula combined with FOLFOX4 regimen chemotherapy. Formula composition: Hedyotis chrysotricha, Smilax, Coxi seed, Yam, Codonopsis, Largehead atractylodes, Poria, Aucklandia, Chinese angelica, White paeony, Liquorice	FOLFOX4 regimen chemotherapy: Oxaliplatin injection 85 mg/m ² intra venous drip on day 1; CF 200 mg/m ² intra venous drip on day 1–2; 5-Fu 400 mg/m ² on day 1, and a 22-h infusion (600 mg/m ² /d) for 2 consecutive days, one cycle for 21 days
Huang (2014)	Jianpi Huayu Decoction combined with FOLFOX4 regimen chemotherapy. Formula composition: Codonopsis, Largehead atractylodes, Dandelion, Perilla frutescens stem, Nardostachys, Snakegourd seed, Pinellia, Gekko, Acraginuous turmeric, Crataegi, Rhei, Magnolia bark, Membrane of chickens gizzard	FOLFOX4 regimen chemotherapy: Oxaliplatin injection 85 mg/m ² intra venous drip on day 1; CF 200 mg/m ² intra venous drip on day 1–2; 5-Fu 400 mg/m ² on day 1, and a 22-h infusion (600 mg/m ² /d) for 2 consecutive days, one cycle for 21 days
Jiang et al. (2021)	Jiedu Sanjie Formula combined with SOX regimen chemotherapy. Formula composition: Dandelion, Prunella, Honeysuckle, Forsythia, Chinese angelica, Figwort, Isatis, Stiff silkworm, Myrrh, Scorpion, Gleditsia sinensis	SOX regimen: S-1 Capsules 40–60 mg, twice daily, taking it for 14 days, stopping for 7 days; Oxaliplatin injection 130 mg/m ² intra venous drip for 3 h on day 1, one cycle for 21 days
Jiao (2019)	Modified Xuezheng Decoction combined with FOLFOX4 regimen chemotherapy. Formula composition: Sparganii, Acraginuous turmeric, Hedyotis diffusa, Smilax, Chinese angelica, Red paeony, Frankincense, Myrrh, Cassia twig	FOLFOX4 regimen chemotherapy: Oxaliplatin injection 85 mg/m ² intra venous drip on day 1; CF 200 mg/m ² intra venous drip on day 1–2; 5-Fu 400 mg/m ² on day 1, and a 22-h infusion (600 mg/m ² /d) for 2 consecutive days, one cycle for 21 days

(Continued on following page)

TABLE 2 (Continued) Intervention details of included RCTs.

Study	Treatment in intervention group	Treatment in intervention group
Li (2016)	Fuzheng Kangai Formula combined with FOLFOX4 regimen chemotherapy. Formula composition: Largehead atractylodes, Morinda, Wolfberry, Drynaria Rehmannia glutinosa, Epimedium, Cornus, Ginseng, Eucommia, Psoralea, Cassia bark, Chinese angelica, Curculigo	FOLFOX4 regimen chemotherapy: Oxaliplatin injection 85 mg/m ² intra venous drip on day 1; CF 200 mg/m ² intra venous drip on day 1–2; 5-Fu 400 mg/m ² on day 1, and a 22-h infusion (600 mg/m ² /d) for 2 consecutive days, one cycle for 21 days
Li Y. et al. (2020)	Shunqi Yiwei Decoction combined with SOX regimen chemotherapy. Formula composition: Bupleurum, Aurantii fructus, White paeony, Liquorice, Poria, Atractylodis, Codonopsis	SOX regimen: S-1 Capsules 40 mg, twice daily, once after breakfast and dinner respectively, taking it for 14 days, stopping for 7 days; Oxaliplatin injection 130 mg/m ² intra venous drip for 3 h on day 1, one cycle for 21 days
Liu et al. (2015)	Jianpi Xiaozheng Formula combined with SOX regimen chemotherapy. Formula composition: Astragalus, Smilax, Hedyotis chrysotricha, Coxi seed, Codonopsis, Poria, Yam, Sparganii, Acraginuous turmeric, Largehead atractylodes, Aucklandia, Tangerine peel, Chinese angelica, White paeony	SOX regimen: S-1 Capsules 40–60 mg, twice daily, taking it for 14 days, stopping for 7 days; Oxaliplatin injection 130 mg/m ² intra venous drip for 3 h on day 1, one cycle for 21 days
Liu et al. (2019)	Jianpi Huayu Formula combined with FOLFOX4 regimen chemotherapy. Formula composition: Largehead atractylodes, Dandelion, Perilla frutescens stem, Nardostachys, Snakegourd seed, Pinellia, Gekko, Acraginuous turmeric, Crataegi, Rhei, Magnolia bark, Membrane of chickens gizzard	FOLFOX4 regimen chemotherapy: Oxaliplatin injection 85 mg/m ² intra venous drip on day 1; CF 200 mg/m ² intra venous drip on day 1–2; 5-Fu 400 mg/m ² on day 1, and a 22-h infusion (600 mg/m ² /d) for 2 consecutive days, one cycle for 21 days
Long (2021)	Yiqi Fuyuan Formula combined with mFOLFOX6 regimen chemotherapy. Formula composition: Astragalus, Codonopsis, Largehead atractylodes, Aucklandia, Tangerine peel, Poria, Chinese angelica, Spine date seed, Yam, Raw ginger, Lotus seed, Liquorice	mFOLFOX6 regimen chemotherapy: Oxaliplatin injection 85 mg/m ² intra venous drip on day 1; CF 400 mg/m ² intra venous drip on day 1; 5-Fu 400 mg/m ² on day 1, and a infusion (2,400 mg/m ²) for 46 consecutive hours, one cycle for 21 days
Qin (2012)	Modified Buzhong Yiqi Decoction combined with SOX regimen chemotherapy. Formula composition: Astragalus, Codonopsis, Largehead atractylodes, Liquorice, Chinese angelica, Sichuan lovase, Tangerine peel, Acraginuous turmeric, Hedyotis diffusa, Coxi seed	SOX regimen: S-1 Capsules 80 mg, twice daily, taking it for 14 days, stopping for 7 days; Oxaliplatin injection 130 mg/m ² intra venous drip for 3 h on day 1, one cycle for 21 days
Sun et al. (2020)	Fuzheng Kangai Formula combined with FOLFOX6 regimen chemotherapy. Formula composition: Codonopsis, Largehead atractylodes, Bupleurum, White paeony, Poria, Tangerine peel, Pinellia, Sichuan lovase, Aurantii fructus, Ligustrum, Ganoderma, Barley sprout, Millet sprout, Paris polyphylla, Scutellaria barbata, Hedyotis diffusa, Liquorice	FOLFOX6 regimen chemotherapy: Oxaliplatin injection 85 mg/m ² intra venous drip on day 1; CF 400 mg/m ² intra venous drip on day 1; 5-Fu 400 mg/m ² on day 1, and a infusion (2,400 mg/m ²) for 46 consecutive hours, one cycle for 21 days
Wang Y. et al. (2018)	Guishao Liu junzi Decoction combined with SOX regimen chemotherapy. Formula composition: Chinese angelica, White paeony, Codonopsis, Poria, Largehead atractylodes, Yam, Coxi seed, Tangerine peel, Pinellia, Hedyotis diffusa, Scutellaria barbata, Sparganii, Acraginuous turmeric, Liquorice	SOX regimen: S-1 Capsules 50 mg, twice daily, taking it for 14 days, stopping for 7 days; Oxaliplatin injection 130 mg/m ² intra venous drip on day 1, one cycle for 21 days
Xie (2019)	Wendan Decoction combined with XELOX regimen chemotherapy. Formula composition: Pinellia, Bambusae caulis, Aurantii fructus Immaturus, Tangerine peel, Poria, Liquorice, Raw ginger, Red date	XELOX regimen for 3 cycles: Capetabine 1,000 mg/m ² , twice daily, once after breakfast and dinner respectively, taking it for 14 days, stopping for 7 days; Oxaliplatin injection 85 mg/m ² intra venous drip on day 1, one cycle for 21 days
Yang et al. (2018)	Shenyu Yangwei Decoction combined with XELOX regimen chemotherapy. Formula composition: Ginseng, Cornus, Dendrobium, Salviae	XELOX regimen for 2 cycles: Capetabine 1,000 mg/m ² , twice daily, once after breakfast and dinner respectively, taking it for 14 days, stopping for 7 days; Oxaliplatin injection 130 mg/m ² intra venous drip on day 1, one cycle for 21 days
Yu et al. (2019)	Modified Shengyang Yiwei Decoction combined with XELOX regimen chemotherapy. Formula composition: Ginseng, Cornus, Dendrobium, Salviae	XELOX regimen for 2 cycles: Capetabine 1,000 mg/m ² , twice daily, once after breakfast and dinner respectively, taking it for 14 days, stopping for 7 days; Oxaliplatin injection 130 mg/m ² intra venous drip on day 1, one cycle for 21 days
Yuan (2011)	Modified Shengyang Yiwei Decoction combined with XELOX regimen chemotherapy. Formula composition: Codonopsis, Largehead atractylodes, Poria, Coxi seed, Pinellia, Tangerine peel, Agaric Yam, Millet sprout, Barley sprout, Poria with hostwood, Loquat leaf, Liquorice	XELOX regimen for 2 cycles: Capetabine 1,000 mg/m ² , twice daily, once after breakfast and dinner respectively, taking it for 14 days, stopping for 7 days; Oxaliplatin injection 130 mg/m ² intra venous drip for 2 h on day 1, one cycle for 21 days
Yuan (2018)	Yiqi Jiedu Formula combined with SOX regimen chemotherapy. Formula composition: Ginseng, Gekko, Paris polyphylla, Pinellia, Tangerine peel, Magnolia bark, Liquorice	SOX regimen: S-1 Capsules 40 mg, twice daily, taking it for 14 days, stopping for 7 days; Oxaliplatin injection 130 mg/m ² intra venous drip on day 1, one cycle for 21 days
Zhai (2019)	Huayu Jiedu Formula combined with SOX regimen chemotherapy. Formula composition: Scorpion, Gekko, Sanchi, Nitroum, Scutellaria barbata, Membrane of chickens gizzard	SOX regimen: S-1 Capsules 40–60 mg, twice daily, once after breakfast and dinner respectively, taking it for 14 days, stopping for 7 days; Oxaliplatin injection 130 mg/m ² intra venous drip for 3 h on day 1, one cycle for 21 days
Zhang (2021a)	Modified Shiquan Dabu Decoction combined with XELOX regimen chemotherapy. Formula composition: Astragalus, Coxi seed, Largehead atractylodes, Poria, Chinese angelica, Pinellia, White paeony, Rehmannia glutinosa, Sparganii, Acraginuous turmeric, Sichuan lovase, Ginseng, Cassia bark, Villous amomum, Liquorice	XELOX regimen: Capetabine 1,000 mg/m ² , twice daily, once after breakfast and dinner respectively, taking it for 14 days, stopping for 7 days; Oxaliplatin injection 130 mg/m ² intra venous drip for 2 h on day 1, one cycle for 21 days

(Continued on following page)

TABLE 2 (Continued) Intervention details of included RCTs.

Study	Treatment in intervention group	Treatment in intervention group
Zhang (2021a)	TCM syndrome differentiation treatment combined with XELOX regimen chemotherapy	XELOX regimen for 3 cycles: Capetabine 1,000 mg/m ² , twice daily, once after breakfast and dinner respectively, taking it for 14 days, stopping for 7 days; Oxaliplatin injection 130 mg/m ² intra venous drip for 2 h on day 1, one cycle for 21 days
Zhang (2021b)	Shugan Yangwei Decoction combined with SOX regimen chemotherapy. Formula composition: Bupleurum, White paeony, Scutellaria, Aurantii fructus Immaturus, Coptis, Dried ginger, Pinellia, Aucklandia, Rhei, Salviae, Toosendan Corydalis Codonopsis, Katsumada galangal, Liquorice	SOX regimen: S-1 Capsules 40–60 mg, twice daily, taking it for 14 days, stopping for 7 days; Oxaliplatin injection 130 mg/m ² intra venous drip on day 1, one cycle for 21 days
Zhang et al. (2020)	Shengyang Yiwei Decoction combined with SOX regimen chemotherapy. Formula composition: Astragalus, Pinellia, Ginseng, Liquorice, Angelicae tuhuo, Divaricate saposhniovia, White paeony, Notopterygium, Tangerine peel, Poria, Bupleurum, Alisma orientale, Largehead atractylodes, Coptis	SOX regimen: S-1 Capsules 60 mg, twice daily, taking it for 14 days, stopping for 7 days; Oxaliplatin injection 130 mg/m ² intra venous drip on day 1, one cycle for 21 days
Zhang (2019)	Erteng Sanjie Capsule combined with SOX regimen chemotherapy. Formula composition: Pseudostellaria, Largehead atractylodes, Coxi seed, Pinellia, Tangerine peel, Villous amomum, Gekko, Sargentgloryvine Smilax, Amur grape vines, Actinidia root, Prunella, Ostrea concha, Acruginous turmeric, Areca, Liquorice	SOX regimen: S-1 Capsules 40–60 mg, twice daily, taking it for 14 days, stopping for 7 days; Oxaliplatin injection 130 mg/m ² intra venous drip on day 1, one cycle for 21 days
Zhao (2011)	Kun Shen Granule combined with FOLFOX regimen chemotherapy. Formula composition: Laminaria, Actinidia root, Agrimony, Ginseng	FOLFOX regimen chemotherapy for 2 cycles: Oxaliplatin injection 200 mg intra venous drip on day 1; CF 300 mg intra venous drip on day 1–5; 5-Fu 750 mg on day 1–5, one cycle for 21 days
Zhao (2016)	Jianpi Huayu Formula combined with SOX regimen chemotherapy. Formula composition: Pseudostellaria, Largehead atractylodes, Paris polyphylla, Salviae, Scutellaria barbata, Salvia chinensis, Hedyotis diffusa, Poria, Nightshade, Dendrobium, Yam	SOX regimen: S-1 Capsules 60–80 mg, twice daily, taking it for 14 days, stopping for 7 days; Oxaliplatin injection 65 mg/m ² intra venous drip for 3 h on day 1 and day 8, one cycle for 21 days
Zhao (2021)	Wenyang Jianpi Decoction combined with SOX regimen chemotherapy. Formula composition: Pseudostellaria, Hedyotis diffusa, Largehead atractylodes, Acruginous turmeric, Nightshade, Millet sprout, Barley sprout, Pinellia, Poria, Tangerine peel, Aurantii fructus, Cassia twig, Dried ginger, Liquorice	SOX regimen: S-1 Capsules 40 mg, twice daily, taking it for 14 days, stopping for 7 days; Oxaliplatin injection 130 mg/m ² intra venous drip on day 1, one cycle for 21 days
Zhong et al. (2021)	Jianpi Fuzheng Xiaoliu Formula combined with XELOX regimen chemotherapy. Formula composition: Pseudostellaria, Coxi seed, Largehead atractylodes, Hedyotis diffusa, Smilax, Scutellaria barbata, Sparganii, Acruginous turmeric, Poria, Yam, Chinese angelica, Crataegi, Liquorice, Membrane of chickens gizzard	XELOX regimen for 4 cycles: Capetabine 1,000 mg/m ² , twice daily, taking it for 14 days, stopping for 7 days; Oxaliplatin injection 130 mg/m ² intra venous drip for on day 1, one cycle for 21 days
Zhong et al. (2019)	Modified Shenling Baizhu Decoction combined with FOLFOX4 regimen chemotherapy. Formula composition: Tangerine peel, Cimicifuga, Bupleurum, Platycodon, Liquorice, Lotus seed, Villous amomum, Chinese angelica, Largehead atractylodes, Dolichos, Poria, Yam, Codonopsis, Astragalus, Coxi seed	FOLFOX4 regimen chemotherapy: Oxaliplatin injection 85 mg/m ² intra venous drip on day 1; CF 200 mg/m ² intra venous drip on day 1; 5-Fu 400 mg/m ² on day 1, and a 22-h infusion (600 mg/m ² /d) for 2 consecutive days, one cycle for 21 days
Zhu (2011)	Jianpi Yiqi Decoction combined with FOLFOX regimen chemotherapy. Formula composition: Astragalus, Crataegi, Scorch-fried medicated leaven, Barley sprout, Adenophorae, Glehnia, Solomonseal, Tangerine peel, Pinellia, Finger citron, Magnolia bark, Membrane of chickens gizzard, Villous amomum, Whitefruit amomim, Liquorice	FOLFOX regimen chemotherapy for 2 cycles: Oxaliplatin injection 135 mg/m ² intra venous drip on day 1; CF 100 mg/m ² intra venous drip on day 1–5; 5-Fu 500 mg/m ² on day 1–5, one cycle for 21 days

(Qin, 2012; Guo, 2014; Liu et al., 2015; Zhao et al., 2016; Feng, 2017; Wang N. et al., 2018; Yuan, 2018; Zhai, 2019; Zhang, 2019; Bao, 2020; Gong, 2020; Li Y. et al., 2020; Zhang et al., 2020; Zhang, 2021a; Jiang et al., 2021; Zhao, 2021), FOLFOX regimen was adopted in 14 trials (Chen et al., 2007; Chi et al., 2010; Zhao, 2011; Zhu et al., 2011; Huang, 2014; Li et al., 2016; Chu et al., 2017; Huang et al., 2017; Gu et al., 2019; Jiao, 2019; Liu et al., 2019; Zhong et al., 2019; Sun et al., 2020; Long, 2021), and XELOX regimen in 10 trials (Hu, 2011; Yuan, 2011; Yang et al., 2018; Cai et al., 2019; Xie, 2019; Yu et al., 2019; Zhang, 2021b;

Feng et al., 2021; Zhang H. O. et al., 2021; Zhong et al., 2021). Intervention details of included RCTs were shown in Table 2. The Chinese phonetic transcription, scientific name, Latin drug name, and English name of herbs adopted in the prescriptions of included trials were shown in Table 3.

3.1.2 Risk of bias of included trials

RoB 2 was used to assess the quality of 40 included trials. Two trials were assessed as “High” risk of bias (Zhao, 2011; Zhang, 2019), and 38 trials were assessed as “Some

TABLE 3 The names of Herbs.

Phonetic transcription	Scientific name	Latin drug name	English name
Bajitian	<i>Morinda officinalis</i> How	Morindae Officinalis Radix	Morinda
Baqia	<i>Smilax china</i> L.	Smilacis Chinae Rhizoma	Smilax
Baibiandou	<i>Dolichos lablab</i> L.	Lablab Semen Album	Dolichos
Baidoukou	<i>Amomum kravanh</i> Pierre ex Gagnep.	Amomi Fructus Rotundus	Whitefruit Amomim
Baihuasheshecao	<i>Hedyotis diffusa</i> Willd.	Hedyotis Diffusa Herba	Hedyotis diffusa
Baiji	<i>Bletilla striata</i> (Thunb.) Reichb.f.	Bletillae Rhizoma	Bletilla
Baishao	<i>Paeonia lactiflora</i> Pall.	Paeoniae Radix Alba	White Paeony
Baizhu	<i>Atractylodes macrocephala</i> Koidz.	Atractylodis Macrocephalae Rhizoma	Largehead Atractylodes
Banlangen	<i>Isatis indigotica</i> Fort.	Isatidis Radix	Isatis
Banxia	<i>Pinellia ternata</i> (Thunb.) Makino.	Pinelliae Rhizoma	Pinellia
Banzhilian	<i>Scutellaria barbata</i> D.Don	Scutellariae Barbatae Herba	Scutellaria barbata
Beishanshen	<i>Glehnia littoralis</i> Fr. Schmidtex Miq.	Glehniae Radix	Glehnia
Bihu	<i>Gekko swinhonis</i> Guenther	Gekko Swinhonis	Gekko
Binlang	<i>Areca catechu</i> L.	Arecae Semen	Areca
Buguzhi	<i>Psoralea corylifolia</i> L.	Psoraleae Fructus	Psoralea
Caodoukou	<i>Alpinia katsumadai</i> Hayata	Alpiniae Katsumadai Semen	Katsumada Galangal
Chaihu	<i>Bupleurum chinense</i> DC.	Bupleuri Radix	Bupleurum
Chenpi	<i>Citrus reticulata</i> Blanco	Citri Reticulatae Pericarpium	Tangerine Peel
Chishao	<i>Paeonia lactiflora</i> Pall.	Paeoniae Radix Rubra	Red paeony
Chuanlianzi	<i>Melia toosendan</i> Sieb.et Zucc.	Toosendan Fructus	Toosendan
Chuanxiong	<i>Ligusticum chuanxiong</i> Hort.	Chuanxiong Rhizoma	Sichuan lovase
Dahuang	<i>Rheum officinale</i> Baill.	Rhei Radix et Rhizoma	Rhei
Daxueteng	<i>Sargentodoxa cuneata</i> (Oliv.) Rehd. et Wils.	Sargentodoxae Caulis	Sargentgloryvine
Dazao	<i>Ziziphus jujuba</i> Mill.	Jujubae Fructus	Red date
Dansheng	<i>Salvia miltiorrhiza</i> Bunge	Salviae Miltiorrhizae Radix et Rhizoma	Salviae
Danggui	<i>Angelica sinensis</i> (Oliv.) Diels	Angelicae Sinensis Radix	Chinese Angelica
Dangshen	<i>Codonopsis pilosula</i> (Franch.) Nannf.	Codonopsis Radix	Codonopsis
Duhuo	<i>Angelica pubescens</i> Maxim.f. biserrata Shan et Yuan	Angelicae Pubescentis Radix	Angelicae tuhuo
Duzhong	<i>Eucommia ulmoides</i> Oliv.	Eucommiae Cortex	Eucommia
Ezhu	<i>Curcuma phaeocaulis</i> Val.	Curcuma Rhizoma	Acruginous Turmeric
Fangfeng	<i>Saposhnikovia divaricata</i> (Turcz.) Schischk.	Saposhnikoviae Radix	Divaricate Saposhniovia
Fangji	<i>Stephania tetrandra</i> S.Moore	Stephaniae Tetrandrae Radix	Fourstamen Stephania
Foshou	<i>Citrus medica</i> L. var. sarco- dactylis Swingle	Citri Sarcodactylis Fructus	Finger Citron
Fuling	<i>Poria cocos</i> (Schw.) Wolf	Poria	Poria
Fushen	<i>Poria cocos</i> (Schw.) Wolf	Poria Cum Radix Pini	Poria with hostwood
Gancao	<i>Glycyrrhiza uralensis</i> Fisch.	Glycyrrhizae Radix et Rhizoma Praeparata Cum Melle	Liquorice
Gansong	<i>Nardostachys jatamansi</i> DC.	Nardostachys Radix et Rhizoma	Nardostachys
Ganjiang	<i>Zingiber officinale</i> Roscoe	Zingiberis Rhizoma	Dried Ginger
Gouqi	<i>Lycium barbarum</i> L.	Lycii Fructus	Wolfberry
Guya	<i>Setaria italica</i> (L.) Beauv.	Setariae Fructus Germinatus	Millet sprout
Gusuibu	<i>Drynaria fortunei</i> (Kunze) J.Sm.	Drynariae Rhizoma	Drynaria
Gualou	<i>Trichosanthes kirilowii</i> Maxim.	Trichosanthis Semen	Snakegourd seed
Guizhi	<i>Neolitsea cassia</i> (L.) Kosterm.	Cinnamomi Ramulus	Cassia twig
Hehuanpi	<i>Albizia julibrissin</i> Durazz.	Albiziae Cortex	Silktree bark
Houpu	<i>Magnolia officinalis</i> Rehder & E.H.Wilson	Magnoliae Officinalis Cortex	Magnolia bark
Huangjing	<i>Polygonatum kingianum</i> Coll.et Hemsl.	Polygonati Rhizoma	Solomonseal

(Continued on following page)

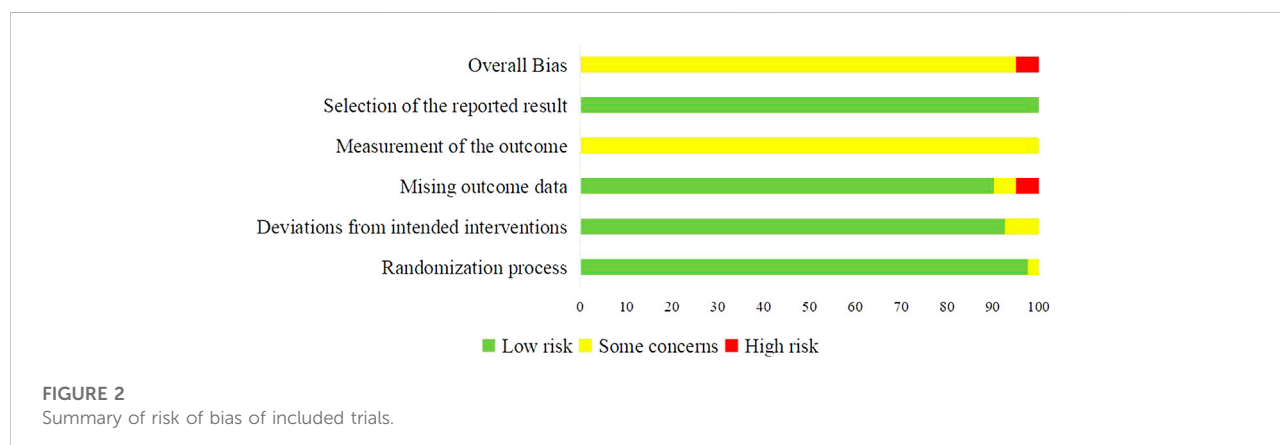
TABLE 3 (Continued) The names of Herbs.

Phonetic transcription	Scientific name	Latin drug name	English name
Huanglian	<i>Coptis chinensis</i> Franch.	Coptidis Rhizoma	Coptis
Huangqi	<i>Astragalus mongholicus</i> Bunge	Astragali Radix	Astragalus
Huangqin	<i>Scutellaria baicalensis</i> Georgi	Scutellariae Radix	Scutellaria
Jineijin	—	Galli Gigerii Endothelium Corneum	Membrane of Chickens Gizzard
Jixueteng	<i>Spatholobus suberectus</i> Dunn	Spatholobi Caulis	Suberect Spatholobus
Jiangcan	—	Bombyx Batryticatus	Stiff Silkworm
Jiaoshenqu	—	—	Scorch-fried medicated leaven
Jinyinhua	<i>Lonicera japonica</i> Thunb.	Lonicerae Japonicae Flos	Honeysuckle
Jiegeng	<i>Platycodon grandiflorus</i> (Jacq.) A.DC.	Platycodonis Radix	Platycodon
Kushen	<i>Sophora flavescens</i> Ait.	Sophorae Flavescents Radix	Lightyellow Sophora
Kuxingren	<i>Prunus armeniaca</i> L.	Armeniacae Semen Amarum	Bitter Apricot Seed
Lianqiao	<i>Forsythia suspensa</i> (Thunb.) Vahl	Forsythiae Fructus	Forsythia
Lianzi	<i>Nelumbo nucifera</i> Gaertn.	Nelumbinis Semen	Lotus seed
Lingzhi	<i>Ganoderma lucidum</i> (Leyss.ex Fr.) Karst.	Ganoderma	Ganoderma
Longkui	<i>Solanum nigrum</i> L.	Solani Nigri Herba	Nightshade
Maiya	<i>Hordeum vulgare</i> L.	Hordei Fructus Germinatus	Barley Sprout
Mangxiao	—	Natrii Sulfas	Mirabilite
Moyao	<i>Commiphora myrrha</i> Engl.	Myrrha	Myrrh
Muli	<i>Ostrea gigas</i> Thunberg	Ostreae Concha	Ostreae Concha
Muxiang	<i>Aucklandia lappa</i> Decne.	Aucklandiae Radix	Aucklandia
Nanshashen	<i>Adenophora stricta</i> Miq.	Adenophorae Radix	Adenophorae
Nvzhenzi	<i>Ligustrum lucidum</i> Ait.	Ligustri Lucidi Fructus	Ligustrum
Pipaye	<i>Eriobotrya japonica</i> (Thunb.) Lindl.	Eriobotryae Folium	Loquat Leaf
Pugongying	<i>Taraxacum mongolicum</i> Hand. -Mazz.	Taraxaci Herba	Dandelion
Qianghuo	<i>Notopterygium incisum</i> Ting ex H. T. Chang	Notopterygii Rhizoma et Radix	Notopterygium
Quanxie	<i>Buthus martensii</i> Karsch	Scorpio	Scorpion
Renshen	<i>Panax ginseng</i> C. A. Mey.	Ginseng Radix et Rhizoma	Ginseng
Rougui	<i>Cinnamomum cassia</i> Presl	Cinnamomi Cortex	Cassia Bark
Ruxiang	<i>Boswellia carterii</i> Birdw.	Olibanum	Frankincense
Sanleng	<i>Sparganium stoloniferum</i> Buch.-Ham.	Sparganii Rhizoma	Sparganii
Sanqi	<i>Panax notoginseng</i> (Burk.) F. H. Chen	Notoginseng Radix et Rhizoma	Sanchi
Sharen	<i>Amomum villosum</i> Lour.	Amomi Fructus	villous amomum
Shangcigu	<i>Cremastra appendiculata</i> (D.Don) Makino	Cremastrae Pseudobulbus Pleiones Pseudobulbus	Cremastra
Shandougen	<i>Sophora tonkinensis</i> Gagnep.	Sophorae Tonkinensis Radix et Rhizoma	Vietnamese Sophora Root
Shanyao	<i>Dioscorea opposita</i> Thunb.	Dioscoreae Rhizoma	Common Yam
Shanzha	<i>Crataegus pinnatifida</i> Bge.	Crataegi Fructus	Crataegi
Shanzhuyu	<i>Cornus officinalis</i> Sieb. et Zucc.	Corni Fructus	Cornus
Shengma	<i>Cimicifuga heracleifolia</i> Kom.	Cimicifugae Rhizoma	Cimicifuga
Shengjiang	<i>Zingiber officinale</i> Roscoe	Zingiberis Rhizoma Recens	Raw Ginger
Shidachuan	<i>Hedyotis chrysotricha</i> (Palib.) Merr.	Hedyotis Chrysotrichae Herba	Hedyotis Chrysotricha
Shihu	<i>Dendrobium nobile</i> Lindl.	Dendrobii Caulis	Dendrobium
Shudihuang	<i>Rehmannia glutinosa</i> Libosch.	Rehmanniae Radix Praeparata	Rehmannia Glutinosa
Suanzaoren	<i>Ziziphus jujuba</i> Mill. var. <i>spinosa</i> (Bunge) Hu ex H. F. Chou	Ziziphi Spinosa Semen	Spine Date Seed
Taizishen	<i>Pseudostellaria heterophylla</i> (Miq.) Pax	Pseudostellariae Radix	Pseudostellaria
Taoren	<i>Prunus persica</i> (L.) Batsch	Persicae Semen	Peach kernel
Tengligen	<i>Actinidia chinensis</i> Planch. var. <i>hispida</i> C.F.Liang	Actinidiae Chinensis Radix	Actinidia root

(Continued on following page)

TABLE 3 (Continued) The names of Herbs.

Phonetic transcription	Scientific name	Latin drug name	English name
Tusizi	<i>Cuscuta chinensis</i> Lam.	Cuscutae Semen	Cuscuta
Walengzi	<i>Arca subcrenata</i> Lischke	Arcae Concha	Arcae concha
Weilingxian	<i>Clematis chinensis</i> Osbeck	Clematidis Radix et Rhizoma	Chinese Clematis
Wumei	<i>Prunus mume</i> (Siebold) Siebold et Zucc.	Mume Fructus	Dark plum
Wugong	<i>Scolopendra subspinipes mutilans</i> L. Koch	Scolopendra	Scolopendra
Xiakucao	<i>Prunella vulgaris</i> L.	Prunellae Spica	Prunella
Xianmao	<i>Curculigo orchoides</i> Gaertn.	Curculiginis Rhizoma	Curculigo
Xuanshen	<i>Scrophularia ningpoensis</i> Hemsl.	Scrophulariae Radix	Figwort
Xuanfuhua	<i>Inula japonica</i> Thunb.	Inulae Flos	Inula
Yeputaoteng	<i>Vitis amurensis</i> Rupr.	Vitis Amurensis Caulis	Amur grape vines
Yiyiren	<i>Coix lacryma-jobi</i> L.	Coicis Semen	Coxi seed
Yinyanghuo	<i>Epimedium brevicornu</i> Maxim.	Epimedii Folium	Epimedium
Yanhusuo	<i>Corydalis yanhusuo</i> W.T.Wang	Corydalis Rhizoma	Corydalis
Zaojiaoci	<i>Gleditsia sinensis</i> Lam.	Gleditsiae Spina	Gleditsia sinensis
Zexie	<i>Alisma plantago-aquatica</i> subsp. orientale (Sam.) Sam.	Alismatis Rhizoma	Alisma orientale
Zhebeimu	<i>Fritillaria thunbergii</i> Miq.	Fritillariae Thunbergii Bulbus	Thunberg fritillary
Zhiqiao	<i>Citrus × aurantium</i> L.	Aurantii Fructus	Aurantii Fructus
Zhishi	<i>Citrus × aurantium</i> L.	Fructus Aurantii Immaturus	Aurantii Fructus Immaturus
Chonglou	<i>Paris polyphylla</i> Smith var. yunnanensis (Franch.) Hand.-Mazz.	Paridis Rhizoma	Paris Polyphylla
Zhuling	<i>Polyporus umbellatus</i> (Pers.) Fries	Polyporus	Agaric
Zhuru	<i>Bambusa tuldoidea</i> Munro	Bambusae Caulis in Taenias	Bambusae Caulis
Zisugeng	<i>Perilla frutescens</i> (L.) Britt.	Perillae Caulis	Perilla frutescens stem



concerns” (Chen et al., 2007; Chi et al., 2010; Hu, 2011; Yuan, 2011; Zhu et al., 2011; Qin, 2012; Guo, 2014; Huang, 2014; Liu et al., 2015; Li et al., 2016; Zhao et al., 2016; Chu et al., 2017; Feng, 2017; Huang et al., 2017; Wang Y. et al., 2018; Yang et al., 2018; Yuan, 2018; Cai et al., 2019; Gu et al., 2019; Jiao, 2019; Liu et al., 2019; Xie, 2019; Yu et al.,

2019; Zhai, 2019; Zhong et al., 2019; Bao, 2020; Gong, 2020; Li D. H. et al., 2020; Sun et al., 2020; Zhang et al., 2020; Zhang, 2021a; Zhang, 2021b; Feng et al., 2021; Jiang et al., 2021; Long, 2021; Zhang L. et al., 2021; Zhao, 2021; Zhong et al., 2021). Most concerns were caused by the measurement of the outcomes, since the assessment of

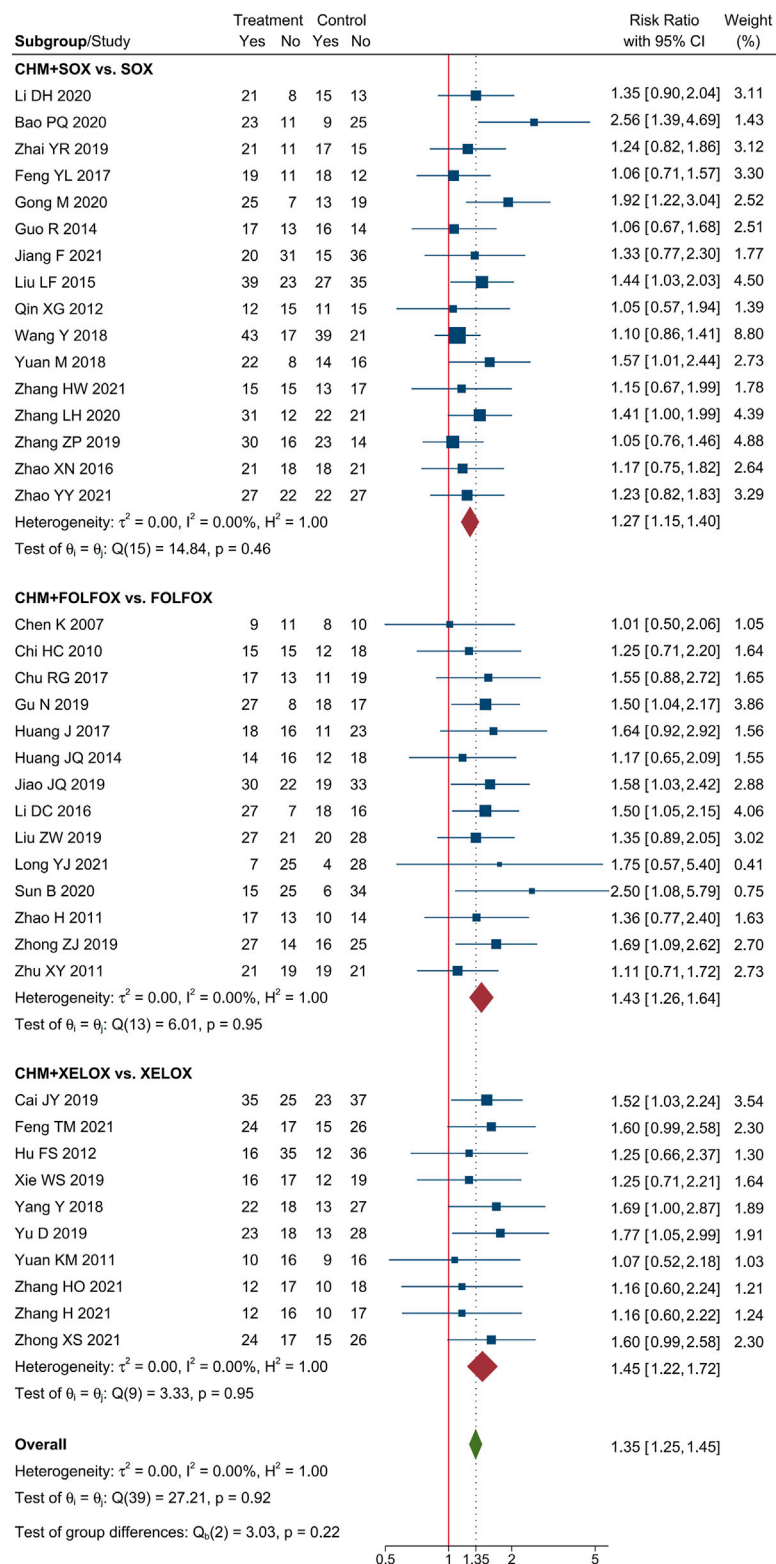


FIGURE 3
Forest plot of ORR.

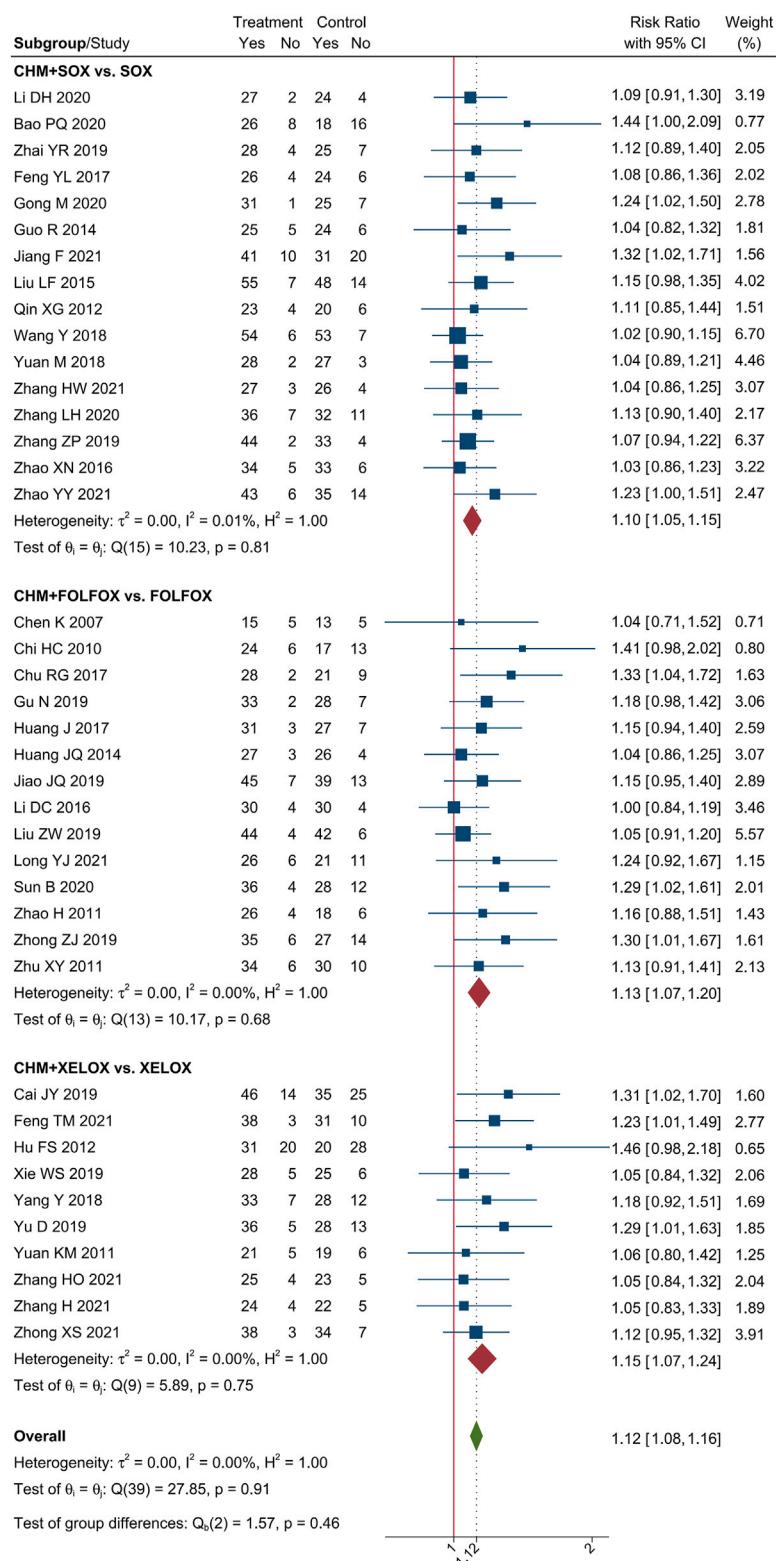


FIGURE 4
Forest plot of DCR.

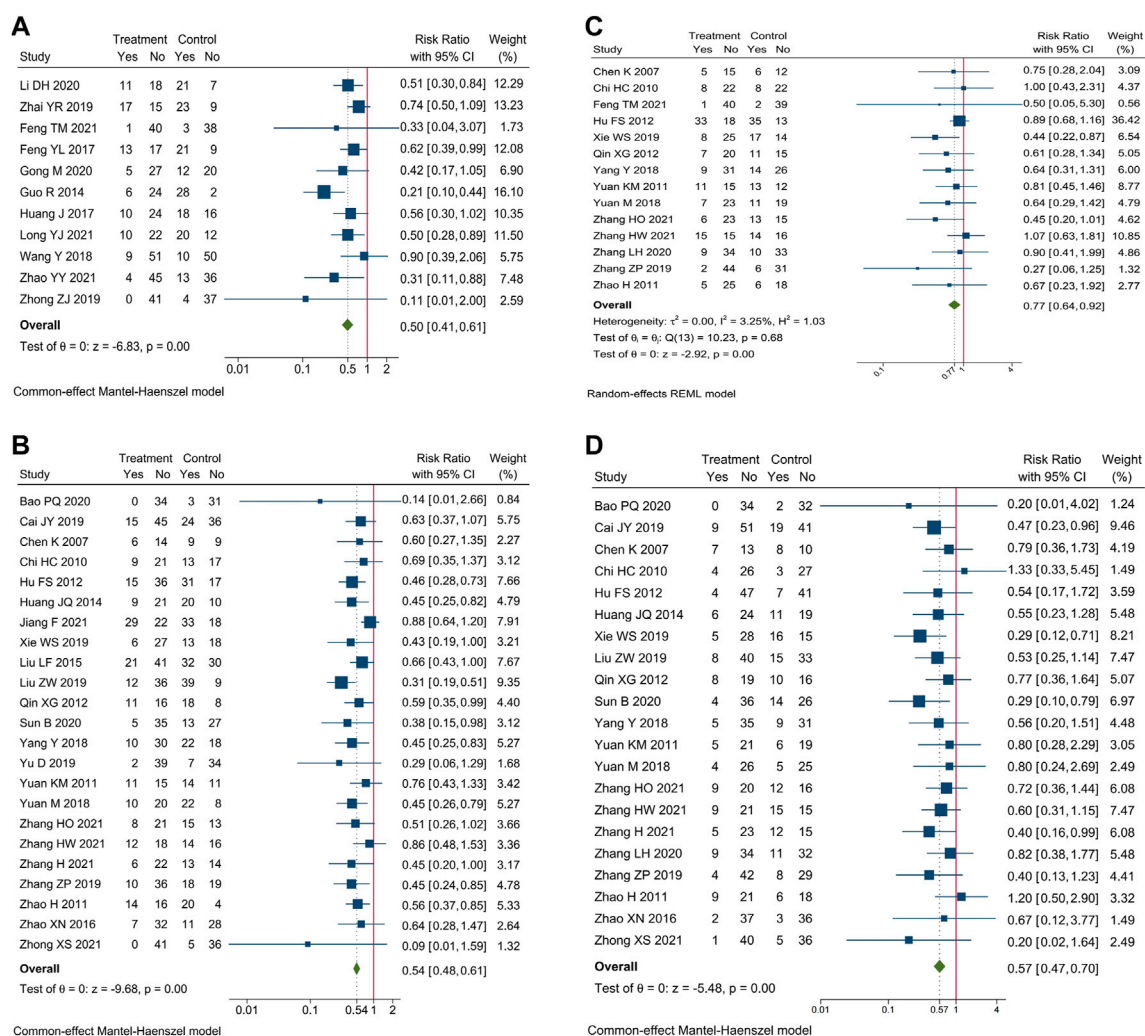


FIGURE 5

Forest plot of incidence of AEs of blood system. Incidence of (A) myelosuppression, (B) leucopenia, (C) anemia, and (D) thrombocytopenia.

outcomes could be influenced by knowledge of interventions patients received. The imbalanced missing data in two trials lead to the “High” risk in domain of missing outcome data, and in overall bias. The summary of RoB was shown in Figure 2.

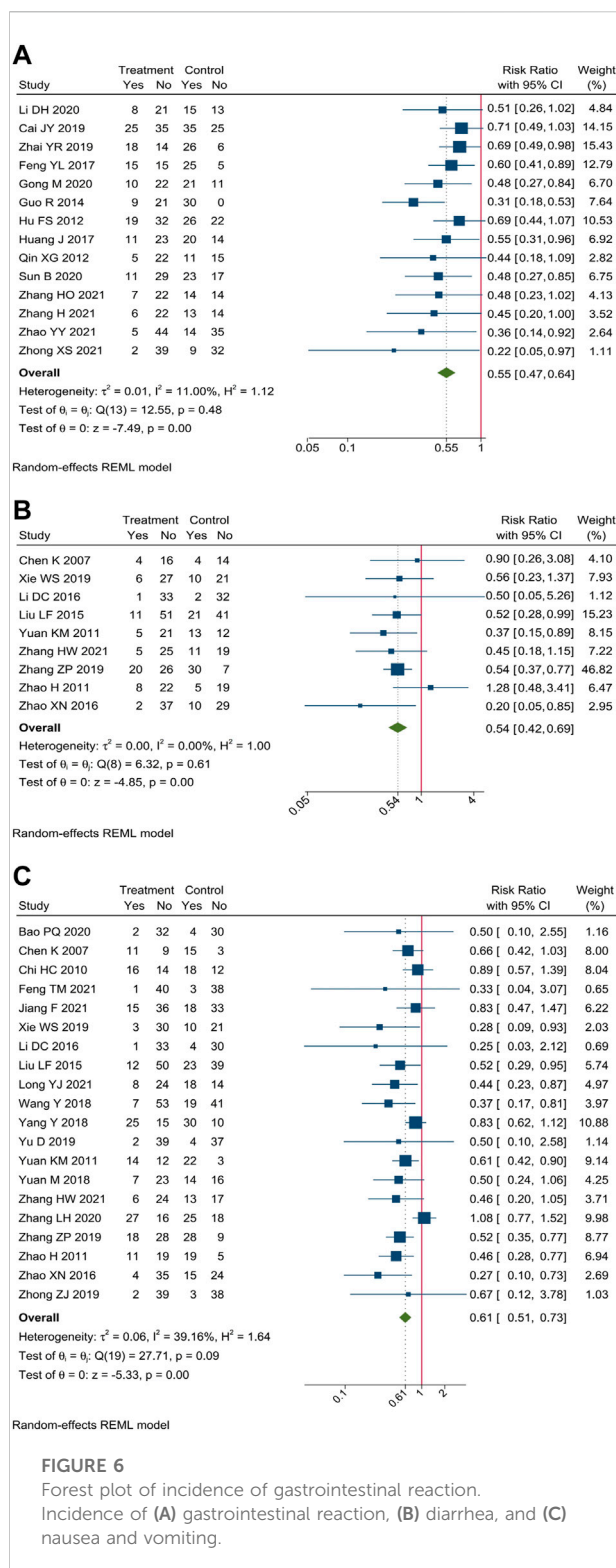
3.2 The tumor response of CHM combined with oxaliplatin-based chemotherapy in AGC

Meta-analysis of 40 trials showed that CHM combined with oxaliplatin-based chemotherapy could increase the ORR by 35% [RR = 1.35, 95% CI (1.25, 1.45)]. The value of $I^2 = 0$ indicates that there was no statistical heterogeneity

among these trials. The forest plot of ORR was shown in Figure 3. Meta-analysis of 40 trials showed that CHM combined with oxaliplatin-based chemotherapy could increase the DCR by 12% [RR = 1.12, 95% CI (1.08, 1.16)]. $I^2 = 0$ indicates that there was no statistical heterogeneity among these trials. The forest plot of DCR was shown in Figure 4.

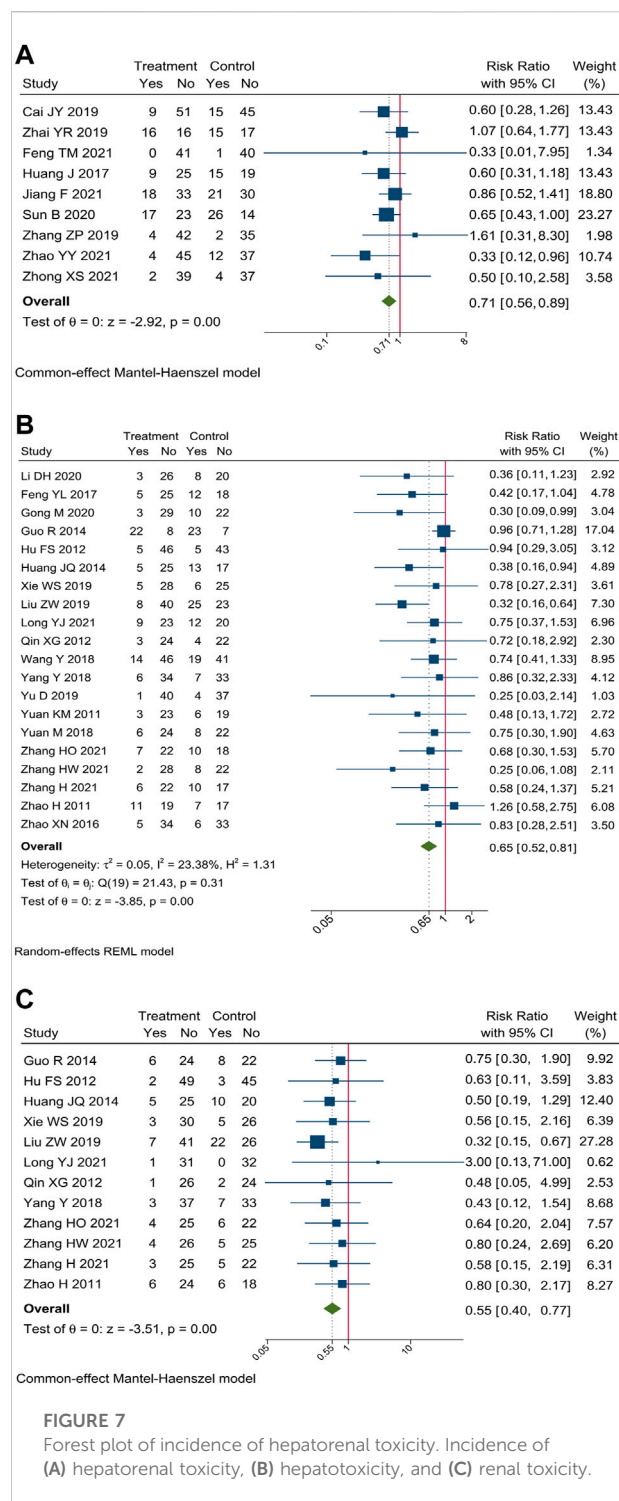
3.3 The safety of CHM combined with oxaliplatin-based chemotherapy in AGC

Safety outcomes were reported in 37 trials. We evaluated the incidence of AEs of blood system, gastrointestinal reaction, hepatorenal toxicity, and peripheral neurotoxicity.



3.3.1 AEs of blood system

Incidence of AEs of blood system were reported in 35 trials. Meta-analysis showed that compare oxaliplatin-



based chemotherapy alone, CHM combined with oxaliplatin-based chemotherapy could decrease the incidence of myelosuppression by 50% [RR = 0.50, 95% CI (0.41, 0.61)], leucopenia by 46% [RR = 0.54, 95% CI (0.48, 0.61)], anemia by 23% [RR = 0.77, 95% CI (0.64, 0.92)], and

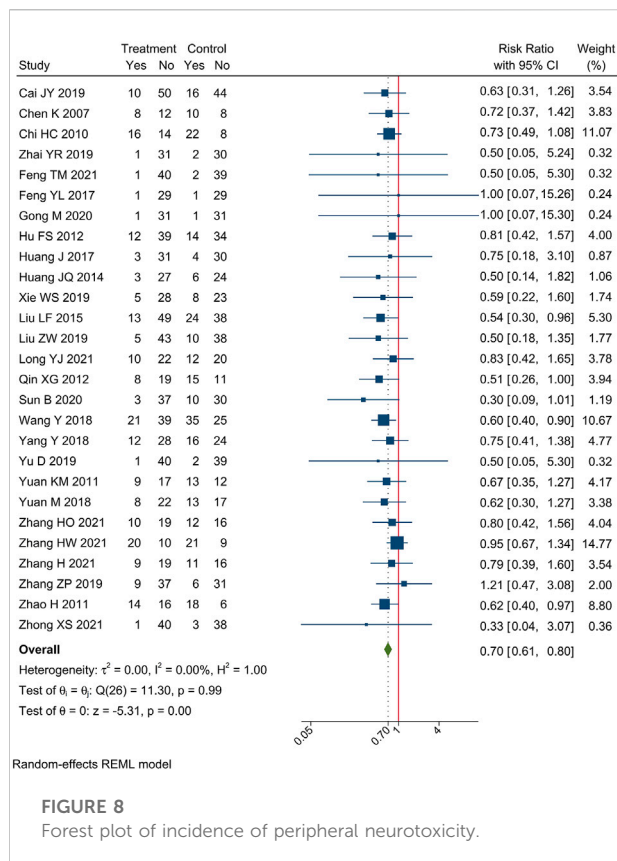


FIGURE 8

Forest plot of incidence of peripheral neurotoxicity.

thrombocytopenia by 43% [RR = 0.57, 95% CI (0.47, 0.70)]. Forest plots of incidence of AEs of blood system were shown in Figure 5.

3.3.2 Gastrointestinal reaction

Incidence of gastrointestinal reaction were reported in 34 trials. Meta-analysis showed that compare oxaliplatin-based chemotherapy alone, CHM combined with oxaliplatin-based chemotherapy could decrease the incidence of gastrointestinal reaction by 45% [RR = 0.55, 95% CI (0.47, 0.64)], nausea and vomiting by 39% [RR = 0.61, 95% CI (0.51, 0.73)], and diarrhea by 46% [RR = 0.54, 95% CI (0.42, 0.69)]. Forest plots of incidence of gastrointestinal reaction were shown in Figure 6.

3.3.3 Hepatorenal toxicity

Incidence of hepatorenal toxicity were reported in 29 trials. Meta-analysis showed that compare oxaliplatin-based chemotherapy alone, CHM combined with oxaliplatin-based chemotherapy could decrease the incidence of hepatorenal toxicity by 29% [RR = 0.71, 95% CI (0.56, 0.89)], hepatotoxicity by 35% [RR = 0.65, 95% CI (0.52, 0.81)], and renal toxicity by 45% [RR = 0.55, 95% CI (0.40, 0.77)]. Forest plots of incidence of hepatorenal toxicity were shown in Figure 7.

3.3.4 Peripheral neurotoxicity

Incidences of peripheral neurotoxicity were reported in 27 trials. Meta-analysis showed that compare oxaliplatin-based chemotherapy alone, CHM combined with oxaliplatin-based chemotherapy could decrease the incidence of peripheral neurotoxicity by 30% [RR = 0.70, 95% CI (0.61, 0.80)]. Forest plots of incidence of hepatorenal toxicity were shown in Figure 8.

3.4 Subgroup analysis

We performed subgroup analysis of the outcomes of tumor-response, according to the different regimen of chemotherapy that patients received. Compare to SOX regimen alone, CHM combined with SOX regimen chemotherapy could increase the ORR by 27% [RR = 1.27, 95% CI (1.15, 1.40)], and DCR by 10% [RR = 1.10, 95% CI (1.05, 1.15)]. Compare to FOLFOX regimen alone, CHM combined with FOLFOX regimen chemotherapy could increase the ORR by 43% [RR = 1.43, 95% CI (1.26, 1.64)], and DCR by 14% [RR = 1.13, 95% CI (1.07, 1.20)]. Compare to XELOX regimen alone, CHM combined with XELOX regimen chemotherapy could increase the ORR by 27% [RR = 1.35, 95% CI (1.26, 1.45)], and DCR by 12% [RR = 1.12, 95% CI (1.09, 1.16)]. The details were shown in Figures 3, 4.

3.5 Sensitivity analysis

We performed sensitivity analysis to investigate the potential contributions of specific herbs to tumor response. Three trials which adopted multiple core prescriptions were excluded from sensitivity analysis, and we analyzed the composition of core prescriptions in other 37 trials that adopted single core prescription. There are 114 herbs in the formulas of included trials, 47 of these herbs were used only in one trial and were excluded from the sensitivity analysis. Among 67 herbs analyzed, 43 herbs were only used with other herbs as a combination, which means that when herb was used in several formulas, there was always an herb in the same formulas. RRs of the group of trials that included each specific herb or herb combination were calculated. Among 380 sensitivity analyses performed, 21 single herbs and 129 herb combinations were located, and 3 single herbs along with 227 herb combinations were excluded according to the predetermined principle.

3.5.1 Tier 1: Single herbs

The five most frequently used single herbs were Largehead Atractylodes ($n = 26$), Liquorice ($n = 23$), Poria ($n = 21$), Pinellia ($n = 20$), and Codonopsis Pilosula ($n = 18$). The single herbs with the five highest RR were Dandelion [RR = 1.47, 95% CI (1.17, 1.83), $n = 5$], Paris Polyphylla [RR = 1.47, 95% CI (1.07, 2.02), $n =$

TABLE 4 Sensitivity analysis of specific contributions of herbs.

Tier	Composition	No. of RCTs	Effect estimates (EE)	95% CI of EE	I ² statistics (%)
1	Dandelion	5	1.47	1.17, 1.83	0.00
1	Paris Polyphylla	3	1.47	1.07, 2.02	10.95
1	Red paeony	4	1.46	1.13, 1.88	0.00
1	Chinese Angelica	14	1.44	1.27, 1.64	9.33
1	Astragalus	13	1.43	1.25, 1.64	0.00
1	Scutellaria Barbata	8	1.41	1.18, 1.69	28.11
1	Villous Amomum	7	1.40	1.13, 1.73	33.15
1	Smilax	6	1.40	1.17, 1.67	8.17
1	White Paeony	10	1.39	1.20, 1.61	14.62
1	Ginseng	6	1.39	1.17, 1.65	0.00
1	Codonopsis	18	1.38	1.23, 1.55	5.92
1	Acruginous Turmeric	15	1.36	1.20, 1.54	16.12
1	Poria	21	1.35	1.23, 1.49	0.00
1	Largehead Atractylodes	26	1.34	1.23, 1.47	0.00
1	Gekko	6	1.33	1.10, 1.60	14.72
1	Tangerine Peel	17	1.32	1.18, 1.47	6.29
1	Hedyotis Diffusa	12	1.32	1.16, 1.50	3.56
1	Membrane of Chickens Gizzard	7	1.32	1.11, 1.57	0.00
1	Salviae	4	1.32	1.04, 1.67	0.00
1	Liquorice	23	1.30	1.18, 1.42	0.00
1	Pinellia	20	1.28	1.17, 1.41	0.00
2	Codonopsis + Villous Amomum	4	1.70	1.34, 2.16	0.00
2	Ginseng + Cornus	2	1.56	1.16, 2.10	0.00
2	Acruginous Turmeric + Astragalus	7	1.55	1.28, 1.88	0.00
2	Chinese Angelica + Astragalus	7	1.55	1.28, 1.89	0.00
2	Chinese Angelica + Smilax	5	1.55	1.27, 1.88	0.00
2	Acruginous Turmeric + Cassia Twig	4	1.54	1.23, 1.91	0.00
2	Scutellaria Barbata + Membrane of Chickens Gizzard	3	1.53	1.18, 1.98	0.00
2	Chinese Angelica + Myrrh	3	1.52	1.15, 2.00	0.00
2	Largehead Atractylodes + Wolfberry	4	1.51	1.22, 1.89	0.00
2	Astragalus + Villous Amomum	4	1.50	1.11, 2.03	25.93
2	Codonopsis + Astragalus	8	1.47	1.23, 1.76	0.00
2	Liquorice + Bupleurum	5	1.46	1.19, 1.79	0.00
2	Codonopsis + Chinese Angelica	8	1.46	1.20, 1.77	27.05
2	Codonopsis + Aucklandia	6	1.46	1.20, 1.77	0.00
2	Largehead Atractylodes + Scutellaria Barbata	7	1.44	1.19, 1.74	27.24
2	Largehead Atractylodes + White Paeony	9	1.41	1.21, 1.63	12.42
2	Largehead Atractylodes + Ginseng	3	1.41	1.21, 1.78	0.00
2	Largehead Atractylodes + Membrane of Chickens Gizzard	5	1.40	1.14, 1.73	0.00
2	Acruginous Turmeric + Hedyotis Diffusa	8	1.40	1.16, 1.70	21.43
2	Membrane of Chickens Gizzard + Gekko	4	1.40	1.12, 1.76	0.00
2	Largehead Atractylodes + Yam	9	1.38	1.18, 1.62	13.56
2	Liquorice + Poria	17	1.36	1.22, 1.52	0.00
2	Pinellia + Gekko	5	1.35	1.10, 1.65	14.01
2	Pinellia + Magnolia Bark	4	1.30	1.04, 1.64	0.00
2	Pinellia + Dried Ginger	4	1.29	1.03, 1.61	1.47

(Continued on following page)

TABLE 4 (Continued) Sensitivity analysis of specific contributions of herbs.

Tier	Composition	No. of RCTs	Effect estimates (EE)	95% CI of EE	I ² statistics (%)
3	Chinese Angelica + Astragalus + Villous Amomum	3	1.73	1.26, 2.36	0.00
3	Largehead Atractylodes + Wolfberry + Psoralea	2	1.65	1.24, 2.19	0.00
3	Codonopsis + Chinese Angelica + Astragalus	6	1.60	1.30, 1.97	0.00
3	Liquorice + Codonopsis + Bupleurum	3	1.57	1.14, 2.15	0.00
3	Pinellia + White Paeony + Dried Ginger	2	1.56	1.10, 2.21	0.00
3	Codonopsis + Acruginous Turmeric + Astragalus	5	1.53	1.22, 1.91	0.00
3	Largehead Atractylodes + Astragalus + White Paeony	5	1.52	1.26, 1.84	0.00
3	Largehead Atractylodes + Poria + Aucklandia	5	1.51	1.22, 1.86	0.00
3	Largehead Atractylodes + Acruginous Turmeric + Membrane of Chickens Gizzard	4	1.51	1.19, 1.91	0.00
3	Acruginous Turmeric + Chinese Angelica + Astragalus	5	1.51	1.21, 1.89	0.00
3	Acruginous Turmeric + Hedyotis Diffusa + Red paeony	3	1.51	1.14, 2.01	0.00
3	Scutellaria Barbata + Membrane of Chickens Gizzard + Gekko	2	1.51	1.11, 2.04	0.00
3	Largehead Atractylodes + Pinellia + Scutellaria Barbata	5	1.50	1.18, 1.92	39.55
3	Largehead Atractylodes + Astragalus + Villous Amomum	2	1.50	1.04, 2.16	0.00
3	Largehead Atractylodes + Pinellia + Dandelion	4	1.49	1.17, 1.91	0.00
3	Largehead Atractylodes + Acruginous Turmeric + Astragalus	6	1.47	1.20, 1.80	0.00
3	Liquorice + Codonopsis + Aucklandia	5	1.47	1.15, 1.86	0.00
3	Largehead Atractylodes + Acruginous Turmeric + Scutellaria Barbata	4	1.46	1.12, 1.89	39.92
3	Largehead Atractylodes + Chinese Angelica + Astragalus	6	1.46	1.19, 1.80	0.00
3	Largehead Atractylodes + Astragalus + Coxi Seed	6	1.46	1.21, 1.78	0.00
3	Largehead Atractylodes + Pinellia + Astragalus	5	1.44	1.17, 1.77	0.00
3	Largehead Atractylodes + Tangerine Peel + White Paeony	6	1.44	1.19, 1.74	27.78
3	Acruginous Turmeric + Hedyotis Diffusa + Cassia Twig	3	1.44	1.12, 1.84	0.00
3	Largehead Atractylodes + Pinellia + White Paeony	6	1.43	1.15, 1.77	29.02
3	Codonopsis + White Paeony + Aucklandia	3	1.41	1.09, 1.82	0.00
3	Liquorice + White Paeony + Bupleurum	4	1.40	1.11, 1.76	0.00
3	Largehead Atractylodes + Poria + Suberect Spatholobus	3	1.39	1.05, 1.83	0.00
3	Pinellia + Tangerine Peel + Barley Sprout	5	1.39	1.10, 1.75	4.55
3	Pinellia + Gekko + Magnolia Bark	3	1.39	1.06, 1.81	0.00
3	Largehead Atractylodes + Tangerine Peel + Yam	6	1.38	1.13, 1.69	22.74
3	Largehead Atractylodes + Liquorice + Poria	16	1.37	1.22, 1.53	0.00
3	Largehead Atractylodes + Pinellia + Membrane of Chickens Gizzard	4	1.36	1.08, 1.72	0.00
4	Codonopsis + Chinese Angelica + Astragalus + Villous Amomum	2	1.95	1.36, 2.78	0.00
4	Largehead Atractylodes + Pinellia + Tangerine Peel + Dandelion	2	1.76	1.24, 2.52	0.00
4	Acruginous Turmeric + Chinese Angelica + Astragalus + Villous Amomum	2	1.75	1.01, 3.03	34.11
4	Liquorice + Pinellia + Tangerine Peel + Paris Polyphylla	2	1.74	1.18, 2.56	0.00
4	Largehead Atractylodes + Tangerine Peel + Astragalus + Yam	4	1.63	1.30, 2.05	0.00
4	Codonopsis + Acruginous Turmeric + Chinese Angelica + Astragalus	4	1.57	1.24, 1.99	0.00
4	Largehead Atractylodes + Liquorice + Poria + Aucklandia	4	1.55	1.19, 2.02	0.00
4	Largehead Atractylodes + Tangerine Peel + Acruginous Turmeric + Astragalus	4	1.54	1.23, 1.93	0.00
4	Largehead Atractylodes + Poria + Chinese Angelica + Astragalus	5	1.53	1.23, 1.91	0.00
4	Largehead Atractylodes + Astragalus + Wolfberry + Cuscuta	3	1.53	1.12, 2.08	0.00
4	Acruginous Turmeric + Chinese Angelica + Sparganii + Smilax	4	1.53	1.24, 1.89	0.00
4	Largehead Atractylodes + Liquorice + Poria + Villous Amomum	4	1.52	1.19, 1.93	0.00
4	Largehead Atractylodes + Liquorice + Poria + Bupleurum	4	1.51	1.22, 1.89	0.00
4	Largehead Atractylodes + Poria + Codonopsis + Aucklandia	5	1.51	1.22, 1.86	0.00

(Continued on following page)

TABLE 4 (Continued) Sensitivity analysis of specific contributions of herbs.

Tier	Composition	No. of RCTs	Effect estimates (EE)	95% CI of EE	I ² statistics (%)
4	Largehead Atractylodes + Pinellia + Tangerine Peel + Barley Sprout	4	1.50	1.15, 1.97	3.91
4	Largehead Atractylodes + Codonopsis + Chinese Angelica + Astragalus	5	1.50	1.21, 1.87	0.00
4	Largehead Atractylodes + Liquorice + Chinese Angelica + Astragalus	5	1.48	1.14, 1.02	0.00
4	Largehead Atractylodes + Pinellia + Tangerine Peel + Astragalus	4	1.47	1.19, 1.83	0.00
4	Liquorice + Pinellia + Tangerine Peel + Ginseng	2	1.47	1.12, 1.93	0.00
4	Largehead Atractylodes + Poria + Tangerine Peel + Astragalus	6	1.45	1.21, 1.73	0.00
4	Largehead Atractylodes + Poria + Codonopsis + Astragalus	6	1.44	1.18, 1.75	0.00
4	Liquorice + Pinellia + Codonopsis + Aucklandia	3	1.42	1.08, 1.85	0.00
4	Liquorice + Pinellia + White Paeony + Bupleurum	3	1.42	1.08, 1.88	0.00
4	Largehead Atractylodes + Poria + Codonopsis + White Paeony	5	1.40	1.13, 1.73	23.16
4	Largehead Atractylodes + Acruiginous Turmeric + Coxi Seed + Yam	4	1.39	1.12, 1.72	30.94
4	Largehead Atractylodes + Liquorice + Poria + Aurantii Fructus	3	1.38	1.05, 1.81	0.00
4	Largehead Atractylodes + Acruiginous Turmeric + Membrane of Chickens Gizzard + Crataegi	3	1.38	1.05, 1.82	0.00
5	Largehead Atractylodes + Pinellia + Acruiginous Turmeric + Astragalus + White Paeony	3	1.67	1.23, 2.27	0.00
5	Largehead Atractylodes + Acruiginous Turmeric + Astragalus + Wolfberry + Cuscuta	2	1.66	1.15, 2.41	0.00
5	Largehead Atractylodes + Liquorice + Poria + Chinese Angelica + Astragalus	4	1.59	1.19, 2.13	0.00
5	Acruiginous Turmeric + Chinese Angelica + Hedyotis Diffusa + Sparganii + Smilax	3	1.59	1.22, 2.08	0.00
5	Largehead Atractylodes + Liquorice + Poria + Codonopsis + Villous Amomum	3	1.58	1.22, 2.05	0.00
5	Largehead Atractylodes + Liquorice + Poria + Tangerine Peel + Bupleurum	3	1.58	1.22, 2.05	0.00
5	Largehead Atractylodes + Liquorice + Poria + Codonopsis + Aucklandia	4	1.55	1.19, 2.02	0.00
5	Largehead Atractylodes + Codonopsis + Tangerine Peel + Chinese Angelica + Astragalus	5	1.50	1.21, 1.87	0.00
5	Largehead Atractylodes + Poria + Codonopsis + Tangerine Peel + Aucklandia	3	1.49	1.12, 1.97	0.00
5	Largehead Atractylodes + Poria + Codonopsis + Acruiginous Turmeric + Astragalus	3	1.48	1.14, 1.93	0.00
5	Largehead Atractylodes + Liquorice + Poria + White Paeony + Bupleurum	3	1.46	1.13, 1.88	0.00
5	Largehead Atractylodes + Liquorice + Poria + Pinellia + Coptis	2	1.45	1.08, 1.94	0.00
5	Largehead Atractylodes + Liquorice + Poria + Tangerine Peel + Astragalus	5	1.45	1.17, 1.78	0.00
5	Largehead Atractylodes + Liquorice + Poria + Codonopsis + White Paeony	4	1.44	1.07, 1.93	33.23
5	Largehead Atractylodes + Poria + Codonopsis + Hedyotis Diffusa + Suberect Spatholobus	2	1.43	1.04, 1.97	0.00
5	Largehead Atractylodes + Liquorice + Poria + Hedyotis Diffusa + Scutellaria Barbata	5	1.42	1.14, 1.77	26.53
6	Largehead Atractylodes + Pinellia + Tangerine Peel + White Paeony + Scutellaria Barbata + Barley Sprout	2	2.04	1.37, 3.05	0.00
6	Largehead Atractylodes + Liquorice + Poria + Codonopsis + Tangerine Peel + Bupleurum	2	1.84	1.24, 2.72	0.00
6	Largehead Atractylodes + Acruiginous Turmeric + Coxi Seed + Yam + Scutellaria Barbata + Membrane of Chickens Gizzard	2	1.76	1.27, 2.45	0.00
6	Largehead Atractylodes + Pinellia + Coxi Seed + Inula + Haematitum	2	1.68	1.25, 2.25	0.00
6	Largehead Atractylodes + Poria + Codonopsis + Tangerine Peel + Chinese Angelica + Astragalus	4	1.59	1.25, 2.01	0.00
6	Largehead Atractylodes + Liquorice + Codonopsis + Tangerine Peel + Chinese Angelica + Astragalus	4	1.55	1.16, 2.06	0.00
6	Largehead Atractylodes + Liquorice + Poria + Pinellia + Codonopsis + Villous Amomum	2	1.53	1.11, 2.10	0.00
6	Largehead Atractylodes + Liquorice + Poria + White Paeony + Bupleurum + Aurantii Fructus	2	1.52	1.05, 2.20	0.00
6	Largehead Atractylodes + Poria + Chinese Angelica + Coxi Seed + Yam + Smilax	3	1.52	1.18, 1.95	0.00
6	Largehead Atractylodes + Liquorice + Poria + Pinellia + Codonopsis + Aucklandia	2	1.51	1.11, 2.06	0.00
6	Largehead Atractylodes + Liquorice + Poria + Tangerine Peel + Astragalus + Bupleurum	2	1.51	1.15, 1.98	0.00
6	Largehead Atractylodes + Poria + Codonopsis + Chinese Angelica + Yam + Aucklandia	3	1.51	1.13, 2.00	0.00
6	Largehead Atractylodes + Tangerine Peel + Acruiginous Turmeric + Barley Sprout + Cassia Twig + Dried Ginger	2	1.49	1.10, 2.03	3.12
6	Largehead Atractylodes + Pinellia + Acruiginous Turmeric + Membrane of Chickens Gizzard + Gekko + Dandelion	3	1.48	1.13, 1.95	0.00

(Continued on following page)

TABLE 4 (Continued) Sensitivity analysis of specific contributions of herbs.

Tier	Composition	No. of RCTs	Effect estimates (EE)	95% CI of EE	I ² statistics (%)
6	Largehead Atractylodes + Liquorice + Poria + Codonopsis + Tangerine Peel + Astragalus	4	1.47	1.13, 1.91	0.00
6	Largehead Atractylodes + Poria + Acrogenous Turmeric + Chinese Angelica + Astragalus + White Paeony	3	1.47	1.13, 1.91	0.00
6	Largehead Atractylodes + Liquorice + Poria + Pinellia + Tangerine Peel + Coptis	2	1.45	1.08, 1.94	0.00
7	Largehead Atractylodes + Liquorice + Poria + Codonopsis + Tangerine Peel + Chinese Angelica + Astragalus	3	1.75	1.25, 2.38	0.00
7	Largehead Atractylodes + Liquorice + Poria + Pinellia + Tangerine Peel + White Paeony + Bupleurum	2	1.53	1.11, 2.11	0.00
7	Largehead Atractylodes + Liquorice + Poria + Chinese Angelica + Coxi Seed + Yam + Smilax	2	1.61	1.12, 2.34	0.00
7	Largehead Atractylodes + Pinellia + Tangerine Peel + Acrogenous Turmeric + Astragalus + White Paeony + Scutellaria Barbata	2	1.86	1.31, 2.62	0.00
8	Largehead Atractylodes + Liquorice + Poria + Pinellia + Tangerine Peel + Astragalus + White Paeony + Alisma Orientale	2	1.51	1.13, 2.02	0.00
8	Largehead Atractylodes + Poria + Codonopsis + Tangerine Peel + Acrogenous Turmeric + Chinese Angelica + Astragalus + White Paeony	2	1.53	1.15, 2.04	0.00
8	Largehead Atractylodes + Poria + Codonopsis + Tangerine Peel + Chinese Angelica + Astragalus + Yam + Aucklandia	2	1.47	1.06, 2.04	0.00
8	Largehead Atractylodes + Poria + Acrogenous Turmeric + Chinese Angelica + Coxi Seed + Yam + Sparganii + Smilax	2	1.50	1.13, 1.97	0.00
9	Largehead Atractylodes + Liquorice + Poria + Codonopsis + Tangerine Peel + Chinese Angelica + Astragalus + Yam + Lotus Seed	2	1.70	1.12, 2.56	0.00
9	Acrogenous Turmeric + Chinese Angelica + Hedyotis Diffusa + Sparganii + Smilax + Red paeony + Cassia Twig + Myrrh + Frankincense	2	1.59	1.15, 2.18	0.00
10	Largehead Atractylodes + Poria + Codonopsis + Chinese Angelica + Coxi Seed + White Paeony + Yam + Aucklandia + Smilax + Hedyotis Chrysotricha	2	1.49	1.11, 2.00	0.00

3], Red Paeony [RR = 1.46, 95% CI (1.13, 1.88) $n = 4$], Chinese Angelica [RR = 1.44, 95% CI (1.27, 1.64), $n = 14$], and Astragalus [RR = 1.43, 95% CI (1.27, 1.64), $n = 13$]. Other details of the contributions of single herbs were shown in Table 4.

3.5.2 Tier 2: Combination of 2 herbs

The three most frequently used combination of 2 herbs were: Liquorice + Poria ($n = 17$), Largehead Atractylodes + White Paeony ($n = 9$), and Largehead Atractylodes + Yam ($n = 9$). The combination of 2 herbs with the five highest RR were Codonopsis Pilosula + Villous Amomum [RR = 1.70, 95% CI (1.34, 2.16), $n = 4$], Cornus + Ginseng [RR = 1.56, 95% CI (1.16, 2.10), $n = 2$], Acrogenous Turmeric + Astragalus [RR = 1.55, 95% CI (1.28, 1.88), $n = 7$], Chinese Angelica + Astragalus [RR = 1.55, 95% CI (1.28, 1.89), $n = 7$], and Chinese Angelica + Smilax [RR = 1.55, 95% CI (1.27, 1.88), $n = 5$]. Other sensitivity analysis of combination of 2 herbs were shown in Table 4.

3.5.3 Tier 3: Combination of 3 herbs

The combination of 3 herbs with the five highest RR were Chinese Angelica + Astragalus + Villous Amomum [RR = 1.73, 95% CI (1.26, 2.36), $n = 3$], Largehead Atractylodes + Wolfberry + Psoralea [RR = 1.65, 95% CI (1.24, 2.19), $n = 2$], Codonopsis + Chinese Angelica + Astragalus [RR = 1.60, 95% CI (1.30, 1.97),

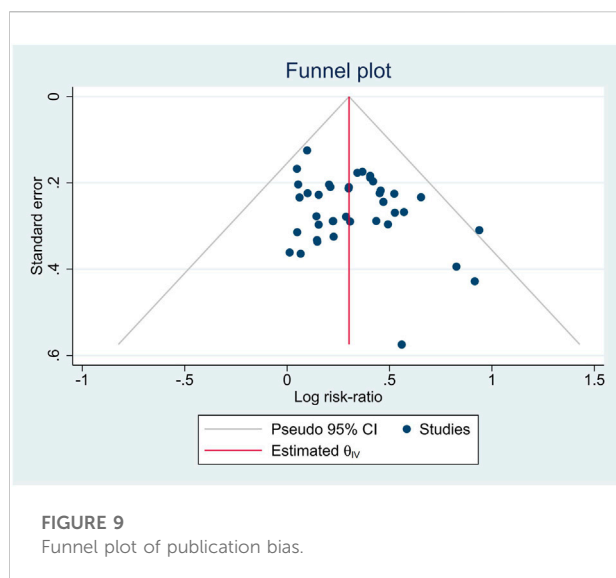
$n = 6$], Liquorice + Codonopsis + Bupleurum [RR = 1.57, 95% CI (1.14, 2.15), $n = 3$], and Pinellia + White Paeony + Dried Ginger [RR = 1.56, 95% CI (1.10, 2.21), $n = 2$]. Other sensitivity analysis of combination of 3 herbs were shown in Table 4.

3.5.4 Tier 4: Combination of 4 herbs

Two combination of 4 herbs were used more than five times: Largehead Atractylodes + Poria + Tangerine Peel + Astragalus ($n = 6$), and Largehead Atractylodes + Poria + Codonopsis + Astragalus ($n = 6$). The combination of 3 herbs with the five highest RR were Codonopsis + Chinese Angelica + Astragalus + Villous Amomum [RR = 1.95, 95% CI (1.36, 2.78), $n = 2$], Largehead Atractylodes + Pinellia + Tangerine Peel + Dandelion [RR = 1.76, 95% CI (1.24, 2.52), $n = 2$], Acrogenous Turmeric + Chinese Angelica + Astragalus + Villous Amomum [RR = 1.75, 95% CI (1.01, 3.03), $n = 2$], Liquorice + Pinellia + Tangerine Peel + Paris Polyphylla [RR = 1.74, 95% CI (1.18, 2.56), $n = 2$], and Largehead Atractylodes + Tangerine Peel + Astragalus + Yam [RR = 1.63, 95% CI (1.30, 2.05), $n = 4$]. Other sensitivity analyses were shown in Table 4.

3.5.5 Tier 5: Combination of 5 herbs

The three most frequently used combination of 5 herbs were: Largehead Atractylodes + Codonopsis + Tangerine Peel + Chinese Angelica + Astragalus ($n = 5$), Largehead



Atractylodes + Liquorice + Poria + Tangerine Peel + Astragalus ($n = 5$), and Largehead Atractylodes + Liquorice + Poria + Hedyotis Diffusa + Scutellaria Barbata ($n = 5$). The combination of 5 herbs with the two highest RR were Largehead Atractylodes + Pinellia + Acruginous Turmeric + Astragalus + White Paeony [RR = 1.67, 95% CI (1.23, 2.27), $n = 3$] and Largehead Atractylodes + Acruginous Turmeric + Astragalus + Wolfberry + Cuscuta [RR = 1.66, 95% CI (1.15, 2.41), $n = 2$]. Other sensitivity analyses were shown in Table 4.

3.5.6 Tier 6: Combination of 6 herbs or above

The three most frequently used combination of 6 or more herbs were Largehead Atractylodes + Poria + Codonopsis + Tangerine Peel + Chinese Angelica + Astragalus ($n = 4$), Largehead Atractylodes + Liquorice + Codonopsis + Tangerine Peel + Chinese Angelica + Astragalus ($n = 4$), and Largehead Atractylodes + Liquorice + Poria + Codonopsis + Tangerine Peel + Astragalus ($n = 4$). Other combination of 6 or more herbs only used 2 or 3 times in the formulas. The combination of 6 or more herbs with the three highest RR were Largehead Atractylodes + Pinellia + Tangerine Peel + White Paeony + Scutellaria Barbata + Barley Sprout [RR = 2.04, 95% CI (1.37, 3.05), $n = 2$], Largehead Atractylodes + Pinellia + Tangerine Peel + Acruginous Turmeric + Astragalus + White Paeony + Scutellaria Barbata [RR = 1.86, 95% CI (1.31, 2.62), $n = 2$], and Largehead Atractylodes + Liquorice + Poria + Codonopsis + Tangerine Peel + Bupleurum [RR = 1.84, 95% CI (1.24, 2.72), $n = 2$]. Other sensitivity analyses were shown in Table 4.

3.6 Publication bias

We assessed the publication bias with a funnel plot and Egger test. The funnel plot was shown in Figure 9A p -value = 0.1197 in

Egger test indicated that no serious publication bias was observed.

3.7 Quality of evidence

We assessed the quality of synthesized evidence of tumor response with GRADE approach. The results in subgroup analysis were adopted, since the subgroup of different chemotherapy regimen minimize the clinical heterogeneity. We got moderate to low quality of evidence, and the reasons to downgrade were that the majority of the evidence was from the trials with moderate methodological quality, and small sample size. The summary of findings was shown in Table 5.

4 Discussion

4.1 Meta-analysis of trial results

Our study showed with a moderate certainty that compare with SOX, FOLFOX or XELOX regimen alone, CHM combined with SOX, FOLFOX or XELOX could significantly improve the ORR without heterogeneity, which has a practical guiding value for the clinical application of CHM synergistic chemotherapy regimen. In addition, we also found that although the relative effect of SOX regimen was lower than that of FOLFOX and XELOX, which was due to the higher anticipated absolute effects of SOX regimen alone than that of FOLFOX and XELOX, so the improvement was not particularly significant. When SOX combined with CHM, the anticipated absolute effects had increased to 60.5%, which was higher than about 50% of other regimens. The results of our study were consistent with another previously published meta-analysis of CHM combined with paclitaxel-based chemotherapy in the treatment of AGC (Li Y. et al., 2020). Compared with paclitaxel-based chemotherapy, TCM combined with paclitaxel-based chemotherapy could also significantly improve the ORR [RR = 1.39, 95% CI (1.24–1.57), $I^2 = 12\%$]. But the prescriptions of CHM included in the above studies are not consistent, which brings more uncertain factors to the comparison.

In reducing the incidence of AEs, CHM combined with oxaliplatin-based chemotherapy showed consistent efficacy in leukopenia, thrombocytopenia, nausea and vomiting with paclitaxel-based chemotherapy, but had more improvement advantages in anemia, gastrointestinal reactions, diarrhea, hepatorenal toxicity and peripheral neurotoxicity. It is worth noting that both paclitaxel-based and oxaliplatin-based chemotherapy are clinically useful chemotherapy regimens that easily lead to peripheral neurotoxicities (Yamashita et al., 2021). However, inconsistent clinical outcomes occurred between these regimens. CHM prescriptions in our study were effective in reducing the incidence of peripheral neurotoxicity, indicating that different herbal combinations may have different effects in reducing

TABLE 5 Summary of findings.

Outcome No. of participants (studies)	Relative effect (95% CI)	Anticipated absolute effects (95% CI)			Certainty
		Oxaliplatin-based chemotherapy alone (%)	CHM combined with oxaliplatin-based chemotherapy	Risk difference	
ORR (CHM + SOX vs. SOX) of participants: 1,237 (16 RCTs)	RR 1.27 (1.15–1.40)	47.6	60.5% (54.8–66.7)	12.9% more (7.1 more to 19.1 more)	⊕⊕⊕○ Moderate ^a
ORR (CHM + FOLFOX vs. FOLFOX) No. of participants: 1,064 (15 RCTs)	RR 1.45 (1.27–1.66)	36.2	52.5% (45.9–60)	16.3% more (9.8 more to 23.9 more)	⊕⊕⊕○ Moderate ^a
ORR (CHM + XELOX vs. XELOX) No. of participants: 772 (10 RCTs)	RR 1.45 (1.22–1.72)	34.6	50.1% (42.2–59.4)	15.5% more (7.6 more to 24.9 more)	⊕⊕○○ Low ^{a,b}
DCR (CHM + SOX vs. SOX) No. of participants: 1,237 (16 RCTs)	RR 1.10 (1.05–1.15)	78.0	85.8% (81.9–89.7)	7.8% more (3.9 more to 11.7 more)	⊕⊕⊕○ Moderate ^a
DCR (CHM + FOLFOX vs. FOLFOX) No. of participants: 1,064 (15 RCTs)	RR 1.14 (1.08–1.21)	72.9	83.1% (78.8–88.2)	10.2% more (5.8 more to 15.3 more)	⊕⊕⊕○ Moderate ^a
ORR (CHM + XELOX vs. XELOX) No. of participants: 772 (10 RCTs)	RR 1.12 (1.09–1.16)	69.4	77.7% (73.7–78.4)	8.3% more (6.1 more to 10.8 more)	⊕⊕⊕○ Moderate ^a

^aMost information is from studies at moderate (Some concerns) risk of bias.

^bSmall sample size, the number of events is less than 200.

CI, confidence interval; RR, risk ratio.

Explanations.

The meaning of the bold is to highlighted the clinical value of the outcomes.

the incidence of AEs. Therefore, it is important to excavate the effects of herbs and their combinations which may affect the efficacy to guide clinical application. In addition, this study also found that the interventions of CHM was safe in AGC patients, and the participation of CHM did not increase the occurrence of AEs.

Furthermore, in order to explore the effect of CHM on the survival time of AGC, we reviewed the following studies and hope that will provide a useful reference, which is also the focus for future studies. A cohort study that 1:1 matched in Taiwan found that CHM could improve the OS rate of GC and reduce the risk of death by 45% (Hung et al., 2017). Afterward, using propensity score matching according to 1:3 also found that regardless of short-term or long-term application of TCM, compared with non-users, it could effectively reduce the risk of death by 41% or 59%, and pointed out that the most frequently used single herbal medicine was Astragalus (11.8%), and the most frequently used formula was Xiangsha Liujunzi Decoction (15.5%) [Codonopsis pilosula, Largehead Atractylodes, Poria, Liquorice, Muxiang, Amomum villosum] (Shih et al., 2021). Interestingly, these single herbs or formulas were generally consistent with the listed herbs in our study. In addition, a meta-analysis evaluating the efficacy of Astragalus-containing TCM combined with platinum-based chemotherapy for AGC suggested that compare with platinum-based chemotherapy alone, chemotherapy combined with Astragalus-containing TCM could improve ORR, DCR, 1 or 2-year survival rate, QoL and lower incidence of AEs (Cheng et al., 2021). These above studies strongly corroborated the credibility of the herbal compositions obtained in this study.

4.2 Analysis of TCM contribution

It is well-known that CHM formulas were prescriptions composed of varieties of herbs, which plays a complex and multiple effect role in clinical efficacy. Based on the characteristics of syndrome differentiation treatment, the CHM prescriptions issued by different physicians for the same disease may be different from others. Similarly, this unique treatment characteristic is significantly highlighted in this study: the specific herbs of interventions is inconsistent in clinical studies of different CHM treatments for AGC. It should be emphasized that the same herbs may be used in different studies, which provides an important basis for findings the special contribution of different herbs.

However, these herbs are not only focused on improving ORR, and perhaps some herbs pay more attention to the reduction of the occurrence of AEs to chemotherapy, or the improvement of QoL. Therefore, to eliminate the interference of other herbs, we applied sensitivity analysis to explore the effect of individual herbs on ORR in AGC one by one firstly. Then analyze the multi-herb combination containing the same herbs to further evaluate which specific herbs and their combinations are most likely to improve the ORR of chemotherapy for AGC.

Inferred to previous studies (Chen et al., 2016a; Chen et al., 2016b; Chen MH. et al., 2016), to analyze the results more cautiously, our selected herbs and compositions must have more significant differences, no heterogeneity, and equal or higher RRs within each level. Based on the above criteria,

from the results of multiple sensitivity analyses, we identified seven herbs as potential effect of synergistic action with chemotherapy for AGC: Astragalus ($n = 13$), Liquorice ($n = 23$), Poria ($n = 21$), Largehead Atractylodes ($n = 26$), Chinese Angelica ($n = 14$), Codonopsis ($n = 18$), and Tangerine Peel ($n = 17$). Among them, Dandelion and Paris Polyphylla possessed the highest effect estimate ($RR = 1.47$) in individual herb analysis. In addition, this study also analyzed the combination of herbs. It is reported that the composition of Codonopsis and Liquorice, and the composition of Codonopsis, Liquorice, Largehead Atractylodes and Poria both significantly improved the ORR of TCM combined with paclitaxel-based chemotherapy, which also provided supporting evidence for our study (Li Y. et al., 2020).

Surprisingly, some relatively high-frequency herbs such as Pinellia ($n = 20$), Acruginous Turmeric ($n = 15$), or some herbs with relatively high RR such as Dandelion [1.47 (1.17, 1.83)], Paris Polyphylla [1.47 (1.07, 2.02)], and Red Paeony [1.46 (1.13, 1.88)] in the individual herb analysis were not included in the final combination. We found that compared to the ORR under multi-herb combinations, the above potential herbs may not show a consistent effect with other herbs under multi-herb combinations. Nevertheless, these herbs also have the potential to contribute to ORR, and we found that these individual herbs with relatively high RR were mostly combined with the above 7 herbs in multi-herb combinations showing higher ORR value. Therefore, these herbs can also be considered for subsequent development.

In addition, we also excluded some highly heterogeneous herbs, such as Panax notoginseng ($I^2 = 73.56\%$), although commonly used in AGC, which seems to significantly reduce ORR [1.71, (0.84, 3.48)], but only two studies were evaluated. Notably, no negative RRs emerged for any of the herbs or combinations, suggesting that these herbs did not impair the effects of chemotherapy.

4.3 Strength and limitations

To our knowledge, this is the first meta-analysis evaluating the efficacy and safety of CHM combined with oxaliplatin-based chemotherapy in AGC. Our study suggests that the synergistic treatment of CHM may be more TRR-improving on FOLFOX and XELOX regimens, and has high safety for clinical application. In addition, this study complied strict inclusion and exclusion criteria to exclude studies without a clear randomization method, which reduces the RoB in studies and improves the reliability of results. Therefore, quality of only one outcome was classified as low, and other qualities of evidence were moderate. There was also no serious publication bias.

At the same time, our study also has several limitations. Firstly, lacks multi-center, large-sample RCTs and some of the original study sample sizes are small, which causes bias in the

results, which requires the publication of more high-quality clinical studies. Secondly, the included studies had an insufficient assessment of long-term survival indicators (OS, PFS), and our study showed that CHM could improve TRR in AGC, but whether it could translate into a benefit in long-term outcomes, also requires reassessment. In addition, CHMs are a part of TCM preparations, including Chinese patent medicines and TCM injections, and these preparation types should also be widely evaluated. Even if there have been studies on the anti-tumor efficacy of TCM preparations such as cinobufotalin (Sun et al., 2019) and brucea javanica oil injection (Wang et al., 2021) for AGC. A more comprehensive evaluation of CHM is needed to obtain more real, effective and safe evidence.

In addition, an obvious innovation point lies in exploring special herbs that have a synergistic action with chemotherapy on the ORR for AGC. The advantage of this methodology is based on the contribution of each herb to the contribution of ORR and is not simply based on the total frequency of herb emergence. A sensitivity analysis was chosen to identify the contribution of each herb in the study to ORR without missing it at a lower frequency. In summary, one cannot simply choose according to the overall frequency or the order of effect sizes of herbs in the dataset, but rather needs to consider the overall effect sizes at multiple levels simultaneously. For the selection process of final results, these herbs do not show improvement in ORR in only one clinical intervention study. In contrast, these herbs have shown consistent or higher effects in multiple studies and multiple combinations. Another limitation is that all possible combinations cannot be evaluated, and as the number of multi-herb combinations increases, the number of combinations with a significant difference and no heterogeneity is smaller, the number of corresponding clinical studies and their sample size is also reduced, and the interpretation of the results should be more cautious. And there is no clear clinical trial to evaluate the clinical efficacy of this formula, and the corresponding RCT should be carried out for evaluation in the future.

4.4 Review of anti-gastric cancer mechanisms of seven selected herbs

Similarly, we cannot clarify that the listed herbs are all for improving the efficacy of chemotherapy, however, seven herbs have been used for AGC treatment in clinical in China (Cao et al., 2009). Among them, four herbs constitute a typical formula in China, Sijunzi decoction, which has been shown to reduce the nuclear accumulation and DNA-binding activity of β -catenin, thereby repressing cell growth and inducing apoptosis in human GC MKN74 and MKN45 cells (Li et al., 2021). Network pharmacology and experimental validation suggested that Sijunzi decoction could inhibit tumor proliferation and angiogenesis by down-regulating the expression of VEGFA, iNOS, COX-2, and Bax/Bcl2 proteins in NCG-bearing mice

with human gastric adenocarcinoma cell NUGC-4, regulate the PI3K/AKT pathway, and induce apoptosis (Ding et al., 2022). To further explore how seven herbs improve the short-term efficacy of platinum-based chemotherapy for AGC, we will review each herb to assess the mechanistic evidence of the specific anti-tumor activity. We found that the number of published mechanistic studies of these herbs was uneven, with Astragalus and Liquorice being more intensively studied.

4.4.1 Astragalus

Previous study has shown that Astragalus dose-dependently stimulates dendritic cells (DCs) to express Toll-like receptor 4 (TLR4), thereby enhancing cellular immune function, and inhibiting I κ B- α protein expression and regulating NF- κ B signaling pathways (Tian et al., 2014). Secondly, after co-culture with MKN45 *in vitro*, MTT showed that Astragalus could reduce cell viability and induce apoptosis, and significantly reduce the number of cells. *In vitro* experiments also confirmed that Astragalus could significantly inhibit tumor diameter and weight, with a tumor inhibition rate of 57.1%. Another study also found that the aqueous extract of Astragalus could mediate antigen-presenting cells (APCs) to stimulate CXCR5 + Tfh-like cells to highly express IL-21, enhance humoral immunity and regulate CD8 + T cell activity (Dong et al., 2021).

In addition, the pharmacologically active components of Astragalus include polysaccharides, saponins and flavonoids, of which Astragalus polysaccharide (APS) is the most widely studied (Ma et al., 2002). In one study evaluating the anti-tumor activity of APS combined with adriamycin in human GC cell SGC-7901 and SGC-7901/ADR, the results showed that APS reduced cell viability and enhanced the rate of apoptosis in a time-dosage dependent manner, up-regulated p-AMPK and caspase-3 expression levels, induced apoptosis through the AMPK pathway, and improved the sensitivity of GC cells to adriamycin, suggesting that APS can be used as a chemosensitizer (Song et al., 2020). This paper speculated that the effect may be related to the decreased expression of MDR1, and the overexpression of tumor suppressor genes such as SEMA3F, P21^{WAF1/CIP1} and FBXW7. Similarly, APS can also inhibit the expression of phosphorylated AKT (p-AKT) and MMP-9, and then inhibit the proliferation, migration and invasion of GC AGS cells through the AKT pathway, and also induce autophagy (Wu et al., 2018). In addition, APS also has a variety of immunoregulatory activities, such as regulating B lymphocytes and cytokines, especially inducing the activation and differentiation of splenic DCs, followed by the completion of Th2 to Th1 transition and enhancing the immune function of T lymphocytes (Liu et al., 2011).

4.4.2 Liquorice

A large number of bioactive components can be isolated from Liquorice, including triterpenoid saponins, flavonoids,

isoflavones and chalcone (Asl et al., 2008). Glycyrrhizic acid (GA) is usually considered to be the main active component. The study has shown that GA can induce G1/S phase arrest of cell cycle and apoptosis by down-regulating the expression of cyclin D1, D2, D3, E1, E2, Bcl-2, survivin and p65, up-regulating the protein levels of Bax, PARP and pro-caspase-3, -8, -9. The proliferation of human GC cells (MGC-803, BGC-823, SGC-7901) has a time- and dose-dependent inhibitory effect by down-regulating PI3K/AKT signaling pathway (Wang et al., 2020).

Isoliquiritigenin (ISL) is a flavonoid extracted from Liquorice. Studies have shown that ISL can down-regulate Bcl-2 protein and p62, up-regulate Bax protein, caspase-3, Beclin 1 and LC3II/LC3I ratio, mediate apoptosis and autophagy of human GC MKN28 cells by inhibiting PI3K/AKT/mTOR signaling pathway, thereby inhibiting cell proliferation, and reducing invasion and migration (Zhang et al., 2018). ISL can also induce apoptosis in human GC MGC-803 cells by increasing free calcium concentration and decreasing mitochondrial transmembrane potential (Ma et al., 2001). However, licochalcone A (LCA), as a cytotoxic flavonoid, alone or in combination with 5-FU, increased the expression levels of Bax, PARP, tumor proteins 21, 27, 53 and caspase 3, and decreased the expression levels of Bcl-2, cyclin A, cyclin B and MDM2, which in turn blocked G 2/M cell cycle progression and induced apoptosis, inhibiting SGC7901 and MKN-45 cell proliferation in a time-dependent manner (Xiao et al., 2011; Lin et al., 2017). In addition, LCA can also increase the level of reactive oxygen species (ROS) and induce oxidative stress and apoptosis of BGC-823 cells through PI3K/AKT/mTOR and MAPK signaling cascades (Hao et al., 2015).

In addition, glycyrrhetic acid (GA) can inhibit the viability of GC cells in a dose- and time-dependent manner, but its toxic and side effects limit its wide application, thus making many beneficial explorations on related derivatives (Xu et al., 2017). For example, 11-deoxy glycyrrhetic acid can effectively inhibit GC formation by up-regulating p21 and down-regulating cdc2 and cyclin B1, mediating BID translocation from the nucleus to mitochondria, thereby inducing apoptosis and G2 phase arrest in GC cell (Lin et al., 2014). For another example, 18 β -glycyrrhetic acid (18 β -GA) can inhibit MMP-2 and MMP-9 activities in a dose-dependent manner, up-regulate E-cadherin expression and down-regulate vimentin expression, and reduce the metastatic potential of human GC cell line SGC-7901 cells through ROS/PKC- α /ERK signaling pathway and inhibition of EMT (Cai et al., 2018). In addition, new isoliquiritigenin (ISL) analogues (Huang et al., 2020), licochalcone A derivatives (LCA) (Shibata, 1994) can also provide more options for anti-GC drug research and development.

4.4.3 Poria

In vitro studies confirmed that Poria combined with oxaliplatin significantly decreased Snail, Twist, vimentin, and

N-cadherin mRNA and protein expression, significantly increased E-cadherin mRNA and protein expression, inhibited the EMT process, and decreased the invasion and migration of SGC7901 (Wang N. et al., 2018). This study also found that *Poria* could reduce the tumor volume, and improve the morphological parameters of GC cells. In addition, both dehydroeburonic acid and dehydrotrametenonic acid found from *Poria sclerotia* inhibited the growth of GC cells by arresting the G1 phase of the cell cycle, with LD (50) values of 63.6 and 38.4 microM, respectively (Mizushima et al., 2004).

4.4.4 Largehead Atractylodes

Atractylolide (AT) is the main anticancer active ingredient of Largehead Atractylodes. Atractylolide I (AT-I) has been found to inactivate the Notch signaling pathway by down-regulating the protein and mRNA expression of Notch1, Jagged1, Hes1, Hey1 and CD44, inhibiting the sphere formation ability and cell viability of HGC-27, MGC-803 and MKN-45, thereby inhibiting the self-renewal ability and cell proliferation of GC stem-like cells (GCSC) and inducing apoptosis (Ma et al., 2014). A randomized controlled trial also verified the therapeutic effect of AT-1 on GC cachexia (Liu et al., 2008). Similarly, for Atractylolide II (AT-II), Bax expression could also be up-regulated, and B-cell lymphoma 2 (Bcl-2), phosphorylated protein kinase B (p-Akt), and phosphorylated ERK (p-ERK) expression could be down-regulated, which induced apoptosis and inhibited proliferation and migration of HGC-27 and AGS in a concentration- and time-dependent manner by inactivating Ras/ERK and PI3K/Akt signaling pathways (Tian et al., 2017). AT-1 and AT-2 also inhibit Akt/I κ Ba/NF- κ B signaling pathway to play a role, thereby inhibiting gastritis to GC transformation (Amin et al., 2022). In addition, the aqueous extract of Largehead Atractylodes could inhibit the proliferation of BGC-823 and SGC-7901, decrease the mitochondrial transmembrane potential, and induce apoptosis and cell cycle arrest in a dose- and time-dependent manner (Zhao et al., 2014).

4.4.5 Chinese Angelica

Decursin is one of the active components of Chinese Angelica, which has been confirmed to down-regulate CXCR7 and Bcl-2 expression in a dose-dependent manner, mediate STAT3/c-Myc signaling pathway, induce apoptosis, and inhibit the proliferation, migration, and invasion of SNU484 and SNU216 (Kim et al., 2019). Another study by the same team also confirmed that Decursin could reduce cell viability, inhibited cell growth and induce G0/G1 arrest *in vitro* in a dose- and time-dependent manner (Kim et al., 2021). And by promoting the accumulation of LC3 and SQSTM1, inhibiting CTSC and E2F3 expression, and reducing the activity of lysosomal protein cathepsin C (CTSC), thereby inducing autophagic flux disorders. While *in vivo* studies, Decursin decreased the growth of tumor spheroids and patient-derived gastric organoids, and regulated the

expression of CTSC and autophagy-related proteins, which in turn validated the *in vivo* experimental results.

In addition, a clinical data from Taiwan verified that Chinese Angelica could prolong the survival rate of GC patients [adjusted hazard ratio (HR) 0.72 [95% CI, 0.57–0.92] ($p = 0.009$)], and experimental studies also found that N-butylidenephthalide (BP), the active component of Chinese Angelica, could induce increased REDD1 expression, inhibit mTOR signaling, activate apoptosis through the mitochondrial pathway, and inhibit the proliferation and EMT of AGS, NCI-N87, and TSGH-9201 cells (Liao et al., 2018).

4.4.6 Codonopsis

Lobetyolin (LBT) and Lobetyol are the essential components of Codonopsis. The anti-GC activity of LBT mainly depends on the regulation of glutamine metabolism, the decrease of mRNA and protein expression of amino acid transporter alanine-serine-cysteine transporter 2 (ASCT2), the induction of apoptosis and the inhibition of GC cell proliferation (Bailly, 2021). Lobetyol induced apoptosis and G1/S phase cell cycle arrest in MKN45 cells by mediating MAPK signaling pathway in a time- and dose-dependent manner (Shen et al., 2016). Both can be further considered as potential anti-GC active ingredients. In addition, the Chinese medicine formula “Weikang Keli”, containing Codonopsis and Largehead Atractylodes, can induce autophagic cell death in SGC-7901 cells. *In vitro* experiments showed that compared with the positive control of 5-FU, “Weikang Keli” aqueous extract could reduce the tumor volume in the GC model. Although the difference was not statistically significant, the motility, response sensitivity and food intake were increased (Huo et al., 2013).

4.4.7 Tangerine Peel

Nobiletin (Nob), a poly methoxy flavonoid extracted from Tangerine Peel, has been shown to inhibit MMP-9 activity in a concentration-dependent manner and to significantly reduce the total weight and number of disseminated nodules in a SCID mouse model (0.07g vs. 0.78g, $p = 0.0059$; 7.5 vs. 69.3/body, $p = 0.0001$), thereby inhibiting the proliferation of TMK-1 cell with peritoneal disseminated nodule formation, which is beneficial in preventing GC metastasis (Minagawa et al., 2001). In addition, it could also up-regulate E-cadherin protein expression and down-regulate vimentin, fibronectin, MMP-9 protein and p-STAT3 expression in SGC-7901 cell, by inhibiting the STAT3 pathway, followed by inhibiting EMT (Yang et al., 2020).

In addition, Nob-induced apoptosis is mediated by activating ER stress, decreasing phosphorylated Akt and mTOR, and mediating protective autophagy, thereby inhibiting GC proliferation in SNU-16 cells (Moon et al., 2016). And it increased Bax/Bcl-2 ratio, caspase-3/9 proteolytic activation

with degradation of poly (ADP-ribose) polymerase (PARP) protein, induced apoptosis and had a synergistic anticancer effect with 5-fluorouracil in p53-mutant SNU-16 cell (Moon et al., 2013).

5 Conclusion

Overall, CHM has a positive effect on improving oxaliplatin-based chemotherapy for AGC, which can improve short-term efficacy and reduce the incidence of AEs. In the sensitivity analysis of herbal medicines, it was found that herbal medicines such as Astragalus, Liquorice, Poria, Largehead Atractylodes, Chinese Angelica, Codonopsis, and Tangerine Peel had more advantages in increasing ORR. Previous mechanistic studies also confirmed their anti-GC activity, and the results of our study will provide beneficial evidence support for the combination therapy of CHM. Considering factors such as low quality of literature and insufficient sample size for clinical trials corresponding to shortlisted herbal medicines, quality of evidence was not high, definite conclusions cannot be drawn. More rigorously designed, large-sample, multi-center RCTs of herbal synergistic chemotherapy are needed in the future to better validate the action characteristics of CHM and its potential herbal medicines.

Author contributions

YT conceived this study. YT and HW registered the protocol and performed the search, screen, inclusion, and quality assessment of the included trials. HW and BX performed the evidence synthesis. YT, HW, and BX drafted the first version of this manuscript. XZ, GZ, YG, and TL provided critical revisions and edited the manuscript. JL and

RG revised the manuscript. All authors read and approved the final manuscript for submission.

Funding

This work was supported by Scientific and technological innovation project of China Academy of Chinese Medical Sciences (grant number CI2021A01802).

Conflict of interest

The authors declare that the research was conducted in the absence of any commercial or financial relationships that could be construed as a potential conflict of interest.

The reviewer SC declared a shared parent affiliation with the authors BX, GZ, YG, and TL at the time of review.

Publisher's note

All claims expressed in this article are solely those of the authors and do not necessarily represent those of their affiliated organizations, or those of the publisher, the editors and the reviewers. Any product that may be evaluated in this article, or claim that may be made by its manufacturer, is not guaranteed or endorsed by the publisher.

Supplementary material

The Supplementary Material for this article can be found online at: <https://www.frontiersin.org/articles/10.3389/fphar.2022.977708/full#supplementary-material>

References

- Ajani, J. A., D'Amico, T. A., Almhanna, K., Bentrem, D. J., Chao, J., Das, P., et al. (2016). Gastric cancer, version 3.2016, NCCN clinical practice guidelines in oncology. *J. Natl. Compr. Canc. Netw.* 10, 1286–1312. doi:10.6004/jncn.2016.0137
- Ajani, J. A., D'Amico, T. A., Bentrem, D. J., Chao, J., Cooke, D., Corvera, C., et al. (2022). Gastric cancer, version 2.2022, NCCN clinical practice guidelines in oncology. *J. Natl. Compr. Canc. Netw.* 20, 167–192. doi:10.6004/jncn.2022.0008
- Ajani, J. A., Moiseyenko, V. M., Tjulandin, S., Majlis, A., Constenla, M., Boni, C., et al. (2007). Clinical benefit with docetaxel plus fluorouracil and cisplatin compared with cisplatin and fluorouracil in a phase III trial of advanced gastric or gastroesophageal cancer adenocarcinoma: The V-325 study group. *J. Clin. Oncol.* 22, 3205–3209. doi:10.1200/JCO.2006.10.4968
- Al-Batran, S. E., Hartmann, J. T., Probst, S., Schmalenberg, H., Hollerbach, S., Hofheinz, R., et al. (2008). Phase III trial in metastatic gastroesophageal adenocarcinoma with fluorouracil, leucovorin plus either oxaliplatin or cisplatin: A study of the arbeitsgemeinschaft internistische onkologie. *J. Clin. Oncol.* 9, 1435–1442. doi:10.1200/JCO.2007.13.9378
- Amin, A., Hossen, M. J., Fu, X. Q., Chou, J. Y., Wu, J. Y., Wang, X. Q., et al. (2022). Inhibition of the Akt/NF- κ B pathway is involved in the anti-gastritis effects of an ethanolic extract of the rhizome of *Atractylodes macrocephala*. *J. Ethnopharmacol.* 293, 115251. doi:10.1016/j.jep.2022.115251
- Asl, M. N., and Hosseinzadeh, H. (2008). Review of pharmacological effects of *Glycyrrhiza* sp. and its bioactive compounds. *Phytother. Res.* 6, 709–724. doi:10.1002/ptr.2362
- Bailly, C. (2021). Anticancer properties of lobetyolin, an essential component of radix *Codonopsis* (dangshen). *Nat. Prod. Bioprospect.* 2, 143–153. doi:10.1007/s13659-020-00283-9
- Bang, Y. J., Kang, Y. K., Catenacci, D. V., Muro, K., Fuchs, C. S., Geva, R., et al. (2019). Pembrolizumab alone or in combination with chemotherapy as first-line therapy for patients with advanced gastric or gastroesophageal junction adenocarcinoma: Results from the phase II nonrandomized KEYNOTE-059 study. *Gastric Cancer* 4, 828–837. doi:10.1007/s10120-018-00909-5
- Bao, P. Q. (2020). Effect of Yiqi Huoxue Recipe combined with SOX chemotherapy on serum tumor markers, T lymphocyte subsets and quality of life in patients with stage III-IV gastric cancer. *Int. Med. Health Guid.* 2, 241–243+248. doi:10.3760/cma.j.issn.1007-1245.2020.02.028

- Cai, H., Chen, X., Zhang, J., and Wang, J. (2018). 18 β -glycyrrhetic acid inhibits migration and invasion of human gastric cancer cells via the ROS/PKC- α /ERK pathway. *J. Nat. Med.* 1, 252–259. doi:10.1007/s11418-017-1145-y
- Cai, J. Y., Jin, Y., Lin, H., Gan, J. W., Yue, S. B., and Chen, Q. T. (2019). Efficacy of tumor response and quality of life of traditional Chinese medicine of strengthening spleen and reinforcing qi in the treatment of advanced gastric cancer. *Mod. J. Integr. Traditional Chin. West. Med.* 33, 3711–3714. doi:10.3969/j.issn.1008-8849.2019.33.016
- Cao, W., and Zhao, A. G. (2009). Prescription rules of Chinese herbal medicines in treatment of gastric cancer. *Zhong Xi Yi Jie He Xue Bao* 1, 1–8. doi:10.3736/jcim20090101
- Chen, K., Wang, Q. C., Yin, H., Duan, W. M., and Gao, Y. (2007). Clinical observation of chemotherapy combined with TCM syndrome differentiation treatment in advanced gastric cancer. *Chin. J. Clin. Healthc.* 3, 275–277. doi:10.3969/j.issn.1672-6790.2007.03.021
- Chen, M., May, B. H., Zhou, I. W., Sze, D. M., Xue, C. C., and Zhang, A. L. (2016a). Oxaliplatin-based chemotherapy combined with traditional medicines for neutropenia in colorectal cancer: A meta-analysis of the contributions of specific plants. *Crit. Rev. Oncol. Hematol.* 105, 18–34. doi:10.1016/j.critrevonc.2016.07.002
- Chen, M., May, B. H., Zhou, I. W., Xue, C. C., and Zhang, A. L. (2016b). Meta-analysis of oxaliplatin-based chemotherapy combined with traditional medicines for colorectal cancer: Contributions of specific plants to tumor response. *Integr. Cancer Ther.* 1, 40–59. doi:10.1177/1534735415596424
- Chen, M. H., May, B. H., Zhou, I. W., Zhang, A. L., and Xue, C. C. (2016c). Integrative medicine for relief of nausea and vomiting in the treatment of colorectal cancer using oxaliplatin-based chemotherapy: A systematic review and meta-analysis. *Phytother. Res.* 5, 741–753. doi:10.1002/ptr.5586
- Cheng, M. Q., Hu, J. Q., Zhao, Y., Jiang, W. J. L., Qi, R. Z., Chen, S. T., et al. (2021). Efficacy and safety of astragalus-containing traditional Chinese medicine combined with platinum-based chemotherapy in advanced gastric cancer: A systematic review and meta-analysis. *Front. Oncol.* 11, 632168. doi:10.3389/fonc.2021.632168
- Chi, H. C., Zhao, W. S., Yang, Z., Hu, F. S., and Zhang, Q. (2010). Effective observation on treating advanced gastric cancer by Yiqi Huoxue plus FOLFOX4. *Clin. J. Chin. Med.* 11, 77–79. doi:10.3969/j.issn.1674-7860.2010.11.047
- Chu, R. G., Guo, H. F., Xie, H., Wu, L., Wu, H. Y., Shi, M., et al. (2017). Effect of zhangshi yiwei decoction on T-lymphocyte subsets of advanced gastric cancer. *Guangming J. Chin. Med.* 4, 499–502. doi:10.3969/j.issn.1003-8914.2017.04.018
- Cunningham, D., Starling, N., Rao, S., Iveson, T., Nicolson, M., Coxon, F., et al. (2008). Capecitabine and oxaliplatin for advanced esophagogastric cancer. *N. Engl. J. Med.* 1, 36–46. doi:10.1056/NEJMoa073149
- Diao, Z., Wang, C., Liu, X. C., and Tang, Y. H. (2018). The clinic effects of Shenlian capsule, trastuzumab combined with SOX regimen in the treatment for HER-2 positive advanced gastric carcinoma. *Int. J. Trad. Chin. Med.* 11, 1020–1024. doi:10.13288/j.11-2166/r.2015.02.009
- Digkila, A., and Wagner, A. D. (2016). Advanced gastric cancer: Current treatment landscape and future perspectives. *World J. Gastroenterol.* 8, 2403–2414. doi:10.3748/wjg.v22.i8.2403
- Ding, P., Guo, Y., Wang, C., Chen, J., Guo, C., Liu, H., et al. (2022). A network pharmacology approach for uncovering the antitumor effects and potential mechanisms of the Sijunzi decoction for the treatment of gastric cancer. *Evid. Based. Complement. Altern. Med.* 2022, 9364313. doi:10.1155/2022/9364313
- Dong, Q., Pu, J., Du, T., Xu, S., Liu, W., Liu, L., et al. (2021). Astragalus-mediated stimulation on antigen-presenting cells could result in higher IL-21 production from CXCR5+ Tfh-like cells and better IL-21-mediated effector functions. *Hum. Immunol.* 6, 429–437. doi:10.1016/j.humimm.2021.03.012
- Egger, M., Smith, G. D., Schneider, M., and Minder, C. (1997). Bias in meta analysis detected by a simple, graphical test. *BMJ* 315, 629–634. doi:10.1136/bmj.315.7109.629
- Fan, J. L., Li, D. F., Jiao, J., Tang, J. Y., Hou, F. F., and Hu, Y. (2015). Effect of combined treatment of Weifu formula and chemotherapy on the quality of life in advanced gastric carcinoma patients with spleen deficiency and toxin accumulation syndrome. *J. Tradit. Chin. Med.* 2, 120–123. doi:10.13288/j.11-2166/r.2015.02.009
- Feng, T. M., Wang, E. Q., and Wu, D. P. (2021). Effects of modified xuezheng decoction combined with western medicine on serum CEA and CA199 in patients with advanced gastric cancer. *West. J. Traditional Chin. Med.* 8, 126–129. doi:10.12174/j.issn.2096-9600.2021.08.29
- Feng, Y. L. (2017). *Clinical observation of gancao xiexin decoction combined with SOX chemotherapy in treating gastric adenocarcinoma (syndrome of dampness-heat due to spleen deficiency)*. Chendu: Chendu University of Traditional Chinese Medicine.
- Gong, M. (2020). Efficacy and safety of wenyang sanjie decoction combined with chemotherapy in the treatment of advanced gastric adenocarcinoma. *Chongqing Yixue* S02, 248–250.
- Gu, N., Wang, Z. X., and Li, Z. G. (2019). Clinical efficacy of chemotherapy combined with traditional Chinese medicine in advanced gastric cancer. *Henan Med. Res.* 18, 3383–3385. doi:10.3969/j.issn.1004-437X.2019.18.066
- Guo, R. (2014). *The clinical research of jianpi xiaoji decoction combined with S-1 combined oxaliplatin chemotherapy in the treatment of advanced middle-late gastric cancer*. Zhengzhou: Zhengzhou University.
- Guyatt, G. H., Oxman, A. D., Vist, G. E., Kunz, R., Falck-Ytter, Y., Alonso-Coello, P., et al. (2008). Grade: An emerging consensus on rating quality of evidence and strength of recommendations. *BMJ* 7650, 924–926. doi:10.1136/bmj.39489.470347.AD
- Hao, W., Yuan, X., Yu, L., Gao, C., Sun, X., Wang, D., et al. (2015). Licochalcone A-induced human gastric cancer BGC-823 cells apoptosis by regulating ROS-mediated MAPKs and PI3K/AKT signaling pathways. *Sci. Rep.* 5, 10336. doi:10.1038/srep10336
- Hu, F. S. (2011). *Summary of professor Yu rencun's academic thought and clinical experience and clinical observation of yiqi huoxue jiedu recipe combined with chemotherapy in the treatment of advanced gastric cancer*. Beijing: Beijing University of Chinese Medicine.
- Hu, F., Li, C., Yang, G., Yang, Z., Zhao, W., and Zhang, Q. (2012). Clinical observation of yiqi huoxue jiedu formula combined with chemotherapy on advanced gastric cancer. *Int. J. Trad. Chin. Med.* 34, 1024–1026. doi:10.3760/cma.j.issn.1673-4246.2012.11.023
- Huang, F., Wang, J., Xu, Y., Zhang, Y., Xu, N., and Yin, L. (2020). Discovery of novel isoliquiritigenin analogue ISL-17 as a potential anti-gastric cancer agent. *Biosci. Rep.* 6, BSR20201199. doi:10.1042/BSR20201199
- Huang, J., and Hu, K. (2017). Clinical observation of jianpi yangwei prescription combined with FOLFOX4 regimen for advanced gastric cancer. *J. New Chin. Med.* 4, 121–124. doi:10.13457/j.cnki.jncm.2017.04.043
- Huang, J. Q. (2014). *Clinical observation of jianpi huayu decoction combined with chemotherapy for advanced gastric cancer of spleen deficiency and phlegm stasis syndrome*. Changsha: Hunan University of Chinese Medicine.
- Hung, K. F., Hsu, C. P., Chiang, J. H., Lin, H. J., Kuo, Y. T., Sun, M. F., et al. (2017). Complementary Chinese herbal medicine therapy improves survival of patients with gastric cancer in taiwan: A nationwide retrospective matched-cohort study. *J. Ethnopharmacol.* 199, 168–174. doi:10.1016/j.jep.2017.02.004
- Huo, J., Qin, F., Cai, X., Ju, J., Hu, C., Wang, Z., et al. (2013). Chinese medicine formula "Weikang Keli" induces autophagic cell death on human gastric cancer cell line SGC-7901. *Phytomedicine.* 2, 159–165. doi:10.1016/j.phymed.2012.10.001
- J. P. T. Higgins, J. Thomas, J. Chandler, M. Cumpston, T. Li, M. J. Page, et al. Editors (2019). *Cochrane handbook for systematic reviews of interventions version 6.0 (updated July 2019)* (London, United Kingdom: Cochrane). Available at: <http://www.training.cochrane.org/handbook>.
- Jiang, F., Liu, X. F., Gao, Y. W., Sun, X. H., and Jiang, S. Q. (2021). Effect of Jiedu sanjie recipe combined with chemotherapy on patients with advanced gastric cancer and the effect of serum VEGF and VEGFR-1. *Shaanxi J. Traditional Chin. Med.* 5, 582–585. doi:10.3969/j.issn.1000-7369.2021.05.009
- Jiao, J. Q. (2019). Application of dialectical addition and subtraction of xuezheng decoction combined with chemotherapy in patients with advanced gastric cancer and its effects on serum tumor markers and immune status. *J. Sichuan Traditional Chin. Med.* 12, 99–101.
- Johnston, F. M., and Beckman, M. (2019). Updates on management of gastric cancer. *Curr. Oncol. Rep.* 21, 67. doi:10.1007/s11912-019-0820-4
- Joshi, S. S., and Badgwell, B. D. (2021). Current treatment and recent progress in gastric cancer. *Ca. Cancer J. Clin.* 3, 264–279. doi:10.3322/caac.21657
- Kang, Y. K., Kang, W. K., Shin, D. B., Chen, J., Xiong, J., Wang, J., et al. (2009). Capecitabine/cisplatin versus 5-fluorouracil/cisplatin as first-line therapy in patients with advanced gastric cancer: A randomised phase III noninferiority trial. *Ann. Oncol.* 4, 666–673. doi:10.1093/annonc/mdn717
- Kim, S., Kim, J. E., Kim, N., Joo, M., Lee, M. W., Jeon, H. J., et al. (2019). Decursin inhibits tumor growth, migration, and invasion in gastric cancer by down-regulating CXCR7 expression. *Am. J. Cancer Res.* 9, 2007–2018.
- Kim, S., Lee, S. I., Kim, N., Joo, M., Lee, K. H., Lee, M. W., et al. (2021). Decursin inhibits cell growth and autophagic flux in gastric cancer via suppression of cathepsin C. *Am. J. Cancer Res.* 4, 1304–1320.
- Koizumi, W., Narahara, H., Hara, T., Takagane, A., Akiya, T., Takagi, M., et al. (2008). S-1 plus cisplatin versus S-1 alone for first-line treatment of advanced gastric cancer (SPIRITS trial): A phase III trial. *Lancet. Oncol.* 3, 215–221. doi:10.1016/S1470-2045(08)70035-4
- Leong, T. (2005). Chemotherapy and radiotherapy in the management of gastric cancer. *Curr. Opin. Gastroenterol.* 6, 673–678. doi:10.1097/01.mog.0000179833.28158.b7

- Li, D. C., and Xiong, Y. J. (2016). Fuzheng kang'ai prescription combined with mFOLFOX4 chemotherapy in treatment of advanced gastric cancer. *Acta Chin. Med.* 9, 1253–1257. doi:10.16368/j.issn.1674-8999.2016.09.352
- Li, D. H., Su, Y. F., Sun, C. X., and Fan, H. F. (2020). Effect of shunqi yiwei decoction combined with sox chemotherapy on advanced gastric cancer. *Acta Medica Mediterr.* 36, 2313. doi:10.19193/0393-6384_2020_4_360
- Li, Y., Sui, X., Su, Z., Yu, C., Shi, X., Johnson, N. L., et al. (2020). Meta-analysis of paclitaxel-based chemotherapy combined with traditional Chinese medicines for gastric cancer treatment. *Front. Pharmacol.* 11, 132. doi:10.3389/fphar.2020.00132
- Li, Y. J., Liao, L. L., Liu, P., Tang, P., Wang, H., and Peng, Q. H. (2021). Sijunzi decoction inhibits stemness by suppressing β -catenin transcriptional activity in gastric cancer cells. *Chin. J. Integr. Med.* 28, 702–710. doi:10.1007/s11655-021-3314-9
- Liao, K. F., Chiu, T. L., Huang, S. Y., Hsieh, T. F., Chang, S. F., Ruan, J. W., et al. (2018). Anti-cancer effects of radix Angelica sinensis (danggui) and N-butylidenephthalide on gastric cancer: Implications for REDD1 activation and mTOR inhibition. *Cell. Physiol. biochem.* 6, 2231–2246. doi:10.1159/000492641
- Lin, D., Zhong, W., Li, J., Zhang, B., Song, G., and Hu, T. (2014). Involvement of BID translocation in glycyrrhetic acid and 11-deoxy glycyrrhetic acid-induced attenuation of gastric cancer growth. *Nutr. Cancer* 3, 463–473. doi:10.1080/01635581.2013.877498
- Lin, X., Tian, L., Wang, L., Li, W., Xu, Q., and Xiao, X. (2017). Antitumor effects and the underlying mechanism of licochalcone A combined with 5-fluorouracil in gastric cancer cells. *Oncol. Lett.* 3, 1695–1701. doi:10.3892/ol.2017.5614
- Liu, L. F., Liu, Z. R., Cheng, Z. R., and Wang, C. X. (2015). Jianpi-Xiaozheng recipe combined with chemotherapy for late gastric cancer. *Int. J. Traditional Chin. Med.* 2, 126–129. doi:10.3760/cma.j.issn.1673-4246.2015.02.008
- Liu, Q. Y., Yao, Y. M., Zhang, S. W., and Sheng, Z. Y. (2011). Astragalus polysaccharides regulate T cell-mediated immunity via CD11c(high) CD45RB(low) DCs *in vitro*. *J. Ethnopharmacol.* 3, 457–464. doi:10.1016/j.jep.2010.06.041
- Liu, Y., Jia, Z., Dong, L., Wang, R., and Qiu, G. (2008). A randomized pilot study of atractylenolide I on gastric cancer cachexia patients. *Evid. Based. Complement. Altern. Med.* 3, 337–344. doi:10.1093/ecam/nem031
- Liu, Z. M., Yang, X. L., Jiang, F., Pan, Y. C., and Zhang, L. (2020). Matrine involves in the progression of gastric cancer through inhibiting miR-93-5p and upregulating the expression of target gene AHNK. *J. Cell. Biochem.* 3, 2467–2477. doi:10.1002/jcb.29469
- Liu, Z. W., Wang, D. L., Zhao, X. F., and Zhao, P. (2019). Effect of jianpi huayu decoction on immune function and toxicity for patients with gastric cancer before and after chemotherapy. *J. Sichuan Traditional Chin. Med.* 10, 92–96.
- Long, Y. J. (2021). *Clinical observation of yiqi fuyuan paste combined with chemotherapy in the treatment of advanced gastric cancer of spleen qi deficiency syndrome*. Changsha: Hunan University of Chinese Medicine.
- Ma, J., Fu, N. Y., Pang, D. B., Wu, W. Y., and Xu, A. L. (2001). Apoptosis induced by isoliquiritigenin in human gastric cancer MGC-803 cells. *Planta Med.* 8, 754–757. doi:10.1055/s-2001-18361
- Ma, L., Mao, R., Shen, K., Zheng, Y., Li, Y., Liu, J., et al. (2014). Atractylenolide I-mediated Notch pathway inhibition attenuates gastric cancer stem cell traits. *Biochem. Biophys. Res. Commun.* 1, 353–359. doi:10.1016/j.bbrc.2014.05.110
- Ma, X. Q., Shi, Q., Duan, J. A., Dong, T. T., and Tsim, K. W. (2002). Chemical analysis of radix astragali (huangqi) in China: A comparison with its adulterants and seasonal variations. *J. Agric. Food Chem.* 17, 4861–4866. doi:10.1021/jf0202279
- Minagawa, A., Otani, Y., Kubota, T., Wada, N., Furukawa, T., Kumai, K., et al. (2001). The citrus flavonoid, nobiletin, inhibits peritoneal dissemination of human gastric carcinoma in SCID mice. *Jpn. J. Cancer Res.* 12, 1322–1328. doi:10.1111/j.1349-7006.2001.tb02156.x
- Mizushima, Y., Akihisa, T., Ueki, M., Murakami, C., Kuriyama, I., Xu, X., et al. (2004). A novel DNA topoisomerase inhibitor: Dehydroeburonic acid, one of the lanostane-type triterpene acids from *Poria cocos*. *Cancer Sci.* 4, 354–360. doi:10.1111/j.1349-7006.2004.tb03215.x
- Moher, D., Liberati, A., Tetzlaff, J., and Altman, D. G. (2009). Preferred reporting items for systematic reviews and meta-analyses: The PRISMA statement. *PLoS Med.* 7, e1000097. doi:10.1371/journal.pmed.1000097
- Moon, J. Y., Cho, M., Ahn, K. S., and Cho, S. K. (2013). Nobiletin induces apoptosis and potentiates the effects of the anticancer drug 5-fluorouracil in p53-mutated SNU-16 human gastric cancer cells. *Nutr. Cancer* 2, 286–295. doi:10.1080/01635581.2013.756529
- Moon, J. Y., and Cho, S. K. (2016). Nobiletin induces protective autophagy accompanied by ER-stress mediated apoptosis in human gastric cancer SNU-16 cells. *Molecules* 7, 914. doi:10.3390/molecules21070914
- Peng, W. H., Tien, Y. C., Huang, C. Y., Huang, T. H., Liao, J. C., Kuo, C. L., et al. (2010). Fraxinus rhynchophylla ethanol extract attenuates carbon tetrachloride-induced liver fibrosis in rats via down-regulating the expressions of uPA, MMP-2, MMP-9 and TIMP-1. *J. Ethnopharmacol.* 3, 606–613. doi:10.1016/j.jep.2009.12.016
- Qin, X. G. (2012). Clinical observation of buzhang yiqi decoction combined with SOX therapy on the patient with advanced gastric cancer. *J. Pract. Traditional Chin. Intern. Med.* 10, 39–41. doi:10.3969/j.issn.1671-7813.2012.10.24
- Ren, L. Q., Li, Q., and Zhang, Y. (2020). Luteolin suppresses the proliferation of gastric cancer cells and acts in synergy with oxaliplatin. *Biomed. Res. Int.* 2020, 9396512. doi:10.1155/2020/9396512
- Shen, J., Lu, X., Du, W., Zhou, J., Qiu, H., Chen, J., et al. (2016). Lobetyol activate MAPK pathways associated with G1/S cell cycle arrest and apoptosis in MKN45 cells *in vitro* and *in vivo*. *Biomed. Pharmacother.* 81, 120–127. doi:10.1016/j.biopha.2016.03.046
- Shibata, S. (1994). Anti-tumorigenic chalcones. *Stem Cells* 1, 44–52. doi:10.1002/stem.5530120109
- Shih, W. T., Yang, P. R., Shen, Y. C., Yang, Y. H., and Wu, C. Y. (2021). Traditional Chinese medicine enhances survival in patients with gastric cancer after surgery and adjuvant chemotherapy in taiwan: A nationwide matched cohort study. *Evid. Based. Complement. Altern. Med.* 2021, 7584631. doi:10.1155/2021/7584631
- Shitara, K., Özgüroğlu, M., Bang, Y. J., Di Bartolomeo, M., Mandalà, M., Ryu, M. H., et al. (2018). Pembrolizumab versus paclitaxel for previously treated, advanced gastric or gastro-oesophageal junction cancer (KEYNOTE-061): A randomised, open-label, controlled, phase 3 trial. *Lancet* 10142, 123–133. doi:10.1016/S0140-6736(18)31257-1
- Smyth, E. C., Verheij, M., Allum, W., Cunningham, D., Cervantes, A., Arnold, D., et al. (2016). Gastric cancer: ESMO clinical practice guidelines for diagnosis, treatment and follow-up. *Ann. Oncol.* 27 (5), v38–v49. doi:10.1093/annonc/mdw350
- Song, J., Chen, Y., He, D., Tan, W., Lv, F., Liang, B., et al. (2020). Astragalus polysaccharide promotes adriamycin-induced apoptosis in gastric cancer cells. *Cancer Manag. Res.* 12, 2405–2414. doi:10.2147/CMAR.S237146
- Song, Z., Wu, Y., Yang, J., Yang, D., and Fang, X. (2017). Progress in the treatment of advanced gastric cancer. *Tumour Biol.* 7, 1010428317714626. doi:10.1177/1010428317714626
- Sterne, J. A. C., Savović, J., Page, M. J., Elbers, R. G., Blencowe, N. S., Boutron, I., et al. (2019). RoB 2: A revised tool for assessing risk of bias in Randomised Trials. *BMJ* 366, 14898. doi:10.1136/bmj.14898
- Sun, B., Zhou, L., Wang, X. L., Zhou, D. Y., and Li, Z. Q. (2020). Clinical study of self-made fuzheng kang'ai decoction combined with FOLFOX6 chemotherapy on symptoms, signs and quality of life for patients with stage III-IV gastric cancer. *J. Sichuan Traditional Chin. Med.* 12, 101–104.
- Sun, H., Wang, W., Bai, M., and Liu, D. (2019). Cinobufotalin as an effective adjuvant therapy for advanced gastric cancer: A meta-analysis of randomized controlled trials. *Onco. Targets. Ther.* 12, 3139–3160. doi:10.2147/OTT.S196684
- Sung, H., Ferlay, J., Siegel, R. L., Laversanne, M., Soerjomataram, I., Jemal, A., et al. (2021). Global cancer statistics 2020: GLOBOCAN estimates of incidence and mortality worldwide for 36 cancers in 185 countries. *Ca. Cancer J. Clin.* 3, 209–249. doi:10.3322/caac.21660
- Thuss-Patience, P. C., Shah, M. A., Ohtsu, A., Van Cutsem, E., Ajani, J. A., Castro, H., et al. (2017). Trastuzumab emtansine versus taxane use for previously treated HER2-positive locally advanced or metastatic gastric or gastro-oesophageal junction adenocarcinoma (GATSBY): An international randomised, open-label, adaptive, phase 2/3 study. *Lancet. Oncol.* 5, 640–653. doi:10.1016/S1470-2045(17)30111-0
- Tian, S., and Yu, H. (2017). Atractylenolide II inhibits proliferation, motility and induces apoptosis in human gastric carcinoma cell lines HGC-27 and AGS. *Molecules* 11, 1886. doi:10.3390/molecules22111886
- Tian, Y., Li, X., Li, H., Lu, Q., Sun, G., and Chen, H. (2014). Astragalus mongholicus regulate the Toll-like-receptor 4 mediated signal transduction of dendritic cells to restrain stomach cancer cells. *Afr. J. Tradit. Complement. Altern. Med.* 3, 92–96. doi:10.4314/ajtcam.v11i3.13
- Van Cutsem, E., Moiseyenko, V. M., Tjulandin, S., Majlis, A., Constenla, M., Boni, C., et al. (2006). Phase III study of docetaxel and cisplatin plus fluorouracil compared with cisplatin and fluorouracil as first-line therapy for advanced gastric cancer: A report of the V325 study group. *J. Clin. Oncol.* 31, 4991–4997. doi:10.1200/JCO.2006.06.8429
- Van Cutsem, E., Valderrama, A., Bang, Y. J., Fuchs, C. S., Shitara, K., Janjigian, Y. Y., et al. (2021). Quality of life with first-line pembrolizumab for PD-L1-positive advanced gastric/gastroesophageal junction adenocarcinoma: Results from the randomised phase III KEYNOTE-062 study. *ESMO Open* 4, 100189. doi:10.1016/j.esmoop.2021.100189
- Wagner, A. D., Grothe, W., Haerting, J., Kleber, G., Grothey, A., and Fleig, W. E. (2006). Chemotherapy in advanced gastric cancer: A systematic review and meta-

analysis based on aggregate data. *J. Clin. Oncol.* 18, 2903–2909. doi:10.1200/JCO.2005.05.0245

Wang, H., Ge, X., Qu, H., Wang, N., Zhou, J., Xu, W., et al. (2020). Glycyrrhizic acid inhibits proliferation of gastric cancer cells by inducing cell cycle arrest and apoptosis. *Cancer Manag. Res.* 12, 2853–2861. doi:10.2147/CMAR.S244481

Wang, N., Liu, D., Guo, J., Sun, Y., Guo, T., and Zhu, X. (2018). Molecular mechanism of Poria cocos combined with oxaliplatin on the inhibition of epithelial-mesenchymal transition in gastric cancer cells. *Biomed. Pharmacother.* 102, 865–873. doi:10.1016/j.biopha.2018.03.134

Wang, X., Wang, H., Cao, L., Wu, J., Lu, T., Li, S., et al. (2021). Efficacy and safety of brucea javanica oil emulsion injection in the treatment of gastric cancer: A systematic review and meta-analysis. *Front. Nutr.* 8, 784164. doi:10.3389/fnut.2021.784164

Wang, Y., Li, Z. P., Qian, W. T., Jia, Z. J., Li, W. B., He, Y. M., et al. (2018). Treated HER2 negative advanced metastatic gastric cancer by combining guishao Liujuanzi decoction with SOX regimen. *J. Anhui Sci. Technol. Univ.* 5, 48–52.

Wu, J., Yu, J., Wang, J., Zhang, C., Shang, K., Yao, X., et al. (2018). Astragalus polysaccharide enhanced antitumor effects of Apatinib in gastric cancer AGS cells by inhibiting AKT signalling pathway. *Biomed. Pharmacother.* 100, 176–183. doi:10.1016/j.biopha.2018.01.140

Xiang, S., Zhao, Z., Zhang, T., Zhang, B., Meng, M., Cao, Z., et al. (2020). Triptonide effectively suppresses gastric tumor growth and metastasis through inhibition of the oncogenic Notch1 and NF- κ B signaling pathways. *Toxicol. Appl. Pharmacol.* 388, 114870. doi:10.1016/j.taap.2019.114870

Xiao, X. Y., Hao, M., Yang, X. Y., Ba, Q., Li, M., Ni, S. J., et al. (2011). Licochalcone A inhibits growth of gastric cancer cells by arresting cell cycle progression and inducing apoptosis. *Cancer Lett.* 1, 69–75. doi:10.1016/j.canlet.2010.12.016

Xie, W. S. (2019). *The clinical observation of wendan decoction combined with chemotherapy in the treatment of advanced gastric cancer with the type of phlegm-damp coagulation*. Taiyuan: Shanxi University of Chinese Medicine.

Xu, B., Wu, G. R., Zhang, X. Y., Yan, M. M., Zhao, R., Xue, N. N., et al. (2017). An overview of structurally modified glycyrrhetinic acid derivatives as antitumor agents. *Molecules* 6, 924. doi:10.3390/molecules22060924

Yamashita, K., Hosoda, K., Niihara, M., and Hiki, N. (2021). History and emerging trends in chemotherapy for gastric cancer. *Ann. Gastroenterol. Surg.* 4, 446–456. doi:10.1002/ags3.12439

Yang, X. Z., Zhang, H., Cui, X. Y., Su, P. Z., and Li, Z. T. (2020). Study on the mechanism of nobiletin inhibiting the invasiveness of SGC-7901 gastric cancer cells. *Mod. Oncol.* 18, 3099–3104. doi:10.3969/j.issn.1672-4992.2020.18.001

Yang, Y., Ma, J., and Zhang, H. Y. (2018). Clinical study on 40 cases of advanced gastric cancer treated with shenyang yangwei decoction combined with capecitabine chemotherapy. *Jiangsu J. Traditional Chin. Med.* 4, 40–43. doi:10.3969/j.issn.1672-397X.2018.04.017

Yoshino, T., Arnold, D., Taniguchi, H., Pentheroudakis, G., Yamazaki, K., Xu, R. H., et al. (2018). Pan-asian adapted ESMO consensus guidelines for the management of patients with metastatic colorectal cancer: A JSMO-ESMO initiative endorsed by CSCO, KACO, MOS, SSO and TOS. *Ann. Oncol.* 1, 44–70. doi:10.1093/annonc/mdx738

Yu, D., Huang, L. P., Shao, L. L., and Tian, Y. Z. (2019). Effect of shengyang yiwei decoction combined with chemotherapy on advanced gastric cancer and its effect on immune function. *Chin. J. Traditional Med. Sci. Technol.* 4, 556–557.

Yuan, K. M. (2011). *The clinical research of effect of WD-3 combined with XELOX scheme on the quality of life in treating patients with IV period gastric carcinoma*. Nanjing: Nanjing University of Chinese Medicine.

Yuan, M. (2018). *Clinical observation of YiQi Jiedu decoction combined with chemotherapy for gastric cancer in stage IIIB-IV*. Zhengzhou: Henan University of Chinese Medicine.

Zhai, Y. R. (2019). *Clinical observation on treatment of advanced Gastric Cancer (syndrome of intermin-gled phlegm and bloodstasis) by huayu jiedu method*. Zhengzhou: Henan University of Chinese Medicine.

Zhang, H. O., Chen, W. J., Yang, S. W., Huang, H. Q., Huang, M. H., Tang, S. H., et al. (2021). Evaluation of curative effect of traditional Chinese medicine treatment for advanced gastric cancer. *Fujian J. Traditional Chin. Med.* 11, 15–17. doi:10.3969/j.issn.1000-338X.2021.11.004

Zhang, H. (2021b2021). *The clinical observation of all nourishing decoction combined with chemotherapy in the treatment of advanced gastric cancer with qi blood deficiency and stasis syndrome*. Fuzhou: Fujian University of Traditional Chinese Medicine.

Zhang, H. W. (2021a2021). *Pei's shugan yangwei decoction combined with SOX regimen chemotherapy under treatment clinical observation of advanced gastric cancer*. Lanzhou: Gansu University of Chinese Medicine.

Zhang, L., Xiao, Y., Yang, R., Wang, S., Ma, S., Liu, J., et al. (2021). Systems pharmacology to reveal multi-scale mechanisms of traditional Chinese medicine for gastric cancer. *Sci. Rep.* 1, 22149. doi:10.1038/s41598-021-01535-5

Zhang, L. H., Zhao, C. J., Wu, H., Dang, Y. Y., and Zheng, J. (2020). Exploration on the effect of shengyang yiwei decoction plus reduction in chemotherapy for advanced gastric cancer patients with wet resistance syndrome of Yang deficiency. *World Chin. Med.* 24, 3792–3796. doi:10.3969/j.issn.1673-7202.2020.24.012

Zhang, X. R., Wang, S. Y., Sun, W., and Wei, C. (2018). Isoliquiritigenin inhibits proliferation and metastasis of MKN28 gastric cancer cells by suppressing the PI3K/AKT/mTOR signaling pathway. *Mol. Med. Rep.* 3, 3429–3436. doi:10.3892/mmr.2018.9318

Zhang, Z. P. (2019). *Clinical observation of erteng sanjie capsule combined with SOX regimen in the treatment of advanced gastric cancer with spleen deficiency and phlegm stasis syndrome*. Taiyuan: Shanxi Provincial Institute of Traditional Chinese Medicine.

Zhao, H. (2011). *Experimental research on effect of kunshen granule to antiangiogenesis factors and clinical research on it treating advanced gastric cancer*. Jinan: Shandong University of Traditional Chinese Medicine.

Zhao, M., Wang, Q., Ouyang, Z., Han, B., Wang, W., Wei, Y., et al. (2014). Selective fraction of Atractylodes lancea (Thunb.) DC. and its growth inhibitory effect on human gastric cancer cells. *Cytotechnology* 2, 201–208. doi:10.1007/s10616-013-9559-1

Zhao, X. N., and Xue, W. H. (2016). Effect of jianpi huayu decoction combined with chemotherapy on advanced gastric cancer and its impact on quality of life. *Acta Chin. Med. Pharmacol.* 3, 105–108. doi:10.19664/j.cnki.1002-2392.2016.03.034

Zhao, Y. Y. (2021). Clinical efficacy of wenyang jianpi decoction supplemented with SOX regimen in the treatment of patients with advanced gastric cancer. *Acta Med. Sin.* 4, 63–67. doi:10.19296/j.cnki.1008-2409.2021-04-016

Zhong, X. S., Shen, G. Z., Qin, H. H., Liang, W. J., and Zhou, Z. L. (2021). Clinical effect of weijixiao combined with chemotherapy in advanced gastric cancer and its effect on MDSCs, treg cells and immune factors. *Mod. J. Integr. Traditional Chin. West. Med.* 9, 974–978. doi:10.3969/j.issn.1008-8849.2021.09.015

Zhong, Z. J., Hu, C., and Liu, J. Y. (2019). Efficacy of shenling baizhu san plus FOLFOLX4 on advanced gastric cancer. *Clin. J. Chin. Med.* 31, 84–86. doi:10.3969/j.issn.1674-7860.2019.31.029

Zhou, X., Wang, W., Li, P., Zheng, Z., Tu, Y., Zhang, Y., et al. (2016). Curcumin enhances the effects of 5-fluorouracil and oxaliplatin in inducing gastric cancer cell apoptosis both *in vitro* and *in vivo*. *Oncol. Res.* 1–2, 29–34. doi:10.3727/096504015X14452563486011

Zhu, X. Y., and Chen, B. S. (2011). Clinical research of traditional Chinese medicine combined with chemotherapy following palliative gastrectomy for gastric cancer. *Chin. J. Prim. Med. Pharm.* 2, 208–209. doi:10.3760/cma.j.issn.1008-6706.2011.02.033



OPEN ACCESS

EDITED BY

Massimo Lucarini,
Council for Agricultural Research and
Economics, Italy

REVIEWED BY

Michael VanSaun,
University of Kansas Medical Center,
United States
Ana Sandoval-Rodriguez,
University of Guadalajara, Mexico

*CORRESPONDENCE

Chang-Gue Son,
ckson@dju.ac.kr

SPECIALTY SECTION

This article was submitted to
Ethnopharmacology,
a section of the journal
Frontiers in Pharmacology

RECEIVED 29 March 2022

ACCEPTED 25 July 2022

PUBLISHED 29 August 2022

CITATION

Lee S-B, Hwang S-J and Son C-G
(2022), CGX, a standardized herbal
syrup, inhibits colon-liver metastasis by
regulating the hepatic
microenvironments in a splenic
injection mouse model.
Front. Pharmacol. 13:906752.
doi: 10.3389/fphar.2022.906752

COPYRIGHT

© 2022 Lee, Hwang and Son. This is an
open-access article distributed under
the terms of the [Creative Commons
Attribution License \(CC BY\)](#). The use,
distribution or reproduction in other
forums is permitted, provided the
original author(s) and the copyright
owner(s) are credited and that the
original publication in this journal is
cited, in accordance with accepted
academic practice. No use, distribution
or reproduction is permitted which does
not comply with these terms.

CGX, a standardized herbal syrup, inhibits colon-liver metastasis by regulating the hepatic microenvironments in a splenic injection mouse model

Sung-Bae Lee, Seung-Ju Hwang and Chang-Gue Son*

Institute of Bioscience and Integrative Medicine, Daejeon University, Daejeon, Korea

Background: Colon-liver metastasis is observed in approximately 50% of patients with colorectal cancer and is a critical risk factor for a low survival rate. Several clinical studies have reported that colon-liver metastasis is accelerated by pathological hepatic microenvironments such as hepatic steatosis or fibrosis. Chunggan syrup (CGX), a standardized 13-herbal mixture, has been prescribed to patients with chronic liver diseases, including fatty liver, inflammation and fibrotic change, based on preclinical and clinical evidence.

Aim of the study: In the present study, we investigated anti-liver metastatic the effects of CGX in a murine colon carcinoma (MC38)-splenic injection mouse model.

Materials and methods: C57BL/6N mice were administered with CGX (100, 200 or 400 mg/kg) for 14 days before or after MC38-splenic injection under normal and high-fat diet (HFD) fed conditions. Also, above experiment was repeated without MC38-splenic injection to explore underlying mechanism.

Results: The number of tumor nodules and liver weight with tumors were suppressed by preadministration of CGX in both normal and HFD fed mice. Regarding its mechanisms, we found that CGX administration significantly activated epithelial-cadherin (E-cadherin), but decreased vascular endothelial-cadherin (VE-cadherin) in hepatic tissues under MC38-free conditions. In addition, CGX administration significantly reduced hepatic steatosis, via modulation of lipolytic and lipogenic molecules, including activated adenosine monophosphate activated protein kinase (AMPK) and peroxisome proliferator activated receptor-alpha (PPAR α).

Conclusion: The present data indicate that CGX exerts an anti-colon-liver metastatic property via modulation of hepatic lipid related microenvironments.

KEYWORDS

colon-liver metastasis, hepatic microenvironment, chuggan syrup (CGX), herbal medicine, hepatic steatosis

Introduction

Metastasis is a critical process that determines the success or failure of cancer treatment; more than 60% of cancer-derived deaths are related to metastasis (Dillekås et al., 2019). Liver metastasis is most commonly observed by approximately 50% of colon cancer patients worldwide, while the average 5-years survival rate is notably decreased by 30%, even after surgical re-section of metastatic cancer (Simmonds et al., 2006; De Greef et al., 2016). The liver is a major target of metastasis in gastrointestinal-originated tumors because of the anatomical feature of blood flow called the portal vein (Tan, 2019). One clinical study showed that 35% of colon cancer patients who underwent a complete resection experienced liver-metastasis in 40 months (Sotelo et al., 2015).

In general, the risk of metastasis is associated with advanced levels of tumors, and an increasing number of studies have shown that the metastatic process starts at a very early stage of cancer, even when tumors are 5 mm in diameter (Kokubo et al., 2018; Takemoto et al., 2020). Researchers found that circulating tumor cells were observed in the blood of patients even after 30 days of resection of breast tumors (Sandri et al., 2010). These findings strongly suggest the importance of host-side determinants of cancer metastasis, called tumor microenvironments (TMEs) (Baghban et al., 2020). During colon-liver metastasis, colon cancer cells interact with various constituents of the liver microenvironments, such as extracellular matrix (ECM), cell adhesion molecules (CAMs), and many cellular components, including natural killer (NK) cells, Kupffer cell (KC), hepatic stellate cells (HSCs), and liver sinusoidal endothelial cells (LSECs) (Zeng et al., 2021).

Accordingly, liver microenvironments are undeniable components for metastasis. Several clinical studies have reported that pathological conditions such as hepatic steatosis, inflammation and fibrosis accelerate colon-liver metastasis (Kondo et al., 2016; Chen et al., 2021). These pathologic alterations in hepatic tissues make the liver microenvironment favorable for liver metastasis, as evidenced by animal studies (Matsusue et al., 2009; Li et al., 2020). We have previously reported that alcohol consumption aggravated the colon-liver metastatic seeding phase by upregulating the inter-cellular adhesion molecule 1 (ICAM1) and mild inflammatory changes in hepatic tissue (Im et al., 2016). These findings indicate that controlling liver microenvironments may be a strategy to reduce colon-liver metastasis.

Chunggan syrup (CGX), a multiherbal drug derived from traditional Korean medicine (TKM), has been prescribed for patients with chronic hepatic disorders. We previously observed anti-steatotic and anti-inflammatory effects *via* reducing hepatic lipid and oxidative stress in animal models (Shin et al., 2006; Kim

et al., 2013; Park et al., 2013) as well as anti-fibrotic effects of CGX in a clinical trial (Joung et al., 2020). However, how the hepatoprotective effects of CGX affect the risk of colon-liver metastasis has not yet been studied.

In the present study, we aimed to investigate the pharmaceutical effects of CGX against colon-liver metastasis using a murine colon carcinoma (MC)38-splenic injection mouse model under both normal and fat diet conditions.

Materials and methods

Preparation and fingerprinting of CGX

CGX, which consisted of 13 kinds of herbal plants that complied with the Korean Pharmacopoeia standards, was manufactured by Kyung-bang Pharmacy according to the guidelines of the Korean Food and Drug Administration (Table 1). To confirm the chemical composition of CGX, ultrahigh-performance liquid chromatography tandem mass spectrometry (UHPLC-MS/MS, Thermo Scientific, Waltham, CA, United States) was performed according to a previous study (Kim et al., 2014). The chromatogram indicated that the main chemical components of CGX were scopoletin, liquiritin, naringin, esculetin, rosmarinic acid, salvianolic acid B, poncirin, and tanshinone IIA (Sigma Aldrich, MO, United States, Figures 1A–C).

Cell culture

Murine colon carcinoma (MC)38 was purchased from Kerafast (MA, United States) and cultured at 37°C in a 5% CO₂ chamber in Dulbecco's modified Eagle medium (DMEM) with 10% fetal bovine serum (FBS) and 1% penicillin/streptomycin solution (WelGENE Inc., Kyeong-book, Korea).

Animals and experimental designs

Male C57BL/6N mice (8 weeks of age, 22–25 g) purchased from Daehan Biolink (Choong-book, Korea) were housed in a room maintained at 22 ± 2°C under a 12 h light/12 h dark cycle with a free-accessing standard diet (Zeigler Co. PA, United States) and tap water. The animal experiments were conducted in accordance with the Guide for the Care and Use of Laboratory Animals prepared by the US National Institutes of Health and were approved by the Institutional Animal Care and Use Committee of Daejeon University (DJUARB 2022-002). A total of 99 mice were used according to four different experimental de-signs (Figure 1D).

In this study, colon-liver metastasis was performed *via* splenic injection of MC38 cells according to a previous study

TABLE 1 Components of CGX.

Herbal name	Scientific name	Amounts (g)
Artemisiae Capillaris Herba	<i>Artemisia capillaris</i> Thunberg	5
Amydae Carapax	<i>Amyda sinensis</i> (Wiegmann)	5
Raphanus Seed	<i>Raphanus sativus</i> L	5
Atractylodis Rhizoma Alba	<i>Atractylodes macrocephala</i> Koidz	3
Hoelen	<i>Poria cocos</i> Wolf	3
Alismatis Rhizoma	<i>Alisma orientalis</i> (Sam.) Juzepczuk	3
Atractylodis Rhizoma	<i>Atractylodes chinensis</i> Koidzumi	3
Salviae Miltiorrhizae Radix	<i>Salvia miltiorrhiza</i> Bunge	3
Polyporus	<i>Polyporus umbellatus</i> Fries	2
Aurantii Immaturus Fructus	<i>Poncirus trifoliata</i> Rafin	2
Amomi Fructus	<i>Amomum villosum</i> Lour	2
Glycyrrhizae Radix	<i>Glycyrrhiza uralensis</i> Fisch	1
Aucklandiae Radix	<i>Aucklandia lappa</i> Decne	1

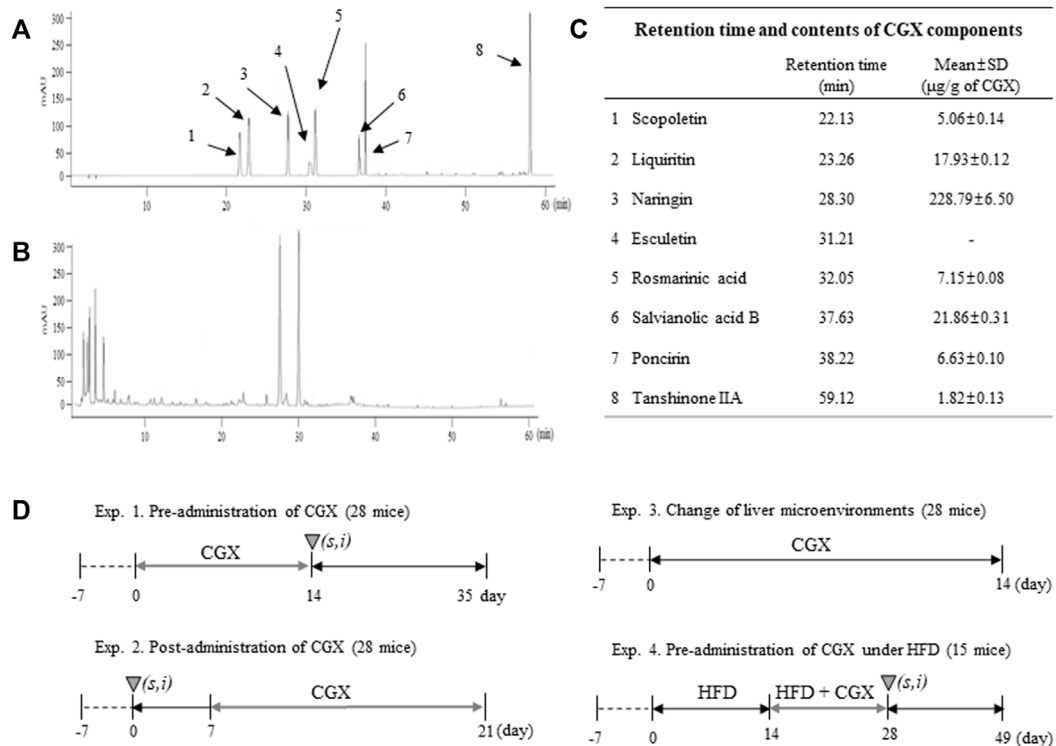


FIGURE 1

Fingerprinting of CGX and animal experimental designs. Eight reference compounds (A) in CGX (B) were analyzed using HPLC, and semiquantitative analysis was performed using their standard curves (C). The mice (99 mice in total) were used according to four different experimental designs (D).

(VanSaun et al., 2009). Briefly, the spleen was exteriorized by an incision of the left upper abdomen under anesthetization using a ketamine/xylazine mixture (90/10 mg/kg for one mouse). Then, MC38 cells (1×10^5) in 100 μL of Dulbecco's phosphate-buffered

saline (DPBS, WelGENE Inc., Kyeong-book, Korea) were slowly injected into the spleen. To allow the cells to arrive at the liver, the needle was left without removal for 90 sec, followed by removal of the spleen and ligation of the splenic vein/artery.

TABLE 2 Composition of normal chow diet and 60% high-fat diet.

Composition	Normal diet		High-fat diet	
	g %	kcal %	g %	kcal %
Carbohydrate	72	73	26	20
Protein	18	18	26	20
Fat	4	9	34	60
kcal/g	4.0		5.2	

(high fat diet/water) and HFD + CGX (high fat diet/CGX 400 mg/kg). The HFD and HFD + CGX groups were free-fed a 60% high-fat diet (HFD, Research Diets Inc. NJ, United States) for 4 weeks. Compositions of normal chow diet and HFD were described in Table 2. Beginning 2 weeks after feeding HFD, mice were orally administered water or CGX 400 mg/kg for 14 days. For all mice, splenic injection of MC38 cells (1×10^5 /mouse) was performed evenly one by one for four groups on the day of final administration of CGX. After 21 days without any manipulation, the mice were sacrificed in a CO₂ chamber. The liver weights and numbers of nodules were evaluated by two researchers who were blinded to group allocations.

Animal experiment 1

In total, 28 mice were randomly divided into four groups (each with seven mice), and all mice were orally administered water or CGX (100, 200 or 400 mg/kg) for 14 days. For all mice, a splenic injection of MC38 cells (1×10^5 /mouse) was performed evenly one by one for four groups on the day of the final administration of CGX. After 21 days without any manipulation, the mice were sacrificed in a CO₂ chamber. The liver weights and numbers of nodules were evaluated by two researchers who were blinded to group allocations.

Animal experiment 2

In total, 28 mice were administered a splenic injection of MC38 cells (1×10^5 /mouse) and allowed to recover for 7 days. Then, the mice were randomly divided into four groups (each with seven mice), and all mice were orally administered water or CGX (100, 200 or 400 mg/kg) for 14 days. Twenty-one days after the MC38 injection, all mice were sacrificed in a CO₂ chamber, and the liver weights and numbers of nodules were evaluated by two re-searchers who were blinded to group allocations.

Animal experiment 3

In total, 28 mice were randomly divided into four groups (each with seven mice), and all mice were orally administered water or CGX (100, 200 or 400 mg/kg) for 14 days. Body weights were measured once a week. After 14 days without splenic injection of MC38 cells, mice were sacrificed in a CO₂ chamber. The liver and three abdominal fats (epididymal, retroperitoneal and visceral fat) were respectively weighed, and then the blood and liver were acquired for PCR, ELISA, western blotting, and histological analysis.

Animal experiment 4

In total, 15 mice were randomly divided into three groups (each with five mice): control (normal chow diet/water), HFD

Histological analysis in hepatic tissue

To evaluate histology and fat accumulation, hepatic tissues were fixed in 10% formalin solution. The formalin in tissue was removed by storing in 10, 20, and 30% sucrose solution in a stepwise manner, and then cryosections of tissue were performed using a Leica CM3050 cryostat (Leica Microsystems). The sections were stained with hematoxylin and eosin (H&E, Sigma Aldrich, MO, United States) and Oil red O (Sigma Aldrich, MO, United States). The staining slides were visualized using microscope (Leica, Wetzlar, Germany) at 100× (H&E) and ×200 (Oil red O) magnifications, respectively.

Fat composition and lipid levels in the liver tissue

The fat composition was measured using dual-energy X-ray absorptiometry (DEXA) with an InAlyzer (Medikors Co., Seongnam, Korea). Briefly, large leaves of liver tissue were placed on the scanner bed and then scanned according to the instructions for operating the InAlyzer system. The fat mass in liver tissue was calculated as 100% of the control group, and the percentage was compared other groups. TG and TC levels were determined in normal liver tissue for normal diet feeding mice or liver tissue containing tumor for HFD feeding mice using commercial kits (ASAN pharmacy, Seoul, Korea) according to a previous method (Carr et al., 1993).

Western blotting

50 mg of hepatic tissues were dissolved in Radioimmunoprecipitation assay (RIPA) buffer and adjusted to a concentration of 1 mg/ml using the Bio-Rad protein assay reagent (Hercules, CA, United States), and then 25 µL of samples were separated by seven or 15% poly-acrylamide gel electrophoresis and transferred to polyvinylidene fluoride (PVDF) mem-branes. After blocking in 5% skim milk or bovine serum albumin (BSA) for 1 h,

TABLE 3 Primer sequences.

Primer name	Forward	Reverse
DGAT1	CATCATGTTCTCTCAAGCTTTATTCCT	ACTGACCTTCTCCCTGTAGAGACA
DGAT2	CACCCTGAAGAACCGCAA	RCTGCTTGTATACCTCATTCTCTCCAA
HMGCR	GGGCCCCACATTCACCTCTT	GCCGAAGCAGCACATGATCT
LIPE	ATGAAGGACTCACCGCTGACTT	CGGATGGCAGGTGTGAACT
MGLL	TGGTGTCTGGACTTCCAAGTTT	GAGTGGCCCAGGAGGAAGAT
ACAA2	CTCTGCCACCGATTAACTGAA	CATGACATTGCCACGATGA

DGAT1 and 2, diacylglycerol acyltransferase 1 and 2; HMGCR, hydroxy-methyl-glutaryl coenzyme A reductase; LIPE, hormone-stimulated lipase; MGLL, monoglyceride lipase; ACAA2, acetyl-coenzyme A acyltransferase 2.

the membranes were probed with primary antibodies against pAMPK (Cell Signaling, Cambridge, United Kingdom), PPAR α (Abcam, Cambridge, United Kingdom), E-cadherin (Cell Signaling, Cambridge, United Kingdom), VE-cadherin (Abcam, Cambridge, United Kingdom) and actin (Thermo Fisher Scientific, PA, United States) at 4°C overnight. Then, the membranes were washed three times for 15 min each and incubated for 2 h with HRP-conjugated anti-rabbit or anti-mouse secondary antibody. Blots were developed using an enhanced chemiluminescence (ECL) advanced kit and visualized using UV fluorescence autoexposure in the Fusion Solo S system (VILBER ROURMAT, France). Protein expression was semiquantified using ImageJ software (NIH). In the present study, Western blot data were presented with one of them as representative image.

Real-time PCR

Total RNA from the hepatic tissues was extracted using QIAzol reagent (Qiagen, Hil-den, Germany). Complementary DNA (cDNA) was synthesized using a High-Capacity cDNA Reverse Transcription Kit (Ambion, TX, United States). Real-time PCR was 40 cycles performed on diacylglycerol acyltransferase 1, 2 (DGAT one and 2), hydroxy-methyl-glutaryl coenzyme A reductase (HMGCR), hormone-sensitive lipase (LIPE), monoglyceride lipase (MGLL), acetyl-coenzyme A acyltransferase 2 (ACAA2) and β -actin under the condition below; denaturation (95°C, 15 sec), annealing (60°C, 15 sec) and extension (72°C, 1 min) using SYBR Green PCR Master Mix (Applied Biosystems, CA, United States) and Rotor-Gene Q (Qiagen, Hilden, Germany). All CT-values for above genes were normalized by β -actin and presented as fold-value. The primer sequences used in the gene expression analyses were summarized in Table 3.

Statistical analysis

The results are expressed as the means \pm standard deviation (SD, $n = 3\sim 7$). All statistical significance among the groups was

analyzed by one-way ANOVA followed by post hoc multiple comparisons (Tukey HSD) using Statistical Package for the Social Sciences (PRISM). For all analyses, $*p < 0.05$ or $**p < 0.01$ indicated statistical significance of each group compared to another group.

Results

Effects of pre- and post-administration of CGX on colon-liver metastasis

Using an MC38-splenic injection mouse model, we evaluated the anti-liver metastatic effects of both pre- or postadministration of CGX for 14 days. The preadministration of CGX significantly reduced the numbers of metastatic tumor nodules in the liver compared to the control group ($p < 0.01$, Figures 2A,B), along with a significant decrease in liver weights ($p < 0.05$ or 0.01 , Figure 2C). The postadministration of CGX also showed a slight re-duction in these parameters, but the difference did not reach statistical significance ($p > 0.05$, Figures 2D–F). The anti-liver metastatic effects of the preadministration of CGX were consistent with hematoxylin and eosin (H&E) staining in hepatic tissue (Figures 2G,H).

Effects of CGX on lipid content-related microenvironments in hepatic tissue

To investigate how CGX affected the anti-liver metastatic effects, we examined the changes in whole body and hepatic microenvironments using MC38-free conditions. There was no change in body and abdominal fat weights by CGX ($p > 0.05$, Figures 3A,B), while CGX administration (especially 400 mg/kg) significantly reduced liver weights compared to the control group ($p < 0.01$ Figure 3D). This result was confirmed by fat composition imaging ($p < 0.05$, Figures 3C,E), quantity of triglyceride (TG, $p < 0.05$ or 0.01 , Figure 3F) and total cholesterol (TC, $p < 0.05$, Figure 3G) in hepatic tissue.

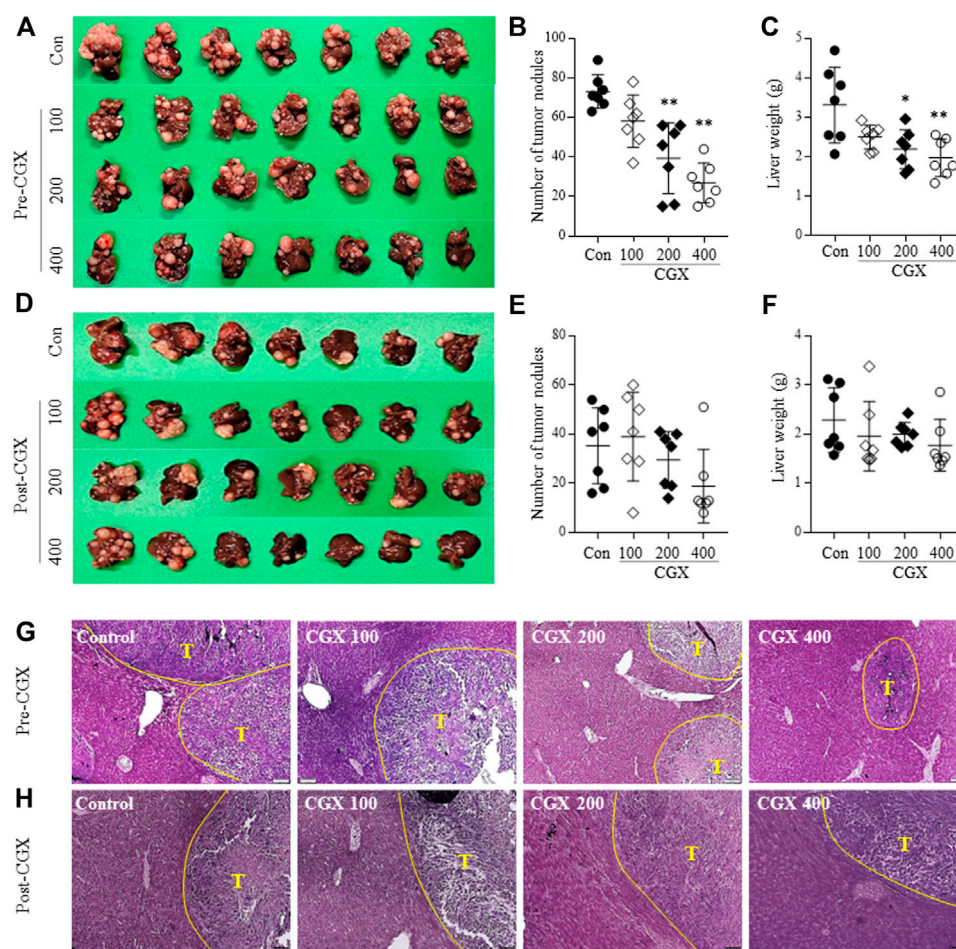


FIGURE 2

Anti-metastatic effects of pre- and postadministration of CGX. Mice were given pre- (A–C) and (G) or postadministered (D–F) CGX (100, 200 or 400 mg/kg, 14 days) via MC38-splenic injection. After 21 days of MC38-splenic injection (1×10^5 /mouse), the numbers of tumor nodules and liver weight were measured. H&E staining was performed in liver tissue and visualized at $\times 100$ magnifications (G–H). The data are expressed as the means \pm SD ($n = 7$). * $p < 0.05$ or ** $p < 0.01$ indicates statistical significance compared to the control group. T; Tumor nodule.

Effects of CGX on adherent and lipid-related molecules in hepatic tissue

To investigate the mechanisms underlying the anti-liver metastatic effects of CGX, we examined the two-representative cell-adherent molecules. CGX administration activated epithelial-cadherin (E-cadherin) in a dose-dependent manner but suppressed vascular endothelial-cadherin (VE-cadherin) at the protein level in hepatic tissues ($p < 0.01$, Figures 4A,B). In addition, we confirmed that CGX administration (especially 400 mg/kg) modulated two typical lipid metabolism-related molecules, phospho adenosine monophosphate kinase (pAMPK) and peroxisome proliferator-activated receptor alpha (PPAR α) in hepatic tissue under general condition ($p < 0.01$, Figures 4A,B). These results were supported by analyses of mRNA expression for both lipogenesis genes ($p < 0.01$ in

DGAT1) and lipolysis genes ($p < 0.05$ or $p < 0.01$ in LIPE, MGLL and ACAA2, Figure 4C).

Effects of preadministration with CGX on colon-liver metastasis under high-fat diet conditions

We confirmed the anti-liver metastatic effects of CGX (400 mg/kg) under high-fat diet (HFD)-induced fatty liver conditions. HFD dramatically accelerated the liver metastasis of colon tumors, as measured by both the number of tumor nodules and liver weight ($p < 0.01$). Then, these were effects significantly attenuated by the administration of CGX ($p < 0.05$, Figures 5A–C). As expected, the TG and TC contents in hepatic tissues were significantly reduced in CGX ($p < 0.05$, Figures

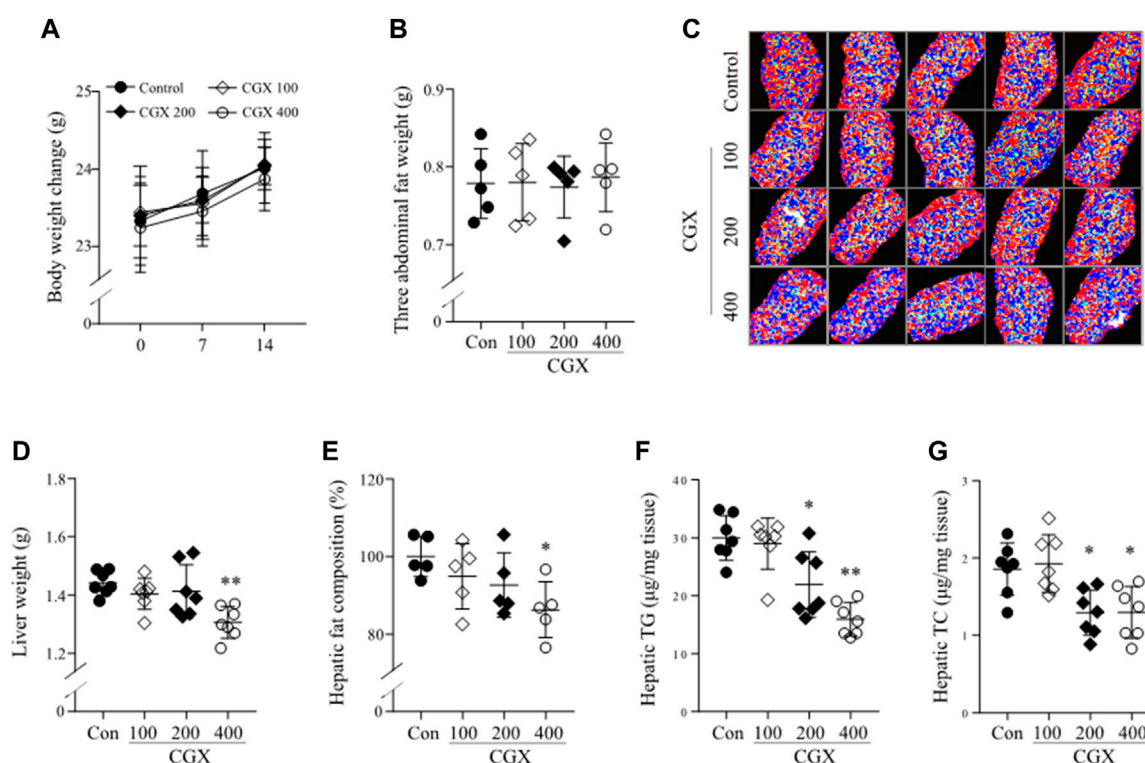


FIGURE 3

Effects of CGX on lipid components in body and hepatic tissue. Under MC38-free conditions, mice were administered with CGX (100, 200 or 400 mg/kg, 14 days). Body weight (A) was measured once a week, and the three abdominal fats (epididymal, retroperitoneal and visceral fat, (B) and liver (D) were weighed after sacrifice. The hepatic fat composition was measured using a DEXA analyzer and expressed as a relative value compared to the control group (C,E). Hepatic TG and TC were determined using commercial kits (F,G). The data are expressed as the means \pm SD ($n = 5$ or 7). * $p < 0.05$ or ** $p < 0.01$ indicates statistical significance compared to the control group. DEXA; dual energy X-ray absorptiometry, TC; total cholesterol, TG; triglyceride.

5F,G), which was confirmed by Oil Red O staining ($p < 0.05$, Figures 5D,E).

Discussion

Although therapeutic strategies for cancer have advanced, metastasis remains the main cause of cancer-related death. Metastasis is a multistep process of intravasation, survival in blood, extravasation and colonization of cancer cells (Sahai, 2007). The interaction between the tumor and the TME is known to play a key role in the success or failure of those metastatic processes (Fontebasso and Dubinett, 2015; Chandra et al., 2021). Accordingly, many recent studies emphasize the importance of the TME as a therapeutic target (Steege, 2016; Fares et al., 2020). In addition to TME in tumor-originated sites, the circumstance of liver tissue (i.e., the metastatic target-region of colorectal tumors) also markedly affects the end step of metastasis likely the acceleration of liver metastasis in inflammation, steatosis, or fibrotic change (Rossetto et al., 2019). Furthermore, symptomatic dormant cancer cells in the liver disseminated from the primary

lesion could be reactivated to proliferate into histologic metastasis under certain alterations of hepatic microenvironments (Llovet et al., 2021). From this aspect, we evaluated the anti-colon-liver metastatic effects of CGX which has been proven to exert hepatoprotective effects in many studies. Preadministration of CGX resulted in a significant reduction in liver metastasis among cancer cells (Figures 2A–C). Even though the postadministration of CGX also showed a similar pattern, the effect was weaker than the preadministration results of CGX (Figures 2D–F). These findings indicate that CGX exerts preventive but not therapeutic effects against colon-liver metastasis.

In the present study, we adapted a splenic injection-derived colon-liver metastasis model established previously (VanSaun et al., 2009). The experimental model mimics the clinical phenotype of liver metastasis, in which most tumor cells in the gastrointestinal tract mainly enter the portal vein and spread into liver tissue (Kok et al., 2021). Colon and liver metastasis occur *via* the pas-sage portal vein, which cancer cells can reach and contact LSECs (Vidal-Vanaclocha et al., 1993). CAMs in LSECs play key roles in calling the tumor cells inside the sinusoid bloodstream into hepatic tis-sue for extravasation (Paschos et al., 2009; Leong

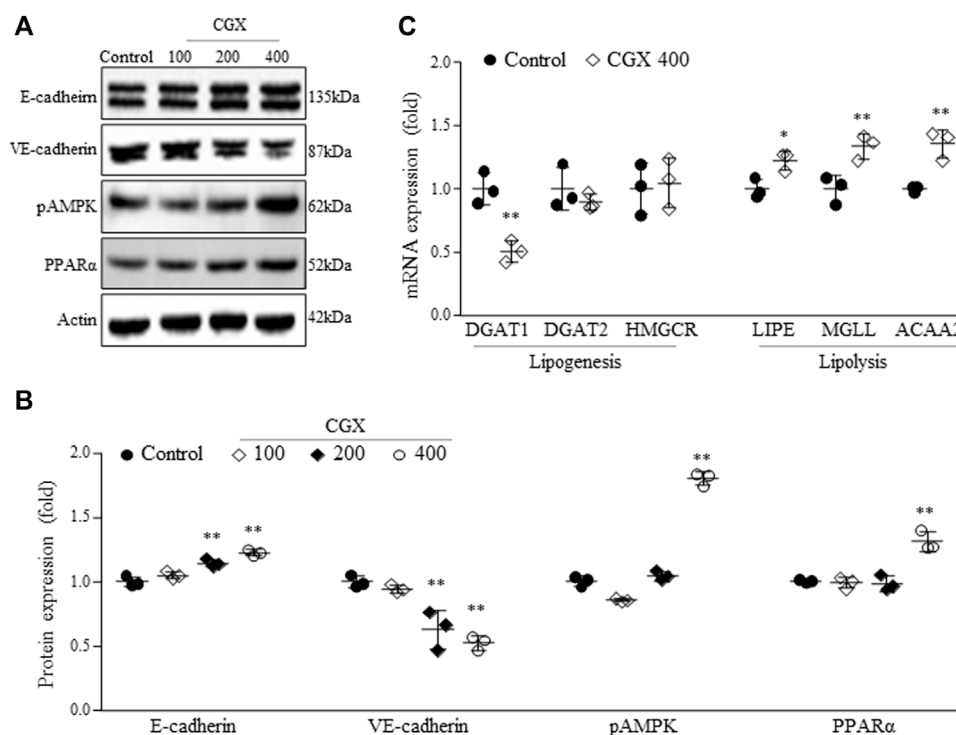


FIGURE 4

Effects of CGX on cell adhesion- and lipid metabolism-related molecules. The protein (A,B) and mRNA levels (C) were determined using western blotting and PCR, and normalized to β -actin, respectively. The data are expressed as the means \pm SD ($n = 3$). * $p < 0.05$ or ** $p < 0.01$ indicates statistical significance compared to the control group. E-cadherin; epithelial cadherin, VE-cadherin; vascular endothelial cadherin, pAMPK; phospho adenosine monophosphate kinase, PPAR α ; peroxisome proliferator-activated receptor alpha, DGAT1 and two; diacylglycerol acyltransferase 1 and 2, HMGCR; hydroxy-methyl-glutaryl coenzyme A reductase, LIPE; hormone-sensitive lipase, MGLL; monoglyceride lipase, ACAA2; acetyl-coenzyme A acyltransferase 2.

et al., 2014). CAMs in endothelial cells are also implicated in both the detachment and settlement of cancer cells in distant sites (Harjunpää et al., 2019). We found that CGX treatment significantly down- and upregulated two typical metastasis-related CAMs, VE-cadherin and E-cadherin, in liver tissue (Figures 4A,B). In fact, clinical studies have reported a significant correlation between the risk of liver metastasis and high blood levels of VE-cadherin but low levels of E-cadherin (Velikova et al., 1998; Dymicka-Piekarska and Kemonia, 2009; Okugawa et al., 2012; Rochefort et al., 2017). E-cadherin works especially at cell-cell junctions, so it protects against the extravasation of tumor cells into tissues of secondary sites (Onder et al., 2008; Samanta and Almo, 2015). Another group showed that cancer cells need to incorporate with VE-cadherin into vascular endothelial cells in the initial step of extravasation using a VE-cadherin knockout model, (Hamilla et al., 2014). Based on these facts, our data indicate that CGX may inhibit the extravasation step of colon cancer in hepatic sinusoidal vessels. Additionally, we confirmed that CGX has no effects on metastatic parameters such as intercellular adhesion molecule 1 (ICAM1), vascular cell adhesion protein 1 (VCAM1) and E-selectin (data not shown).

Components of liver including hepatocytes, KCs and HSCs play key roles colon-liver metastasis. Especially, fat excessive accumulation in hepatocyte lead to hepatic inflammation which allow those tumor cells to escape immune surveillance to colonize liver tissue (Brodt, 2016). Furthermore, it leads to activate HSCs which promote tumor growth and metastasis in liver (Matsusue et al., 2009). In clinic, nonalcoholic fatty liver disease (NAFLD) is known as an accelerator of liver metastasis, increasing the metastatic incidence by 2.5-fold in patients with colorectal cancer (Lv and Zhang, 2020). Our 28 days HFD feeding model showed dramatically increase in body weight (Supplementary Figure S1C) and mild hepatic steatosis (Figures 5D–G) which are accordance with our previous study (Hwi-Jin Im et al., 2020). Also, our HFD model severely accelerated colon-liver metastasis; the number of tumor nodules and liver weight was approximately 1.6-fold higher in the NAFLD model than in the normal diet model (Figure 5A). Then, we confirmed the anti-metastatic effects of CGX in both normal and HFD-fed mouse models. Interestingly, anti-metastatic effects showed in preadministration of CGX but not postadministration (Figures 2, 5). These effects are explained by changing the liver environment into a state that inhibits metastasis before the tumor invades the liver. Also, our results are supported by role and importance of host

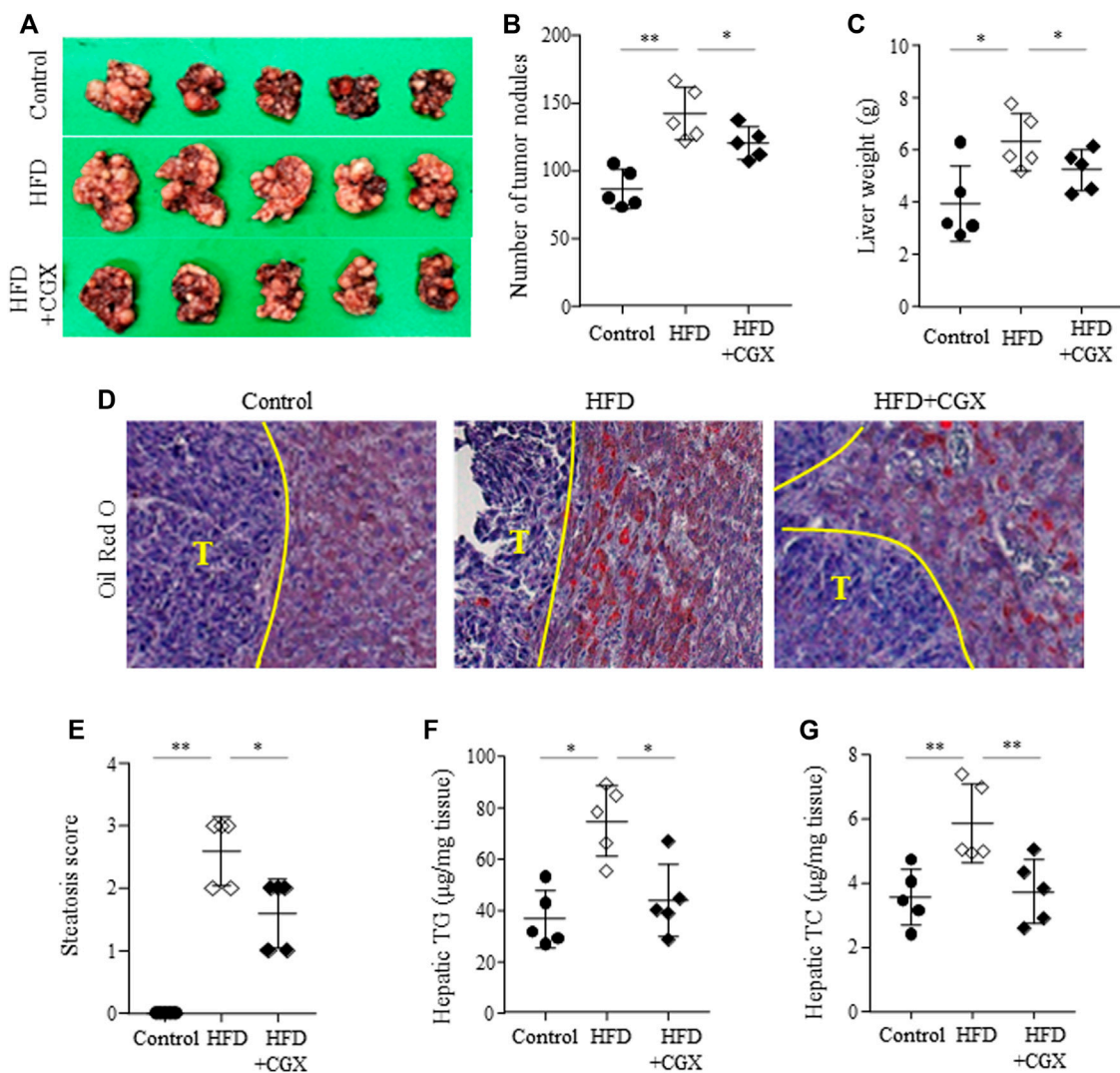


FIGURE 5

Effects of anti-metastatic effects of CGX in the HFD-induced metastasis model. Beginning 2 weeks after HFD feeding, the mice were orally administered water or CGX (400 mg/kg) for 14 days. A splenic injection of MC38 cells (1×10^5 /mouse) was performed on the day of the final administration of CGX. The liver weights and numbers of nodules were evaluated by two researchers who were blinded to group allocations (A–C). Oil red O staining was performed in the liver tissue and visualized at $\times 200$ magnifications (D). Steatosis area was scored according to the nonalcoholic steatohepatitis (NASH) clinical research network scoring system (E). Hepatic TG and TC were determined using common kits (F) and (G). The data are expressed as the means \pm SD ($n = 5$). * $p < 0.05$ or ** $p < 0.01$ indicates statistical significance compared to each group. T; Tumor nodule.

microenvironment in metastasis based on seed and soil theory (Brodt, 2016; Liu et al., 2017). In fact, our previous animal and clinical studies reported the hepatoprotective effects of CGX against hepatic inflammation and fibrosis as well as HFD or alcohol-induced hepatic steatosis (Shin et al., 2006; Kim et al., 2013; Park et al., 2013; Joung et al., 2020). These results indicate that CGX prevent metastasis *via* modulation of liver environments, especially hepatic lipid.

Regarding the anti-liver metastatic effects of CGX in the present study, we anticipated that the modulation of hepatic lipid profiles might contribute to the reduction of colon-liver metastasis (Figures 3, 4). Tumor cells require an aberrantly high supply of energy from

carbohydrates and lipids for fast growth; therefore, alteration of lipid contents and metabolism is considered one of the hallmarks of tumors (Beloribi-Djefafila et al., 2016; Jeong et al., 2021). Recent studies have showed that hepatic lipids promote liver metastasis *via* excessive increased metabolism in tumor cells (Li et al., 2020). Fatty liver conditions are also known to alter CAMs, including E-selectin, ICAM1 and VCAM1, into favorable metastasis directions in hepatic tissues (Lin et al., 2010; Oktay Bilgir, 2014). In particular, several research groups showed that VE-cadherin in liver sinusoid endothelial cells was activated in patients with NAFLD (Kan et al., 2016), and steatotic hepatocytes suppress E-cadherin

compared to normal hepatocytes (Pan et al., 2015). These facts support that CGX's inhibition of liver metastasis involves actions on hepatic lipid contents, thereby leading to modulations of VE-cadherin and E-cadherin in hepatic tissue.

CGX is an herbal syrup composed of multiple medicinal plants and is standardized as eight chemical compounds, including scopoletin, liquiritin, naringin, esculetin, rosmarinic acid, salvianolic acid B, poncirin and tanshinone IIA (Figures 1A–C). Some data using the above compounds support our results. In addition, naringin and esculetin inhibited lipid accumulation in hepatocytes *via* the modulation of gut microbiota in mouse models (Park et al., 2017; Mu et al., 2020). In the present study, although active compounds for anti-metastatic effects may be predicted *via* previous studies, it further need to identifying active compounds of CGX which have antimetastatic effects.

Taken together, our findings indicate that CGX has an anti-colon-liver metastatic effect. Its underlying mechanisms involve the modulation of liver microenvironments, including hepatic lipids and their mediated adhesion molecules (VE-cadherin and E-cadherin), and these effects is preventive but not therapeutic.

Data availability statement

The original contributions presented in the study are included in the article/Supplementary Materials, further inquiries can be directed to the corresponding author.

Ethics statement

The animal study was reviewed and approved by Institutional Animal Care and Use Committee of Daejeon University (DJUAR2022-002).

Author contributions

SL performed the overall experiments and wrote the manuscript. SH conducted H&E and Oil red O staining. CS supervised this study and edited the manuscript.

References

- Baghban, R., Roshangar, L., Jahanban-Esfahlan, R., Seidi, K., Ebrahimi-Kalan, A., Jaymand, M., et al. (2020). Tumor microenvironment complexity and therapeutic implications at a glance. *Cell Commun. Signal.* 18, 59. doi:10.1186/s12964-020-0530-4
- Beloribi-Djefafli, S., Vasseur, S., and Guillaumond, F. (2016). Lipid metabolic reprogramming in cancer cells. *Oncogenesis* 5, e189. doi:10.1038/onsis.2015.49
- Brodt, P. (2016). Role of the microenvironment in liver metastasis: From pre-to prometastatic niches. *Clin. Cancer Res.* 22, 5971–5982. doi:10.1158/1078-0432.CCR-16-0460
- Carr, T. P., Andresen, C. J., and Rudel, L. L. (1993). Enzymatic determination of triglyceride, free cholesterol, and total cholesterol in tissue lipid extracts. *Clin. Biochem.* 26, 39–42. doi:10.1016/0009-9120(93)90015-x
- Chandra, R., Karalis, J. D., Liu, C., Murimwa, G. Z., Voth Park, J., Heid, C. A., et al. (2021). The colorectal cancer tumor microenvironment and its impact on liver and lung metastasis. *Cancers* 13, 6206. doi:10.3390/cancers13246206
- Chen, H., Dai, S., Fang, Y., Chen, L., Jiang, K., Wei, Q., et al. (2021). Hepatic steatosis predicts higher incidence of recurrence in colorectal cancer liver metastasis patients. *Front. Oncol.* 11, 631943. doi:10.3389/fonc.2021.631943
- De Greef, K., Rolfó, C., Russo, A., Chapelle, T., Bronte, G., Passiglia, F., et al. (2016). Multidisciplinary management of patients with liver metastasis from colorectal cancer. *World J. Gastroenterol.* 22, 7215–7225. doi:10.3748/wjg.v22.i32.7215
- Dillekäs, H., Rogers, M. S., and Straume, O. (2019). Are 90% of deaths from cancer caused by metastases? *Cancer Med.* 8, 5574–5576. doi:10.1002/cam4.2474

Funding

This study was supported by the National Research Foundation of Korea (grant number: 2019R1A2C2088201).

Conflict of interest

The authors declare that the research was conducted in the absence of any commercial or financial relationships that could be construed as a potential conflict of interest.

Publisher's note

All claims expressed in this article are solely those of the authors and do not necessarily represent those of their affiliated organizations, or those of the publisher, the editors and the reviewers. Any product that may be evaluated in this article, or claim that may be made by its manufacturer, is not guaranteed or endorsed by the publisher.

Supplementary material

The Supplementary Material for this article can be found online at: <https://www.frontiersin.org/articles/10.3389/fphar.2022.906752/full#supplementary-material>

Supplementary Figure 1

MC38 and AML12 cells seeded in 96-well plate (2×10^3 /well), 60-mm culture dish (1×10^5 /dish) or 100-mm culture dish (3×10^5 /dish) for determination of cell viability, mRNA or protein expression. The cells were exposed CGX (1, 10, 100 or 1000 μ g/mL) for 24 h. Cell viabilities were measured using cell-based assay kit (EZ-Cytox, DoGenBio, Seoul, Korea, A). In vitro model, PCR on Ki67 (B) and western blot analysis on E-cadherin (C, D) were performed according to method of main article. In vivo, western blot analysis on E-cadherin and VE-cadherin in individual-hepatic tissue was performed according to method of main article (E). Mice were weighed on the 28 days of HFD feeding (F). * $p < 0.05$ or ** $p < 0.01$ indicates statistical significance compared to the control group. ## $p < 0.01$ indicates statistical significance compared to the HFD group. AML1; alpha mouse liver 12, CGX; chunggan syrup, E-cadherin; epithelial cadherin, HFD; high-fat diet, VE-cadherin; vascular endothelial cadherin.

- Dymicka-Piekarska, V., and Kemon, H. (2009). Does colorectal cancer clinical advancement affect adhesion molecules (sP-selectin, sE-selectin and ICAM-1) concentration? *Thromb. Res.* 124, 80–83. doi:10.1016/j.thromres.2008.11.021
- Fares, J., Fares, M. Y., Khachfe, H. H., Salhab, H. A., and Fares, Y. (2020). Molecular principles of metastasis: A hallmark of cancer revisited. *Signal Transduct. Target. Ther.* 5, 28–17. doi:10.1038/s41392-020-0134-x
- Fontebasso, Y., and Dubinett, S. M. (2015). Drug development for metastasis prevention. *Crit. Rev. Oncog.* 20, 449–473. doi:10.1615/CritRevOncog.v20.i5-6.150
- Hamilla, S. M., Stroka, K. M., and Aranda-Espinoza, H. (2014). VE-Cadherin-Independent cancer cell incorporation into the vascular endothelium precedes transmigration. *PLoS One* 9, e109748. doi:10.1371/journal.pone.0109748
- Harjunpää, H., Lloort Asens, M., Guenther, C., and Fagerholm, S. C. (2019). Cell adhesion molecules and their roles and regulation in the immune and tumor microenvironment. *Front. Immunol.* 10, 1078. doi:10.3389/fimmu.2019.101078
- Im, H.-J., Hwang, S.-J., Lee, J.-S., Lee, S.-B., Kang, J.-Y., and Son, C.-G. (2020). Ethyl acetate fraction of amomum xanthioides ameliorates nonalcoholic fatty liver disease in a high-fat diet mouse model. *Nutrients* 13(8), 2433. doi:10.3390/nut12082433
- Im, H.-J., Kim, H.-G., Lee, J.-S., Kim, H.-S., Cho, J.-H., Jo, I.-J., et al. (2016). A preclinical model of chronic alcohol consumption reveals increased metastatic seeding of colon cancer cells in the liver. *Cancer Res.* 76, 1698–1704. doi:10.1158/0008-5472.CAN-15-2114
- Jeong, D.-W., Lee, S., and Chun, Y.-S. (2021). How cancer cells remodel lipid metabolism: Strategies targeting transcription factors. *Lipids Health Dis.* 20, 163. doi:10.1186/s12944-021-01593-8
- Joung, J.-Y., Kim, H.-G., Lee, J.-S., Cho, J.-H., Ahn, Y.-C., Lee, D.-S., et al. (2020). Anti-hepatofibrotic effects of CGX, a standardized herbal formula: A multicenter randomized clinical trial. *Biomed. Pharmacother.* 126, 110105. doi:10.1016/j.biopha.2020.110105
- Kan, X., Liu, G., Yang, Y., Yang, Q., Li, Y., and Wang, F. (2016). Serum vascular endothelial cadherin and thrombomodulin are markers of non-alcoholic fatty liver disease in children. *J. Pediatr. Endocrinol. Metab.* 29, 1331–1335. doi:10.1515/jpem-2015-0328
- Kim, H.-G., Kim, J.-M., Han, J.-M., Lee, J.-S., Choi, M.-K., Lee, D.-S., et al. (2014). Chunggan extract, a traditional Korean herbal formula, ameliorated alcohol-induced hepatic injury in rat model. *World J. Gastroenterol.* 20, 15703–15714. doi:10.3748/wjg.v20.i42.15703
- Kim, H. G., Wang, J. H., Han, J. M., Hwang, S. Y., Lee, D. S., and Son, C. G. (2013). Chunggan extract (CGX), a traditional Korean herbal medicine, exerts hepatoprotective effects in a rat model of chronic alcohol consumption. *Phytother. Res.* 27, 1854–1862. doi:10.1002/ptr.4935
- Kok, S. Y., Oshima, H., Takahashi, K., Nakayama, M., Murakami, K., Ueda, H. R., et al. (2021). Malignant subclone drives metastasis of genetically and phenotypically heterogeneous cell clusters through fibrotic niche generation. *Nat. Commun.* 12, 863. doi:10.1038/s41467-021-21160-0
- Kokubo, S., Ohnuma, S., Suzuki, H., Imoto, H., Yamamura, A., Karasawa, H., et al. (2018). A small rectal neuroendocrine tumor of less than 5mm with lymph node metastasis. *Gan Kagaku Ryoho.* 45, 1985–1987.
- Kondo, T., Okabayashi, K., Hasegawa, H., Tsuruta, M., Shigeta, K., and Kitagawa, Y. (2016). The impact of hepatic fibrosis on the incidence of liver metastasis from colorectal cancer. *Br. J. Cancer* 115, 34–39. doi:10.1038/bjc.2016.155
- Leong, H. S., Robertson, A. E., Stoletov, K., Leith, S. J., Chin, C. A., Chien, A. E., et al. (2014). Invadopodia are required for cancer cell extravasation and are a therapeutic target for metastasis. *Cell Rep.* 8, 1558–1570. doi:10.1016/j.celrep.2014.07.050
- Li, Y., Su, X., Rohatgi, N., Zhang, Y., Brestoff, J. R., Shoghi, K. I., et al. (2020). Hepatic lipids promote liver metastasis. *JCI Insight* 5, e136215. doi:10.1172/jci.insight.136215
- Lin, G., Duan, X., Cai, X., Tian, L., Xu, Z., and Fan, J. (2010). Hepatocyte steatosis increases the expression of adhesion molecules in endothelial cells. *Asian Biomed.* 4, 757–763. doi:10.2478/abm-2010-0098
- Liu, Q., Zhang, H., Jiang, X., Qian, C., Liu, Z., and Luo, D. (2017). Factors involved in cancer metastasis: A better understanding to “seed and soil” hypothesis. *Mol. Cancer* 16, 176. doi:10.1186/s12943-017-0742-4
- Llovet, J. M., Kelley, R. K., Villanueva, A., Singal, A. G., Pikarsky, E., Roayaie, S., et al. (2021). Hepatocellular carcinoma. *Nat. Rev. Dis. Prim.* 7, 16018–16028. doi:10.1038/nrdp.2016.18
- Lv, Y., and Zhang, H. (2020). Effect of non-alcoholic fatty liver disease on the risk of synchronous liver metastasis: Analysis of 451 consecutive patients of newly diagnosed colorectal cancer. *Frontiers in oncology* 10. Available at: <https://www.frontiersin.org/article/10.3389/fonc.2020.00251>. (Accessed March 6, 2022).
- Matsusue, R., Kubo, H., Hisamori, S., Okoshi, K., Takagi, H., Hida, K., et al. (2009). Hepatic stellate cells promote liver metastasis of colon cancer cells by the action of SDF-1/CXCR4 Axis. *Ann. Surg. Oncol.* 16, 2645–2653. doi:10.1245/s10434-009-0599-x
- Mu, H., Zhou, Q., Yang, R., Zeng, J., Li, X., Zhang, R., et al. (2020). Naringin attenuates high fat diet induced non-alcoholic fatty liver disease and gut bacterial dysbiosis in mice. *Frontiers in microbiology* 11. Available at: <https://www.frontiersin.org/article/10.3389/fmicb.2020.585066>. (Accessed March 8, 2022).
- Oktay Bilgir, F. B. (2014). The levels of soluble intercellular adhesion molecule, vascular adhesion molecule and Se-selectin levels in patients with non-alcoholic fatty liver disease. *J. Autacoids* 05. doi:10.4172/2161-0479.1000108
- Okugawa, Y., Toiyama, Y., Inoue, Y., Iwata, T., Fujikawa, H., Saigusa, S., et al. (2012). Clinical significance of serum soluble E-cadherin in colorectal carcinoma. *J. Surg. Res.* 175, e67–e73. doi:10.1016/j.jss.2011.11.009
- Onder, T. T., Gupta, P. B., Mani, S. A., Yang, J., Lander, E. S., and Weinberg, R. A. (2008). Loss of E-cadherin promotes metastasis via multiple downstream transcriptional pathways. *Cancer Res.* 68, 3645–3654. doi:10.1158/0008-5472.CAN-07-2938
- Pan, X., Wang, P., Luo, J., Wang, Z., Song, Y., Ye, J., et al. (2015). Adipogenic changes of hepatocytes in a high-fat diet-induced fatty liver mice model and non-alcoholic fatty liver disease patients. *Endocrine* 48, 834–847. doi:10.1007/s12020-014-0384-x
- Park, H.-J., Han, J.-M., Kim, H.-G., Choi, M.-K., Lee, J.-S., Lee, H.-W., et al. (2013). Chunggan extract (CGX), methionine and choline-deficient (MCD) diet-induced hepatosteatosis and oxidative stress in C57BL/6 mice. *Hum. Exp. Toxicol.* 32, 1258–1269. doi:10.1177/0960327113485253
- Park, Y., Sung, J., Yang, J., Ham, H., Kim, Y., Jeong, H.-S., et al. (2017). Inhibitory effect of esculetin on free-fatty-acid-induced lipid accumulation in human HepG2 cells through activation of AMP-activated protein kinase. *Food Sci. Biotechnol.* 26, 263–269. doi:10.1007/s10068-017-0035-0
- Paschos, K. A., Canovas, D., and Bird, N. C. (2009). The role of cell adhesion molecules in the progression of colorectal cancer and the development of liver metastasis. *Cell. Signal.* 21, 665–674. doi:10.1016/j.cellsig.2009.01.006
- Rochefort, P., Chabaud, S., Pierga, J.-Y., Tredan, O., Brain, E., Bidard, F.-C., et al. (2017). Soluble VE-cadherin in metastatic breast cancer: An independent prognostic factor for both progression-free survival and overall survival. *Br. J. Cancer* 116, 356–361. doi:10.1038/bjc.2016.427
- Rossetto, A., De Re, V., Steffan, A., Ravaioli, M., Miolo, G., Leone, P., et al. (2019). Carcinogenesis and metastasis in liver: Cell physiological basis. *Cancers* 11, 1731. doi:10.3390/cancers11111731
- Sahai, E. (2007). Illuminating the metastatic process. *Nat. Rev. Cancer* 7, 737–749. doi:10.1038/nrc2229
- Samanta, D., and Almo, S. C. (2015). Nectin family of cell-adhesion molecules: Structural and molecular aspects of function and specificity. *Cell. Mol. Life Sci.* 72, 645–658. doi:10.1007/s00018-014-1763-4
- Sandri, M. T., Zorzino, L., Cassatella, M. C., Bassi, F., Luini, A., Casadio, C., et al. (2010). Changes in circulating tumor cell detection in patients with localized breast cancer before and after surgery. *Ann. Surg. Oncol.* 17, 1539–1545. doi:10.1245/s10434-010-0918-2
- Shin, J.-W., Son, J.-Y., Oh, S.-M., Han, S.-H., Wang, J.-H., Cho, J.-H., et al. (2006). An herbal formula, CGX, exerts hepatotherapeutic effects on dimethylnitrosamine-induced chronic liver injury model in rats. *World J. Gastroenterol.* 12, 6142–6148. doi:10.3748/wjg.v12.i38.6142
- Simmonds, P. C., Primrose, J. N., Colquitt, J. L., Garden, O. J., Poston, G. J., and Rees, M. (2006). Surgical resection of hepatic metastases from colorectal cancer: A systematic review of published studies. *Br. J. Cancer* 94, 982–999. doi:10.1038/sj.bjc.6603033
- Sotelo, M. J., Sastre, J., Maestro, M. L., Véganzones, S., Viéitez, J. M., Alonso, V., et al. (2015). Role of circulating tumor cells as prognostic marker in resected stage III colorectal cancer. *Ann. Oncol.* 26, 535–541. doi:10.1093/annonc/mdl568
- Steeg, P. S. (2016). Targeting metastasis. *Nat. Rev. Cancer* 16, 201–218. doi:10.1038/nrc.2016.25
- Takemoto, K., Harada, K., Toma, A., Imura, T., Ochiai, T., and Otsuji, E. (2020). Case of a 5mm rectal neuroendocrine tumor (G1) with lymph node metastasis. *Gan Kagaku Ryoho.* 47, 652–654.

Tan, Z. (2019). Recent advances in the surgical treatment of advanced gastric cancer: A review. *Med. Sci. Monit.* 25, 3537–3541. doi:10.12659/MSM.916475

VanSaun, M. N., Lee, I. K., Washington, M. K., Matrisian, L., and Gorden, D. L. (2009). High fat diet induced hepatic steatosis establishes a permissive microenvironment for colorectal metastases and promotes primary dysplasia in a murine model. *Am. J. Pathol.* 175, 355–364. doi:10.2353/ajpath.2009.080703

Velikova, G., Banks, R. E., Gearing, A., Hemingway, I., Forbes, M. A., Preston, S. R., et al. (1998). Serum concentrations of soluble adhesion

molecules in patients with colorectal cancer. *Br. J. Cancer* 77, 1857–1863. doi:10.1038/bjc.1998.309

Vidal-Vanaclocha, F., Rocha, M. A., Asumendi, A., and Barberá-Guillem, E. (1993). Role of periportal and perivenous sinusoidal endothelial cells in hepatic homing of blood and metastatic cancer cells. *Semin. Liver Dis.* 13, 60–71. doi:10.1055/s-2007-1007338

Zeng, X., Ward, S. E., Zhou, J., and Cheng, A. S. L. (2021). Liver immune microenvironment and metastasis from colorectal cancer-pathogenesis and therapeutic perspectives. *Cancers (Basel)* 13, 2418. doi:10.3390/cancers13102418



The Antigastric Cancer Effect of Triptolide is Associated With H19/NF- κ B/FLIP Axis

Weiwei Yuan¹, Jinxi Huang¹, Shanshan Hou², Huahua Li¹, Liangyu Bie³, Beibei Chen³, Gaofeng Li¹, Yang Zhou^{4*} and Xiaobing Chen^{3*}

¹Department of General Surgery, The Affiliated Cancer Hospital of Zhengzhou University & Henan Cancer Hospital, Zhengzhou, China, ²Department of Pharmacy, Zhejiang Pharmaceutical College, Ningbo, China, ³Department of Medical Oncology, The Affiliated Cancer Hospital of Zhengzhou University and Henan Cancer Hospital, Zhengzhou University, Zhengzhou, China, ⁴Children's Hospital Affiliated to Zhengzhou University, Henan Children's Hospital, Zhengzhou Children's Hospital, Zhengzhou University, Zhengzhou, China

OPEN ACCESS

Edited by:

Muhammad Faisal Nadeem,
University of Veterinary and Animal
Sciences, Pakistan

Reviewed by:

Hafiz Ishfaq Ahmad,
University of Veterinary and Animal
Sciences, Pakistan
Hamid Saeed Shah,
University of Veterinary and Animal
Sciences, Pakistan

*Correspondence:

Xiaobing Chen
zlyychenxb0807@zzu.edu.cn
Yang Zhou
zyangcpu@163.com

Specialty section:

This article was submitted to
Ethnopharmacology,
a section of the journal
Frontiers in Pharmacology

Received: 12 April 2022

Accepted: 02 June 2022

Published: 30 August 2022

Citation:

Yuan W, Huang J, Hou S, Li H, Bie L,
Chen B, Li G, Zhou Y and Chen X
(2022) The Antigastric Cancer Effect of
Triptolide is Associated With H19/NF- κ B/FLIP Axis.
Front. Pharmacol. 13:918588.
doi: 10.3389/fphar.2022.918588

Background and Objective: Triptolide (TP), one of the fat-soluble components extracted from the Chinese medicinal herb *Tripterygium wilfordii* Hook F. (TWHF), possesses strong antitumor bioactivities, but its dose-dependent side effects restrict its wide application. This study was designed to investigate whether inflammatory factors increased the antitumor effects of the nontoxic dose of TP on gastric cancer cells and tried to explore the possible molecular mechanisms.

Method: AGS and MKN45 cells were treated with different doses of TP and TNF- α . Cell viability and apoptosis were detected *in vitro*. In addition, NF- κ B mediated prosurvival signals and cytoprotective proteins, especially FLICE-inhibitory protein (FLIP), were detected to determine their effects on TP/TNF- α -induced apoptosis. Moreover, the function of lncRNA H19/miR-204-5p/NF- κ B/FLIP axis was investigated *in vitro*, and the antigastric cancer effect of TP plus TNF- α was proved in the mice xenograft model.

Result: *In vitro* experimental results showed that TP pretreatment promoted apoptosis in AGS and MKN45 cells upon TNF- α exposure. TP/TNF- α -mediated apoptosis was partly mediated by the inhibitory effect of NF- κ B-mediated FLIP expression. Oncogene H19 lying in the upstream pathway of NF- κ B played a vital role upon TNF- α exposure, and bioinformatics analysis proved that H19 participated in TP/TNF- α -induced apoptosis via binding of miR-204-5p. Lastly, a low dose of TP and TNF- α inhibited the tumor weight and tumor volume of AGS and MKN45 cells *in vivo*.

Conclusion: TP pretreatment increased apoptosis in TNF- α -stimulated gastric cancer cells, which are dependent on the disruption of the H19/miR-204-5p/NF- κ B/FLIP axis. Cotreatment of TP and TNF- α is a better option for enhancing the anticancer effect and lowering the side effect of TP.

Keywords: triptolide, TNF- α , gastric cancer, H19, NF- κ B

Abbreviations: CIAP1, Cellular inhibitor of apoptosis protein 1; CIAP2, Cellular inhibitor of apoptosis protein 2; FADD, Fas-associated protein with death domain; FLIP, Cellular FLICE-inhibitory protein; LPS, Lipopolysaccharide; lncRNA, Long Noncoding RNA; NFKBIA, NFKB Inhibitor Alpha; TP, Triptolide; TNF- α , Tumor necrosis factor- α ; TNFAIP3, TNF Alpha-Induced Protein 3; TRAF2, TNF receptor-associated factor 2; XIAP, X-linked inhibitor of apoptosis protein.

INTRODUCTION

The development of cancer and cancer therapy response is tightly regulated by inflammation, which facilitates tumor progression upon continuous inflammatory stimulation and accelerates cancer recovery by provoking immune response (Zhao et al., 2021). Inflammatory stimulation could also strengthen the efficacy of antitumor drugs. For example, 5-fluorouracil enhances the chemosensitivity of gastric cancer to TRAIL, and Tanshinone IIA sensitizes TRAIL-induced apoptosis in glioblastoma through death receptor (Zhou X. et al., 2021; Li et al., 2021). Natural products extracted from plants, animals, or microbes play an essential role in the human struggle against diseases for centuries (Rao et al., 2019; Wang et al., 2020). It is reported that triptolide (TP), an active ingredient of a Chinese herbal plant *Tripterygium wilfordii* Hook F (TWHF), has antimicrobial, immunomodulatory, antitumor, antirheumatic, and antiinflammatory activities associated with serious systemic toxicity (Tong et al., 2021). Although TP possesses strong antitumor bioactivity, the dose-dependent side effects limit its application. Exploring a better solution for enhancing the antitumor bioactivity and lowering the side effects of TP has great significance. Previously research found that TP pretreatment increased the sensitivity of hepatocytes upon TNF- α /LPS stimulation (Yuan et al., 2019). The mechanistic study revealed that TP/TNF- α (TP/LPS) induced apoptosis in hepatocytes *via* downregulating NF- κ B-mediated cellular FLICE-inhibitory protein (FLIP) expression (Yuan et al., 2019; Yuan Z. et al., 2020). However, whether we can take advantage of this feature of TP to increase its antitumor activity remains elusive.

Gastric cancer is ranked second among other cancers in terms of incidence and mortality in the population of China. Statistical data show that the incidence of stomach cancer is 679.1 per 0.1 million and mortality is 498 per 0.1 million. Late-stage diagnosis along with poor prognosis is the main cause of the high mortality rate in gastric cancer patients. Therefore, understanding the biological mechanisms and seeking a better treatment plan is the need of the hour. Previous antitumor studies of TP on gastric carcinoma mainly focused on the direct cytotoxicity of TP, while a high dose of TP might also affect the physiological function of normal cells (Jiang et al., 2001; Chang et al., 2007; Wang et al., 2014). Thus, a scientific approach for improving the antitumor effects of TP along with lessening its side effects is desired.

When TNF- α binds to TNF-R1, it leads to the activation of NF- κ B with a subsequent increase in the protein expression of FLIP. This cellular FLICE-like inhibitory protein has the main role in regulating cell fate. After the cytoplasmic transfer of the TNF receptor-associated death domain, receptor-interacting protein kinase 1 (RIPK1), and TNF receptor-associated factor 2 (TRAF2) through their death domains, coupled with Fas-associated death domain (FADD) and Caspase-8, create a complex named complex-IIa (Micheau and Tschopp, 2003).

When NF- κ B synthesizes FLIP, the formation of Caspase-8/FLIP dimer arrests the activity of Caspase-8. However, the inactivation of NF- κ B leads to the activation of Caspase-8, which can cause cell death through the apoptosis pathway upon TNF- α stimulation. Previous studies revealed that TP/TNF- α (TP/LPS) induced apoptosis in hepatocytes *via* downregulating NF- κ B-mediated FLIP expression (Yuan et al., 2019). However, the mechanism behind TP-induced NF- κ B inhibition is still unknown, and whether TNF- α can enhance the antitumor effect of TP remains unclear.

Among 75% of transcribed RNA molecules, long noncoding RNA (lncRNA) is supposed to be involved in various biomolecular processes, such as transcriptional modulation, translational regulation, and epigenetic mechanism. Research studies have discovered that the expression of lncRNAs, including MALAT1, H19, MEG3, and TUSC7, markedly control gastric cancer cell migration, proliferation, invasion, metastasis, cell cycle, tumorigenicity, and apoptosis (Huang and Yu, 2015; Yang et al., 2015; Deng et al., 2016; Xie et al., 2016). In addition, targeting miRNA for binding to mRNA following protein regulation is an important process for lncRNAs to exert their physiological functions (Chen et al., 2021). It is widely accepted that some lncRNAs regulate the activity of NF- κ B and ultimately participate in inflammation and immune response (Gupta et al., 2020). H19 is one of the most studied lncRNAs in carcinogenesis that plays a key role in the multistep process of carcinogenesis including genomic irregularity, translational fluctuation, unstable proliferation, stress management, and metastasis (Raveh et al., 2015a). It is widely accepted that the function of H19 can be divided into two parts: the reservoir of miR-675 to suppress its target genes and the binding to miRNAs or proteins to modulate their function (Raveh et al., 2015b). The previous study showed that TNF- α treatment also increased the level of H19, which in turn led to the activation of the NF- κ B pathway by stimulating the phosphorylation of TAK1, which implied that H19 might be involved in TP/TNF- α -induced apoptosis (Yang et al., 2020b).

In this study, we explored whether TNF- α enhanced the antitumor effect of TP against gastric carcinoma. Moreover, we screened lncRNAs related to the pathogenesis of gastric cancer and tried to investigate the effect of the H19/miR-204-5p/NF- κ B axis in TP/TNF- α -induced apoptosis in gastric carcinoma.

MATERIALS AND METHODS

Materials

TP (CAS number 38748-32-2, purity > 98%) was supplied by SelleckChem (Houston, TX, United States). Human recombinant TNF- α (300-01A) and Cell Counting Kit-8 (CCK-8, HY-K0301) were obtained from Peprotech Inc. (Rocky Hill, NJ, United States) and MedChemExpress (Madison, WI, United States), respectively. Trizol reagent (R401-01), SYBR Green Master

Mix (Q111-03), and Reverse Transcription Kit (R312-02) were obtained from Vazyme Biotech Co., Ltd. (Nanjing, Jiangsu, China).

Antibodies against FLIP (56343), X-linked inhibitor of apoptosis protein (XIAP, 2042), cleaved caspase-8 (9746), and cleaved caspase-3 (9661) were purchased from Cell Signaling Technology (Boston, MA, United States). Antibody against NF- κ B p65 (ab16502) was purchased from Abcam (Cambridge, United Kingdom). Antibodies against cellular inhibitor of apoptosis protein 1 (CIAP1) and cellular inhibitor of apoptosis protein 2 (CIAP2) (10022-1-AP), Lamin B1 (12987-1-AP), and β -Actin (HRP-60008) were purchased from Proteintech (Chicago, IL, United States).

Animal and Pharmacological Treatments

All experimental procedures involving mice complied with the ARRIVE guidelines and were permitted by the Animal Ethics Committee, Zhengzhou University. To explore the antitumor effects of TP, six-week-old female athymic BALB/c nude mice were purchased from SPF (Beijing) Biotechnology Co., Ltd. and maintained under pathogen-free conditions. Nude mice were subcutaneously injected into the inguinal region with 5×10^6 AGS and MKN45 cells (6 mice per group). When tumor volume reached 30–50 mm³, the mice were administered with TP intragastrically (125 μ g/kg or 250 μ g/kg) or 0.5% CMC–Na at the volume of 10 ml/kg once a day. Tumor volumes were measured every 3 days, and all the mice were sacrificed 3 weeks after TP treatment. Tumors were collected for further detection.

To investigate the antitumor effects of TP and TNF- α , nude mice were subcutaneously injected into the inguinal region with 1×10^7 AGS and MKN45 cells (6 mice per group). The mice were administered with TP (125 μ g/kg) and TNF- α (5 μ g/kg). TP was administered once a day, and an intratumoral injection of TNF- α was administered twice a week. Mice used in this experiment were sacrificed 3 weeks after TP administration.

Cell Culture and Cell Viability Assay

Cell lines used in this experiment, including AGS, MKN45, and HEK293T cells, were purchased from China Cell Culture Center (Shanghai, China). Cells were cultured in Dulbecco Modified Eagle's medium (DMEM) with 10% fetal bovine serum (FBS) provided by Gibco (Grand Island, NY, United States) and incubated at 37°C in a humidified atmosphere with 5% CO₂. TP was added 2 h before the addition of human recombinant TNF- α in all *in vitro* experiments.

Cell viability was detected with the CCK-8 assay in the 96-well plates. In brief, exponentially growing cells were plated at the density of 5×10^3 in each well. Fresh DMEM without FBS containing different concentrations of TP as well as human recombinant TNF- α was added to replace the old medium 24 h after seeding. CCK-8 reagents were added at the indicated time, and cell viability was detected with Varioskan LUX (Thermo Fisher Scientific, Waltham, MA, United States).

TABLE 1 | Sequence of target miR-204-5p.

Gene	Gene sequence (5'-3')
NC inhibitor	CAGUACUUUUGUGUAGUACAA
miR-204-5p inhibitor	AGGCAUAGGAUGACAAAGGGAA

Cell Transfection

Cell transfection was carried out according to our published research (Zhou Y. et al., 2021). Briefly, for gene silencing of miR-204-5p or overexpression of human FLIP and H19, miRNA inhibitor or plasmid carrying the corresponding sequence were purchased from Genepharma (Shanghai, China). H19 siRNA (SR319206) and its negative control (SR30004) were purchased from Origene Technologies (Beijing, China). miRNA inhibitor or plasmid were transfected into the cells using Lipofectamine 3000 (Invitrogen, Carlsbad, CA, United States) according to the manufacturer's protocol. AGS and MKN45 cells cultured in 12-well plates were transfected with scrambled control sequence, miR-204-5p inhibitor, H19 siRNA, pLVX-EF1 α -IRES-puro vector, or pEX-1 vector carrying H19 sequence. Fresh DMEM medium was added to the plates to replace the transfection medium after a 24-h transfection. Next, TP (25 nmol/L) and TNF- α (5 ng/ml) were added to the medium 48 h after transfection. Then, cell supernatant was collected at the indicated time after TNF- α application. The sequences of miR-204-5p, H19 siRNA, and their negative controls are presented in **Table 1**.

Dual-Luciferase Reporter Assay

Dual-luciferase reporter assay was conducted according to the published research (Gao et al., 2019). In brief, to confirm that miR-204-5p was the direct target of H19, the sequence of wild-type H19 and the corresponding H19 mutants were inserted into psiCHECK-2 plasmid obtained from Genepharma. HEK293T cells were co-transfected with either psiCHECK-2-H19 wt or psiCHECK-2-H19 mut together with miR-204-5p inhibitor or negative control (NC) using Lipofectamine 3000. Dual-luciferase reporter assay was conducted according to the Dual-luciferase Reporter Assay System Kit (E1960) obtained from Promega (Madison, WI, United States).

RNA Extraction and qPCR

Cellular RNA was isolated using Trizol reagent, and complementary DNA was synthesized from 1- μ g RNA for each sample with Reverse Transcription Kit after the quantification of RNA concentration with Nanodrop 2000 (Thermo Fisher Scientific), according to the manufacturer's instructions. The experiment was conducted on Applied Biosystems 7500 Real-Time PCR Systems (Thermo Fisher Scientific) using SYBR Green Master Mix and normalized with U6 for the detection of miR-204-5p and β -actin for the detection of H19. The relative mRNA expression was calculated using the $\Delta\Delta$ CT method, and the primers used for qPCR are listed in **Table 2**.

TABLE 2 | Primer sequences used for qPCR assay in mice.

Gene	Forward primer (5'-3')	Reverse primer (5'-3')
<i>β-actin</i>	CCATGTACGTTGCTATCCAG	CTTCATGAGGTAGTCAGTCAG
<i>LncRN H19</i>	ACCACTGCACTACCTGACTC	CCGCAGGGGGTGGCCATGAA
<i>U6</i>	GCTTCGGCAGCACATATACTAAAT	CGCTTCACGAATTTGCGTGTCTAT
<i>miR-204-5p</i>	CCTTTGTCATCCTATGCC	GAACATGTCTGCGTATCTC
<i>TNFAIP3</i>	CTCAACTGGTGTGCGAGAAGTCC	TTCTTTGAGCGTGTGGAACAGC
<i>NFKBIA</i>	TCCACTCCATCCTGAAGGCTAC	CAAGGACACCAAAGCTCCACG

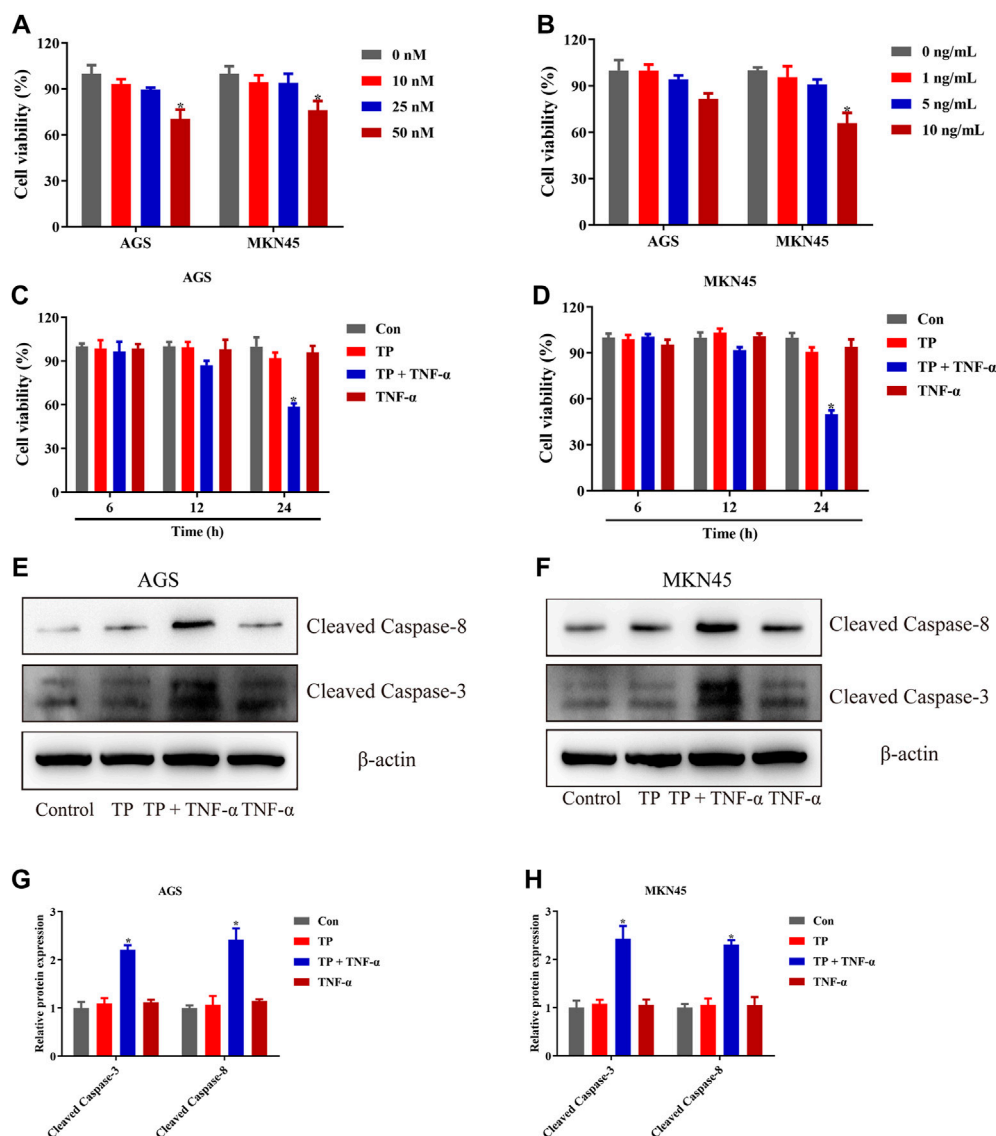


FIGURE 1 | TP pretreatment increased the sensitivity of AGS and MKN45 cells to TNF- α . **(A)** Cell viability of AGS and MKN45 cells treated with different concentrations of TP between 10 and 50 nM for 24 h. **(B)** Cell viability of AGS and MKN45 cells treated with different concentrations of TNF- α ranging from 1 ng/ml to 10 ng/ml for 24 h. **(C–D)** Cell viability of AGS and MKN45 cells treated with TP (25 nM) and TNF- α (5 ng/ml) for 6, 12, and 24 h. **(E–H)** Representative Western blots and relative intensity of protein bands of cleaved caspase-3 and cleaved caspase-8 of AGS and MKN45 cells treated with TP (25 nM) and TNF- α (5 ng/ml), 24 h after TNF- α application, with β -actin as the loading control. Results were expressed as mean \pm SEM, and statistical analysis was performed using one-way ANOVA or two-way ANOVA followed by Tukey's multiple comparison test. * $p < 0.05$ ($n \geq 3$). * p compared with the control group.

Western Blot Analysis

Total cellular protein was extracted from cell lines or tumor tissues with radio-immunoprecipitation assay lysis buffer (P0013C) purchased from Beyotime Biotechnology (Shanghai, China). Nuclear proteins were separated with Nuclear Plasma Separation Kit (P0028, Beyotime Biotechnology). The concentration of protein was quantified using a BCA Kit (P0012, Beyotime Biotechnology). The cell lysate was then mixed with 5× loading buffer (P0015, Beyotime Biotechnology) and separated using SDS-PAGE with gels ranging from 8% to 12%. After transferring the proteins onto poly(vinylidene fluoride) membranes (Millipore, Danvers, MA, United States) and blocking with 5% BSA at room temperature for 1 h, the membranes were incubated with primary antibodies overnight at 4°C. The membranes were then incubated with secondary antibodies for 1 h and visualized in Tanon 5200 Chemiluminescent Imaging System (Shanghai, China) using an ECL Detection Kit (Millipore). Relative protein expression was normalized with Lamin B1 for the detection of NF- κ B p65 or β -actin for the detection of the whole protein lysate and analyzed with Image J 1.52a (NIH, Bethesda, MD, United States).

NF- κ B Transcription Factor Activation Assay

Cell lysates were collected at the indicated time and then extracted and quantified with the kit purchased from Beyotime Biotechnology, as described above. NF- κ B transcription factor activation was detected using the kit from Abcam (ab176648), according to the manufacturer's instructions.

Statistical Analysis

Data were analyzed using GraphPad Prism 8.01 (GraphPad Software, San Diego, CA, United States) and presented in the form of mean \pm SEM. One-way analysis of variance (ANOVA) and two-way ANOVA followed by Tukey's multiple comparison test was performed to analyze the differences between groups. p -values < 0.05 were considered to be statistically significant.

RESULTS

TP Pretreatment Increased the Sensitivity of AGS and MKN45 Cells to TNF- α

TP has been recognized as an antitumor active ingredient for various cancers (Noel et al., 2019). The result in **Figure 1A** showed that TP decreased the cell viability of two gastric cancer cell lines, AGS and MKN45, in a concentration-dependent manner. However, low doses of TP (10 and 25 nM) had little effect on cell viability. However, 50-nM concentration significantly decreased the cell viability in both cell lines. In addition, researchers reported that a high dose of TNF- α induces cell death, while a low dose of TNF- α induces cell survival instead of cell death (Brenner et al., 2015; Annibaldi and Meier, 2018). The result of **Figure 1B** showed that only a 10-ng/ml concentration of TNF- α had remarkably decreased the cell viability of MKN45 cells, which was consistent with the published articles (Oberst et al., 2011; Suda et al., 2016).

Next, we treated both the cell lines with nontoxic concentrations of TP (25 nM) and TNF- α (5 ng/ml) for further experiments. Time-dependent results revealed that the combination of TP and TNF- α decreased the cell viability at 24-h time interval (**Figures 1C,D**). To confirm the results of cell viability experiments, protein expressions of cleaved caspase-3 and cleaved caspase-8 were analyzed using western blot. The results showed that TP/TNF- α cotreatment increased the expression of cleaved caspase-3 and cleaved caspase-8 (**Figures 1E–H**). These results confirmed that TP pretreatment sensitized AGS and MKN45 cells to TNF- α in gastric cancer.

Triptolide Treatment Inhibited NF- κ B-Mediated Prosurvival Signals Induced by TNF- α

It has been widely accepted that TNF- α is the inducer of apoptosis and necroptosis (Pasparakis and Vandenabeele, 2015; Peltzer et al., 2016). However, under a physiological state, TNF- α induces cell survival instead of cell death because of the checkpoints in the TNF- α -TNF-R1 pathway. Several checkpoints determine cell fate, and NF- κ B-mediated prosurvival signals are one of them (Annibaldi and Meier, 2018). To determine the NF- κ B activity, both cell lines were treated with TNF- α (5 ng/ml) for different time intervals. The result illustrated that NF- κ B activity was increased in a time-dependent manner, restored to normal at the 6-h time interval, and peaked at the 30-min time interval (**Figure 2A**). Based on these observations, NF- κ B activity was determined 30 min after TNF- α stimulation. The result in **Figure 2B** showed that TP/TNF- α cotreatment decreased NF- κ B activity compared to TNF- α treatment alone, indicating that TP pretreatment inhibited the activity of NF- κ B induced by TNF- α . Similar results were obtained after the detection of the protein level of NF- κ B p65 (**Figures 2C,D**). NF- κ B mediated prosurvival function depends on the expression of several prosurvival proteins. Thus, we detected the expressions of prosurvival proteins related to NF- κ B, including CIAP1, CIAP2, XIAP, and FLIP. The results revealed that TP and TNF- α had little effect on the expressions of CIAP1 and CIAP2. In contrast, XIAP and FLIP protein expressions were decreased in the TP/TNF- α cotreatment group compared to the TNF- α treatment alone, and TNF- α induced the upregulation of FLIP in both the cell lines (**Figures 2E–H**). However, previous results implied that CIAP1, CIAP2, and XIAP cooperated to maintain embryonic development and protected cells from TNF- α -induced cell death (Moulin et al., 2012). Thus, we excluded the role of XIAP in TP/TNF- α -induced apoptosis in gastric cancer and supposed that FLIP might play an essential role in TP/TNF- α -induced apoptosis in AGS and MKN45 cells.

Overexpression of FLIP Protected AGS and MKN45 Cells From TP/TNF- α -Induced Apoptosis

To evaluate the function of FLIP in TP/TNF- α -induced apoptosis in AGS and MKN45 cells, both cell lines were

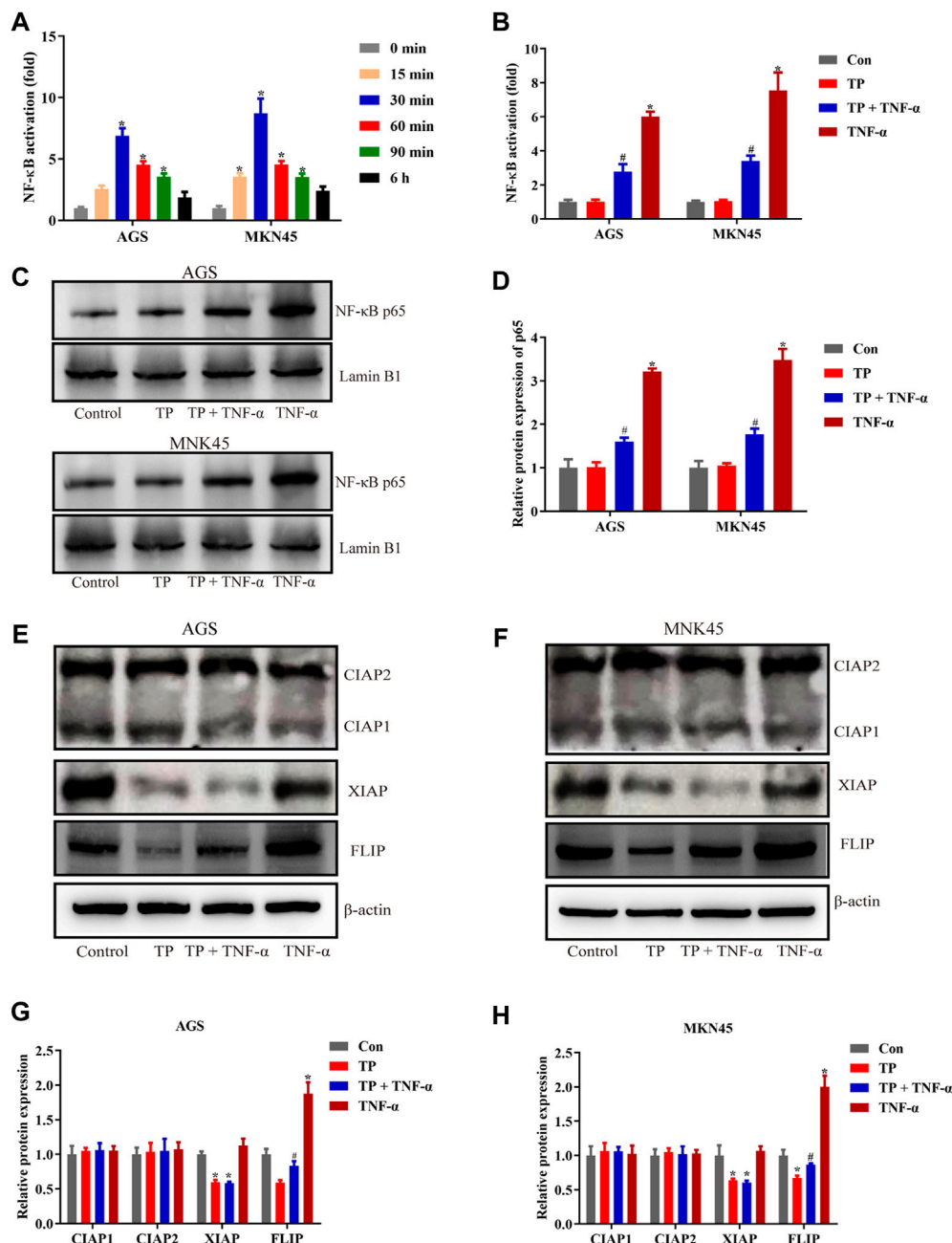


FIGURE 2 | TP treatment inhibited NF-κB-mediated prosurvival signals induced by TNF-α. **(A)** Time-dependent NF-κB activation induced by TNF-α (5 ng/ml). **(B)** Relative NF-κB activity induced by TP (25 nM) and TNF-α (5 ng/ml), 30 min after TNF-α treatment. **(C–D)** Representative western blots and relative intensity of protein bands of NF-κB p65 nuclear protein, with Lamin B1 as the loading control, 30 min after TNF-α (5 ng/ml) treatment. **(E–H)** Representative western blots and relative intensity of protein bands of CIAP1, CIAP2, XIAP, and FLIP in AGS and MKN45 cells treated with TP (25 nM) and TNF-α (5 ng/ml), 24 h after TNF-α application, with β-actin as the loading control. Results were expressed as mean ± SEM, and statistical analysis was performed using one-way ANOVA or two-way ANOVA followed by Tukey's multiple comparison test. **p* < 0.05 (*n* ≥ 3). **p* compared with the control group and #*p* compared with the TNF-α-treated group.

transfected with the FLIP expression plasmid. The results showed that FLIP overexpression significantly increased the cell viability (Figure 3A). Relative protein expressions of cleaved caspase-3, cleaved caspase-8, and FLIP also revealed

that FLIP overexpression protected the cells from TP/TNF-α-induced apoptosis (Figures 3B–E). These results showed that NF-κB-mediated FLIP expression had a protective role in TP/TNF-α-induced apoptosis.

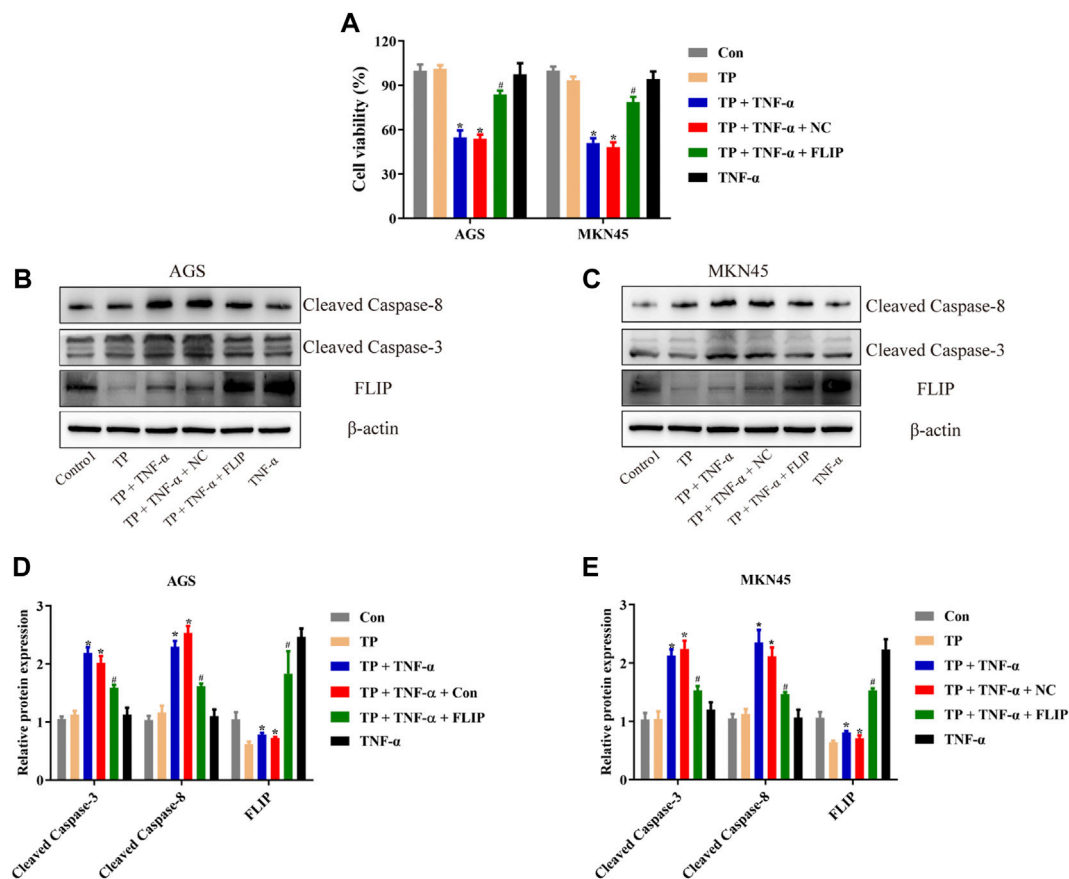


FIGURE 3 | Overexpression of FLIP protected AGS and MKN45 cells from TP/TNF- α -induced apoptosis. **(A)** Cell viability of AGS and MKN45 cells transfected with a plasmid carrying FLIP sequence or its negative control with subsequent treatment with TP (25 nM) and TNF- α (5 ng/ml) for 24 h. **(B–E)** Representative western blots and relative intensity of protein bands of cleaved caspase-3, cleaved caspase-8, and FLIP in AGS and MKN45 cells transfected with FLIP plasmid and treated with TP (25 nM) and TNF- α (5 ng/ml), 24 h after TNF- α application, with β -actin as the loading control. Results were expressed as mean \pm SEM, and statistical analysis was performed using two-way ANOVA followed by Tukey's multiple comparison test. *, # $p < 0.05$ ($n \geq 3$). * p compared with the control group and # p compared with TP/TNF- α /NC-treated group.

LncRNA H19 Acted as the Upstream Component of the NF- κ B Pathway in TP/TNF- α -Stimulated AGS and MKN45 Cells

Numerous studies implied that abnormal expression of lncRNA participated in the tumorigenesis and tumor progression of multitype cancer cells, including gastric cancer (Yu and Rong, 2018; Yuan L. et al., 2020; Wei et al., 2020). The regulation of lncRNAs and their bioactivity has attracted researchers' attention for their function in cancer diagnosis, prognosis, as well as chemotherapy (Wei et al., 2020). To identify the unrevealed lncRNA that might participate in TP/TNF- α -induced antigastric cancer effect, we screened the generally accepted lncRNAs that related to NF- κ B activation (Gupta et al., 2020). Among them, we found that lncRNA H19 and Lethe were both increased by TNF- α in AGS and MKN45 cells (Figure 4A). LncRNA H19 was recognized as the oncogene of gastric cancer. Existing scientific research pointed out that overexpression of H19 promoted gastric cancer cell invasion and migration, while the inhibition of H19 inhibited gastric cancer cell growth (Liu et al., 2016; Zhang et al., 2017; Gan

et al., 2019). As H19 was reported to be the upstream member of the NF- κ B pathway upon TNF- α stimulation, we speculated that H19 might play an essential role in TP/TNF- α -induced apoptosis in gastric cancer cells. Researchers found that TNF- α treatment significantly enhanced the expression of H19, while TP pretreatment inhibited this process (Figure 4B). To identify whether H19 acted as the upstream component of the NF- κ B under the stimulation of TNF- α in gastric cancer cells, H19 siRNA was transfected into AGS and MKN45 cells before TNF- α treatment. qPCR analysis revealed that two NF- κ B targeting genes, *NFKBIA* and *TNFAIP3*, were significantly increased in TNF- α treated cells, while H19 siRNA obstructed this process (Supplementary Figures S1A,B). Moreover, H19 siRNA pretreatment decreased the translocation of p65 from the cytoplasm into the nucleus in TNF- α -treated AGS and MKN45 cells (Supplementary Figures S1C,D). We also transfected the H19 plasmid into these two cell lines. The results revealed that cells transfected with H19 overexpression plasmid showed a relative increase in H19 expression and

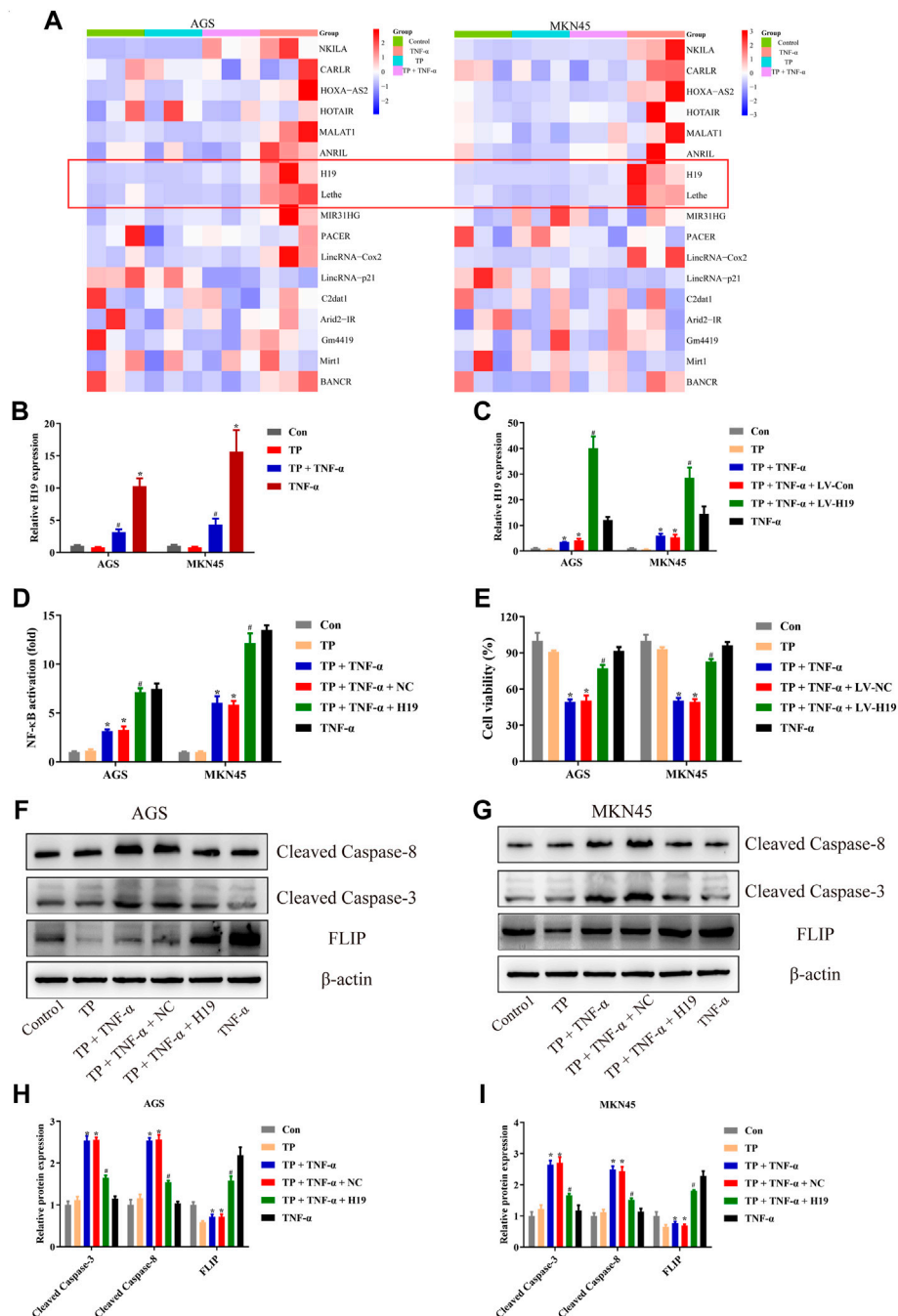


FIGURE 4 | LncRNA H19 acted as the upstream component of the NF-κB pathway in TP/TNF-α-stimulated AGS and MKN45 cells. **(A)** NF-κB-related lncRNA was detected with qPCR 30 min after TNF-α stimulation. **(B)** Relative mRNA expression of H19 on cells treated with TP (25 nM) and TNF-α (5 ng/ml) for 24 h. **(C)** Relative mRNA expression of H19 on cells transfected with a plasmid carrying H19 sequence or its negative control treated with TP (25 nM) and TNF-α (5 ng/ml) for 24 h. **(D)** Relative NF-κB activity of cells transfected with H19 plasmid and treated with TP (25 nM) and TNF-α (5 ng/ml), 30 min after TNF-α treatment. **(E)** Cell viability of AGS and MKN45 cells transfected with a plasmid carrying H19 sequence or its negative control and treated with TP (25 nM) and TNF-α (5 ng/ml) for 24 h. **(F–I)** Representative western blots and relative intensity of protein bands of cleaved caspase-3, cleaved caspase-8, and FLIP in AGS and MKN45 cells transfected with H19 plasmid and treated with TP (25 nM) and TNF-α (5 ng/ml), 24 h after TNF-α application, with β-actin as the loading control. Results were expressed as mean ± SEM, and statistical analysis was performed using two-way ANOVA followed by Tukey's multiple comparison test. *, #p < 0.05 (n ≥ 3). *p compared with the control group and #p compared with TP/TNF-α/NC-treated group.

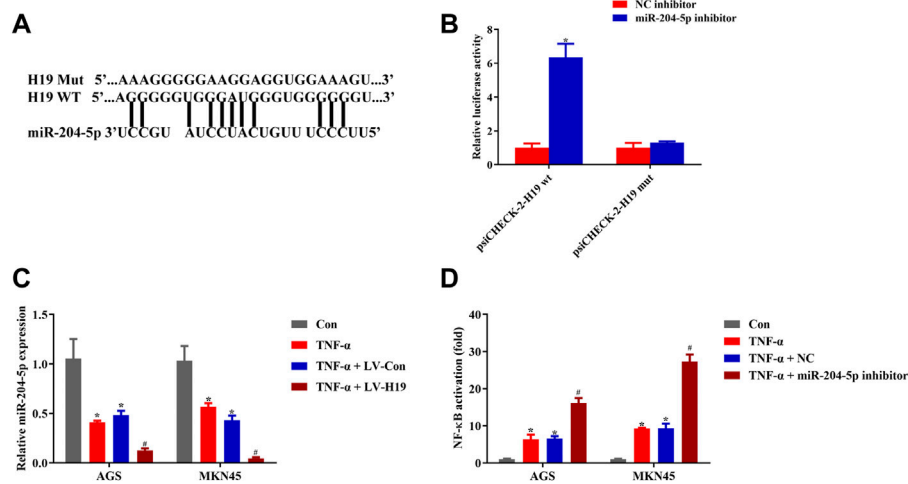


FIGURE 5 | H19 showed direct binding to miR-204-5p. **(A)** Predicted binding sites between miR-204-5p and H19. **(B)** Dual-luciferase reporter assay of psiCHECK-2-H19 wt and psiCHECK-2-H19 mut HEK 293T cell cotransfected with miR-204-5p inhibitor or its negative control. **(C)** Relative mRNA expression of miR-204-5p in cells transfected with H19 or its negative control and treated with TNF- α (5 ng/ml) for 24 h. **(D)** Relative NF- κ B activity of cells transfected with miR-204-5p inhibitor or its negative control and treated with TNF- α (5 ng/ml) for 24 h. Results were expressed as mean \pm SEM, and statistical analysis was performed using two-way ANOVA followed by Tukey's multiple comparison test. * $p < 0.05$ ($n \geq 3$). * p compared with the control group and # p compared with TNF- α /LV-Con or TNF- α /NC-treated group.

significantly increased the activity of NF- κ B (Figures 4C,D). Moreover, H19 overexpression increased the cell viability of the cells treated with TP/TNF- α (Figure 4E). Western blot results also confirmed that H19 overexpression exhibits a cytoprotective effect in both cell lines as cleaved caspase-3 and cleaved caspase-8 levels were decreased, while the FLIP level was increased in TP/TNF- α /H19 group (Figures 4F–I). These results explained that TP-induced sensitivity of AGS and MKN45 cells to TNF- α was dependent on H19.

H19 Showed Direct Binding to miR-204-5p

To identify how H19 regulated NF- κ B activity upon TNF- α stimulation, we screened the candidate miRNA that related to NF- κ B and selected the most suitable eight miRNAs for our study (Mirzaei et al., 2021). We used RNAhybrid to predict the binding of the selected miRNAs to H19, finding that miR-204-5p binding to H19 needed the minimum MFE (Supplementary Material). According to the prediction, there is a putative binding site of miR-204-5p in H19 (Figure 5A). Dual-luciferase reporter assay conducted in HEK293T cells implied that miR-204-5p inhibitor significantly increased H19 WT luciferase activity while having little effect on H19 Mut cells (Figure 5B). In addition, TNF- α treatment inhibited the expression of miR-204-5p, and transfection of H19 plasmid into both cell lines decreased the relative miR-204-5p expression (Figure 5C). NF- κ B activity assay revealed that the miR-204-5p inhibitor decreased the upregulation of NF- κ B induced by TNF- α (Figure 5D). These results revealed that H19 inhibited the expression of miR-204-5p, which acted as the activator of the upstream pathway of NF- κ B upon TNF- α stimulation in AGS and MKN45 cells.

miR-204-5p Inhibitor Protected AGS and MKN45 Cells From Triptolide/TNF- α -Induced Apoptosis

To investigate the role of miR-204-5p in TP/TNF- α -induced apoptosis in gastric cancer cells, AGS and MKN45 cells were additionally treated with miR-204-5p inhibitor or its NC. According to the results in Figures 6A–C, the miR-204-5p inhibitor group showed a decrease in the relative expression of miR-204-5p and an increase in NF- κ B activity and cell viability in TP/TNF- α treated AGS and MKN45 cells. Western blot results also illustrated that miR-204-5p inhibitor treatment had a cytoprotective role by decreasing the protein expressions of cleaved caspase-3 and cleaved caspase-8 and increasing the level of FLIP (Figures 6D–G). These results firmly proved that miR-204-5p was the upstream member of the NF- κ B pathway and was negatively correlated to NF- κ B activation.

Triptolide/TNF- α Inhibited the Growth of AGS and MKN45 Cells *in vivo*

Lastly, the antagastric cancer effects of TP were investigated *in vivo*. Mice were subcutaneously injected with AGS cells and MKN45 cells and were treated with different doses of TP (125 μ g/kg and 250 μ g/kg) for 21 days. Two doses of TP inhibited the tumor volume and tumor weight of AGS and MKN45 cells in a dose-dependent manner (Figures 7A–F). Western bolt analysis revealed that TP inhibited the expression of FLIP at both doses (Figures 7G,H). Then, we treated mice with TP (125 μ g/kg) for 3 weeks and TNF- α (5 μ g/kg) twice a week. Three weeks after TP administration, we found that TNF- α alone has little effect on the tumor weight and volume. However, TP/

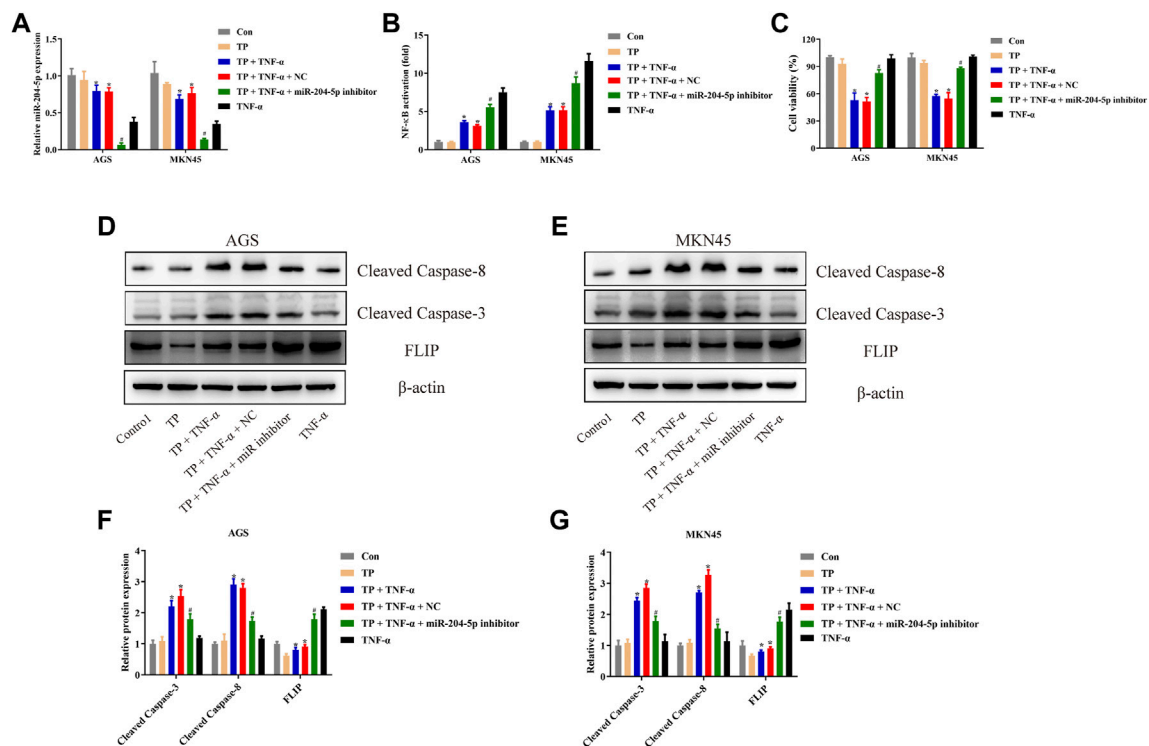


FIGURE 6 | miR-204-5p inhibitor protected AGS and MKN45 cells from TP/TNF- α -induced apoptosis. **(A)** Relative mRNA expression of miR-204-5p in cells transfected with miR-204-5p inhibitor and treated with TP (25 nM) and TNF- α (5 ng/ml) for 24 h. **(B)** Relative NF- κ B activity of cells transfected with miR-204-5p inhibitor and treated with TP and TNF- α for 30 min. **(C)** Cell viability of AGS and MKN45 cells transfected with miR-204-5p inhibitor and treated with TP (25 nM) and TNF- α (5 ng/ml) for 24 h. **(D–G)** Representative western blots and relative intensity of protein bands of cleaved caspase-3, cleaved caspase-8, and FLIP in AGS and MKN45 cells transfected with miR-204-5p inhibitor and treated with TP (25 nM) and TNF- α (5 ng/ml), 24 h after TNF- α application, with β -actin as the loading control. Results were expressed as mean \pm SEM, and statistical analysis was performed using two-way ANOVA followed by Tukey's multiple comparison test. * $p < 0.05$ ($n \geq 3$). * p compared with the control group and # p compared with TP/TNF- α /miR-204-5p inhibitor-treated group.

TNF- α cotreatment dramatically inhibited the tumor growth of AGS and MKN45 cells and firmly proved that TP treatment increased the sensitivity of AGS and MKN45 cells to TNF- α *in vivo* (Figures 7I–L).

DISCUSSION

TP and its derivatives, such as Minnelide and PG490-88, attracted researchers' attention because of their multiple pharmacological activities. The antitumor activity of TP is associated with the inhibition of tumor cell growth, induction of tumor cell death, or cell cycle arrest in diverse types of cancers, such as breast cancer, acute myeloid leukemia, lung cancer, ovarian cancer, neuroblastoma, prostate cancer, osteosarcoma, and gastric cancer (Pigneux et al., 2008; Krosch et al., 2013; Rivard et al., 2014; Shao et al., 2014; Jiang et al., 2016; Isharwal et al., 2017; Jiang et al., 2018). However, the application of TP and its derivatives was restricted due to their side effects. Structural modifications, reduction in the dose, or improving the delivery system of TP may be the better choices for therapeutic uses of TP. Previous research found that TP increased the sensitivity of hepatocytes upon TNF- α exposure, and we wanted to utilize this characteristic of TP to increase its antitumor efficiency (Yuan et al., 2019). This study was designed to explore whether TP increased the

sensitivity of gastric cancer cells to the TNF- α stimulation and tried to find the mechanisms behind it.

Experimental results of Figures 1A–D showed that TP pretreatment sensitized gastric cancer cell lines to TNF- α in a time-dependent manner, and we selected nontoxic doses of TP and TNF- α for further experiments. In most cases, cells exposed to the low dose of TNF- α did not experience cell death until the checkpoints of the TNF- α pathway became out of control, keeping the NF- κ B-mediated prosurvival signal indispensable. Next, mechanistic studies revealed that TP inhibited NF- κ B-mediated FLIP expression that was upregulated by the stimulation of TNF- α , and this observation was the same as reported in the previous study (Yuan Z. et al., 2020). However, the mechanism behind TP-induced inhibition of NF- κ B-mediated FLIP expression leading to an increase in gastric cancer cell sensitivity to TNF- α stimulation remained unclear.

Some experimental reports revealed that lncRNA may not only participate in the progress of gastric cancer but also control the activity of NF- κ B (Lin et al., 2014; Sun et al., 2017). After screening the lncRNAs, we found that H19 might be the appropriate candidate for our study. H19, expressed only on maternal allele and imprinted in both humans as well as mice, was the first lncRNA gene to be discovered. It has been reported that an elevated level of H19 is present in gastric cancer and bladder cancer, while the decreased level is

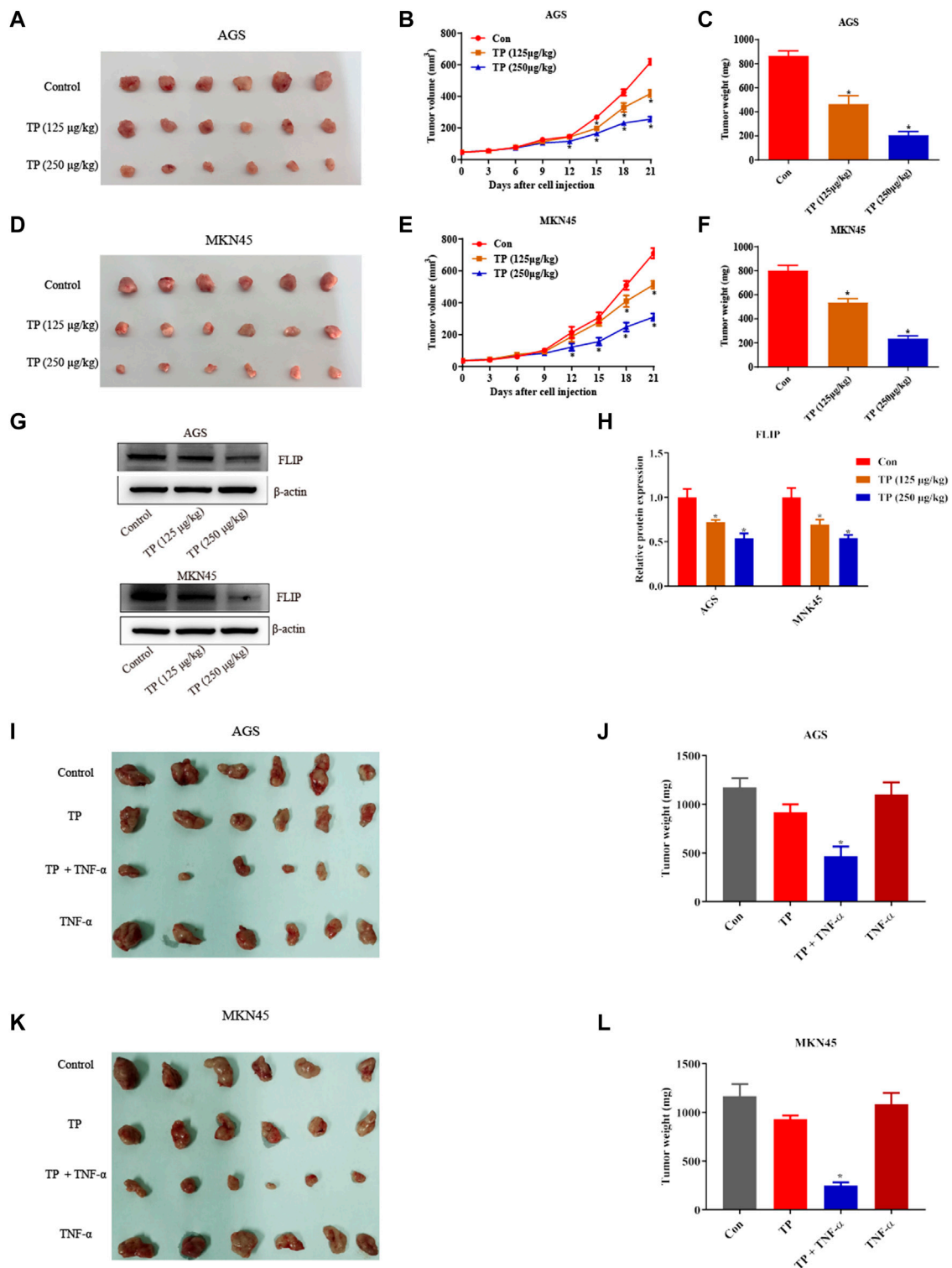


FIGURE 7 | TP inhibited the growth of AGS and MKN45 cells *in vivo*. **(A)** Images of tumor size when nude mice were subcutaneously injected with AGS cells and treated with TP (125 µg/kg or 250 µg/kg) for 3 weeks. **(B–C)** Tumor volume and weight of mice injected with AGS cells treated with TP. **(D)** Images of tumor size when nude mice were subcutaneously injected with MKN45 cells and treated with TP (125 µg/kg or 250 µg/kg) for 3 weeks. **(E–F)** Tumor volume and weight of mice injected with MKN45 cells treated with TP. **(G–H)** Representative western blots and relative intensity of protein bands of FLIP in mice injected with AGS and MKN45 cells and treated with TP (125 µg/kg or 250 µg/kg). **(I–L)** Images of tumor size and weight of nude mice injected with TP (125 µg/kg) and TNF-α (5 µg/kg) for 3 weeks. Results were expressed as mean ± SEM, and statistical analysis was performed using one-way ANOVA or two-way ANOVA followed by Tukey's multiple comparison test. **p* < 0.05 (*n* ≥ 3). **p* compared with the control group.

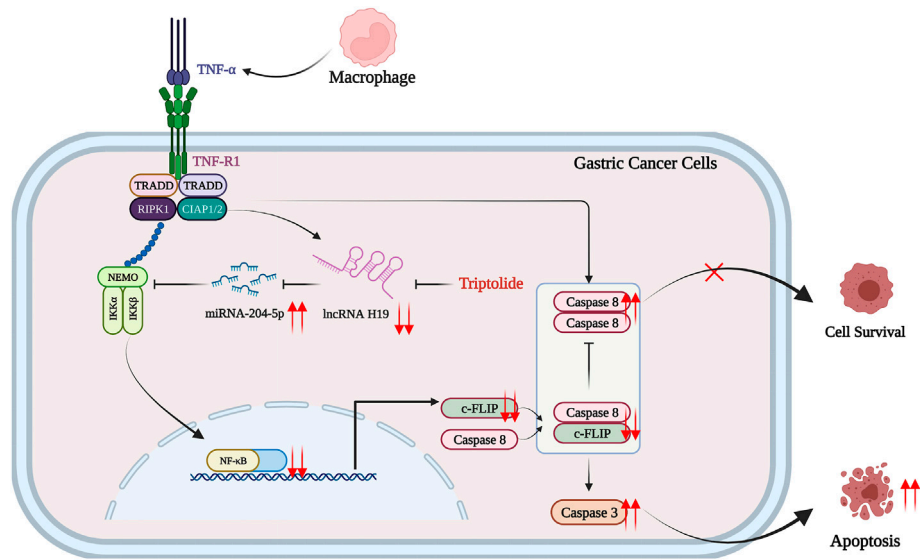


FIGURE 8 | Schematic presentation indicating the suggested mechanisms by which TP/TNF- α -induced gastric cancer cell death. Under a physiological state, a low dose of TNF- α stimulates both cell survival signals via H19/miR-204-5p/NF- κ B/FLIP pathway and cell death signals via activating caspase-8. The upregulation of FLIP inhibits caspase-8-dependent apoptosis, and the consequence of a low dose of TNF- α is cell survival. However, TP pretreatment inhibited H19/miR-204-5p/NF- κ B/FLIP signals, and the insignificant level of FLIP could not counteract the prodeath signals induced by TNF- α , leading to gastric cancer cell death. The figure was created using BioRender.com (Agreement number: IQ23Z4T0E3).

present in hepatocellular carcinoma, indicating that H19 has both tumor suppressor as well as oncogenic properties (Iizuka et al., 2004; Yang et al., 2012; Song et al., 2013b; Luo et al., 2013). Overexpression of H19 in kidney tumor cells reduced the growth rate along with the absence of neoplasm in mice, suggesting the tumor suppressor capacity of H19 in renal carcinogenesis (Matouk et al., 2005). A scientific study on the effect of H19 on gastric cancer showed that the H19 level was significantly elevated in AGS gastric cancer cell line. This increased level of H19 led to an increase in cell proliferation, while the use of H19 siRNA caused cell death in AGS cells (Yang et al., 2012). Another experimental study on gastric cancer illustrated that H19 expression was markedly increased in gastric tumor tissues compared with noncancer tissues. The increased level of H19 in gastric cancer tissues and gastric cancer cell lines suggested a main role of H19 in gastric cancer pathology (Song et al., 2013a). Based on these scientific developments, H19 has proven itself a diagnostic and therapeutic marker in various cancers, and its main role in carcinogenesis has been established. Moreover, it has been reported that H19 activates NF- κ B via TAK1 phosphorylation and promotes gastric cancer cell growth via NF- κ B activation (Zhang et al., 2019; Yang et al., 2020a). To identify whether H19 is the upstream member of the NF- κ B pathway in AGS and MKN45 cells, we transfected the H19 plasmid into these cell lines. The results revealed that cells transfected with H19 overexpression plasmid showed a relative increase in H19 expression and a significant increase in the activity of NF- κ B (Figure 4D). H19 overexpression also increased the cell viability after TP/TNF- α treatment (Figure 4E). Our experimental design for the first time depicted that H19 is the upstream member of NF- κ B signaling in gastric cancer cells upon TNF- α stimulation. However, no existing research reveals that H19 deficit mice are sensitive to LPS or TNF- α , which needs to be proved in future studies.

It has been revealed that an abnormal level of miRNAs is involved in the development of neoplasm, and some of them are associated with gastric carcinogenesis by regulating cancer-related genes. Moreover, they also prove to be important cancer biomarkers (Li et al., 2011; Shin and Chu, 2014). Most of the miRNAs are engaged in critical cellular processes, including proliferation and invasion, by controlling the posttranscriptional level of target gene expressions. For instance, miR-589 remarkably promoted gastric cancer proliferation and invasion through miR-589-P13/AKT-c-Jun signaling (Zhang et al., 2018). MiRNA-21 enhanced gastric cancer cell growth by regulating PEG2 (Qi et al., 2018). To find out the physiological mechanism of H19, we used RNAhybrid to predict the binding of H19 to biochemically suitable miRNA and found that miR-204-5p was the ideal candidate. Our results found that transfection with H19 overexpression plasmid inhibited the miR-204-5p level upon TNF- α stimulation in AGS and MKN45 cells (Figure 5). In addition, the miR-204-5p inhibitor increased the activity of NF- κ B and cell viability upon TP/TNF- α treatment. Western blot results also showed a decrease in the protein expression of proapoptotic cleaved caspase-3 and cleaved caspase-8 proteins and an increase in the protein expression of the prosurvival protein, FLIP (Figure 6). Other studies have also reported the frequent downregulation of miR-204-5p in other tumor cells, including colorectal cancer cells and head and neck squamous cell carcinoma, indicating a similar effect of miR-204-5p in carcinogenesis (Shuai et al., 2018; Zhuang Z. et al., 2020).

In this hypothesis, we proved that TP-induced sensitivity of AGS and MKN45 cells to the TNF- α treatment was dependent on H19/miR-204-5p/NF- κ B signaling. It is known that the injection of TNF- α via the tail vein quickly distributes in multiple organs that may cause some side effects. We investigated the effect of

cotreatment of TP and TNF- α *in vivo*; however, the distribution of TNF- α in the tissue is so quick that there is no difference in the level of TNF- α in the serum and tumor tissue groups after iv injection of TNF- α (10 μ g/kg) into the tail vein, although there might be some differences in the levels of miR-204-5p and H19 between the TP/TNF- α and TNF- α -treatment groups. Moreover, iv injection of TNF- α into the tail vein slightly upregulated NF- κ B target genes (compared with the published articles), *NFKBIA*, and *TNFAIP3*, which were observed to examine the effect of TNF- α on the tumor NF- κ B activity (Supplementary Figure S2). Due to the rapid tissue distribution of TNF- α , intratumoral injection of TNF- α was administered *in vivo*. The result proved that TP/TNF- α inhibited the growth of AGS and MKN45 cells. Considering the poor accessibility of intratumoral injection, we supposed that exosome-based antibodies or other formulations for TNF- α delivery might be the optional plan (Probst et al., 2019a; Zhuang et al., 2020a). In addition, researchers proved that TNF- α delivery can enhance the antitumor activity of antibody-dependent cell-mediated cytotoxicity of an anti-Melanoma Immunoglobulin, peptide anticancer vaccine, and cancer cell membrane targeting therapy (Probst et al., 2019b; Murer et al., 2019; Zhuang et al., 2020b). We believe that new formulations focusing on the codelivery of TP and TNF- α nanomaterials for targeting tumor tissues can be a better solution for the antitumor effects of TP.

CONCLUSION

Pretreatment with a nontoxic dose of TP promoted apoptosis in AGS and MKN45 cells upon TNF- α treatment. The inhibition of FLIP by lncRNA H19 and miR-204-5p interaction lying upstream of NF- κ B is indispensable for inflammatory sensitization (Figure 8). In addition, codelivery of TP and TNF- α nanomaterial might be the better solution for the antitumor effects of TP.

DATA AVAILABILITY STATEMENT

The original contributions presented in the study are included in the article/Supplementary Material. Further inquiries can be directed to the corresponding authors.

REFERENCES

- Annibaldi, A., and Meier, P. (2018). Checkpoints in TNF-Induced Cell Death: Implications in Inflammation and Cancer. *Trends Mol. Med.* 24, 49–65. doi:10.1016/j.molmed.2017.11.002
- Brenner, D., Blaser, H., and Mak, T. W. (2015). Regulation of tumour necrosis factor signalling: live or let die. *Nat. Rev. Immunol.* 15, 362–374. doi:10.1038/nri3834
- Chang, H. J., Kim, M. H., Baek, M. K., Park, J. S., Chung, I. J., Shin, B. A., et al. (2007). Triptolide Inhibits Tumor Promoter-Induced uPAR Expression via Blocking NF-kappaB Signaling in Human Gastric AGS Cells. *Anticancer Res.* 27, 3411–3417.
- Chen, Y., Li, Z., Chen, X., and Zhang, S. (2021). Long Non-coding RNAs: From Disease Code to Drug Role. *Acta Pharm. Sin. B* 11, 340–354. doi:10.1016/j.apsb.2020.10.001

ETHICS STATEMENT

The animal study was reviewed and approved by the Animal Ethics Committee, Zhengzhou University.

AUTHOR CONTRIBUTIONS

WY, YZ, XC, and JH participated in the research design. WY, JH, SH, HL, YZ, BC, GL, and LB carried out the experiments. WY, YZ, XC, and JH performed the data analysis. WY, JH, and XC wrote the manuscript.

FUNDING

This study was supported by the Medical Science and Technique Foundation of Henan Province (SB201901101), the 1000 Talents Program of Central plains (204200510023), and the Young and Middle-aged Health and Technology Innovation Leading Talent Project of Henan Province (YXKC2020008).

SUPPLEMENTARY MATERIAL

The Supplementary Material for this article can be found online at: <https://www.frontiersin.org/articles/10.3389/fphar.2022.918588/full#supplementary-material>

Supplementary Figure S1 | Relative expression of the mRNA levels of NF- κ B target genes *NFKBIA* and *TNFAIP3* in AGS and MKN45 cells pretreated with H19 siRNA and stimulated with TNF- α for 30 min. **(C,D)** The protein level of NF- κ B in AGS and MKN45 cells pretreated with H19 siRNA and stimulated with TNF- α for 30 min. Results were expressed as mean \pm SEM, and statistical analysis was performed using two-way ANOVA followed by Tukey's Multiple Comparison Test. *, # p < 0.05 ($n \geq 3$). *P compared with the control group and #P compared with the TNF- α -siRNA-NC group.

Supplementary Figure S2 | Serum **(A)** and tumor tissue **(B)** concentration of TNF- α in mice subcutaneously injected with AGS or MKN45 cells and treated with TP (125 μ g/kg, ip) once a day and TNF- α (10 μ g/kg, iv) once a week. **(C–F)** Relative mRNA expression of NF- κ B target genes (*NFKBIA* and *TNFAIP3*), H19, and miR204-5p in mice treated with TP and TNF- α . Results were expressed as mean \pm SEM, and statistical analysis was performed using Two-way ANOVA followed by Tukey's multiple comparison test. *, # p < 0.05 ($n \geq 3$). * p compared with the control group and # p compared with the TNF- α -treated group.

- Deng, K., Wang, H., Guo, X., and Xia, J. (2016). The Cross Talk between Long, Non-coding RNAs and microRNAs in Gastric Cancer. *Acta Biochim. Biophys. Sin. (Shanghai)* 48, 111–116. doi:10.1093/abbs/gmv120
- Gan, L., Lv, L., and Liao, S. (2019). Long Non-coding RNA H19 R-regulates C-ell G-rowth and M-etastasis via the miR-22-3p/Sna11 axis in G-astric C-ancer. *Int. J. Oncol.* 54, 2157–2168. doi:10.3892/ijo.2019.4773
- Gao, L., Guo, Q., Li, X., Yang, X., Ni, H., Wang, T., et al. (2019). MiR-873/PD-L1 axis Regulates the Stemness of Breast Cancer Cells. *EBioMedicine* 41, 395–407. doi:10.1016/j.ebiom.2019.02.034
- Gupta, S. C., Awasthee, N., Rai, V., Chava, S., Gunda, V., and Challagundla, K. B. (2020). Long Non-coding RNAs and Nuclear Factor-Kb Crosstalk in Cancer and Other Human Diseases. *Biochim. Biophys. Acta Rev. Cancer* 1873, 188316. doi:10.1016/j.bbcan.2019.188316
- Huang, Y. K., and Yu, J. C. (2015). Circulating microRNAs and Long Non-coding RNAs in Gastric Cancer Diagnosis: an Update and Review. *World J. Gastroenterol.* 21, 9863–9886. doi:10.3748/wjg.v21.i34.9863

- Iizuka, N., Oka, M., Tamesa, T., Hamamoto, Y., and Yamada-Okabe, H. (2004). Imbalance in Expression Levels of Insulin-like Growth Factor 2 and H19 Transcripts Linked to Progression of Hepatocellular Carcinoma. *Anticancer Res.* 24, 4085–4089.
- Isharwal, S., Modi, S., Arora, N., Uhlrich, C., III, Giri, B., Barlass, U., et al. (2017). Minnelide Inhibits Androgen Dependent, Castration Resistant Prostate Cancer Growth by Decreasing Expression of Androgen Receptor Full Length and Splice Variants. *Prostate* 77, 584–596. doi:10.1002/pros.23298
- Jiang, C., Huang, S., Gao, P., and Chen, D. (2018). Experimental Study on the Bond and Durability Properties of Mortar Incorporating Polyacrylic Ester and Silica Fume. *Adv. Cem. Res.* 30, 56–65. doi:10.1680/jadcr.17.00053
- Jiang, L., Shestov, A. A., Swain, P., Yang, C., Parker, S. J., Wang, Q. A., et al. (2016). Reductive Carboxylation Supports Redox Homeostasis during Anchorage-independent Growth. *Nature* 532, 255–258. doi:10.1038/nature17393
- Jiang, X. H., Wong, B. C., Lin, M. C., Zhu, G. H., Kung, H. F., Jiang, S. H., et al. (2001). Functional P53 Is Required for Triptolide-Induced Apoptosis and AP-1 and Nuclear Factor-kappaB Activation in Gastric Cancer Cells. *Oncogene* 20, 8009–8018. doi:10.1038/sj.onc.1204981
- Krosch, T. C., Sangwan, V., Banerjee, S., Mujumdar, N., Dudeja, V., Saluja, A. K., et al. (2013). Triptolide-mediated Cell Death in Neuroblastoma Occurs by Both Apoptosis and Autophagy Pathways and Results in Inhibition of Nuclear Factor-Kappa B Activity. *Am. J. Surg.* 205, 387–396. doi:10.1016/j.amjsurg.2013.01.008
- Li, H., Lv, J., Guo, J., Wang, S., Liu, S., Ma, Y., et al. (2021). 5-Fluorouracil Enhances the Chemosensitivity of Gastric Cancer to TRAIL via Inhibition of the MAPK Pathway. *Biochem. Biophys. Res. Commun.* 540, 108–115. doi:10.1016/j.bbrc.2021.01.006
- Li, X., Zhang, Y., Zhang, H., Liu, X., Gong, T., Li, M., et al. (2011). miRNA-223 Promotes Gastric Cancer Invasion and Metastasis by Targeting Tumor Suppressor EPB41L3. *Mol. Cancer Res.* 9, 824–833. doi:10.1158/1541-7786.MCR-10-0529
- Lin, X. C., Zhu, Y., Chen, W. B., Lin, L. W., Chen, D. H., Huang, J. R., et al. (2014). Integrated Analysis of Long Non-coding RNAs and mRNA Expression Profiles Reveals the Potential Role of lncRNAs in Gastric Cancer Pathogenesis. *Int. J. Oncol.* 45, 619–628. doi:10.3892/ijo.2014.2431
- Liu, G., Xiang, T., Wu, Q. F., and Wang, W. X. (2016). Long Noncoding RNA H19-Derived miR-675 Enhances Proliferation and Invasion via RUNX1 in Gastric Cancer Cells. *Oncol. Res.* 23, 99–107. doi:10.3727/096504015X14496932933575
- Luo, M., Li, Z., Wang, W., Zeng, Y., Liu, Z., and Qiu, J. (2013). Long Non-coding RNA H19 Increases Bladder Cancer Metastasis by Associating with EZH2 and Inhibiting E-Cadherin Expression. *Cancer Lett.* 333, 213–221. doi:10.1016/j.canlet.2013.01.033
- Matouk, I., Ohana, P., Ayesh, S., Sidi, A., Czerniak, A., De Groot, N., et al. (2005). The Oncofetal H19 RNA in Human Cancer, from the Bench to the Patient. *Cancer Ther.* 3, 249–266.
- Micheau, O., and Tschopp, J. (2003). Induction of TNF Receptor I-Mediated Apoptosis via Two Sequential Signaling Complexes. *Cell* 114, 181–190. doi:10.1016/s0092-8674(03)00521-x
- Mirzaei, S., Zarrabi, A., Hashemi, F., Zabolian, A., Saleki, H., Ranjbar, A., et al. (2021). In Response to "Comment on 'Regulation of Nuclear Factor-KappaB (NF-Kb) Signaling Pathway by Non-coding RNAs in Cancer: Inhibiting or Promoting Carcinogenesis?'" *Cancer Lett.* 2021 May 2; 509 (2021) 63–80". *Cancer Lett.* 516, 36–37. doi:10.1016/j.canlet.2021.05.026
- Moulin, M., Anderton, H., Voss, A. K., Thomas, T., Wong, W. W., Bankovacki, A., et al. (2012). IAPs Limit Activation of RIP Kinases by TNF Receptor 1 during Development. *EMBO J.* 31, 1679–1691. doi:10.1038/emboj.2012.18
- Mur, P., Kiefer, J. D., Plüss, L., Matasci, M., Blümich, S. L., Stringhini, M., et al. (2019). Targeted Delivery of TNF Potentiates the Antibody-dependent Cell-Mediated Cytotoxicity of an Anti-melanoma Immunoglobulin. *J. Invest. Dermatol.* 139, 1339–1348. doi:10.1016/j.jid.2018.11.028
- Noel, P., Von Hoff, D. D., Saluja, A. K., Velagapudi, M., Borazanci, E., and Han, H. (2019). Triptolide and its Derivatives as Cancer Therapies. *Trends Pharmacol. Sci.* 40, 327–341. doi:10.1016/j.tips.2019.03.002
- Oberst, A., Dillon, C. P., Weinlich, R., McCormick, L. L., Fitzgerald, P., Pop, C., et al. (2011). Catalytic Activity of the caspase-8-FLIP(L) Complex Inhibits RIPK3-dependent Necrosis. *Nature* 471, 363–367. doi:10.1038/nature09852
- Pasparakis, M., and Vandenabeele, P. (2015). Necroptosis and its Role in Inflammation. *Nature* 517, 311–320. doi:10.1038/nature14191
- Peltzer, N., Darding, M., and Walczak, H. (2016). Holding RIPK1 on the Ubiquitin Leash in TNFR1 Signaling. *Trends Cell. Biol.* 26, 445–461. doi:10.1016/j.tcb.2016.01.006
- Pigneux, A., Mahon, F. X., Uhalde, M., Jeanneteau, M., Lacombe, F., Milpied, N., et al. (2008). Triptolide Cooperates with Chemotherapy to Induce Apoptosis in Acute Myeloid Leukemia Cells. *Exp. Hematol.* 36, 1648–1659. doi:10.1016/j.exphem.2008.08.002
- Probst, P., Stringhini, M., Ritz, D., Fugmann, T., and Neri, D. (2019a). Antibody-based Delivery of TNF to the Tumor Neovasculature Potentiates the Therapeutic Activity of a Peptide Anticancer Vaccine. *Clin. Cancer Res.* 25, 698–709. doi:10.1158/1078-0432.CCR-18-1728
- Probst, P., Stringhini, M., Ritz, D., Fugmann, T., and Neri, D. (2019b). Antibody-based Delivery of TNF to the Tumor Neovasculature Potentiates the Therapeutic Activity of a Peptide Anticancer Vaccine. *Clin. Cancer Res.* 25, 698–709. doi:10.1158/1078-0432.CCR-18-1728
- Qi, R., Wang, D. T., Xing, L. F., and Wu, Z. J. (2018). miRNA-21 Promotes Gastric Cancer Growth by Adjusting Prostaglandin E2. *Eur. Rev. Med. Pharmacol. Sci.* 22, 1929–1936. doi:10.26355/eurrev_201804_14717
- Rao, T., Tan, Z., Peng, J., Guo, Y., Chen, Y., Zhou, H., et al. (2019). The Pharmacogenetics of Natural Products: A Pharmacokinetic and Pharmacodynamic Perspective. *Pharmacol. Res.* 146, 104283. doi:10.1016/j.phrs.2019.104283
- Raveh, E., Matouk, I. J., Gilon, M., and Hochberg, A. (2015a). The H19 Long Non-coding RNA in Cancer Initiation, Progression and Metastasis - a Proposed Unifying Theory. *Mol. Cancer* 14, 184–214. doi:10.1186/s12943-015-0458-2
- Raveh, E., Matouk, I. J., Gilon, M., and Hochberg, A. (2015b). The H19 Long Non-coding RNA in Cancer Initiation, Progression and Metastasis - a Proposed Unifying Theory. *Mol. Cancer* 14, 184. doi:10.1186/s12943-015-0458-2
- Rivard, C., Geller, M., Schnettler, E., Saluja, M., Vogel, R. I., Saluja, A., et al. (2014). Inhibition of Epithelial Ovarian Cancer by Minnelide, a Water-Soluble Pro-drug. *Gynecol. Oncol.* 135, 318–324. doi:10.1016/j.ygyno.2014.08.031
- Shao, H., Ma, J., Guo, T., and Hu, R. (2014). Triptolide Induces Apoptosis of Breast Cancer Cells via a Mechanism Associated with the Wnt/ β -Catenin Signaling Pathway. *Exp. Ther. Med.* 8, 505–508. doi:10.3892/etm.2014.1729
- Shin, V. Y., and Chu, K. M. (2014). MiRNA as Potential Biomarkers and Therapeutic Targets for Gastric Cancer. *World J. Gastroenterol.* 20, 10432–10439. doi:10.3748/wjg.v20.i30.10432
- Shuai, F., Wang, B., and Dong, S. (2018). MicroRNA-204 Inhibits the Growth and Motility of Colorectal Cancer Cells by Downregulation of CXCL8. *Oncol. Res.* 26, 1295–1305. doi:10.3727/096504018X1517274209020
- Song, H., Sun, W., Ye, G., Ding, X., Liu, Z., Zhang, S., et al. (2013a). Long Non-coding RNA Expression Profile in Human Gastric Cancer and its Clinical Significances. *J. Transl. Med.* 11, 225. doi:10.1186/1479-5876-11-225
- Song, H., Sun, W., Ye, G., Ding, X., Liu, Z., Zhang, S., et al. (2013b). Long Non-coding RNA Expression Profile in Human Gastric Cancer and its Clinical Significances. *J. Transl. Med.* 11, 225–310. doi:10.1186/1479-5876-11-225
- Suda, J., Dara, L., Yang, L., Aghajan, M., Song, Y., Kaplowitz, N., et al. (2016). Knockdown of RIPK1 Markedly Exacerbates Murine Immune-Mediated Liver Injury through Massive Apoptosis of Hepatocytes, Independent of Necroptosis and Inhibition of NF-Kb. *J. Immunol.* 197, 3120–3129. doi:10.4049/jimmunol.1600690
- Sun, Y., Pan, J., Zhang, N., Wei, W., Yu, S., and Ai, L. (2017). Knockdown of Long Non-coding RNA H19 Inhibits Multiple Myeloma Cell Growth via NF-Kb Pathway. *Sci. Rep.* 7, 18079–18110. doi:10.1038/s41598-017-18056-9
- Tong, L., Zhao, Q., Datan, E., Lin, G. Q., Minn, I., Pomper, M. G., et al. (2021). Triptolide: Reflections on Two Decades of Research and Prospects for the Future. *Nat. Prod. Rep.* 38, 843–860. doi:10.1039/d0np00054j
- Wang, B. Y., Cao, J., Chen, J. W., and Liu, Q. Y. (2014). Triptolide Induces Apoptosis of Gastric Cancer Cells via Inhibiting the Overexpression of MDM2. *Med. Oncol.* 31, 270. doi:10.1007/s12032-014-0270-7
- Wang, H. N., Shen, Z., Liu, Q., Hou, X. Y., Cao, Y., Liu, D. H., et al. (2020). Isochlorogenic Acid (ICGA): Natural Medicine with Potentials in Pharmaceutical Developments. *Chin. J. Nat. Med.* 18, 860–871. doi:10.1016/S1875-5364(20)60029-2
- Wei, L., Sun, J., Zhang, N., Zheng, Y., Wang, X., Lv, L., et al. (2020). Noncoding RNAs in Gastric Cancer: Implications for Drug Resistance. *Mol. Cancer* 19, 62. doi:10.1186/s12943-020-01185-7

- Xie, S. S., Jin, J., Xu, X., Zhuo, W., and Zhou, T. H. (2016). Emerging Roles of Non-coding RNAs in Gastric Cancer: Pathogenesis and Clinical Implications. *World J. Gastroenterol.* 22, 1213–1223. doi:10.3748/wjg.v22.i3.1213
- Yang, F., Bi, J., Xue, X., Zheng, L., Zhi, K., Hua, J., et al. (2012). Up-regulated Long Non-coding RNA H19 Contributes to Proliferation of Gastric Cancer Cells. *FEBS J.* 279, 3159–3165. doi:10.1111/j.1742-4658.2012.08694.x
- Yang, J., Li, Y., Wang, L., Zhang, Z., Li, Z., and Jia, Q. (2020a). LncRNA H19 Aggravates TNF- α -Induced Inflammatory Injury via TAK1 Pathway in MH7A Cells. *Biofactors* 46, 813–820. doi:10.1002/biof.1659
- Yang, J., Li, Y., Wang, L., Zhang, Z., Li, Z., and Jia, Q. (2020b). LncRNA H19 Aggravates TNF- α -Induced Inflammatory Injury via TAK1 Pathway in MH7A Cells. *Biofactors* 46, 813–820. doi:10.1002/biof.1659
- Yang, Z. G., Gao, L., Guo, X. B., and Shi, Y. L. (2015). Roles of Long Non-coding RNAs in Gastric Cancer Metastasis. *World J. Gastroenterol.* 21, 5220–5230. doi:10.3748/wjg.v21.i17.5220
- Yu, H., and Rong, L. (2018). Emerging Role of Long Non-coding RNA in the Development of Gastric Cancer. *World J. Gastrointest. Oncol.* 10, 260–270. doi:10.4251/wjgo.v10.i9.260
- Yuan, L., Xu, Z. Y., Ruan, S. M., Mo, S., Qin, J. J., and Cheng, X. D. (2020a). Long Non-coding RNAs towards Precision Medicine in Gastric Cancer: Early Diagnosis, Treatment, and Drug Resistance. *Mol. Cancer* 19, 96. doi:10.1186/s12943-020-01219-0
- Yuan, Z., Yuan, Z., Hasnat, M., Zhang, H., Liang, P., Sun, L., et al. (2020b). A New Perspective of Triptolide-Associated Hepatotoxicity: the Relevance of NF- κ B and NF- κ B-Mediated Cellular FLICE-Inhibitory Protein. *Acta Pharm. Sin. B* 10, 861–877. doi:10.1016/j.apsb.2020.02.009
- Yuan, Z., Zhang, H., Hasnat, M., Ding, J., Chen, X., Liang, P., et al. (2019). A New Perspective of Triptolide-Associated Hepatotoxicity: Liver Hypersensitivity upon LPS Stimulation. *Toxicology* 414, 45–56. doi:10.1016/j.tox.2019.01.005
- Zhang, F., Li, K., Pan, M., Li, W., Wu, J., Li, M., et al. (2018). miR-589 Promotes Gastric Cancer Aggressiveness by a LIFR-Pi3k/akt-C-Jun Regulatory Feedback Loop. *J. Exp. Clin. Cancer Res.* 37, 152. doi:10.1186/s13046-018-0821-4
- Zhang, L., Zhou, Y., Huang, T., Cheng, A. S., Yu, J., Kang, W., et al. (2017). The Interplay of LncRNA-H19 and its Binding Partners in Physiological Process and Gastric Carcinogenesis. *Int. J. Mol. Sci.* 18. doi:10.3390/ijms18020450
- Zhang, Y., Yan, J., Li, C., Wang, X., Dong, Y., Shen, X., et al. (2019). LncRNA H19 Induced by helicobacter Pylori Infection Promotes Gastric Cancer Cell Growth via Enhancing NF-Kb-Induced Inflammation. *J. Inflamm. (Lond)* 16, 23. doi:10.1186/s12950-019-0226-y
- Zhao, H., Wu, L., Yan, G., Chen, Y., Zhou, M., Wu, Y., et al. (2021). Inflammation and Tumor Progression: Signaling Pathways and Targeted Intervention. *Signal Transduct. Target Ther.* 6, 263. doi:10.1038/s41392-021-00658-5
- Zhou, X., Lv, L., Tan, Y., Zhang, Z., Wei, S., and Xiao, S. (2021a). Tanshinone IIA Sensitizes TRAIL-Induced Apoptosis in Glioblastoma through Inducing the Expression of Death Receptors (And Suppressing STAT3 Activation). *Brain Res.* 1766, 147515. doi:10.1016/j.brainres.2021.147515
- Zhou, Y., Yan, H., Zhou, Q., Feng, R., Wang, P., Yang, F., et al. (2021b). Beta-Lapachone Attenuates BMSC-Mediated Neuroblastoma Malignant Transformation by Inhibiting Gal-3/Gal-3BP/IL6 Axis. *Front. Pharmacol.* 12, 766909. doi:10.3389/fphar.2021.766909
- Zhuang, M., Chen, X., Du, D., Shi, J., Deng, M., Long, Q., et al. (2020a). SPION Decorated Exosome Delivery of TNF- α to Cancer Cell Membranes through Magnetism. *Nanoscale* 12, 173–188. doi:10.1039/c9nr05865f
- Zhuang, M., Chen, X., Du, D., Shi, J., Deng, M., Long, Q., et al. (2020b). SPION Decorated Exosome Delivery of TNF- α to Cancer Cell Membranes through Magnetism. *Nanoscale* 12, 173–188. doi:10.1039/c9nr05865f
- Zhuang, Z., Yu, P., Xie, N., Wu, Y., Liu, H., Zhang, M., et al. (2020c). MicroRNA-204-5p Is a Tumor Suppressor and Potential Therapeutic Target in Head and Neck Squamous Cell Carcinoma. *Theranostics* 10, 1433–1453. doi:10.7150/thno.38507

Conflict of Interest: The authors declare that the research was conducted in the absence of any commercial or financial relationships that could be construed as a potential conflict of interest.

Publisher's Note: All claims expressed in this article are solely those of the authors and do not necessarily represent those of their affiliated organizations, or those of the publisher, editors, and reviewers. Any product that may be evaluated in this article, or claim that may be made by its manufacturer, is not guaranteed or endorsed by the publisher.

Copyright © 2022 Yuan, Huang, Hou, Li, Bie, Chen, Li, Zhou and Chen. This is an open-access article distributed under the terms of the Creative Commons Attribution License (CC BY). The use, distribution or reproduction in other forums is permitted, provided the original author(s) and the copyright owner(s) are credited and that the original publication in this journal is cited, in accordance with accepted academic practice. No use, distribution or reproduction is permitted which does not comply with these terms.



OPEN ACCESS

Edited by:

Muhammad Hasnat,
University of Veterinary and Animal
Sciences, Pakistan

Reviewed by:

Hafiz Ishfaq Ahmad,
University of Veterinary and Animal
Sciences, Pakistan
Faisal Raza,
Shanghai Jiao Tong University, China

*Correspondence:

Lúcio Roberto Cançado Castellano
luciocastellano2@gmail.com

†ORCID:

Renaly Ivyna de Araújo Rêgo
orcid.org/0000-0002-1085-0127
Geovana Ferreira Guedes Silvestre
orcid.org/0000-0002-5783-0449
Demis Ferreira de Melo
orcid.org/0000-0001-8486-5578
Sonaly Lima Albino
orcid.org/0000-0002-2904-036X
Marcela Monteiro Pimentel
orcid.org/0000-0001-9059-1120
Sara Brito Silva Costa Cruz
orcid.org/0000-0003-1509-900X
Sabrina Daniela Silva Wurzba
orcid.org/0000-0002-3742-2819
Wellington Francisco Rodrigues
orcid.org/0000-0002-3426-2186
Bolívar Ponciano Goulart de Lima
Damasceno
orcid.org/0000-0002-0747-0297
Lúcio Roberto Cançado Castellano
orcid.org/0000-0003-0851-5298

Specialty section:

This article was submitted to
Ethnopharmacology,
a section of the journal
Frontiers in Pharmacology

Received: 23 May 2022

Accepted: 20 June 2022

Published: 31 August 2022

Citation:

Ivyna de Araújo Rêgo R,
Guedes Silvestre GF,
Ferreira de Melo D, Albino SL,
Pimentel MM, Silva Costa Cruz SB,
Silva Wurzba SD, Rodrigues WF,
Goulart de Lima Damasceno BP and
Cançado Castellano LR (2022)
Flavonoids-Rich Plant Extracts Against
Helicobacter pylori Infection as
Prevention to Gastric Cancer.
Front. Pharmacol. 13:951125.
doi: 10.3389/fphar.2022.951125

Flavonoids-Rich Plant Extracts Against *Helicobacter pylori* Infection as Prevention to Gastric Cancer

Renaly Ivyna de Araújo Rêgo^{1,2,3†}, Geovana Ferreira Guedes Silvestre^{2†},
Demis Ferreira de Melo^{2†}, Sonaly Lima Albino^{4†}, Marcela Monteiro Pimentel^{3†},
Sara Brito Silva Costa Cruz^{5,6,7†}, Sabrina Daniela Silva Wurzba^{6,7†},
Wellington Francisco Rodrigues^{8†}, Bolívar Ponciano Goulart de Lima Damasceno^{2†} and
Lúcio Roberto Cançado Castellano^{1,2,5,6,7*†}

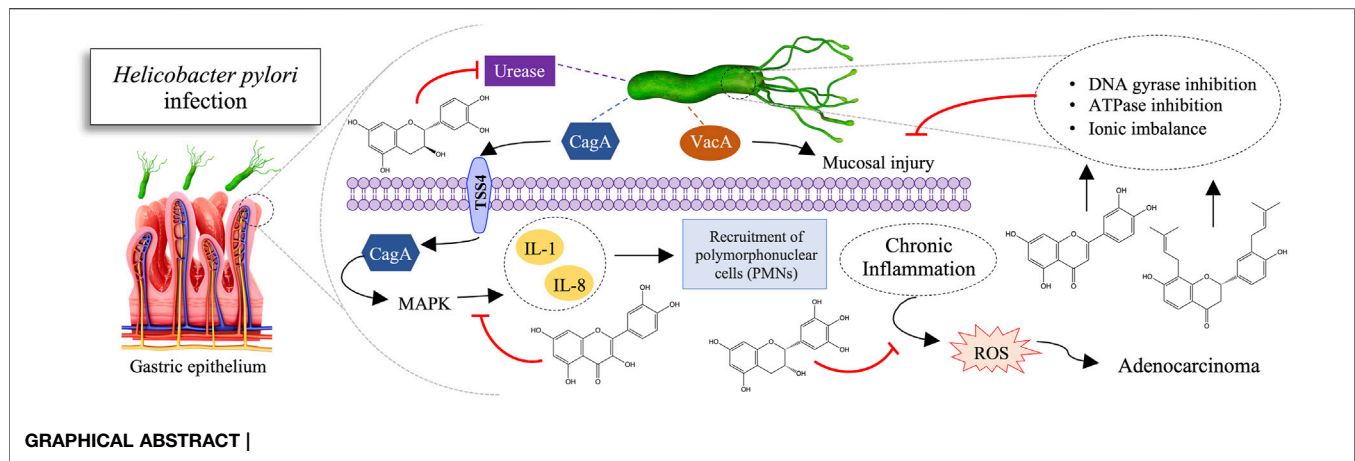
¹Human Immunology Research and Education Group-GEPIH, Federal University of Paraíba, João Pessoa, Brazil, ²Postgraduate Program of Pharmaceutical Sciences, State University of Paraíba, Campina Grande, Brazil, ³Postgraduate Program of Science and Technology in Health, State University of Paraíba, Campina Grande, Brazil, ⁴Postgraduate Program of Therapeutic Innovation, Federal University of Pernambuco, Recife, Brazil, ⁵Postgraduate Program in Dentistry, Federal University of Paraíba, João Pessoa, Brazil, ⁶Department of Otolaryngology and Head and Neck Surgery, McGill University, Montreal, QC, Canada, ⁷Segal Cancer Centre and Lady Davis Institute for Medical Research, Departments of Medicine and Oncology, Faculty of Medicine, McGill University, Montreal, QC, Canada, ⁸Postgraduate Course in Health Sciences, Federal University of Triângulo Mineiro, UFTM, Uberaba, Brazil

Gastric cancer is the fifth most common and fourth type to cause the highest mortality rates worldwide. The leading cause is related to *Helicobacter pylori* (*H. pylori*) infection. Unfortunately, current treatments have low success rates, highlighting the need for alternative treatments against carcinogenic agents, specifically *H. pylori*. Noteworthy, natural origin products contain pharmacologically active metabolites such as flavonoids, with potential antimicrobial applications.

Objective: This article overviews flavonoid-rich extracts' biological and pharmacological activities. It focuses on using these substances against *Helicobacter pylori* infection to prevent gastric cancer. For this, PubMed and Science Direct databases were searched for studies that reported the activity of flavonoids against *H. pylori*, published within a 10-year time frame (2010 to August 2020). It resulted in 1,773 publications, of which 44 were selected according to the search criteria. The plant family primarily found in publications was Fabaceae (9.61%). Among the flavonoids identified after extraction, the most prevalent were quercetin (19.61%), catechin (13.72), epicatechin (11.76), and rutin (11.76). The potential mechanisms associated with anti-*H. pylori* activity to the extracts were: inhibition of urease, damage to genetic material, inhibition of protein synthesis, and adhesion of the microorganism to host cells.

Conclusion: Plant extracts rich in flavonoids with anti-*H. pylori* potential proved to be a promising alternative therapy source, reinforcing the relevance of studies with natural products.

Keywords: phytotherapy, stomach neoplasms, anti-infective agents, ethnopharmacology, preventive medicine



INTRODUCTION

Gastric cancer represents the fifth most common type of cancer (1.08 million cases in 2020). It is the fourth most common cause of death among cancers worldwide (768,000 deaths in 2020) due to the advanced stage at diagnosis (Smyth et al., 2020; Sung et al., 2021). Incidence and mortality vary considerably between regions, although it is more prevalent in developing countries, in which the percentage of cases is equivalent to 70%, especially in East Asia. In addition, the incidence of gastric cancer is proportional to population age, with an average of 68 years, and is more common in men (1 in each 96) than in women (1 in each 152) (Herrero et al., 2014; medical and editorial content Team, 2018).

According to the topology, gastric cancer can be classified into cardia, usually associated with gastroesophageal reflux, and non-cardia or distal gastric cancer, caused by the interaction with different factors (Nardone, 2006; de Martel et al., 2013). The latter is histologically subdivided according to Laurén's classification in diffuse and intestinal (Lauren, 1965). The diffuse type consists of individually infiltrated neoplastic cells without glandular structures. In contrast, the intestinal type mimics the intestinal glands. It progresses through a series of histological changes that begin with transitioning from normal mucosa to chronic superficial gastritis, followed by atrophic gastritis, intestinal metaplasia, dysplasia, and adenocarcinoma (Nardone, 2006; Polk and Peek, 2010). For both types of non-cardiac gastric cancer, the main factor associated with developing approximately 90% of adenocarcinomas is the bacterium *Helicobacter pylori* (*H. pylori*) (Peek, 2005; Plummer et al., 2015, 2016; Moss, 2017; Thrift and El-Serag, 2020).

H. pylori is a gram-negative, flagellated, microaerophilic bacteria that infects the epithelial lining of the stomach (Tsukamoto and Tatematsu, 2014; Hooi et al., 2017). The infection is prevalent in approximately 50% of the world population, varying according to geographic region, age, socioeconomic status, education level, environment, and occupation. It is usually contracted in the first years of life and tends to persist until the completion of the appropriate treatment (McColl, 2010; Cui et al., 2013; Wang et al., 2014; Schaalán et al., 2020).

The inflammatory process developed by *H. pylori* infection involves a variety of pathways induced in both gastric epithelial cells and circulating immune cells recruited to the infection site. Activated pathways involve mitogen-activated protein kinase (MAPK), nuclear factor- κ B (NF- κ B), activating protein (AP)-1, Wnt/ β -catenin, PI3K pathways, signal transducers and transcription activators 3 (STAT3). These alterations cause an increase in the production of inflammatory cytokines, such as interleukin 1 (IL-1), IL-6, IL-8, and tumor necrosis factor- α (TNF- α). Also, they alter the apoptosis rate and proliferation and differentiation of epithelial cells. These phenomena result in the oncogenic transformation of epithelial cells and gastric cancer formation (Ding et al., 2010; Lamb and Chen, 2013; Schaalán et al., 2020). In addition, virulence factors contribute to determining the pattern of immune defense performed in response to the infection. It includes the factors named vacuolating cytotoxin (VacA), cytotoxin-associated antigen A (CagA), the Cag pathogenicity island (PAI), HP-NAP, oipA, and dupA (Ding et al., 2010; Sepulveda, 2013; Wang et al., 2014; Yamaoka, 2010, 2012).

The clinical condition produced by the microorganism in question is usually asymptomatic. However, the infection caused is associated with gastrointestinal diseases, such as chronic gastritis, peptic ulcer disease, gastric B-cell mucosa-associated lymphoid tissue lymphoma, and, as aforementioned, gastric adenocarcinoma. Thereby, *H. pylori* was recognized and classified as a definite (group 1) carcinogen by the World Health Organization's International Agency for Research on Cancer in 1994 (WHO, 2010; de Martel et al., 2013; Plummer et al., 2016; Moss, 2017). Additionally, studies demonstrate that eradicating *H. pylori* decreases the risk of developing cancer in individuals without pre-malignant lesions. It reinforces that this infection influences the early stages of gastric carcinogenesis (Polk and Peek, 2010).

Currently, the treatment for gastric cancer consists of surgical intervention associated with chemotherapy using 5-fluorouracil (5-FU), platinum, taxane, irinotecan, and anthracycline (Ma et al., 2016). The treatment options for tumors associated with *H. pylori* are antibiotics (clarithromycin and amoxicillin or metronidazole), proton pump inhibitors, and bismuth (Lamb

and Chen, 2013). However, surgery remains the only curative therapy. At the same time, chemotherapy can improve the outcome, thus emphasizing the importance of employing preventive recourses (Orditura et al., 2014).

Alternatively, there is an increase in the use of natural products. One of the most investigated sources is the plants, representing 25% of the medical industry (Ji et al., 2009; Lahlou, 2013; Calixto, 2019). Botanical drugs contain active metabolites with pharmacological activities capable of relieving symptoms or curing diseases (Trojan-Rodrigues et al., 2012; Ferreira et al., 2014). Thus, the application of ethnopharmacology has collaborated in discovering new chemical entities, mainly through the bioprospecting of secondary metabolites (Albino et al., 2020).

Among the most known and studied ethnobotanical constituents are flavonoids. They possess a polyphenolic benzo- γ -pyrone structure of low molecular weight (Kumar and Pandey, 2013; Jucá et al., 2020). Moreover, these compounds present antioxidant (Babiaka et al., 2020; Joseph Sahayarayan et al., 2020; Liu et al., 2020), hepatoprotective (Ge et al., 2018; Ma Q. et al., 2020; Wei et al., 2020), anti-inflammatory (Maleki et al., 2019; Tian et al., 2019; Wu et al., 2019), anticancer (Imran et al., 2019; Bailly, 2020; Wei et al., 2020), antiviral (Ahmad et al., 2015; Russo et al., 2020), and antibacterial properties (Cushnie and Lamb, 2005; Ahmad et al., 2015; Tian et al., 2019; Biharee et al., 2020). Concerning the antibacterial activity, flavonoids can inhibit the synthesis of nucleic acids, the function of the cytoplasmic membrane, and energy metabolism, among others. These activities prompt their application as antibacterial drugs with a scope of possible mechanisms of action (Cushnie and Lamb, 2005; Xie et al., 2014).

The antimicrobial potential of flavonoids against *H. pylori* has been described in the literature by several studies (Loo, 1997; Bae et al., 1999; Shin et al., 2005; Lee et al., 2006; Cushnie and Lamb, 2011; Pandey and Kumar, 2013; González et al., 2019). In addition to demonstrating an *in vitro* action against this bacterium, these compounds could also promote synergistic interactions with antibiotics commonly used in treatments against *H. pylori* infections (Krzyżek et al., 2021). The pathways of action of flavonoids can be diverse. Some mechanisms in *H. pylori* have already been described, such as inhibition of the essential function of HsrA (González et al., 2019), mediation of the response to oxidative stress (Olekhovich et al., 2013, 2014; Pellicciari et al., 2017), interactions with virulence factors (Kim et al., 2021), recognition of molecular targets including secretion systems (Yeon et al., 2019) and enzymes (Wu et al., 2008; Zhang et al., 2008) acting on pathways that lead to changes in cell morphology of *H. pylori* (Krzyżek et al., 2021). In turn, the broad pharmacotherapeutic and biochemical spectrum of flavonoids and the possible contribution of these compounds to improving human health make such substances increasingly explored (Tungmunthum et al., 2018). Still, these findings support the valuable potential of flavonoids as candidate botanical drugs for novel antibacterial and anticancer strategies. The most promising flavonoid compounds are Catechin, Epicatechin, Kaempferol, Luteolin, Morin, Myricetin, Naringenin, Naringin, Quercetin,

Hyperoside, and Rutin. In this way, this article provides an overview of the biological and pharmacological activities of flavonoid-rich plant extracts with a focus on the use of these substances against *H. pylori* infection in the prevention of gastric cancer.

MATERIALS AND METHODS

The Question Under Analysis

This review was guided by the question: “Are flavonoids-rich plant extracts a promising alternative in treatments against *Helicobacter pylori* infection and preventing gastric cancer?”

Search Strategy and Articles Selection

PRISMA guidelines were followed (Liberati et al., 2009; Moher et al., 2009). In addition, an electronic search was performed in the PubMed and Science Direct databases from studies published between 2010 to August 2020, with the keywords “flavonoids” and “*Helicobacter pylori*.”

Studies Selection

Eligible studies followed the criteria: 1) pre-clinical *in vitro* and *in vivo*; 2) studies with rodents and cells; 3) any type of treatment that used plant extracts containing flavonoids in its composition; 4) studies with positive or negative control; 5) no language restriction. Clinical research, studies with other than flavonoids that did not determine the value of the tested dose, with flavonoids in their isolated form, and studies that used flavonoids as control compounds, were excluded.

Two independent reviewers selected the studies. In the first screening, titles and abstracts were evaluated, and studies considered irrelevant were excluded. The two reviewers read the articles for each potential manuscript and evaluated them based on the inclusion criteria. Duplicate studies between the bases were excluded. A third reviewer was contacted in the presence of inconsistency between the two examiners. Thus, 44 articles were selected for this review that reports the activity of plant species extracts containing flavonoids against *H. pylori*.

RESULTS

The initial search of the databases (with the strategies presented in **Table 1**) allowed the identification of 1,773 publications. Review studies, meta-analyses, encyclopedias, book chapters, abstracts, conference proceedings, editorials/letters, and case reports were excluded. The 567 articles left were screened based on titles and abstracts for the inclusion criteria mentioned above. At this stage, 128 articles remained, following the exclusion of 439 articles. Subsequently to the removal of 25 repeated articles, 103 remained. These studies were afterward entirely read. Finally, 44 articles were selected, as 59 articles did not meet all inclusion criteria (**Figure 1**). The selected studies were concentrated between 2010 and 2020 and are considered current.

TABLE 1 | Pharmacobotanical information, extracts and tests involving activity against *H. pylori* of flavonoids contained in plant species.

Species	Family	Extracted part	Identified flavonoids	Study model	Pharmacological evaluation	Country	References
<i>Qualea parviflora</i>	Vochysiaceae	Bark	—	<i>In vitro</i>	Agar well diffusion	Brazil	Mazzolin et al. (2010)
<i>Camellia sinensis</i>	Theaceae	Leaves	Catechin; Epicatechin Epigallocatechin; Quercetin	<i>In vitro</i>	Agar diffusion	USA	Ankolekar et al. (2011)
<i>Hypericum erectum</i>	Hypericaceae	Whole plant	Quercetin-3'-O-β-D-galactopyranoside	<i>In vitro</i>	MIC	South Korea	Moon et al. (2011)
<i>Bridelia micranta</i>	Phyllanthaceae	Stem bark	—	<i>In vitro</i>	Agar well diffusion, MIC, rate of kill	South Africa	Okeleye et al. (2011)
<i>Byrsonima intermedia</i>	Malpighiaceae	Leaves	Catechin; Epicatechin; Quercetin Quercetin-3-(2''-O-galloyl)-O-α-galactopyranoside; Quercetin-3-O-(2''-O-galloyl)-α-arabinopyranoside; Quercetin-3'-O-(2''-acetyl)-β-D-glucopyranoside; Quercetin-3-O-α-arabinopyranoside; Quercetin-3'-O-β-D-galactopyranoside 7,3'-di-O-methyletheriodictyol	<i>In vitro</i>	MIC	Brazil	Santos et al. (2012)
<i>Glycyrrhiza Glabra</i>	Fabaceae	Roots	Glabridin; Glabrol	<i>In vitro</i>	MIC	India	Asha et al. (2013)
<i>Amygdalus communis</i>	Rosaceae	Fruit	Epicatechin; Naringenin	<i>In vitro</i>	MIC	Italy	Bisignano et al. (2013)
<i>Vitis rotundifolia</i>	Vitaceae	Fruit	—	<i>In vitro</i>	Disk diffusion	USA	Brown and Jiang, (2013)
<i>Polygala cyparissias</i>	Polygalaceae	Whole plant	—	<i>In vitro</i>	MIC	Brazil	Klein-Júnior et al. (2013)
<i>Lythrum salicaria</i>	Lythraceae	Leaves, flowers and stem	—	<i>In vitro</i>	Disk diffusion	Iran	Manayi et al. (2013)
<i>Caesalpinia pyramidalis</i>	Leguminosae	Inner bark	—	<i>In vitro</i>	MIC, MBC	Brazil	Ribeiro et al. (2013)
<i>Hippocratea celastroides</i>	Hippocrateaceae	Leaves, stems, and root bark	—	<i>In vitro</i>	MIC	Mexico	Escobedo Hinojosa et al. (2014)
<i>Theobroma cacao</i>	Malvaceae	Seeds	—	<i>In vitro</i>	MIC	Nigeria	Lawal et al. (2014)
<i>Lippia integrifolia</i>	Lythraceae	Leaves and flowers	Salvagenin; 6-Hydroxyluteolin 7-hexoside; 6-Methoxyluteolin-hexoside 6-Methylscutellarein 7-hexoside B-ring-dimethoxylated Flavone-hexoside; Methoxylated apigenin-hexoside	<i>In vitro</i>	Agar diffusion	Argentina	Marcial et al. (2014)
<i>Cuphea aequipetala</i>	Lythraceae	Leaves and flowers	—	<i>In vitro</i>	MIC	Brazil	Palacios-Espinosa et al. (2014)
<i>Peumus boldus</i>	Monimiaceae	Leaves	Catechin; Epicatechin	<i>In vitro</i>	MIC	Chile	Pastene et al. (2014)
<i>Solanum cernuum</i>	Solanaceae	Leaves	Atzelin; Quercitrin	<i>In vitro</i>	MIC, MBC	Brazil	Miranda et al. (2015)
<i>Copaifera malmey</i>	Fabaceae	Leaves	Rutin; Catechin; Quercetin	<i>In vitro</i>	MIC	Brazil	Adzu et al. (2015)
<i>Parthenium hysterophorus</i>	Asteraceae	Roots	—	<i>In vitro</i>	MIC	Mexico	Espinosa-Rivero et al. (2015)
<i>Lithraea molleoides</i>	Anacardaceae	Leaves	Rutin	<i>In vitro</i>	MIC	Argentina	Garro et al. (2015)
<i>Syzygium aromaticum</i> ; <i>Piper nigrum</i> ; <i>Cuminum cyminum</i> ; <i>Salvia officinalis</i> ; <i>Punica granatum</i> ; <i>Zingiber officinale</i> ; <i>Commiphora</i>	Myrtaceae; Piperaceae; Apiaceae; Lamiaceae; Punicaceae; Zingiberaceae; Burseraceae Fabaceae	Flowers; Fruit; Seeds; Leaves; Peel; Roots; Resin; Roots	Catechin	<i>In vitro</i>	MIC	Egypt	Hamad et al. (2015)

(Continued on following page)

TABLE 1 | (Continued) Pharmacobotanical information, extracts and tests involving activity against *H. pylori* of flavonoids contained in plant species.

Species	Family	Extracted part	Identified flavonoids	Study model	Pharmacological evaluation	Country	References
<i>myrrha</i> ; <i>Glycyrrhiza glabra</i>							
<i>Maytenus robusta</i>	Celastraceae	Leaves	—	<i>In vitro</i>	MIC	Brazil	Mota Da Silva et al. (2015)
<i>Leonotis nepetifolia</i>	Lamiaceae	Whole plant	Kaempferol; Morin; Myricetin; Naringin; Naringenin; Quercetin; Rutin	<i>In vitro</i>	MIC, MBC	Brazil	Oliveira et al. (2015)
<i>Piper umbellatum</i>	Piperaceae	Leaves	—	<i>In vitro</i>	MIC	Brazil	da Silva Junior et al. (2016)
<i>Euphorbia umbellata</i>	Euphorbiaceae	Bark	—	<i>In vitro</i>	Disk diffusion	Brazil	Minozzo et al. (2016)
<i>Rosa hybrida</i>	Rosaceae	Flowers	—	<i>In vitro</i>	MIC	Korea	Park et al. (2016)
<i>Agrimonia eupatoria</i> ; <i>Fragaria vesca</i>	Rosaceae	Leaves and stems; flowers and fruit	—	<i>In vitro</i>	MIC	Portugal	Cardoso et al. (2018)
<i>Heterotheca inuloides</i>	Asteraceae	Leaves, stems and flowers	Quercetin; 7,3'-di-O-methyletheriodictyol	<i>In vitro</i>	MIC	Mexico	Egas et al. (2018)
<i>Anoda cristata</i> ; <i>Cnidioscolus aconitifolius</i> ; <i>Crotalaria pumila</i>	Malvaceae; Euphorbiaceae; Fabaceae	Leaves	Acacetin; Diosmetin	<i>In vitro</i>	MIC	Mexico	Gomez-Chang et al. (2018)
<i>Desmostachya bipinnata</i>	Poaceae	Leaves and flowers	—	<i>In vitro</i>	MIC	Saudi Arabia	Ibrahim et al. (2018)
<i>Oryza sativa</i>	Poaceae	Grain	—	<i>In vitro</i>	Western blotting	South Korea	Kim et al. (2018)
<i>Ixeris chinensis</i>	Asteraceae	Whole plant	Kaempferol; Luteolin; Myricetin; Naringenin; Naringin; Rutin	<i>In vitro</i>	Disk diffusion	Taiwan	Lu et al. (2018)
<i>Physalis alkekengi</i>	Solanaceae	Leaves and flowers	Kaempferol; Quercetin	<i>In vitro</i>	MIC	China	Wang et al. (2018)
<i>Cannabis sativa</i>	Cannabaceae	Flowers	Catechin; Epicatechin; Naringenin; Naringin; Quercetin; Rutin	<i>In vitro</i>	MIC, MBC	Italy	Zengin et al. (2018)
<i>Cochlospermum regium</i>	Cochlospermaceae	Leaves	Kaempferol; Morin; Myricetin; Rutin	<i>In vitro</i>	MIC	Brazil	Arunachalam et al. (2019)
<i>Azadirachta indica</i>	Meliaceae	Fruit and seeds	—	<i>In vitro</i>	MIC	Italy	Cesa et al. (2019)
<i>Viola elongata</i>	Myristicaceae	Stems	—	<i>In vitro</i>	MIC	Brazil	de Almeida et al. (2019)
<i>Byrsonima intermedia</i>	Malpighiaceae	Leaves	Catechin; Epicatechin; Quercetin	<i>In vitro</i>	MIC	Brazil	de Cássia dos Santos et al. (2019)
<i>Diospyros virginiana</i>	Ebenaceae	Pedicels	—	<i>In vitro</i>	MIC	South Korea	Saravanakumar et al. (2019)
<i>Casearia sylvestris</i>	Salicaceae	Leaves	—	<i>In vitro</i>	MIC	Brazil	Spósito et al. (2019)
<i>Plectranthus barbatus</i>	Lamiaceae	Leaves	Luteolin; Quercetin	<i>In vitro</i>	MIC, MBC	Brazil	Borges et al. (2020)
<i>Berberis aristata</i>	Berberidaceae	Stems	—	<i>In vitro</i>	Disk diffusion	India	Das et al. (2020)
<i>Erythrina speciosa</i>	Fabaceae	Leaves	—	<i>In vitro</i>	MIC	Egypt	Fahmy et al. (2020)
<i>Alpinia Officinarum</i>	Zingiberaceae	Rhizomes	Apigenin; Galangin; Galangin-3-methylether; Kaempferol; Kaempferide; Pinobaksin; Ponocembrin; Quercetin; Quercetin-3-methylether; Salvagenin	<i>In vivo</i>	<i>H. pylori</i> -associated gastritis (HAG) model (mice)	China	Ma et al. (2020)

There was variability in the study regions for the selected manuscripts, with 25% of the papers coming from Asia (Moon et al., 2011; Asha et al., 2013; Manayi et al., 2013; Wang et al., 2014; Park et al., 2016; Ibrahim et al., 2018; Kim et al., 2018; Lu et al., 2018; Saravanakumar et al., 2019; Ma X. et al., 2020; Das et al., 2020), 56.82% from America, of which 40.91% were from South America (Adzu et al., 2015; Almeida et al., 2019;

Arunachalam et al., 2019; Borges et al., 2020; da Silva Junior et al., 2016; de Cássia dos Santos et al., 2019; Garro et al., 2015; Klein-Júnior et al., 2013; Marcial et al., 2014; Mazzolin et al., 2010; Minozzo et al., 2016; Miranda et al., 2015; Mota Da Silva et al., 2015; Oliveira et al., 2015; Pastene et al., 2014; Ribeiro et al., 2013; Santos et al., 2012; Spósito et al., 2019) and 15.91% from North America (Ankolekar et al., 2011; Brown and Jiang, 2013;

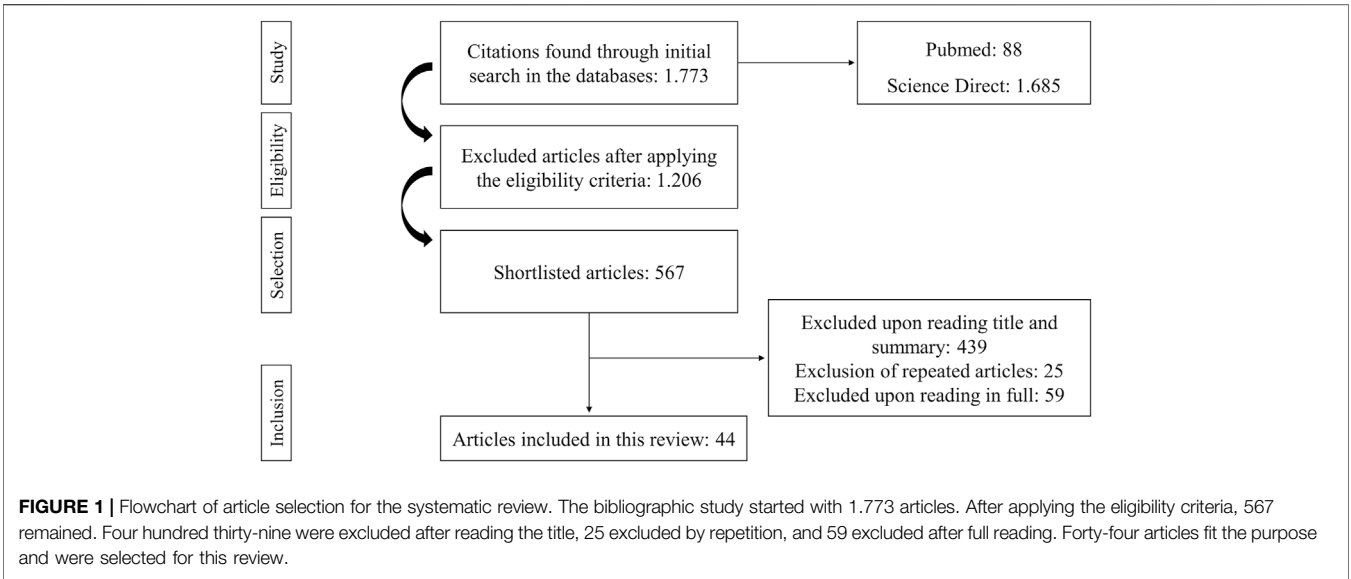
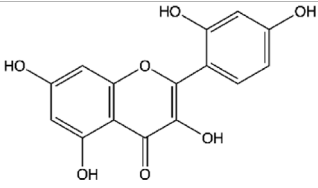
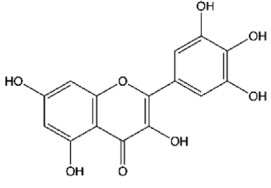
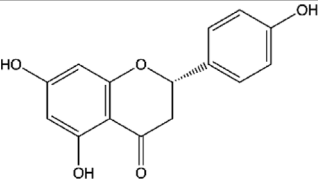
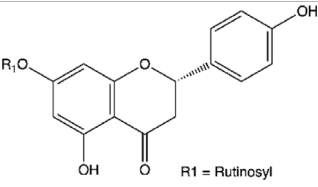
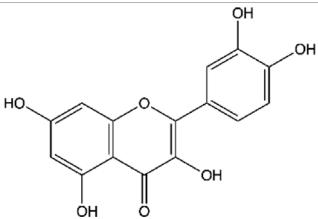
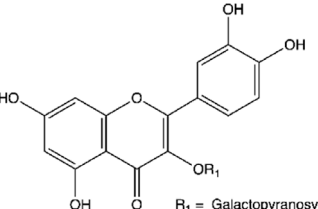
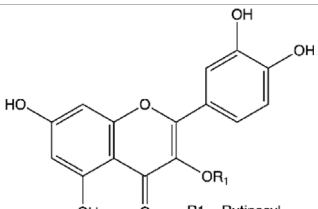


TABLE 2 | Main flavonoids identified in the articles included in this review.

ID	Name	Structure	Reference
01	Catechin		Adzu et al. (2015); Ankolekar et al. (2011); de Cássia dos Santos et al. (2019); Hamad et al. (2015); Pastene et al. (2014); Santos et al. (2012); Zengin et al. (2018)
02	Epicatechin		Ankolekar et al. (2011); Bisignano et al. (2013); de Cássia dos Santos et al. (2019); Pastene et al. (2014); Santos et al. (2012); Zengin et al. (2018)
03	Kaempferol		Arunachalam et al. (2019); Lu et al. (2018); Ma et al. (2020); Oliveira et al. (2015); Wang et al. (2018)
04	Luteolin		Borges et al. (2020); Fahmy et al. (2020); Lu et al. (2018)
05	Morin		Arunachalam et al. (2019); Oliveira et al. (2015)

(Continued on following page)

TABLE 2 | (Continued) Main flavonoids identified in the articles included in this review.

ID	Name	Structure	Reference
			
06	Myricetin		Arunachalam et al. (2019); Lu et al. (2018); Oliveira et al. (2015)
07	Naringenin		Bisignano et al. (2013); Lu et al. (2018); Oliveira et al. (2015); Zengin et al. (2018)
08	Naringin	 R ₁ = Rutinosyl	Lu et al. (2018); Oliveira et al. (2015); Zengin et al. (2018)
09	Quercetin		Adzu et al. (2015); Ankolekar et al. (2011); Borges et al. (2020); de Cássia dos Santos et al. (2019); Egas et al. (2018); Ma et al. (2020); Oliveira et al. (2015); Santos et al. (2012); Wang et al. (2018); Zengin et al. (2018)
10	Hyperoside	 R ₁ = Galactopyranosyl	Moon et al. (2011); Santos et al. (2012)
11	Rutin	 R ₁ = Rutinosyl	Adzu et al. (2015); Arunachalam et al. (2019); Garro et al. (2015); Lu et al. (2018); Oliveira et al. (2015); Zengin et al. (2018)

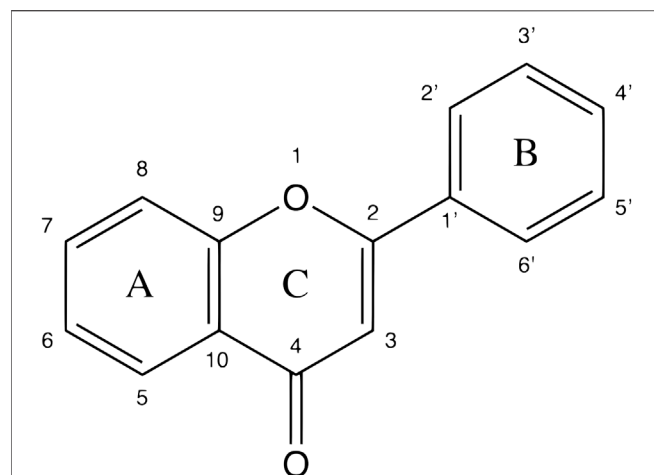


FIGURE 2 | A basic chemical skeleton of flavonoids. General structural representation of a flavonoid, characteristic of 15 carbon atoms in its basic skeleton, corresponding to two benzene rings (A and B) linked by a pyran ring (C).

TABLE 3 | Advantages of flavonoid-rich extracts with antimicrobial activities compared to other extracts.

Advantages	References
Diverse microbial cell targets	Baker, (2020)
Different mechanisms of conventional antimicrobial drugs	Pandey and Kumar, (2013)
Modulation of antimicrobial resistance mechanisms	Górnica et al. (2019)
Greater possibility of synergistic association with traditional antimicrobials	Cushnie and Lamb, (2011)

Escobedo Hinojosa et al., 2014; Palacios-Espinosa et al., 2014; Espinosa-Rivero et al., 2015; Egas et al., 2018; Gomez-Chang et al., 2018), 9.09% of the articles originated from the Africa (Okeleye et al., 2011; Lawal et al., 2014; Hamad et al., 2015; Fahmy et al., 2020), and 9.09% from the Europe (Bisignano et al., 2013; Cardoso et al., 2018; Zengin et al., 2018; Cesa et al., 2019).

Among the Asian countries, South Korea represented 9.09% of the publications (Moon et al., 2011; Park et al., 2016; Kim et al., 2018; Saravanakumar et al., 2019), India (Asha et al., 2013; Das et al., 2020) and China (Wang et al., 2018; Ma X. et al., 2020) both 4.55%, Iran (Manayi et al., 2013), Saudi Arabia (Ibrahim et al., 2018), and Taiwan (Lu et al., 2018) 2.27%. In South America, Brazil (Adzu et al., 2015; Almeida et al., 2019; Arunachalam et al., 2019; Borges et al., 2020; da Silva Junior et al., 2016; de Cássia dos Santos et al., 2019; Klein-Júnior et al., 2013; Mazzolin et al., 2010; Minozzo et al., 2016; Miranda et al., 2015; Mota Da Silva et al., 2015; Oliveira et al., 2015; Ribeiro et al., 2013; Santos et al., 2012; Spósito et al., 2019) represented 34.09%, Argentina (Marcial et al., 2014; Garro et al., 2015) 4.55%, and Chile (Pastene et al., 2014) 2.27%. In North America, Mexico (Escobedo Hinojosa et al., 2014; Palacios-Espinosa et al., 2014; Espinosa-Rivero et al., 2015; Egas et al., 2018; Gomez-Chang et al., 2018) represented 11.36% and the United States (Ankolekar et al., 2011; Brown and Jiang,

2013) 4.55%. In the Africa, Egypt (Hamad et al., 2015; Fahmy et al., 2020) represented 4.55%, Nigeria (Lawal et al., 2014) and South Africa (Okeleye et al., 2011) both 2.27%. In the Europe, Italy (Bisignano et al., 2013; Zengin et al., 2018; Cesa et al., 2019) represented 6.82% and Portugal (Cardoso et al., 2018) 2.27% of publications.

The plant families used in the studies were Anacardaceae (Garro et al., 2015), Apiaceae (Hamad et al., 2015), Asteraceae (Espinosa-Rivero et al., 2015; Egas et al., 2018; Lu et al., 2018), Berberidaceae (Das et al., 2020), Burseraceae (Hamad et al., 2015), Cannabaceae (Zengin et al., 2018), Celastraceae (Mota Da Silva et al., 2015), Cochlospermaceae (Arunachalam et al., 2019), Ebenaceae (Saravanakumar et al., 2019), Euphorbiaceae (Minozzo et al., 2016; Gomez-Chang et al., 2018), Fabaceae (Asha et al., 2013; Adzu et al., 2015; Hamad et al., 2015; Gomez-Chang et al., 2018; Fahmy et al., 2020), Hippocrateaceae (Escobedo Hinojosa et al., 2014), Hypericaceae (Moon et al., 2011), Lamiaceae (Oliveira et al., 2015), Leguminosae (Ribeiro et al., 2013), Lythraceae (Manayi et al., 2013; Marcial et al., 2014; Palacios-Espinosa et al., 2014), Malpighiaceae (Santos et al., 2012; de Cássia dos Santos et al., 2019), Malvaceae (Lawal et al., 2014; Gomez-Chang et al., 2018), Meliaceae (Cesa et al., 2019), Monimiaceae (Pastene et al., 2014), Myristicaceae (de Almeida et al., 2019), Myrtaceae (Hamad et al., 2015), Phyllanthaceae (Okeleye et al., 2011), Piperaceae (da Silva Junior et al., 2016; Hamad et al., 2015), Poaceae (Ibrahim et al., 2018; Kim et al., 2018), Polygalaceae (Klein-Júnior et al., 2013), Rosaceae (Bisignano et al., 2013; Park et al., 2016; Cardoso et al., 2018), Salicaceae (Spósito et al., 2019), Solanaceae (Abreu Miranda et al., 2015; Wang et al., 2018), Theaceae (Ankolekar et al., 2011), Vitaceae (Brown and Jiang, 2013), Vochysiaceae (Mazzolin et al., 2010) and Zingiberaceae (Hamad et al., 2015; Ma X. et al., 2020). The most prominent family in these studies was the Fabaceae.

Between the flavonoids identified in the extracts (Table 2), quercetin (Ankolekar et al., 2011; Santos et al., 2012; Adzu et al., 2015; Oliveira et al., 2015; Egas et al., 2018; Wang et al., 2018; Zengin et al., 2018; de Cássia dos Santos et al., 2019; Ma X. et al., 2020; Borges et al., 2020), catechin (Ankolekar et al., 2011; Santos et al., 2012; Pastene et al., 2014; Adzu et al., 2015; Hamad et al., 2015; Zengin et al., 2018; de Cássia dos Santos et al., 2019), epicatechin (Ankolekar et al., 2011; Santos et al., 2012; Bisignano et al., 2013; Pastene et al., 2014; Zengin et al., 2018; de Cássia dos Santos et al., 2019), rutin (Adzu et al., 2015; Garro et al., 2015; Oliveira et al., 2015; Lu et al., 2018; Zengin et al., 2018; Arunachalam et al., 2019), kaempferol (Oliveira et al., 2015; Lu et al., 2018; Wang et al., 2018; Arunachalam et al., 2019; Ma X. et al., 2020), naringenin (Bisignano et al., 2013; Oliveira et al., 2015; Lu et al., 2018; Zengin et al., 2018), naringin (Oliveira et al., 2015; Lu et al., 2018; Zengin et al., 2018), luteolin (Lu et al., 2018; Borges et al., 2020; Fahmy et al., 2020), myricetin (Oliveira et al., 2015; Lu et al., 2018; Arunachalam et al., 2019), morin (Oliveira et al., 2015; Arunachalam et al., 2019), and quercetin-3'-O- β -D-galactopyranoside (Moon et al., 2011; Santos et al., 2012) stood out.

The tests for determination of antimicrobial activity included the evaluation of minimum inhibitory concentration (MIC) (Adzu et al., 2015; Arunachalam et al., 2019; Asha et al., 2013;

Bisignano et al., 2013; Borges et al., 2020; Cardoso et al., 2018; Cesa et al., 2019; da Silva Junior et al., 2016; de Almeida et al., 2019; de Cássia dos Santos et al., 2019; Egas et al., 2018; Escobedo Hinojosa et al., 2014; Espinosa-Rivero et al., 2015; Fahmy et al., 2020; Garro et al., 2015; Gomez-Chang et al., 2018; Hamad et al., 2015; Ibrahim et al., 2018; Klein-Júnior et al., 2013; Lawal et al., 2014; Moon et al., 2011; Mota Da Silva et al., 2015; Okeleye et al., 2011; Oliveira et al., 2015; Palacios-Espinosa et al., 2014; Park et al., 2016; Pastene et al., 2014; Ribeiro et al., 2013; Santos et al., 2012; Saravanakumar et al., 2019; Spósito et al., 2019; Wang et al., 2018; Zengin et al., 2018), minimum bactericidal concentration (MBC) (Ribeiro et al., 2013; Abreu Miranda et al., 2015; Oliveira et al., 2015; Zengin et al., 2018; Borges et al., 2020), disk diffusion (Brown and Jiang, 2013; Manayi et al., 2013; Minozzo et al., 2016; Lu et al., 2018; Das et al., 2020), well agar diffusion (Mazzolin et al., 2010; Okeleye et al., 2011), agar diffusion (Ankolekar et al., 2011; Marcial et al., 2014), rate of kill (Okeleye et al., 2011), and *H. pylori*-associated gastritis (HAG) *in vivo* model (mice) (Ma X. et al., 2020).

DISCUSSION

The use of natural products and synthetic variations of their structures is the primary source of novel chemical entities approved as drugs by federal regulatory agencies. Despite the significant advance in combinatorial chemistry, discovering new active compounds through exclusively synthetic routes does not fulfill the role of presenting itself as a primary source of therapeutic innovation. *In silico* analysis has been used as an optimization tool to identify natural compounds as a valuable alternative to the pharmaceutical industry (Newman and Cragg, 2020).

Natural products and their derivatives represent more than a third of all newly discovered molecular entities approved by the FDA (Food and Drugs Administration). Notably, about 25% are of plant origin (Patridge et al., 2016). Sixty-four percent of these compounds have been used to treat neoplastic diseases. For example, of the 126 drugs discovered between 1981 and 2019, 78 (48%) are natural products for antibacterials.

Flavonoids

The pharmacological potential of medicinal plants is given by the chemical structures produced by secondary plant metabolism. It presents several biosynthesis mechanisms capable of supplying substances with complex chemical structures. In addition, these structures are responsible for specialized intrinsic functions, favoring the activity in biological environments. They generally possess pharmacophoric regions, which are intricate to create or reproduce through organic synthesis (Mendes et al., 2012).

Flavonoids are among the main classes of secondary metabolites with pharmacological relevance (Wang et al., 2019). These phenolic compounds act on plants as adaptive agents, playing a crucial role in the survival of species against environmental stresses and in response to invasions by microorganisms. This natural function of flavonoids explains

the growing interest in studying these compounds in searching for new drugs with antimicrobial activity, mainly due to the lack of effective therapies in the current clinical scenario (Biharee et al., 2020).

Moreover, flavonoids represent one of the most important and diversified phenolic groups among natural metabolites. Its occurrence is often associated with the color of plants, and it is frequently found in flowers, fruits, leaves, stems, and seeds (Zuanazzi and Montanha, 2007). The word “Flavonoid” derives from the Latin “Flavus,” which means light yellow. However, the color of the flavonoid often varies according to the species. The basic skeleton of the flavonoids (**Figure 2**) has a tricyclic structure with 15 carbon atoms, with a chromatic ring (A) fused to a pinane ring (C) connected to an aromatic ring (B), leading to the subcategories of flavonoids (Zuanazzi and Montanha, 2007; Batra and Sharma, 2013; Biharee et al., 2020).

Literature reports have shown that flavonoids play a role in plant survival by preventing the spread of fungal and bacterial pathogens (Cho and Lee, 2015; Piasecka et al., 2015). Furthermore, flavonoid biosynthesis is closely related to defense responses in plant tissues. Significantly, it interferes in the vascular strands of leaves, which are most exposed and susceptible to contamination (Beck and Stengel, 2016). These findings support the hypothesis that flavonoids are potential antimicrobial agents that may be effective against human pathogens.

Due to the great diversity of compounds within the flavonoid group, the highly concentrated extracts exhibit more diverse mechanisms of antimicrobial activity. In other words, they target more components and functions of bacterial cells than other plant secondary metabolites (Cushnie and Lamb, 2005; Górniak et al., 2019). Other advantages of flavonoid-rich extracts with antimicrobial action compared to others are summarized in **Table 3**.

Catechin and Epicatechin

Catechins, such as catechin and epicatechin, are flavonoids in plants, fruits (e.g., apple, strawberry, kiwi), black and green tea, red wine, beer, chocolate, and cocoa, among others (Grzesik et al., 2018). For example, green tea has a high catechin concentration (Botten et al., 2015), about 1 g/ml in a teacup (Rahardiyani, 2019). Approximately 5–7% of this concentration is epicatechin (Braicu et al., 2013).

Catechins' antimicrobial activity is related to the interaction of this compound with the cell wall and inner membrane of bacteria and hydrogen peroxide production. One of the proposed mechanisms of action is related to the formation of high molecular mass complexes between this compound and proteins on the surface of the bacterial cell wall. It interrupts substrate transit between the intra and extracellular environment, inhibiting bacterial cell activity (Nakayama et al., 2013).

Some studies report catechin's antimicrobial activity against gram-positive and gram-negative bacteria. It includes species like *Escherichia coli* (*E. coli*) (Bernal-Mercado et al., 2018), *H. pylori* (Díaz-Gómez et al., 2013), *Staphylococcus aureus* (*S. aureus*) (Martins et al., 2011; Sinsinwar and Vadivel, 2020), and *Bacillus subtilis* (*B. subtilis*) (Fathima and Rao, 2016).

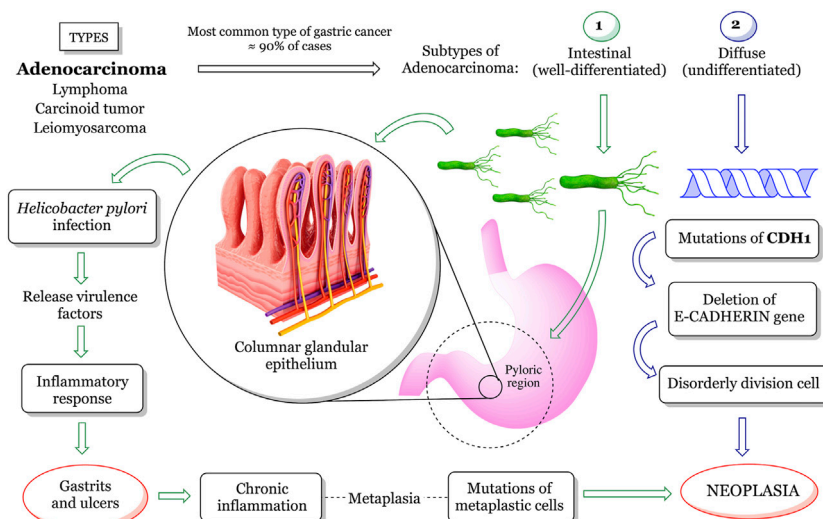


FIGURE 3 | General overview of *H. pylori*-associated gastric cancer development. According to its topology, gastric cancer can be classified into adenocarcinoma, lymphoma, carcinoid tumor, and leiomyosarcoma. Adenocarcinoma is the type of gastric cancer most affecting the population, subdivided into (1) intestinal and (2) diffuse. Type (1) is mainly elicited by an acute immune response induced by *H. pylori* infection. The silent persistence of the bacteria provides a picture of chronic inflammation, consequently inducing gastritis and ulcers that can lead to gastric perforation. As a result, epithelial tissue undergoes metaplasia (cell differentiation) and behaves like intestinal cells, losing function. Metaplastic cells begin a process of disordered division by undergoing gene mutation that ends up in the formation of malignant neoplastic tissue. Type (2) adenocarcinoma is caused by genetic factors that affect the expression of the intercellular adhesion proteins. For example, E-cadherin is responsible for keeping gastric epithelial cells interconnected and controls the cell cycle.

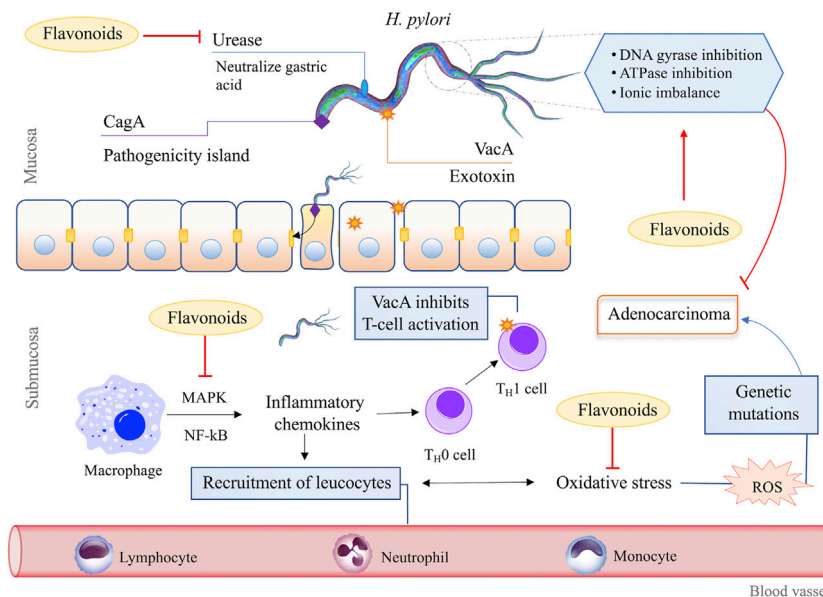


FIGURE 4 | Mechanisms of action of flavonoids against *H. pylori*. The pathogenesis of *H. pylori* depends on several virulence factors, including urease. This enzyme neutralizes the acidic pH of the gastric medium and facilitates bacteria adhesion to the epithelium. Flavonoids can block this process once they inhibit urease activity. Flavonoids also act by inhibiting enzymes crucial for the reproduction and survival of *H. pylori*, such as DNA gyrase and ATPase. In addition, it induces ionic and metabolic imbalances at the cytoplasmic level, causing bacterial cell wall disruption, which leads to cell death or latency. Once adhered to the gastric epithelium, *H. pylori* induces the release of proinflammatory cytokines and the generation of specific genetic mutations which promote cell apoptosis. Flavonoids have anti-inflammatory activities. They inhibit MAPK and NF- κ B pathways and regulate the oxidative stress response in phagocytes and other cells. In addition, some flavonoids act as antioxidant agents, scavenging free radicals and reestablishing the ionic balance. The Establishment of adenocarcinoma from successive gene mutations caused by chronic inflammation and the inhibition of any stage of this process can attenuate, delay or prevent the onset of gastric cancer.

Kaempferol

Kaempferol is a natural flavonol present in many edible plants (e.g., broccoli, cabbage, beans, tomatoes, and strawberries) as well as in traditional medicine (e.g., *Ginkgo biloba* L. (Ginkgoaceae); *Moringa oleifera* Lamarck (Moringaceae) (Saldanha et al., 2019). This compound and its glycosides possess several pharmacological properties, such as antioxidant, anti-inflammatory, antidiabetic, anticancer, cardioprotective, neuroprotective, anti-steroidal, anxiolytic, estrogenic/anti-estrogenic, analgesic, anti-allergic and antimicrobial (Mbaveng et al., 2014; Shields, 2017).

Kaempferol's antimicrobial activity may be associated with its ability to form complexes with the bacterial cell wall, which causes the inhibition of microbial growth (Tatsimo et al., 2012). In addition, the compound blocked the formation of *S. aureus* biofilm in the initial adhesion stage (Ming et al., 2017). This inhibition probably occurs due to the inhibition of enzymes responsible for the beginning of biofilm formation and promoting suppression of the expression of genes of some surface proteins involved in adhesion.

In addition to *S. aureus*, kaempferol and its glycosides have reported activity against *H. pylori* (Escandón et al., 2016), *E. coli* (Wu et al., 2013), *Pseudomonas aeruginosa* (*P. aeruginosa*) (Tatsimo et al., 2012), *Vibrio parahaemolyticus* (*V. parahaemolyticus*), *Bacillus cereus* (*B. cereus*), *Bacillus licheniformis* (*B. licheniformis*) (Sivasothy et al., 2013), and *Enterococcus faecalis* (*E. faecalis*) (del Valle et al., 2016).

Luteolin

Luteolin is a flavone naturally found in its glycosylated structure in many edible plant species (e.g., carrot, pepper, peppermint, and oregano) (Omar, 2017). Its pharmacological activities include antioxidant, anti-inflammatory, neuroprotective, anticancer, antidiabetic, and antimicrobial (Dong et al., 2017; Shukla et al., 2019).

Luteolin demonstrates antimicrobial activity against the uropathogenic *E. coli* (UPEC) strain (fei Shen et al., 2014). The compound reduces UPEC adhesion to urinary epithelium cells by decreasing the expression of adhesion proteins in the microorganism's fimbriae. Furthermore, Luteolin reduced the expression of adhesion-related genes and increased the hydrophilicity, inhibiting biofilm formation.

Other studies also describe the activities of luteolin against *H. pylori* (Tran Trung et al., 2020), *S. aureus* (Qiu et al., 2011; Joung et al., 2016; Liu et al., 2020), *Listeria monocytogenes* (*L. monocytogenes*) (Qian et al., 2020), *P. aeruginosa*, *B. cereus*, and *Salmonella typhimurium* (*S. typhimurium*) (Rashed et al., 2014).

Morin

Morin is a flavone in many fruits and plants of the Moraceae and Myrtaceae families, such as *Maclura pomifera* (Rafinesque) C. K. Schneider (Moraceae); *Maclura tinctoria* L. D. Don ex Steudel (Moraceae); *Psidium guajava* L. (Myrtaceae); and *Morus alba* L. (Moraceae) (Mbaveng et al., 2014; Shivashankara et al., 2015; Baliga et al., 2019). This flavonoid is attributed to antioxidant, anti-inflammatory, antidiabetic, antihistamine, antitumor,

antihypertensive, antiuricemic, neuroprotective, antiviral, and antimicrobial activities (Al-Numair et al., 2014; Caselli et al., 2016).

The antimicrobial activity of morin was demonstrated against *Listeria monocytogenes* can be explained by two mechanisms (Sivaranjani et al., 2016). Firstly, it reduces biofilm formation by inhibiting microbial motility and adhesion and compromising cell-surface and cell-cell interactions. The second mechanism is the interruption of listeriolysin O secretion. It reduces the pathogenicity of *L. monocytogenes* in epithelial cells and macrophages.

Morin acts against *S. aureus* (Amin et al., 2015), *B. cereus*, *Salmonella enteritidis* (*S. enteritidis*) (Arima and Danno, 2002), *E. coli* (Kopacz et al., 2016), and *H. pylori* (Tombola et al., 2003).

Myricetin

Myricetin is a flavone encountered in many fruits, vegetables, teas, berries, and red wine (Omar, 2017). Biological activities attributed to this flavone include hypoglycemic (Eddouks et al., 2014), anti-inflammatory (Shukla et al., 2019), anticarcinogenic, and antiviral (Dormán et al., 2016), and antimicrobial (Puupponen-Pimiä et al., 2001).

This compound reduces the expression of genes that encode some virulence factors responsible for bacterial colonization. Moreover, it inactivates host defenses, tissue damage, and nutrient uptake genes in pathogenic strains of *Porphyromonas gingivalis* (*P. gingivalis*) (Grenier et al., 2015). Moreover, myricetin activity was demonstrated against *E. coli* (Puupponen-Pimiä et al., 2001), *S. aureus*, and *Proteus vulgaris* (*P. vulgaris*) (Mori et al., 1987), and *H. pylori* (Tran Trung et al., 2020).

Naringenin and Naringin

The flavanone naringenin and its glycoside (naringin) are abundant in the peels of citrus fruits, mainly grapefruit and orange (Jadeja and Devkar, 2013). They present antioxidant, antidiabetic (Srinivasan et al., 2019), anti-inflammatory (Shukla et al., 2019), hypolipemic, antihypertensive, and antifibrotic (Casas-Grajales and Muriel, 2017), and antimicrobial (Céliz et al., 2011) activities.

Naringenin and naringin act against *Salmonella enteritidis* (Yin et al., 2012). The study reported the synergism of these grapefruit juice components with the acidic pH generated. In combination, these factors reduced the adhesion of *S. enteritidis* by inhibiting the bacterium's acid tolerating response mechanism.

Moreover, other studies reported the activity of naringenin and naringin against *E. coli*, *P. aeruginosa* (Adamczak et al., 2019), *Proteus mirabilis* (*P. mirabilis*), *Acinetobacter baumannii* (*A. baumannii*), *Klebsiella pneumonia* (*K. pneumoniae*), *S. aureus*, *B. subtilis*, *E. faecalis* (Özçelik et al., 2011), and *H. pylori* (Tran Trung et al., 2020).

Quercetin

Quercetin is a bioflavonoid obtained from various plant sources (e.g., apple, onion, citrus fruits, and vegetables) (Shankar et al., 2015; Horwitz, 2018). It has several biological activities, such as

antioxidant, anti-inflammatory, anticancer (Ay et al., 2016), antiviral (Sathya and Devi, 2017), and antimicrobial (Jaisinghani, 2017).

Feasible antimicrobial mechanisms of action of quercetin have been described (Adeyemi et al., 2020) in *S. aureus* and *E. coli*. Quercetin can initiate the peroxidation of the outer lipid membrane in gram-negative bacteria, such as *E. coli*. It compromises the integrity of the bacterial cell barrier, leading to cell lysis. Additionally, in gram-positive bacteria, quercetin causes oxidative stress and activates the kynurenine pathway. It depletes L-tryptophan reserves, leading to a reduction in bacterial growth.

Studies also report quercetin activity against *P. aeruginosa*, *P. vulgaris* (Jaisinghani, 2017), *P. mirabilis*, *A. baumannii*, *K. pneumoniae*, *E. faecalis*, *B. subtilis* (Özçelik et al., 2011) and *H. pylori* (Brown and Jiang, 2013).

Hyperoside and Rutin

Hyperoside (quercetin-3'-O- β -D-galactopyranoside) and rutin (quercetin-3-O-rutinoside) are quercetin glycosides found in vegetables, citrus fruits, and berries. They exhibit several biological activities, such as anti-inflammatory, antithrombotic, antidiabetic, hepatoprotective, antioxidant, antihistamine, antitumor, antiplatelet, antihypertensive, antispasmodic, antiprotozoal, and antimicrobial (Patel and Patel, 2019; Shukla et al., 2019).

Rutin can inhibit biofilm formation in *E. coli* and *S. aureus* (Al-Shabib et al., 2017). The probable mechanism of this activity is related to reducing the production of exopolysaccharides. These molecules are responsible for biofilms' higher resistance to antimicrobials than planktonic cultures and protect the biofilm by forming multiple layers on its surface that aid in adhesion.

Additionally, hyperoside and rutin activities against *P. aeruginosa* (Sun et al., 2017; Adamczak et al., 2019), *Serratia marcescens* (*S. marcescens*) (Vaquero et al., 2007), *E. faecalis* (Jesus et al., 2018), *Actinomyces viscosus* (*A. viscosus*), *Actinomyces naeslundii* (*A. naeslundii*) (Gutiérrez-Venegas et al., 2019), *S. pyogenes* (Van Der Watt and Pretorius, 2001) and *H. pylori* (Jeong, 2009) are also described.

Use of Extracts Containing Flavonoids Against *H. pylori* and Its Advantages

Defined as a group I carcinogen since 1994 by the International Agency for Research on Cancer, *H. pylori* represents about 5% of the total burden of all cancers worldwide (WHO, 2010; Moss, 2017). In addition, *H. pylori* is associated with diseases such as chronic gastritis, peptic ulcer, and gastric mucosa-associated lymphoid tissue lymphoma. This bacterium has a urease enzyme capable of converting the urea present in gastric acid into ammonia, increasing the stomach pH, thus allowing its colonization. Its silent permanence results in chronic inflammation and, consequently, in the appearance of gastritis and ulcers that can lead to gastric perforation. Thereupon, the epithelial tissue begins to undergo metaplasia. The metaplastic cells start the process of uncontrolled division, which undergoes gene mutation and culminate in the formation of malignant

neoplastic tissue (**Figure 3**) (Ladeira et al., 2003; Minozzo et al., 2016).

Among the current treatment strategies for patients with *H. pylori*-associated gastritis and peptic ulcer disease, triple therapy is based on combinations of multiple agents, including bismuth subsalicylate, proton pump inhibitors, H₂ blockers, and antibiotics, mainly clarithromycin. Additionally, the eradication of *H. pylori* is indicated for treating lymphoma. Also, other regimens used as adjunctive therapy include probiotics, bovine lactoferrin, and curcumin (Asha et al., 2013).

As expected, the application of multiple drugs is associated with several side effects, making it impossible for the patient to adhere to and abandon the course of treatment. In addition, these interferents can lead to the emergence of resistant strains (Ustün et al., 2006).

Therefore, the search for new anti-*H. pylori* therapy alternatives promoted the exploration in the field of medicinal plants. As a result, several studies have been conducted, and many natural products have anti-*H. pylori* mechanisms of action proven, such as urease inhibition, DNA damage, protein synthesis inhibition, and anti-inflammatory effects. Moreover, they inhibit some enzymes, such as dihydrofolate reductase and myeloperoxidase N-acetyltransferase (**Figure 4**) (Baker, 2020).

Preparations containing physiologically active constituents in folk medicine support the therapeutic use of flavonoids. Several pharmacological actions include antimicrobial, antitumor, anti-inflammatory, and antioxidant (Asha et al., 2013). For example, flavonoids are effective against different microorganisms by different mechanisms of action. They cause membrane disruption, antibiofilm action, cell envelope synthesis, nucleic acid synthesis, electron transport chain and ATP synthesis, formation of flavonoid-metal complexes, inhibition of bacterial toxins, and others (Górniak et al., 2019).

As mentioned above, pathogenic bacteria may resist antibiotic drugs through different mechanisms. For example, mechanisms might be the prevention of interaction of the drug with the target, efflux of the antibiotic from the cell, and direct destruction or modification of the drug compound. Moreover, bacteria can interchange resistance genes with surrounding colonies. For example, the β -lactamase gene encodes an enzyme that hydrolyzes the amide bond in the β -lactam ring through transformation (incorporation of naked DNA), transduction (phage-mediated), and conjugation. Gram-negative bacteria interfere with β -lactam ring hydrolysis, whereas Gram-positive bacteria modify the target site of antibiotics (Bush and Fisher, 2011; Bush, 2013).

Occasionally the resistance to antimicrobial agents can be obtained via combined mechanisms. For instance, although gentamicin resistance does not rely on antibiotic modification, it is executed by altering the membrane potential and efflux and 16S rRNA methylation (Waglechner and Wright, 2017).

Cistus laurifolius L. (Cistaceae) extract has proved anti-*H. pylori*, including against resistant strains (Ustün et al., 2006). Moreover, the extract of *Glycyrrhiza glabra* L. (Fabaceae)

maintained its action against *H. pylori* even after being clinically used without any drug resistance (Fukai et al., 2002). Such findings infer how flavonoids may be helpful as lead compounds in the development of a new class of anti-*H. pylori* regimens.

Possible Mechanisms of Action of Flavonoids Against *H. pylori*

The urease enzyme is considered a potent *H. pylori* virulence factor. It comprises 6% of the synthesized proteins, representing a significant energy investment in colonization. Moreover, its inhibition hinders the survival of *H. pylori* in the gastric environment, which becomes hostile due to high acidity (Ladeira et al., 2003). *In vitro* experiments demonstrated that the flavonoid quercetin, present in *Heterotheca inuloides* Cassini (Asteraceae) extract, promotes high enzyme inhibition ($IC_{50} = 132.4 \mu\text{g/ml}$) (Egas et al., 2018). Additionally, a complimentary *in silico* study of molecular docking has identified that quercetin interacts with the catalytic site, forming ionic bonds with the zinc cation. Ionic bonds are among the strongest, supporting and inducing high enzyme inhibition activity. Catechin and epicatechin isolated from the *Peumus boldus* extract inhibit urease activity, with IC_{50} values of 66 and $112 \mu\text{g GAE/ml}$, respectively (Pastene et al., 2014). However, due to molecules' sizes and high polarity, they seem to neutralize only the most external pool of urease. It means they could not inhibit the urease cytoplasmic pool, suggesting a more preventive application.

Glabridin and glabrol present in the extract of *Glycyrrhiza glabra* L. (GutGard®) inhibit the dihydrofolate reductase (DHFR) (Asha et al., 2013). DHFR consists of a ubiquitous enzyme in every eukaryotic and prokaryotic cell that plays a crucial role in the synthesis of thymidine. It catalyzes the reduction of 7,8-dihydrofolate to 5,6,7,8-tetrahydrofolate, using NADPH as a cofactor. This reaction is an essential step in the biosynthesis of DNA nucleotide bases and, therefore, plays an essential role in bacteria survival, such as *H. pylori* in the human body. It is interesting to note that in addition to the anti-*H. pylori* activity, GutGard® also has anti-inflammatory (Chandrasekaran et al., 2011) and antioxidant (Mukherjee et al., 2010).

The potential activity of the luteolin-rich extract from *Plectranthus barbatus* (Andrews) Benth. ex G. Don (Lamiaceae) has been proved (Borges et al., 2020). The subinhibitory dose of ethyl acetate (EAF) fraction ($128 \mu\text{g/ml}$) produced similar morphological changes as did the subinhibitory dose of amoxicillin ($0.25 \mu\text{g/ml}$). The filamentous cells found and the production of protrusions indicate a possible action on the bacterial cell wall. These data suggest a possible action on PBPs (Penicillin-Binding Proteins), which are involved in the cell septation process, especially the 63 kDa PBP (PBP63). Besides, observations in producing protrusions and blebs suggest a possible action on other PBPs involved in the peptidoglycan wall.

When assessing the intracellular accumulation of quercetin from *Vitis rotundifolia* Michaux (Vitaceae), it was observed a behavior possibly interspersed in the hydrophobic region of the lipid bilayers of the cell envelope, passively diffused through the

cell membrane into the cytosol (Brown and Jiang, 2013). It may be an interaction with cell membrane proteins or active import into the cytosol, leading to metabolic imbalance, followed by cell death.

Catechin, epicatechin, epigallocatechin, and quercetin flavonoids in white, green, oolong, and black teas deplete membrane electrons responsible for the transport chain (Ankolekar et al., 2011). They disrupt oxidative phosphorylation and inhibit the proton efflux linked to dehydrogenase. Thereby, they interfere with the flow of electrons at the cytochrome level. However, low hydrophobic and simple soluble phenolic compounds may not be effective. The outer lipopolysaccharide layer of *H. pylori* avoids oxidative phosphorylation. As a result, the membrane creates a hydrophobic microenvironment along the bacterial surface. Also, soluble phenols interrupt the H^+ -adenosine triphosphatase required to synthesize adenosine triphosphate. It causes hyperacidification *via* proton donation in the plasma membrane or in the intracellular cytosolic pathway. Another explanation is that the hydrophobic portion of polyphenols adheres to the cell wall. It would cause destabilization and rupture of the membrane and inhibition of transmembrane transport. These mechanisms can act synergistically: the disturbing and destabilizing effect of polyphenols can make it easier for simple soluble phenols to exercise their hyperacidification.

Alpinia officinarum Hance (Zingiberaceae) extracts possess the flavonoids apigenin, galangin, galangin-3-methyl ether, kaempferol, kaempferide, pinobaksin, pinocembrin, quercetin, quercetin-3-methyl ether, and salvagenin (Ma X. et al., 2020). To such metabolites has been attributed the anti-*H. pylori* activity by inhibiting the synthesis of the proinflammatory cytokine interleukin-8 (IL-8) *via* the MAPK pathway, whose gene shows a significant increase in expression in the entire genome of gastric epithelial cells after infection by *H. pylori*. This reduction would result in decreased inflammation and adhesion of the bacteria to the epithelium.

Moreover, the *Lippia integrifolia* (Griseb.) Hieronymus (Verbenaceae) extract demonstrated the flavonoids salvagenin, 6-Hydroxyluteolin 7-hexoside, 6-Methoxyluteolin-hexoside, 6-Methylscutellarein 7-hexoside, B-ring-dimethoxylated Flavone-hexoside and Methoxylated apigenin-hexoside (Marcial et al., 2014). As a result, it exhibited strong antioxidant capacity *in vitro*. Furthermore, it inhibited *H. pylori* adhesion to stomach cells by up to 40%. In comparison, the ethanol-soluble fraction showed up to 60% inhibition rates. Furthermore, the decoction significantly increased the gastric adenocarcinoma cell line (AGS) cell viability at $> 10 \mu\text{g/ml}$ without influencing the proliferation rate. Besides, *H. pylori*-induced IL-8 secretion was significantly reduced by the coincubation of AGS cells with extracts.

Study Relevance

Here, the activity of flavonoid extracts was investigated against *H. pylori* for gastric cancer prevention and treatment. These studies provided a basis for further investigations that may lead to new clinical trials for proper drug administration. In this

perspective, the use of botanical drugs might present as a viable and safe alternative.

Administration of botanic products is a complementary treatment for acute and chronic diseases and preventive care. GutGard® (Asha et al., 2013) is an example currently used to help control indigestion and heartburn and manage *H. pylori* infection at a dosage of 150 mg/day (Ribeiro, 2019). So, using extracts containing flavonoid compounds might be highly relevant to eradicating *H. pylori* as a curative and preventive therapeutic strategy.

Furthermore, botanical drugs are cost-effective compared to synthetic medicines and processed plant derivatives (Maqbool et al., 2019). The focus on the herbal products research encourages the investigation of alternative therapeutic modalities for long-standing and persistent health problems.

Limitations

Studies using pure isolated flavonoids were rare, which required the inclusion of additional extracts in our protocol. Few publications mentioned the mechanism of action of flavonoids on *H. pylori*. Additionally, many articles identified their flavonoids but not their concentration. Furthermore, some studies did not use full botanical taxonomic names, limiting comparative analysis and data translation. Finally, only one *in vivo* study was included in this review, limiting the analytical power of the effectiveness of the flavonoid in the live organism.

FUTURE DIRECTIONS

This review on flavonoids' antimicrobial and anticancer action is in line with recent literature (Al-Ishaq et al., 2021; González et al., 2021; Li et al., 2022). Altogether, data demonstrate the great potential of these compounds in combating *H. pylori* infection and gastric cancer protection. The immense variety of plants that serve as a source of flavonoids can ensure the sustainable production of drugs containing the compounds. In addition, the great potential of these compounds for various health applications is observed. New flavonoids' extraction methods might allow for better profitability and sustainability. Moreover, dosage control and compound stability offered by smart drug delivery systems can further expand the understanding of the activities of flavonoid-rich extracts against various pathogens (de Lima Nascimento et al., 2019; Gondim et al., 2019).

REFERENCES

- Abreu Miranda, M., Lemos, M., Alves Cowart, K., Rodenburg, D., D McChesney, J., Radwan, M. M., et al. (2015). Gastroprotective Activity of the Hydroethanolic Extract and Isolated Compounds from the Leaves of *Solanum Cernuum* Vell. *J. Ethnopharmacol.* 172, 421–429. doi:10.1016/j.jep.2015.06.047
- Abreu Miranda, M., Lemos, M., Alves Cowart, K., Rodenburg, D., D. McChesney, J., Radwan, M. M., et al. (2015). Gastroprotective Activity of the Hydroethanolic Extract and Isolated Compounds from the Leaves of *Solanum Cernuum* Vell. *J. Ethnopharmacol.* 172, 421–429. doi:10.1016/j.jep.2015.06.047

Furthermore, a broader understanding of the interactions of flavonoids with drugs of choice for the treatment of *H. pylori* may help determine the use of the compounds as adjuvant therapy in the fight against the development of gastric cancer. Also, it is imperative to evaluate the effect of flavonoids on the human microbiome and how the metabolic process of the colonizing microbes might interfere with the activities of the compounds against pathogenic strains. Clinical trials testing the action of these compounds in patients with *H. pylori* infection deserve attention.

CONCLUSION

There is no single therapy for *H. pylori* eradication. Instead, an association of an antiulcerogenic drug and two antibiotics with 70–85% success rates. Our data demonstrated the relevance of new studies involving natural products, specifically extracts of plants rich in flavonoids. These compounds have shown promising results in anti-*H. pylori* targeting different mechanisms of action.

AUTHOR CONTRIBUTIONS

All authors contributed to the development of the article. RI, DF, GG, and WR held the bibliographic search and selection of articles. MP and DF performed the methodology of the article. RI, DF, SA, and GG discussed the articles. RI and GG were in charge of generating the tables and figures. BG, SC, SW, and LC were responsible for the general review of the content.

FUNDING

Funds supported this study from the Brazilian Federal Foundation for Support and Evaluation of Graduate Education (CAPES) - Finance Code 001 (fellowships to SC and LC).

ACKNOWLEDGMENTS

Thanks to CAPES, UFPB, and UEPB for the most valuable support given to this research.

- Adamczak, A., Ożarowski, M., and Karpiński, T. M. (2019). Antibacterial Activity of Some Flavonoids and Organic Acids Widely Distributed in Plants. *J. Clin. Med.* 9, 109. doi:10.3390/jcm9010109
- Adeyemi, O. S., Ebugosi, C., Akpor, O. B., Hetta, H. F., Al-Rashed, S., Otohino, D. A., et al. (2020). Quercetin Caused Redox Homeostasis Imbalance and Activated the Kynurenine Pathway (Running Title: Quercetin Caused Oxidative Stress). *Biol. (Basel)* 9, 1–9. doi:10.3390/biology9080219
- Adzu, B., Balogun, S. O., Pavan, E., Ascêncio, S. D., Soares, I. M., Aguiar, R. W., et al. (2015). Evaluation of the Safety, Gastroprotective Activity and Mechanism of Action of Standardised Leaves Infusion Extract of *Copaifera Malmei* Harms. *J. Ethnopharmacol.* 175, 378–389. doi:10.1016/j.jep.2015.09.027

- Ahmad, A., Kaleem, M., Ahmed, Z., and Shafiq, H. (2015). Therapeutic Potential of Flavonoids and Their Mechanism of Action against Microbial and Viral Infections-A Review. *Food Res. Int.* 77, 221–235. doi:10.1016/j.foodres.2015.06.021
- Al-Ishaq, R. K., Liskova, A., Kubatka, P., and Büsselberg, D. (2021). Enzymatic Metabolism of Flavonoids by Gut Microbiota and its Impact on Gastrointestinal Cancer. *Cancers (Basel)* 13. doi:10.3390/cancers13163934
- Al-Numair, K. S., Chandramohan, G., Alsaif, M. A., Veeramani, C., and El Newehy, A. S. (2014). Morin, a Flavonoid, on Lipid Peroxidation and Antioxidant Status in Experimental Myocardial Ischemic Rats. *Afr. J. Tradit. Complement. Altern. Med.* 11, 14–20. doi:10.4314/ajtcam.v11i3.3
- Al-Shabib, N. A., Husain, F. M., Ahmad, I., Khan, M. S., Khan, R. A., and Khan, J. M. (2017). Rutin Inhibits Mono and Multi-Species Biofilm Formation by Foodborne Drug Resistant *Escherichia coli* and *Staphylococcus aureus*. *Food control.* 79, 325–332. doi:10.1016/j.foodcont.2017.03.004
- Albino, S. L., da Silva, J. M., de C NobreNobre, M. S. M. S., de M E Silvae Silva, Y. M. S. Y. M. S., Santos, M. B., de Araújo, R. S. A., et al. (2020). Bioprospecting of Nitrogenous Heterocyclic Scaffolds with Potential Action for Neglected Parasitosis: A Review. *Curr. Pharm. Des.* 26, 4112–4150. doi:10.2174/1381612826666200711160904
- Almeida, G. V. B., Arunachalam, K., Balogun, S. O., Pavan, E., Ascêncio, S. D., Soares, I. M., et al. (2019). Chemical Characterization and Evaluation of Gastric Antiulcer Properties of the Hydroethanolic Extract of the Stem Bark of *Virola Elongata* (Benth.) Warb. *J. Ethnopharmacol.* 231, 113–124. doi:10.1016/j.jep.2018.11.011
- Almeida, G. V. B., Arunachalam, K., Balogun, S. O., Pavan, E., Ascêncio, S. D., Soares, I. M., et al. (2019). Chemical Characterization and Evaluation of Gastric Antiulcer Properties of the Hydroethanolic Extract of the Stem Bark of *Virola Elongata* (Benth.) Warb. *J. Ethnopharmacol.* 231, 113–124. doi:10.1016/j.jep.2018.11.011
- Amin, M. U., Khurram, M., Khattak, B., and Khan, J. (2015). Antibiotic Additive and Synergistic Action of Rutin, Morin and Quercetin against Methicillin Resistant *Staphylococcus aureus*. *BMC Complement. Altern. Med.* 15, 59–12. doi:10.1186/s12906-015-0580-0
- Ankolekar, C., Johnson, D., Pinto, M. S., Johnson, K., Labbe, R., and Shetty, K. (2011). Inhibitory Potential of Tea Polyphenolics and Influence of Extraction Time against *Helicobacter Pylori* and Lack of Inhibition of Beneficial Lactic Acid Bacteria. *J. Med. Food* 14, 1321–1329. doi:10.1089/jmf.2010.0237
- Arima, H., and Danno, G. (2002). Isolation of Antimicrobial Compounds from Guava (*Psidium Guajava* L.) and Their Structural Elucidation. *Biosci. Biotechnol. Biochem.* 66, 1727–1730. doi:10.1271/bbb.66.1727
- Arunachalam, K., Damazo, A. S., Pavan, E., Oliveira, D. M., Figueiredo, F. F., Machado, M. T. M., et al. (2019). Cochlospermum Regium (Mart. Ex Schrank) Pilg.: Evaluation of Chemical Profile, Gastroprotective Activity and Mechanism of Action of Hydroethanolic Extract of its Xylopodium in Acute and Chronic Experimental Models. *J. Ethnopharmacol.* 233, 101–114. doi:10.1016/j.jep.2019.01.002
- Asha, M. K., Debraj, D., Prashanth, D., Edwin, J. R., Srikanth, H. S., Muruganatham, N., et al. (2013). In Vitro anti-*Helicobacter pylori* Activity of a Flavonoid Rich Extract of *Glycyrrhiza Glabra* and its Probable Mechanisms of Action. *J. Ethnopharmacol.* 145, 581–586. doi:10.1016/j.jep.2012.11.033
- Ay, M., Charli, A., Jin, H., Kanthasamy, A., and Kanthasamy, A. G. (2016). Muhammet Ay, Adhithiya Charli, Huajun Jin, Vellareddy Anantharam, Arthi Kanthasamy and Anumantha G. Kanthasamy. 447–452.
- Babiaka, S. B., Nia, R., Abuga, K. O., Mbah, J. A., Nziko, V. d. P. N., Paper, D. H., et al. (2020). Antioxidant Potential of Flavonoid Glycosides from *Manniophyton Fulvum* Müll. (Euphorbiaceae): Identification and Molecular Modeling. *Sci. Afr.* 8, e00423. doi:10.1016/j.sciaf.2020.e00423
- Bae, E. A., Han, M. J., and Kim, D. H. (1999). In Vitro Anti-*Helicobacter pylori* Activity of Some Flavonoids and Their Metabolites. *Planta Med.* 65, 442–443. doi:10.1055/s-2006-960805
- Bailly, C. (2020). Molecular and Cellular Basis of the Anticancer Activity of the Prenylated Flavonoid Icaritin in Hepatocellular Carcinoma. *Chem. Biol. Interact.* 325, 109124. doi:10.1016/j.cbi.2020.109124
- Baker, D. A. (2020). Plants against *Helicobacter pylori* to Combat Resistance: An Ethnopharmacological Review. *Biotechnol. Rep. (Amst)* 26, e00470. doi:10.1016/j.btre.2020.e00470
- Baliga, M. S., Shivashankara, A. R., Venkatesh, S., Bhat, H. P., Palatty, P. L., Bhandari, G., et al. (2019). Phytochemicals in the Prevention of Ethanol-Induced Hepatotoxicity. *Diet. Interv. Liver Dis. Foods, Nutr. Diet. Suppl.*, 79–89. doi:10.1016/B978-0-12-814466-4.00007-0
- Batra, P., and Sharma, A. K. (2013). Anti-cancer Potential of Flavonoids: Recent Trends and Future Perspectives. *3 Biotech.* 3, 439–459. doi:10.1007/s13205-013-0117-5
- Beck, S., and Stengel, J. (2016). Mass Spectrometric Imaging of Flavonoid Glycosides and Biflavonoids in Ginkgo Biloba L. *Phytochemistry* 130, 201–206. doi:10.1016/j.phytochem.2016.05.005
- Bernal-Mercado, A. T., Vazquez-Armenta, F. J., Tapia-Rodriguez, M. R., Islas-Osuna, M. A., Mata-Haro, V., Gonzalez-Aguilar, G. A., et al. (2018). Comparison of Single and Combined Use of Catechin, Protocatechuic, and Vanillic Acids as Antioxidant and Antibacterial Agents against Uropathogenic *Escherichia coli* at Planktonic and Biofilm Levels. *Molecules* 23. doi:10.3390/molecules23112813
- Biharee, A., Sharma, A., Kumar, A., and Jaitak, V. (2020). Antimicrobial Flavonoids as a Potential Substitute for Overcoming Antimicrobial Resistance. *Fitoterapia* 146, 104720. doi:10.1016/j.fitote.2020.104720
- Bisignano, C., Filocamo, A., La Camera, E., Zummo, S., Fera, M. T., and Mandalari, G. (2013). Antibacterial Activities of Almond Skins on *cagA*-Positive And-Negative Clinical Isolates of *Helicobacter pylori*. *BMC Microbiol.* 13, 103. doi:10.1186/1471-2180-13-103
- Borges, A. S., Minozzo, B. R., Santos, H., Ardisson, J. S., Rodrigues, R. P., Romão, W., et al. (2020). Plectranthus Barbatas Andrews as Anti-*Helicobacter pylori* Agent with Activity against Adenocarcinoma Gastric Cells. *Industrial Crops Prod.* 146, 112207. doi:10.1016/j.indcrop.2020.112207
- Botten, D., Fugalto, G., Fraternali, F., and Molteni, C. (2015). Structural Properties of Green Tea Catechins. *J. Phys. Chem. B* 119, 12860–12867. doi:10.1021/acs.jpcc.5b08737
- Braicu, C., Lodomery, M. R., Chedea, V. S., Irimie, A., and Berindan-Neagoe, I. (2013). The Relationship between the Structure and Biological Actions of Green Tea Catechins. *Food Chem.* 141, 3282–3289. doi:10.1016/j.foodchem.2013.05.122
- Brown, J. C., and Jiang, X. (2013). Activities of Muscadine Grape Skin and Polyphenolic Constituents against *Helicobacter pylori*. *J. Appl. Microbiol.* 114, 982–991. doi:10.1111/jam.12129
- Bush, K., and Fisher, J. F. (2011). Epidemiological Expansion, Structural Studies, and Clinical Challenges of New β -lactamases from Gram-Negative Bacteria. *Annu. Rev. Microbiol.* 65, 455–478. doi:10.1146/annurev-micro-090110-102911
- Bush, K. (2013). The ABCD's of β -lactamase Nomenclature. *J. Infect. Chemother.* 19, 549–559. doi:10.1007/s10156-013-0640-7
- Calixto, J. B. (2019). The Role of Natural Products in Modern Drug Discovery. *An. Acad. Bras. Cienc.* 91 Suppl 3, e20190105–7. doi:10.1590/0001-376520190190105
- Cardoso, O., Donato, M. M., Luxo, C., Almeida, N., Liberal, J., Figueirinha, A., et al. (2018). Anti-*Helicobacter pylori* potential of Agrimonia eupatoria L. and Fragaria vesca. *J. Funct. Foods* 44, 299–303. doi:10.1016/j.jff.2018.03.027
- Casas-Grajales, S., and Muriel, P. (2017). The Liver, Oxidative Stress, and Antioxidants. *Liver Pathophysiol. Ther. Antioxidants*, 583–604. doi:10.1016/B978-0-12-804274-8.00043-6
- Caselli, A., Cirri, P., Santi, A., and Paoli, P. (2016). Morin: A Promising Natural Drug. *Curr. Med. Chem.* 23, 774–791. doi:10.2174/0929867323666160106150821
- Céliz, G., Daz, M., and Audisio, M. C. (2011). Antibacterial activity of naringin derivatives against pathogenic strains. *J. Appl. Microbiol.* 111, 731–738. doi:10.1111/j.1365-2672.2011.05070.x
- Cesa, S., Sisto, F., Zengin, G., Scaccabarozzi, D., Kokolakis, A. K., Scaltrito, M. M., et al. (2019). Phytochemical analyses and pharmacological screening of Neem oil. *South Afr. J. Bot.* 120, 331–337. doi:10.1016/j.sajb.2018.10.019
- Chandrasekaran, C. V., Deepak, H. B., Thiyagarajan, P., Kathiresan, S., Sangli, G. K., Deepak, M., et al. (2011). Dual inhibitory effect of *Glycyrrhiza glabra* (GutGard™) on COX and LOX products. *Phytomedicine* 18, 278–284. doi:10.1016/j.phymed.2010.08.001

- Cho, M. H., and Lee, S. W. (2015). Phenolic phytoalexins in rice: Biological functions and Biosynthesis. *Int. J. Mol. Sci.* 16, 29120–29133. doi:10.3390/ijms161226152
- Cui, Y., Chen, J., He, Z., and Xiao, Y. (2013). SUZ12 depletion suppresses the proliferation of gastric cancer cells. *Cell. Physiol. biochem.* 31, 778–784. doi:10.1159/000350095
- Cushnie, T. P., and Lamb, A. J. (2005). Antimicrobial activity of flavonoids. *Int. J. Antimicrob. Agents* 26, 343–356. doi:10.1016/j.ijantimicag.2005.09.002
- Cushnie, T. P., and Lamb, A. J. (2011). Recent advances in understanding the antibacterial properties of flavonoids. *Int. J. Antimicrob. Agents* 38, 99–107. doi:10.1016/j.ijantimicag.2011.02.014
- da Silva Junior, I. F., Balogun, S. O., de Oliveira, R. G., Damazo, A. S., and Martins, D. T. O. (2016). Piper umbellatum L.: A medicinal plant with gastric-ulcer protective and ulcer healing effects in experimental rodent models. *J. Ethnopharmacol.* 192, 123–131. doi:10.1016/j.jep.2016.07.011
- da Silva, L. M., Boeing, T., Somensi, L. B., Curry, B. J., Steimbach, V. M., Silveria, A. C., et al. (2015). Evidence of gastric ulcer healing activity of Maytenus robusta Reissek: In Vitro and In Vivo studies. *J. Ethnopharmacol.* 175, 75–85. doi:10.1016/j.jep.2015.09.006
- Das, S., Das, M. K., Das, R., Gehlot, V., Mahant, S., Mazumder, P. M., et al. (2020). Isolation, characterization of Berberine from Berberis aristata DC for eradication of resistant *Helicobacter pylori*. *Biocatal. Agric. Biotechnol.* 26, 101622. doi:10.1016/j.bcab.2020.101622
- de Cássia dos Santos, R., Bonamin, F., Périco, L. L., Rodrigues, V. P., Zanatta, A. C., Rodrigues, C. M., et al. (2019). Byrsonima intermedia A. Juss partitions promote gastroprotection against peptic ulcers and improve healing through antioxidant and anti-inflammatory activities. *Biomed. Pharmacother.* 111, 1112–1123. doi:10.1016/j.biopha.2018.12.132
- de Lima Nascimento, T. R., de Amoêdo Campos Velo, M. M., Silva, C. F., Costa Cruz, S. B. S., Gondim, B. L. C., Mondelli, R. F. L., et al. (2019). Current Applications of Biopolymer-based Scaffolds and Nanofibers as Drug Delivery Systems. *Curr. Pharm. Des.* 25, 3997–4012. doi:10.2174/1381612825666191108162948
- de Martel, C., Forman, D., and Plummer, M. (2013). Gastric cancer: epidemiology and risk factors. *Gastroenterol. Clin. North Am.* 42, 219–240. doi:10.1016/j.gtc.2013.01.003
- del Valle, P., García-Armesto, M. R., de Arriaga, D., González-Donquiles, C., Rodríguez-Fernández, P., and Rúa, J. (2016). Antimicrobial activity of kaempferol and resveratrol in binary combinations with parabens or propyl gallate against *Enterococcus faecalis*. *Food control.* 61, 213–220. doi:10.1016/j.foodcont.2015.10.001
- Díaz-Gómez, R., López-Solis, R., Obreque-Slier, E., and Toledo-Araya, H. (2013). Comparative antibacterial effect of gallic acid and catechin against *Helicobacter pylori*. *LWT - Food Sci. Technol.* 54, 331–335. doi:10.1016/j.lwt.2013.07.012
- Ding, S. Z., Goldberg, J. B., and Hatakeyama, M. (2010). *Helicobacter pylori* infection, oncogenic pathways and epigenetic mechanisms in gastric carcinogenesis. *Future Oncol.* 6, 851–862. doi:10.2217/fon.10.37
- Dong, H., Yang, X., He, J., Cai, S., Xiao, K., and Zhu, L. (2017). Enhanced antioxidant activity, antibacterial activity and hypoglycemic effect of luteolin by complexation with Manganese(II) and its inhibition kinetics on xanthine oxidase. *RSC Adv.* 7, 53385–53395. doi:10.1039/c7ra11036g
- Dormán, G., Flachner, B., Hajdú, I., and András, C. D. (2016). Target identification and polypharmacology of nutraceuticals. *Nutraceuticals Effic. Saf. Toxic.* 263–286. doi:10.1016/B978-0-12-802147-7.00021-8
- Eddouks, M., Bidi, A., Bouhali, B. E. L., and Zeggwagh, N. A. (2014). Insulin resistance as a target of some plant-derived phytochemicals. *Stud. Nat. Prod. Chem.* 43, 351–373. doi:10.1016/B978-0-444-63430-6.00011-4
- Egas, V., Salazar-Cervantes, G., Romero, I., Méndez-Cuesta, C. A., Rodríguez-Chávez, J. L., and Delgado, G. (2018). Anti-*Helicobacter pylori* metabolites from *Heterotheca inuloides* (Mexican arnica). *Fitoterapia* 127, 314–321. doi:10.1016/j.fitote.2018.03.001
- Escandón, R. A., del Campo, M., López-Solis, R., Obreque-Slier, E., and Toledo, H. (2016). Antibacterial effect of kaempferol and (–)-epicatechin on *Helicobacter pylori*. *Eur. Food Res. Technol.* 242, 1495–1502. doi:10.1007/s00217-016-2650-z
- Espinosa-Rivero, J., Rendón-Huerta, E., and Romero, I. (2015). Inhibition of *Helicobacter pylori* growth and its colonization factors by *Parthenium hysterophorus* extracts. *J. Ethnopharmacol.* 174, 253–260. doi:10.1016/j.jep.2015.08.021
- Fahmy, N. M., Al-Sayed, E., Michel, H. E., El-Shazly, M., and Singab, A. N. B. (2020). Gastroprotective effects of *Erythrina speciosa* (Fabaceae) leaves cultivated in Egypt against ethanol-induced gastric ulcer in rats. *J. Ethnopharmacol.* 248, 112297. doi:10.1016/j.jep.2019.112297
- Fathima, A., and Rao, J. R. (2016). Selective toxicity of Catechin-a natural flavonoid towards bacteria. *Appl. Microbiol. Biotechnol.* 100, 6395–6402. doi:10.1007/s00253-016-7492-x
- Ferreira, T. S., Moreira, C. Z., Cária, N. Z., Victoriano, G., Silva Jr, W. F., and Magalhães, J. C. (2014). Phytotherapy: an introduction to its history, use and application. *Rev. Bras. Plantas Med.* 16, 290–298. doi:10.1590/S1516-05722014000200019
- Fukai, T., Marumo, A., Kaitou, K., Kanda, T., Terada, S., and Nomura, T. (2002). Anti-*Helicobacter pylori* flavonoids from licorice extract. *Life Sci.* 71, 1449–1463. doi:10.1016/S0024-3205(02)01864-7
- Garro, M. F., Salinas Ibáñez, A. G., Vega, A. E., Arismendi Sosa, A. C., Pelzer, L., Saad, J. R., et al. (2015). Gastroprotective effects and antimicrobial activity of *Lithraea molleoides* and isolated compounds against *Helicobacter pylori*. *J. Ethnopharmacol.* 176, 469–474. doi:10.1016/j.jep.2015.11.009
- Ge, L., Li, J., Wan, H., Zhang, K., Wu, W., Zou, X., et al. (2018). NMR data for novel flavonoids from *Lonicera japonica* flower buds. *Data Brief.* 21, 2192–2207. doi:10.1016/j.indcrop.2018.08.07310.1016/j.dib.2018.11.021
- Gomez-Chang, E., Uribe-Estanslao, G. V., Martinez-Martinez, M., Gálvez-Mariscal, A., and Romero, I. (2018). Anti-*Helicobacter pylori* potential of three edible plants known as quelites in Mexico. *J. Med. Food* 21, 1150–1157. doi:10.1089/jmf.2017.0137
- Gondim, B. L. C., Oshiro-Júnior, J. A., Fernanandes, F. H. A., Nóbrega, F. P., Castellano, L. R. C., and Medeiros, A. C. D. (2019). Plant Extracts Loaded in Nanostructured Drug Delivery Systems for Treating Parasitic and Antimicrobial Diseases. *Curr. Pharm. Des.* 25, 1604–1615. doi:10.2174/1381612825666190628153755
- González, A., Casado, J., and Lanas, Á. (2021). Fighting the Antibiotic Crisis: Flavonoids as Promising Antibacterial Drugs Against *Helicobacter pylori* Infection. *Front. Cell. Infect. Microbiol.* 11, 709749. doi:10.3389/fcimb.2021.709749
- González, A., Salillas, S., Velázquez-Campoy, A., Espinosa Angarica, V., Fillat, M. F., Sancho, J., et al. (2019). Identifying potential novel drugs against *Helicobacter pylori* by targeting the essential response regulator HsrA. *Sci. Rep.* 9, 11294. doi:10.1038/s41598-019-47746-9
- Górniak, I., Bartoszewski, R., and Króliczewski, J. (2019). *Comprehensive Review of Antimicrobial Activities of Plant Flavonoids*, 18, 241–272. doi:10.1007/s11101-018-9591-zComprehensive review of antimicrobial activities of plant flavonoids *Phytochem. Rev.*
- Grenier, D., Chen, H., Ben Lagha, A., and Fournier-Larente, M. P. (2015). Dual action of myricetin on *Porphyromonas gingivalis* and the inflammatory response of host cells: A promising therapeutic molecule for periodontal diseases. *PLoS One* 10, e0131758–15. doi:10.1371/journal.pone.0131758
- Grzesik, M., Naparło, K., Bartosz, G., and Sadowska-Bartos, I. (2018). Antioxidant properties of catechins: Comparison with other antioxidants. *Food Chem.* 241, 480–492. doi:10.1016/j.foodchem.2017.08.117
- Gutiérrez-Venegas, G., Gómez-Mora, J. A., Meraz-Rodríguez, M. A., Flores-Sánchez, M. A., and Ortiz-Miranda, L. F. (2019). Effect of flavonoids on antimicrobial activity of microorganisms present in dental plaque. *Heliyon* 5, e03013. doi:10.1016/j.heliyon.2019.e03013
- Hamad, G. M., Taha, T. H., El-Deeb, N. M., and Alshehri, A. M. (2015). Advanced trends in controlling *Helicobacter pylori* infections using functional and therapeutically supplements in baby milk. *J. Food Sci. Technol.* 52, 8156–8163. doi:10.1007/s13197-015-1875-3
- Herrero, R., Park, J. Y., and Forman, D. (2014). The fight against gastric cancer - The IARC Working Group report. *Best. Pract. Res. Clin. Gastroenterol.* 28, 1107–1114. doi:10.1016/j.bpg.2014.10.003
- Hinojosa, W. I., Quiróz, M. A., Álvarez, I. R., Castañeda, P. E., Villarreal, M. L., and Taketa, A. C. (2014). Anti-*Helicobacter pylori*, gastroprotective, anti-inflammatory, and cytotoxic activities of methanolic extracts of five different populations of *Hippocratea celastroides* collected in Mexico. *J. Ethnopharmacol.* 155, 1156–1163. doi:10.1016/j.jep.2014.06.044

- Hooi, J. K. Y., Lai, W. Y., Ng, W. K., Suen, M. M. Y., Underwood, F. E., Tanyingoh, D., et al. (2017). Global Prevalence of *Helicobacter pylori* Infection: Systematic Review and Meta-Analysis. *Gastroenterology* 153, 420–429. doi:10.1053/j.gastro.2017.04.022
- Horwitz, R. J. (2018). "Chapter 30 - The Allergic Patient," in *Integrative Medicine (Fourth Edition)*. Editor D. Rakel (Amsterdam, Netherlands: Elsevier), 300–300.e2.
- Ibrahim, N. H., Awaad, A. S., Alnafisah, R. A., Alqasoumi, S. I., El-Meligy, R. M., and Mahmoud, A. Z. (2018). In - Vitro activity of Desmostachya bipinnata (L.) Stapf successive extracts against *Helicobacter pylori* clinical isolates. *Saudi Pharm. J.* 26, 535–540. doi:10.1016/j.jsps.2018.02.002
- Imran, M., Rauf, A., Abu-Izneid, T., Nadeem, M., Shariati, M. A., Khan, I. A., et al. (2019). Luteolin, a flavonoid, as an anticancer agent: A review. *Biomed. Pharmacother.* 112, 108612. doi:10.1016/j.biopha.2019.108612
- Jadeja, R. N., and Devkar, R. V. (2014). Polyphenols and Flavonoids in Controlling Non-Alcoholic Steatohepatitis. *Polyphenols Hum. Heal. Dis.* 1, 615–623. doi:10.1016/B978-0-12-398456-2.00047-5
- Jaisinghani, R. N. (2017). Antibacterial properties of quercetin. *Microbiol. Res. (Pavia)* 8. doi:10.4081/mr.2017.6877
- Jeong, C.-S. (2009). Evaluation for protective effect of rutin, a natural flavonoid, against Hcl/ethanol-induced gastric lesions. *Biomol. Ther.* 17, 199–204. doi:10.4062/biomolther.2009.17.2.199
- Jesus, R. S., Piana, M., Freitas, R. B., Brum, T. F., Alves, C. F. S., Belke, B. V., et al. (2018). In Vitro antimicrobial and antimycobacterial activity and HPLC-DAD screening of phenolics from *Chenopodium ambrosioides* L. *Braz J. Microbiol.* 49, 296–302. doi:10.1016/j.bjm.2017.02.012
- Ji, H. F., Li, X. J., and Zhang, H. Y. (2009). Natural products and drug discovery. Can thousands of years of ancient medical knowledge lead us to new and powerful drug combinations in the fight against cancer and dementia? *EMBO Rep.* 10, 194–200. doi:10.1038/embor.2009.12
- Joseph Sahayarayan, J., Udayakumar, R., Arun, M., Ganapathi, A., Alwahibi, M. S., Aldosari, N. S., et al. (2020). Effect of different Agrobacterium rhizogenes strains for *in-vitro* hairy root induction, total phenolic, flavonoids contents, antibacterial and antioxidant activity of (*Cucumis anguria* L.). *Saudi J. Biol. Sci.* 27, 2972–2979. doi:10.1016/j.sjbs.2020.08.050
- Joung, D. K., Lee, Y. S., Han, S. H., Lee, S. W., Cha, S. W., Mun, S. H., et al. (2016). Potentiating activity of luteolin on membrane permeabilizing agent and ATPase inhibitor against methicillin-resistant *Staphylococcus aureus*. *Asian pac. J. Trop. Med.* 9, 19–22. doi:10.1016/j.apjtm.2015.12.004
- Jucá, M. M., Cysne Filho, F. M. S., de Almeida, J. C., Mesquita, D. D. S., Barriga, J. R. M., Dias, K. C. F., et al. (2020). Flavonoids: biological activities and therapeutic potential. *Nat. Prod. Res.* 34, 692–705. doi:10.1080/14786419.2018.1493588
- Kim, H. W., Woo, H. J., Yang, J. Y., Kim, J.-B., and Kim, S.-H. (2021). Hesperetin Inhibits Expression of Virulence Factors and Growth of *Helicobacter pylori*. *Ijms* 22, 10035. doi:10.3390/ijms221810035
- Kim, S.-H., Lee, M. H., Park, M., Woo, H. J., Kim, Y. S., Tharmalingam, N., et al. (2018). Regulatory Effects of Black Rice Extract on *Helicobacter pylori* Infection-Induced Apoptosis. *Mol. Nutr. Food Res.* 62, 1700586. doi:10.1002/mnfr.201700586
- Klein-Júnior, L. C., Santin, J. R., Lemos, M., Silveira, A. C., Rocha, J. A., Beber, A. P., et al. (2013). Role of gastric mucus secretion, oxinitrergic system and sulphydryl groups on the gastroprotection elicited by Polygala cyparissias (Polygalaceae) in mice. *J. Pharm. Pharmacol.* 65, 767–776. doi:10.1111/jphp.12038
- Kopacz, M., Woźnicka, E., and Gruszecka, J. (2016). Antibacterial activity of morin and its complexes with La(III), Gd(III) and Lu(III) ions. *Acta Pol. Pharm.* 62, 65–67.
- Krzyżek, P., Migdał, P., Paluch, E., Karwańska, M., Wieliczko, A., and Gościński, G. (2021). Myricetin as an Antivirulence Compound Interfering with a Morphological Transformation into Coccoid Forms and Potentiating Activity of Antibiotics against *Helicobacter pylori*. *Int. J. Mol. Sci.* 22, 2695. doi:10.3390/ijms22052695
- Kumar, S., and Pandey, A. K. (2013). Chemistry and biological activities of flavonoids: An overview. *ScientificWorldJournal* 2013, 162750. doi:10.1155/2013/162750
- Ladeira, M. S. P., Salvadori, D. M. F., and Rodrigues, M. A. M. (2003). Biopatologia Do *Helicobacter pylori*. *J. Bras. Patol. Med. Lab.* 39, 335–342. doi:10.1590/s1676-24442003000400011
- Lahlou, M. (2013). The Success of Natural Products in Drug Discovery. *Pp* 04, 17–31. doi:10.4236/pp.2013.43a003
- Lamb, A., and Chen, L. F. (2013). Role of the *Helicobacter pylori*-Induced inflammatory response in the development of gastric cancer. *J. Cell.Biochem.* 114, 491–497. doi:10.1002/jcb.24389
- Lauren, P. (1965). THE TWO HISTOLOGICAL MAIN TYPES OF GASTRIC CARCINOMA: DIFFUSE AND SO-CALLED INTESTINAL-TYPE CARCINOMA. AN ATTEMPT AT A HISTO-CLINICAL CLASSIFICATION. *Acta Pathol. Microbiol. Scand.* 64, 31–49. doi:10.1111/apm.1965.64.1.31
- Lawal, T. O., Olorunnipa, T. A., and Adeniyi, B. A. (2014). Susceptibility testing and bactericidal activities of Theobroma cacao Linn. (cocoa) on *Helicobacter pylori* in an In Vitro study. *J. Herb. Med.* 4, 201–207. doi:10.1016/j.hermed.2014.09.004
- Lee, H. M., Hong, E., Jeon, B. Y., Kim, D. U., Byun, J. S., Lee, W., et al. (2006). Crystallization and preliminary X-ray crystallographic study of HP1043, a *Helicobacter pylori* orphan response regulator. *Biochim. Biophys. Acta* 1764, 989–991. doi:10.1016/j.bbapap.2005.10.024
- Li, C., Li, X., Jiang, Z., Wang, D., Sun, L., Li, J., et al. (2022). Flavonoids Inhibit Cancer by Regulating the Competing Endogenous RNA Network. *Front. Oncol.* 12, 842790. doi:10.3389/fonc.2022.842790
- Liberati, A., Altman, D. G., Tetzlaff, J., Mulrow, C., Gotzsche, P. C., Ioannidis, J. P., et al. (2009). The PRISMA statement for reporting systematic reviews and meta-analyses of studies that evaluate health care interventions: Explanation and elaboration. *PLoS Med.* 6, e1000100. doi:10.1371/journal.pmed.1000100
- Liu, C., Huang, H., Zhou, Q., Liu, B., Wang, Y., Li, P., et al. (2020). Pithecellobium clypearia extract enriched in gallic acid and luteolin has antibacterial activity against MRSA and reduces resistance to erythromycin, ceftriaxone sodium and levofloxacin. *J. Appl. Microbiol.* 129, 848–859. doi:10.1111/jam.14668
- Loo, V. G., Fallone, C. A., De Souza, E., Lavallée, J., and Barkun, A. N. (1997). In-vitro susceptibility of *Helicobacter pylori* to ampicillin, clarithromycin, metronidazole and omeprazole. *J. Antimicrob. Chemother.* 40, 881–883. doi:10.1093/jac/40.6.881
- Lu, M.-C., Chiu, H.-F., Lin, C.-P., Shen, Y.-C., Venkatakrishnan, K., and Wang, C.-K. (2018). Anti-*Helicobacter pylori* effect of various extracts of ixeris chinensis on inflammatory markers in human gastric epithelial AGS cells. *J. Herb. Med.* 11, 60–70. doi:10.1016/j.hermed.2017.08.002
- Ma, J., Shen, H., Kapesa, L., and Zeng, S. (2016). Lauren classification and individualized chemotherapy in gastric cancer. *Oncol. Lett.* 11, 2959–2964. doi:10.3892/ol.2016.4337
- Ma, Q., Wei, R., Sang, Z., and Dong, J. (2020a). Structural characterization, neuroprotective and hepatoprotective activities of flavonoids from the bulbs of *Heleocharis dulcis*. *Bioorg. Chem.* 96, 103630. doi:10.1016/j.bioorg.2020.103630
- Ma, X., You, P., Xu, Y., Ye, X., Tu, Y., Liu, Y., et al. (2020b). Anti-*Helicobacter pylori*-associated gastritis effect of the ethyl acetate extract of *Alpinia officinarum* Hance through MAPK signaling pathway. *J. Ethnopharmacol.* 260, 113100. doi:10.1016/j.jep.2020.113100
- Maleki, S. J., Crespo, J. F., and Cabanillas, B. (2019). Anti-inflammatory effects of flavonoids. *Food Chem.* 299, 125124. doi:10.1016/j.foodchem.2019.125124
- Manayi, A., Khanavi, M., Saeidnia, S., Saiednia, S., Azizi, E., Mahmoodpour, M. R., et al. (2013). Biological activity and microscopic characterization of *Lythrum salicaria* L. *Daru* 21, 61–67. doi:10.1186/2008-2231-21-61
- Maqbool, M., Amin Dar, M., Gani, I., Ahmad Mir, S., and Khan, M. (2019). Herbal Medicines As An Alternative Source of Therapy: A Review. *World J. Pharm. Pharm. Sci.* 8, 374–380. doi:10.20959/wjpps20192-13108
- Marcial, G., Sendker, J., Brandt, S., De Lampasona, M. P., Catalán, C. A., De Valdez, G. F., et al. (2014). Gastroprotection as an example: Antiadhesion against *Helicobacter pylori*, anti-inflammatory and antioxidant activities of aqueous extracts from the aerial parts of *Lippia integrifolia* Hieron. *J. Ethnopharmacol.* 155, 1125–1133. doi:10.1016/j.jep.2014.06.039
- Martins, A., Vasas, A., Viveiros, M., Molnár, J., Hohmann, J., and Amaral, L. (2011). Antibacterial properties of compounds isolated from *Carpobrotus edulis*. *Int. J. Antimicrob. Agents* 37, 438–444. doi:10.1016/j.ijantimicag.2011.01.016
- Mazzolin, L. P., Nasser, A. L., Moraes, T. M., Santos, R. C., Nishijima, C. M., Santos, F. V., et al. (2010). *Qualea parviflora* Mart.: An integrative study to validate the gastroprotective, antidiarrheal, antihemorrhagic and mutagenic action. *J. Ethnopharmacol.* 127, 508–514. doi:10.1016/j.jep.2009.10.005

- Mbaveng, A. T., Hamm, R., and Kuete, V. (2014). *Harmful and Protective Effects of Terpenoids from African Medicinal Plants*, 557–576. doi:10.1016/B978-0-12-800018-2.00019-4
- McColl, K. E. (2010). Clinical practice. *Helicobacter pylori* infection. *N. Engl. J. Med.* 362, 1597–1604. doi:10.1056/NEJMcp1001110
- medical, and editorial content Team (2018). About Stomach Cancer. *Am. Cancer Soc.*, 1–14. Available at: <https://www.cancer.org/content/dam/CRC/PDF/Public/8838.00.pdf>.
- Mendes, D. B., Lemes, L. S., Carlos, R., Cruz, S., Lúcia, M., Castro, L. De, et al. (2012). Metabólitos secundários e hipertireoidismo. *J. Biotechnol. Biodivers.* 3, 1–69. Available at: <https://www.infoteca.cnptia.embrapa.br/infoteca/handle/doc/951393>.
- Ming, D., Wang, D., Cao, F., Xiang, H., Mu, D., Cao, J., et al. (2017). Kaempferol inhibits the primary attachment phase of biofilm formation in *Staphylococcus aureus*. *Front. Microbiol.* 8, 1–11. doi:10.3389/fmicb.2017.02263
- Minozzo, B. R., Lemes, B. M., Justo, A. D. S., Lara, J. E., Petry, V. E. K., Fernandes, D., et al. (2016). Anti-ulcer mechanisms of polyphenols extract of *Euphorbia umbellata* (Pax) Bruyns (Euphorbiaceae). *J. Ethnopharmacol.* 191, 29–40. doi:10.1016/j.jep.2016.06.032
- Moher, D., Liberati, A., Tetzlaff, J., Altman, D. G., Altman, D., Antes, G., et al. (2009). Preferred reporting items for systematic reviews and meta-analyses: The PRISMA statement. *PLoS Med.* 6, e1000097. doi:10.1371/journal.pmed.1000097
- Moon, H. I., Lee, Y. C., and Lee, J. H. (2011). Phenol glycosides with In Vitro anti-*Helicobacter pylori* activity from hypericum erectum Thunb. *Phytother. Res.* 25, 1389–1391. doi:10.1002/ptr.3453
- Mori, A., Nishino, C., Enoki, N., and Tawata, S. (1987). Antibacterial activity and mode of action of plant flavonoids against *Proteus vulgaris* and *Staphylococcus aureus*. *Phytochemistry* 26, 2231–2234. doi:10.1016/S0031-9422(00)84689-0
- Moss, S. F. (2017). The Clinical Evidence Linking *Helicobacter pylori* to Gastric Cancer. *Cell. Mol. Gastroenterol. Hepatol.* 3, 183–191. doi:10.1016/j.jcmgh.2016.12.001
- Mukherjee, M., Bhaskaran, N., Srinath, R., Shivaprasad, H. N., Allan, J. J., Shekhar, D., et al. (2010). Anti-ulcer and antioxidant activity of GutGard. *Indian J. Exp. Biol.* 48, 269–274.
- Nakayama, M., Shimatani, K., Ozawa, T., Shigemune, N., Tsugukuni, T., Tomiyama, D., et al. (2013). A study of the antibacterial mechanism of catechins: Isolation and identification of *Escherichia coli* cell surface proteins that interact with epigallocatechin gallate. *Food control.* 33, 433–439. doi:10.1016/j.foodcont.2013.03.016
- Nardone, G. (2006). “16 Role of *Helicobacter pylori* in Gastric Cancer,” in *Handbook of Immunohistochemistry and in Situ Hybridization of Human Carcinomas*, 205–220. doi:10.1016/S1874-5784(05)80078-9
- Newman, D. J., and Cragg, G. M. (2020). Natural Products as Sources of New Drugs over the Nearly Four Decades from 01/1981 to 09/2019. *J. Nat. Prod.* 83, 770–803. doi:10.1021/acs.jnatprod.9b01285
- Okeleye, B. I., Bessong, P. O., and Ndip, R. N. (2011). Preliminary phytochemical screening and In Vitro anti-*Helicobacter pylori* activity of extracts of the stem bark of *bridelia micrantha* (Hochst., Baill., Euphorbiaceae). *Molecules* 16, 6193–6205. doi:10.3390/molecules16086193
- Olekhnovich, I. N., Vitko, S., Chertihin, O., Hontecillas, R., Viladomiu, M., Bassaganya-Riera, J., et al. (2013). Mutations to Essential Orphan Response Regulator HP1043 of *Helicobacter pylori* Result in Growth-Stage Regulatory Defects. *Infect. Immun.* 81, 1439–1449. doi:10.1128/IAI.01193-12
- Olekhnovich, I. N., Vitko, S., Valliere, M., and Hoffman, P. S. (2014). Response to Metronidazole and Oxidative Stress Is Mediated through Homeostatic Regulator HsrA (HP1043) in *Helicobacter pylori*. *J. Bacteriol.* 196, 729–739. doi:10.1128/JB.01047-13
- Oliveira, D. M., Melo, F. G., Balogun, S. O., Flach, A., De Souza, E. C., De Souza, G. P., et al. (2015). Antibacterial mode of action of the hydroethanolic extract of *Leonotis nepetifolia* (L.) R. Br. involves bacterial membrane perturbations. *J. Ethnopharmacol.* 172, 356–363. doi:10.1016/j.jep.2015.06.027
- Omar, S. H. (2018). Biophenols. *Biophenols Impacts Prospects Anti-Alzheimer Drug Discov.*, 103–148. doi:10.1016/B978-0-12-809593-5.00004-5
- Orditura, M., Galizia, G., Sforza, V., Gambardella, V., Fabozzi, A., Laterza, M. M., et al. (2014). Treatment of gastric cancer. *World J. Gastroenterol.* 20, 1635–1649. doi:10.3748/wjg.v20.i7.1635
- Özcelik, B., Kartal, M., and Orhan, I. (2011). Cytotoxicity, antiviral and antimicrobial activities of alkaloids, flavonoids, and phenolic acids. *Pharm. Biol.* 49, 396–402. doi:10.3109/13880209.2010.519390
- Palacios-Espinosa, J. F., Arroyo-García, O., García-Valencia, G., Linares, E., Bye, R., and Romero, I. (2014). Evidence of the anti-*Helicobacter pylori*, gastroprotective and anti-inflammatory activities of *Cuphea aequipetala* infusion. *J. Ethnopharmacol.* 151, 990–998. doi:10.1016/j.jep.2013.12.012
- Pandey, A. K., and Kumar, S. (2013). Perspective on Plant Products as Antimicrobials Agents: A Review. *Pharmacologia* 4, 469–480. doi:10.5567/pharmacologia.2013.469.480
- Park, D., Shin, K., Choi, Y., Guo, H., Cha, Y., Kim, S. H., et al. (2016). Antimicrobial activities of ethanol and butanol fractions of white rose petal extract. *Regul. Toxicol. Pharmacol.* 76, 57–62. doi:10.1016/j.yrtph.2016.01.011
- Pastene, E., Parada, V., Avello, M., Ruiz, A., and García, A. (2014). Catechin-based Procyanidins from *peumus boldus* mol. aqueous extract inhibit *Helicobacter pylori* urease and adherence to adenocarcinoma gastric cells. *Phytother. Res.* 28, 1637–1645. doi:10.1002/ptr.5176
- Patel, K., and Patel, D. K. (2019). The Beneficial Role of Rutin, A Naturally Occurring Flavonoid in Health Promotion and Disease Prevention: A Systematic Review and Update. *Bioact. Food as Diet. Interv. Arthritis Relat. Inflamm. Dis.*, 457–479. doi:10.1016/b978-0-12-813820-5.00026-x
- Patridge, E., Gareiss, P., Kinch, M. S., and Hoyer, D. (2016). An analysis of FDA-approved drugs: Natural products and their derivatives. *Drug Discov. Today* 21, 204–207. doi:10.1016/j.drudis.2015.01.009
- Peek, R. M. (20052005). Orchestration of aberrant epithelial signaling by *Helicobacter pylori* CagA. *Sci. STKE* 2005, pe14–280. doi:10.1126/stke.2772005pe14
- Pellicciari, S., Pinatel, E., Vannini, A., Peano, C., Puccio, S., De Bellis, G., et al. (2017). Insight into the essential role of the *Helicobacter pylori* HP1043 orphan response regulator: genome-wide identification and characterization of the DNA-binding sites. *Sci. Rep.* 7, 41063. doi:10.1038/srep41063
- Piasecka, A., Jedrzejczak-Rey, N., and Bednarek, P. (2015). Secondary metabolites in plant innate immunity: Conserved function of divergent chemicals. *New Phytol.* 206, 948–964. doi:10.1111/nph.13325
- Plummer, M., de Martel, C., Vignat, J., Ferlay, J., Bray, F., and Franceschi, S. (2016). Global burden of cancers attributable to infections in 2012: a synthetic analysis. *Lancet Glob. Health* 4, e609–16. doi:10.1016/S2214-109X(16)30143-7
- Plummer, M., Franceschi, S., Vignat, J., Forman, D., and De Martel, C. (2015). Global burden of gastric cancer attributable to *Helicobacter pylori*. *Int. J. Cancer* 136, 487–490. doi:10.1002/ijc.28999
- Polk, D. B., and Peek, R. M. (2010). *Helicobacter pylori*: Gastric cancer and beyond. *Nat. Rev. Cancer* 10, 403–414. doi:10.1038/nrc2857
- Puupponen-Pimia, R., Nohynek, L., Meier, C., Kahkonen, M., Heinonen, M., Hopia, A., et al. (2001). Antimicrobial properties of phenolic compounds from berries. *J. Appl. Microbiol.* 90, 494–507. doi:10.1046/j.1365-2672.2001.01271.x
- Qian, W., Liu, M., Fu, Y., Zhang, J., Liu, W., Li, J., et al. (2020). Antimicrobial mechanism of luteolin against *Staphylococcus aureus* and *Listeria monocytogenes* and its antibiofilm properties. *Microb. Pathog.* 142, 104056. doi:10.1016/j.micpath.2020.104056
- Qiu, J., Li, H., Meng, H., Hu, C., Li, J., Luo, M., et al. (2011). Impact of luteolin on the production of alpha-toxin by *Staphylococcus aureus*. *Lett. Appl. Microbiol.* 53, 238–243. doi:10.1111/j.1472-765X.2011.03098.x
- Rahardiyani, D. (2019). Antibacterial potential of catechin of tea (*Camellia sinensis*) and its applications. *Food Res.* 3, 1–6. doi:10.26656/fr.2017.3(1).097
- Rashed, K., Ćirić, A., Glamočlija, J., and Soković, M. (2014). Antibacterial and antifungal activities of methanol extract and phenolic compounds from *Diospyros virginiana* L. *Industrial Crops Prod.* 59, 210–215. doi:10.1016/j.indcrop.2014.05.021
- Ribeiro, A. R., Diniz, P. B., Estevam, C. S., Pinheiro, M. S., Albuquerque-Júnior, R. L., and Thomazzi, S. M. (2013). Gastroprotective activity of the ethanol extract from the inner bark of *Caesalpinia pyramidalis* in rats. *J. Ethnopharmacol.* 147, 383–388. doi:10.1016/j.jep.2013.03.023
- Ribeiro, L. H. L. (2019). Análise dos programas de plantas medicinais e fitoterápicos no Sistema Único de Saúde (SUS) sob a perspectiva territorial. *Ciênc. saúde coletiva* 24, 1733–1742. doi:10.1590/1413-81232018245.15842017

- Russo, M., Moccia, S., Spagnuolo, C., Tedesco, I., and Russo, G. L. (2020). Roles of flavonoids against coronavirus infection. *Chem. Biol. Interact.* 328, 109211. doi:10.1016/j.cbi.2020.109211
- Saldanha, E., Saxena, A., Kaur, K., Kalekhan, F., Venkatesh, P., Fayad, R., et al. (2019). Polyphenols in the Prevention of Ulcerative Colitis. *Diet. Interv. Gastrointest. Dis. Foods, Nutr. Diet.* 2, 277–287. doi:10.1016/B978-0-12-814468-8.00023-5
- Santos, R. C., Kushima, H., Rodrigues, C. M., Sannomiya, M., Rocha, L. R., Bauab, T. M., et al. (2012). Byrsinima intermedia A. Juss.: Gastric and duodenal anti-ulcer, antimicrobial and antidiarrheal effects in experimental rodent models. *J. Ethnopharmacol.* 140, 203–212. doi:10.1016/j.jep.2011.12.008
- Saravankumar, K., Chellia, R., Hu, X., Kathiresan, K., Oh, D. H., and Wang, M. H. (2019). Eradication of *Helicobacter pylori* through the inhibition of urease and peptide deformylase: Computational and biological studies. *Microb. Pathog.* 128, 236–244. doi:10.1016/j.micpath.2019.01.001
- Sathya, S., and Pandima Devi, K. (2018). The Use of Polyphenols for the Treatment of Alzheimer's Disease. *Role Mediterr. Diet. Brain Neurodegener. Dis.*, 239–252. doi:10.1016/B978-0-12-811959-4.00015-8
- Schaalan, M., Mohamed, W., and Fathy, S. (2020). MiRNA-200c, MiRNA-139 and In RNA H19; new predictors of treatment response in H-pylori- induced gastric ulcer or progression to gastric cancer. *Microb. Pathog.* 149, 104442. doi:10.1016/j.micpath.2020.104442
- Sepulveda, A. R. (2013). *Helicobacter*, Inflammation, and Gastric Cancer. *Curr. Pathobiol. Rep.* 1, 9–18. doi:10.1007/s40139-013-0009-8
- Shankar, G. M., Antony, J., and Anto, R. J. (2015). Quercetin and Tryptanthrin: Two Broad Spectrum Anticancer Agents for Future Chemotherapeutic Interventions. *Enzymes* 37, 43–72. doi:10.1016/bs.enz.2015.05.001
- Shen, X. F., Ren, L. B., Teng, Y., Zheng, S., Yang, X. L., Guo, X. J., et al. (2014). Luteolin decreases the attachment, invasion and cytotoxicity of UPEC in bladder epithelial cells and inhibits UPEC biofilm formation. *Food Chem. Toxicol.* 72, 204–211. doi:10.1016/j.fct.2014.07.019
- Shields, M. (2017). Chemotherapeutics. *Chemotherapeutics*, 295–313. doi:10.1016/b978-0-12-802104-0.00014-7
- Shin, J. E., Kim, J. M., Bae, E. A., Hyun, Y. J., and Kim, D. H. (2005). In Vitro Inhibitory Effect of Flavonoids on Growth, Infection and Vacuolation of *Helicobacter pylori*. *Planta Med.* 71, 197–201. doi:10.1055/s-2005-837816
- Shivashankara, A. R., Venkatesh, S., Bhat, H. P., Palatty, P. L., and Baliga, M. S. (2015). Can Phytochemicals be Effective in Preventing Ethanol-Induced Hepatotoxicity in the Geriatric Population? An Evidence-Based Revisit. *Foods Diet. Suppl. Prev. Treat. Dis. Older Adults*, 163–170. doi:10.1016/B978-0-12-418680-4.00017-8
- Shukla, R., Pandey, V., Vadrone, G. P., and Lodhi, S. (2019). Role of Flavonoids in Management of Inflammatory Disorders. *Bioact. Food as Diet. Interv. Arthritis Relat. Inflamm. Dis.*, 293–322. doi:10.1016/b978-0-12-813820-5.00018-0
- Sinsinwar, S., and Vadivel, V. (2020). Catechin isolated from cashew nut shell exhibits antibacterial activity against clinical isolates of MRSA through ROS-mediated oxidative stress. *Appl. Microbiol. Biotechnol.* 104, 8279–8297. doi:10.1007/s00253-020-10853-z
- Sivaranjani, M., Gowrishankar, S., Kamaladevi, A., Pandian, S. K., Balamurugan, K., and Ravi, A. V. (2016). Morin inhibits biofilm production and reduces the virulence of *Listeria monocytogenes* - An In Vitro and In Vivo approach. *Int. J. Food Microbiol.* 237, 73–82. doi:10.1016/j.jfoodmicro.2016.08.021
- Sivasothy, Y., Sulaiman, S. F., Ooi, K. L., Ibrahim, H., and Awang, K. (2013). Antioxidant and antibacterial activities of flavonoids and curcuminoids from Zingiber spectabile Griff. *Food control.* 30, 714–720. doi:10.1016/j.foodcont.2012.09.012
- Smyth, E. C., Nilsson, M., Grabsch, H. I., van Grieken, N. C., and Lordick, F. (2020). Gastric cancer. *Lancet* 396, 635–648. doi:10.1016/S0140-6736(20)31288-5
- Spósito, L., Oda, F. B., Vieira, J. H., Carvalho, F. A., dos Santos Ramos, M. A., de Castro, R. C., et al. (2019). In Vitro and In Vivo anti-*Helicobacter pylori* activity of Casearia sylvestris leaf derivatives. *J. Ethnopharmacol.* 233, 1–12. doi:10.1016/j.jep.2018.12.032
- Srinivasan, S., Vinothkumar, V., and Murali, R. (2019). Antidiabetic Efficacy of Citrus Fruits With Special Allusion to Flavone Glycosides. *Bioact. Food as Diet. Interv. Diabetes*, 335–346. doi:10.1016/b978-0-12-813822-9.00022-9
- Sun, Y., Sun, F., Feng, W., Qiu, X., Liu, Y., Yang, B., et al. (2017). Hyperoside inhibits biofilm formation of *Pseudomonas aeruginosa*. *Exp. Ther. Med.* 14, 1647–1652. doi:10.3892/etm.2017.4641
- Sung, H., Ferlay, J., Siegel, R. L., Laversanne, M., Soerjomataram, I., Jemal, A., et al. (2021). Global Cancer Statistics 2020: GLOBOCAN Estimates of Incidence and Mortality Worldwide for 36 Cancers in 185 Countries. *Ca. Cancer J. Clin.* 71, 209–249. doi:10.3322/caac.21660
- Tatsimo, S. J., Tamokou, J. D., Havyarimana, L., Csupor, D., Forgo, P., Hohmann, J., et al. (2012). Antimicrobial and antioxidant activity of kaempferol rhamnoside derivatives from Bryophyllum pinnatum. *BMC Res. Notes* 5, 1–6. doi:10.1186/1756-0500-5-158
- Thrift, A. P., and El-Serag, H. B. (2020). Burden of Gastric Cancer. *Clin. Gastroenterol. Hepatol.* 18, 534–542. doi:10.1016/j.cgh.2019.07.045
- Tian, C., Chang, Y., Zhang, Z., Wang, H., Xiao, S., Cui, C., et al. (2019). Extraction technology, component analysis, antioxidant, antibacterial, analgesic and anti-inflammatory activities of flavonoids fraction from Tribulus terrestris L. leaves. *Heliyon* 5, e02234. doi:10.1016/j.heliyon.2019.e02234
- Tombola, F., Campello, S., De Luca, L., Ruggiero, P., Del Giudice, G., Papini, E., et al. (2003). Plant polyphenols inhibit VacA, a toxin secreted by the gastric pathogen *Helicobacter pylori*. *FEBS Lett.* 543, 184–189. doi:10.1016/S0014-5793(03)00443-5
- Tran Trung, H., Truong Thi Huynh, H., Nguyen Thi Thuy, L., Nguyen Van Minh, H., Thi Nguyen, M. N., and Luong Thi, M. N. (2020) 20080–20089). Growth-inhibiting, bactericidal, antibiofilm, and urease inhibitory activities of hibiscus rosa sinensis L. flower constituents toward antibiotic sensitive- And resistant-strains of helicobacter pylori. *ACS Omega* 5, 20080–20089. doi:10.1021/acsomega.0c01640
- Trojan-Rodrigues, M., Alves, T. L., Soares, G. L., and Ritter, M. R. (2012). Plants used as antidiabetics in popular medicine in Rio Grande Do Sul, southern Brazil. *J. Ethnopharmacol.* 139, 155–163. doi:10.1016/j.jep.2011.10.034
- Tsukamoto, T., and Tatematsu, M. (2014). Role of *Helicobacter pylori* in gastric neoplasia. *Curr. Infect. Dis. Rep.* 16, 402–406. doi:10.1007/s11908-014-0402-4
- Tungmunthum, D., Thongboonyou, A., Pholboon, A., and Yangsabai, A. (2018). Flavonoids and Other Phenolic Compounds from Medicinal Plants for Pharmaceutical and Medical Aspects: An Overview. *Med. (Basel)* 5, 93. doi:10.3390/medicines5030093
- Ustün, O., Özçelik, B., Akyön, Y., Abbasoglu, U., and Yesilada, E. (2006). Flavonoids with anti-*Helicobacter pylori* activity from Cistus laurifolius leaves. *J. Ethnopharmacol.* 108, 457–461. doi:10.1016/j.jep.2006.06.001
- Van Der Watt, E., and Pretorius, J. C. (2001). Purification and identification of active antibacterial components in *Carpobrotus edulis* L. *J. Ethnopharmacol.* 76, 87–91. doi:10.1016/S0378-8741(01)00197-0
- Vaquero, M. J. R., Alberto, M. R., and de Nadra, M. C. M. (2007). Antibacterial effect of phenolic compounds from different wines. *Food control.* 18, 93–101. doi:10.1016/j.foodcont.2005.08.010
- Waglechner, N., and Wright, G. D. (2017). Antibiotic resistance: it's bad, but why isn't it worse? *BMC Biol.* 15, 84–88. doi:10.1186/s12915-017-0423-1
- Wang, F., Meng, W., Wang, B., and Qiao, L. (2014). *Helicobacter pylori*-induced gastric inflammation and gastric cancer. *Cancer Lett.* 345, 196–202. doi:10.1016/j.canlet.2013.08.016
- Wang, S., Alseekh, S., Fernie, A. R., and Luo, J. (2019). The Structure and Function of Major Plant Metabolite Modifications. *Mol. Plant* 12, 899–919. doi:10.1016/j.molp.2019.06.001
- Wang, Y., Zhang, J. Y., Song, X. N., Zhang, Z. Y., Li, J. F., and Li, S. (2018). Anti-ulcer and anti-*Helicobacter pylori* potentials of the ethyl acetate fraction of Physalis alkekengi L. var. franchetii (Solanaceae) in rodent. *J. Ethnopharmacol.* 211, 197–206. doi:10.1016/j.jep.2017.09.004
- Wei, R., Ma, Q., Zhong, G., He, J., and Sang, Z. (2020). Isolation and characterization of flavonoid derivatives with anti-prostate cancer and hepatoprotective activities from the flowers of Hosta plantaginea (Lam.) Aschers. *J. Ethnopharmacol.* 253, 112685. doi:10.1016/j.jep.2020.112685
- Wu, B.-L., Wu, Z.-W., Yang, F., Shen, X.-F., Wang, L., Chen, B., et al. (2019). Flavonoids from the seeds of Oroxylum indicum and their anti-inflammatory and cytotoxic activities. *Phytochem. Lett.* 32, 66–69. doi:10.1016/j.phytol.2019.05.003
- Wu, D., Kong, Y., Han, C., Chen, J., Hu, L., Jiang, H., et al. (2008). d-Alanine:d-alanine ligase as a new target for the flavonoids quercetin and apigenin. *Int. J. Antimicrob. Agents* 32, 421–426. doi:10.1016/j.ijantimicag.2008.06.010
- Wu, T., Zang, X., He, M., Pan, S., and Xu, X. (2013). Structure-activity relationship of flavonoids on their anti-Escherichia coli activity and inhibition of DNA gyrase. *J. Agric. Food Chem.* 61, 8185–8190. doi:10.1021/jf402222v
- Xie, Y., Yang, W., Tang, F., Chen, X., and Ren, L. (2014). Antibacterial Activities of Flavonoids: Structure-Activity Relationship and Mechanism. *Curr. Med. Chem.* 22, 132–149. doi:10.2174/0929867321666140916113443

- Yamaoka, Y. (2010). Mechanisms of disease: *Helicobacter pylori* virulence factors. *Nat. Rev. Gastroenterol. Hepatol.* 7, 629–641. doi:10.1038/nrgastro.2010.154
- Yamaoka, Y. (2012). Pathogenesis of *Helicobacter pylori*-Related Gastrointestinal Diseases from Molecular Epidemiological Studies. *Gastroenterology Res. Pract.* 2012, 1–9. doi:10.1155/2012/371503
- Yeon, M. J., Lee, M. H., Kim, D. H., Yang, J. Y., Woo, H. J., Kwon, H. J., et al. (2019). Anti-inflammatory effects of Kaempferol on *Helicobacter pylori*-induced inflammation. *Biosci. Biotechnol. Biochem.* 83, 166–173. doi:10.1080/09168451.2018.1528140
- Yin, X., Gyles, C. L., and Gong, J. (2012). Grapefruit juice and its constituents augment the effect of low pH on inhibition of survival and adherence to intestinal epithelial cells of *Salmonella enterica* serovar Typhimurium PT193. *Int. J. Food Microbiol.* 158, 232–238. doi:10.1016/j.ijfoodmicro.2012.07.022
- Zengin, G., Menghini, L., Di Sotto, A., Mancinelli, F., Carradori, S., Cesa, S., et al. (2018). Chromatographic analyses, In Vitro biological activities, and cytotoxicity of cannabis sativa L. Essential oil: A multidisciplinary study. *Molecules* 23. doi:10.3390/molecules23123266
- Zhang, L., Kong, Y., Wu, D., Zhang, H., Wu, J., Chen, J., et al. (2008). Three flavonoids targeting the beta-hydroxyacyl-acyl carrier protein dehydratase from *Helicobacter pylori*: crystal structure characterization with enzymatic inhibition assay. *Protein Sci.* 17, 1971–1978. doi:10.1110/ps.036186.108
- Zuanazzi, J. A. S., and Montanha, J. A. (2007). “Flavonóides,” in *Farmacognosia - Da Planta Ao Medicamento* (Porto Alegre: Editora da UFRGS), 577–614.
- Zuckerman, A. J. (1995). IARC monographs on the evaluation of carcinogenic risks to humans. *J. Clin. Pathology* 48, 691. doi:10.1136/jcp.48.7.691-a

Conflict of Interest: The authors declare that the research was conducted in the absence of any commercial or financial relationships that could be construed as a potential conflict of interest.

Publisher’s Note: All claims expressed in this article are solely those of the authors and do not necessarily represent those of their affiliated organizations, or those of the publisher, the editors and the reviewers. Any product that may be evaluated in this article, or claim that may be made by its manufacturer, is not guaranteed or endorsed by the publisher.

Copyright © 2022 Ivyana de Araújo Rêgo, Guedes Silvestre, Ferreira de Melo, Albino, Pimentel, Silva Costa Cruz, Silva Wurzba, Rodrigues, Goulart de Lima Damasceno and Cançado Castellano. This is an open-access article distributed under the terms of the Creative Commons Attribution License (CC BY). The use, distribution or reproduction in other forums is permitted, provided the original author(s) and the copyright owner(s) are credited and that the original publication in this journal is cited, in accordance with accepted academic practice. No use, distribution or reproduction is permitted which does not comply with these terms.



OPEN ACCESS

EDITED BY

Muhammad Hasnat,
University of Veterinary and Animal
Sciences, Pakistan

REVIEWED BY

Hafiz Ishfaq Ahmad,
University of Veterinary and Animal
Sciences, Pakistan
Hamid Saeed Shah,
University of Veterinary and Animal
Sciences, Pakistan
Walied Abdo,
Kafrelsheikh University, Egypt

*CORRESPONDENCE

Jinyang He,
303877469@qq.com

SPECIALTY SECTION

This article was submitted to
Ethnopharmacology,
a section of the journal
Frontiers in Pharmacology

RECEIVED 26 May 2022

ACCEPTED 09 August 2022

PUBLISHED 01 September 2022

CITATION

Xie L, Luo M, Li J, Huang W, Tian G,
Chen X, Ai Y, Zhang Y, He H,
Jinyang He (2022), Gastroprotective
mechanism of modified lvdou gancao
decoction on ethanol-induced gastric
lesions in mice: Involvement of Nrf-2/
HO-1/NF- κ B signaling pathway.
Front. Pharmacol. 13:953885.
doi: 10.3389/fphar.2022.953885

COPYRIGHT

© 2022 Xie, Luo, Li, Huang, Tian, Chen,
Ai, Zhang, He and Jinyang He. This is an
open-access article distributed under
the terms of the [Creative Commons
Attribution License \(CC BY\)](https://creativecommons.org/licenses/by/4.0/). The use,
distribution or reproduction in other
forums is permitted, provided the
original author(s) and the copyright
owner(s) are credited and that the
original publication in this journal is
cited, in accordance with accepted
academic practice. No use, distribution
or reproduction is permitted which does
not comply with these terms.

Gastroprotective mechanism of modified lvdou gancao decoction on ethanol-induced gastric lesions in mice: Involvement of Nrf-2/HO-1/NF- κ B signaling pathway

Lei Xie¹, Minyi Luo¹, Junlin Li¹, Wenguan Huang¹,
Guangjun Tian², Xiuyun Chen¹, Ying Ai³, Yan Zhang⁴,
Haolan He⁵ and Jinyang He^{1*}

¹Science and Technology Innovation Center, Guangzhou University of Chinese Medicine, Guangzhou, Guangdong, China, ²Liver Diseases Center, Guangdong Provincial Hospital of Chinese Medicine, Zhuhai, Guangdong, China, ³Artemisinin Research Center, Guangzhou University of Chinese Medicine, Guangzhou, Guangdong, China, ⁴First Clinical Medical College, Guangzhou University of Chinese Medicine, Guangzhou, Guangdong, China, ⁵Guangzhou Eighth People's Hospital, Guangzhou, Guangdong, China

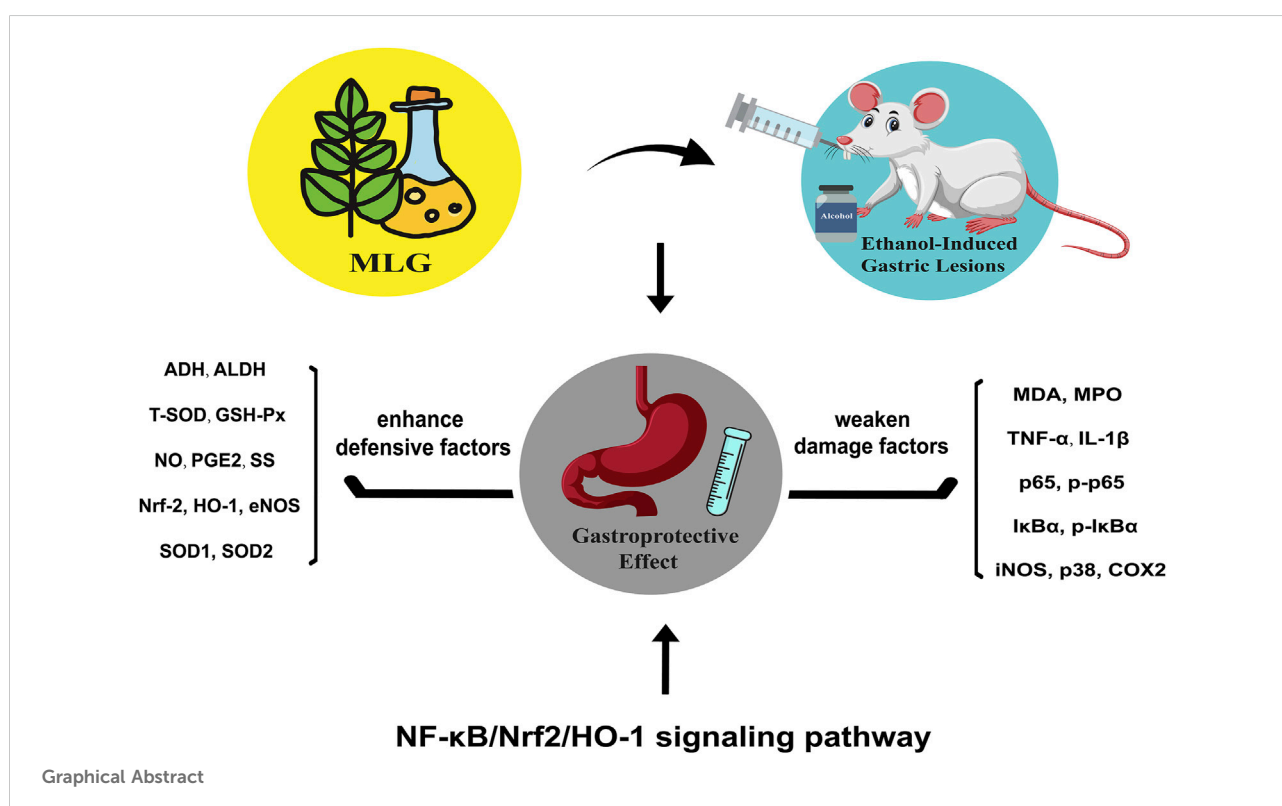
Modified Lvdou Gancao decoction (MLG), a traditional Chinese medicine formula, has been put into clinical use to treat the diseases of the digestive system for a long run, showing great faculty in gastric protection and anti-inflammatory, whereas its protective mechanisms have not been determined. The current study puts the focus on the protective effect and its possible mechanisms of MLG on ethanol-induced gastric lesions in mice. In addition to various gastric lesion parameters and histopathology analysis, the activities of a list of relevant indicators in gastric mucosa were explored including ALDH, ADH, MDA, T-SOD, GSH-Px, and MPO, and the mechanisms were clarified using RT-qPCR, ELISA Western Blot and immunofluorescence staining. The results showed that MLG treatment induced significant increment of ADH, ALDH, T-SOD, GSH-Px, NO, PGE2 and SS activities in gastric tissues, while MPO, MDA, TNF- α and IL-1 β levels were on the decline, both in a dose-dependent manner. In contrast to the model group, the mRNA expression of Nrf-2 and HO-1 in the MLG treated groups showed an upward trend while the NF- κ B, TNF α , IL-1 β and COX2 in the MLG treated groups had a downward trend simultaneously. Furthermore, the protein levels of p65, p-p65, I κ B α , p-I κ B α , iNOS, COX2 and p38 were inhibited, while Nrf2, HO-1, SOD1, SOD2 and eNOS

Abbreviations: ADH, alcohol dehydrogenase; ALDH, aldehyde dehydrogenase; CBP, Colloidal Bismuth Pectin; Elisa, Enzyme-linked immunosorbent assay; GSH-Px, glutathione peroxidase; GUI, gastric ulcer index; H&E, hematoxylin and eosin; IL-1 β , interleukin-1 β ; MDA, malondialdehyde; MLG, Modified Lv-dou-Gan-cao decoction; MLG-L, low dose of MLG; MLG-M, medium dose of MLG; MLG-H, high dose of MLG; NO, nitric oxide; TCM, traditional Chinese medicine; PGE2, prostaglandin E2; ROS, reactive oxygen species; SS, somatostatin; T-SOD, total superoxide dismutase; TNF α , tumor necrosis factor- α .

were ramped up in MLG treatment groups. Immunofluorescence intensities of Nrf2 and HO-1 in the MLG treated groups were considerably enhanced, with p65 and I κ B α diminished simultaneously, exhibiting similar trends to that of qPCR and western blot. To sum up, MLG could significantly ameliorate ethanol-induced gastric mucosal lesions in mice, which might be put down to the activation of alcohol metabolizing enzymes, attenuation of the oxidative damage and inflammatory response to maintain the gastric mucosa. The gastroprotective effect of MLG might be achieved through the diminution of damage factors and the enhancement of defensive factors involving NF- κ B/Nrf2/HO-1 signaling pathway. We further confirmed that MLG has strong potential in preventing and treating ethanol-induced gastric lesions.

KEYWORDS

ethanol-induced gastric lesions, Ivdou gancao decoction, ROS, vasodilation, inflammatory response, oxidative stress



Introduction

Excessive alcohol consumption can pose serious challenges to a cascade of vital organs, including the liver, brain, heart, and gastrointestinal tract (Hyun et al., 2021). Similar to chronic abuse, acute alcohol consumption is toxic to many organs, the stomach being particularly vulnerable in this process, predisposing to gastrointestinal disorders, including acute gastric mucosal lesion (AGML), gastritis, gastric ulcers, and gastric bleeding (Gonçalves et al., 2017). The role of

gastroprotective effect in protecting the body against alcohol-related toxicity, oxidative stress as well as inflammation response cannot be overlooked.

Ethanol could result in severe gastric mucosal damage through direct toxic action or free radicals to activate oxidative stress, leading to acute hemorrhagic lesions, edema of the mucus membrane, epithelial exfoliation and the release of inflammatory cells (Wang et al., 2015; Li J et al., 2017). This acute gastric mucosal damage may be attributed to the low activity of defensive factors such as nitric oxide (NO), prostaglandins (PG),

mucosal microcirculation, antioxidants and certain cytokines, or is due to the overproduction of reactive oxygen species (ROS), lipid peroxidation and infiltration of neutrophils (Escobedo-Hinojosa et al., 2018; Magierowska et al., 2018; Zaghlool et al., 2019). NO, working as a mixed blessing in the alimentary system, is synthesized with the participation of nitric oxide synthase (NOS) (Mohamed et al., 2022). It is widely recognized that, in the digestive system, NO generated by constitutive NOS (cNOS) is related to cytoprotective effect, whereas inducible NOS (iNOS)-produced NO, by contrast, is cytotoxic (Motawi et al., 2007). Excessive alcohol consumption may intensify gastric mucosal damage via down-modulating the levels of defensive factors, represented by NO and prostaglandin E2 (PGE2), which contribute to the improvement of gastric mucosal blood flow and mucosal microcirculation under normal conditions (Xie et al., 2019).

Several studies reported that oxidative stress and inflammatory responses play a significant role in the development and progression of alcohol-induced gastric mucosal damage (Arda-Pirincci et al., 2006; Pan et al., 2008; Wu et al., 2018). As two interplaying systems regulating the equilibrium of cellular redox status, Nrf-2/HO-1 signaling axis and NF- κ B could modulate both oxidative stress and inflammatory response indeed (Casili et al., 2020; Kim et al., 2021). They express at relatively low levels normally while are upregulated under stress conditions. It is well-founded that Nrf2/HO-1 signaling are protecting factors against oxidative stress and inflammatory responses in gastric mucosal damage, while NF- κ B plays an opposite role (Dimauro et al., 2021). Furthermore, Nrf2 activation and its anti-inflammatory effect are closely related to the transcription of antioxidant factor through NF- κ B. Deficiency of Nrf2 could increase the activity of NF- κ B, leading to increased cytokine production associated with increased oxidative stress (Sandberg et al., 2014). The production and removal of ROS equilibrates dynamically in the gastric mucosa under the physiology condition (Lebda et al., 2018). Induced by a series of factors such as ethanol exposure, inflammatory stimuli lead to the excessive production of ROS along with the decline of antioxidative enzymes, which disrupts the equilibrium of oxidation and anti-oxidation systems, thereby supervening the gastric lesions (Jeon et al., 2014). Considering the molecular crosstalk of NF- κ B/Nrf-2/HO-1 is indispensable for the ROS-mediated inflammatory cascades and the regulation of ethanol-induced gastric lesions, it is fair enough to believe that mitigating the NF- κ B activation or supporting Nrf2 activation may be effective strategies for treatment of ethanol-induced gastric lesions. It is well established that ethanol and metabolite acetaldehyde would attack the gastric mucosa, inducing microcirculatory disturbance and hypoxia, along with consequent propagation of the inflammatory cascade (De Araújo et al., 2018; Yu Y et al., 2020). ADH and ALDH, as crucial alcohol metabolism enzymes, could oxidize acetaldehyde to harmless acetic acid to

accelerate alcohol metabolism and ameliorate the ethanol-induced gastric lesions. Some natural plant extracts have been shown to activate ADH and ALDH in previous studies (Martin and Maricle, 2015; Jang et al., 2018).

Current common-used treatments for ethanol-induced gastric lesions treatment largely include potentiating the protective mechanism of gastric mucosa and improving the gastric mucosal microcirculation to repair of gastric mucosa (Association, 2015). H2 receptor antagonists, such as cimetidine, roxatidine, ranitidine, and famotidine, continue to be the first-line therapy for peptic ulcer disease, which has been proven effective for AGML through suppressing gastric acid secretion. However, in ethanol-induced AGML, some H2 receptor antagonists could block gastric first-pass ethanol metabolism, resulting in slightly higher blood alcohol levels than normal after consuming alcohol (Weathermon and Crabb, 1999; Breslow et al., 2015). Colloid Bismuth Pectin (CBP) could protect the gastric mucosa by reacting with the complexes of biOCl and bismuth citrate to form a protective film (Li and Sun, 2012; Adeyemi and Onwudiwe, 2020). Nevertheless, the side effect of CBP is not to be ignored that grumbles from the users about constipation and other adverse reactions have gained prominence. Therefore, it is of great significance to screen out better drugs, particularly extracted from plants or herbs which display higher efficiency and lower toxicity.

The research on natural products is all the rage for their great efficacy and low toxicity, and the natural compounds they contain have been regarded as superior compatibility with the human body (Ashktorab et al., 2019). The first appearance of Lvdu Gancao decoction (LGD), a famous traditional Chinese medicine prescription, was found in Wen Cheng's *Jijiu Bianfang* in the Qing Dynasty. LGD exerts a good detoxification effect in traditional use and has a reliable therapeutic effect against acute organophosphorus pesticide poisoning (AOPP) (Cailin, 1999; Wang, 2002), drug poisoning (Zhou, 2009; Wenxue, 2018), mushroom poisonings (Zhang, 2000) and digestive system diseases such as toxic hepatitis (Li and Tang, 1997; Wenquan, 2007; Weifeng and Jia, 2022) and acute pancreatitis (Wei et al., 2013). Based on this classic LGD, the modified Lvdu Gancao decoction (MLG) is made of several components and could be effective in gastropathy (Minqing and Mingwei, 2002; Dan et al., 2018; Yuewen and Qiang, 2018), liver complaints (Wang, 2017; Xie et al., 2022) and alcohol-induced conditions (Sun, 2015; Takei et al., 2015; Zhang and Zhang, 2017). Many of the herbs applied by MLG have been put into clinical use to treat the diseases of the digestive system for a long run and have shown their faculty in gastric protection and anti-inflammatory (Wang et al., 2012; Lv et al., 2018; Cao et al., 2020; Meng et al., 2020). Although their therapeutic mechanisms have not yet been known, their therapeutic efficacy has been speculated to be largely related to their antioxidant effect, for example, Dangshen (Wang et al., 1997; Li L et al., 2017), Shanyao (Qiao et al., 2018), Dingxiang (Agboola et al., 2022), Banxia (Yu L et al.,

2020; Fu et al., 2021), Tianma (Dong et al., 2021), and Shengjiang (Haniadka et al., 2013). Previous studies indicated these herbs can effectively remove free radicals and inhibit the occurrence of lipid peroxidation, so as to protecting gastrointestinal mucosa. Our previous study has confirmed that MLG can efficaciously ameliorate alcohol-induced hepatotoxicity, accelerate the metabolism of alcohol and weaken inflammatory and oxidative stress responses in mice liver (Xie et al., 2022). The current study shifted its focus towards demonstrating the gastroprotective effect and mechanisms of MLG to further explore the value of clinical applications of MLG.

Materials and methods

Preparation and composition of MLG

Modified Lydou Gancao decoction (MLG) is similar to the one in our previous studies (Xie et al., 2022), all herbs come from the same preparation and share the same batch number respectively. MLG consists of a mixture of 14 well-defined herbs, namely, Lvdu (Vigna radiata (L.) R.Wilczek [Fabaceae]); Gancao (Glycyrrhiza glabra L. [Fabaceae]); Baishao (Paeonia lactiflora Pall. [Paeoniaceae]); Huang Jiezi (Brassica juncea (L.) Czern. [Brassicaceae]); Chuanxiong (Conioselinum anthriscoides 'Chuanxiong' [Apiaceae]); Gansong (Nardostachys jatamansi (D.Don) DC. [Caprifoliaceae]); Dangshen (Codonopsis pilosula (Franch.) Nannf. [Campanulaceae]); Lianfang (Nelumbo nucifera Gaertn. [Nelumbonaceae]); Shanyao (Dioscorea oppositifolia L. [Dioscoreaceae]); Dingxiang (Syzygium aromaticum (L.) Merr. & L.M.Perry [Myrtaceae]); Jiangbanxia (Pinellia ternata (Thunb.) Makino [Araceae]); Tianma (Gastrodia elata Blume [Orchidaceae]); Shengjiang (Zingiber officinale Roscoe [Zingiberaceae]) and Dazao (Ziziphus jujuba Mill. [Rhamnaceae]). Detailed ingredients are listed in [Appendix A](#). These Chinese Herbal Medicine Slices were purchased from Kangmei Traditional Chinese Medicine Pieces Co., Ltd. (Guangdong, China) and identified by Professor Ping Ding (School of Pharmaceutical Sciences, Guangzhou University of Chinese Medicine, Guangdong, China). We deposited a voucher specimen (NO. 20201127002) in the public herbaria of Guangzhou University of Chinese Medicine. Herbal decoction of MLG was made according to conventional TCM decocting methods, and concentrating filtrates was extracted by condensing and stored at 4 °C.

Animals

Kunming mice of specific-pathogen-free (SPF) grade (6–8 weeks old, weighing 20–25 g, male and female in equal number) were supplied and housed by the Experimental Animal

Center of Guangzhou University of Chinese Medicine (No.SYXK (Yue) 2018–0001; No.SCXK (Yue) 2018–0034) and kept under a constant temperature (22–24°C), invariable humidity (50–60%) and a fixed 12 h light/dark cycle, with free access to food and water. Animal experiments followed the guidelines of the humane, ethical treatment of animals set forth by the World Health Organization and were approved by the Ethics Committee for Animal Studies of Guangzhou University of Chinese Medicine (NO. 20210316001).

Reagents

The 56 percent liquor used in our study was provided by Baiyunbian Wine Industry Co. LTD. (Hubei, China); Colloidal Bismuth Pectin (CBP) was obtained from Guangdong Bidi Pharmaceutical Co. (Guangzhou, China); Hematoxylin eosin (H-E) staining reagents were purchased from Guangzhou Yiqiao Biotechnology Co., Ltd. (Guangzhou, China); kits used for determination of ADH, ALDH, T-SOD, MDA, NO, GSH-Pxt, MPO were purchased from Nanjing Jiancheng Biotechnology (Nanjing, China); ELISA kits for determining TNF- α (70-EK282/4–96) and IL-1 β (70-EK201B/3–96) were purchased from MultiSciences (Lianke) Biotech Co. (Hangzhou, China); ELISA kits for mouse PGE2 (Prostaglandin E2) (E-EL-0034c) and mouse SS (Somatostatin) (E-EL-M1086c) were obtained from Elabscience biotechnology (Wuhan, China). BCA protein concentration determination kit and protein extraction kit were provided by Beijing Beyotime Biotechnology (Beijing, China). Trizol RNA isolation reagent, RevertAid Reverse Transcriptase and SYBR Green Real time PCR Master Mix was purchased from Thermo Fisher Scientific (NY, United States). The rabbit anti-Nrf2 antibody (AF0639), rabbit anti-HO-1 antibody (AF5393), rabbit anti-I κ B α antibody (AF5002), rabbit anti-NF- κ B p65 antibody (AF5006), rabbit anti-p-I κ B α antibody (AF 2002), rabbit anti-p-p65 antibody (AF 2006), rabbit anti-SOD1 Antibody (AF5198), rabbit anti-SOD2/MnSOD Antibody (AF5144), rabbit anti-iNOS Antibody (AF0199), rabbit anti-nNOS Antibody (AF6249), rabbit anti-eNOS Antibody (AF0096), rabbit anti-Cox2 Antibody (AF7003), rabbit anti-p38 MAPK Antibody (AF6456) and rabbit anti-GAPDH antibody (AF7021) was obtained from Affinity Biosciences (OH, United States).

Mice groupings and drug administration

Six mice per group were distributed among the 36 Kunming mice: model group, MLG-H (high-dose MLG-treated group, 20 g/kg body weight), MLG-M (medium-dose MLG-treated group, 10 g/kg body weight), MLG-L (low-dose MLG-treated group, 5 g/kg body weight), CBP (Colloidal Bismuth Pectin treatment group, 57 mg/kg body weight) and control

TABLE 1 Primer sequence of qRT-PCR.

Gene	Forward	Reverse
Nrf-2	5'-AGACATTCCCATTTGTAGATGACC-3'	5'-CTCCAGAGAGCTATTGAGGGACT-3'
NF-κB	5'-CTGGAAGTCACATCTGGTTTGAT-3'	5'-CAACCCTCAGCAAATCCTCTAC-3'
HO-1	5'-ACCGCCTTCCTGCTCAACATTG-3'	5'-CTCTGACGAAGTGACGCCATCTG-3'
TNFα	5'-TGTCTCAGCCTCTTCTCATTCC-3'	5'-GGTCTGGGCCATAGAACTGAT-3'
IL-1β	5'-TCCACCTCAATGGACAGAATATC-3'	5'-CCGTCTTTCATTACACAGGACA-3'
COX2	5'-CGGTGGATGTGAGTCTAGCTAC-3'	5'-CGGTGGATGTGAGTCTAGCTAC-3'
GAPDH	5'-GACAACTCACTCAAGATTGTCAGC-3'	5'-AGTCTTCTGGGTGGCAGTGAT-3'

Nrf-2, nuclear factor-erythroid 2-related factor 2; NF-κB, nuclear factor-kappa B; HO-1, heme oxygenase-1; TNFα, tumor necrosis factorα; IL-1β, interleukin-1β; COX2, cyclooxygenase two; GAPDH, glyceraldehyde-3-phosphate dehydrogenase.

group. Pretreatment of the mice with MLG and CBP was given by oral gavage after 24 h of fasting, while the other groups received the same dose of physiological saline in the same way. Two hours later, model group, MLG-L group, MLG-M group and MLG-H group were treated with alcohol (13.25 ml/kg body weight) by intragastric administration, the control group received the same volume of physiological saline. After 30 minutes, each group were administrated orally with corresponding drugs (MLG, CBP, or physiological saline) once again as described previously.

Evaluation of the gastric ulcer index

Using isoflurane anesthesia, all mice were euthanized 5 hours after being given alcohol. Gastric tissues were collected and washed clean by 0.9% pre-cooling normal saline after gastric acidity (pH) was measured. Weight was measured for an empty stomach, and a stomach index was calculated. Also, the surface damage of gastric mucosa was observed, including bleeding, erosion and ulcer; the gastric ulcer index (GUI) was calculated macroscopically according to the Guth standard (Guth et al., 1979; El-Maraghy et al., 2015; Raish et al., 2018): we recorded one point for spot erosion; two points for erosion lengths up to 1mm; three points for erosion lengths between 1 and 2 mm, four points for those from 2 to 3 mm; five points for those more than 3 mm. If the erosion width is greater than 1 mm, the scores are doubled. Method for calculating ulcer inhibition rate: ulcer inhibition rate (%) = (GUI in control group - GUI in administration group)/GUI in control group × 100%.

Gastric tissues histopathology assay

Fresh gastric tissues were fixed for 12–24 h at room temperature in 4% paraformaldehyde. Tissues were routinely dehydrated, transparent, and paraffin embedded before being sliced into sections of 4 or 5 μm thickness for haematoxylin and eosin staining. Hetopathologists reviewed slides under a 200X microscope under the supervision of an expert.

Gastric tissues biochemical assays

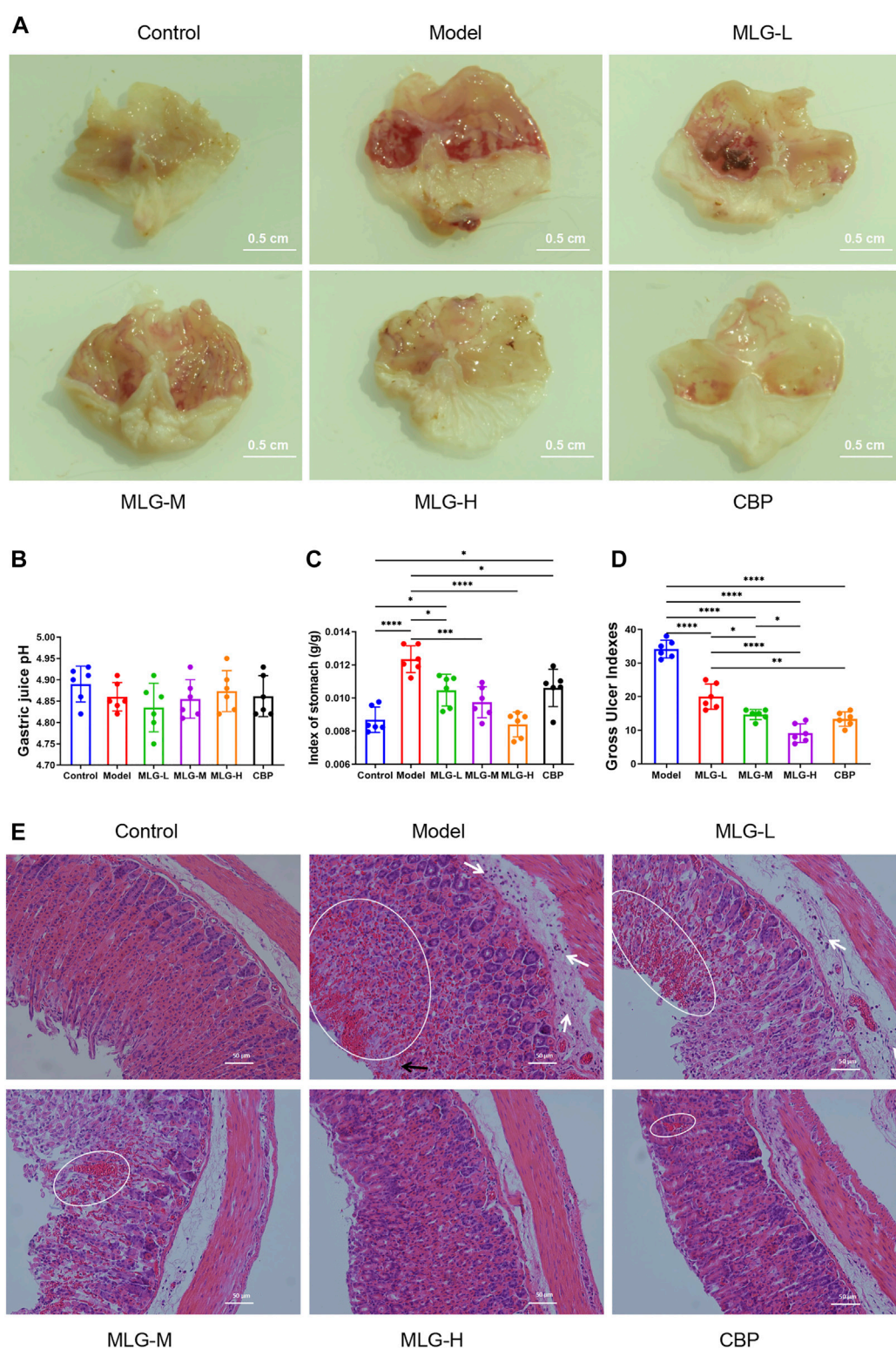
A homogenate of 10% gastric tissues homogenates was obtained by homogenizing gastric tissues (100 mg) in 0.9% physiological saline, and the proteins in 10% homogenate were measured using the BCA protein assay kit (Beyotime Biotechnology, Beijing, China). The activity of T-SOD, GSH-Px, MDA, NO, MPO, ADH and ALDH were colorimetrically detected in gastric tissues homogenates using commercial kits (Nanjing Jiancheng Biotechnology, Nanjing, China) according to manufacturer directions.

Enzyme-linked immunosorbent assay

TNF-α, IL-1β, PGE2 and SS levels in gastric tissues were detected using mouse ELISA kits. A 96-well plate was washed three times using PBST and subsequently incubated for 2 hours at room temperature with either 100 μl diluted serum or a standard. Add 100 μl of diluted detection antibody to each well and incubate for 1 h after washing the wells three times. The levels of TNF-α, IL-1β, PGE2 and SS levels in gastric tissues were read at 450 nm and the antibody concentrations were calculated based on a standard curve.

Quantitative real-time polymerase chain reaction

Gastric tissues were homogenized in 1 ml of TRIzol and flash frozen in dry ice and stored at -80 °C until the total RNA of all samples were isolated according to the manufacturer's protocol. Total RNA samples were reverse transcribed into complementary DNA (cDNA) with oligo dT18 primer using RevertAid Reverse Transcriptase and then were amplified using SYBR Real time PCR Master Mix (TAKARA, Shiga, Japan) in a Bio-rad fluorescence quantitative PCR instrument (Bio-rad, United States). The mRNA expression of Nrf-2, NF-κB, HO-1, TNFα, IL-1β, and COX2 were measured using reverse

**FIGURE 1**

Gross evaluation in mice gastric tissue (A); effects of MLG on gastric acidity (B), stomach index (C) and gastric ulcer index (D); H&E-stained in the gastric tissues of mice (E), white arrows highlight inflammatory cell infiltration, black arrows highlight epithelial cell loss, and highlighted circles indicate hemorrhage. Control: negative control group; Model: the group induced by intragastric administration of ethanol (13.25 ml/kg BW); MLG-L: the group treated with low dose MLG (5 g/kg BW); MLG-M: the group treated with medium dose MLG (10 g/kg BW); MLG-H: the group treated with high dose MLG (20 g/kg BW); CBP: the group treated with CBP (57 mg/kg BW). Data was expressed as mean \pm standard deviation (SD), $n = 6$ for each group. By one-way analysis of variance (ANOVA) test, $*p < 0.05$, $***p < 0.001$, $****p < 0.0001$.

transcription quantitative real-time polymerase chain reaction (qRT-PCR) with GAPDH as internal reference gene. The reaction conditions were set as follows: one cycle at 50°C for 2 min and 95°C for 1 min; 40 cycles at 95°C for 15 s, 60°C for 15 s and 72°C for 30 s; with a dissolution curve being produced in the last cycle: 95°C, 15 s; 60°C, 1 min; 95°C, 15 s. RT-qPCR data were analyzed using relative quantification by standard curve method based on mRNA copy number ratio (R) of target gene versus reference genes GAPDH. The primers were designed with ABI Primer Express 3.0 software and synthesized by Suzhou Jinweizhi Biotechnology (Suzhou, China) and the sequences are shown in Table 1.

Western blot

Following the homogenization of the tissue samples, a BCA protein assay kit was used to determine the protein concentration. Protein was isolated from gastric mucosa isolated from mice stomach using a protein extraction kit (Beyotime Biotechnology, Beijing, China). Equal amounts of protein (30 µg) were separated by 10% SDS-polyacrylamide gel electrophoresis and were transferred onto a polyvinylidene fluoride (PVDF) membrane. Membranes were blocked in TBST (Tris-buffered saline, pH 7.6, 0.1% Tween 20) supplemented with 5% (w/v) BSA at room temperature (RT) for 1 h before incubation with rabbit anti-Nrf2 antibody (AF0639; 1:2000; Affinity, OH, United States), rabbit anti-HO-1 antibody (AF5393; 1:2000; Affinity), rabbit anti-IκBα antibody (AF5002; 1:2000; Affinity), rabbit anti-NF-κB p65 antibody (AF5006; 1:2000; Affinity), rabbit anti-p-IκBα antibody (AF 2002; 1:2000; Affinity), rabbit anti-p-p65 antibody (AF 2006; 1:2000; Affinity), rabbit anti-SOD1 Antibody (AF5198; 1:2000; Affinity), rabbit anti-SOD2/MnSOD Antibody (AF5144; 1:2000; Affinity), rabbit anti-iNOS Antibody (AF0199; 1:2000; Affinity), rabbit anti-nNOS Antibody (AF6249; 1:2000; Affinity), rabbit anti-eNOS Antibody (AF0096; 1:2000; Affinity), rabbit anti-Cox2 Antibody (AF7003; 1:2000; Affinity), rabbit anti-p38 MAPK Antibody (AF6456; 1:2000; Affinity) and rabbit anti-GAPDH antibody (AF7021; 1:2000; Affinity) overnight at 4°C, followed by incubation with a secondary antibody Goat Anti-Rabbit IgG (H + L) HRP (S0001; 1:10,000; Affinity) at RT for 1 h. The ECL enhanced chemiluminescence Plus Western blotting detection system was used for detecting immunoblots.

Immunofluorescence analysis

Immunofluorescence staining was performed on gastric tissue sections for the detection of Nrf2 (rabbit anti-Nrf2, AF0639), HO-1 (rabbit anti-HO-1, AF5393), IκBα (rabbit anti-IκBα, AF5002), NF-κB (rabbit anti-NF-κB p65, AF5006) proteins according to standard protocols. Fresh

gastric tissues were fixed in 4% paraformaldehyde for 24 h at 4°C, dehydrated in 15 and 30% sucrose solutions sequentially overnight at 4°C. Frozen sections preserved in OCT were cut into 10 µm sections using frozen section machine (Leica, Weztlar, Germany). Slides were rehydrated in PBS for 10 min, blocked in 5% BSA/PBS/0.1% Triton-X 100 for 1 h, and then with primary antibodies overnight at 4°C. Slides were washed three times with PBS for 10 min each and incubated with Goat Anti-Rabbit IgG (H + L) FITC-conjugated (Affinity, S0008) for 1 h at room temperature and then mounted with DAPI counterstain (Vector Laboratories, Burlingame, CA, United States).

Statistical analysis

Three independent experiments were conducted, and data from one representative experiment was shown. The data were presented as the mean ± standard deviation (SD) and were analyzed using one-way analysis of variance (ANOVA). Statistically significant difference was assumed to be $p < 0.05$, while $p < 0.01$ indicated a statistically significant difference of greater magnitude.

Result

Effects of MLG on gross evaluation in gastric mucosa

As shown in Figure 1A, the gastric mucosal surfaces of mice in the normal group were pink, smooth and glossy, while the gastric mucosae of mice in model group were observed with extensive bleeding, edema, accompanied by local ulcer and erosion. Compared with model group, mice treated with MLG and CBP showed varied degrees of gastric tissue injury, most obvious in MLG-L group, but mild in the other three. The gastric mucosa of mice treated with high-dose MLG and CBP were light pink, with basically smooth surface and no bleeding and erosion, which showed obviously relieved in the injury of gastric mucosa.

Effects of MLG on gastric acidity, stomach index and gastric ulcer index

According to Figures 1B–D, there was no significant difference between the groups when it came to gastric acidity (pH) values ($p > 0.05$). From the comparison with the control group, strikingly higher stomach indexes and ulcer gastric indexes are associated with acute alcohol exposure, however, the indexes in the groups treated with MLG and CBP were significantly lower than those of the model group ($p < 0.05$),

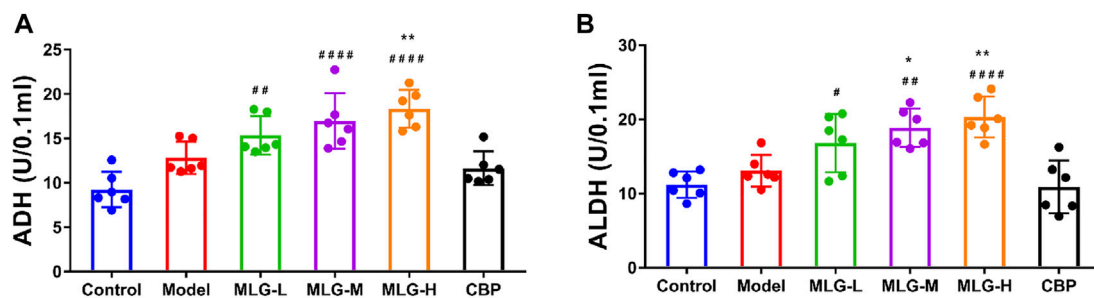


FIGURE 2

ADH activity (A) and ALDH activity (B) in mice gastric tissues. Control: the group administered zero ethanol; Model: the group administered ethanol intragastrically (13.25 ml/kg BW); MLG-L: low-dose (5 g/kg body weight) MLG-treated group; MLG-M: medium-dose (10 g/kg body weight) MLG-treated group; MLG-H: high-dose (20 g/kg body weight) MLG-treated group; CBP: the group receiving Colloid Bismuth Pectin (57 mg/kg body weight). Each group's data was expressed as mean \pm standard deviation (SD), $n = 6$. By one-way analysis of variance (ANOVA) test, * $p < 0.05$, ** $p < 0.01$ vs. model group; # $p < 0.05$, ## $p < 0.01$, ### $p < 0.0001$ versus the control group.

especially in the MLG-M group ($p < 0.001$) and the MLG-H group ($p < 0.0001$). The ulcer inhibition rate was mushroomed markedly in MLG groups and CBP group compared to the model group, exhibiting an obvious dose-effect relationship in MLG's gastroprotective effects.

Effects of MLG on mice gastric tissues histopathology

As is shown in Figure 1E, the gastric tissue structure in control group was normal with a continuous and integral mucosa, and the cells were arranged neatly with clear morphology. Gastric tissues in the Model group displayed obvious alterations primarily caused by epithelial cell loss, structural disorders of glandular tissues, submucosal edema, hemorrhage, and infiltration of inflammatory cells. Nevertheless, the pathological changes in MLG treated groups were milder to a dose-dependent extent. Moreover, both the MLG-M and MLG-H groups maintain gastroprotective effects comparable to that of the CBP group. Our results showed that MLG possessed a significant gastric protection effect and could effectively alleviate the pathological changes of gastric tissues in acute ethanol exposure mice.

Effects of MLG on the metabolism of alcohol in the gastric tissues

The activities of ADH and ALDH in gastric tissue were slightly elevated in response to acute alcohol exposure (Figure 2) due to the short-term and superfluous alcohol intake, but there was no significant statistical difference ($p > 0.05$). Comparatively to the model group, ADH and

ALDH levels in gastric tissue of the MLG treated groups can be seen a remarkable upward trend, especially in MLG-M ($p < 0.05$) and MLG-H ($p < 0.01$) groups with no significant changes showed in CBP group ($p > 0.05$). Our results demonstrated MLG was extraordinarily effective on accelerating the metabolism of alcohol.

Effects of MLG on T-SOD, MDA, GSH-Px, NO and MPO levels in gastric tissues

As can be seen in Figure 3, acute alcohol administered in mice significantly down-regulated T-SOD, GSH-Px, and NO levels ($p < 0.0001$) but up-regulated MDA and MPO level ($p < 0.0001$). Whereas the mice treated with MLG and CBP, especially in CBP ($p < 0.01$ or $p < 0.0001$), MLG-M ($p < 0.05$) and MLG-H ($p < 0.01$ or $p < 0.0001$) groups, had a reversed trend in comparison to the Model group. In the MLG-H group, particularly, the effect proved to be comparable or even more efficient than that of the CBP group, with T-SOD, GSH-Px and NO levels shooting up to 165.03 ± 4.08 , 19.51 ± 5.06 and 2.86 ± 0.34 , respectively, while MDA and MPO level dropping to 2.14 ± 0.14 and 4.43 ± 1.24 respectively. Our results revealed that MLG could abate the oxidative damage of gastric tissues caused by acute alcoholism via cutting the production of oxidative damage products and improving the levels of antioxidant enzymes.

Effect of MLG on mRNA expression of Nrf2, NF- κ B, HO-1, TNF- α , IL-1 β , and COX2 in gastric tissues

As shown in Figure 4, quantitative polymerase chain reaction analysis indicated that acute alcohol administered

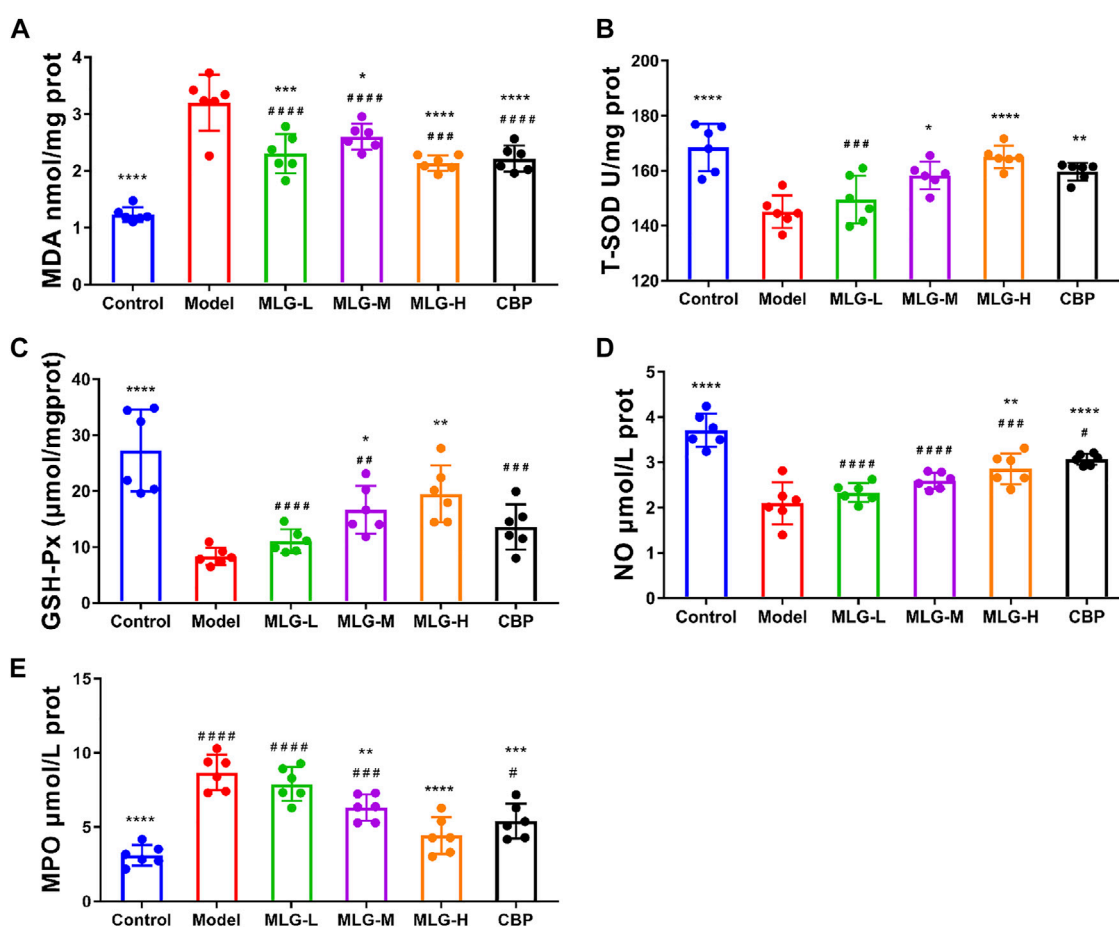


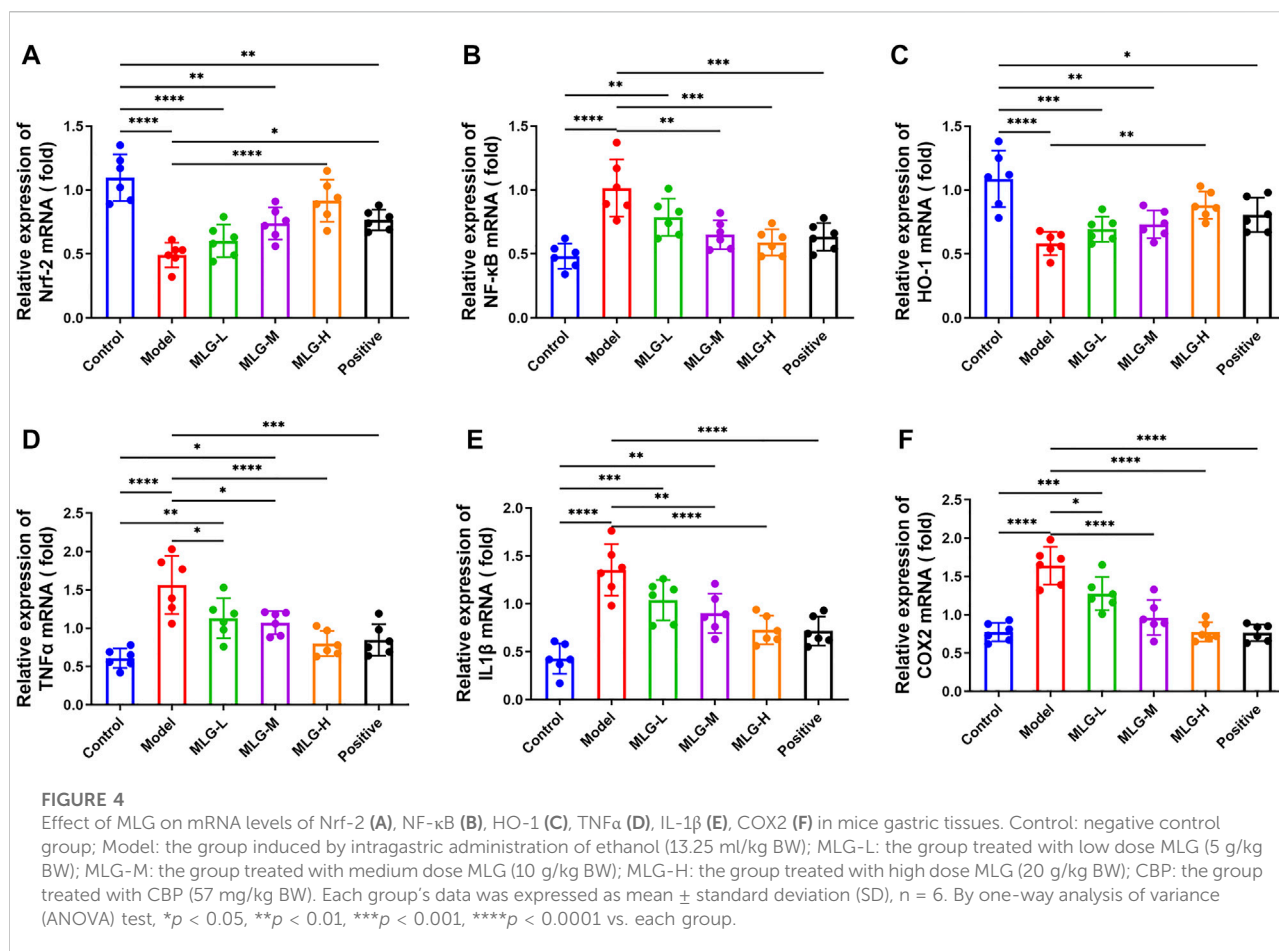
FIGURE 3

MDA (A), T-SOD (B), GSH-Px (C) NO (D) and MPO (E) levels in mice gastric tissues. Control: negative control group; Model: the group induced by intragastric administration of ethanol (13.25 ml/kg BW); MLG-L: the group treated with low dose MLG (5 g/kg BW); MLG-M: the group treated with medium dose MLG (10 g/kg BW); MLG-H: the group treated with high dose MLG (20 g/kg BW); CBP: the group treated with CBP (57 mg/kg BW). Each group's data was expressed as mean \pm standard deviation (SD), $n = 6$. By one-way analysis of variance (ANOVA) test, * $p < 0.05$, ** $p < 0.01$, *** $p < 0.001$, **** $p < 0.0001$ versus the model group, # $p < 0.05$, ## $p < 0.01$, ### $p < 0.001$, #### $p < 0.0001$ versus the control group.

in mice induced significant enhance ($p < 0.0001$) in the mRNA expression levels of NF- κ B, TNF- α , IL-1 β and COX2, with the Nrf2 and HO-1 mRNA expression levels, especially in MLG-M and MLG-H groups, showing a downward trend ($p < 0.0001$). The mRNA expression levels of NF- κ B, TNF- α , IL-1 β and COX2 in the gastric tissue of the MLG-treated mice, for the MLG-H group particularly, dropped to 0.59 ± 0.1 , 0.80 ± 0.16 , 0.72 ± 0.15 and 0.78 ± 0.13 , respectively, were lower than those in the model group ($p < 0.001$ or $p < 0.0001$) and comparable to or even lower than that of the positive group. Meanwhile, the mRNA expression levels of Nrf2 and HO-1 mRNA in MLG-H group raise to 0.92 ± 0.16 and 0.88 ± 0.11 , were higher than those in the model group ($p < 0.01$ or $p < 0.0001$).

Effects of MLG on TNF- α , IL-1 β , PGE2 and SS levels in gastric tissues

As determined by ELISA assays, acute alcohol exposure significantly increased TNF- α and IL-1 β protein levels ($p < 0.0001$) and reduced the protein levels of PGE2 and SS ($p < 0.0001$) synchronously (Figure 5). The levels of TNF- α and IL-1 β were dwindled in MLG treated groups ($p < 0.0001$), but the levels of PGE2 and SS were remarkably increased ($p < 0.01$ or $p < 0.0001$) comparatively to the model group, which indicated that MLG could effectively relieve the expression of TNF- α and IL-1 β to inhibit the inflammatory response of gastric tissues caused by acute ethanol exposure, protect gastric mucosa and increase blood supply of gastric tissues. Evidently, acute alcohol



exposure can stimulate the secretion of inflammatory mediators, such as TNF-α and IL-1β, and inhibit the flow of the gastric mucosal microcirculation. In contrast, when MLG was administered, this trend was reversed.

Effect of MLG on Nrf-2/HO-1/NF-κB signaling pathway in gastric tissues

As illustrated in Figure 6 and Figure 7, the levels of Nrf-2, HO-1, SOD1 (Cu/Zn-SOD), SOD2 (SOD2/Mn SOD) and eNOS proteins were reduced after alcohol exposure ($p < 0.0001$) in the mice gastric tissues, whereas the levels of p65, p-p65, p-p65/p65 (the ratio is 0.93 ± 0.09), p-IκBα, p-IκBα/IκBα (the ratio is 1.47 ± 0.14), iNOS, nNOS, COX2 and p38 were elevated ($p < 0.0001$). In MLG treated groups, however, the inclination was observed to be reversed. Our results suggested that Nrf-2, HO-1, SOD1 (Cu/Zn-SOD), SOD2 (SOD2/Mn SOD) and eNOS expression were significantly increased ($p < 0.001$, $p < 0.01$ or $p < 0.05$) in mice gastric tissues by the treatment of MLG after alcohol exposure, whereas p65, p-p65, p-IκBα, p-p65/p65, p-IκBα/IκBα, iNOS, nNOS, COX2, and p38 levels decreased partially

but significantly ($p < 0.0001$, $p < 0.001$, $p < 0.01$ or $p < 0.05$). We also found that this regulation of Nrf-2/HO-1/NF-κB signaling pathway with the treatment of MLG was in a dose-dependent manner. Together, the results revealed that MLG has potent anti-oxidative and anti-inflammatory properties via the suppression of the NF-κB phosphorylation and activation of Nrf-2/HO-1 antioxidant pathway to attenuate the oxidative damage and inflammatory response and improve the defensive factors in response to ethanol-induced gastric lesions.

Effects of MLG on mice gastric tissues immunofluorescence staining

Immunofluorescence staining was performed on gastric tissue sections for the detection of Nrf2, HO-1, IκBα and NF-κB proteins (as shown in Figure 8). The immunofluorescence results showed the expression of IκBα and NF-κB was increased while the expression of Nrf2 and HO-1 was decreased in model group. The relative quantitative analysis of NF-κB/Nrf2/HO-1 signaling pathway-related proteins displayed a reversal trend after MLG treatment. The expression of Nrf2 and HO-1 were up-

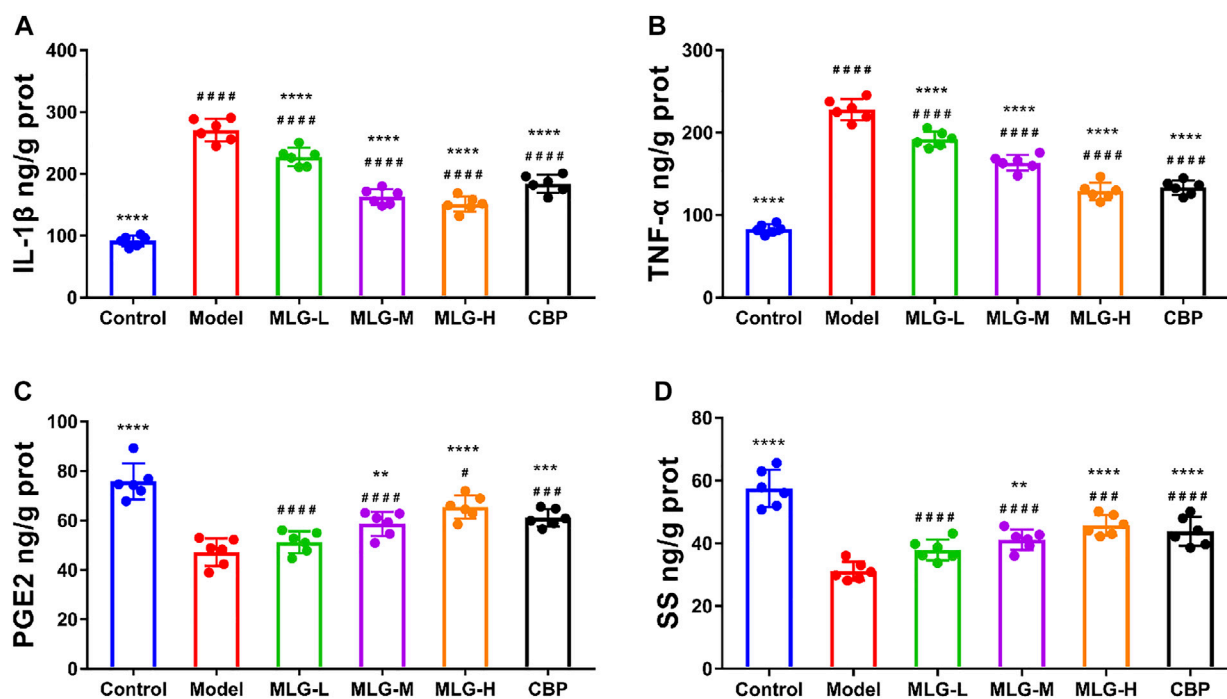


FIGURE 5

IL-1 β (A), TNF- α (B), PGE2 (C) and SS (D) levels in mice gastric tissues. Control: negative control group; Model: the group induced by intragastric administration of ethanol (13.25 ml/kg BW); MLG-L: the group treated with low dose MLG (5 g/kg BW); MLG-M: the group treated with medium dose MLG (10 g/kg BW); MLG-H: the group treated with high dose MLG (20 g/kg BW); CBP: the group treated with CBP (57 mg/kg BW). Each group's data was expressed as mean \pm standard deviation (SD), $n = 6$. By one-way analysis of variance (ANOVA) test, $^{*}p < 0.01$, $^{***}p < 0.001$, $^{****}p < 0.0001$ versus the model group, $^{#}p < 0.05$, $^{###}p < 0.001$, $^{####}p < 0.0001$ versus the control group.

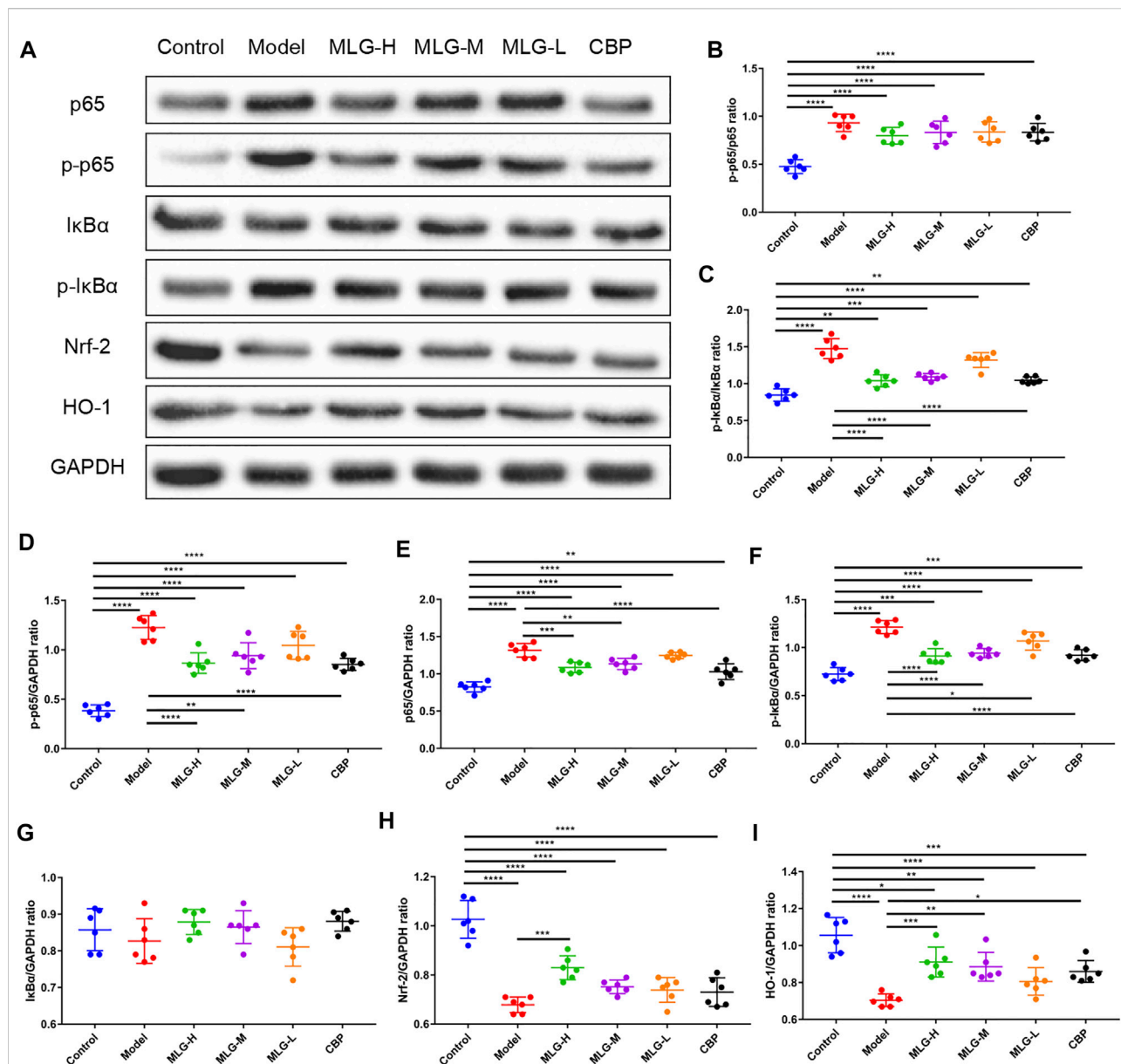
regulated ($p < 0.0001$, $p < 0.001$ or $p < 0.05$) and simultaneously, I κ B α and NF- κ B expression were down-regulated ($p < 0.0001$, $p < 0.001$, $p < 0.01$ or $p < 0.05$), showing the results that agree with the qPCR and western blot. Moreover, the relative fluorescence intensity of Nrf2 and HO-1, the key components of the cellular antioxidant defense system, in MLG-H group were increased considerably ($p < 0.001$, $p < 0.0001$). Noticeably, the treatment of MLG could activate Nrf2/HO-1 signaling pathway and inhibit NF- κ B signaling pathway, reversing the trend of acute alcohol exposure.

Discussion

Ethanol-induced gastric lesion is a ubiquitous emergency worldwide, and the request for more effective therapeutic drugs still keeps impending. Although MLG shows great competence in treating alcohol-induced symptoms and gastric lesions in clinical practice, the exact mechanism remains ambiguous.

In our study, we mainly discussed that: 1) MLG could prevent acute alcohol intoxication and promote wakefulness after acute ethanol exposure; 2) MLG showed a significant gastric protection effect, which is able to drastically abate the gastric ulcer index,

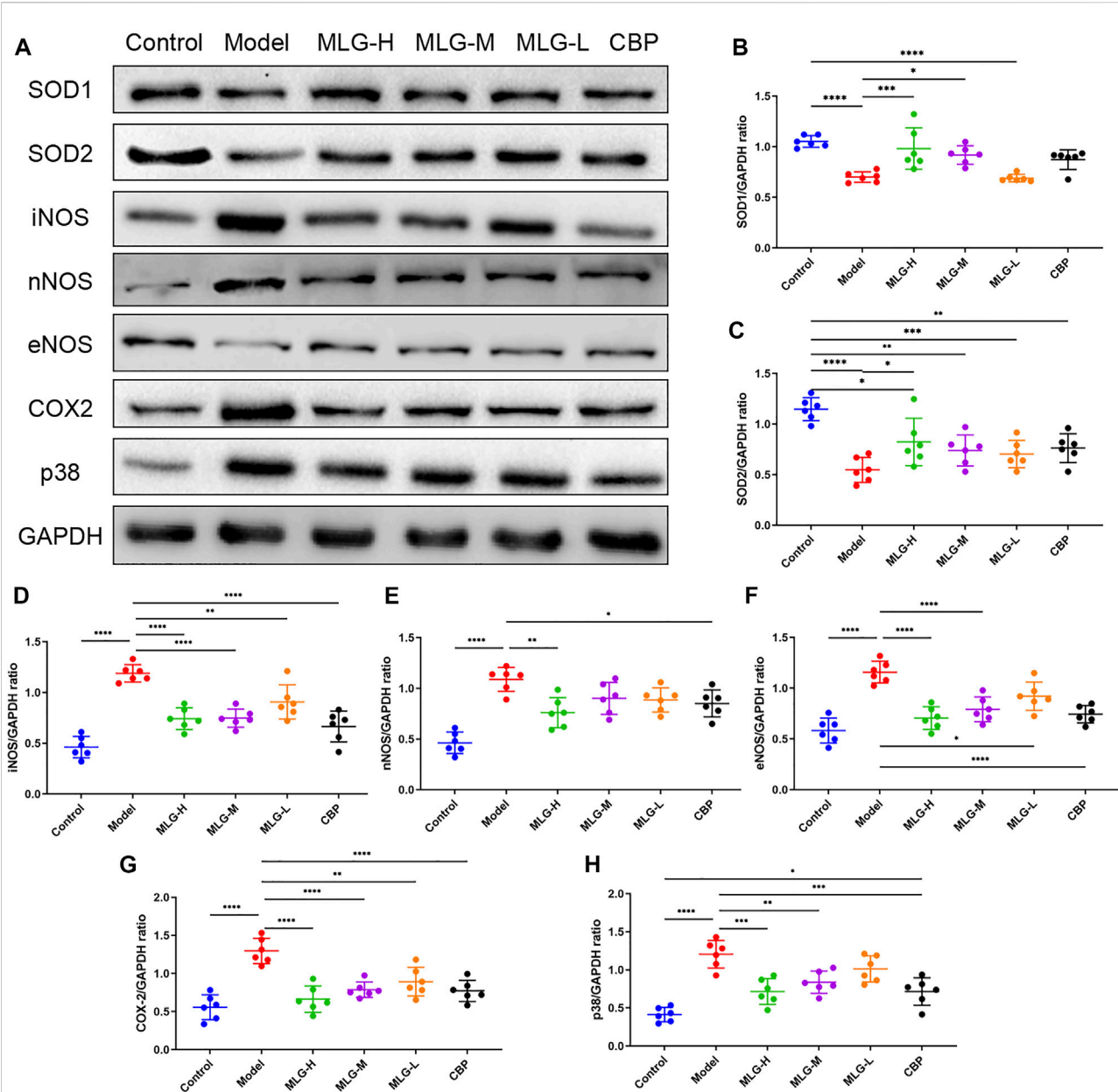
raise the ulcer inhibition rate and alleviate the pathological changes of gastric tissues in mice effectively; 3) ADH and ALDH levels in gastric tissue of the MLG treated groups showed a upward remarkably, which revealed a significant effect of MLG on accelerating the alcohol metabolism; 4) MLG could reduce the oxidative damage for gastric tissues by decreasing the production of oxidative damage products and increasing the levels of antioxidant enzymes; 5) MLG might aid the repair of the damaged gastric mucosa by inhibiting the release of inflammatory mediators and accelerating microcirculation of the gastric mucosa, NO and PGE2 possibly involved in the process; 6) MLG could attenuate the oxidative damage and inflammatory response and improve the defensive factors, which might be associated with the activation of the Nrf2/HO-1 signaling and the repression of the NF- κ B signaling pathway. In general, MLG could significantly accelerate the metabolism of alcohol and attenuate ethanol-induced gastric mucosal lesions in mice, which might be put down to the activation of alcohol metabolizing enzymes, the inhibition of oxidative damage and the maintenance of gastric mucosa involving the regulation of Nrf-2/HO-1/NF- κ B signaling pathway. It is worth mentioning that the protection effects of MLG for ethanol-induced gastric lesions appears to be



comparable to the classical gastric mucosal protection agent Colloidal Bismuth Pectin (CBP). Moreover, MLG could significantly accelerate the metabolism of alcohol and reduce the toxicity of alcohol, a property not shared by CBP.

ADH and ALDH are crucial enzymes involved in alcohol metabolism, which convert about 90% of ethanol to acetaldehyde, and the resulting acetaldehyde is further

oxidized into harmless acetic acid. This biological process plays a critical role in the rate of alcohol metabolism and the detoxification of alcohol (Gizer et al., 2011; Meng et al., 2019). We recorded the elevation of the activities of ADH and ALDH in gastric tissues after alcohol administration in mice, which could be considered as an adaptive response to alcohol stimulation. In comparison, the raise of ADH and ALDH levels in gastric tissues



were more significant in mice treated with MLG, and a dose-dependent manner is showed with the increment of MLG-M and MLG-H groups being especially arresting. The marvelous results revealed that MLG can stimulate alcohol metabolism, which is

convincingly supported by the enhance ADH and ALDH levels in the gastric tissues of MLG-treated group.

Ethanol, a recognized necrotizing agent, could directly irritate and damage the gastric mucosa, making the gastric

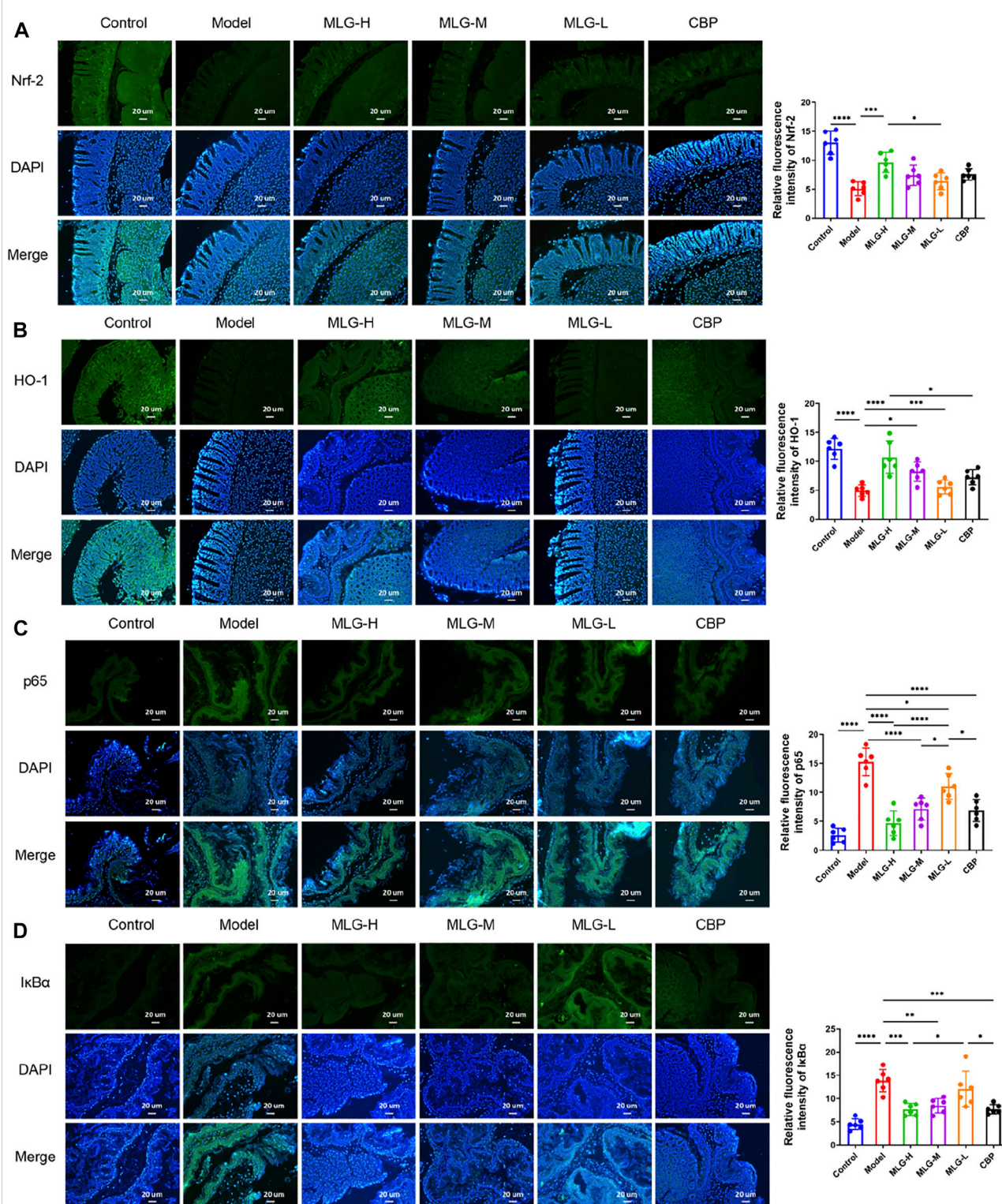


FIGURE 8

Representative immunofluorescence pictures and relative quantitative analysis on mice gastric tissues of Nrf-2 (A), HO-1 (B), p65 (C) and IκBα (D). The blue immunofluorescence is DAPI, showing nuclei. Graphs showing relative quantitative analysis of NF-κB/Nrf2/HO-1 signaling pathway-related proteins, performed with ImageJ software. Control: the group administered zero ethanol; Model: the group administered ethanol intragastrically (13.25 ml/kg BW); MLG-L: low-dose (5 g/kg body weight) MLG-treated group; MLG-M: medium-dose (10 g/kg body weight) MLG-treated group; MLG-H: high-dose (20 g/kg body weight) MLG-treated group; CBP: the group receiving Colloid Bismuth Pectin (57 mg/kg body weight). Each group's data was expressed as mean \pm standard deviation (SD), $n = 6$. By one-way analysis of variance (ANOVA) test, $*p < 0.05$, $***p < 0.001$, $****p < 0.0001$ vs. each group.

mucosal epithelium more susceptible to degeneration and necrosis. We observed that, compared with the model group, MLG-treated groups exhibited lower gastric ulcer index, higher ulcer inhibition rate and milder gastric tissue injury, suggesting that MLG could efficaciously ameliorate ethanol-induced gastric lesions in mice. The histopathological examination of gastric tissues shown a similar tendency. A series of pathological changes that indicated severe gastric lesions, including epithelial cell loss, hemorrhage, structural disorders of glandular tissues, submucosal edema, and inflammatory cells infiltration, could be seen in the model group. The administration of MLG certainly mitigated the situation in a dose-dependent manner. The pathological changes including epithelial cell loss, structural disorder of glandular tissues, submucosal edema and hemorrhage were observed to a milder extent within all MLG-treated group, and, strikingly, the effect of MLG-H group is comparable (and even better) to CBP.

The pathogenesis for ethanol-induced gastric lesions is manifold and complicated, but chief among them is oxidative stress-mediated aggravated inflammatory response. It is well established that ethanol and its metabolite acetaldehyde attack the gastric mucosa causing microcirculatory disturbance and hypoxia, along with the propagation of the inflammatory cascade due to the depletion of mucus and bicarbonate, eventually resulting in cellular necrosis and the excessive production of ROS (Périco et al., 2020). It is ROS that is responsible for the pathogenesis of ethanol-induced gastric lesions mediated by oxidative stress (Sistani Karampour et al., 2019), which interferes with the antioxidant systems of endogenous cells in mucosa, induces leukocyte recruitment and boosts inflammatory response. In the gastric mucosa, the relation, between ROS generation and antioxidant protection mediated through antioxidant enzymes, maintains homeostasis. Oxidative stress triggers a cascade, bringing on the excessive production of ROS and the accumulation of malondialdehyde (MDA). MDA is a significant marker of ROS peroxidation due to its role as a primary lipid peroxidation end product, which manifests the damage of ROS on gastric mucosa directly and is mediated by the development of gastric lesions (Yuksel et al., 2012). ROS also stimulates inhibitor Kappa B (I κ B) kinase to trigger the proteasomal breakdown of I κ B α , the release of NF- κ B p65, and, at length, the activation of NF- κ B. NF- κ B serves as a catalyst for the transcription of a host of inflammatory cytokines and chemokines, being responsible for the high expression of inflammatory factors including TNF- α , IL-6, and IL-1 β (Wardyn et al., 2015; Mitchell et al., 2016; Akanda and Park, 2017). TNF- α and IL-1 β , multifunctional pro-inflammatory cytokines, conduce to the activation and migration of inflammatory cells into the gastric mucosa as well as the gastric inflammatory process (Sugimoto et al., 2009). The secretion of inflammatory mediators, including TNF- α and IL-1 β , is consistent with the activation of polymorphonuclear neutrophil leukocytes, inflammatory infiltration of lymphocytes, and macrophages in gastric tissue after acute ethanol exposure (Bagheri et al., 2015).

When oxidative stress transpires, antioxidant defense system acts actively as well to scavenge ROS, defend against oxidative stress in cell and guard the body. Nuclear factor erythroid 2-related factor 2 (Nrf2) is a crucial transcriptional regulator for cellular defenses against oxidant-associated damage. Excessive ROS phosphorylates Nrf2 and dissociates it from its inhibitor, Kelch-like epichlorohydrin-associated protein 1 (Keap1); the activated Nrf2 will translocate to the nucleus and bind with Maf proteins, to stimulate antioxidant response elements (AREs) and activate downstream antioxidant enzymes such as heme oxygenase-1 (HO-1), superoxide dismutase (SOD), catalase (CAT) and glutathione peroxidase (GSH-Px) (Takei et al., 2015; Kim et al., 2022). HO-1, a stress-inducible enzyme, is considered as a reliable anti-oxidative and cytoprotective agent, which catalyzes the breakdown of heme into equimolar amounts of biliverdin, ferrous iron and carbon monoxide (Puentes-Pardo et al., 2020). Signaling pathways associated with inflammation and oxidative stress, mainly including Nrf2 and NF- κ B, control the expression of HO-1. SODs are universal and essential enzymes for organisms that live in the presence of oxygen, and they are widely recognized as the first hurdle in the fight against oxygen free radicals (Wang et al., 2018). Characterized by requiring for different catalytic metal ions, SODs are divided into three classes in various organisms including copper/zinc SOD (Cu/Zn SODs), manganese/iron SOD (Mn SOD/Fe SODs), and nickel SOD (Ni SODs) (Wang et al., 2018). GSH-Px is highly concentrated in gastric tissue, which is also a vital member of antioxidant system, and gastric mucosa GSH loss may further exacerbate lipid peroxidation along with cell membrane and gastric mucosa damage (Zhang et al., 2013).

The mitogen-activated protein kinases (MAPKs) are important cellular signaling molecules transferring various extracellular signals to intracellular responses by sequential phosphorylation cascades. Several distinct but parallel subgroups have been identified, including C-Jun N-terminal kinase (JNK), Extracellular signal-regulating kinases (ERKs) and p38 MAPK (Bak et al., 2016). MAPKs are involved in a variety of cell biological processes, such as cell proliferation, differentiation, stress response, apoptosis, cell migration, and survival. p38 MAPK is closely related to multiple pathways related to oxidative stress, which is activated and phosphorylated under environmental influence. It is well founded that p38 MAPK is activated and phosphorylated by oxidative stress. Tissue damage and other external stimuli will trigger the secretion of multiple pro-inflammatory cytokines such as TNF- α , IL-1 β , as well as IL-6, and subsequently, the activation of p38 (Chaparro Huerta et al., 2008). The relation between p38 MAPK and NF- κ B has been reported that a variety of pro-inflammatory factors can give rise to the modified I κ Bs degradation and the p65 translocation into the nucleus directly or via the activated p38-MAPK to activate NF- κ B pathway (Xie et al., 2019). Recent studies have found that high expression of P38 can threaten the integrity of gastrointestinal mucosa, and, in

contrast, the inhibition of p38 MAPK phosphorylation can regulate claudin expression, thereby improving the function of gastrointestinal mucosal epithelial barrier (Carrozzino et al., 2009). Increased TNF- α level leads to the disruption of tight epithelial cells and the phosphorylation of P38. HO-1 can keep the barrier intact by blocking tight junction disruption caused by TNF- α and phosphorylation of ERK, P38, and JNK (Zhang Z et al., 2021). Furthermore, MAPK cascades are found to be involved in HO-1 activation. It has been reported that p38 MAPK takes part in the protein synthesis of HO-1 as well as the activation and translocation of Nrf2 to help the body resist oxidative stress (Bak et al., 2016).

The destruction of gastric mucosal integrity can be considered as the disequilibrium between multiple endogenous aggressive factors (such as hydrochloric acid, leukotrienes, and ROS) and defensive factors, including a functional mucus-bicarbonate barrier, nitric oxide (NO), prostaglandins (PG), mucosal microcirculation, antioxidants and some growth factors (Ibrahim et al., 2016). Prostaglandin E2 (PGE2) and NO are postulated to be important defenders of the gastric epithelial mucosal barrier. PGE2, a production of arachidonic acid, is well recognized as a protective factor essential for the repair of damaged gastric mucosa. PGE2 synthesis involves two steps: arachidonic acid is converted into prostaglandin H2 (PGH2) by cyclooxygenase-1 (COX-1) and cyclooxygenase-2 (COX-2), and then PGH2 is isomerized to PGE2 by prostaglandin E synthases (Kloska et al., 2020). As a recognized vasodilator factor, PGE2 has been shown to inhibit platelet aggregation and thrombosis, as well as increase blood flow to the mucosa surface of the stomach, restrain gastric acid secretion, regenerate cells, mediate adaptive immune protective functions and promote mucosal repair (Chen et al., 2016; Fang et al., 2019). COX isoenzymes mainly exist in two isoforms: the constitutive form (COX-1) and the inducible form (COX-2). COX-2 is restricted at the site of inflammation, acting as a proinflammatory enzyme, and its expression could vary drastically as reacting to inflammatory stimuli or growth factors (Zhang J et al., 2021). It is well known that NO plays an indispensable role in maintaining the integrity of the gastric mucosal, which can repair damaged gastric mucosa by regulating gastric mucosal blood flow, acid and alkaline secretion as well as mucus secretion (Ismail Suhaimy et al., 2017). Paradoxically, NO also triggers mucosal damage. NOS, playing a pivotal role in the synthesis of NO by transforming L-arginine to L-citrulline, mainly can be divided into three forms including neuronal NOS (nNOS, type I), inducible NOS (iNOS, type II), and endothelial NOS (eNOS, type III), whereby each of them participates in multiple biological processes. nNOS and eNOS can both be grouped into constitutive NOS (cNOS), characterized by calcium dependence, while iNOS is calcium independent (Kumar and Chanana, 2017; Mohamed et al., 2022). In the digestive system, cNOS-generated NO and iNOS-produced NO are related to contradictory outcomes, with the former one displaying the cytoprotective effect and the latter being cytotoxic (Motawi et al., 2007). eNOS-generated NO facilitates the healing of ulcer via scavenging the damaging free radicals, eliciting angiogenesis,

increasing vasodilation, and attenuating leukocyte infiltration, thereby aiding mucous secretion and epithelial tissue integrity restoration (Khattab et al., 2001; Abd El-Rady et al., 2021). iNOS usually generates NO in response to a wide range of stimuli, such as the production of inflammatory cytokines (IL-1 β , TNF- α). iNOS-produced NO is found to be highly involved in gastric damage, which reacts with superoxide directly to form a potent cytotoxic oxidant, peroxynitrite (Abdel-Raheem, 2010; Kumar and Chanana, 2017). Somatostatin (SS), an important gastrointestinal hormone, could directly inhibit the secretion of acid and indirectly suppress the secretion of histamine and gastrin to protect the gastric mucosa (El-Salhy et al., 2014). Myeloperoxidase (MPO) is mainly found in neutrophils and therefore becomes the specific marker of neutrophils. During the initial inflammatory response, the accumulation of neutrophils results in high expression of MPO, and the activity of MPO can in turn reflect the severity of inflammation in tissues (Al-Quraishy et al., 2017). Moreover, MPO can induce oxidative stress by stimulating the production of reactive oxygen species (ROS) and active nitrogen (RNS) (Chen et al., 2020).

As our observation in the current study, ethanol exposure induced a drastic augment in the MDA level, while GSH-Px and T-SOD concentrations suffered a dramatic decline, signifying the enhancement of oxidative stress as well as lipid peroxidation. This, in turn, serves as a catalyst in the wreck of the antioxidant defense system, making the gastric mucosa more susceptible to injury. MLG has significant antioxidant activity, represented by significantly inhibiting the elevation of MDA while promoting the T-SOD and GSH-Px levels even in a small dose (Figures 5A–C), which effectively reduced the production of oxidative damage products, inhibited the activity of antioxidant enzymes, and protected the mucosa of the stomach from alcohol-induced damage. Our results demonstrated that MLG could inhibit the secretion of inflammatory mediators (TNF- α , IL-1 β , iNOS, MPO, p38-MAPK, and COX-2) and up-regulate the activities of defensive factors (PEG2, NO, eNOS, and SS) in gastric tissues after ethanol exposure, which could attenuate the inflammation response and accelerate the flow of gastric mucosal microcirculation to repair the damaged gastric mucosa. On this account, we speculated that MLG could reduce the infiltration of inflammatory lymphocyte cells in gastric mucosa, which is consistently supported by the amelioration of inflammatory cells infiltration in mice gastric tissue histomorphology examination of MLG-treated groups. We found that MLG treatment markedly blocked the NF- κ B expression and suppressed the phosphorylation of p65 and I κ B α indicating that MLG alleviates ethanol-induced gastric lesions by inhibition of the ROS-mediated inflammatory signaling cascade. Synchronously, Nrf2 and HO-1 levels were observed up-regulated in MLG treatment groups, which demonstrated that the cytoprotective factors were activated to defense the oxidative stress damage and improve the gastric healing of ethanol-induced gastric lesions at the same time. In other words, MLG might have defensive effects on gastric mucosa by counterbalancing ROS generation and antioxidant defense systems in the gastric mucosa, which might rely on reducing the

oxidative stress and strengthening the antioxidant defense concurrently via the molecular cross-talk of NF- κ B/Nrf-2/HO-1. Taken together, our results demonstrated that MLG, as natural antioxidants, could help protect the gastric mucosa from oxidative stress and improve its defenses in order to moderate gastric mucosal microcirculation and preserve gastric mucosa.

Conclusion

Taken together, our study delivered a point of view that MLG could effectively protect the gastric mucosa of mice against the gastric damage of ethanol-induced gastric lesions, mainly presented as the activation of alcohol metabolizing enzymes, attenuation of oxidative damage and inflammatory response, up-regulation of the defensive factors and improvement of vasodilation. Most glaring of all, MLG could remarkably accelerate the metabolism of alcohol and reduce the toxicity of alcohol, a property not shared by CBP. The gastroprotective effect of MLG on ethanol-induced gastric lesions may be achieved through the weakened of damage factors (TNF- α , IL-1 β , iNOS, MPO, p38-MAPK, and COX-2) and the enhancement of defensive factors (PEG2, NO, eNOS, and SS) in gastric tissues involving NF- κ B/Nrf2/HO-1 signaling pathway. We further confirmed that MLG has a strong potential in preventing and treating ethanol-induced gastric lesions.

Data availability statement

The original contributions presented in the study are included in the article/Supplementary Material, further inquiries can be directed to the corresponding author.

Ethics statement

The animal study was reviewed and approved by the Ethics Committee for Animal Studies of Guangzhou University of Chinese Medicine (NO. 20210316001).

References

- Abd El-Rady, N. M., Dahpy, M. A., Ahmed, A., Elgamal, D. A., Hadiya, S., Ahmed, M. A. M., et al. (2021). Interplay of biochemical, genetic, and immunohistochemical factors in the etio-pathogenesis of gastric ulcer in rats: A comparative study of the effect of pomegranate loaded nanoparticles versus pomegranate peel extract. *Front. Physiol.* 12, 649462. doi:10.3389/fphys.2021.649462
- Abdel-Raheem, I. T. (2010). Gastroprotective effect of rutin against indomethacin-induced ulcers in rats. *Basic Clin. Pharmacol. Toxicol.* 107 (3), 742–750. doi:10.1111/j.1742-7843.2010.00568.x
- Adeyemi, J. O., and Onwudiwe, D. C. (2020). Chemistry and some biological potential of bismuth and antimony dithiocarbamate complexes. *Mol. (Basel, Switz.)* 25 (2), 305. doi:10.3390/molecules25020305
- Agboola, J. B., Ehigie, A. F., Ehigie, L. O., Ojienyi, F. D., and Olayemi, A. A. (2022). Ameliorative role of *Syzgium aromaticum* aqueous extract on

Author contributions

LX: Conceptualization, Methodology, Writing—original draft; ML: Validation, Investigation; JL: Investigation, Writing—original draft; WH: Validation, Data curation; GT: Investigation; XC: Investigation; YZ: Data curation; YA: Investigation; HH: Writing-review and editing; JH: Conceptualization, Methodology, Writing-review and editing.

Funding

This study was supported by the National Natural Science Foundation of China (Nos. 81573861).

Conflict of interest

The authors declare that the research was conducted in the absence of any commercial or financial relationships that could be construed as a potential conflict of interest.

Publisher's note

All claims expressed in this article are solely those of the authors and do not necessarily represent those of their affiliated organizations, or those of the publisher, the editors and the reviewers. Any product that may be evaluated in this article, or claim that may be made by its manufacturer, is not guaranteed or endorsed by the publisher.

Supplementary material

The Supplementary Material for this article can be found online at: <https://www.frontiersin.org/articles/10.3389/fphar.2022.953885/full#supplementary-material>

synaptosomal tyrosine hydroxylase activity, oxidative stress parameters, and behavioral changes in lead-induced neurotoxicity in mice. *J. Food Biochem.* 46 (7), e14115. doi:10.1111/jfbc.14115

Akanda, M. R., and Park, B. (2017). Involvement of MAPK/NF- κ B signal transduction pathways: *Camellia japonica* mitigates inflammation and gastric ulcer. *Biomed. Pharmacother.* 95, 1139–1146. doi:10.1016/j.biopha.2017.04.069

Al-Quraishy, S., Othman, M. S., Dkhil, M. A., and Abdel Moneim, A. E. (2017). Olive (*Olea europaea*) leaf methanolic extract prevents HCl/ethanol-induced gastritis in rats by attenuating inflammation and augmenting antioxidant enzyme activities. *Biomed. Pharmacother.* 91, 338–349. doi:10.1016/j.biopha.2017.04.069

Arda-Pirinci, P., Bolkent, S., and Yanardag, R. (2006). The role of zinc sulfate and metallothionein in protection against ethanol-induced gastric damage in rats. *Dig. Dis. Sci.* 51 (12), 2353–2360. doi:10.1007/s10620-006-9301-3

- Ashktorab, H., Soleimani, A., Singh, G., Amr, A., Tabatabaei, S., Latella, G., et al. (2019). Saffron: The golden spice with therapeutic properties on digestive diseases. *Nutrients* 11 (5), 943. doi:10.3390/nu11050943
- Association, C. M. D. (2015). Emergency experts consensus on acute gastric mucosal lesions in China. *Chin. J. Emerg. Med.* 10 (24), 1072–1077.
- Bagheri, N., Azadegan-Dehkordi, F., Shirzad, M., Zamanzad, B., Rahimian, G., Taghikhani, A., et al. (2015). Mucosal interleukin-21 mRNA expression level is high in patients with *Helicobacter pylori* and is associated with the severity of gastritis. *Cent. Eur. J. Immunol.* 40 (1), 61–67. doi:10.5114/ceji.2015.50835
- Bak, M. J., Truong, V., Ko, S., Nguyen, X. N. G., Jun, M., Hong, S., et al. (2016). Induction of Nrf2/ARE-mediated cytoprotective genes by red ginseng oil through ASK1–MKK4/7–JNK and p38 MAPK signaling pathways in HepG2 cells. *J. Ginseng Res.* 40 (4), 423–430. doi:10.1016/j.jgr.2016.07.003
- Breslow, R. A., Dong, C., and White, A. (2015). Prevalence of alcohol-interactive prescription medication use among current drinkers: United States, 1999 to 2010. *Alcohol. Clin. Exp. Res.* 39 (2), 371–379. doi:10.1111/acer.12633
- Cailin, Z. (1999). 31 cases of Lvdu Gancao decoction in the treatment of the pesticide poisoning. *Chin. Folk. Remed* 1 (11), 29–32.
- Cao, Y., Zheng, Y., Niu, J., Zhu, C., Yang, D., Rong, F., et al. (2020). Efficacy of Banxia xiexin decoction for chronic atrophic gastritis: A systematic review and meta-analysis. *PLoS One* 15 (10), e0241202. doi:10.1371/journal.pone.0241202
- Carrozzino, F., Pugnale, P., Féraille, E., and Montesano, R. (2009). Inhibition of basal p38 or JNK activity enhances epithelial barrier function through differential modulation of claudin expression. *Am. J. Physiol. Cell Physiol.* 297 (3), C775–C787. doi:10.1152/ajpcell.00084.2009
- Casili, G., Lanza, M., Filippone, A., Campolo, M., Paterniti, I., Cuzzocrea, S., et al. (2020). Dimethyl fumarate alleviates the nitroglycerin (NTG)-induced migraine in mice. *J. Neuroinflammation* 17 (1), 59. doi:10.1186/s12974-020-01736-1
- Chaparro Huerta, V., Flores Soto, M. E., Gudiño Cabrera, G., Rivera Cervantes, M. C., Bitzer Quintero, O. K., and Beas Zárate, C. (2008). Role of p38 MAPK and pro-inflammatory cytokines expression in glutamate-induced neuronal death of neonatal rats. *Int. J. Dev. Neurosci.* 26 (5), 487–495. doi:10.1016/j.jidvneu.2008.02.008
- Chen, S., Chen, H., Du, Q., and Shen, J. (2020). Targeting myeloperoxidase (MPO) mediated oxidative stress and inflammation for reducing brain ischemia injury: Potential application of natural compounds. *Front. Physiol.* 11, 433. doi:10.3389/fphys.2020.00433
- Chen, Z., Wu, J., Xu, D., Huang, M., Sun, S., Zhang, H., et al. (2016). Epidermal growth factor and prostaglandin E2 levels in *Helicobacter pylori*-positive gastric intraepithelial neoplasia. *J. Int. Med. Res.* 44 (2), 241–247. doi:10.1177/0300060515611535
- Dan, Z., Donghui, C., Meishan, J., Menghui, W., Yueqi, W., Na, Y., et al. (2018). Inhibitory effect of β -glycyrrhetic acid in inflammation related gastric cancer and its mechanism. *J. Jilin Univ.* 06 (44), 1150–1155.
- De Araújo, E. R. D., Guerra, G. C. B., Araújo, D. F. D. S., de Araújo, A. A., Fernandes, J. M., de Araújo Júnior, R. F., et al. (2018). Gastroprotective and antioxidant activity of *kalanchoe brasiliensis* and *kalanchoe pinnata* leaf juices against indomethacin and ethanol-induced gastric lesions in rats. *Int. J. Mol. Sci.* 19 (5), 1265. doi:10.3390/ijms19051265
- Dimauro, I., Grazioli, E., Lisi, V., Guidotti, F., Fantini, C., Antinozzi, C., et al. (2021). Systemic response of antioxidants, heat shock proteins, and inflammatory biomarkers to short-lasting exercise training in healthy male subjects. *Oxid. Med. Cell. Longev.* 2021, 1938492. doi:10.1155/2021/1938492
- Dong, Z., Bian, L., Wang, Y., and Sun, L. (2021). Gastrodin protects against high glucose-induced cardiomyocyte toxicity via GSK-3 β -mediated nuclear translocation of Nrf2. *Hum. Exp. Toxicol.* 40 (9), 1584–1597. doi:10.1177/09603271211002885
- El-Maraghy, S. A., Rizk, S. M., and Shahin, N. N. (2015). Gastroprotective effect of crocin in ethanol-induced gastric injury in rats. *Chem. Biol. Interact.* 229, 26–35. doi:10.1016/j.cbi.2015.01.015
- El-Salhy, M., Gilja, O. H., Hatlebakk, J. G., and Hausken, T. (2014). Stomach antral endocrine cells in patients with irritable bowel syndrome. *Int. J. Mol. Med.* 34 (4), 967–974. doi:10.3892/ijmm.2014.1887
- Escobedo-Hinojosa, W. I., Gomez-Chang, E., García-Martínez, K., Guerrero Alquicira, R., Cardoso-Taketa, A., and Romero, I. (2018). Gastroprotective mechanism and ulcer resolution effect of *Cyrtocarpa procera* methanolic extract on ethanol-induced gastric injury. *Evidence-based complementary Altern. Med. eCAM* 2018, 2862706. doi:10.1155/2018/2862706
- Fang, Y. F., Xu, W. L., Wang, L., Lian, Q. W., Qiu, L. F., Zhou, H., et al. (2019). Effect of hydrotalcite on indomethacin-induced gastric injury in rats. *Biomed. Res. Int.* 2019, 4605748. doi:10.1155/2019/4605748
- Fu, Y., Zhou, J., Sang, X., and Zhao, Q. (2021). Gualou-Xiebai-Banxia decoction protects against type II diabetes with acute myocardial ischemia by attenuating oxidative stress and apoptosis via PI3K/Akt/eNOS signaling. *Chin. J. Nat. Med.* 19 (3), 161–169. doi:10.1016/S1875-5364(21)60017-1
- Gizer, I. R., Edenberg, H. J., Gilder, D. A., Wilhelmsen, K. C., and Ehlers, C. L. (2011). Association of alcohol dehydrogenase genes with alcohol-related phenotypes in a Native American community sample. *Alcohol. Clin. Exp. Res.* 35 (11), 2008–2018. doi:10.1111/j.1530-0277.2011.01552.x
- Gonçalves, J. L., Lacerda-Queiroz, N., Sabino, J. F. L., Marques, P. E., Galvão, I., Gamba, C. O., et al. (2017). Evaluating the effects of refined carbohydrate and fat diets with acute ethanol consumption using a mouse model of alcoholic liver injury. *J. Nutr. Biochem.* 39, 93–100. doi:10.1016/j.jnutbio.2016.08.011
- Guth, P. H., Aures, D., and Paulsen, G. (1979). Topical aspirin Plus HCl gastric lesions in the rat. *Gastroenterology* 76 (1), 88–93. doi:10.1016/s0016-5085(79)80133-x
- Haniadka, R., Saldanha, E., Sunita, V., Palatty, P. L., Fayad, R., and Baliga, M. S. (2013). A review of the gastroprotective effects of ginger (*Zingiber officinale* Roscoe). *Food Funct.* 4 (6), 845–855. doi:10.1039/c3fo30337c
- Hyun, J., Han, J., Lee, C., Yoon, M., and Jung, Y. (2021). Pathophysiological aspects of alcohol metabolism in the liver. *Int. J. Mol. Sci.* 22 (11), 5717. doi:10.3390/ijms22115717
- Ibrahim, M. Y., Hashim, N. M., Dhiyaaldeen, S. M., Al-Obaidi, M. M. J., El-Ferjani, R. M., Adam, H., et al. (2016). Acute toxicity and gastroprotection studies of a new Schiff base derived manganese (II) complex against HCl/Ethanol-Induced gastric ulcerations in rats. *Sci. Rep.-UK*. 6, 26819. doi:10.1038/srep26819
- Ismail Suhaimy, N. W., Noor Azmi, A. K., Mohtarrudin, N., Omar, M. H., Tohid, S. F. M., Cheema, M. S., et al. (2017). Semipurified ethyl acetate partition of methanolic extract of *Melastoma malabathricum* leaves exerts gastroprotective activity partly via its antioxidant-antisecretory-anti-inflammatory action and synergistic action of several flavonoid-based compounds. *Oxid. Med. Cell. Longev.* 2017, 6542631. doi:10.1155/2017/6542631
- Jang, A. J., Lee, J., Yotsu-Yamashita, M., Park, J., Kye, S., Benza, R. L., et al. (2018). A novel compound, "FA-1" isolated from *Prunus mume*, protects human bronchial epithelial cells and keratinocytes from cigarette smoke extract-induced damage. *Sci. Rep.* 8 (1), 11504. doi:10.1038/s41598-018-29701-2
- Jeon, W., Shin, I., Shin, H., and Lee, M. (2014). Gastroprotective effect of the traditional herbal medicine, *Sipjeondaebo*-tang water extract, against ethanol-induced gastric mucosal injury. *BMC Complement. Altern. Med.* 14, 373. doi:10.1186/1472-6882-14-373
- Khattab, M. M., Gad, M. Z., and Abdallah, D. (2001). Protective role of nitric oxide in indomethacin-induced gastric ulceration by a mechanism independent of gastric acid secretion. *Pharmacol. Res.* 43 (5), 463–467. doi:10.1006/phrs.2001.0801
- Kim, H. S., Lim, J. W., and Kim, H. (2022). Korean red ginseng extract inhibits IL-8 expression via Nrf2 activation in *Helicobacter pylori*-infected gastric epithelial cells. *Nutrients* 14 (5), 1044. doi:10.3390/nu14051044
- Kim, M. J., Kim, D. W., Kim, J. G., Shin, Y., Jung, S. K., and Kim, Y. (2021). Analysis of the chemical, antioxidant, and anti-inflammatory properties of pink pepper (*Schinus molle* L.). *Antioxidants (Basel, Switz.)* 10 (7), 1062. doi:10.3390/antiox10071062
- Kloska, A., Malinowska, M., Gabig-Cimińska, M., and Jakóbkiewicz-Banecka, J. (2020). Lipids and lipid mediators associated with the risk and pathology of ischemic stroke. *Int. J. Mol. Sci.* 21 (10), 3618. doi:10.3390/ijms21103618
- Kumar, A., and Chanana, P. (2017). Role of nitric oxide in stress-induced anxiety: From pathophysiology to therapeutic target. *Vitam. Horm.* 103, 147–167. doi:10.1016/bs.vh.2016.09.004
- Lebda, M. A., El-Far, A. H., Noreldin, A. E., Elewa, Y. H. A., Al Jaouni, S. K., and Mousa, S. A. (2018). Protective effects of miswak (*Salvadora persica*) against experimentally induced gastric ulcers in rats. *Oxid. Med. Cell. Longev.* 2018, 6703296. doi:10.1155/2018/6703296
- Li, H., and Sun, H. (2012). Recent advances in bioinorganic chemistry of bismuth. *Curr. Opin. Chem. Biol.* 16 (1–2), 74–83. doi:10.1016/j.cbpa.2012.01.006
- Li, J., Wang, T., Zhu, Z., Yang, F., Cao, L., and Gao, J. (2017). Structure features and anti-gastric ulcer effects of inulin-type fructan CP-A from the roots of *Codonopsis pilosula* (franch.) Nannf. *Franch.) Nannf. Mol.* 22 (12), 2258. doi:10.3390/molecules22122258
- Li, L., Kong, L., and Song, H. (2017). The therapeutic effect of zerumbone on chronic gastritis via antioxidant mechanisms. *Exp. Ther. Med.* 14 (3), 2505–2510. doi:10.3892/etm.2017.4795
- Li, X., and Tang, C. (1997). 15 cases of clinical effect observation on Lvdu Gancao decoction in the treatment of drug-induced hepatitis. *Guangdong Med. J.* 10, 691–692.
- Lv, C., Shi, C., Li, L., Wen, X., and Xian, C. J. (2018). Chinese herbal medicines in the prevention and treatment of chemotherapy-induced nausea and vomiting. *Curr. Opin. Support. Palliat. Care* 12 (2), 174–180. doi:10.1097/SPC.0000000000000348

- Magierowska, K., Wojcik, D., Chmura, A., Bakalarz, D., Wierdak, M., Kwiecien, S., et al. (2018). Alterations in gastric mucosal expression of calcitonin gene-related peptides, vanilloid receptors, and heme oxygenase-1 mediate gastroprotective action of carbon monoxide against ethanol-induced gastric mucosal lesions. *Int. J. Mol. Sci.* 19 (10), 2960. doi:10.3390/ijms19102960
- Martin, N. M., and Maricle, B. R. (2015). Species-specific enzymatic tolerance of sulfide toxicity in plant roots. *Plant physiology Biochem. PPB.* 88, 36–41. doi:10.1016/j.plaphy.2015.01.007
- Meng, B., Zhang, Y., Wang, Z., Ding, Q., Song, J., and Wang, D. (2019). Hepatoprotective effects of morchella esculenta against alcohol-induced acute liver injury in the C57bl/6 mouse related to nrf-2 and NF- κ B signaling. *Oxid. Med. Cell. Longev.* 2019, 6029876. doi:10.1155/2019/6029876
- Meng, J., Liu, J., Chen, D., Kang, J., Huang, Y., Li, D., et al. (2020). Integration of lncRNA and mRNA profiles to reveal the protective effects of Codonopsis pilosula extract on the gastrointestinal tract of mice subjected to D-galactose-induced aging. *Int. J. Mol. Med.* 47 (3), 1. doi:10.3892/ijmm.2020.4834
- Minqing, Z., and Mingwei, Z. (2002). *Modern clinical Chinese pharmacy*. Shanghai: Shanghai University of Traditional Chinese Medicine Press, 603–608.
- Mitchell, S., Vargas, J., and Hoffmann, A. (2016). Signaling via the NF κ B system. *Wiley Interdiscip. Rev. Syst. Biol. Med.* 8 (3), 227–241. doi:10.1002/wsbm.1331
- Mohamed, Y. T., Naguib, I. A., Abo-Saif, A. A., Elkomy, M. H., Alghamdi, B. S., and Mohamed, W. R. (2022). Role of ADMA/DDAH-1 and iNOS/eNOS signaling in the gastroprotective effect of tadalafil against indomethacin-induced gastric injury. *Biomed. Pharmacother.* 150, 113026. doi:10.1016/j.biopha.2022.113026
- Motawi, T. K., Abd Elgawad, H. M., and Shahin, N. N. (2007). Modulation of indomethacin-induced gastric injury by spermine and taurine in rats. *J. Biochem. Mol. Toxicol.* 21 (5), 280–288. doi:10.1002/jbt.20194
- Pan, J., He, S., Xu, H., Zhan, X., Yang, X., Xiao, H., et al. (2008). Oxidative stress disturbs energy metabolism of mitochondria in ethanol-induced gastric mucosa injury. *World J. Gastroenterol.* 14 (38), 5857–5867. doi:10.3748/wjg.14.5857
- Périco, L. L., Emílio-Silva, M. T., Ohara, R., Rodrigues, V. P., Bueno, G., Barbosa-Filho, J. M., et al. (2020). Systematic analysis of monoterpenes: Advances and challenges in the treatment of peptic ulcer diseases. *Biomolecules* 10 (2), 265. doi:10.3390/biom10020265
- Puentes-Pardo, J. D., Moreno-Sanjuan, S., Carazo, Á., and León, J. (2020). Heme oxygenase-1 in gastrointestinal tract health and disease. *Antioxidants* 9 (12), 1214. doi:10.3390/antiox9121214
- Qiao, Y., Xu, L., Tao, X., Yin, L., Qi, Y., Xu, Y., et al. (2018). Protective effects of dioscin against fructose-induced renal damage via adjusting Sirt3-mediated oxidative stress, fibrosis, lipid metabolism and inflammation. *Toxicol. Lett.* 284, 37–45. doi:10.1016/j.toxlet.2017.11.031
- Raish, M., Ahmad, A., Ansari, M. A., Alkharfy, K. M., Aljenoobi, F. I., Jan, B. L., et al. (2018). Momordica charantia polysaccharides ameliorate oxidative stress, inflammation, and apoptosis in ethanol-induced gastritis in mucosa through NF- κ B signaling pathway inhibition. *Int. J. Biol. Macromol.* 111, 193–199. doi:10.1016/j.ijbiomac.2018.01.008
- Sandberg, M., Patil, J., D'Angelo, B., Weber, S. G., and Mallard, C. (2014). NRF2-regulation in brain health and disease: Implication of cerebral inflammation. *Neuropharmacology* 79, 298–306. doi:10.1016/j.neuropharm.2013.11.004
- Sistani Karampour, N., Arzi, A., Rezaie, A., Pashmforoosh, M., and Kordi, F. (2019). Gastroprotective effect of zingerone on ethanol-induced gastric ulcers in rats. *Med. Kaunas. Lith.* 55 (3), 64. doi:10.3390/medicina55030064
- Sugimoto, M., Ohno, T., Graham, D. Y., and Yamaoka, Y. (2009). Gastric mucosal interleukin-17 and -18 mRNA expression in Helicobacter pylori-induced Mongolian gerbils. *Cancer Sci.* 100 (11), 2152–2159. doi:10.1111/j.1349-7006.2009.01291.x
- Sun, S. (2015). *Zhonghua yifang*. Beijing: Scientific and Technical Documentation Press, 1819.
- Takei, K., Hashimoto-Hachiya, A., Takahara, M., Tsuji, G., Nakahara, T., and Furue, M. (2015). Cynaropicrin attenuates UVB-induced oxidative stress via the AhR-Nrf2-Nqo1 pathway. *Toxicol. Lett.* 234 (2), 74–80. doi:10.1016/j.toxlet.2015.02.007
- Wang, C., Zhu, M., Xia, W., Jiang, W., and Li, Y. (2012). Meta-analysis of Traditional Chinese Medicine in treating functional dyspepsia of liver-stomach disharmony syndrome. *J. Tradit. Chin. Med.* 32 (4), 515–522. doi:10.1016/S0254-6272(13)60063-1
- Wang, F. (2002). 11 cases of Lv dou Gancao decoction in the adjuvant treatment of the organophosphorus pesticide poisoning. *China's Naturop.* 1 (08), 37.
- Wang, Q., Zhu, X., Jiang, H., Wang, G., and Cui, Y. (2015). Protective effects of alginate-chitosan microspheres loaded with alkaloids from Coptis chinensis Franch. and Evodia rutaecarpa (Juss.) Benth. (Zuojin Pill) against ethanol-induced acute gastric mucosal injury in rats. *Drug Des. devel. Ther.* 9, 6151–6165. doi:10.2147/DDDT.S96056
- Wang, Y., Branicky, R., Noë, A., and Hekimi, S. (2018). Superoxide dismutases: Dual roles in controlling ROS damage and regulating ROS signaling. *J. Cell Biol.* 217 (6), 1915–1928. doi:10.1083/jcb.201708007
- Wang, Z. (2017). *Chinese medicinal diet dictionary*. Dalian: Dalian Publishing House.
- Wang, Z., Du, Q., Xu, G., Wang, R., Fu, D., and Ng, T. (1997). Investigations on the protective action of Condonopsis pilosula (Dangshen) extract on experimentally-induced gastric ulcer in rats. *Gen. Pharmacol.* 28 (3), 469–473. doi:10.1016/S0306-3623(96)00047-X
- Wardyn, J. D., Ponsford, A. H., and Sanderson, C. M. (2015). Dissecting molecular cross-talk between Nrf2 and NF- κ B response pathways. *Biochem. Soc. Trans.* 43 (4), 621–626. doi:10.1042/BST20150014
- Weathermon, R., and Crabb, D. W. (1999). Alcohol and medication interactions. *Alcohol Res. Health.* 23 (1), 40–54.
- Wei, W., Zhang, H., Wang, J., and Jing, Z. (2013). Clinical efficacy analysis of acute pancreatitis treating by Lv dou Gancao decoction. *Mod. Tradit. Chin. Med.* 33 (04), 25–27.
- Weifeng, M., and Jia, S. (2022). Discussion on the treatment of liver disease in traditional Chinese medicine base on Wang Xugao's Night talk record of Xixi bookstore. *Hepatology J. Integr. Traditional Chin. West. Med.* 01 (32), 1–7.
- Wenquan, L. (2007). *Liver-protection and detoxication of mungbean Huang*. Guangzhou: Guangzhou University Of Chinese Medicine.
- Wenxue, Z. (2018). *Food poisoning or drug poisoning*. Suzhou: Healthy Living, 25(06).
- Wu, X., Huang, Q., Xu, N., Cai, J., Luo, D., Zhang, Q., et al. (2018). Antioxidative and anti-inflammatory effects of water extract of *Acrostichum aureum* linn. Against ethanol-induced gastric ulcer in rats. *Evidence-based complementary Altern. Med. eCAM* 2018, 3585394. doi:10.1155/2018/3585394
- Xie, L., Huang, W., Li, J., Chen, G., Xiao, Q., Zhang, Y., et al. (2022). The protective effects and mechanisms of modified Lv dou Gancao decoction on acute alcohol intoxication in mice. *J. Ethnopharmacol.* 282, 114593. doi:10.1016/j.jep.2021.114593
- Xie, W., Huang, X., Chen, R., Chen, R., Li, T., Wu, W., et al. (2019). Esomeprazole alleviates the damage to stress ulcer in rats through not only its antisecretory effect but its antioxidant effect by inactivating the p38 MAPK and NF- κ B signaling pathways. *Drug Des. devel. Ther.* 13, 2969–2984. doi:10.2147/DDDT.S193641
- Yu, L., Li, R., Liu, W., Zhou, Y., Li, Y., Qin, Y., et al. (2020). Protective effects of wheat peptides against ethanol-induced gastric mucosal lesions in rats: Vasodilation and anti-inflammation. *Nutrients* 12 (8), 2355. doi:10.3390/nu12082355
- Yu, Y., Zhang, G., Han, T., and Huang, H. (2020). Analysis of the pharmacological mechanism of Banxia Xiexin decoction in treating depression and ulcerative colitis based on a biological network module. *BMC Complement. Med. Ther.* 20 (1), 199. doi:10.1186/s12906-020-02988-3
- Yuewen, L., and Qiang, W. (2018). Mechanism of licoflavone in protecting human gastric mucosal epithelial cells from aspirin-induced injury. *Chin. General Pract.* 32 (21), 3971–3975.
- Yuksel, M. B., Kavak, S., Gecit, I., Basel, H., Gümrükçüoğlu, H. A., Demir, H., et al. (2012). Short-term levosimendan treatment protects rat testes against oxidative stress. *Braz. J. Med. Biol. Res. = Revista brasileira de pesquisas medicas e Biol.* 45 (8), 716–720. doi:10.1590/s0100-879x2012007500075
- Zaghloul, S. S., Abo-Seif, A. A., Rabeh, M. A., Abdelmohsen, U. R., and Messiha, B. A. S. (2019). Gastro-protective and anti-oxidant potential of althaea officinalis and Solanum nigrum on pyloric ligation/indomethacin-induced ulceration in rats. *Antioxidants (Basel, Switz.)* 8 (11), 512. doi:10.3390/antiox8110512
- Zhang, C., Gu, C., Peng, F., Liu, W., Wan, J., Xu, H., et al. (2013). Preparation and optimization of triptolide-loaded solid lipid nanoparticles for oral delivery with reduced gastric irritation. *Mol. (Basel, Switz.)* 18 (11), 13340–13356. doi:10.3390/molecules181113340
- Zhang, F., and Zheng, Y. (2017). *The first batch of national-level famous traditional Chinese medicine doctors' effective prescription*. Beijing: China Medical Science Press.
- Zhang, H. (2000). 88 cases of Lv dou Gancao decoction treating the mycetism heteroptics. *J. Emerg. Traditional Chin. Med.* 1 (01), 17.
- Zhang, J. J., Wang, J., Fang, H., Yu, H., Zhao, Y., Shen, J., et al. (2021). Pterostilbene inhibits deoxynivalenol-induced oxidative stress and inflammatory response in bovine mammary epithelial cells. *Toxicon* 189, 10–18. doi:10.1016/j.toxicon.2020.11.002
- Zhang, Z. Z., Zhang, Q., Li, F., Xin, Y., and Duan, Z. (2021). Contributions of HO-1-Dependent MAPK to regulating intestinal barrier disruption. *Biomol. Ther.* 29 (2), 175–183. doi:10.4062/biomolther.2020.112
- Zhou, S. (2009). Lv dou Gancao decoction treating the kusnezoff monkshood poisoning. *J. Emerg. Traditional Chin. Med.* 18 (03), 347–383.

Appendix A: Contents of MLG.

Chinese name	Accepted name	Weight (g)	Medicinal part	Plantchemical composition
Lvdou	<i>Vigna radiata</i> (L.) R.Wilczek [Fabaceae]	50	Seeds	sitosterol, beta-carotene, vitamin-e, vitexin_qt, vitexin_qtPQN
Gancao		10	Roots and rhizomes	Glycyrol, Glycyrol, licopyranocoumarin, shinpterocarpin, Phaseol, Licochalcone B, glyasperin F, Inermine, Vestitol, Glyasperins M
Dangshen	<i>Glycyrrhiza glabra</i> L. [Fabaceae]	10	Root	Perlolyrine, Perlolyrine, glycitein, glycitein
	<i>Codonopsis pilosula</i> (Franch.) Nannf. [Campanulaceae]			
Shanyao		15	Tuber	diosgenin, diosgenin, Isofucosterol, Stigmasterol, hancinone C, Denudatin B, Kadsurenone, hancinol, (-)-taxifolin
	<i>Dioscorea oppositifolia</i> L. [Dioscoreaceae]			
Chuanxiong	<i>Conioselinum anthriscoides</i> 'Chuanxiong' [Apiaceae]	10	Rhizome	sitosterol, Myricanone, Mandenol, wallichilide, senkyunone, PerlolyrineFA
Gansong		15	Roots and rhizomes	(2R)-5,7-dihydroxy-2-(4-hydroxyphenyl)chroman-4-one, acaciin, acacetin, sitosterol, sitosterol
	<i>Nardostachys jatamansi</i> (D.Don) DC. [Caprifoliaceae]			
Dingxiang		10	Flower Bud	Strictosamide_qt, ZINC03860434, beta-sitosterol, kaempferol, Stigmasterol, quercetin
	<i>Syzygium aromaticum</i> (L.) Merr. & L.M.Perry [Myrtaceae]			
Jiangbanxia		10	Tuber	Baicalin, (3S,6S)-3-(benzyl)-6-(4-hydroxybenzyl)piperazine-2,5-quinone, beta-D-Ribofuranoside, xanthine-9, Stigmasterol, Stigmasterol, 10,13-eicosadienoic, Cycloartenol, beta-sitosterol, 24-Ethylcholest-4-en-3-one, Cavidine, baicalein, coniferin, gondoic acid
	<i>Pinellia ternata</i> (Thunb.) Makino [Araceae]			
Baishao		30	Root	11alpha,12alpha-epoxy-3beta-23-dihydroxy-30-norolean-20-en-28,12beta-olide, paeoniflorgenone, (3S,5R,8R,9R,10S,14S)-3,17-dihydroxy-4,4,8,10,14-pentamethyl-2,3,5,6,7,9-hexahydro-1H-cyclopenta[a]phenanthrene-15,16-dione, Lactiflorin, paeoniflorin, paeoniflorin_qt, albiflorin_qt, benzoyl paeoniflorin, Mairin, beta-sitosterol, sitosterol, kaempferol, (+)-catechin
	<i>Paeonia lactiflora</i> Pall. [Paeoniaceae]			
Lianfang		10	Receptacle	procyanidin, Hyperin, quercetin
	<i>Nelumbo nucifera</i> Gaertn. [Nelumbonaceae]			
Tianma	<i>Gastrodia elata</i> Blume [Orchidaceae]	10	Tuber	gastrodin, P-hydroxybenzyl alcohol, Parisin E, Parisin A, Parisin B, Parisin C
huang Jiezi	<i>Brassica juncea</i> (L.) Czern. [Brassicaceae]	10	Seeds	Uniflex BYO, 2-(2-phenylethyl)-6-[[[(5S,6R,7R,8S)-5,6,7-trihydroxy-4-keto-2-(2-phenylethyl)-5,6,7,8-tetrahydrochromen-8-yl]oxy]chromone, Sinoacutine
Shengjiang		5	Fresh rhizome	beta-sitosterol, 6-methylgingediacetate2, Stigmasterol, Stigmasterol, Dihydrocapsaicin
	<i>Zingiber officinale</i> Roscoe [Zingiberaceae]			
Dazao		5	Pulp and seeds	Spiradine A, Mauratine D, Moupinamide, Ziziphin_qt, Fumarine, malkangunin, Mairin, (+)-catechin, (-)-catechin, Daechuine S6, Daechuine S6, Daechuine S7, Stigmasterol, (S)-Coclaurine
	<i>Ziziphus jujuba</i> Mill. [Rhamnaceae]			



OPEN ACCESS

EDITED BY

Muhammad Hasnat,
University of Veterinary and Animal
Sciences, Pakistan

REVIEWED BY

Min Chen,
University of Kentucky, United States
Francesca Bianchini,
University of Florence, Italy

*CORRESPONDENCE

Mehdi Shakibaei,
mehdi.shakibaei@med.uni-
muenchen.de

SPECIALTY SECTION

This article was submitted to
Ethnopharmacology,
a section of the journal
Frontiers in Pharmacology

RECEIVED 26 June 2022

ACCEPTED 11 August 2022

PUBLISHED 02 September 2022

CITATION

Brockmueller A, Mueller A-L, Shayan P
and Shakibaei M (2022), β 1-Integrin
plays a major role in resveratrol-
mediated anti-invasion effects in the
CRC microenvironment.
Front. Pharmacol. 13:978625.
doi: 10.3389/fphar.2022.978625

COPYRIGHT

© 2022 Brockmueller, Mueller, Shayan
and Shakibaei. This is an open-access
article distributed under the terms of the
[Creative Commons Attribution License](https://creativecommons.org/licenses/by/4.0/)
(CC BY). The use, distribution or
reproduction in other forums is
permitted, provided the original
author(s) and the copyright owner(s) are
credited and that the original
publication in this journal is cited, in
accordance with accepted academic
practice. No use, distribution or
reproduction is permitted which does
not comply with these terms.

β 1-Integrin plays a major role in resveratrol-mediated anti-invasion effects in the CRC microenvironment

Aranka Brockmueller¹, Anna-Lena Mueller¹, Parviz Shayan² and Mehdi Shakibaei^{1*}

¹Musculoskeletal Research Group and Tumor Biology, Faculty of Medicine, Institute of Anatomy, Chair of Vegetative Anatomy, Ludwig-Maximilians-University Munich, Munich, Germany, ²Department of Parasitology, Faculty of Veterinary Medicine, University of Tehran, Tehran, Iran

Background: Tumor microenvironment (TME) is one of the most important factors in tumor aggressiveness, with an active exchange between tumor and other TME-associated cells that promotes metastasis. The tumor-inhibitory effect of resveratrol on colorectal cancer (CRC) cells has been frequently reported. However, whether resveratrol can specifically suppress TME-induced CRC invasion via β 1-integrin receptors has not been fully elucidated yet.

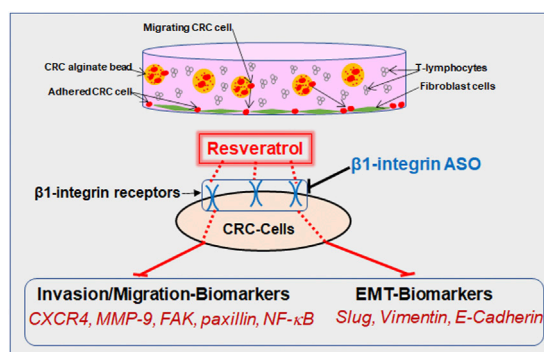
Methods: Two CRC cell lines (HCT116, RKO) were cultured in multicellular, pro-inflammatory 3D-alginate TME cultures (containing fibroblasts, T-lymphocytes) to investigate the role of β 1-integrin receptors in the anti-invasive and anti-metastatic effect of resveratrol by antisense oligonucleotides (ASO).

Results: Our results show that resveratrol dose-dependently suppressed the migration-promoting adhesion adapter protein paxillin and simultaneously enhanced the expression of E-cadherin associated with the phenotype change of CRC cells, and their invasion. Moreover, resveratrol blocked TME-induced phosphorylation and nuclear translocation of p65-NF- κ B, which was associated with changes in the expression pattern of epithelial-mesenchymal-transition-related biomarkers (slug, vimentin, E-cadherin), metastasis-related factors (CXCR4, MMP-9, FAK), and apoptosis (caspase-3). Finally, transient transfection of β 1-integrin, in contrast to knockdown of NF- κ B, abrogated most anti-invasive, anti-metastatic effects as well as downstream signaling of resveratrol, resulting in a concomitant increase in CRC cell invasion, indicating a central role of β 1-integrin receptors in the anti-invasive function of resveratrol.

Conclusion: These results demonstrate for the first time that silencing β 1-integrins may suppress, at least in part the inhibitory effects of resveratrol on invasion and migration of CRC cells, underscoring the crucial homeostatic role of β 1-integrin receptors.

KEYWORDS

β 1-integrin, CRC, inflammation, invasion, metastasis, NF- κ B, tumor microenvironment, resveratrol



GRAPHICAL ABSTRACT

Introduction

Cancer is one of the most commonly diagnosed diseases that causes many deaths among populations worldwide. According to global cancer statistics, there were over 19 million new cancer cases and 10 million cancer deaths globally in 2020 (Sung et al., 2021). Herein, colorectal cancer (CRC) represented 10% and the total number is expected to further increase within the next 20 years (Sung et al., 2021). In fact, CRC is the second leading cause of cancer deaths in the United States (Siegel et al., 2020). It is known that not only patients of advanced age are at risk, but also unhealthy lifestyle, sedentary behavior, excessive obesity or smoking play a decisive role in the development of cancer disease (Siegel et al., 2020). Moreover, despite the rising prevalence of screening and the growing number of colonoscopies (Siegel et al., 2020), more investment is needed to detect CRC at an early stage. Indeed, it has been reported that when a CRC is first diagnosed, up to 25% of patients already have been developing metastases, and as the disease progresses, as many as half of all affected individuals develop metastases (Vatandoust et al., 2015).

In that regard, metastatic tumors are cells that have spread outside of the colorectal tract *via* the blood or lymphatic system and are then located predominantly in the liver or lungs. The metastatic process, which is one of the six hallmarks of cancer, is usually a sign of a high-progressive disease and explains why patients die more often from secondary than from primary tumors (Koklesova et al., 2020). Furthermore, these lethal complications can also be triggered by metastases damaging affected organs, leading to dysfunction, organ failure, and ultimately to death in patients.

As inflammatory processes are one of the major underlying mechanisms of cancer diseases, colorectal tumors also contain

large numbers of cells that can trigger excessive immune responses and cytokine production, leading to increased activation of pro-inflammatory and oncogenic transcription factors such as nuclear factor kappa-light-chain-enhancer of activated B-cells (NF- κ B) (Rasool et al., 2021). In the advanced cascade of tumor invasion and metastasis, epithelial-mesenchymal transition (EMT) plays an essential role, which describes the process of cells changing their polarity from epithelial to mesenchymal characteristics, thus are able to migrate. While this transformation is a physiological process during the embryonic phase, it is considered highly pathological in the context of cancer development and migration (Koklesova et al., 2020). In addition, there are numerous signs of EMT, such as reduced E-cadherin expression acting as an epithelial marker with simultaneously increased vimentin expression as a mesenchymal marker (Koklesova et al., 2020). Moreover, it has been reported that the inflamed multicellular microenvironment of CRC significantly promotes expression of EMT proteins and transcription factors such as slug (Buhrmann et al., 2015). Indeed, this complex disease process requires therapy that attacks various levels in a multi-faceted manner, thus it is advisable to incorporate the power of nature-derived substances into treatment, such as the polyphenol and phytoalexin resveratrol. Resveratrol was found as a stilbenoid in several plants such as grapevines and peanuts, where it is synthesized in order to protect plants against pathogens (Fritzemeier et al., 1983; Hain et al., 1993).

Based on preclinical studies in CRC, resveratrol has already been shown promising effects in the subject of anti-inflammatory, anti-proliferative and anti-invasive properties in tumor cells (Brockmueller et al., 2022), and its clinical application

is currently under intense investigation (Brockmueller et al., 2021). Thus, previous studies by our group among others have shown that resveratrol is able to suppress the dangerous and tumor-promoting cross-talk between CRC cells and stromal cells in a pro-inflammatory tumor microenvironment (TME) *in vitro*. Furthermore, resveratrol, as a multi-target molecule has been reported to interfere and negatively affect NF- κ B signaling pathways, which is one of the major inflammatory transcription factors and markers promoted by the TME, that was shown to affect invasion behavior matrix metalloproteinase 9 (MMP-9) and metastasis process chemokine receptor type 4 (CXCR4) in CRC cells (Bergman et al., 2013; Buhrmann et al., 2016; Suh et al., 2018; Buhrmann et al., 2020).

Moreover, the prevention of EMT mechanisms in tumor cells is one of the most important goals in cancer research and therapy and has been increasingly attributed to be of fundamental importance. In this context, resveratrol has been frequently reported to possess potent and targeted subcellular modulatory effects on EMT, particularly the inhibition of EMT-promoting proteins (vimentin, slug) and simultaneous promotion of the epithelial protein, E-cadherin (Buhrmann et al., 2015), thus showing an inhibitory effect on the highly metastatic tumors.

Resveratrol has also been announced to make use of integrins as both, surface receptors and signaling molecules, for exerting its anti-tumor effects (Lin et al., 2006; Belleri et al., 2008; Varoni et al., 2016). Integrin families are heterodimeric cell adhesion and signaling molecules that play a central role as signal transducers in the interaction between cells and extracellular matrix (Shakibaei et al., 1997; Shakibaei, 1998; Shakibaei and Merker, 1999; Mueller et al., 2022), thus display a crucial role in the differentiation and function of cells in healthy tissues (Carter et al., 1990; Chen, 1990; Shakibaei, 1995). Moreover, these specific compounds are remarkably up-regulated in cancer cells, what is associated with increased risk for tumor migration and metastasis (Huang et al., 2021). Researchers aim to take advantage of this property and thus are investigating the chance of using integrins as tumor markers (Jones et al., 1992). Specifically for colorectal carcinoma, α 1-integrin has already been shown to be associated with increased tumorigenesis, CRC cell migration and invasion (Li et al., 2020), and β 6-integrin provided even more accurate prognosis than the already established tumor marker carcinoembryonic antigen (CEA) for tumor surveillance of patients with advanced CRC stage (Bengs et al., 2019). Furthermore, there are indications that inhibition of α v β 6-integrin could reduce the risk of liver metastasis in diabetic CRC patients (Wang et al., 2021) and that resveratrol-binding α v β 3-integrin inhibits tumor growth and metastasis as promising target for cancer therapy (Cheng et al., 2021; Chen et al., 2022). Moreover, down-regulation of focal adhesion kinase (FAK), a specific subcellular target protein of integrins (Lipfert et al., 1992) that is also of great importance in cell migration and invasion (Buhrmann et al., 2017), represents

an important mechanism here (Cheng et al., 2021) and resveratrol modulates FAK phosphorylation (Buhrmann et al., 2017).

Recently, we have demonstrated that resveratrol shows one of its important anti-proliferative and -viable properties *via* modulation of the β 1-integrin pathway by rearrangement of β 1-integrin receptors to use them for signal transduction as well as for exertion of resveratrol's proliferation- and viability-inhibitory capabilities (Brockmueller et al., 2022) in CRC cells.

In the present work, we address the question of whether and how resveratrol can affect the invasion and metastasis potential and thus the EMT of CRC cells *via* β 1-integrin axis. Within this study, implications of β 1-integrin-SO/ASO (β 1-SO/ASO) and NF- κ B-SO/ASO in HCT116 and RKO CRC cells were compared in a multicellular, pro-inflammatory TME *in vitro*. This 3D-tumor cultures, composed of cancer cells, T-lymphocytes and fibroblasts have been established throughout our previous studies (Buhrmann et al., 2020; Brockmueller et al., 2021) as well as in other research groups (Gao et al., 2021).

Material and methods

Antibodies and reagents

Monoclonal antibodies to NF- κ B (#MAB5078), and phospho-specific p65-NF- κ B (#MAB7226), MMP-9 (#MAB911), polyclonal caspase-3 (#AF835) were purchased from R&D Systems (Heidelberg, Germany). Monoclonal antibodies to anti-FAK (#610088), anti-phospho-FAK (#558540) were from Becton Dickinson (Heidelberg, Germany). Monoclonal antibodies to β -actin (#A4700), resveratrol, alginate, DAPI, Fluoromount were from Sigma-Aldrich (Taufkirchen, Germany). Monoclonal anti-E-cadherin (#sc-21791), anti-vimentin (#sc-53464), anti-slug (#sc-166476), anti-paxillin (#sc-365059) normal mouse IgG (#sc-2025) were from Santa Cruz Biotechnology (Dallas, Texas, United States). Monoclonal anti- β 1-integrin (#14-0299-82) and anti-CXCR4 (#35-8800) were from Thermo Fisher Scientific (Langensfeld, Germany). Secondary rhodamine-coupled antibodies for immunofluorescence were from Dianova (Hamburg, Germany), and alkaline phosphatase-linked antibodies for Western blotting were from EMD Millipore (Schwalbach, Germany). Resveratrol was prepared in 100 mM stocks with ethanol and directly diluted in the cell culture medium for CRC cell treatment, without exceeding an ethanol concentration of 0.1% during the investigations.

Cells and preparation

For the presented studies, two different human CRC cell lines [HCT116 from European Collection of Cell Cultures (Salisbury, United Kingdom) and RKO from American Type Culture Collection (Manassas, Virginia, United States)], human

T-lymphocytes [Jurkat from DSMZ-German Collection of Microorganisms and Cell Cultures (Braunschweig, Germany)] and human fibroblasts [MRC-5 from European Collection of Cell Cultures (Salisbury, United Kingdom)] were used. The cell culture setting and preparation corresponds to the one already described earlier (Buhrmann et al., 2020; Brockmueller et al., 2022). 3% fetal bovine serum (FBS) or 10% FBS, 1% glutamine, 1% penicillin/streptomycin solution (10.000 IU/10.000 IU), 75 µg/ml ascorbic acid, 1% essential amino acids and 0.5% amphotericin B solution were added to Dulbecco's modified Eagle's medium/F-12 from Sigma-Aldrich (Taufkirchen, Germany) and used as cell culture medium.

Transfection

To study the effects of transfection, 0.5 µM antisense oligonucleotides (ASO) or control sense oligonucleotides (SO) was incubated in Lipofectin transfection reagent (Invitrogen, Karlsruhe, Germany) and added into the experimental well-plate. Oligonucleotides from Eurofins MWG Operon (Ebersberg, Germany) were modified with phosphonothioate to preserve the oligonucleotides from cell nucleases, the exact procedure has already been described (Buhrmann et al., 2016; Buhrmann et al., 2020), and used for transient transfection with antisense/sense oligonucleotides (ASO/SO) based on β1-integrin or p65-NF-κB:

- a) β1-integrin-ASO (5'-TAGTTGGGGTTGCACTCACAC A-3'),
- b) β1-integrin-SO (5'-TGTGTGAGTGCAACCCCACTA-3'),
- c) NF-κB/p65-subunit-ASO (5'-gGAGATGCGCACTGTCCC TGGTC-3'),
- d) NF-κB/p65-subunit-SO (5'-gACCAGGGACAGTGC GCA TCTC-3').

3D-alginate tumor culture *in vitro*

In the current investigations, the *in vivo* condition of a cancerous patient was simulated by a 3D-alginate culture model *in vitro*. This enables an animal-free investigation of resveratrol's anti-tumor effect in a pro-inflammatory tumor microenvironment. The present study focuses on the exploration of resveratrol's β1-integrin-mediated effects on the migration and invasion of CRC cells using β1-integrin-ASO/SO as well as NF-κB-ASO/SO for comparison.

The experiments were carried out with CRC-alginate balls comprising an average size of 4 mm which were produced as described in numerous publications of our research group (Buhrmann et al., 2020; Brockmueller et al., 2022). Then they were assembled in a composition of MRC-5 fibroblasts as monolayer on the bottom of 12-well-plates, and Jurkat

T-lymphocytes floating in the cell culture medium, which has been established as a suitable TME simulation for other cancer cells as well (Gao et al., 2021). In the present work, the alginate balls were made from HCT116 or RKO cells in 12-well-plates and the alginate coating ensures that the CRC cells do not mix with the other cell types during the experiments. A control without TME (Ba. Co.) and a TME control (TME Co.) without treatment additives were established. The treated cells received resveratrol (1, 5 µM), β1-integrin-ASO/SO (0.5 µM), NF-κB-ASO/SO (0.5 µM) or a combination thereof as supplements to 3% FBS (serum-starved) cell culture medium with a running time of 10–14 days for all samples.

Three invasion attempts

To observe the invasion and to draw conclusions about CRC's metastatic properties, HCT116 and RKO were treated as explained before (Ba. Co., TME Co., resveratrol, β1-integrin-SO/ASO, NF-κB-SO/ASO) for 10–14 days and evaluated using three different invasion assays:

- A) Firstly, the bottom of 12-well-plates was photographed in phase contrast with a Zeiss Axiovert 40 CFL microscope (Oberkochen, Germany) in order to compare the CRC cell colonies that had settled. To determine the average size of settled colonies, 25 colonies of each treatment were measured.
- B) Secondly, the 12-well-plates were fixated with Karnovsky solution for 30 min, stained with toluidine blue. To determine the average colony, count of stained colonies, labelled as invasion, colonies were counted from three wells at each treatment.
- C) Thirdly, the experiment was set up with identical treatments in 6-well-plates. As a special feature, a square cover glass was placed in each well on which the migrating CRC cell colonies settled. The glass slides were fixated with methanol for 30 min, then rinsed with Hank's solution (3 times), incubated for 15 min in the dark with DAPI and covered in Fluoromount for photographic analysis using a Leica DM 2000 microscope (Wetzlar, Germany).

Immunofluorescence investigation

Leica (Wetzlar, Germany) DM 2000 microscope with LAS V4.12 software was used for the generation of immunofluorescence images. For preparation, 6000 CRC cells (HCT116 or RKO) were sown on a small round glass plate. After 24 h, the TME was recreated in a modified manner by placing the small glass plates on a meshed bridge in a 6-well-plate containing fibroblasts as monolayer, floating T-lymphocytes and reagents according to the treatment pattern described above. After 1 day,

the glass slides were removed from well-plates and washed with Hank's salt solution three times, ensuring that only CRC cells were left for immunolabelling. Then, CRC-glass plates were fixated in methanol for 30 min and prepared for immunofluorescence microscopy as described in detail before (Brockmueller et al., 2022; Mueller et al., 2022). In the present work, CRC cells were immunolabeled with E-cadherin-, NF- κ B-paxillin- or slug-antibodies. The primary antibody dilution was 1:80 and the secondary antibody dilution was 1:100 each. To reveal the cell nuclei, each slide was stained with DAPI for 15 min and then fixated with Fluoromount.

Immunoblotting

For Western blot analysis, HCT116 or RKO 3D-alginate balls were treated with the aforementioned substances. After 10–14 days, the alginate balls were removed from 12-well-plates with bent tweezers, transferred to 12-well-plates containing Hank's salt solution, and washed on a gentle waving shaker. This procedure was repeated at least three times, ensuring that no T-lymphocytes adhered to the CRC-alginate balls which was verified by observation with a phase contrast microscope. Then, the clean CRC-alginate balls were dissolved in sodium citrate (55 mM) for 30 min to isolate CRC cells which were resuspended in lysis buffer as described before (Brockmueller et al., 2022). After 30 min of centrifugation, the liquid supernatant was kept frozen (-80°C) and samples were further processed with a Bio-Rad (Munich, Germany) transblot apparatus for densitometric evaluation with Bio-Rad Quantity One analysis software as explained in detail in our earlier work (Brockmueller et al., 2022; Mueller et al., 2022). In the current study, the beforementioned antibodies were used in 1:10.000 dilution and β -actin served as loading control.

Statistical analysis

We performed all assays as three independent repetitions and used an unpaired student's t-test for statistical analysis. Results matched by one-way ANOVA followed by post hoc test to compare parameters within the groups. At the outcomes, a *p*-value less than 0.05 was considered as statistically significant.

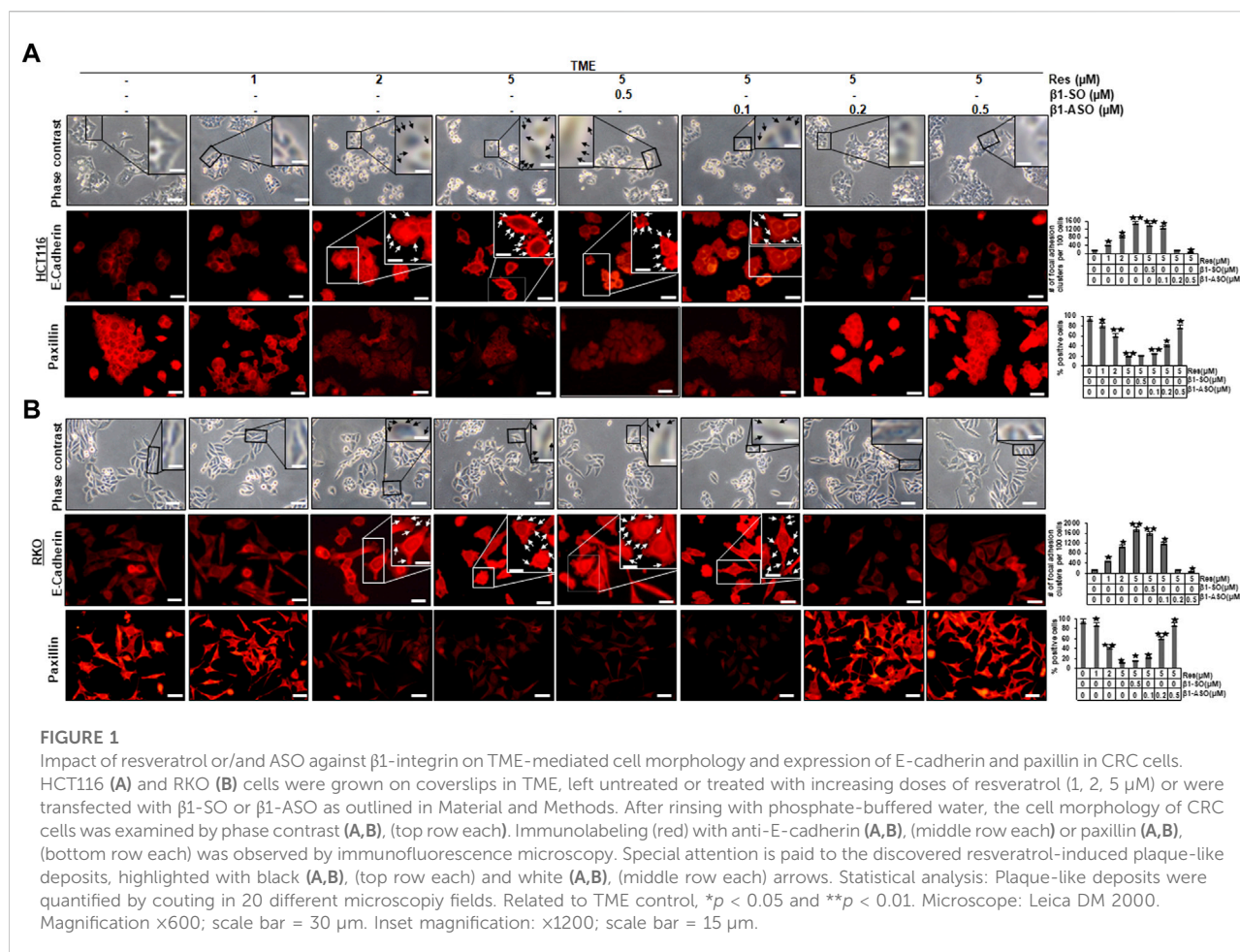
Results

The aim of our study was to determine the role of β 1-integrin receptors in the anti-invasive, anti-metastatic and anti-inflammatory effects of resveratrol in two CRC cell lines (HCT116, RKO) in a pro-inflammatory, multicellular, *in vivo*-like tumor microenvironment *in vitro* by β 1-integrin

knockdown and NF- κ B knockdown via antisense oligonucleotides (ASO).

Resveratrol targets the β 1-integrin receptors to promote TME-down-regulated E-cadherin expression and suppress up-regulated paxillin expression in CRC cells

Investigations on CRC primary tumors showed that they were prone to have a dedifferentiated, mesenchymal phenotype, a noticeably reduced E-cadherin expression, an increased paxillin expression, and a high tendency to metastasize (Kaiharu et al., 2003; Buhrmann et al., 2015; Wen et al., 2020). Therefore, we examined HCT116 and RKO cells, grown on glass slides, in more detail using the phase contrast microscope, and observed that the HCT116 and RKO control cultures exhibited evenly distributed cell colonies with a slightly epithelial morphology, smooth surface, and close cell to cell contacts (Figures 1A,B), similar to treatment with only β 1-integrin-SO or -ASO (β 1-SO or -ASO). In contrast, the RKO control cells showed a more fibroblast-like to mesenchymal morphology, less colony formation, and fewer cell to cell contacts. Interestingly, treatment of both CRC cells with resveratrol resulted in 1) increased cell to cell contact (epithelial shape) and a rounder shape of CRC cells though and 2) the development of small conspicuous plaque-like deposits of the cell membrane on HCT116 (Figure 1A, top row, black arrows) and RKO cells (Figure 1B, top row, black arrows) in a dose-dependent (1, 2, 5 μM resveratrol) manner, similar to the combined treatment with resveratrol (5 μM) and/or β 1-SO (0.5 μM). Even more interestingly, treatment with resveratrol and β 1-ASO significantly decreased or resolved the development of small conspicuous plaque-like deposits of the cell membrane on HCT116 (Figure 1A, top row) and RKO cells (Figure 1B, top row) in a dose-dependent (0.1, 0.2, 0.5 μM β 1-ASO) manner in both cell lines. Together, these findings indicate that the detected resveratrol-induced plaque formation in CRC cells by targeting β 1-integrin receptors was related to an increased E-cadherin expression, leading to a more stable local adhesion and therefore rather epithelial shape. We wondered whether this resveratrol-induced plasma membrane plaques contain the biomarker for epithelial phenotype, E-cadherin, and therefore examined its expression by immunofluorescence analysis (Figures 1A,B; middle row each). The untreated CRC cells in TME showed minimal E-cadherin expression on the surface, similar to treatment with β 1-SO (0.5 μM) or β 1-ASO (0.5 μM) alone. On the other hand, the expression of E-cadherin on the surface of CRC cells treated with resveratrol (1, 2, 5 μM) alone showed a significant increase in E-cadherin expression in a concentration-dependent manner, which was regulated similar

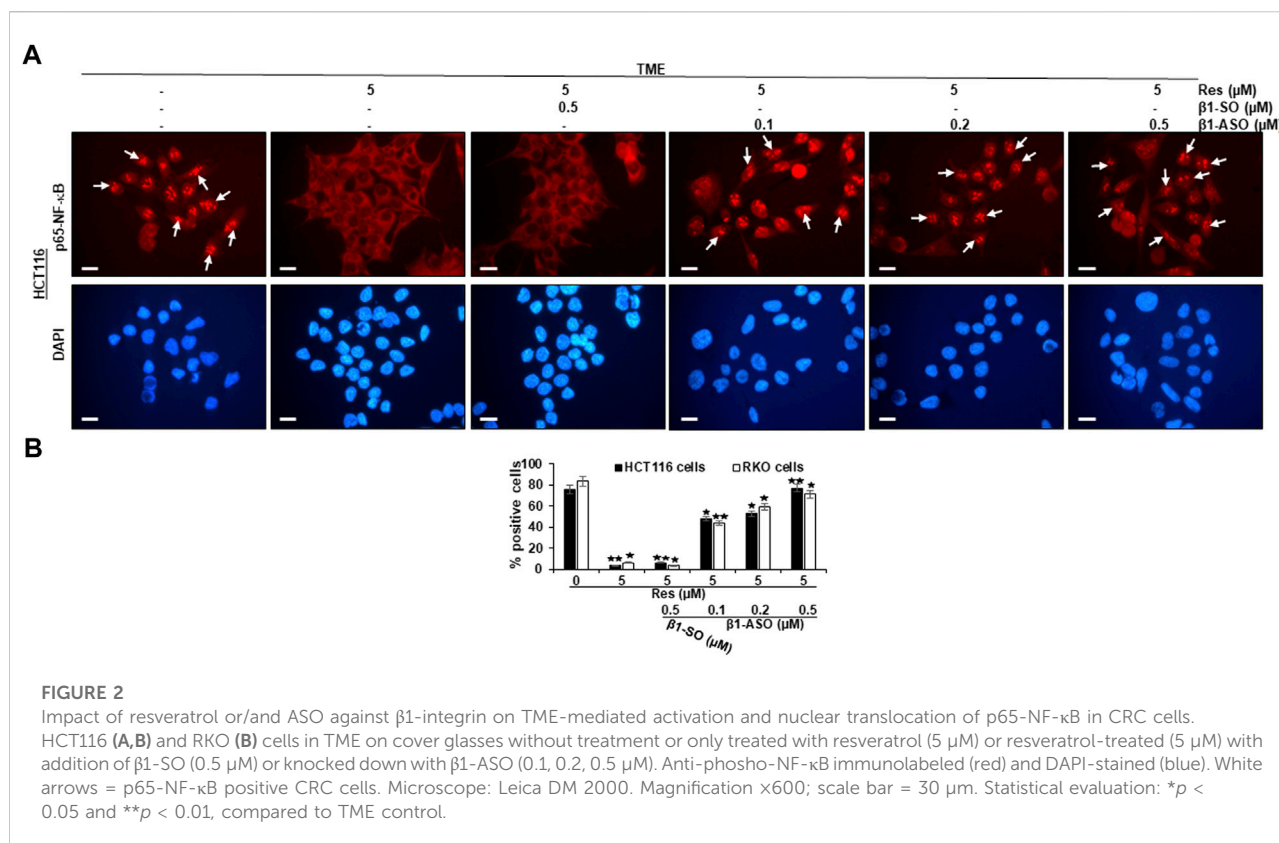


to cells treated with $\beta 1$ -SO and resveratrol in combination (Figures 1A,B; middle row each, white arrows). In contrast, knockdown of $\beta 1$ -integrin with $\beta 1$ -ASO in a concentration-dependent (0.1, 0.2, 0.5 μM) manner abolished the blocking effect of resveratrol on the expression of the above-mentioned epithelial biomarkers. To further investigate the impact of the $\beta 1$ -integrin-mediated effect of resveratrol on EMT processes in CRC cells, we also immunolabelled HCT116 as well as RKO cells with an antibody against the cell migration marker paxillin (Figures 1A,B; bottom row each). Confirming previous results, both CRC cell lines showed high paxillin expression in the untreated TME control, which decreased significantly with increasing resveratrol (1, 2, 5 μM) concentration. The largely suppressed expression of paxillin by resveratrol (5 μM) in CRC cells remained low even with combined treatment of the CRC cells with 0.5 μM $\beta 1$ -SO. However when $\beta 1$ -ASO (0.1, 0.2, 0.5 μM) was added to resveratrol-treated HCT116 or RKO cells, paxillin expression became increasingly intense. In summary, these results indicate a strong migration inhibitory effect of resveratrol on CRC cells (Figures 1A,B) and the important role of $\beta 1$ -integrin receptors in resveratrol-

enhancing anti-tumor effect on CRC cells in TME, whereby these effects were not cell line specific.

Resveratrol targets $\beta 1$ -integrin receptors and suppresses TME-up-regulated phosphorylation and nuclear NF- κB translocation in CRC cells

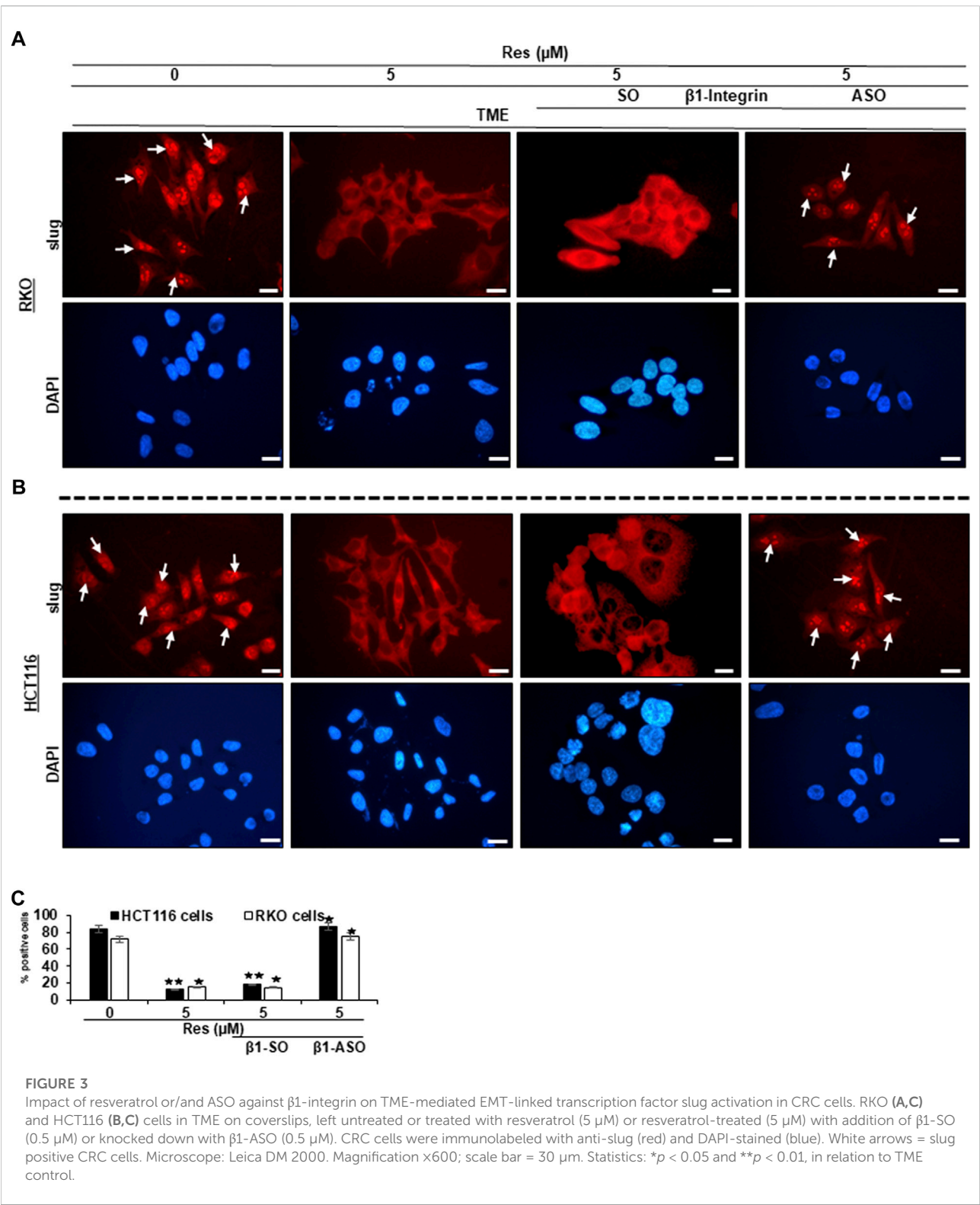
As resveratrol is known to be a compound that inhibits inflammation in CRC cells (Buhrmann et al., 2016), we wanted to examine its influence on NF- κB activation and furthermore the role of $\beta 1$ -integrin receptors in this context. For this purpose, CRC cells (HCT116, RKO) were cultured on round glass coverslips and examined by immunofluorescence microscopy as described in the Material and Methods section. Here, HCT116 cells in untreated TME (TME control) showed a distinct, luminescent immunolabeling (Figure 2A, exemplary marked with white arrows) as a sign of high, inflammation-induced NF- κB phosphorylation and nuclear translocation in the majority of CRC cells (Figures



2A,B) and confirmatory, this expression was similar to TME-HCT116 cells treated with $\beta 1$ -SO (0.5 μ M) or $\beta 1$ -ASO (0.5 μ M) alone. Moreover, treatment with resveratrol (5 μ M) led to impressive changes in TME grown CRC cells with a significant down-regulation of NF- κ B phosphorylation and nuclear translocation compared to the TME control, resulting in barely labeled, pale cell nuclei (Figure 2A). This effect remained the same with $\beta 1$ -SO (0.5 μ M) addition to resveratrol-treated HCT116 cells in TME, validating $\beta 1$ -SO as suitable control substance (Figures 2A,B). However, when $\beta 1$ -ASO (0.1, 0.2, 0.5 μ M) was added to resveratrol-treated TME cultures for the purpose of $\beta 1$ -integrin knockdown, a concentration-dependent increase of phosphorylation and nuclear translocation of NF- κ B was found in CRC cell nuclei, due to the gradual removal of resveratrol's effect (Figures 2A,B). Interestingly, the statistical analysis of RKO CRC cells undergoing same treatments (Figure 2B) confirmed our observations made on HCT116 (Figures 2A,B), leading to the assumption that these are transferable to other CRC cell lines, whereas DAPI staining verified the vitality of the photographed CRC cells by blue DNA labeling. Altogether, these results demonstrate a strong, non-cell line specific anti-inflammatory effect of resveratrol and furthermore suggest a significant limitation of resveratrol's anti-inflammatory impact by $\beta 1$ -integrin knockdown.

Resveratrol targets $\beta 1$ -integrin receptors and suppresses TME-induced activation of EMT-related transcription factor (slug) in CRC cells

Since we have already found out that a pro-inflammatory, multicellular TME promotes EMT and resveratrol is able to intervene this conversion (Buhmann et al., 2015), we were then interested in the extend of major EMT transcription factor slug expression, the influence of resveratrol and especially the role of $\beta 1$ -integrin receptors in this process. In Figure 3, RKO (Figure 3A) and HCT116 are shown (Figure 3B), which were grown on small cover glasses in TME, subsequently immune-marked with anti-slug antibody and analyzed by immunofluorescence microscopy as described in the Material and Methods section. We observed same significant expression tendencies in both cell lines, RKO and HCT116: In the TME (TME control), the majority of CRC cells showed cell nuclei with bright, slug-positive labeling, exemplary highlighted with white arrows (Figures 3A,B), whereas $\beta 1$ -SO (0.5 μ M) or $\beta 1$ -ASO (0.5 μ M) addition had no visible influence. However, resveratrol-treatment (5 μ M), remarkably suppressed slug expression in the TME compared to TME control, leading to pale labelled inconspicuous cell nuclei. Interestingly, addition of 5 μ M resveratrol to $\beta 1$ -SO (0.5 μ M) treated CRC cells did not change this expression pattern, leading to confirmation of $\beta 1$ -SO as suitable



control substance (Figures 3A,B). In contrast, in the combined treatment consisting of 5 μ M resveratrol and 0.5 μ M β 1-ASO, there were almost as many slug-positive labeled CRC cells found as in the TME control (Figures 3A,B), underscoring that resveratrol was not able to fully exert its EMT-inhibitory effect when β 1-integrin was knocked down. The direct statistical comparison of RKO and

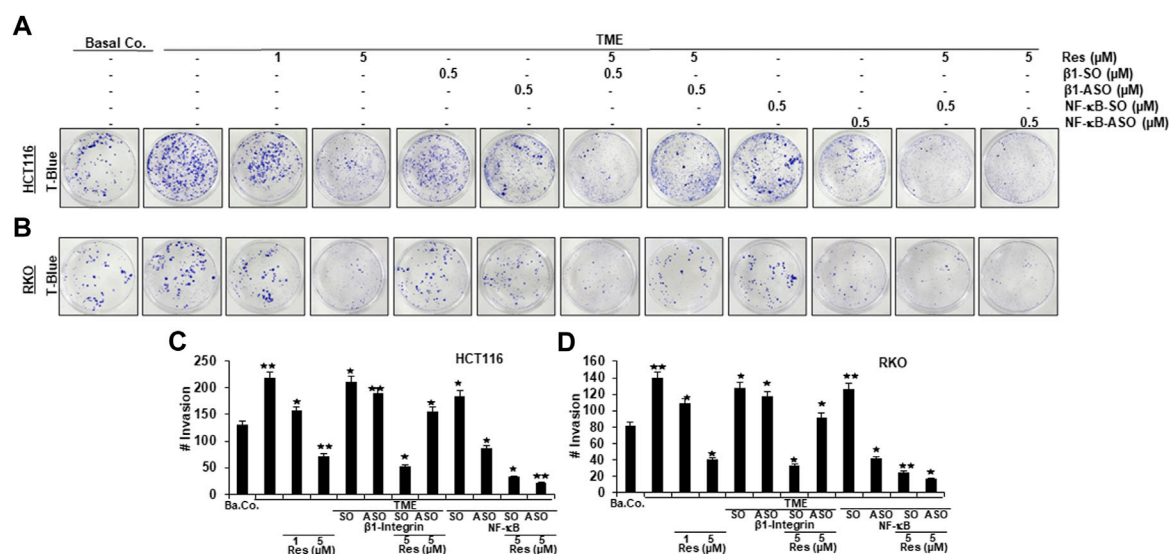


FIGURE 4

Impact of resveratrol or/and ASO against $\beta 1$ -integrin or against NF- κ B on TME-promoted CRC cell invasion in alginate cultures. Serum-starved HCT116 (A) and RKO (B) cells, cultured in 3D-alginate, emigrated under following treatments: untreated (Basal Co.), TME control, resveratrol (1, 5 μ M), $\beta 1$ -SO/ASO (0.5 μ M), NF- κ B-SO/ASO (0.5 μ M) or co-treatment of sense or antisense oligonucleotides with resveratrol (5 μ M). CRC cells were stained with toluidine blue (T-Blue) after settling on the bottom of 12-well-plates. Statistical evaluation: Compared to TME control, * $p < 0.05$ and ** $p < 0.01$ for HCT116 (C) and RKO (D).

HCT116 (Figure 3C) proved the described non-cell line specific effects. To ensure the viability of evaluated CRC cells, supplementary DAPI staining (blue) was performed (Figures 3A,B). In summary, these results highlight the significant EMT-inhibitory and reproducible effect of resveratrol in the two CRC cell lines RKO and HCT116, and point out the major role of $\beta 1$ -integrin receptors in mediating these effects.

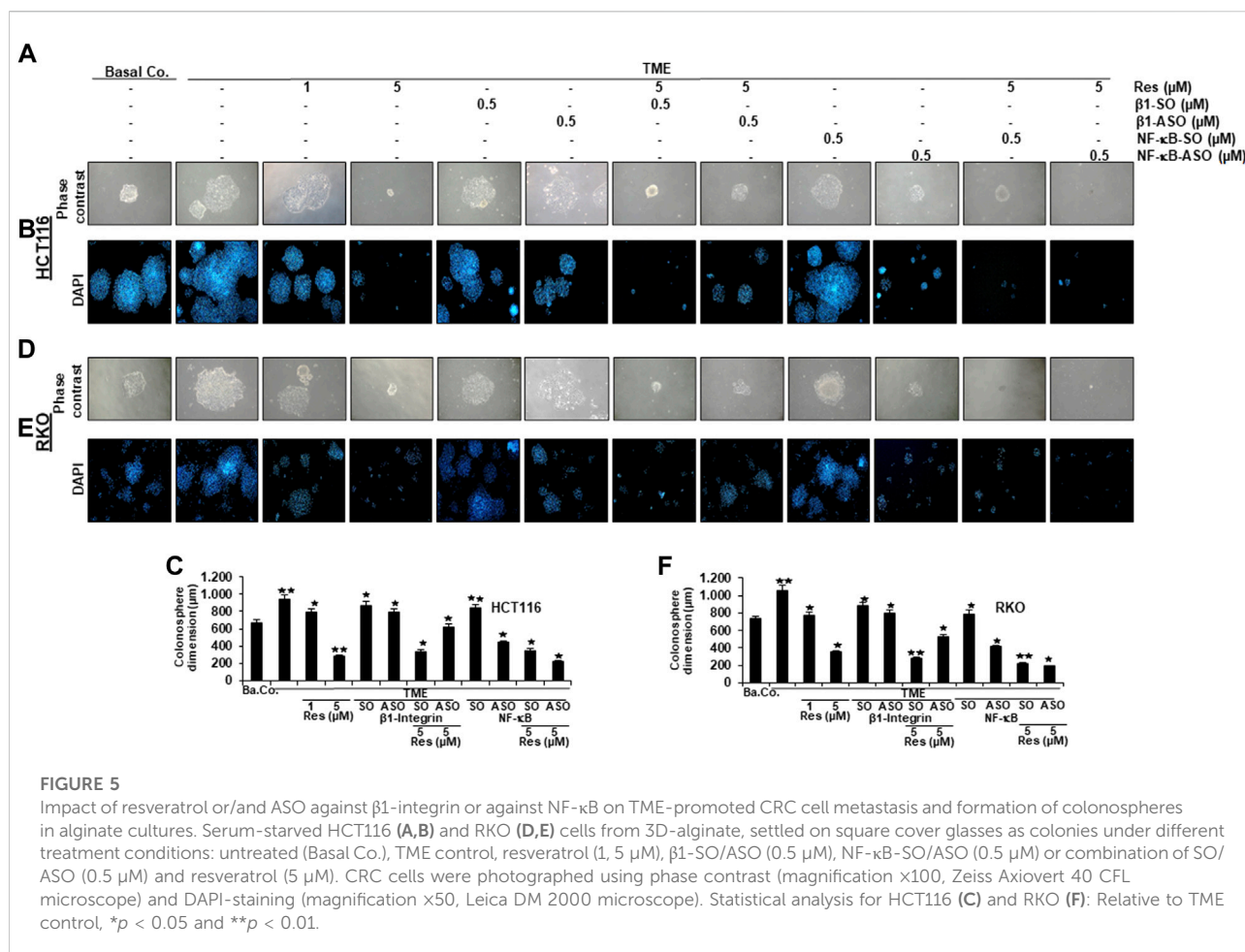
Resveratrol-promoted repression of TME-induced migration and invasion, similarly to knockdown of NF- κ B, is blocked by knockdown of $\beta 1$ -integrin in CRC cells

In order to further investigate the role of $\beta 1$ -integrin receptors in mediating the anti-metastatic and anti-invasive effects of resveratrol, we carried out three invasion assays of HCT116 (Figures 4A,C, Figures 5A–C) and RKO (Figures 4B,D, Figures 5D–F) as described in the Material and Methods section. For this purpose, $\beta 1$ -integrin was knocked down *via* $\beta 1$ -ASO and because of its important role in inflammation and tumor progression (Rasool et al., 2021), NF- κ B was knocked down as well using NF- κ B-ASO.

The focus of our invasion assays was the observation of spheres of CRC cells that have been migrated from 3D-alginate beads, which represent an *in vivo*-like simulation of metastasis and invasion in an *in vitro* culture model. The emigrated CRC-colonies that had attached to the bottom of well-plates were stained with toluidine

blue (Figure 4), whereas colonies that had settled on square cover glasses were analyzed by phase contrast (Figures 5A,D) or additionally stained with the before mentioned DAPI-method (Figures 5B,E), in order to demonstrate the vitality of CRC cells. Cross-methodology, based on invasion assays and statistical analysis, showed that the pro-inflammatory, multicellular TME increased both, the number of invaded colonies and the average diameter of colonies compared to the baseline control (Ba.Co.) without fibroblasts and T-lymphocytes (Figures 4A,B Figures 5A,B,D,E). The administration of $\beta 1$ -SO (0.5 μ M) or $\beta 1$ -ASO (0.5 μ M) alone had no significant modifying effects on the CRC-colonies in TME. Apart from that, a concentration-dependent reduction of invaded colonies and colony size by resveratrol (1, 5 μ M) treatment in the TME was clearly visible, and could also be observed in concomitant treatment of resveratrol (5 μ M) together with $\beta 1$ -SO (0.5 μ M), validating $\beta 1$ -SO as an appropriate control agent. However, the knockdown of $\beta 1$ -integrin *via* $\beta 1$ -ASO strongly reduced the inhibitory effect of resveratrol, barely affecting colony size and number of migrated CRC cells. Even TME-treatment using a lower concentration of resveratrol (1 μ M) and without $\beta 1$ -integrin knockdown, did show greater effects (Figures 4A,B, Figures 5A,B,D,E).

Simultaneously, resveratrol (5 μ M), comparable to the knockdown of NF- κ B (0.5 μ M NF- κ B-ASO), significantly reduced the number of CRC cell migration and their average size, highlighting resveratrol's anti-invasive effect and its ability to even intensify the inhibitory effect of NF- κ B-ASO (0.5 μ M). Moreover, it was found



that there was no significant difference between co-treatment of resveratrol (5 μ M) and NF- κ B-SO (0.5 μ M) or resveratrol (5 μ M) alone on reduced inhibition of migration and invasion and their size on CRC cells (Figures 4A,B, Figures 5A,B,D,E). These findings were further supported by the quantification of colonosphere formation, migrated CRC cells and their size. All of the described results were reproducible in both cell lines, HCT116 and RKO, indicating a non-cell line specific effect. Altogether, these findings further support the idea that resveratrol uses $\beta 1$ -integrin receptors to repress the pro-inflammatory TME-induced migration, invasion and signaling pathway of CRC cells.

Resveratrol targets $\beta 1$ -integrin receptors to block TME-induced expression of metastasis-related factors and p65-NF- κ B phosphorylation in CRC cells

To screen changes in protein expressions and associated modulation of various signaling pathways, we carried out extensive Western blot analyses. Samples were obtained from

CRC cells (HCT116 or RKO) grown as alginate bead cultures and treated as described in Material and Methods for 10–14 days.

At first, we found that the metastasis parameters CXCR4 and phosphorylated FAK as well as inflammation parameter phosphorylated NF- κ B were highly expressed in HCT116 or RKO cells grown in TME without any treatment. Interestingly, compared to TME control, same biomarkers were significantly down-regulated by resveratrol (5 μ M) in TME-cultures, similar to $\beta 1$ -SO-cultures (0.5 μ M) co-treated with 5 μ M resveratrol, (Figure 6). Contrarily, in CRC cultures with $\beta 1$ -integrin knockdown (0.5 μ M $\beta 1$ -ASO), no suppression of CXCR4, phosphorylated FAK and phosphorylated NF- κ B could be observed by resveratrol co-treatment (5 μ M) so that their expression pattern resembled the TME control (Figure 6). In addition, cultures solely treated with resveratrol (5 μ M) or with resveratrol (5 μ M) in combination with $\beta 1$ -SO (0.5 μ M) clearly showed increased apoptosis, manifested by a high caspase-3 level in the TME compared to a low apoptosis rate in the untreated TME control. In $\beta 1$ -integrin knockdown (0.5 μ M $\beta 1$ -ASO) cultures, however, resveratrol's anti-apoptotic effect could not be detected and a low apoptosis rate was observed again

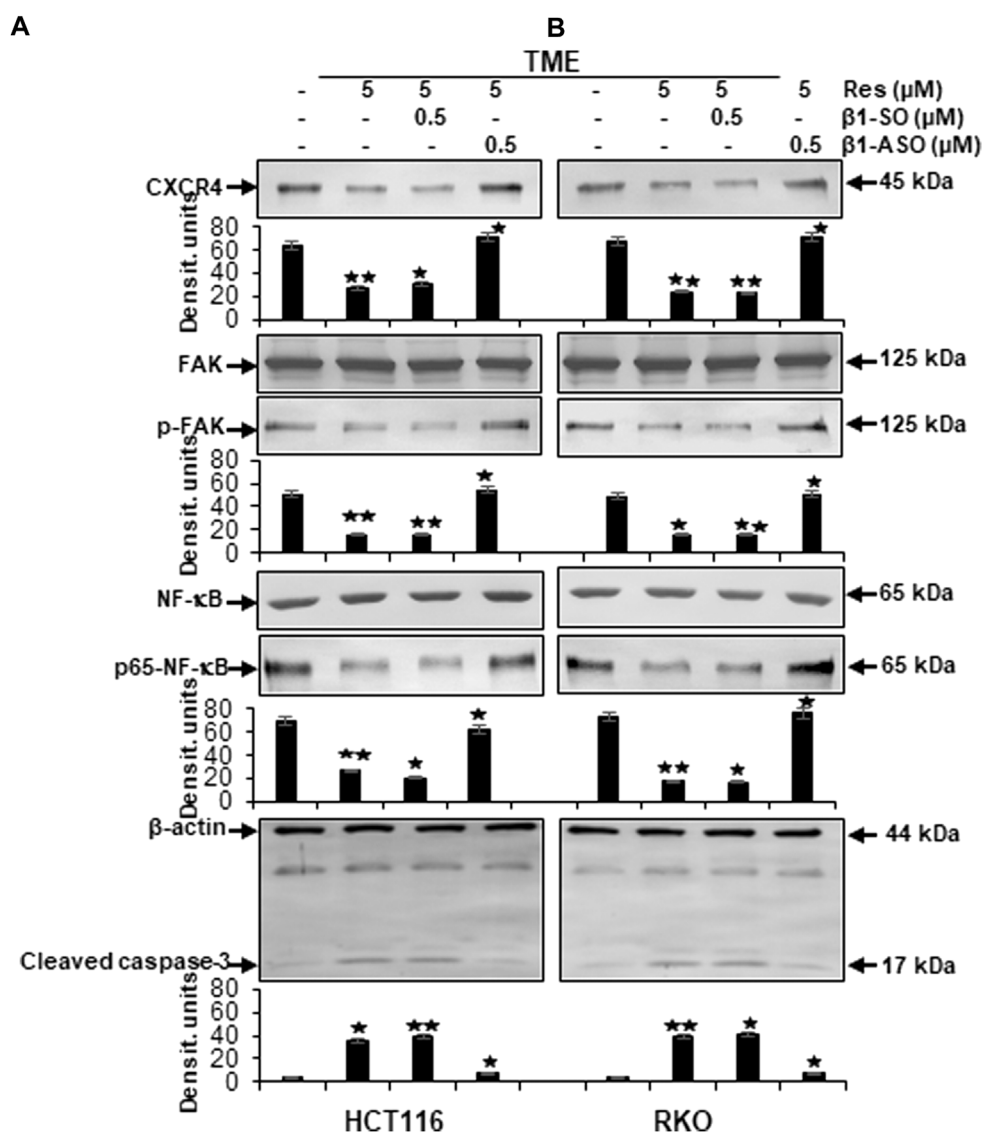


FIGURE 6

Impact of resveratrol or/and ASO against β 1-integrin on TME-promoted activation of metastasis and apoptosis parameters in CRC cells. HCT116 (A) and RKO (B) derived from 3D-alginate cultures were grown untreated or treated with 5 μ M resveratrol alone or in combination with 0.5 μ M β 1-SO or 0.5 μ M β 1-ASO (x-axis) and probed with antibodies against CXCR4, FAK, p-FAK, NF- κ B, p65-NF- κ B and cleaved caspase-3. Loading control: β -actin. Densitometric units complementing Western blot results (y-axis). For densitometric analysis, data were compared to TME control: * $p < 0.05$ and ** $p < 0.01$.

(Figure 6). Our results were supported by the consistent expression of non-phosphorylated FAK and NF- κ B in all of the treatments, serving as reference control, and consistent expression of β -actin serving as loading control (Figure 6).

Furthermore, to reassure the effectiveness of β 1-integrin knockdown (β 1-ASO) and control substance (β 1-SO), or NF- κ B knockdown (NF- κ B-ASO) and the control substance (NF- κ B-SO), we also performed immunoblots with anti- β 1-integrin or with anti-p65-NF- κ B that confirmed the chosen

dosages (0.5 μ M β 1- and NF- κ B-SO/ASO) in both cell lines (HCT116 and RKO), by demonstrating significant β 1-integrin or NF- κ B down-regulation of β 1-ASO or NF- κ B-ASO treated CRC cells, respectively, whereas β 1-integrin and NF- κ B were up-regulated in untreated TME or TME-CRC cells treated with β 1-SO or NF- κ B-SO (Figures 7A,B). These results, supporting our assumption that resveratrol uses β 1-integrin receptors and NF- κ B transcription factor to inhibit metastasis in CRC cells, encouraged us to further investigate the level of EMT-protein expression.

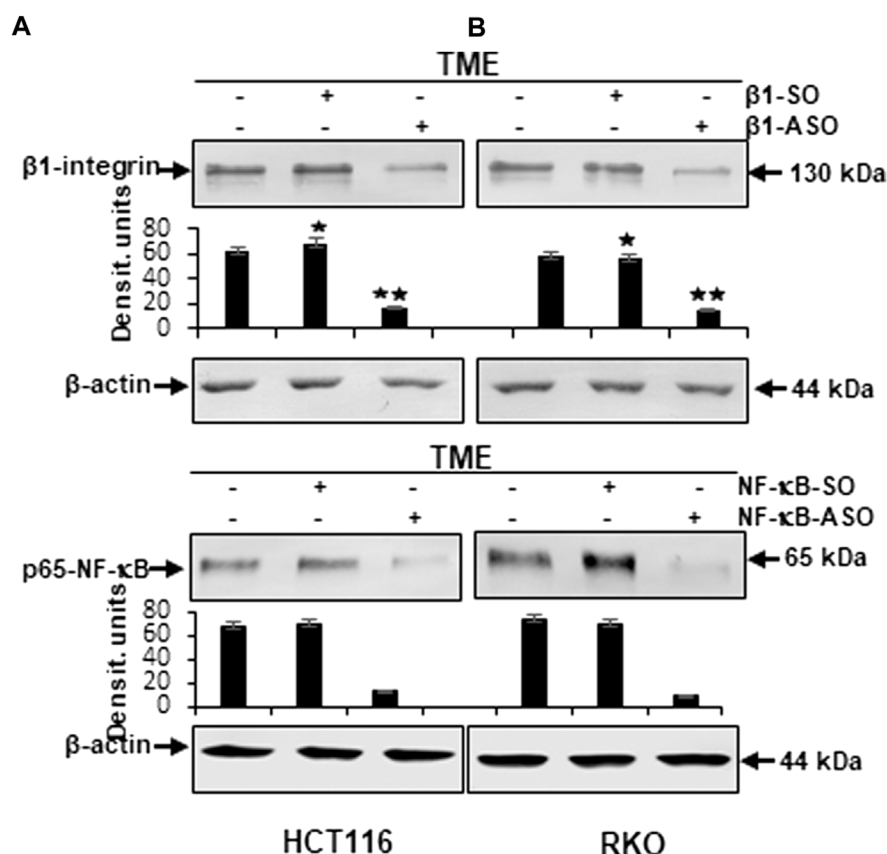


FIGURE 7

Western blot investigation on the efficacy of $\beta 1$ -integrin and NF- κ B knockdown by antisense oligonucleotides in CRC cells. X-axis: HCT116 (A) and RKO (B) samples from 3D-alginate TME were untreated or treated with $\beta 1$ -SO/NF- κ B-SO or $\beta 1$ -ASO/NF- κ B-ASO (0.5 μ M). Immunoblotting with anti- $\beta 1$ -integrin or with anti-p-65-NF- κ B and β -actin as a loading control. Y-axis: Densitometric units (y-axis) complementing Western blot results. Statistical analysis: * $p < 0.05$ and ** $p < 0.01$, comparison to TME control.

Resveratrol modulates TME-triggered inflammation, EMT, invasion, and TME-suppressed apoptosis and acts synergistically with NF- κ B-ASO in CRC cells but not by knockdown of $\beta 1$ -integrin in CRC cells

Whether and by which pathway resveratrol can modulate TME-induced EMT, invasion, migration as well as upregulation of NF- κ B, NF- κ B-dependent inflammation and apoptosis, was investigated by using HCT116 and RKO CRC cells. Analogous to previously explained invasion assays (Figure 4), cells were left untreated in alginate beads as a baseline control (Ba.Co.) or in TME (TME control) or treated with different concentrations of resveratrol (1, 5 μ M) or with NF- κ B-SO/-ASO (0.5 μ M) or with $\beta 1$ -SO/-ASO (0.5 μ M) or with a combination of resveratrol (5 μ M) and NF- κ B-SO/-ASO (0.5 μ M) or $\beta 1$ -SO/-ASO (0.5 μ M) for 10–14 days as described in Methods.

Resveratrol targets $\beta 1$ -integrin and blocks TME-induced expression of EMT-related biomarkers in the same way as NF- κ B-ASO in CRC cells

Initially, with Western blot studies of previously described cell samples we aimed to visualize EMT-reflective parameters (E-cadherin, vimentin, slug) to further elucidate the importance of resveratrol as well as its effect *via* $\beta 1$ -integrin receptors and the NF- κ B signaling pathway.

The expression of E-cadherin, representing epithelial phenotype, was low in untreated baseline control (Ba.Co.) and untreated TME control as well as in TME culture treated with $\beta 1$ -SO (0.5 μ M) or $\beta 1$ -ASO (0.5 μ M) alone (Figures 8A,B). However, resveratrol when added developed a concentration-dependent (1, 5 μ M), strong enhancing effect of E-cadherin expression in both, RKO (Figure 8A) and HCT116 (Figure 8B) cells, compared to cells of the TME control. As this increase was also distinct with

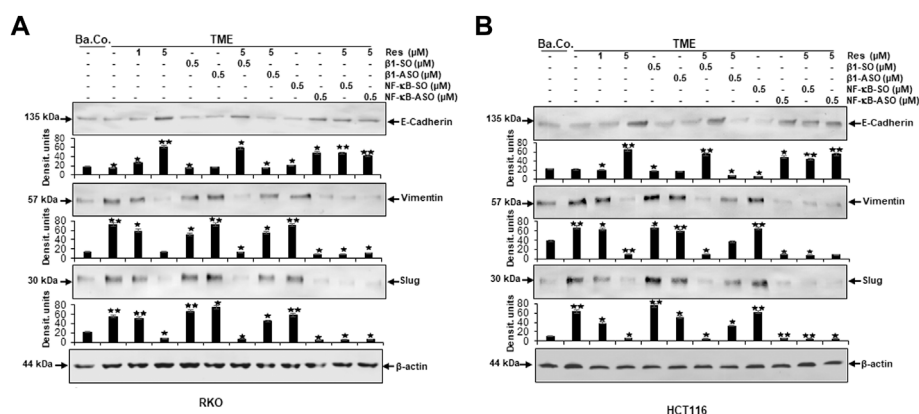


FIGURE 8

Impact of resveratrol or/and ASO against β 1-integrin or against NF- κ B on TME-promoted activation of EMT-linked biomarkers in CRC cells. 3D-alginate RKO (A) and HCT116 (B) CRC cells were detected against E-cadherin, vimentin, slug and loading controlled with β -actin after 10–14 days of treatment. X-axis: untreated (Ba.Co.), TME control, resveratrol (1, 5 μ M), β 1-SO/ASO (0.5 μ M), NF- κ B-SO/ASO (0.5 μ M) or combination of 0.5 μ M SO/ASO and resveratrol (5 μ M). Y-axis: Densitometric units (y-axis) complementing Western blot results and for analysis, data were compared to TME control: * p < 0.05 and ** p < 0.01 were considered statistically significant.

combined administration of resveratrol (5 μ M) and β 1-SO (0.5 μ M) to the TME, β 1-SO proved to be a reliable control reagent. When TME was treated with resveratrol (5 μ M) and β 1-ASO (0.5 μ M), though, E-cadherin expression remained down-regulated because resveratrol could not exert its full epithelial-stabilizing effect in both CRC cell lines (Figures 8A,B). It was noted that treatment with NF- κ B-SO (0.5 μ M) did not alter the low E-cadherin level in TME. In contrast, addition of NF- κ B-ASO (0.5 μ M) to the TME, resulted in down-regulation of inflammatory spread and, concurrently, increased E-cadherin expression. Furthermore, resveratrol-treatment (0.5 μ M) of NF- κ B-SO/-ASO-TME (0.5 μ M) also reduced inflammation and markedly promoted epithelial features of RKO or HCT116 cells (Figures 8A,B). The mesenchymal markers vimentin and slug showed opposite results. Both biomarkers were significantly increased in TME compared to baseline control (Ba.Co.) and not significantly affected by β 1-SO/-ASO addition (0.5 μ M each) in both CRC cell lines (Figures 8A,B). Impressively, resveratrol treatment led to a significant down-regulation of these parameters, which also persisted with combined treatment of resveratrol and β 1-SO (0.5 μ M). With β 1-integrin knockdown by β 1-ASO (0.5 μ M), however, resveratrol (5 μ M) could no longer fully exert its anti-EMT effects, what resulted in a strong increase of vimentin and slug (Figures 8A,B). Whereas the high expression of both biomarkers in TME was unaffected by treatment with NF- κ B-SO (0.5 μ M), both, NF- κ B knockdown (0.5 μ M NF- κ B-ASO) and the combination treatment of resveratrol and NF- κ B-SO or NF- κ B-ASO lead to strong down-regulation in HCT116 and RKO, compared with TME control (Figures 8A,B). For all examinations, β -actin served as an internal control. In summary, resveratrol showed a considerable anti-EMT effect

(Figures 8A,B) and, supported by the immunofluorescence results (Figures 1, 3), these findings suggest the use of β 1-integrin receptors by resveratrol to exert its anti-invasion impact in CRC cells which was not cell line specific.

Resveratrol targets β 1-integrin receptors, modulates TME-induced NF- κ B phosphorylation and NF- κ B-associated migration, metastasis and apoptosis proteins in the same manner as NF- κ B-ASO in CRC cells

In the next step, same Western blot samples as used before were examined for the influence of resveratrol's unfolding effects *via* β 1-integrin receptors on metastasis and apoptosis markers. In addition, the effects of NF- κ B knockdown (with NF- κ B/p65-subunit-ASO as outlined in Material and Methods) were also taken into account, whereby RKO (Figure 9A) and HCT116 (Figure 9B) presented similar results:

Compared to untreated baseline control (Ba.Co.), TME significantly promoted the expression of phosphorylated NF- κ B (p-NF- κ B), phosphorylated FAK (p-FAK), MMP-9 as well as CXCR4 in both CRC cell lines, which are all known as inflammation- and metastasis-related factors. This effect was confirmed in both, the untreated TME and the control treatments with 0.5 μ M β 1-SO or 0.5 μ M β 1-ASO alone (Figures 9A,B). Resveratrol's concentration-dependent (1, 5 μ M) down-regulation of all these parameters was surprising and equally observed in the presence of the control substance β 1-SO (0.5 μ M). In β 1-ASO (0.5 μ M) treated CRC cells, resveratrol was unable to exert its effect properly though, so that the

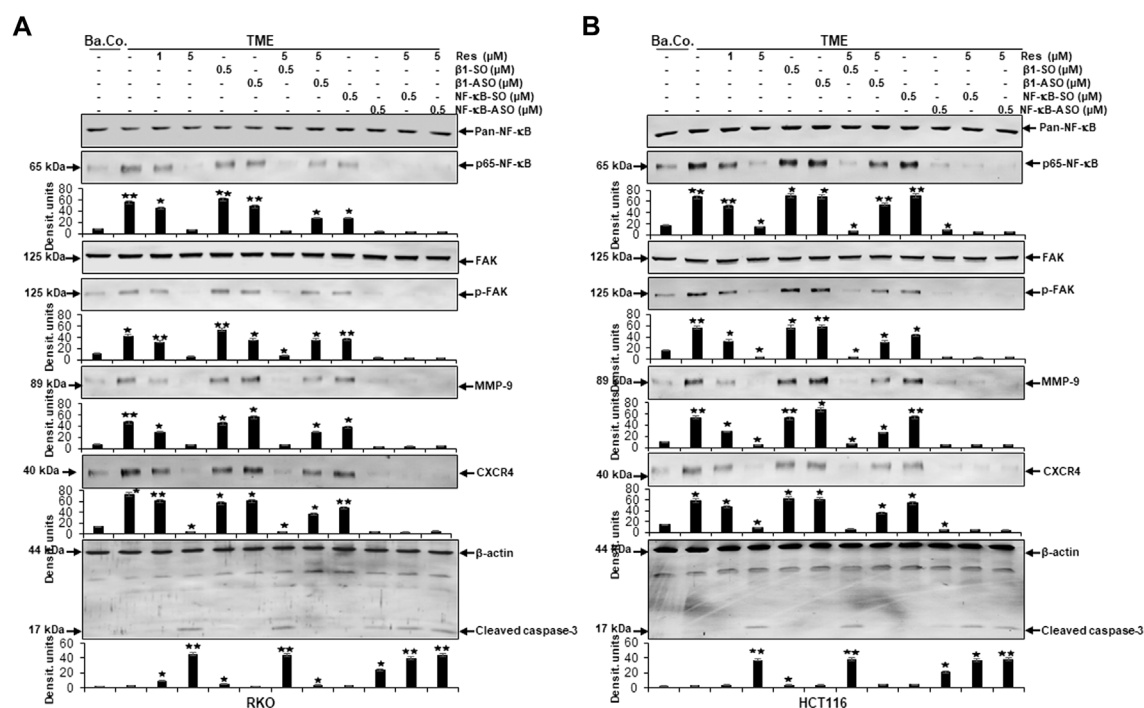


FIGURE 9

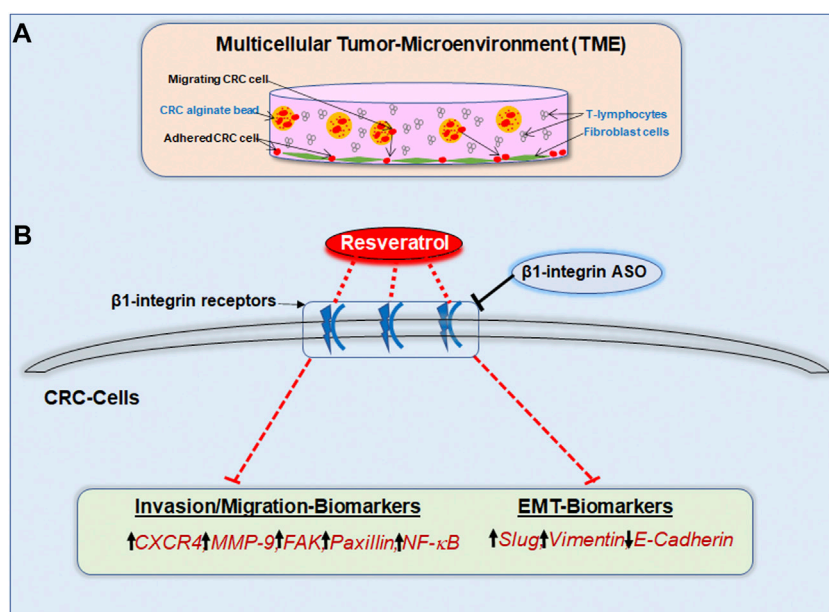
Impact of resveratrol or/and ASO against β 1-integrin or against NF- κ B on TME-promoted activation of metastasis- and apoptosis-linked biomarkers in CRC cells. Serum-starved RKO (A) and HCT116 (B) CRC cells, grown in 3D-alginate and differently treated for 10–14 days [untreated (Ba.Co.), TME control, resveratrol (1, 5 μ M), β 1-SO/ASO (0.5 μ M), NF- κ B-SO/ASO (0.5 μ M) or combination of 0.5 μ M SO/ASO and resveratrol (5 μ M); x-axis] were investigated with antibodies against pan-NF- κ B, p65-NF- κ B, FAK, p-FAK, MMP-9, CXCR4 and cleaved caspase-3. β -actin served as loading control and statistical significance is shown by: * p < 0.05 and ** p < 0.01 compared with the TME control. Y-axis: Densitometric units (y-axis) complementing Western blot results.

expression of metastasis-related and inflammatory biomarkers was up-regulated instead of suppressed. Furthermore, NF- κ B-SO (0.5 μ M) addition barely affected TME, whereas NF- κ B knockdown with 0.5 μ M NF- κ B-ASO or combined treatment with resveratrol and NF- κ B-SO or NF- κ B-ASO suppressed indicators of inflammation and invasion in RKO and HCT116 (Figures 9A,B). In line with these observations, the complementary study of apoptosis presented inverse results with low caspase-3 detection in all control samples, meaning baseline control (Ba.Co.), TME control as well as TME-CRC cells treated with 0.5 μ M β 1-SO or 0.5 μ M β 1-ASO (Figures 9A,B). Also in this regard, resveratrol showed a major modulatory effect by significantly increasing caspase-3 levels in a concentration-dependent (1, 5 μ M) manner, both in TME-CRC cells and in β 1-SO-treated (0.5 μ M) TME-CRC cells, which was inhibited by β 1-integrin knockdown (0.5 μ M β 1-ASO), visible by very low caspase-3 expression. Although the apoptosis rate was low in TME control treated with 0.5 μ M NF- κ B-SO, caspase-3 expression increased by NF- κ B knockdown (0.5 μ M NF- κ B-ASO) and was maintained at a high level by resveratrol (5 μ M) in both, NF- κ B-SO- and NF- κ B-ASO-treated RKO and HCT116 cells (Figures 9A,B).

The results described were supported by the consistent expression of non-phosphorylated FAK and NF- κ B (pan-NF- κ B) in all treatments, serving as a reference control while the uniform β -actin expression functions as a loading control. Overall, these findings indicate the utilization of β 1-integrin receptors by resveratrol to unfold its strong anti-metastasis effects in CRC cells. Furthermore, it is noticeable that resveratrol developed its strongly anti-apoptotic effect even beyond NF- κ B knockdown, suggesting resveratrol to powerfully complement its action. In summary, all Western blot results presented (Figures 6–9) were reproducible in both cell lines, HCT116 and RKO.

Discussion

After revealing the significance of β 1-integrin in the context of resveratrol's anti-viability and anti-proliferative impact on CRC cells *in vitro* in our latest work (Brockmueller et al., 2022), the present study was devoted to the role of β 1-integrin in association with anti-invasive and anti-metastatic resveratrol treatment, focusing on metastasis formation to detect a

**FIGURE 10**

(A) Study model of the pro-inflammatory 3D-tumor microenvironment consisting of a fibroblast monolayer, floating T-lymphocytes in cell culture medium and CRC cells encapsulated in alginate. (B) Graphical outcome of resveratrol's anti-invasive, anti-metastasis and anti-EMT effects by using $\beta 1$ -integrin receptors for signal transmission. The black arrows illustrate the biomarker situation within unaffected CRC cells. The red dashed lines show the modulatory effect of resveratrol on invasion-, migration- as well as EMT-parameters via $\beta 1$ -integrin receptors. $\beta 1$ -integrin-ASO can weaken this effect of resveratrol through $\beta 1$ -integrin receptor inhibition.

potential association. The central new, and in two CRC cell lines reproducible, insights gained within our study were: 1) resveratrol uses $\beta 1$ -integrin receptors to shift the balance from mesenchymal to epithelial morphology in CRC cells; 2) resveratrol uses $\beta 1$ -integrin receptors to down-regulate invasion as well as metastasis of CRC cells; 3) furthermore, resveratrol uses $\beta 1$ -integrin receptors to suppress inflammation in CRC cells; 4) and finally, resveratrol synergistically amplifies NF- κ B knockdown, thereby increasing the anti-inflammatory effect on CRC cells.

EMT together with its associated phenotype alteration pave the way for tumor cells to metastasize and invade peripheral tissue, serving as an indicator for severe disease progression. The EMT process, when tumor cells lose E-cadherin as epithelial organizer and instead take on a mesenchymal character, symbolized by slug overexpression, plays a strong role in CRC cells. It is known that EMT-promoting factors, such as cytokines and growth factors, are mainly generated by the cross-talk between tumor and immune cells (Buhrmann et al., 2020; Vuletić et al., 2021). Therefore, the ability of resveratrol to interrupt this exchange in our 3D-alginate model (Figure 10) represents a very important finding and simultaneously serves as encouragement for further investigation. The present results confirmed that resveratrol is able to prevent EMT-driven changes in the TME mainly by up-regulating the expression

of E-cadherin and the down-regulation of the expression of multifunctional regulatory adhesion protein paxillin, intermediate filament vimentin and EMT-associated master transcription factor slug. These results confirm that paxillin as known downstream intracellular target protein of FAK, controls the interaction of integrin and extracellular ligands (Deakin et al., 2012). Interestingly, stimulation of paxillin has also been reported to alter the functional composition of focal adhesions, thereby significantly increasing cell motility (Devreotes and Horwitz, 2015). As these EMT-inhibitory properties are rendered impossible by $\beta 1$ -integrin knockdown, it can be assumed that resveratrol uses $\beta 1$ -integrin receptors in order to shift the balance from mesenchymal to epithelial phenotype in CRC cells, strongly highlighting the potential of resveratrol as an effective agent for cancer and metastasis prophylaxis via the utilization of $\beta 1$ -integrin receptors. The significance becomes even clearer in light of the fact that paxillin is considered a migration marker in CRC cells due to its direct connection to EMT (Wen et al., 2020).

Moreover, further evidence that previously described the relationship between integrin family members and EMT is provided by the finding of $\beta 4$ -integrin being responsible for the organization of vimentin filaments in lung cancer cells (Colburn and Jones, 2018). In addition, $\alpha \beta 3$ -integrin is known to be a necessary essential condition for slug activation

in breast cancer cells (Desgrosellier et al., 2014). To concretely link molecular events with the clinically diagnosable course of a cancer disease, ten factors of tumorigenesis, that have become known as hallmarks of cancer (Hanahan and Weinberg, 2011), were noted by Hanahan and Weinberg further highlighting the importance of inflammation and invasion. Recently, Welch and Hurst complemented these factors by adding four hallmarks of metastasis including motility/invasion, modulated microenvironment, plasticity and colonization (Welch and Hurst, 2019), underlining their high relevance in the search of alternative treatment strategies for targeting metastatic tumors. Invasion and metastasis involve cell adhesion, cell growth, and degradation of tissue barriers and are inseparable in tumor progress (Gupta et al., 2010). Our invasion assays confirmed the already demonstrated increase of the invasion capacity of CRC cells in TME and highlighted how this process was down-regulated by resveratrol treatment. Impressively, the metastasis-inhibiting impact of resveratrol was significantly abrogated by β 1-integrin knockdown, what was further reinforced by Western blot results. Moreover, resveratrol treatment alone was able to down-regulate the metastasis-related factors including FAK, of which cascade activation is known to be integrin-dependent (Lipfert et al., 1992; Cheng et al., 2021) as well as CXCR4, shown to up-regulate α v β 6-integrin in CRC cells, thus promoting metastasis (Wang et al., 2014). Furthermore, resveratrol was able to up-regulate apoptosis-marker caspase-3, but all these effects were not detectable in β 1-integrin knockdown CRC cells.

Interestingly, the down-regulation of caspase-3 by integrin knockdown in *Helicobacter pylori* infected gastric epithelial cells has been previously reported too (Li et al., 2021). Overall, it is apparent that resveratrol reduced CRC cell invasion and migration via β 1-integrin receptors, what leads to the assumption that its signaling pathway might be a suitable co-treatment for CRC that is urgently needed, since at least 50% of CRC cases are associated with metastases (Vatandoust et al., 2015). The aforementioned hallmarks of CRC progression, EMT and metastasis, are promoted by chronic inflammatory processes (Vuletić et al., 2021) indicating the great importance of NF- κ B, which is considered a major inflammatory and tumorigenesis marker (Ko et al., 2017) in its phosphorylated, thereby activated form. Our results clearly demonstrated that resveratrol suppresses NF- κ B activation in pro-inflammatory TME, what is consistent with previous results (Buhrmann et al., 2020). However, a new observation found is that both, immunofluorescence and Western blot analysis, reproducibly displayed an abolition of resveratrol's anti-inflammatory effect by β 1-integrin knockdown, making it obvious that resveratrol uses β 1-integrin receptors to exert its inflammation-suppressing effect in CRC cells, in turn, leading to lower metastatic potential. On this background, the β 1-integrin pathway

represents a promising target in the fight against inflammation-based cancer.

Moreover, due to the strong association between phosphorylated NF- κ B and cancer progression, we finally investigated on resveratrol's impact on CRC cells in an inflammatory environment when NF- κ B was knocked down. Here, we found that NF- κ B knockdown led to a decreased inflammatory spread and invasion capacity in both CRC cell lines HCT116 and RKO, whereby resveratrol treatment of NF- κ B down-regulated CRC cells significantly enhanced their ability to act in a synergistic, powerful anti-inflammatory way. Based on this finding, it is worth considering the potential of resveratrol in the future with regard to the treatment of cancer and other chronic inflammatory diseases such as rheumatoid arthritis, where NF- κ B activation also plays a crucial role or Crohn's disease, where dysregulation of NF- κ B, physiologically necessary for intestinal homeostasis, triggers an inflammatory cascade (Nissim-Eliraz et al., 2021; Mueller et al., 2022). The fact that integrin receptors physiologically occur and are necessary in the embryonic development is also exploited by malignant cancer cells in the event of disease, thus for treatment of hepatocellular carcinoma, reduction of α 2-, β 1-, and β 3-integrin expression has been proposed as a possible option (Relja et al., 2011). Also in neuroblastoma cells, up-regulated α 2-, α 3- and β 1-integrin expression was shown and invasion and migration could be inhibited mainly by silencing β 1-integrin (Lee et al., 2013). Moreover, the correlation between β 1-integrin upregulation and the migration of triple negative breast cancer cells has been demonstrated in previous research (Schlienger et al., 2015).

Altogether, β 1-integrin has already been shown to act as a fundamentally important receptor in various types of cancer in the digestive tract and other organ systems. Extremely high CRC case numbers underline the urgency to explore the exact mechanisms underlying colorectal cancer, whereby already existing studies of other cancer types support the potential of our observations made in HCT116 and RKO cells. Our findings show evidence that high β 1-integrin expression in cancer cells can be considered as a promising target to be used in CRC therapy. For the first time we suggest to rather use β 1-integrin receptors as promising gateways for CRC co-treatment with the bio-active phytopharmaceutical resveratrol, especially due to its anti-invasive potential.

Conclusion

The presented results shed light on β 1-integrin's role in resveratrol-mediated increased E-cadherin, caspase-3 expression and decreased phosphorylated NF- κ B, phosphorylated FAK, vimentin, slug, paxillin, CXCR4, MMP-9 expression (Figure 10) in HCT116 and RKO cells leading to a noticeable reduction in their invasion and metastasis activity. Resveratrol has been shown to stabilize epithelial balance and to prevent metastasis of CRC cells, whereby these effects were significantly weakened by the knockdown of β 1-integrin. Overall, we conclude that resveratrol exerts its anti-

inflammatory, anti-invasive and thus cancer-inhibiting effect, to a relevant extent, *via* β 1-integrin receptors. Therefore, we are convinced of the helpfulness of clinical studies to determine whether β 1-integrin is suitable as a tumor marker for CRC and to emphasize the great opportunity of innovative, resveratrol-based drugs against highly metastatic CRC *via* the β 1-integrin action mechanism.

Data availability statement

The original contributions presented in the study are included in the article/Supplementary Material, further inquiries can be directed to the corresponding author.

Author contributions

Conceptualization AB and MS; investigation AB and PS; methodology, validation and formal analysis AB and PS; writing—original draft preparation AB and MS; writing—review and editing AB, A-LM and MS; project administration MS. All authors have read and agreed to the published version of the manuscript.

References

- Belleri, M., Ribatti, D., Savio, M., Stivala, L. A., Forti, L., Tanghetti, E., et al. (2008). α v β 3 Integrin-dependent antiangiogenic activity of resveratrol stereoisomers. *Mol. Cancer Ther.* 7, 3761–3770. doi:10.1158/1535-7163.MCT-07-2351
- Bengs, S., Becker, E., Busenhardt, P., Spalinger, M. R., Raselli, T., Kasper, S., et al. (2019). β (6) -integrin serves as a novel serum tumor marker for colorectal carcinoma. *Int. J. Cancer* 145, 678–685. doi:10.1002/ijc.32137
- Bergman, M., Levin, G. S., Bessler, H., Djaldetti, M., and Salman, H. (2013). Resveratrol affects the cross talk between immune and colon cancer cells. *Biomed. Pharmacother.* 67, 43–47. doi:10.1016/j.biopha.2012.10.008
- Brockmueller, A., Sameri, S., Liskova, A., Zhai, K., Varghese, E., Samuel, S. M., et al. (2021). Resveratrol's anti-cancer effects through the modulation of tumor glucose metabolism. *Cancers (Basel)* 13, E188. doi:10.3390/cancers13020188
- Brockmueller, A., Shayan, P., and Shakibaei, M. (2022). Evidence that β 1-integrin is required for the anti-viability and anti-proliferative effect of resveratrol in CRC cells. *Int. J. Mol. Sci.* 23, 4714. doi:10.3390/ijms23094714
- Buhrmann, C., Shayan, P., Brockmueller, A., and Shakibaei, M. (2020). Resveratrol suppresses cross-talk between colorectal cancer cells and stromal cells in multicellular tumor microenvironment: A bridge between *in vitro* and *in vivo* tumor microenvironment study. *Molecules* 25, E4292. doi:10.3390/molecules25184292
- Buhrmann, C., Shayan, P., Goel, A., and Shakibaei, M. (2017). Resveratrol regulates colorectal cancer cell invasion by modulation of focal adhesion molecules. *Nutrients* 9, E1073. doi:10.3390/nu9101073
- Buhrmann, C., Shayan, P., Krahe, P., Popper, B., Goel, A., and Shakibaei, M. (2015). Resveratrol induces chemosensitization to 5-fluorouracil through up-regulation of intercellular junctions, Epithelial-to-mesenchymal transition and apoptosis in colorectal cancer. *Biochem. Pharmacol.* 98, 51–68. doi:10.1016/j.bcp.2015.08.105
- Buhrmann, C., Shayan, P., Popper, B., Goel, A., and Shakibaei, M. (2016). Sirt1 is required for resveratrol-mediated chemopreventive effects in colorectal cancer cells. *Nutrients* 8, 145. doi:10.3390/nu8030145
- Carter, W. G., Wayner, E. A., Bouchard, T. S., and Kaur, P. (1990). The role of integrins α 2 β 1 and α 3 β 1 in cell-cell and cell-substrate adhesion of human epidermal cells. *J. Cell Biol.* 110, 1387–1404. doi:10.1083/jcb.110.4.1387
- Chen, W. T. (1990). Transmembrane interactions at cell adhesion and invasion sites. *Cell Differ. Dev.* 32, 329–335. doi:10.1016/0922-3371(90)90047-z
- Chen, Y. F., Yang, Y. N., Chu, H. R., Huang, T. Y., Wang, S. H., Chen, H. Y., et al. (2022). Role of integrin α v β 3 in doxycycline-induced anti-proliferation in breast cancer cells. *Front. Cell Dev. Biol.* 10, 829788. doi:10.3389/fcell.2022.829788
- Cheng, T. M., Chang, W. J., Chu, H. Y., De Luca, R., Pedersen, J. Z., Incerpi, S., et al. (2021). Nano-strategies targeting the integrin α v β 3 network for cancer therapy. *Cells* 10, 1684. doi:10.3390/cells10071684
- Colburn, Z. T., and Jones, J. C. R. (2018). Complexes of α 6 β 4 integrin and vimentin act as signaling hubs to regulate epithelial cell migration. *J. Cell Sci.* 131, jcs214593. doi:10.1242/jcs.214593
- Deakin, N. O., Pignatelli, J., and Turner, C. E. (2012). Diverse roles for the paxillin family of proteins in cancer. *Genes Cancer* 3, 362–370. doi:10.1177/1947601912458582
- Desgrosellier, J. S., Lesperance, J., Seguin, L., Gozo, M., Kato, S., Franovic, A., et al. (2014). Integrin α v β 3 drives slug activation and stemness in the pregnant and neoplastic mammary gland. *Dev. Cell* 30, 295–308. doi:10.1016/j.devcel.2014.06.005
- Devreotes, P., and Horwitz, A. R. (2015). Signaling networks that regulate cell migration. *Cold Spring Harb. Perspect. Biol.* 7, a005959. doi:10.1101/cshperspect.a005959
- Fritzemeier, K. H., Rölfs, C. H., Pfau, J., and Kindl, H. (1983). Action of ultraviolet-C on stilbene formation in callus of *Arachis hypogaea*. *Planta* 159, 25–29. doi:10.1007/BF00998810
- Gupta, S. C., Kim, J. H., Prasad, S., and Aggarwal, B. B. (2010). Regulation of survival, proliferation, invasion, angiogenesis, and metastasis of tumor cells through modulation of inflammatory pathways by nutraceuticals. *Cancer Metastasis Rev.* 29, 405–434. doi:10.1007/s10555-010-9235-2
- Hain, R., Reif, H. J., Krause, E., Langebartels, R., Kindl, H., Vornam, B., et al. (1993). Disease resistance results from foreign phytoalexin expression in a novel plant. *Nature* 361, 153–156. doi:10.1038/361153a0
- Hanahan, D., and Weinberg, R. A. (2011). Hallmarks of cancer: The next generation. *Cell* 144, 646–674. doi:10.1016/j.cell.2011.02.013
- Huang, M. W., Lin, C. D., and Chen, J. F. (2021). Integrin activation, focal adhesion maturation and tumor metastasis. *Sheng Li Xue Bao* 73, 151–159.

Acknowledgments

We thank Andreas Eimannsberger for excellent technical assistance. We note, that the research was conducted as a part of the doctoral thesis of AB to be submitted to Fachbereich Humanmedizin, Ludwig-Maximilians-University Munich, Germany.

Conflict of interest

The authors declare that the research was conducted in the absence of any commercial or financial relationships that could be construed as a potential conflict of interest.

Publisher's note

All claims expressed in this article are solely those of the authors and do not necessarily represent those of their affiliated organizations, or those of the publisher, the editors and the reviewers. Any product that may be evaluated in this article, or claim that may be made by its manufacturer, is not guaranteed or endorsed by the publisher.

- Jones, J. L., Critchley, D. R., and Walker, R. A. (1992). Alteration of stromal protein and integrin expression in breast—a marker of premalignant change? *J. Pathol.* 167, 399–406. doi:10.1002/path.1711670409
- Kaihara, T., Kusaka, T., Nishi, M., Kawamata, H., Imura, J., Kitajima, K., et al. (2003). Dedifferentiation and decreased expression of adhesion molecules, E-cadherin and ZO-1, in colorectal cancer are closely related to liver metastasis. *J. Exp. Clin. Cancer Res.* 22, 117–123.
- Ko, J. H., Sethi, G., Um, J. Y., Shanmugam, M. K., Arfuso, F., Kumar, A. P., et al. (2017). The role of resveratrol in cancer therapy. *Int. J. Mol. Sci.* 18, E2589. doi:10.3390/ijms18122589
- Koklesova, L., Liskova, A., Samec, M., Zhai, K., Abotaleb, M., Ashrafizadeh, M., et al. (2020). Carotenoids in cancer metastasis—status quo and outlook. *Biomolecules* 10, E1653. doi:10.3390/biom10121653
- Lee, S., Qiao, J., Paul, P., and Chung, D. H. (2013). Integrin $\beta 1$ is critical for gastrin-releasing peptide receptor-mediated neuroblastoma cell migration and invasion. *Surgery* 154, 369–375. doi:10.1016/j.surg.2013.04.067
- Li, B., Rong, Q., Du, Y., Zhang, R., Li, J., Tong, X., et al. (2021). Regulation of $\beta 1$ -integrin in autophagy and apoptosis of gastric epithelial cells infected with *Helicobacter pylori*. *World J. Microbiol. Biotechnol.* 38, 12. doi:10.1007/s11274-021-03199-9
- Li, H., Wang, Y., Rong, S. K., Li, L., Chen, T., Fan, Y. Y., et al. (2020). Integrin $\alpha 1$ promotes tumorigenicity and progressive capacity of colorectal cancer. *Int. J. Biol. Sci.* 16, 815–826. doi:10.7150/ijbs.37275
- Lin, H. Y., Lansing, L., Merillon, J. M., Davis, F. B., Tang, H. Y., Shih, A., et al. (2006). Integrin $\alpha 5\beta 3$ contains a receptor site for resveratrol. *Faseb J.* 20, 1742–1744. doi:10.1096/fj.06-5743fj
- Lipfert, L., Haimovich, B., Schaller, M. D., Cobb, B. S., Parsons, J. T., and Brugge, J. S. (1992). Integrin-dependent phosphorylation and activation of the protein tyrosine kinase pp125FAK in platelets. *J. Cell Biol.* 119, 905–912. doi:10.1083/jcb.119.4.905
- Mueller, A. L., Brockmueller, A., Kunnumakkara, A. B., and Shakibaei, M. (2022). Curcumin A, a compound of turmeric, down-regulates inflammation in tenocytes by NF- κ B/Scleraxis signaling. *Int. J. Mol. Sci.* 23, 1695. doi:10.3390/ijms23031695
- Nissim-Eliraz, E., Nir, E., Marsiano, N., Yagel, S., and Shpigel, N. Y. (2021). NF- κ B activation unveils the presence of inflammatory hotspots in human gut xenografts. *PLoS One* 16, e0243010. doi:10.1371/journal.pone.0243010
- Rasool, M., Malik, A., Waquar, S., Ain, Q. T., Rasool, R., Asif, M., et al. (2021). Assessment of clinical variables as predictive markers in the development and progression of colorectal cancer. *Bioengineered* 12, 2288–2298. doi:10.1080/21655979.2021.1933680
- Relja, B., Meder, F., Wang, M., Blaheta, R., Henrich, D., Marzi, I., et al. (2011). Simvastatin modulates the adhesion and growth of hepatocellular carcinoma cells via decrease of integrin expression and ROCK. *Int. J. Oncol.* 38, 879–885. doi:10.3892/ijo.2010.892
- Schlienger, S., Ramirez, R. A., and Claing, A. (2015). ARF1 regulates adhesion of MDA-MB-231 invasive breast cancer cells through formation of focal adhesions. *Cell. Signal.* 27, 403–415. doi:10.1016/j.cellsig.2014.11.032
- Shakibaei, M., De Souza, P., and Merker, H. J. (1997). Integrin expression and collagen type II implicated in maintenance of chondrocyte shape in monolayer culture: An immunomorphological study. *Cell Biol. Int.* 21, 115–125. doi:10.1006/cbir.1996.0118
- Shakibaei, M. (1998). Inhibition of chondrogenesis by integrin antibody *in vitro*. *Exp. Cell Res.* 240, 95–106. doi:10.1006/excr.1998.3933
- Shakibaei, M. (1995). Integrin expression on epiphyseal mouse chondrocytes in monolayer culture. *Histol. Histopathol.* 10, 339–349.
- Shakibaei, M., and Merker, H. J. (1999). Beta1-integrins in the cartilage matrix. *Cell Tissue Res.* 296, 565–573. doi:10.1007/s004410051318
- Siegel, R. L., Miller, K. D., Goding Sauer, A., Fedewa, S. A., Butterly, L. F., Anderson, J. C., et al. (2020). Colorectal cancer statistics, 2020. *Ca. Cancer J. Clin.* 70, 145–164. doi:10.3322/caac.21601
- Suh, J., Kim, D. H., and Surh, Y. J. (2018). Resveratrol suppresses migration, invasion and stemness of human breast cancer cells by interfering with tumor-stromal cross-talk. *Arch. Biochem. Biophys.* 643, 62–71. doi:10.1016/j.abb.2018.02.011
- Sung, H., Ferlay, J., Siegel, R. L., Laversanne, M., Soerjomataram, I., Jemal, A., et al. (2021). Global cancer statistics 2020: GLOBOCAN estimates of incidence and mortality worldwide for 36 cancers in 185 countries. *Ca. Cancer J. Clin.* 71, 209–249. doi:10.3322/caac.21660
- Varoni, E. M., Lo Faro, A. F., Sharifi-Rad, J., and Iriti, M. (2016). Anticancer molecular mechanisms of resveratrol. *Front. Nutr.* 3, 8. doi:10.3389/fnut.2016.00008
- Vatandoust, S., Price, T. J., and Karapetis, C. S. (2015). Colorectal cancer: Metastases to a single organ. *World J. Gastroenterol.* 21, 11767–11776. doi:10.3748/wjg.v21.i41.11767
- Vuletić, A., Mirjačić Martinović, K., Tišma Miletić, N., Zoidakis, J., Castellvi-Bel, S., and Čavić, M. (2021). Cross-talk between tumor cells undergoing epithelial to mesenchymal transition and natural killer cells in tumor microenvironment in colorectal cancer. *Front. Cell Dev. Biol.* 9, 750022. doi:10.3389/fcell.2021.750022
- Wang, B., Wang, S., Wang, W., Liu, E., Guo, S., Zhao, C., et al. (2021). Hyperglycemia promotes liver metastasis of colorectal cancer via upregulation of integrin $\alpha 5\beta 6$. *Med. Sci. Monit.* 27, e930921. doi:10.12659/MSM.930921
- Wang, B., Wang, W., Niu, W., Liu, E., Liu, X., Wang, J., et al. (2014). SDF-1/CXCR4 axis promotes directional migration of colorectal cancer cells through upregulation of integrin $\alpha 5\beta 6$. *Carcinogenesis* 35, 282–291. doi:10.1093/carcin/bgt331
- Welch, D. R., and Hurst, D. R. (2019). Defining the hallmarks of metastasis. *Cancer Res.* 79, 3011–3027. doi:10.1158/0008-5472.CAN-19-0458
- Wen, L., Zhang, X., Zhang, J., Chen, S., Ma, Y., Hu, J., et al. (2020). Paxillin knockdown suppresses metastasis and epithelial-mesenchymal transition in colorectal cancer via the ERK signalling pathway. *Oncol. Rep.* 44, 1105–1115. doi:10.3892/or.2020.7687
- Gao, H., Tian, Q., Zhu, L., Feng, J., Zhou, Y., and Yang, J. (2021). 3D Extracellular Matrix Regulates the Activity of T Cells and Cancer Associated Fibroblasts in Breast Cancer. *Front. Oncol.* 11, 764204. doi:10.3389/fonc.2021.764204



OPEN ACCESS

EDITED BY

Aftab Ullah,
Jiangsu University, China

REVIEWED BY

Chao-Zhan Lin,
Guangzhou University of Chinese
Medicine, China
Tao Yang,
Shanghai University of Traditional
Chinese Medicine, China

*CORRESPONDENCE

Zhengli Jiang,
jiangzl@enzemed.com

SPECIALTY SECTION

This article was submitted to
Ethnopharmacology,
a section of the journal
Frontiers in Pharmacology

RECEIVED 26 June 2022

ACCEPTED 15 August 2022

PUBLISHED 06 September 2022

CITATION

Chen J, Shen B and Jiang Z (2022),
Traditional Chinese medicine
prescription Shenling BaiZhu powder to
treat ulcerative colitis: Clinical evidence
and potential mechanisms.
Front. Pharmacol. 13:978558.
doi: 10.3389/fphar.2022.978558

COPYRIGHT

© 2022 Chen, Shen and Jiang. This is an
open-access article distributed under
the terms of the [Creative Commons
Attribution License \(CC BY\)](#). The use,
distribution or reproduction in other
forums is permitted, provided the
original author(s) and the copyright
owner(s) are credited and that the
original publication in this journal is
cited, in accordance with accepted
academic practice. No use, distribution
or reproduction is permitted which does
not comply with these terms.

Traditional Chinese medicine prescription Shenling BaiZhu powder to treat ulcerative colitis: Clinical evidence and potential mechanisms

Jing Chen¹, Bixin Shen² and Zhengli Jiang^{1*}

¹Department of Pharmacy, Taizhou Hospital of Zhejiang Province Affiliated to Wenzhou Medical University, Lin Hai, China, ²Department of Pharmaceutics, School of Pharmaceutical Sciences, Wenzhou Medical University, Wenzhou, China

Ulcerative colitis (UC), characterized by syndromes including abdominal pain, bloody stool, diarrhea, weight loss, and repeated relapse, is a non-specific inflammatory intestinal disease. In recent years, with the changing dietary habits in China, the incidence of UC has shown an upward trend. UC belongs to the category of recorded as “diarrhea,” “chronic dysentery,” and “hematochezia” in traditional Chinese medicine (TCM), and Shenling BaiZhu powder (SLBZP) is one of the most effective and commonly used prescriptions. In this review, we aim to systematically summarize the clinical application and pharmacological mechanism of SLBZP in the treatment of UC to provide a theoretical basis for its clinical use and experimental evaluation of SLBZP. Our results showed that both SLBZP and SLBZP in combination with chemical drugs, have a significant therapeutic effect against UC with few adverse reactions. Furthermore, combined therapy was better than western medicine. Further, pathophysiological studies indicated that SLBZP has anti-inflammatory, immunomodulatory, antioxidant effects, regulation relative cell signal transduction and regulation of gut microbiota. Although evidence suggests superior therapeutic efficacy of SLBZP for treating UC and the relative mechanism has been studied extensively, various shortcomings limit the existing research on the topic. There is a lack of UC animal models, especially UC with TCM syndromes, with no uniform standard and certain differences between the animal model and clinical syndrome. The dosage, dosage form, and therapeutic time of SLBZP are inconsistent and lack pharmacological verification, and clinical trial data are not detailed or sufficiently rigorous. In addition, SLSZP is composed of multiple Chinese drugs that contain massive numbers of ingredients and which or several components contribute to therapeutic effects. How they work synergistically together remains unknown. Therefore, on the one hand, large sample prospective cohort studies to clarify the clinical efficacy and safety of SLBZP in the treatment of UC are needed. In contrast, researchers should strengthen the study of the molecular biological mechanism of active ingredients and its

synergistic actions, clarifying the mechanism of SLBZP in treating UC by multi-component, multi-target, and multi-pathway.

KEYWORDS

shenling baizhu powder, ulcerative colitis, clinical evidence, mechanism, signal pathway

1. Introduction

Ulcerative colitis (UC) is a non-specific inflammatory intestinal disease typically characterized by inflammation of the mucosa and submucosa of the rectum and colon (Ungaro et al., 2017). The primary clinical symptoms of UC include abdominal pain, bloody stools, diarrhea, weight loss, and repeated relapse and remission, which seriously affects the quality of life (Ungaro et al., 2017). Currently, the pathogenesis of UC is not adequately clarified and is considered to be associated with the genetic background, environmental factors, and immune dysregulation. In recent years, with changing dietary habits and lifestyle, the incidence of UC has increased in both developed and developing countries, for example in China (Kobayashi et al., 2020). Current treatments of UC mainly include pharmacotherapy and surgical treatment. The therapeutic options include corticosteroids, aminosalicylates, immunosuppressives, such as mesalazine, 5-aminosalicylates, sulfasalazine. Although these drugs could improve symptoms in patients with UC, long-term treatment can lead to vomiting and other adverse effects, resulting in poor compliance. Therefore, there is an urgent need to identify highly efficient drugs with less adverse effects to treat UC.

Traditional Chinese medicine (TCM) as a treatment option is widely used to manage UC. In recent years, numerous studies have confirmed that TCM has been characterized by multi-component, multi-target, and multi-pathway approaches for treating UC and does not carry side effects (Liu et al., 2022a). UC has not been defined in the classics of TCM, and UC falls under the category of “diarrhea,” “chronic dysentery,” and “hematochezia” in TCM (Liu et al., 2021a). With syndrome differentiation, TCM divides UC into seven categories: large intestine damp-heat type, heat toxin type, spleen deficiency and dampness type, cold-heat complex pattern type, liver depression and spleen deficiency type, spleen and kidney Yang deficiency type, and deficiency of both blood and yin type (Zhang et al., 2017). The spleen deficiency and dampness type is the common category of UC, and Shenling BaiZhu powder (SLBZP) is one of the effective remedies used for its treatment (Ma et al., 2019).

SLBZP is a TCM compound commonly used in Chinese clinical practice, originally documented in the Song Dynasty “Taiping Huimin Hejiju Fang” (Yang, 2018). The formula is composed of *Atractylodes macrocephala* Koidz. (Bai Zhu), *Poria cocos* (Schw.) Wolf (Fu Ling), *Glycyrrhiza uralensis*

Fisch. (Gan Cao), *Platycodon grandiflorum* (Jacq.) A. DC. (Jie Geng), *Panax ginseng* C.A.Mey. (Ren Shen), *Amomum villosum* Lour. (Sha Ren), *Dioscorea opposita* Thunb. (Shan Yao), *Coix lacryma-jobi* L. var. *mayuen* (Roman.) Stapf (Yi Yi Ren), *Nelumbo nucifera* Gaertn. (Lian Zi) and *Dolichos lablab* L. (Bai Bian Dou), and stopping diarrhea, SLBZP has long been used to treat digestive system disease in clinical practice. Additionally, SLBZP is also used to treat disease such as chronic obstructive pulmonary disease (Mao et al., 2021a), non-alcoholic fatty liver disease (Zhang et al., 2018), diabetes (Zhou et al., 2019). Recently, numerous clinical and experimental studies have reported the efficacy and mechanism of SLBZP in the treatment of UC (Ma et al., 2019; Chen et al., 2020; Li et al., 2021a; Li et al., 2021b).

However, further in-depth research on SLBZP for the treatment of UC is needed, focusing on the molecular and cellular mechanism of action with more exhaustive pharmacological studies to substantiate the efficacy of this TCM. This review highlights the studies on the pharmacological properties and clinical applications of SLBZP for the treatment of UC. This review may help expand the application of SLBZP to treat UC in clinical practice, and also provide the reference for further study of classical formulas. Moreover, the review of pharmacological effects of single Chinese herb and its active ingredients from SLBZP for UC performed in this study, which may help clarify the effective ingredients and their synergistic actions when formulated in SLBZP.

2 Ulcerative colitis and Shenling BaiZhu powder

2.1 Understanding of UC in TCM

Combining with UC clinical manifestations, including abdominal pain, diarrhea, mucus pus, bloody stool, and tenesmus, UC belongs to the “diarrhea,” “chronic dysentery,” and “hematochezia” category in TCM (Zhang, 2010). Since UC is a chronic disease with recurrence, “chronic dysentery” can describe UC more precisely. Practitioners of TCM believe that the pathogenetic basis of UC is the deficiency of spleen *qi*, and the primary triggers include invasion of external evils, internal injury of emotions, improper diet, and stress (He et al., 2012a). The active phase of UC resembles the TCM excessive syndrome, and the primary pathogenesis is the intestinal accumulation of damp-

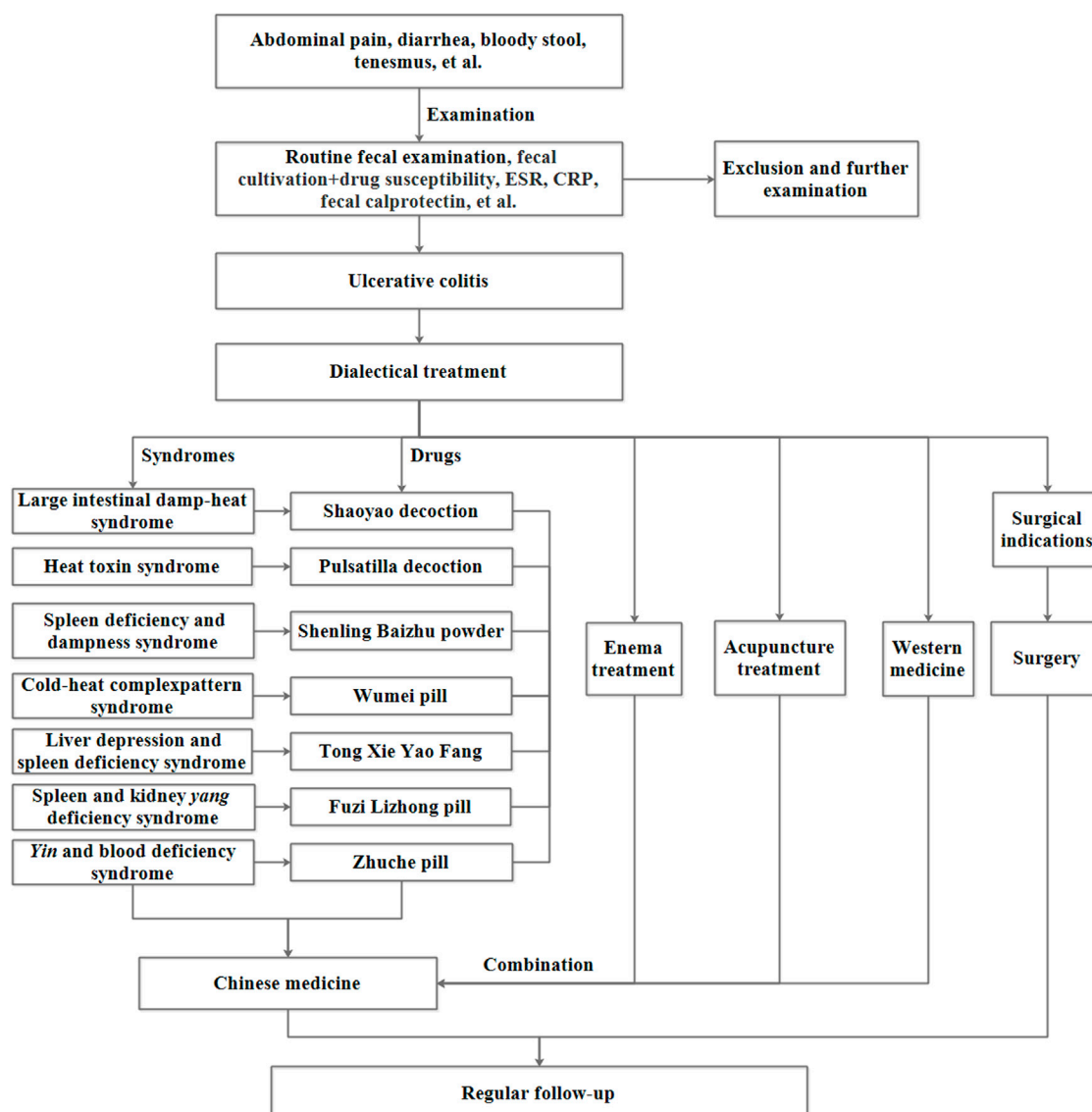
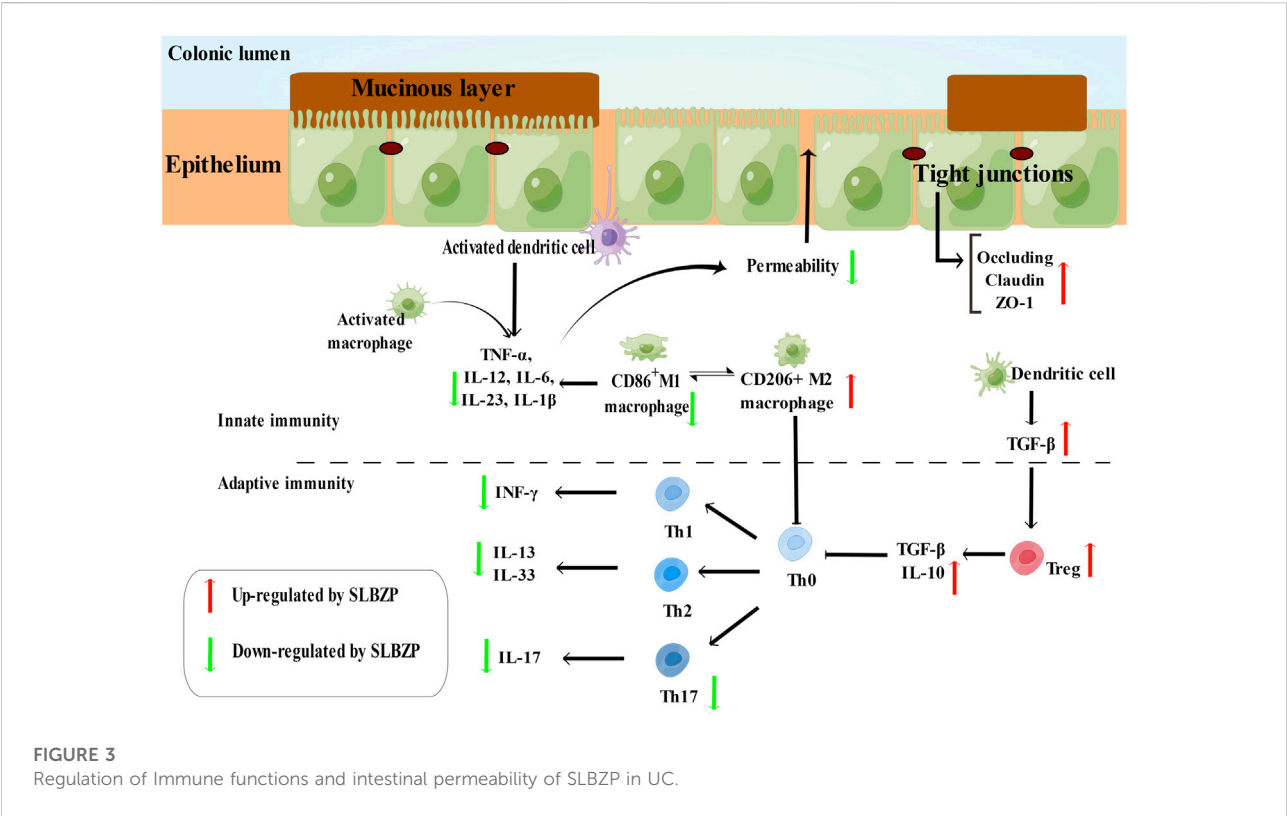
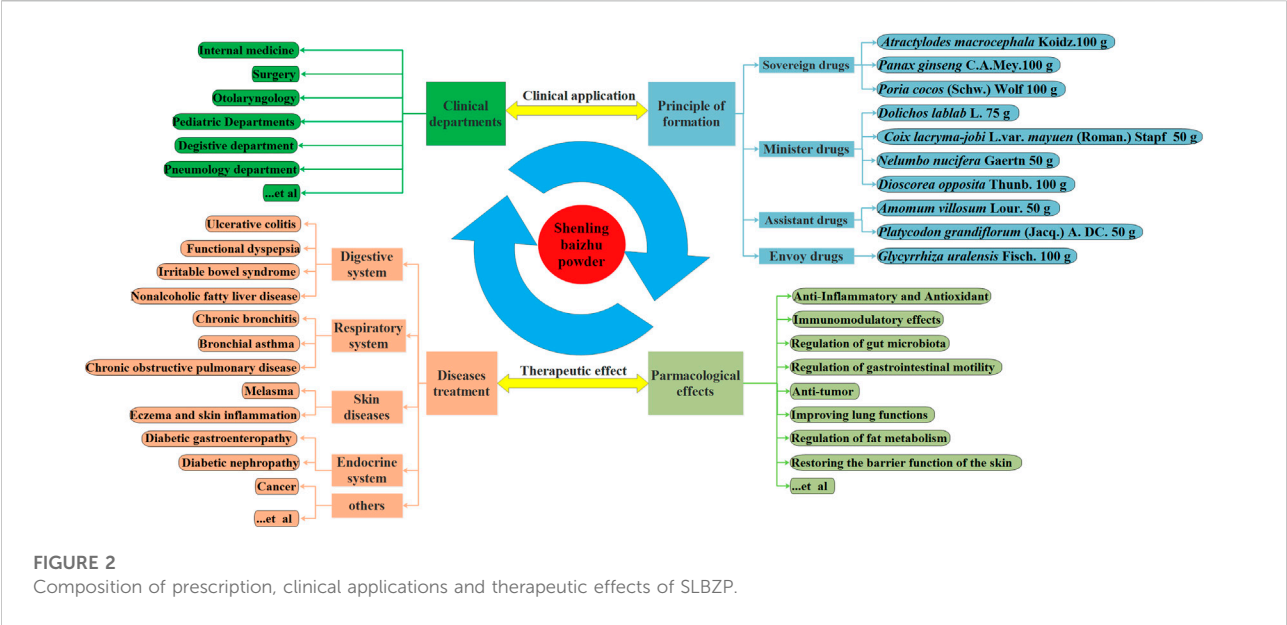


FIGURE 1
The processes of diagnosis and treatment of UC.

heat and disturbance of *qi* and blood. The pathogenesis of severe UC is *heat*-toxic and stagnant *heat*, and refractory UC with relapse should be blood stasis and turbid phlegm. In remission periods, spleen deficiency is the primary pathogenesis of UC (Liu et al., 2021b). Based on the clinical manifestations and “dialectical treatment” of TCM outcomes, UC is classified into seven subtypes: large intestinal damp-heat syndrome, heat toxin syndrome, spleen deficiency and dampness syndrome, cold-heat complicated syndrome, liver depression and spleen deficiency, spleen and kidney *yang* deficiency, and *yin* and blood deficiency syndrome (Zhang et al., 2017). The process for the diagnosis and treatment of UC is shown in Figure 1.

2.2 Shenling Baizhu powder

SLBZP is composed of 10 Chinese herbal drugs, including *Atractylodes macrocephala* Koidz., *Poria cocos* (Schw.) Wolf, *Glycyrrhiza uralensis* Fisch., *Platycodon grandiflorum* (Jacq.) A. DC., *Panax ginseng* C.A.Mey., *Amomum villosum* Lour., *Dioscorea opposita* Thunb., *Coix lacryma-jobi* L. var. *mayuen* (Roman.) Stapf, *Nelumbo nucifera* Gaertn. and *Dolichos lablab* L., which are mainly targeted at spleen deficiency and dampness syndrome. Additionally, SLBZP is a representative prescription of “supplementing spleen to nourish lung” and can be used to treat cough and asthma caused by lung deficiency.



The use of SLBZP is widespread in clinical practice and embraces internal medicine, surgery, and postoperative recovery (Lu et al., 2022). Currently, SLBZP is commonly employed to prevent and treat various diseases including

UC, irritable bowel syndrome, diabetic gastroenteropathy, diabetic nephropathy, chronic obstructive pulmonary disease, allergic rhinitis, otitis media, non-alcoholic fatty liver disease (Zhang et al., 2018; Ma et al., 2019; Mao et al.,

TABLE 1 Overview of clinical studies of SLBZP.

Classification	Therapeutic intervention		Treatment time (days)	Evaluation index	Results	References
	Treatment group (UC cases/treatment drugs)	Control group (UC cases/treatment drugs)				
Monotherapy	49 cases; Flavored SLBZP (1 dose per day, decocted in water, thrice daily)	41 cases; Sulfasalazine (oral 2 g, 3 times a day), norfloxacin (oral 0.2 g, 3 times a day) and enema (150 ml, once a day)	30	Clinical efficacy	1) The response in the treatment group was higher than control group	Ren, (2010)
	75 cases; SLBZP (1 dose per day, decocted in water, twice daily)	75 cases; Sulfasalazine (oral 0.5 g, 4 times a day)	60		2) The recurrence rate in the treatment group was lower than control group	Qin, (2012)
	53 cases; Flavored SLBZP (1 dose per day, decocted in water, twice daily)	53 cases; Sulfasalazine (oral 1 g, 4 times a day)	60			Xie, et al. (2015)
	24 cases; SLBZP (according to the prescription powder the herbs and mixed, 6 g each dose, thrice daily)	24 cases; Mesalazine (oral 1 g, 4 times a day)	90	Clinical efficacy, inflammatory factors and gut microbiota	1) The response in the treatment group is higher than control group	He, (2014)
	50 cases; Flavored SLBZP (1 dose per day, decocted in water, twice daily)	50 cases; Mesalazine (oral 1 g, 4 times a day)	168		2) It could decrease the levels of IL-17, TNF- α , IL-23, CRP, ESR and increase the levels of IL-10	Quan and Tan, (2017)
	30 cases; SLBZP (according to the prescription powder the herbs and mixed, 6 g each dose, thrice daily)	30 cases; Mesalazine (oral 1 g, 4 times a day)	84		3) It could promote the growth of probiotics and inhibit the proliferation and colonization of pathogenic bacteria	Yang, (2017)
	26 cases; SLBZP (1 dose per day, decocted in water, twice daily)	26 cases; Mesalazine (oral 1 g, 3 times a day)	30			Yang, et al. (2021)
	84 cases; Flavored SLBZP (1 dose per day, decocted in water, twice daily)	84 cases; Mesalazine (oral 1 g, 3 times a day)	56			Xu, (2021)
	43 cases; Flavored SLBZP (1 dose per day, decocted in water, twice daily)	42 cases; Domperidone (oral 10 mg, 3 times a day)	30	Clinical efficacy	1) The response in the treatment group is higher than control group	Sun and Chen, (2014)
	41 cases; Flavored SLBZP (1 dose per day, decocted in water, twice daily)	41 cases; Compound Sulfamethoxazole and tetracycline	7			Tian and Song, (2015)
	55 cases; Flavored SLBZP (1 dose per day, decocted in water, twice daily)	55 cases; Norfloxacin (oral 0.4 g, 2 times a day)	20			Wang, (2019)
Combination therapy	48 cases; SLBZP (according to the prescription powder the herbs and mixed, 6 g each dose, thrice daily) and Mesalazine (oral 1 g, 4 times a day)	48 cases; Mesalazine (oral 1 g, 4 times a day)	60	Clinical efficacy, inflammatory factors, antioxidation, immune function	1) The response in the treatment group is higher than control group	Chen, et al. (2013)
	23 cases; SLBZP (according to the prescription powder the herbs and mixed, 6 g each dose, thrice daily) and Mesalazine (oral 1 g, 4 times a day)	23 cases; Mesalazine (oral 1 g, 4 times a day)	84		2) The response in the treatment group is lower than control group	Wei, et al. (2013)
	42 cases; SLBZP (according to the prescription powder the herbs and mixed, 6 g each dose, thrice daily) and Mesalazine (oral 1 g, 4 times a day)	36 cases; Mesalazine (oral 1 g, 4 times a day)	84		3) It could reduce the levels of IL-17, TNF- α and IL-23, CRP, ESR, IL-1 β , IL-6 and IL-18, IL-2, IFN- γ and increase levels of IL-4	Ma, et al. (2015)
	66 cases; SLBZP (granule, 6 g each dose, thrice daily) and Mesalazine (oral 1 g, 3 times a day)	66 cases; Mesalazine (oral 1 g, 3 times a day)	84		4) It could inhibit the expression of NLRP3, ASC and caspase-1 mRNA.	Tian, et al. (2019)
	40 cases; SLBZP (according to the prescription powder the herbs and mixed, 6 g each dose, thrice daily) and Mesalazine (oral 1 g, 4 times a day)	40 cases; Mesalazine (oral 1 g, 4 times a day)	56		5) It could reduce the serum MDA and increase the serum SOD levels	Wang, (2016)
	50 cases; SLBZP (according to the prescription powder the herbs and mixed, 6 g each dose, thrice daily) and Mesalazine (oral 1 g, 4 times a day)	50 cases; Mesalazine (oral 1 g, 4 times a day)	56		6) It could reduce percentage of Th17 cells, IgA, IgM levels and increase the ratio of CD4 ⁺ , CD4 ⁺ /CD8 ⁺ T cells, the percentage of Treg cells	Zhou, et al. (2018)
	49 cases; Flavored SLBZP (1 dose per day, decocted in water, twice daily)	45 cases; Mesalazine (oral 1 g, 3 times a day)	180		7) It could reduce the MMP-2, MMP-9 levels of UC patients	Shi et al. (2018b)
	31 cases; SLBZP (according to the prescription powder the herbs and mixed, 6 g each dose, thrice daily) and Mesalazine (oral 1 g, 4 times a day)	31 cases; Mesalazine (oral 1 g, 4 times a day)	60			Qian and Zhang, (2019)
	45 cases; Flavored SLBZP (1 dose per day, decocted in water, twice daily)	45 cases; Mesalazine (oral 0.5 g, 3 times a day)	56			Li and Wang, (2021)
	51 cases; SLBZP (1 dose per day, decocted in water, thrice daily) and Sulfasalazine (oral 0.5 g, 3 times a day)	51 cases; Sulfasalazine (oral 0.5 g, 3 times a day)	28	Clinical efficacy, inflammatory factors, antioxidation, immune function	1) The response in the treatment group is higher than control group	Yang, (2012)
	47 cases; SLBZP (1 dose per day, decocted in water, twice daily) and Sulfasalazine (oral 0.5 g, 3 times a day)	47 cases; Sulfasalazine (oral 0.5 g, 3 times a day)	28		2) The recurrence rate and incidence of adverse reactions in the treatment group is lower than control group	Ouyang, (2015)

(Continued on following page)

TABLE 1 (Continued) Overview of clinical studies of SLBZP.

Classification	Therapeutic intervention		Treatment time (days)	Evaluation index	Results	References
	Treatment group (UC cases/treatment drugs)	Control group (UC cases/treatment drugs)				
	28 cases; SLBZP (according to the prescription powder the herbs and mixed, 6 g each dose, thrice daily) and Sulfasalazine (enema 3 g/50 ml, one time a day)	28 cases; Sulfasalazine (enema 3 g/50 ml, one time a day)	56		3) It could reduce the levels of TNF- α , IL-1 β , IL-2, IL-6, IL-8, TNF- α , INF- γ , HIF- α , IGF-1 and MMP-9 and increase levels of IL-10	Wang, et al. (2016)
	25 cases; Flavored SLBZP (1 dose per day, decocted in water, thrice daily) and Sulfasalazine (oral 1 g, 4 times a day)	25 cases; Sulfasalazine (oral 1 g, 4 times a day)	28		4) It could inhibit the expression of NF- κ B p65 and promote the expression of β 2AR and β -arrestin2 of intestinal mucosa	Yu, (2017)
	31 cases; Flavored SLBZP (1 dose per day, decocted in water, thrice daily) and Sulfasalazine (oral 1 g, 4 times a day)	31 cases; Sulfasalazine (oral 1 g, 4 times a day)	30		5) It could increase the CD3 ⁺ , CD4 ⁺ , CD8 ⁺ T cells levels	Zhang, (2017)
	46 cases; SLBZP (1 dose per day, decocted in water, thrice daily) and Sulfasalazine (oral 1 g, 4 times a day)	46 cases; Sulfasalazine (oral 1 g, 4 times a day)	56			Xu, et al. (2018)
	53 cases; SLBZP (granule, 6 g each dose, thrice daily) and Sulfasalazine (oral 1 g, 4 times a day)	53 cases; Sulfasalazine (oral 1 g, 4 times a day)	90			Chen, et al. (2020)
	57 cases; Flavored SLBZP + Tao hua decoction (1 dose per day, decocted in water, thrice daily)	57 cases; Mesalazine (oral 1 g, 4 times a day)	90	Clinical efficacy	1) The response in the treatment group is higher than control group	Jiang, (2019)
	64 cases; Flavored SLBZP + Tong Xie Yao Fang (1 dose per day, decocted in water, thrice daily)	40 cases; Compound Diphenoxylate Tablets (oral 50 mg, 3 times a day) and oryzanol (oral 20 mg, 3 times a day)	42			Zhou, (2009)
	20 cases; SLBZP + Shaoyao Gancao decoction (1 dose per day, decocted in water, thrice daily)	16 cases; Sulfasalazine (oral 1 g, 3 times a day)	28			Li, (2013)
	30 cases; Sishen Pills + SLBZP (1 dose per day, decocted in water, thrice daily) + Mesalazine (oral 1 g, 4 times a day)	30 cases; Mesalazine (oral 1 g, 4 times a day)	56	Clinical efficacy, inflammatory factors and intestinal flora	1) The response in the treatment group is higher than control group ($p < 0.05$) 2) It could increase the numbers of bifidobacterium and <i>Lactobacillus</i> and reduce the number of <i>Escherichia coli</i> and the levels of ET, D-lactate and DAO in serum	Shen, et al. (2021)
	32 cases; Shaoyao decoction + flavored SLBZP (1 dose per day, decocted in water, thrice daily)	34 cases; Mesalazine (oral 1 g, 4 times a day)	168	Clinical efficacy and recurrence rate	1) The total effects of two groups have no significantly difference 2) Recurrence rate in treatment group were lower than in control group	Luo, et al. (2014)
	30 cases; Flavored SLBZP + Gegenqinlian decoction (1 dose per day, decocted in water, thrice daily)	30 cases; Sulfasalazine (oral 1 g, 3 times a day)	90	Clinical efficacy	1) The response in the treatment group is higher than control group	Zhang, et al. (2022a)
	55 cases; SLBZP (1 dose per day, decocted in water, thrice daily) + kangfuxin solution (Enema, 50 ml)	55 cases; Sulfasalazine (oral 0.5g, 3 times a day) + Trimebutine Maleate (oral 0.5g, 3 times a day) + Albumin tannate tablet (oral 0.5g, 3 times a day)	30	Clinical efficacy	The response in the treatment group is higher than control group	Chen, (2012)
	43 cases; Flavored SLBZP (1 dose per day, decocted in water, thrice daily) + enema (100 ml, 2 times a day)	37 cases; enema (100 ml, 2 times a day)	42	Clinical efficacy	1) The response in the treatment group is higher than control group	Tian, (2019)
	59 cases; Flavored SLBZP (1 dose per day, decocted in water, thrice daily) + Mesalazine (oral 1 g, 3 times a day) + acupuncture	59 cases; Mesalazine (oral 1 g, 3 times a day)	84	Clinical efficacy and inflammatory factors	1) The response in the treatment group is higher than control group	Hua, (2022)
	47 cases; Flavored SLBZP (1 dose per day, decocted in water, thrice daily) + Mesalazine (oral 1 g, 3 times a day) + warm acupuncture	46 cases; Mesalazine (oral 1 g, 3 times a day)	28		2) it could decrease the serum 5-HT and SP, numbers of intestinal yeast, serum IL-6 and TNF- α levels and increase the levels of SS and VIP, intestinal bifidobacterium, <i>Lactobacillus</i> , and numbers of <i>Peptococcus</i> 3) It exhibited immunomodulatory effects by regulating the levels of Th17, Treg, Th17/Treg, HMGB-1, HIF-1 α , IGF-1	Zhou et al. (2021b)

2021b), and in disease mainly involving digestive system, respiratory system, endocrine system, and skin diseases. As showed as in Figure 2.

SLBZP is modified by *Sijunzi* Tang and comes from the “*Taiping Huimin Hejiju Fang*” (Song Dynasty) (Yang, 2018). In this prescription, *Atractylodes macrocephala* Koidz., *Poria cocos*

(Schw.) Wolf, and *Panax ginseng* C.A.Mey., are the sovereign drugs, which can strengthen the spleen and eliminate dampness. As minister drugs, *Dioscorea opposita* Thunb. and *Nelumbo nucifera* Gaertn can help sovereign drugs strengthen the spleen, tonify the *qi*, and relieve diarrhea; *Coix lacryma-jobi* L. var. *mayuen* (Roman.) Stapf and *Dolichos lablab* L. can help sovereign drugs strengthen the spleen and excrete dampness. *Amomum villosum* Lour. and *Platycodon grandiflorum* (Jacq.) A. DC. are the assistant drugs; the former can enliven the spleen and regulate the stomach, promote *qi*, and relieve dyspepsia, and the latter can diffuse lung and facilitate *qi*, regulate waterways, take herbs bottom-up, and supplement spleen to nourish the lung. *Glycyrrhiza uralensis* Fisch., as the envoy drug, can invigorate the spleen and stomach and coordinate the drug's actions (Ma et al., 2019). Based on the interactions of these medicines, SLBZP exerts the effects of tonifying the stomach and spleen, eliminating dampness and promoting *qi*, to achieve the aim of treating disease. Modern pharmacological studies have shown that SLBZP has anti-inflammatory (Sun et al., 2020a), antioxidant (Xiong et al., 2021), and immunomodulatory (Li et al., 2014a) effect. It helps regulate gut microbiota (Mao et al., 2021a) and gastrointestinal motility (Lv et al., 2022) and also has anti-tumor (Chen et al., 2018a) potential. Generally, SLBZP is composed of mixed powders of 10 drugs in definite proportions (*Panax ginseng* C.A.Mey.: *Poria cocos* (Schw.) Wolf: *Atractylodes macrocephala* Koidz.: *Dioscorea opposita* Thunb.: *Dolichos lablab* L.: *Nelumbo nucifera* Gaertn: *Coix lacryma-jobi* L. var. *mayuen* (Roman.) Stapf: *Platycodon grandiflorum* (Jacq.) A. DC.: *Glycyrrhiza uralensis* Fisch. = 100: 100: 100: 100: 75: 50: 50: 50: 50: 100) and is to be consumed orally 2–3 times a day at a dose of 3–9 g (Ma et al., 2019).

3 Clinical research of SLBZP in treatment of UC

In the clinical prevention and treatment of UC, SLBZP can regulate immune function, decrease pro-inflammatory factors, increase anti-inflammatory factors, and regulate oxidative stress and the balance of gut microbiota (Ma et al., 2019). Additionally, SLBZP can reduce the MMP-2 and MMP-9 levels and ameliorate intestinal mucosal permeability (Wang, 2016). SLBZP, in combination with chemical drugs (such as mesalazine and sulfasalazine) and prescriptions (such as Tong Xie Yao Fang and Sishen pills), is generally prescribed in the current clinical practice. Studies indicated that SLBZP could enhance the therapeutic effects of chemical drugs and reduce side effects and recurrence rates (Xu et al., 2018; Tian et al., 2019). Moreover, powder and decoction are the most commonly used pharmaceutical dosage form of SLBZP, and there are fewer examples of SLBZP pills. Representative clinical studies and its pharmacological data including groups, dosage, treatment time and therapeutic effect are shown in Table 1.

3.1 Monotherapy

Clinical research has shown that both SLBZP and flavored SLBZP can significantly alleviate the symptoms in UC patients, including diarrhea, abdominal pain, and hematochezia, without significant adverse reactions. Moreover, SLBZP has fewer adverse reactions and better efficacy than chemical drugs. Studies showed that the combined efficacy of SLBZP was significantly higher than sulfasalazine (Ren, 2010; Qin, 2012; Xie et al., 2015). For example, among 150 patients with UC, 75 cases were given SLBZP (treatment group, 1 dose per day, decocted in water, twice daily), while another 75 were treated with sulfasalazine (control group, sulfasalazine, 0.5, 4 times a day), 1 month is a course of treatment, both groups were given medication for 2 courses before reexamination of colonoscopy. The results showed that the total efficiency in treatment group (96.4%) was better than that in control group (80.4%) (Qin, 2012). In another study, 106 cases with UC randomly divided into treatment group (SLBZP, 1 dose per day, decocted in water, twice daily) and control group (sulfasalazine, 1 g, 4 times a day) for 8 weeks. The total effective rate of treatment in the treatment group was higher than the control group, and the recurrence rate in the treatment group was considerably lower than sulfasalazine (Xie et al., 2015). Meanwhile, researchers also compared the efficacy of SLBZP and mesalazine for use in UC (He, 2014; Quan and Tan, 2017; Yang, 2017; Yang et al., 2021). For instance, 48 cases with UC randomly divided into treatment group (SLBZP, according to the prescription powder the herbs and mixed, 6 g each dose, 3 times a day) and control group (mesalazine, 1 g/time, 4 times a day) for 90 days. The total effective rate of treatment in the treatment group (91.67%) was higher than the control group (70.83%) (He, 2014). In addition, flavored SLBZP (1 dose per day, decocted in water, twice daily) could decrease the levels of IL-17, TNF- α , IL-23, CRP, and ESR and increase the levels of IL-10 in UC patients, and these effects were superior to mesalazine (1 g/time, 4 times a day) (Xu, 2021). Furthermore, flavored SLBZP (1 dose per day, decocted in water, twice daily) could promote the growth of probiotics and inhibit the proliferation and colonization of pathogenic bacteria by improving the intestinal microecological environment and protecting intestinal mucosa (Yang et al., 2021). Similarly, several studies indicated that the therapeutic effects of flavored SLBZP (1 dose per day, decocted in water, twice daily) were better than other chemical medicines, including domperidone (Sun and Chen, 2014), sulfamethoxazole and tetracycline combination (Tian and Song, 2015), and norfloxacin (Wang, 2019). The above research showed that SLBZP was superior to chemotherapeutics in improving the pathological changes and clinical manifestations of UC by reducing the inflammatory factors and regulating the balance of gut mucosa. However, there are some differences in the treatment time and dosage form of SLBZP, which may affect the results of the evaluation of therapeutic effects. Meanwhile,

the mechanism of action underlying SLBZP monotherapy needs further exploration.

3.2 Combination therapy

3.2.1 Combining with chemical drugs

Combination therapy is the most frequently used treatment modality of SLBZP, and mesalazine and sulfasalazine are the most commonly used chemical medicines combined with SLBZP in treating UC. In a trial, 96 cases of UC patients were randomly divided into control group and treatment group, and control group was treated with mesalazine (oral 1 g, 4 times a day) for 8 weeks, while treatment group was treated with the original treatment plan and combined with SLBZP (according to the prescription powder the herbs and mixed, 6 g each dose, 3 times a day) for 8 weeks. Results showed that the total effective rate of treatment in the treatment group was higher than the control group. While some adverse reactions were associated with SLBZP (powder, oral 6 g each dose, 3 times a day) and mesalazine (oral 1 g, 4 times a day) combination treatment, these were not significant (Chen et al., 2013). Meanwhile, numerous studies have now found that combined SLBZP and mesalazine could decrease the levels of CRP, ESR, IL-17, TNF- α , IL-23, IL-1 β , IL-18, IL-2, IL-6, IFN- γ and increase the levels of IL-4 (Wei et al., 2013; Ma et al., 2015; Zhou et al., 2018; Tian et al., 2019; Li et al., 2021c). Meanwhile, SLBZP (powder, oral 6 g each dose, 3 times a day) and mesalazine (oral 1 g, 4 times a day) in combination could inhibit the expression of NLRP3, ASC, and caspase-1 mRNA in UC patients (Zhou et al., 2018). Studies showed that SLBZP (flavored SLBZP, 1 dose per day, decocted in water, twice daily) and mesalazine (oral 1 g, 4 times a day) in combination exerted the antioxidant effects by increasing the serum MDA and serum SOD levels (Shi et al., 2018a). Meanwhile, SLBZP (granule/powder, oral 6 g each dose, 3 times a day) and mesalazine (oral 1 g, 3–4 times a day) combination exert immunomodulatory effect by changing the serum IgA and IgM levels as well as the ratio of Th17, Treg, CD4⁺ T, and CD8⁺ T cells (Qian and Zhang, 2019; Tian et al., 2019). In addition, SLBZP (powder, oral 6 g each dose, 3 times a day) and mesalazine (oral 1 g, 3–4 times a day) in combination could decrease the serum MMP-2 and MMP-9 levels, ameliorate intestinal mucosa permeability, and improve the symptoms of UC patients (Wang, 2016).

Compared with mesalazine, the side effects of sulfasalazine were commonly observed in clinical practice (Ungaro et al., 2017). However, studies indicated that flavored SLBZP and sulfasalazine in combination could significantly decrease the side effects such as nausea, emesis, and inappetence, which were caused by sulfasalazine alone when treating UC. Among 56 patients with UC, 28 cases were given sulfasalazine (control group, 1 g/time, 4 times a day), while another 28 were treated with the original treatment plan and combined with flavored SLBZP (treatment

group, flavored SLBZP, 1 dose per day, decocted in water, twice daily) for 30 days. The results showed that the total efficiency in treatment group was better than that in control group, and flavored SLBZP and sulfasalazine in combination could significantly decrease the side effects such as nausea, emesis, and inappetence, which were caused by sulfasalazine alone when treating UC (Zhang, 2017). Meanwhile, the recurrence rate was significantly lower than sulfasalazine alone (Yang, 2012; Ouyang, 2015; Yu, 2017). Further, SLBZP (pill, oral 6 g each dose, 3 times a day) and sulfasalazine (oral 1 g, 3–4 times a day) in combination could significantly decrease the levels of IL-2 and INF- γ , and increase the levels of IL-10 in older adults with UC (Zhao et al., 2017). Studies showed that SLBZP (1 dose per day, decocted in water, thice daily) and sulfasalazine (oral 1 g, 4 times a day) in combination could improve immune function and reduce inflammatory response by downregulating the levels of IL-6, IL-8, CD8⁺ T cells and upregulating the levels of CD3⁺, CD4⁺, CD4⁺/CD8⁺ (Xu et al., 2018). In addition, SLBZP (granule, oral 6 g each dose, 3 times a day) and sulfasalazine (oral 1 g, 4 times a day) combination could downregulate the levels of IL-1 β , IL-6, IL-8, TNF- α , INF- γ , HIF- α , IGF-1, and MMP-9, the expression of NF- κ B p65, β 2AR, and β -arrestin 2 protein, in turn, restore the injured intestinal mucosa and achieving therapeutic effects (Chen et al., 2020; Chen and Zhang, 2020).

Furthermore, in combination, SLBZP, lacteol fort, and sulfasalazine could improve the syndromes and promote intestinal mucosal repair, and it has no significant adverse effects (Xiang et al., 2017). Moreover, SLBZP combined with bifid triple viable capsule powder composed of *Bifidobacterium*, *Lactobacillus*, and *Streptococcus faecalis* has also been used to treat UC. Studies indicated that in combination, SLBZP and bifid triple viable capsule powder had good therapeutical effects on UC and were better than sulfasalazine (Zhu, 2012; Ma, 2019).

3.2.2 Combining with TCM prescriptions

Besides using a combination of chemical medicines, some studies have been conducted on the SLBZP combination with other TCM prescriptions for treating UC in the clinic. Studies showed that combining flavored SLBZP with TCM prescriptions such as Taohong Siwu decoction, Tong Xie Yao Fang, and Shaoyao Gancao decoction could improve the syndromes of UC patients and the therapeutic effects were superior to monotherapy with chemical medicines (Zhou, 2009; Li, 2013; Jiang, 2019).

Additionally, the different syndromes of UC patients in TCM, including spleen and kidney *yang* deficiency syndrome, *hot* and dampness syndrome, spleen deficiency and dampness syndrome, and liver depression and spleen deficiency syndrome, were respectively treated by combining SLBZP with Sishen pills (Ma, 2021; Shen et al., 2021), Shaoyao decoction (Luo et al., 2014), Gegenqinlian decoction (Zhang et al., 2022a), and Tong Xie Yao Fang (Zhu and Li, 2012). Meanwhile, researchers showed that SLBZP and Sishen pill in combination could significantly decrease CRP and ESR levels, reduce the number of *Escherichia*

coli, decrease the levels of ET, D-lactate, and DAO in serum, and increase the numbers of *Bifidobacterium* and *Lactobacillus*, in turn decreasing the inflammatory response and improving the intestinal flora structure and promoting repair of intestinal mucosal barrier (Ma, 2021; Shen et al., 2021).

3.2.3 Combining with enema and acupuncture

Other than oral delivery of therapeutic agents, some studies have examined the combination of SLBZP with enema and acupuncture for treating UC in clinical practice. Treatments involving enema using the kangfuxin liquid (enema, 200 ml, once a day) combined with SLBZP (1 dose per day, decocted in water, twice daily) and mesalazine (oral 1 g, 4 times a day) showed that the effects of combination therapy were better, and the occurrence of adverse reactions was lower than mesalazine alone (Lai et al., 2014; Mu and Xiao, 2016). Meanwhile, combining SLBZP or other prescription enemas, SLBZP and mesalazine in combination for treating UC was widely used to treat UC, and it was found to be highly effective (Chen, 2014; Tian, 2019; Sun and Guo, 2022). Furthermore, a study found that flavored SLBZP (1 dose per day, decocted in water, twice daily), mesalazine (oral 1 g, 3 times a day), and enema (100 ml, once a day) could improve TCM syndrome score and Mayo score, decrease the levels of IL-2, IL-17, TNF- α , INF- γ , and increase the levels of IL-10 in UC patients (Yi et al., 2021). Additionally, warm acupuncture combined with flavored SLBZP (1 dose per day, decocted in water, twice daily) could decrease the serum 5-HT and SP, numbers of intestinal yeast, serum IL-6 and TNF- α levels, and increase the levels of IL-10, SS, and VIP, intestinal *Bifidobacterium*, *Lactobacillus*, and the number of *Peptococcus*, in turn improving the clinical symptoms that may be related to the correction of abnormal brain-gut axis and antagonistic inflammatory response (Zhou et al., 2021a). Meanwhile, flavored SLBZP (1 dose per day, decocted in water, twice daily) and acupuncture in combination exhibited immunomodulatory effects by regulating the levels of Th17, Treg, Th17/Treg, TNF- α , HMGB-1, HIF-1 α , and IGF-1 (Hua, 2022).

3.3 Meta-analysis on effectiveness and safety of SLBZP in treatment of UC

Evidence based medicine (EBM) is the dominant paradigm in assessing the effectiveness of clinical treatments. The processes of EBM mainly contain several steps: 1) pose questions; 2) search relative data; 3) quantitative statistical analysis; 4) systematic evaluation; 5) promote the effective treatment methods and abandon ineffective, or even harmful, treatment methods (Djulgovic and Guyatt, 2017). Systematic reviews, including a quantitative and qualitative evaluation, are currently considered to be the best evidences. Meta-analyses are the

most common form of quantitative evaluation. Compare with traditional literature review, meta-analyses can improve the power of test by summarizing results and increasing sample size, and thus closer to reality (Hernandez et al., 2020). In recent years, several studies had been performed to evaluate the effectiveness and safety of SLBZP in treatment of UC by meta-analyses (Wu et al., 2017; Yang et al., 2018). For example, a meta-analysis conducted by Xiangtao Wen et al., included thirteen randomized controlled trials (RCTs) containing of 659 UC patients treated with SLBZP therapy and 598 patients treated with western medicine. The results showed the effectiveness of SLBZP was higher than that of western medicine (RR = 1.17, 95%CI [1.13, 1.22], $p < 0.001$), could significantly improve time of diarrhea (RR = -12.32, 95% CI [-14.27, -10.37], $p < 0.001$), abdominal pain (RR = -8.06, 95%CI [-9.88, -6.24], $p < 0.001$), sepsis (RR = -9.89, 95%CI [-10.77, -9.00], $p < 0.001$), and fever (RR = -8.29, 95%CI [-9.59, -6.98], $p < 0.001$), and significantly decrease the adverse events (RR = 0.06, 95%CI [0.01, 0.40], $p = 0.004$) (Wen et al., 2017). In addition, another meta-analysis had been conducted by Yin et al., included seventeen RCTs with a total sample of 1263 UC treated with mesalazine (control group) and SLBZP combined with mesalazine (test group) (Yin et al., 2021). Results indicated that the total effective rate of patients in the combination group was higher than that in the mesalazine group (OR = 2.03, 95%CI [1.60, 2.58], $p < 0.05$). And the level of IL-17 (MD = -88.29, 95%CI [-100.37, -76.21], $p < 0.00001$), IL-23 (MD = -115.34, 95%CI [-130.69, -99.99], $p < 0.00001$), TNF- α (MD = -10.64, 95%CI [-11.65, -9.64], $p < 0.00001$), ESR (MD = -8.22, 95%CI [-9.31, -7.12], $p < 0.00001$), and CRP (MD = -6.74, 95%CI [-9.99, -3.48], $p < 0.00001$) in the combination group were significantly lower than those in the mesalazine group. Based on these findings, SLBZP or SLBZP combined with mesalazine proved superior to mesalazine in treating UC, and can also reduce inflammatory factors in UC. However, more large-sample-size double-blind RCTs shall be included to support this conclusion.

4 Studies assessing the mechanism of SLBZP in the treatment of UC

SLBZP helps prevent and treat UC by exerting immunomodulatory and antioxidant effects, repairing the intestinal mucosal damage, protecting the gut mucosa barrier, regulating relative signal pathways (including MAPK signaling pathway, toll-like receptors (TLR)/NF- κ B signaling pathway, JAK/STAT signaling pathway, endoplasmic reticulum stress, autophagy pathway, and pyroptosis), regulating the balance of gut microbiota, promoting the targeting of BMSCs to the colonic mucosa, and regulating the levels of AQP.

4.1 Immunomodulatory effects

4.1.1 Immune cells

Immune cells, including cells of the innate and adaptive immune response, play a critical role in the processes of UC. In the case of innate immune response cells, dendritic cells (DCs) and macrophages have an important role in UC development (Kalužna et al., 2022). Antigen-presenting cells like macrophages and DCs, express a diverse repertoire of pattern recognition receptors, such as Toll-like receptors (TLRs), which play critical roles in the development of immune responses. So far, ten TLRs (TLR1–TLR10) have been identified in humans, which can recognize pathogens such as bacteria, viruses, LPS and endogenous DNA or RNA (Vijay, 2018). The mutation and maladjustment of TLRs is a key factor underlying susceptibility to UC (Kordjazy et al., 2018). According to some studies, higher levels of TLR2 and TLR4 mRNA and protein were observed in UC patients, suggesting that these receptors may play an important role in the pathogenesis of this disease (Fan and Liu, 2015; Kobayashi et al., 2020). Meanwhile, TLRs except for TLR3 activate the adaptor myeloid differentiation factor 88 (MyD88), resulting in NF- κ B activation, cytokine secretion and inducing DCs maturation; these cytokines further activate TLRs/NF- κ B signal pathway, which in turn further aggravate the inflammatory response (Dalod et al., 2014; Ungaro et al., 2017). Several studies showed that SLBZP efficiently inhibited the expression of TLRs and contributed to alleviate UC-induced inflammation. For example, the UC model mice (Kunming mice, SPF, male, weighing 34 ± 2 g) were induced by 3% dextran sodium sulfate (DSS), and oral administration with mesalazine (0.4 g/kg), SLBZP (31.2, 15.6, 7.8 g/kg, powder of SLBZP was dissolved in saline, the dose expression is equivalent to the weight of the original medicine, medicine, the dosage expression of SLBZS in the following is the same as this), and vehicle (water) once a day for 14 days. The results indicated that SLBZP could improve the symptoms of UC rats by decreasing the levels of TNF- α and MIF in serum, inhibiting the expression of TLR4 and NF- κ B protein in colon tissue, and increasing the IL-10 and EGF levels (Sun et al., 2020a). Further, rats (Wistar rats, SPF, weighing 200 ± 20 g) were randomly divided into five groups: normal group, UC model group, SLBZP group, SLBZS + TLR2 agonist (Pam3csk4) group, and SLBZS + TLR2 antagonist (T2.5) group. All except the normal group were induced by environment and diet intervention combined with composite trinitrobenzene sulfonic acid (TNBS), ethanol in enema. Rats in normal group and UC model group orally given vehicle (0.9% sodium chloride injection, 10 ml/kg). Rats in SLBZP group orally given SLBZS (15.6 g/kg, concentrated water decoction). Prior to the oral administration with SLBZS (15.6 g/kg), rats in SLBZS + TLR2 agonist group and SLBZS + TLR2 antagonist group received respectively TLR2 agonist dose of 50 μ g/mice and TLR2 antagonist dose of 2.4 μ g/mice injected IV via the tail vein. Results showed that the IL-6, IL-1 β ,

and TNF- α levels, the protein and mRNA expression of TLR2, MyD88, and COX-2 of UC rats were significantly increased in the UC model group; the levels significantly decreased in UC rats treated with SLBZP and TLR2 antagonist (Li et al., 2021a).

Macrophages also show significant functional differences depending on the tissue environment. During inflammation, the cytokines responsible for macrophage activation are secreted, and depending on the activation method, macrophages can be divided into classically activated (M1) or alternatively activated (M2). A murine model of experimental colitis showed that DSS increased the proportion of P1 peritoneal macrophages, which was restored by SLBZP (1.8, 3.6 g/kg) treatment. Moreover, a co-culturing system was established to decipher the interaction between BMDMs and NCM460 cells treated with TNF- α and/or SLBZP serum (the serum was obtained from colitis mice subjected to 3.6 g/kg SLBP treatment). Consistently, the proportion of P2-P4 macrophages was higher in the SLBZ group, concomitant with a decreased migration capacity, implying the transition to M2 macrophages (Yu et al., 2022).

Unlike the innate immune system, the adaptive immune system must be activated before a specific immune response can occur. Upon being stimulated by inflammatory cytokines, the naive T cells begin to differentiate into different lineages, including Th cells, Th1 cells, Th2 cells, Th17 cells, and Treg cells, which play a key role in the development and progression of UC. Depending on the expression of the CD4 and CD8 cell surface molecules, lymphocytes can be divided into T CD8⁺ (mainly cytotoxic cells) and T CD4⁺ cells (Rabe, et al., 2019). UC model mice (Kunming mice, SPF, male, weighing 20 ± 2 g) were induced by TNBS, and oral administration with dexamethasone (1 mg/kg), SLBZP (1.4, 2.8, 5.6 g/kg, powder of SLBZP was dissolved in saline), and vehicle (water) once a day for 10 days. Results indicated that high dosage of SLBZP (5.6 g/kg) could significantly increase the serum IL-10 level and the ratio of CD4⁺, CD25⁺, and Foxp3⁺ cells to CD4⁺ T cells and decrease serum IL-1 β and TNF- α levels, in turn, treating UC mice (Li et al., 2014b). Further, a study showed that SLBZP (7.5, 15, 30 g/kg, concentrated water decoction) could regulate the balance of Th17/Treg and restore the immune function of UC rats by downregulating the levels of IL-17, IL-23, IL-6, TNF- α and upregulating the levels of IL-10 (Li et al., 2017). Another study also showed that after 21 days treatment of SLBZP (6, 12, 24 g/kg, concentrated water decoction), high dose of SLBZP could ameliorate the symptoms of UC rats by regulating the balance of Th17/Treg and decreasing the expression of c-fos in colon tissue (Yu et al., 2018). In addition, UC model rats were induced by TNBS, and oral administration with mesalazine (0.4 g/kg), SLBZP (11.3, 22.6, 45.2 g/kg, concentrated water decoction), and vehicle (0.9% sodium chloride injection) once a day for 14 days. Results showed that middle dosage and high dosage of SLBZP had a therapeutic effects on UC, and it was related to the regulation of expression of ROR γ t/FoxP3 and

correction of the imbalance of Th17/Treg (Qi et al., 2022). As shown in Figure 3.

4.1.2 Inflammatory factors

The imbalance of pro-inflammatory and anti-inflammatory cytokines remains one of the key factors causing UC (Xu et al., 2016). Lamina propria macrophages and T cells are activated when the intestinal mucosal barrier is damaged. These secrete pro-inflammatory cytokines such as IL-1, IL-6, IL-17, IL-23, and TNF- α . Meanwhile, these pro-inflammatory cytokines stimulate immune cells to secrete more pro-inflammatory cytokines. Ultimately, the balance of pro-inflammatory and anti-inflammatory cytokines is disturbed, leading to a cytokine storm, and causing continuous inflammation of intestinal mucosa and ulcer (Isidro et al., 2014). Studies showed that SLBZP (1.4, 2.8, 5.6 g/kg, powder of SLBZP was dissolved in saline) could downregulate TNF- α and IL-1 β levels and upregulate IL-10 levels in the colon tissue of TNBS-induced rats (Li et al., 2014a). Another study indicated that the levels of IL-6, IL-8, TNF- α , and the expression of NF- κ B and p65 increased significantly in UC rats; these levels decreased significantly in rats treated with SLBZP (12 g/kg, concentrated water decoction) (Li et al., 2015a). Additionally, a large amount of literature also suggests that SLBZP affects the levels of other cytokines (IL-3, IL-13, IL-33, TGF- β , IL-4, IL-17, IL-23) (Li et al., 2015b; Bi et al., 2017; Chen et al., 2018a; Ding et al., 2018), and the major cytokines involved in SLBZP treatment for UC are shown in Supplementary Table S1.

4.2 Gut mucosa barrier

The gut mucosal barrier, consisting of mechanical, chemical, immunological, and biological barriers, is an important system of intestinal defense and maintains the integrity of the intestinal barrier and gut homeostasis by isolating the harmful elements. The mechanical barrier includes intestinal mucosa epithelial cells (ICEs) covered with mucosal layer and intercellular tight junctions (with components such as occludin, claudin, and ZO-1) and is the structural foundation for protecting against pathogen invasion and maintaining the intestinal permeability. Intestinal lymph and secretion immune proteins, resident flora, glycoproteins, and digestive juices secreted by ICEs, respectively, are the components of chemical, immunological, and biological barriers. Research has confirmed that mechanical, chemical, immunological, and biological barriers are involved in the pathogenesis of UC (Actis et al., 2014). When the gut mucosa barrier is damaged in UC, many inflammatory factors are produced. These factors can not only induce the apoptosis of ICEs, but can also influence the expression and distribution of tight junction proteins through MLCK and PKC signaling pathways, damage the structure of the mechanical mucosal barrier, and induce intestinal immune response (Actis et al., 2014).

One study found that SLBZP (3, 6, 12 g/kg, concentrated water decoction) could help heal the tight junction of UC mice by increasing the expression of colonic components such as occludin, claudin, ZO-1, as well as JAM gene and protein (Liu et al., 2015). Another study showed that the expression levels of occludin in the colonic tissue were significantly downregulated and expression levels of P65, MLCK, MLC2, P-MLC were significantly upregulated in UC mice. Following treatment with sulfasalazine (0.52 g/kg) and SLBZP (7.8, 15.6, 31.2 g/kg, concentrated water decoction), these indicators improved significantly, in particular, high dosage of SLBZP (Liu et al., 2018a). These results indicated that SLBZP downregulates the expression of occludin, claudin, ZO-1, and JAM protein in the colon tissue, thus maintaining the normal permeability of the intestinal mucosa and repairing the intestinal mucosal damage, which may involve inhibition of the MLCK/MLC signaling pathway. Additionally, extracellular matrix degradation can increase intestinal permeability and decrease the barrier function of the intestinal mucosa, which plays an important role in the pathogenesis of UC (Kirov et al., 2019). Matrix metalloproteinases (MMPs) are proteolytic enzymes that degrade ECM proteins. The pro-inflammatory factor can stimulate the proteolytic enzymes, and activated MMPs can further aggravate the inflammatory response of the intestinal tract (Bai et al., 2020). MMP-2 and MMP-9 are the major gelatinases among MMPs, which can degrade collagen type IV to prevent cell infiltration and inflammatory proliferation. A clinical study indicated that SLBZP (1 dose per day, decocted in water, twice daily) could improve the symptoms of UC patients, and the mechanism may involve a decrease in the expression of MMP-2 and MMP-9 (Wang, 2016).

4.3 Mesenchymal stem cells and cell adhesion molecules

Repair and reconstruction of the damaged colonic mucosa are central to UC treatment. The repair and reconstruction of colonic mucosa rely primarily on colonic mucosa stem cells that can differentiate into mature colonic mucosa cells (He et al., 2012b). Bone mesenchymal stem cells (BMSCs) have good immune regulatory effects and homing feature that promotes migration to the injury site, adhesion, and colonization, in turn repairing and reconstructing the colonic mucosal tissue of UC (Zheng and Wang, 2022). The differentiation, growth, migration, and homing of BMSCs are regulated by a combination of various factors, including several chemokines and adhesion molecules (such as ICAM-1, VCAM-1, and VLA-4) (He et al., 2012a). The study revealed that inflammatory damage to UC could promote homing of BMSCs to colon tissue; however, it did not play a role in the repair and regeneration of the tissue injured due to UC. Research indicated that SLBZP (22.6 g/kg, concentrated water decoction) could not only promote BMSCs homing to colon tissue but also help repair and regenerate tissue injured due to UC, which may involve the

enhancement of the SDF-1/CXCR4 signaling pathway (Cui et al., 2020). Meanwhile, studies have shown that SLBZP (22.6 g/kg, concentrated water decoction) could promote the proliferation and migration of BMSCs and increase the adhesion properties by regulating the expression of VCAM-1 and VLA-4 (Liu et al., 2018b; Shi et al., 2018a).

4.4 Antioxidant effect

Reactive oxygen species (ROS) and reactive nitrogen species (RNS) are produced during oxygen metabolism, and low-to medium-concentration ROS and RNS are molecular signals of mitogenic response or defense responses against invasion by pathogens; excessive expression of these factors can induce oxidative stress (Li et al., 2020a). Oxidative stress altering the inflammatory response causes damage to lipids, proteins, and DNA, and also results in cell apoptosis and cancer cell transformation, which is potentially dangerous. Research showed that oxidative stress is a key factor involved in the progression of many diseases such as UC (Piechota-Polanczyk and Fichna, 2014). Antioxidants inhibit the process of cell oxidation or scavenge ROS, such as free radicals. When antioxidants are inadequate or exhibit lower activity, oxidant molecules can prevail, disrupting the cell functions and leading to cell death. The endogenous cellular antioxidant defense system consists of enzymatic antioxidants (SOD, CAT, GSH-Px, and GR) and non-enzymatic antioxidants (antioxidant vitamins, trace elements, coenzymes, and cofactors) (Wang et al., 2019). Abnormal free radical metabolism is generally observed in UC patients, and the ROS can induce excess lipid oxidation in UC, exacerbating the damage to intestinal mucosa (Pavlick et al., 2002). Therefore, maintaining the oxidant/antioxidant status balance is critical to treating UC and SOD, and MDA plays a significant role in balancing the system. SOD represents the ability to scavenge free radicals and can inhibit the response of excess lipid peroxidation. MDA levels reflect the degree of lipid peroxidation in the body and indirectly reflect the degree of cellular damage (Deng et al., 2016). In a study UC model rats were induced by environment and diet intervention combined with composite TNBS and ethanol, and oral administration with sulfasalazine (0.5 g/kg), SLBZP (12 g/kg, concentrated water decoction), and vehicle (0.9% sodium chloride injection) once a day for 14 days results showed that SLBZP could increase the SOD levels and decrease MDA levels, subsequently leading to clinical benefits in UC rats (Li et al., 2012). In another study, UC model rats were treated with SLBZP (0.472, 0.945, 1.89 g/kg, granule of SLBZP was dissolved in water). Compared with the control group, the levels of PCT, CRP, EPO, and HIF-1 α were significantly upregulated, and levels of iNOS, MPO, SOD, and MDA were significantly downregulated in the model group. Compared with the model group, the levels of PCT, CRP, EPO, and HIF-1 α were significantly downregulated, and

levels of iNOS, MPO, SOD, and MDA were significantly upregulated in the SLBZP group, in particular, high dosage SLBZP group (Xiong et al., 2021).

4.5 Regulation of signaling pathways

4.5.1 MAPK signaling pathway

MAPK is a highly conservative signal-transducing module in eukaryotic cells and is an important member involved in the interaction between the inner and outer in cell reaction, which can mediate extracellular signals stimulation to intracellular and regulate the progress of cell growth, differentiation, migration, and inflammation. The MAPK family is composed of the extracellular regulated kinase (ERK) 1/2, JNK, and p38 MAPK. MAPK pathway can be activated by several stimuli such as inflammatory cytokines, growth factors, and cellular stress. MAPK pathway can activate the c-Jun and c-fos through a cascade of ERK, JNK, and p38 MAPK, which regulate the expression of inflammatory cytokines including IL-1, TNF- α , and IL-6 and contribute to intestinal mucosal inflammation (Jing et al., 2019). In an animal experiment, UC rats were induced by the environment and diet intervention combined with composite TNBS and ethanol in enema and treated with SLBZP (12 g/kg, concentrated water decoction). ERK and p38MAPK protein expression were significantly increased in the model group, while SLBZP could reserve those indicators (Li et al., 2013). Another experiment showed that the expression of p38 MAPK, and TNF- α levels were significantly downregulated, and IL-4 protein of UC rats were significantly upregulated in the SLBZP group (24 g/kg, concentrated water decoction) (Bi et al., 2017). These findings indicated that upregulation of IL-4 concentration as well as downregulation of TNF- α concentration by the MAPK pathway might be a part of the mechanism of SLBZP to treat UC.

4.5.2 TLRs/NF- κ B signaling pathway

Studies have confirmed that the expression of relative genes (TLR4, MyD88, NF- κ B), mRNA, and proteins from the TLR/MyD88-dependent pathway were significantly upregulated in UC. In contrast, negative regulation of the TLRs/NF- κ B signaling pathway was effective in alleviating UC clinical syndromes (Li et al., 2019). Under normal physiological conditions, NF- κ B is inhibited by binding I κ B and is retained in the cytoplasm. Upon cellular stimulation, the active signal of NF- κ B can activate the IKK to induce phosphorylation and degradation of I κ B, so as to prevent the inhibition of NF- κ B by I κ B. Thus, NF- κ B protein when activated, facilitates the transcription and expression of downstream genes, playing a regulatory role in body immunity, cell inflammatory, cell survival, cell growth, cell differentiation, and apoptosis (Wullaert et al., 2011). Studies also showed that SLBZP could ameliorate clinical syndromes of UC by upregulating serum IL-

10 and EGF levels, downregulating serum TNF- α and MIF levels, and the expression of TLR4 and NF- κ B proteins (Sun et al., 2020b). Another study indicated that SLBZP (15.6 g/kg, concentrated water decoction) could decrease the levels of serum TNF- α , IL-6, IL-1 β , and the expression of TLR2, MyD88, COX-2 mRNA and proteins in UC rats (Li et al., 2021b). Moreover, SLBZP (15.6 g/kg, concentrated water decoction) could decrease the concentrations of IL-17, IL-23, IL-6, TNF- α , and IL-1 β , decrease the expression of NF- κ B p65, I κ B β , and increase the expression of I κ B α protein in the UC (Chen et al., 2018b; Li et al., 2020b). These results indicated that SLBZP could reduce the inflammatory response through the negative regulation of the TLRs/NF- κ B signaling pathway, which might be an important mechanism through which SLBZP helps treat UC.

4.5.3 JAK/STAT signaling pathway

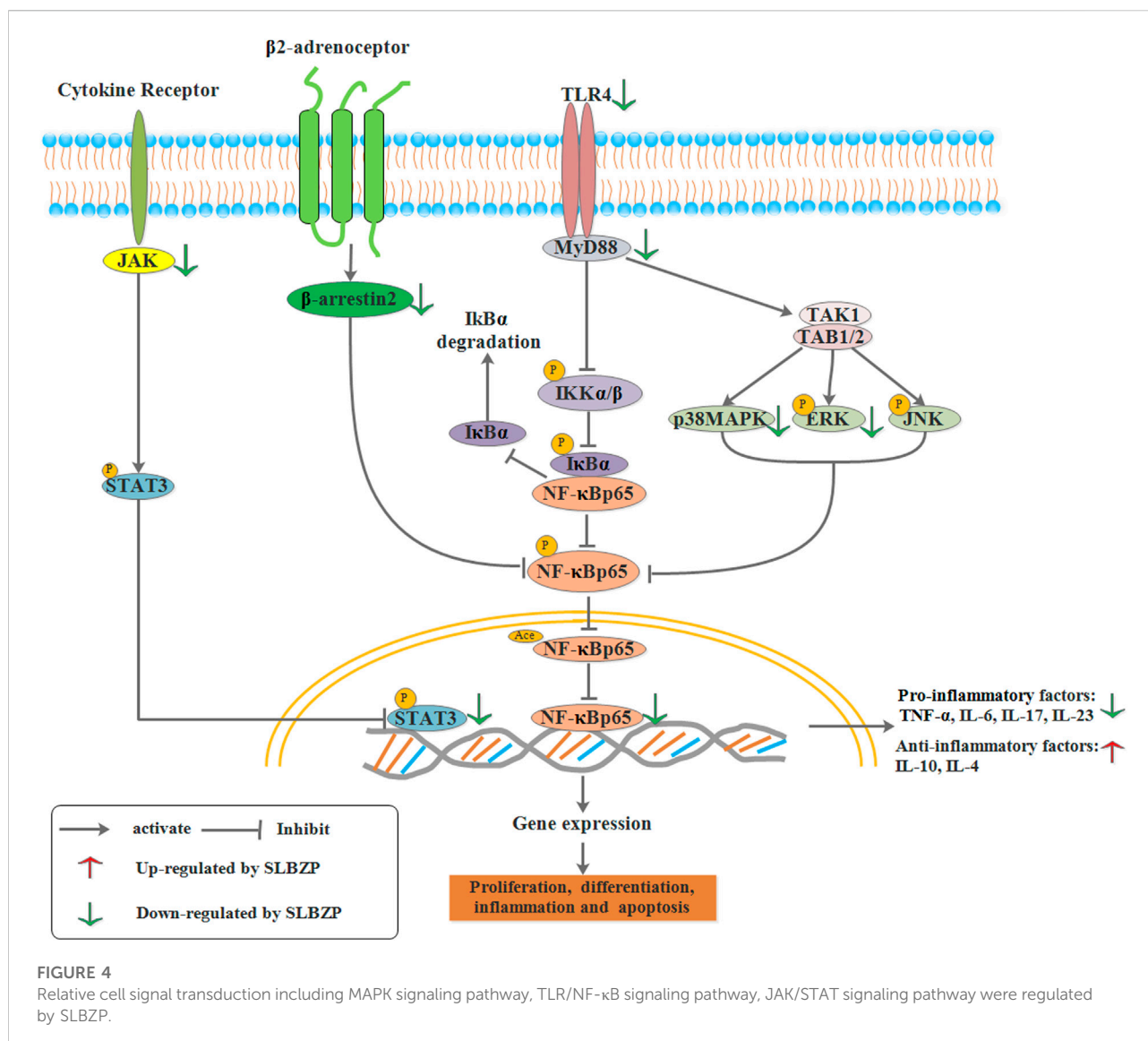
JAK/STAT signaling pathway consists of tyrosine kinase-associated receptor, JAK/STAT, and tyrosine kinase-coupled receptors is a common pathway underlying numerous cellular signal transduction pathways. It plays an important role in physiology and pathology, including immune defense, cell differentiation, cell growth, cell apoptosis, and tumorigenesis (Xin et al., 2020). The JAK family includes JAK1, JAK2, JAK3, and TYK2. JAK1, JAK2, and TYK2 are present in various cells and tissues, while JAK3 only exists in the bone marrow and lymphatic system. STATs, a family of latent cytoplasmic proteins, are the substrate of JAK, which can couple with the signaling pathway of tyrosine phosphorylation, thus exerting biological effects through transcription control (Xin et al., 2020). JAK plays a role in the inflammatory response, while JAK inhibitor can relieve the UC to some extent, a potential therapeutic approach to treat UC (Cordes et al., 2020). According to current research, STAT3 is known to be related to colonic inflammation and activated by different cytokines and growth factors (Jin et al., 2017). Increased STAT3 phosphorylation at tyrosine residues is found in the UC model induced by DSS and in the epithelial tissue and lamina propria cells of UC patients (Aggarwal et al., 2009). Animal experiments showed that the concentration of serum IL-6, and the expression of STAT3 and JAK2 protein in SLBZP (12, 24 g/kg, concentrated water decoction) and mesalazine (0.3 g/kg) groups were significantly lower than those in the model group. In comparison, the concentration of serum IL-10 was significantly higher than that in the UC model group. It showed that the mechanism of SLBZP in treating UC might involve inhibition of the JAK/STAT3 signal pathway (Tong, 2021). As shown in Figure 4.

4.5.4 Endoplasmic reticulum stress pathway and autophagy

The endoplasmic reticulum (ER) is an important subcellular organelle involved in protein synthesis, post-translational modification, and proper folding. When the intracellular

environment changes, the endoplasmic reticulum stress (ERs) is activated to combat the protein misfolding and synthesis damage through multiple ways. While holding the balance of the endoplasmic reticulum, excessive ERs will induce cell apoptosis. ERs alleviate the cell burden in two ways: they strengthen the ability of folding and processing to relieve the accumulation of protein and also relieve the synthesis of new protein. The process is finished by unfolded protein responses (UPR) that can activate the unfolded protein receptors, including IRE1, PERK, and ATF-6. Under the normal conditions, IRE1, PERK, and ATF-6 exhibit an inactive state by binding to the glucose-regulated protein 78 (GRP78). UPR can disaggregate the three proteins from GRP78, thus receiving and inhibiting ERs through the IRE1-XBP1 pathway, PERK-eIF2 α -ATF-4 pathway, and ATF-6 pathway. In addition, the CHOP pathway, IRE1-TRAF2-ASK1 pathway, and caspase pathway are pathways mediated by ERs and lead to cell apoptosis (Yap et al., 2021). ERs as a regulation mechanism widely exist in the body, which similarly plays an essential role in the pathological process of IBD (Bogaert et al., 2011). Research has shown that the expression of GRP78 and XBP1 increased significantly in UC patients (Shkoda et al., 2007; Tréton et al., 2011). ERs can activate NF- κ B to promote the inflammatory response, which can also induce ERs by active oxygen and TNF- α . A study found that phosphorylation of GRP78, IRE1, and the levels of CHOP were upregulated, and the cell apoptosis was increased in ATF6 α -/- mice, ultimately exhibiting severe damage of intestinal epithelial mucosa (Brandl et al., 2009). In cell and animal experiments, ERS of IEC-6 cells and UC mice were induced by LPS, and 5% DSS, respectively. The former was administered with the serum containing SLBZP (the serum was obtained from colitis mice subjected to 3.6 g/kg SLBP treatment), and the latter was administered with SLBZP (3, 6, 12 g/kg, concentrated water decoction). The results indicated that the expression of GRP78, IRE1, P-IRE1, PERK, pJNK, P-eIF2 α , and CHOP proteins were significantly increased in ERS of IEC-6 cell and UC mice while they decreased significantly in ERs of IEC-6 cell and UC mice treated with SLBZP (Xu, 2020). This suggests that SLBZP could regulate the ERs level of colon tissue through ERs pathways such as IRE1-XBP1, PERK-eIF2 α , and ATF-6 pathways, to alleviate intestinal injury in UC.

Autophagy involving the formation of autophagosomes, fusion with lysosomes, and degradation, is a ubiquitous phenomenon in eukaryotic cytoplasmic and plays a role in maintaining the cell survival and update, re-utilizing materials, and maintaining cellular environmental homeostasis (Zhao and Zhang, 2018). Autophagy-related genes (ATG), such as ATG5, ATG6, ATG8, and ATG12, play a very important role in autophagy (Lee and Tournier, 2011). The PI3K/Akt/mTOR pathway is a classical signal pathway involved in the regulation of autophagy. The PI3K is divided into three types: I, II, and III. The activation of PI3K type I can activate the downstream signaling pathway to block autophagy. Beclin1



(ATG6) activation by PI3K type III is an important step in the initiation of autophagy. p62 is an autophagic substrate protein that can bind to LC3, forming a complex followed by autophagic degradation (Liu et al., 2018c). LC3 converts to LC3-I and distributes in autophagic vesicle and autophagosome under normal conditions. When autophagy is induced, LC3-I is modified to LC3-II, which is integrated into the autophagosome membrane (Liu et al., 2016). In the IBD pathologic process, damage to the intestinal epithelial barrier and increased mucosal permeability lead to swelling and alimentary deficiency of intestinal epithelial cells, inhibiting autophagy (Liu et al., 2016). In a cell-based study, IEC-6 injury induced by LPS was treated with the serum containing SLBZP (the serum was obtained from rats subjected to 41.6 g/kg SLBP treatment). Results showed that the concentrations of IL-

1β, IL-8, and the expression of ATG5, ATG13, and ATG16 mRNA were significantly increased, and the level of IL-10 was significantly decreased in the model group compared with the blank group. These indicators were reversed in the SLBZP group, indicating that SLBZP could induce the inflammatory damage to IEC-6 cells through the autophagy pathway (Liu et al., 2019). In another animal experiment, UC was induced in mice by dosing with 5% DSS, and oral administration with mesalazine (2 g/kg), rapamycin (4 mg/kg), SLBZP (3, 6, 12 g/kg, concentrated water decoction), and vehicle (water) once a day for 15 days. The results showed that SLBZP could ameliorate UC syndrome by increasing the LC3-II, beclin1 phosphorylation, and 4EBP protein expression and inhibiting PI3K, mTOR, p-p62 phosphorylation, and ULK1 protein expression. These results were observed in

mesalazine group and rapamycin group. The above indicated that SLBZP helps treat UC by regulating the phosphorylation of PI3K, mTOR, and p-p62 proteins in the autophagy pathway of intestinal epithelial cells (You et al., 2019). These findings indicate that SLBZP regulates the ERs and autophagy signaling pathways, thus contributing to healing in UC (As shown in Figure 5).

4.5.5 Pyroptosis

Pyroptosis is a caspase-1-dependent (classical pathway) and caspase-11, -4/5-dependent (non-classical pathway) pathway of programmed cell death. It is characterized by the cytoplasmic membrane rupture in a short period and the release of cellular content and pro-inflammatory mediators, including IL-1 β , IL-18, and HMGB-1 (Walle and Lamkanfi, 2016). The pyroptosis process relies on caspase-1, -11, -4/5, vesicular shedding, and the cleavage of proteins like GSDMD that create pores in the cell membrane, which leads to cellular rupture and discharge of contents under osmotic pressure and cell membrane movement (Ding et al., 2016). Caspase-11 cleaves GSDMD and generates amino-terminal fragments, increasing the reliance on caspase-1 for pyroptosis and NLRP3 dependence in a cell-intrinsic manner. GSDMD-N is considered a key target of caspase-11 and a critical mediator of the host to gram-negative bacteria (Kayagaki et al., 2015). Demon D et al. found that caspase-1, -11, -4/5, and NLRP were highly expressed in intestinal cells and positively correlated with the severity of inflammation in UC (Demon et al., 2014). LPS from the wall of gram-negative bacteria could enter the cell, specifically activating the reliance on caspase 11 and IL-18 secretion of pyroptosis, resulting in cell death. Similarly, both caspase 1 and caspase 11 could lead to cell death. These results showed that caspase-11 and GSDMD-N drove the pro-immunogenic cell death signal (Shi et al., 2014). Animal experiments showed that SLBZP (1.18 g/kg, powder of SLBZP was dissolved in saline) could significantly decrease the levels of serum IL-18, TNF- α caspase-1, caspase-11, and the expression of GSDMD-N and NLRP3 protein in UC mice induced with DSS. These results indicated that the mechanism of SLBZP was related to the regulation of classical (caspase-1) and non-classical (caspase-11) pathways in pyroptosis, in which the non-classical (caspase-11) pathways may play a significant role (Li, 2019).

4.6 Aquaporins

The expression of aquaporins (AQPs) in the intestinal tissue is closely related to UC pathogenesis. Studies indicated that the low expression of AQPs was observed in the early stage of UC before the appearance of intestinal epithelial injury. AQPs are distributed extensively in the intestinal

tract and play an important in regulating water transport, permeability, secretion, and absorption of fluid in the intestinal tract (Cohly et al., 2008). Evidence showed that inhibiting the expression of AQP3 and AQP4 could cause diarrhea, leading to an inflammatory response, ultimately resulting in UC (Hardin et al., 2004; Planell et al., 2013). Additionally, the MAPK pathway consists of p38MAPK, ERK, and JUK, which can regulate cell growth, differentiation, and apoptosis, and take part in the regulation of AQP3 and AQP4 (Li et al., 2015c). Animal experiments indicated that SLBZP (12 g/kg, concentrated water decoction) could increase the expression of AQP3 and AQP4 in UC, and this effect was partially inhibited by U0126 (ERK1/2 inhibitor) or SB203580 (p38MAPK inhibitor). This suggests that SLBZP can ameliorate UC by increasing the expression of AQP3 and AQP4 through ERK/P38MAPK pathway (Li et al., 2015a).

4.7 Regulation of gut microbiota

Gut microbiota has important immune, metabolic, and intestinal protective functions. Moreover, gut microbiota can inhibit the growth of potentially pathogenic bacteria by producing antibacterial factors and colonization resistance. Gut microbiota in healthy individuals is in a dynamic equilibrium state. In contrast, UC patients or mice showed imbalance, manifested as the abundance of enteropathogenic bacteria and lack of beneficial bacteria in the intestinal tract (Yu, 2018). Studies have shown that *Escherichia/Shigella* and especially *Escherichia coli*, which belongs to the family Enterobacteriaceae, are enriched in patients or mice with UC. At the same time, firmicutes are in reduced quantity, particularly Blautia, Clostridium, Coprococcus, and Roseburia (Bian et al., 2020). In recent years, regulation of gut microbiota for UC treatment has added a new therapeutic strategy and has increased the possibility of curing UC patients (Chen et al., 2014). Animal experiments have shown that high dosage of SLBZP (24 g/kg, concentrated water decoction) could increase Prevotella and Oscillospira that produce SCFAs and decrease the opportunistic pathogens, including Desulfovibrio and Bilophila, which reduce the diversity of gut microbiota and increase abundance (Gu et al., 2021). Another clinical experiment showed that SLBZP combined mesalazine with (6 g of SLBZP particles three times a day; 6 g of mesalazine a day for 8 weeks) could improve the clinical syndrome of UC by regulating the gut microbiota and increasing the microbial levels of tryptophan metabolites, including indole-3-propionic acid and indole-3-acetic acid (Jiao et al., 2022). Only a few studies have assessed the effect of SLBZP on gut microbiota, and more in-depth and comprehensive research on gut microbiota and SLBZP in UC is needed in the future.

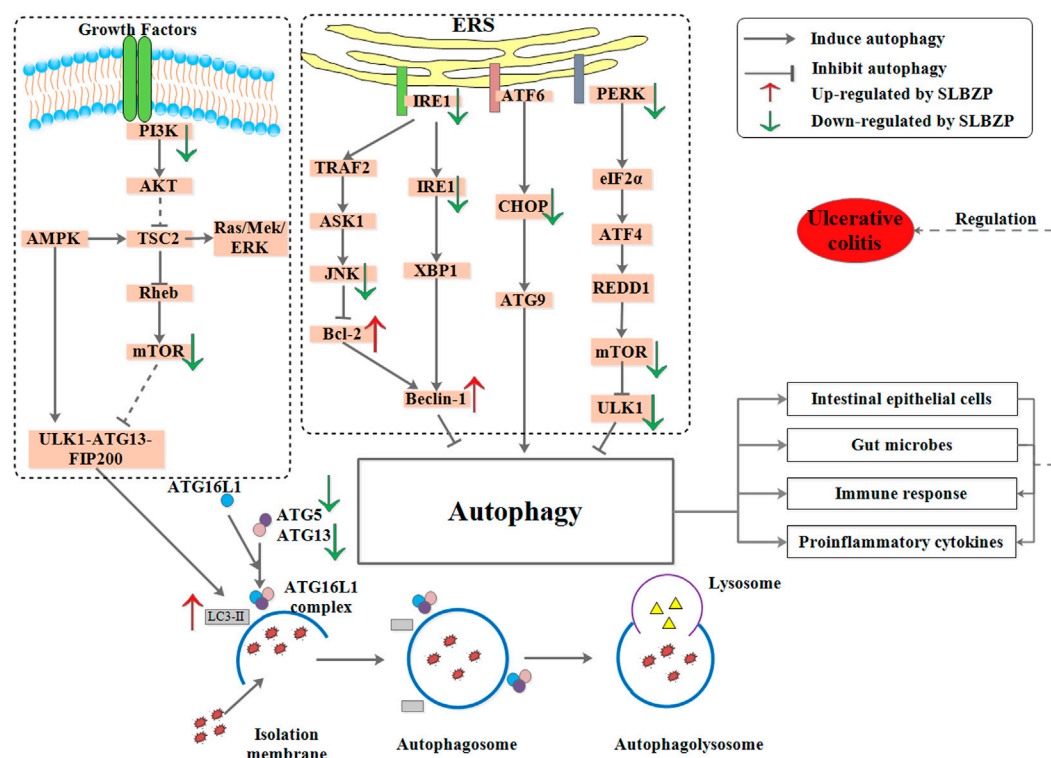


FIGURE 5
Autophagy and endoplasmic reticulum stress were regulated by SLBZP.

5 Pharmacological studies of a single Chinese herb and its active ingredients of SLBZP on UC

SLBZP contains 10 Chinese drugs derived from roots, rhizomes, seeds, seed kernels, fruits, and sclerotium. Over the years, the active components of these Chinese drugs, including triterpenoids, polysaccharides, volatile, flavonoids, alkaloids, and organic acids, have been studied by various researchers. The specific attributes of drugs are shown in [Supplementary Table S2](#), and their mechanisms are summarized in [Figure 6](#). The structures of prototype and metabolites components of herbs in SLBZP are shown in [Figure 7](#).

5.1 *Atractylodes macrocephala* Koidz. (Bai Zhu)

Atractylodes macrocephala Koidz., a common drug in TCM, possesses the effects of tonifying *qi* and strengthening the spleen. It is used to cure patients with splenic asthenia, anorexia, edema, excessive perspiration, and abnormal fetal movement. Modern

research showed that the major constituents of *Atractylodes macrocephala* Koidz. were sesquiterpenes, polyacetylenes, polysaccharides, and organic acids, exhibiting pleiotropic biological activities, including anti-inflammatory, anti-tumor, regulation of gastrointestinal function and immune function ([Yao et al., 2019](#)). In recent studies, *Atractylodes macrocephala* Koidz. and its constituents have demonstrated potential efficacy in different experimental models of UC. A study reported that the water extract of *Atractylodes macrocephala* Koidz. (10 g/kg, concentrated water decoction) could protect against the acetic acid and dinitrochlorobenzene-induced colitis in a rat model by regulating the levels of IL-2, IL-10, and IL-17 cytokines in serum ([Zhu et al., 2014](#)). Meanwhile, another study showed that *Atractylodes macrocephala* Koidz. (10 g/kg, concentrated water decoction) could reduce the expression of TNF- α , IL-6, and IL-1 β and regulate the balance of gut microbiota to treat the DSS-induced UC rats ([Ye et al., 2014a](#)). Similarly, the active ingredients of *Atractylodes macrocephala* Koidz., including polysaccharides, atractylenolide III, and atractylenolide I, exhibited potential efficacy in treating UC mice induced with DSS. Feng et al. reported that polysaccharides from *Atractylodes macrocephala* Koidz. (10, 20, 40 mg/kg) could regulate the

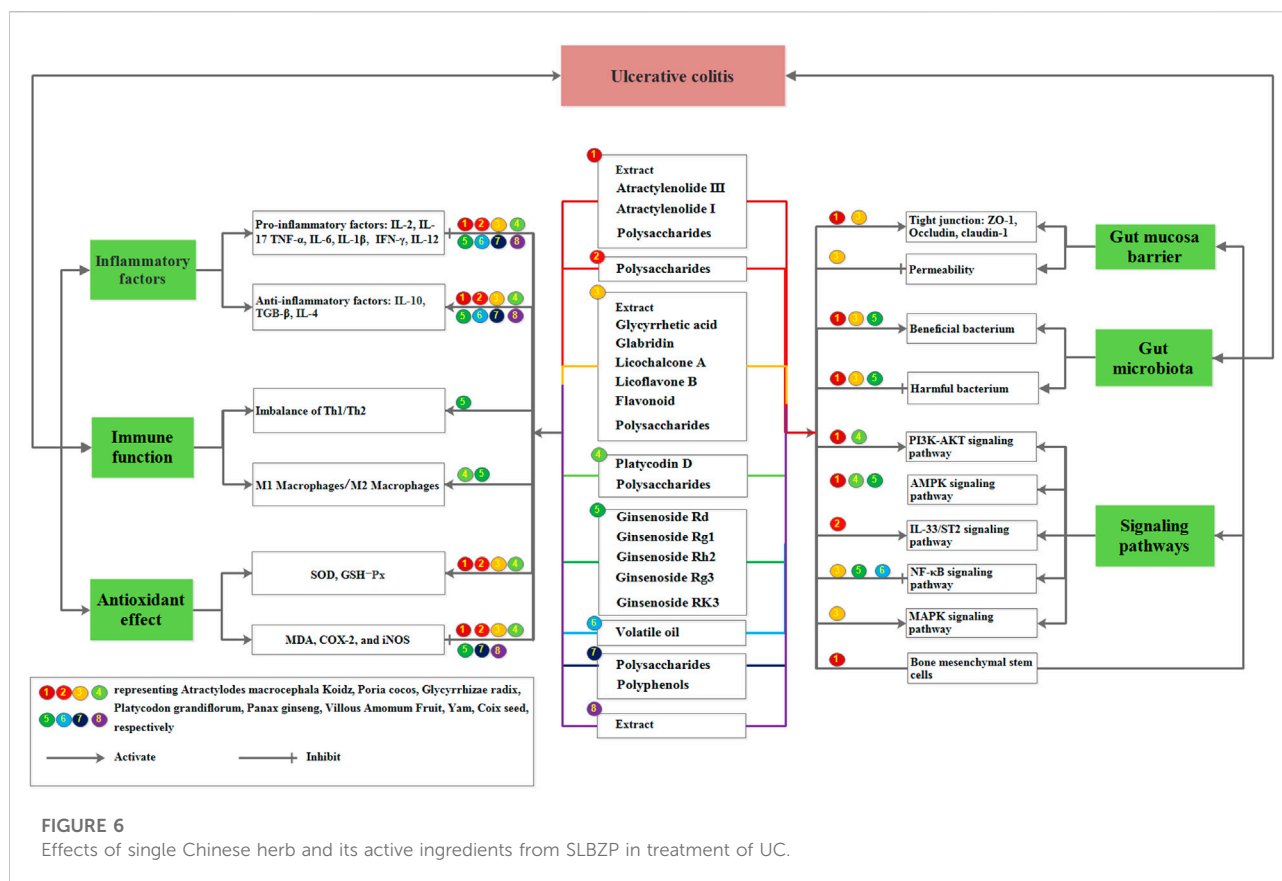


FIGURE 6

Effects of single Chinese herb and its active ingredients from SLBZP in treatment of UC.

balance of gut microbiota and its metabolism to achieve the therapeutic effects of UC (Feng et al., 2020). Additionally, polysaccharides from *Atractylodes macrocephala* Koidz. (540 mg/kg) could not only promote BMSC homing to the injured tissue and regulate cytokines such as IL-6, IL-10, IL-17 A, and TGF- β for preventing TNBS-induced rats colitis but also promote the migration of IEC *in vitro* and influence multiple genes (Zheng and Wang, 2022). Han and colleagues reported that atractylenolide III (5, 10 mg/kg) could ameliorate DSS-induced colitis inflammatory and oxidative stress by regulating the MDA and GSH contents, SOD activity, and the expression of TNF- α , IL-6, COX-2, and iNOS mRNA. Additionally, the intestinal epithelial barrier destruction and mitochondrial dysfunction were decreased. LPS-treated IEC-6 cells and DSS-induced colitis mouse model revealed that the expression of p-AMPK, SIRT1, and PGC-1 α , along with acetylated PGC-1 α , was facilitated by atractylenolide III (40 and 80 μ M) (Han et al., 2022). Linghang Qu et al. demonstrated that atractylenolide I (50 mg/kg) could improve the induction of mucoprotein MUC2, tight junction proteins (ZO-1, Occludin), and inflammatory factors TNF- α , IL-6, IL-1 β in DSS-induced colitis mice. Meanwhile, atractylenolide I could regulate the diversity and abundance of gut microbiota and its metabolism. Furthermore, they found that two genes, SPHK1 and B4GALT2, relating to the metabolism of fructose

and galactose, and the activation of the PI3K-AKT pathway, were inhibited in UC mice treated using atractylenolide I (Qu et al., 2022a).

5.2 *Poria cocos* (SchW.) Wolf. (Fu Ling)

Poria cocos (SchW.) Wolf. can promote diuresis, eliminate dampness, invigorate the spleen, and calm the heart. The polysaccharides of *Poria cocos* (SchW.) Wolf. are its major bioactivity component and account for approximately 70–90% of dry sclerotium, which has proven therapeutic activities such as anti-tumor, anti-inflammatory, and immunomodulation (Deng et al., 2020). A study reported that a carboxymethyl polysaccharide CMP33 from *Poria cocos* (SchW.) Wolf. (100, 300 mg/kg) could improve the syndrome of TNBS-induced colitis mice by regulating the MPO and MDA contents and the levels of pro-inflammatory (TNF- α , IL-6, IL-1 β , IL-12, IFN- γ , IL-2, IL-17) cytokines and anti-inflammatory cytokines (IL-4, IL-10). The results of proteomic and metabolomic studies showed that 2-hydroxybutyric acid-(GPT, GGH)-glutathione-ALB-testosterone-TTR-dihydrotestosterone and (PYY, FABP2, HMGS2)-oleic acid-TTR-dihydrotestosterone were the

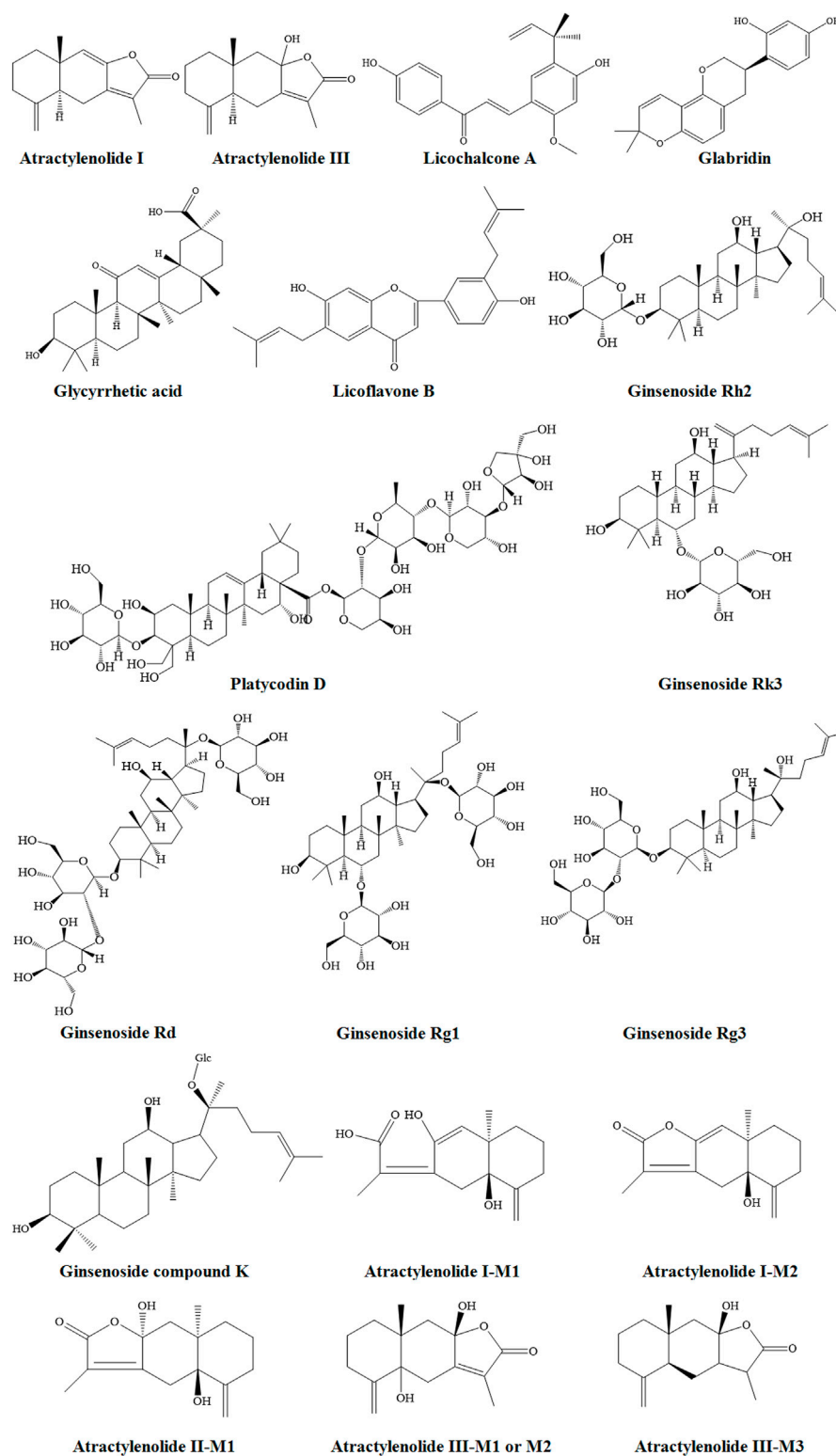


FIGURE 7

The structures of prototype and metabolites components of herbs in SLBZP.

key protein–metabolite pathways (Liu et al., 2018d). Tonger Liang et al. reported that polysaccharides from *Poria cocos* (SchW.) Wolf. (50, 100, 200 mg/kg) could protect against the TNBS-caused colitis in a rat model by decreasing the levels of IL-33, IL-5, IL-13, IL-6 cytokines and expression of IL-33 and ST2 proteins to inhibit the IL-33/ST2 signaling pathway (Liang et al., 2020).

5.3 *Glycyrrhiza uralensis* Fisch. (Gan Cao)

Glycyrrhiza uralensis Fisch. primarily contains triterpenoids, polysaccharides, flavonoids, and coumarins. Modern research has showed that *Glycyrrhiza uralensis* Fisch. has various pharmacological activities, including anti-tumor, anti-inflammatory, antibacterial, and anti-viral properties (Deng et al., 2021). An animal experiment suggested that *Glycyrrhiza uralensis* Fisch. extract (50, 100 mg/kg) is effective against DSS-induced colitis in mice. It functions by decreasing the levels of inflammatory factors, including IL-6 and TNF- α , and suppressing the expression of COX-2, NF- κ B, and PGE2 proteins (Jeon et al., 2016a). Qin Lu and colleagues found that *Glycyrrhiza uralensis* Fisch. extract could inhibit apoptosis by regulating the expression of apoptotic or anti-apoptotic proteins, including muc3, BAX, muc1, bcl-2, FGF-15, P-gp, SHP, and regulating the immune function through FXR/P-gp pathway (Lu et al., 2021). In addition, triterpenoids, polysaccharides, and flavonoids from *Glycyrrhiza uralensis* Fisch. are considered to have a potential therapeutic role in UC. A study reported that glycyrrhetic acid (10, 50 mg/kg) could decrease the levels of IL-6, IL-1 β , and TNF- α , and suppress the expression of COX-2, NF- κ B, and PGE2 protein for treating the DSS-induced colitis mice (Jeon et al., 2016b). Nahla E. El-Ashmawy et al. reported that glabridin (50 mg/kg) exhibits anti-inflammatory and antioxidant effects in DSS-induced colitis mice by regulating the levels of TNF- α and cAMP, the activity of MPO, and gene expression of iNOS in the colon (El-Ashmawy et al., 2018). A report suggested that licochalcone A (20, 40, 80 mg/kg) could reverse the increases in relative levels of inflammatory factors, including TNF- α , IL-1 β and IL-6, MPO activity, and NO level and decrease GSH and SOD levels via the NF- κ B signaling pathway and Nrf2 signaling pathway in DSS-induced colitis mice (Liu et al., 2018e). A report by Juan Zhang et al. suggested that licoflavone B (120 mg/kg) could repair the damage to the colonic barrier by inhibiting colonic cell apoptosis, protecting the expression of occludin, claudin-1, and ZO-1, and suppressing harmful bacteria (such as *Enterococcus*) and boosting beneficial microorganisms (such as *Bacteroides*). Furthermore, licoflavone B could suppress the expression of MAPK pathway-related proteins, including perk, p-p38, and pJNK (Zhang et al., 2022b). *In vitro* experiments have

revealed that a flavonoid-rich extract of *Glycyrrhiza uralensis* Fisch. (6.25, 12.5, 25 mg/kg) could prevent and restore the intestinal barrier dysfunction induced by TNF- α in Caco-2 cell monolayers. Moreover, a flavonoid-rich extract of *glycyrrhiza glabra* could repair intestinal barrier damage by increasing the expression of occluding and ZO-1 protein in TNBS-induced colitis rats (Murugan et al., 2022). Chunying Huang et al. reported that polysaccharides from *Glycyrrhiza uralensis* Fisch. (100, 200, and 400 mg/kg) or the positive control drug sulfasalazine (200 mg/kg) could reduce intestinal permeability and inhibit the inflammatory response (IL-1, IL-6, TNF- α , IL-10 levels) in DSS-induced UC mice (Huang et al., 2022).

5.4 *Platycodon grandiflorum* (Jacq.) A. DC (Jie Geng)

Platycodon grandiflorum (Jacq.) A. DC is commonly used to relieve cough and asthma in clinical practice. The primary components of *Platycodon grandiflorum* (Jacq.) A. DC contain triterpenoid saponins, polysaccharides, and flavonoids, exhibiting antitussive, antiasthmatic, anti-inflammatory, antioxidant, and anti-tumor (Zuo et al., 2019). Platycodin D is a representative triterpenoid saponin component of *Platycodon grandiflorum* (Jacq.) A. DC. A study reported that platycodin D (10 mg/kg) was beneficial in DSS-induced colitis mice, which was related to macrophages. Further, platycodin D (2.5, 5 μ M) could inhibit M1 macrophage polarization and promote M2 macrophage polarization in LPS-stimulated RAW 264.7 cells by PI3K/Akt, NF- κ B, and AMPK-dependent signaling pathways (Guo et al., 2021). In a report by Yang liu et al., the MPO activity, contents of MDA, and expression of IL-1, IL-6, and TNF- α cytokines were inhibited significantly, and expression of IL-10 cytokine and levels of SOD were increased dramatically in UC mice treated with polysaccharides (100, 200, and 400 mg/kg) from *Platycodon grandiflorum* (Jacq.) A. DC (Liu et al., 2022b). In addition, *Platycodon grandiflorum* (Jacq.) A. DC root fermentation broth (0.5, 1 ml per head per day) was suggested to improve UC prognosis by regulating the AMPK/NF- κ B/NLRP3 signaling pathway (Wang et al., 2022).

5.5 *Panax ginseng* C.A.Mey. (Ren Shen)

Panax ginseng C.A.Mey. is a Chinese drug with a high medicinal value. It has the effects of invigorating vital energy, strengthening the spleen, tonifying the lung, engendering liquid, allaying thirst, AND tranquilizing the mind. Modern studies showed that *Panax ginseng* C.A.Mey. has various pharmacological effects such as anti-aging, antioxidant, anti-tumor, and immune enhancement (Yu et al., 2019a).

Ginsenosides are the main activity components of *Panax ginseng* C.A.Mey., exhibiting immunomodulatory and anti-inflammatory activity against UC (Shi, 2011). A study reported that ginsenoside Rd (10, 20 and 40 mg/kg) could improve the syndrome of TNBS-induced colitis rats by enhancing the oxidation resistance of injured colons and inhibiting neutrophil infiltration (Yang et al., 2012). Meanwhile, ginsenoside Rd (10, 20 and 40 mg/kg) could inhibit the NLRP3 inflammasome through the AMPK/ULK1-autophagy signaling pathway in DSS-induced colitis mice (Liu et al., 2018f). In addition, ginsenoside Rd (20 mg/kg) could reduce the levels of TNF- α , IFN- γ , IL-6, IL-12/23p40, IL-17 A, and the expression of relative proteins including pJNK, p-p38, pIkBa, and p65 of NF- κ B and p38 MAPK pathways, which eventually improve the condition of UC mice (Qu et al., 2022b). Weiwei hao et al. reported that ginsenoside Rg1 (50 and 200 mg/kg) could improve the hypercoagulability and microcirculation in DSS-induced colitis mice (Hao et al., 2013). Further, ginsenoside Rg1 (200 mg/kg) could ameliorate the symptoms in DSS-induced UC mice by regulating M1/M2 macrophage polarization associated with inhibition of the Nogo-B/RhoA signaling pathway, microbiota composition, and the balance of Treg/Th9 cells (Long et al., 2022a; Long et al., 2022b). Ginsenoside Rh2 (20 mg/kg) exhibited a potential therapeutic effect on UC, decreasing the mRNA expression of IL-6, TNF α , and INF γ in the DSS-treated colon, and augmenting the TGF β signaling pathway (Ye et al., 2014b). Xuanqing Chen and colleagues suggested that ginsenoside Rh2 (50 mg/kg) is potentially valuable for treating UC, and its mechanism involves the downregulation of STAT3/miR-214 levels (Chen et al., 2021). Meanwhile, Yu Xu et al. successfully encapsulated ginsenoside Rh2 to form Rh2 nanoparticles that exhibit strong anti-inflammatory activity via significantly inhibiting the overproduction of nitric oxide (NO) and inflammatory cytokines (TNF- α , IL-1 β and IL-6). Further, the Rh2 nanoparticles could regulate the oxidant stress levels and intestinal flora of UC mice (Xu et al., 2022). Zhiwei miu et al. reported that ginsenoside Rg3 (40 mg/kg) has significant therapeutic effects on DSS-induced colitis mice. It could regulate the imbalance of Th1/Th2 by decreasing TNF- α and IL-6 levels, increasing IL-10 levels, and suppressing the NF- κ B signaling pathway by decreasing the expression of p-NF- κ B p65 and NF- κ B p65 (Miao et al., 2019). Evelyn Saba and colleagues found that ginsenoside Rg3 (20 mg/kg) could decrease the expression of pro-inflammatory mediators and cytokines including NO, IL-1 β , IL-5, IL-13, and TNF- α , and levels of NLRP3 inflammasome in DSS-induced colitis mice (Saba et al., 2020). Mi Tian et al. reported that ginsenoside RK3 (20, 40 and 60 mg/kg) protected intestinal barrier function and inhibited NLRP3 inflammasome expression in DSS-induced colitis mice by regulating the MPO and iNOS activities and expression of TNF- α , IL-1 β , IL-6, NLRP3, ASC, and Caspase-1 (Tian et al., 2020).

5.6 *Amomum villosum* Lour. (Sha Ren)

Amomum villosum Lour. mainly contains volatile oil, flavonoids, and phenolic acid, exhibiting various pharmacology activities, including gastrointestinal protection, antioxidant, antibacterial, and blood pressure-lowering effects (Qu et al., 2021). Among these, volatile oil and flavonoids from *Amomum villosum* Lour. are the potential drugs used to treat peptic colitis (Qu et al., 2021). Studies reported that volatile oil (0.84, 1.6 g/kg) from *Amomum villosum* Lour. could alleviate the oxidative damage caused by increasing SOD activity and levels of GSH-Px, decreasing the levels of NOS and expression of iNOS, decreasing colonic cell-to-cell adhesion by inhibiting the expression of ICAM, and suppressing inflammatory response by decreasing the expression of TNF- α and NF- κ B p65 (Zhao, 2009; Zhu et al., 2009).

5.7 *Dioscorea opposita* Thunb. (Shan Yao)

Dioscorea opposita Thunb. can help tonify spleen and stomach, benefit the lung and generating fluid, tonify the kidney and essence. Modern studies showed that the chemical composition of yam majorly included polysaccharides, amino acid, fatty acid, dioscin, and polyphenols (Chen et al., 2020). A study showed that polyphenols (240 mg/kg) from *Dioscorea opposita* Thunb. could protect against the DSS-induced colitis mice. Administering *Dioscorea opposita* Thunb. before modeling markedly mitigated colitis as well as intestinal mucosal damage and apoptosis of colonic epithelial cells by regulating the expression of occludin, caspase-8, and COX-2 (Li et al., 2021c).

5.8 *Coix lacryma-jobi* L.var. *mayuen* (Roman.) Stapf (Yi Yi Ren)

Coix lacryma-jobi L. var. *mayuen* (Roman.) Stapf, as a TCM with a homology of medicine and food, has anti-inflammatory, anti-obesity, anti-tumor, and antiallergic activity. It primarily contains lipid acid, polysaccharides, lignans, and phenols (Li et al., 2020c). A study showed that the extract (1.5 g/kg) of *Coix lacryma-jobi* L. var. *mayuen* (Roman.) Stapf has a protective effect on DSS-induced UC rats, which may be related to the antioxidant potential (Hao et al., 2012). Further, Qilyu Zhou and colleagues found that the feed of *Coix lacryma-jobi* L. var. *mayuen* (Roman.) Stapf could not only relieve inflammatory cytokine secretion and alleviate oxidative stress but also change the innate immune cell proportion, which eventually ameliorated immune function disorders for treating UC mice (Zhou et al., 2021a).

5.9 Metabolites of herbs in SLBZP

Therapeutic effects of many constituents of herbs may depend on the transformative components after metabolism *in vivo* rather than prototype components (Yu et al., 2019b). In recent years, in addition to prototype components, metabolites of herbs can often be one of the substances that contribute to the efficacy of the herbs or prescriptions (Kang et al., 2020). Nowadays, lots metabolites of Chinese herbal medicines, such as ginsenoside compound K (CK), have shown various beneficial therapy effects on UC. Ginsenoside CK is the main metabolite of the protopanaxadiol type of ginsenoside (Liu et al., 2022c). Juan Li et al. and colleagues found that Ginsenoside CK (5, 10 and 20 mg/kg) could promote the recovery of the progression of UC and inhibit the inflammatory responses by suppressing NF- κ B activation or regulating the activation of macrophages (Li et al., 2014b). Meanwhile, studies have found that the gut microbial metabolite CK had significant anti-inflammatory effects on UC even at low concentrations, compared to its parent ginsenoside Rb1 (Wang et al., 2018a). In addition, Hao Cai et al. found that the metabolites (Structures were shown in Figure 7) of *Atractylodes macrocephala* Koidz. including atractylenolide I-M1, atractylenolide I-M2, atractylenolide III-M1, atractylenolide III-M2, atractylenolide III-M3 and atractylenolide II-M1 were high degree correlated with the levels of TNF- α , IL-6, IL-10, and TGF- β 1, demonstrating strong anti-UC effects (Cai et al., 2019). And further study is required to verify the effectiveness of Metabolites of *Atractylodes macrocephala* Koidz. for treating UC. Nevertheless, no data on the metabolites of SLBZP are currently available. Prototype components and metabolites of SLBZP that contribute to the therapeutic effects of UC and the mechanism need to be further investigated.

6 Summary and outlook

As one of the classic prescriptions for strengthening the spleen and clearing dampness, SLBZP has beneficial effects on the prevention and treatment of UC. Numerous studies have demonstrated that SLBZP alleviates the symptoms and decreases the recurrence rate of UC, thereby improving the quality of life. The mechanism of action of SLBZP could be attributed to anti-inflammatory, antioxidant, and immunomodulatory effects, as well as repair of intestinal mucosal damage and protection of gut mucosal barrier, promotion of BMSCs migration to the colonic mucosa, regulation of some signal pathways, and regulation of the balance of gut microbiota. These studies not only provide a theoretical basis for the clinical application of SLBZP in the treatment of UC and further research on UC mechanisms but also provide more choices for the prevention and treatment of UC, improving the possibility of curing UC. However, these studies still have some limitations and ambiguities. According

to the current research, eight herbs and their ingredients have been reported to exert therapeutic effects, suggesting a multi-component, multi-target, and multi-pathway mode of action of SLBZP in treating UC (As shown in Figure 6).

However, the ingredients that contribute to the therapeutic effects and the mechanism underlying their synergistic activity remain unclear. Moreover, only characterized components (such as ginsenoside Rg1, Rb1, Re, and atractylenolide III) and HPLC fingerprint of SLBZP were analyzed and reported in some studies (Liu and Zhu 2018; Wang et al., 2018b), and the overall components of SLBZP and its pharmacological effects and mechanism remains to be further investigated. Additionally, since the mechanism of SLBZP has not yet been elucidated, further large-scale evaluations assessing the efficacy and safety of SLBZP and its combination with other drugs to prevent and treat UC are required. Furthermore, the ideal dosage form and treatment duration of SLBZP was inconsistent in the clinic. There may be a difference in the quality of Chinese drugs, which could affect the accuracy of our findings. Furthermore, several animal models that have been developed accurately represent certain aspects of UC. However, they do not completely mimic the human UC pathology, especially the TCM syndromes of UC, which can affect our evaluation of the therapeutic effects of SLBZP in the treatment of UC.

In a sum, SLBZP has shown a broad prospect in the prevention and treatment of UC, and further research is required in the future. That should mainly focus on the following aspects: 1) Large sample prospective cohort studies are performed to clarify the clinical efficacy and safety of SLBZP and combination with other drugs in treatment of UC; 2) Researchers should strengthen the study of molecular biological mechanism of active ingredients and its synergistic actions, clarifying the mechanism of SLBZP in treatment of UC by multi-component, multi-target and multi-pathway.

Author contributions

JC analyzed the data and wrote the article. JC, BS, ZJ collect the literature and summarize the results. JC and ZJ modified the final article.

Funding

These studies were supported by funding obtained from Zhejiang Province Science and Technology Project of TCM (2020ZQ050), scientific researching fund of Taizhou Enze Medical Center (Group) (19EZA5) and the Doctoral Start-up Fund of Taizhou Enze Medical Center (Group) (2018BSKYQDJJ06).

Conflict of interest

The authors declare that the research was conducted in the absence of any commercial or financial relationships that could be construed as a potential conflict of interest.

Publisher's note

All claims expressed in this article are solely those of the authors and do not necessarily represent those of their affiliated

organizations, or those of the publisher, the editors and the reviewers. Any product that may be evaluated in this article, or claim that may be made by its manufacturer, is not guaranteed or endorsed by the publisher.

Supplementary material

The Supplementary Material for this article can be found online at: <https://www.frontiersin.org/articles/10.3389/fphar.2022.978558/full#supplementary-material>

References

- Actis, G. C., Pellicano, R., and Rosina, F. (2014). Inflammatory bowel diseases: Current problems and future tasks. *World J. Gastrointest. Pharmacol. Ther.* 5 (3), 169–174. doi:10.4292/wjgpt.v5.i3.169
- Aggarwal, B. B., Kunnumakkara, A. B., Harikumar, K. B., Gupta, S. R., Tharakan, S. T., Koca, C., et al. (2009). Signal transducer and activator of transcription-3, inflammation, and cancer: How intimate is the relationship? *Ann. N. Y. Acad. Sci.* 1171, 59–76. doi:10.1111/j.1749-6632.2009.04911.x
- Bai, X., Bai, G., Tang, L., Liu, L., Li, Y., and Jiang, W. (2020). Changes in MMP-2, MMP-9, inflammation, blood coagulation and intestinal mucosal permeability in patients with active ulcerative colitis. *Exp. Ther. Med.* 20 (1), 269–274. doi:10.3892/etm.2020.8710
- Bi, D., Jia, Y., and Cheng, Y. (2017). Effects of Shenling Baizhu Powder on expression of IL-1 β , IL-4 and p38MAPK gene protein in rats with ulcerative colitis induced by spleen deficiency and dampness. *Pharmacol. Clin. Chin. Materia Medica* 33 (01), 7–11. doi:10.13412/j.cnki.zyyj.2017.01.002
- Bian, X., Yang, L., Wu, W., Lv, L., Jiang, X., Wang, Q., et al. (2020). *Pedococcus pentosaceus* LI05 alleviates DSS-induced colitis by modulating immunological profiles, the gut microbiota and short-chain fatty acid levels in a mouse model. *Microb. Biotechnol.* 13 (4), 1228–1244. doi:10.1111/1751-7915.13583
- Bogaert, S., Vos, M. D., Olivier, K., Peeters, H., Elewaut, D., Lambrecht, B., et al. (2011). Involvement of endoplasmic reticulum stress in inflammatory bowel disease: A different implication for colonic and ileal disease? *PLoS one* 6 (10), e25589. doi:10.1371/journal.pone.0025589
- Brandl, K., Rutschmann, S., Li, X., Du, X., Xiao, N., Schnabl, B., et al. (2009). Enhanced sensitivity to DSS colitis caused by a hypomorphic *Mbtps1* mutation disrupting the ATF6-driven unfolded protein response. *Proc. Natl. Acad. Sci. U. S. A.* 106 (9), 3300–3305. doi:10.1073/pnas.0813036106
- Cai, H., Xu, Y., Xie, L., Duan, Y., Zhou, J., Liu, J., et al. (2019). Investigation on spectrum-effect correlation between constituents absorbed into blood and bioactivities of baizhu Shaoyao san before and after processing on ulcerative colitis rats by UHPLC/Q-TOF-MS/MS coupled with gray correlation analysis. *Mol. Basel, Switz.* 24 (5), E940. doi:10.3390/molecules24050940
- Chen, T., and Zhang, M. (2020). Efficacy of Shenling Baizhu Powder in the treatment of chronic recurrent ulcerative colitis and its mechanism based on β 2 AR/ β -arrestin2/NF- κ B signal transduction pathway. *J. Chin. Med. Mater.* 43 (04), 996–999. doi:10.13863/j.issn1001-4454.2020.04.040
- Chen, G., Huang, H., and Liu, R. (2013). Clinical effect analysis of Shenling baizhu powder combined with mesalazine treating ulcerative colitis of spleen stomach qi deficiency. *China Med. Pharm.* 3 (17), 120–121.
- Chen, W., Ren, L., and Shi, R. (2014). Enteric microbiota leads to new therapeutic strategies for ulcerative colitis. *World J. Gastroenterol.* 20 (42), 15657–15663. doi:10.3748/wjg.v20.i42.15657
- Chen, M., Xie, S., and Dai, W. (2018a). Applications and research progresses of shenling baizhu decoction in digestive system diseases. *J. Liaoning Univ. Traditional Chin. Med.* 20 (10), 164–166. doi:10.13194/j.issn.1673-842x.2018.10.042
- Chen, S., Gong, Y., and Zhang, D. (2018b). Effects of shenling baizhu san and mesalazine on the protein expression of NF- κ Bp65 of colon tissue and inflammatory reaction in the mice of ulcer colitis of spleen deficiency and damp retention type. *World J. Integr. Traditional West. Med.* 13 (11), 1532–1536. doi:10.13935/j.cnki.sjzx.181112
- Chen, M., Liu, W., Yu, G., and Zhao, F. Z. (2020). Incidence of lymph node metastasis at each station in siewert types II/III adenocarcinoma of the esophagogastric junction: A systematic review and meta-analysis. *Surg. Oncol.* 48 (02), 62–70. doi:10.1016/j.suronc.2020.08.001
- Chen, X., Xu, T., Lv, X., Zhang, J., and Liu, S. (2021). Ginsenoside Rh2 alleviates ulcerative colitis by regulating the STAT3/miR-214 signaling pathway. *J. Ethnopharmacol.* 274, 113997. doi:10.1016/j.jep.2021.113997
- Chen, H. (2012). Observation on curative effect of Shenling Baizhu Powder combined with Kangfuxin liquid in treating chronic colitis. *Strait Pharm. J.* 24 (10), 130–131. doi:10.3969/j.issn.1006-3765.2012.10.062
- Chen, H. (2014). Effect of Shenling Baizhu Powder retention enema combined with mesalazine oral treatment on chronic nonspecific ulcerative colitis. *Hebei J. Traditional Chin. Med.* 36 (11), 1643–1644. doi:10.3969/j.issn.1002-2619.2014.11.021
- Cohly, H. H. P., Isokpehi, R., and Rajnarayanan, R. V. (2008). Compartmentalization of aquaporins in the human intestine. *Int. J. Environ. Res. Public Health* 5 (2), 115–119. doi:10.3390/ijerph5020115
- Cordes, F., Foell, D., Ding, J. N., Varga, G., and Bettenworth, D. (2020). Differential regulation of JAK/STAT-signaling in patients with ulcerative colitis and Crohn's disease. *World J. Gastroenterol.* 26 (28), 4055–4075. doi:10.3748/wjg.v26.i28.4055
- Cui, S., Liu, X., and Li, G. (2020). Effects of Shenling Baizhu Powder and Tongxie Yaofang on homing of BMSCs to colonic mucosa in rats with ulcerative colitis. *Chin. Tradit. Pat. Med.* 42 (2), 480–484. doi:10.3969/j.issn.1001-1528.2020.02.040
- Dalod, M., Chelbi, R., Malissen, B., and Lawrence, T. (2014). Dendritic cell maturation: Functional specialization through signaling specificity and transcriptional programming. *EMBO J.* 33 (10), 1104–1116. doi:10.1002/embj.201488027
- Demon, D., Kuchmiy, A., Fossoul, A., and LaMkanfi, M. (2014). Caspase-11 is expressed in the colonic mucosa and protects against dextran sodium sulfate-induced colitis. *Mucosal Immunol.* 7 (6), 1480–1491. doi:10.1038/mi.2014.36
- Deng, Q., Deng, D., Che, J., Zhao, H. R., Yu, J. J., and Lu, Y. Y. (2016). Hypothalamic paraventricular nucleus stimulation reduces intestinal injury in rats with ulcerative colitis. *World J. Gastroenterol.* 22 (14), 3769–3776. doi:10.3748/wjg.v22.i14.3769
- Deng, T., Peng, D., and Yu, N. (2020). Research progress on chemical composition and pharmacological effects of *Poria cocos* and predictive analysis on quality markers. *Chin. Traditional Herb. Drugs* 51 (10), 2703–2717. doi:10.7501/j.issn.0253-2670.2020.10.013
- Deng, T., Peng, C., Peng, D., Yu, N. J., Chen, W. D., and Wang, L. (2021). [Research progress on chemical constituents and pharmacological effects of *Glycyrrhizae Radix* et *Rhizoma* and discussion of Q-markers]. *Radix et Rhizoma and discussion of Q-markers. China J. Chin. Materia Medica* 46 (11), 2660–2676. doi:10.19540/j.cnki.cjcmm.20210304.201
- Ding, J., Wang, K., Liu, W., She, Y., Sun, Q., Shi, J., et al. (2016). Pore-forming activity and structural autoinhibition of the gasdermin family. *Nature* 535 (7610), 111–116. doi:10.1038/nature18590
- Ding, L., Jia, Y., and Cheng, Y. (2018). Effect of shenling baizhu san on expressions of IL-13, IL-23 and COX-2, CREB in ulcerative colitis rats with spleen deficiency and dampness. *Chin. J. Exp. Traditional Med. Formulae* 24 (11), 67–72. doi:10.13422/j.cnki.syfjx.20181058
- Djulfbegovic, B., and Guyatt, G. H. (2017). Progress in evidence-based medicine: A quarter century on. *Lancet (London, Engl.)* 390 (10092), 415–423. doi:10.1016/s0140-6736(16)31592-6

- El-Ashmawy, N. E., Khedr, N. F., El-Bahrawy, H. A., and El-Adawy, S. A. (2018). Downregulation of iNOS and elevation of cAMP mediate the anti-inflammatory effect of glabridin in rats with ulcerative colitis. *Inflammopharmacology* 26 (2), 551–559. doi:10.1007/s10787-017-0373-9
- Fan, Y., and Liu, B. (2015). Expression of Toll-like receptors in the mucosa of patients with ulcerative colitis. *Exp. Ther. Med.* 9 (4), 1455–1459. doi:10.3892/etm.2015.2258
- Feng, W., Liu, J., Tan, Y., Ao, H., Wang, J., and Peng, C. (2020). Polysaccharides from *Atractylodes macrocephala* Koidz. Ameliorate ulcerative colitis via extensive modification of gut microbiota and host metabolism. *Food Res. Int.* 138 (B), 109777. doi:10.1016/j.foodres.2020.109777
- Gu, D., Zhou, S., Yao, L., Tan, Y., Chi, X., Shi, D., et al. (2021). Effects of ShenLing BaiZhu san supplementation on gut microbiota and oxidative stress in rats with ulcerative colitis. *Evid. Based. Complement. Altern. Med.* 2021, 3960989. doi:10.1155/2021/3960989
- Guo, R., Meng, Q., Wang, B., and Li, F. (2021). Anti-inflammatory effects of Platycodin D on dextran sulfate sodium (DSS) induced colitis and *E. coli* Lipopolysaccharide (LPS) induced inflammation. *Int. Immunopharmacol.* 94, 107474. doi:10.1016/j.intimp.2021.107474
- Han, J., Li, W., Shi, G., Huang, Y., Sun, X., Sun, N., et al. (2022). Atractylenolide III improves mitochondrial function and protects against ulcerative colitis by activating AMPK/SIRT1/PGC-1 α . *Mediat. Inflamm.* 2022, 9129984. doi:10.1155/2022/9129984
- Hao, Y., Li, X., and Liu, N. (2012). Effects of coix lacryma-jobi seed extract on the antioxidation in colitis in rats. *China Prev. Med.* 13 (3), 177–180. doi:10.16506/j.1009-6639.2012.03.011
- Hao, W., Wen, H., and Ma, G. (2013). Ginsenoside-Rg1 regulates blood coagulation in DSS-induced colitis mice. *Chin. J. Integr. Traditional West. Med. Dig.* 21 (05), 238–242. doi:10.3969/j.issn.1671-038X.2013.05.004
- Hardin, J. A., Wallace, L. E., Wong, J. F. K., O'Loughlin, E. V., Urbanski, S. J., Gall, D. G., et al. (2004). Aquaporin expression is downregulated in a murine model of colitis and in patients with ulcerative colitis, Crohn's disease and infectious colitis. *Cell Tissue Res.* 318 (2), 313–323. doi:10.1007/s00441-004-0932-4
- He, H., Shen, H., and He, B. (2012a). Pathogenesis and therapeutic methods of the active stage of ulcerative colitis. *J. nanjing Univ. Tradit. Chin. Med.* 28 (06), 504–505+512. doi:10.14148/j.issn.1672-0482.2012.06.008
- He, X., He, X., Lian, L., Wu, X. J., and Lan, P. (2012b). Systemic infusion of bone marrow-derived mesenchymal stem cells for treatment of experimental colitis in mice. *Dig. Dis. Sci.* 57 (12), 3136–3144. doi:10.1007/s10620-012-2290-5
- He, K. (2014). Ulcerative colitis spleen qi deficiency parallel randomized controlled study Shenling baizhu casual treatment. *J. Pract. Traditional Chin. Intern. Med.* 28 (11), 58–59. doi:10.13729/j.issn.1671-7813.2014.11.27
- Hernandez, A. V., Marti, K. M., and Roman, Y. M. (2020). Meta-analysis. *Chest* 158, S97–S102. doi:10.1016/j.chest.2020.03.003
- Hua, H. (2022). Clinical observation opposing needling combined with modified shenling baizhu powder in the treatment of ulcerative colitis of damp-heat due to spleen deficiency type. *J. Guangzhou Univ. Traditional Chin. Med.* 39 (03), 586–593. doi:10.13359/j.cnki.gzxbtcm.2022.03.021
- Huang, C., Luo, X., Li, L., Xue, N., Dang, Y., Zhang, H., et al. (2022). Glycyrrhiza polysaccharide alleviates dextran sulfate sodium-induced ulcerative colitis in mice. *Evid. Based. Complement. Altern. Med.* 2022, 1345852. doi:10.1155/2022/1345852
- Isidro, R. A., Bonilla, F. J., Pagan, H., Cruz, M. L., Lopez, P., Godoy, L., et al. (2014). The probiotic mixture VSL#3 alters the morphology and secretion profile of both polarized and unpolarized human macrophages in a polarization-dependent manner. *J. Clin. Cell. Immunol.* 5 (3), 1000227. doi:10.4172/2155-9899.1000227
- Jeon, Y.-D., Bang, K.-S., Shin, M.-K., Lee, J. H., Chang, Y. N., and Jin, J. S. (2016a). Regulatory effects of glycyrrhizae radix extract on DSS-induced ulcerative colitis. *BMC Complement. Altern. Med.* 16 (1), 459. doi:10.1186/s12906-016-1390-8
- Jeon, Y.-D., Kang, S.-H., Bang, K.-S., Chang, Y. N., Lee, J. H., and Jin, J. S. (2016b). Glycyrrhetic acid ameliorates dextran sulfate sodium-induced ulcerative colitis in vivo. *Mol. Basel, Switz.* 21 (4), 523. doi:10.3390/molecules21040523
- Jiang, B. (2019). Effect of taohua decoction and shenling baizhu powder on ulcerative colitis. *Guide China Med.* 17 (33), 223. doi:10.15912/j.cnki.gocm.2019.33.188
- Jiao, C., Zhang, Q., Yang, M., Ma, J., Zhao, X., Tang, N., et al. (2022). Shenling baizhu san ameliorates ulcerative colitis by regulating the gut microbiota and its tryptophan metabolites: A complementary medicine to mesalamine. *J. Ethnopharmacol.* 291, 115145. doi:10.1016/j.jep.2022.115145
- Jin, B.-R., Chung, K.-S., Cheon, S.-Y., Lee, M., Hwang, S., Noh Hwang, S., et al. (2017). Rosmarinic acid suppresses colonic inflammation in dextran sulphate sodium (DSS)-induced mice via dual inhibition of NF- κ B and STAT3 activation. *Sci. Rep.* 7, 46252. doi:10.1038/srep46252
- Jing, M., Wang, Y., and Xu, L. (2019). Andrographolide derivative AL-1 ameliorates dextran sodium sulfate-induced murine colitis by inhibiting NF- κ B and MAPK signaling pathways. *Oxid. Med. Cell. Longev.* 6138723. doi:10.1155/2019/6138723
- Kaluźna, A., Olczyk, P., and Komosińska-Vassev, K. (2022). The role of innate and adaptive immune cells in the pathogenesis and development of the inflammatory response in ulcerative colitis. *J. Clin. Med.* 11 (2), 400. doi:10.3390/jcm11020400
- Kang, D., Ding, Q., Xu, Y., Yin, X., Guo, H., Yu, T., et al. (2020). Comparative analysis of constituents and metabolites for traditional Chinese medicine using IDA and SWATH data acquisition modes on LC-Q-TOF MS. *J. Pharm. Anal.* 10 (6), 588–596. doi:10.1016/j.jpba.2019.11.005
- Kayagaki, N., Stowe, I. B., Lee, B. L., O'Rourke, K., Anderson, K., Warming, S., et al. (2015). Caspase-11 cleaves gasdermin D for non-canonical inflammasome signalling. *Nature* 526 (7575), 666–671. doi:10.1038/nature15541
- Kirov, S., Sasson, A., Zhang, C., Chasalow, S., Dongre, A., Steen, H., et al. (2019). Degradation of the extracellular matrix is part of the pathology of ulcerative colitis. *Mol. Omics* 15 (1), 67–76. doi:10.1039/c8mo00239h
- Kobayashi, T., Siegmund, B., Le Berre, C., Wei, S. C., Ferrante, M., Shen, B., et al. (2020). Ulcerative colitis. *Nat. Rev. Dis. Prim.* 6 (1), 74. doi:10.1038/s41572-020-0205-x
- Kordjazy, N., Haj-Mirzaian, A., Haj-Mirzaian, A., Rohani, M. M., Gelfand, E. W., Rezaei, N., et al. (2018). Role of toll-like receptors in inflammatory bowel disease. *Pharmacol. Res.* 129, 204–215. doi:10.1016/j.phrs.2017.11.017
- Lai, J., Lin, Q., and Chen, C. (2014). 30 cases of ulcerative colitis treated by Shenling Baizhu Powder combined with Kangfuxin liquid. *Fujian J. TCM* 45 (04), 11–12. doi:10.13260/j.cnki.jfjtc.010697
- Lee, E.-J., and Tournier, C. (2011). The requirement of uncoordinated 51-like kinase 1 (ULK1) and ULK2 in the regulation of autophagy. *Autophagy* 7 (7), 689–695. doi:10.4161/auto.7.7.15450
- Li, L., and Wang, Y. (2021). Clinical observation on shenling baizhu powder and mesalazine in treating ulcerative colitis. *West. J. Traditional Chin. Med.* 34 (10), 124–126. doi:10.12174/j.issn.2096-9600.2021.10.31
- Li, Z., Wang, J., and Cai, R. (2012). Effect of shenling baizhu powder on superoxide dismutase and malondialdehyde in ulcerative colitis rats. *J. Traditional Chin. Med.* 53 (20), 1764–1767. doi:10.13288/j.11-2166/r.2012.20.025
- Li, Z., Wang, J., and Cai, R. (2013). Effects on expression of ERK, p38 MAPK in ulcerative colitis rats with syndrome of dampness stagnancy due to spleen deficiency treated with shenlingbaizhu powder. *J. Yunnan Univ. Traditional Chin. Med.* 36 (06), 7–10. doi:10.19288/j.cnki.issn.1000-2723.2013.06.003
- Li, J., Zhong, W., Wang, W., Hu, S., Yuan, J., Zhang, B., et al. (2014a). Ginsenoside metabolite compound K promotes recovery of dextran sulfate sodium-induced colitis and inhibits inflammatory responses by suppressing NF- κ B activation. *PLoS one* 9 (2), e87810. doi:10.1371/journal.pone.0087810
- Li, X., Cui, L., and Chen, Y. (2014b). Effect of Shenlingbaizhu Powder on immune regulation of intestinal regulatory T cells in mice with ulcerative colitis. *Chin. Tradit. Pat. Med.* 36 (06), 1295–1297. doi:10.3969/j.issn.1001-1528.2014.06.041
- Li, F., Huang, L., Dong, C., Wang, J. P., Wu, H. J., and Shuang, S. M. (2015a). Down-regulation of aquaporin3 expression by lipopolysaccharide via p38/c-Jun N-terminal kinase signalling pathway in HT-29 human colon epithelial cells. *World J. Gastroenterol.* 21 (15), 4547–4554. doi:10.3748/wjg.v21.i15.4547
- Li, Z., Wang, J., and Cai, R. (2015b). Effects of Shenling Baizhu Powder on the expressions of AQP3 and AQP4 in UC rats via EK/p38 MAPK signal pathway. *Chin. Tradit. Pat. Med.* 37 (09), 1883–1888. doi:10.3969/j.issn.1001-1528.2015.09.002
- Li, Z., Wang, J., and Cai, R. (2015c). Effects of Shenling Baizhu San on the protein expression of NF- κ B p65 and the serum level of related inflammatory cytokines in the colon tissue of rats with ulcerative colitis due to dampness retention and spleen deficiency. *J. Beijing Univ. Traditional Chin. Med.* 38 (05), 315–317+360361. doi:10.3969/j.issn.1006-2157.2015.05.006
- Li, Y., Liu, Y., and Yan, S. (2017). Effect of the classical three prescriptions for regulating intestinal function on cytokines as IL-17, IL-23, IL-6, IL-10 and TNF- α in colonic of ulcerative colitis rat. *Mod. J. Integr. Traditional Chin. West. Med.* 26 (09), 920–924. doi:10.3969/j.issn.1008-8849.2017.09.003
- Li, Y., Liu, Q., Tang, J. H., Wen, J. J., and Zhu, J. Q. (2019). Regulatory mechanism of mesalazine on TLR4/MyD88-dependent pathway in mouse ulcerative colitis model. *Eur. Rev. Med. Pharmacol. Sci.* 23 (15), 6637–6644. doi:10.26355/eurrev.201908.18553
- Li, X., Gu, K., and Liang, M. (2020a). Research progress on chemical constituents and pharmacological effects of Coicis Semen. *Chin. Traditional Herb. Drugs* 51 (21), 5645–5657. doi:10.7501/j.issn.0253-2670.2020.21.031

- Li, Z., Cai, R., and Sun, J. (2020b). Effect of shenling baizhusan on protein and mRNA expression of NF- κ B p65, ik ba ik k β in ulcerative colitis rats with syndrome of dampness stagnancy due to spleen deficiency. *Chin. J. Exp. Traditional Med. Formulae* 26 (19), 108–113. doi:10.13422/j.cnki.syfjx.20201936
- Li, Z., Feng, H., Han, L., Ding, L., Shen, B., Tian, Y., et al. (2020c). Chicoric acid ameliorate inflammation and oxidative stress in Lipopolysaccharide and d-galactosamine induced acute liver injury. *J. Cell. Mol. Med.* 24 (5), 3022–3033. doi:10.1111/jcmm.14935
- Li, K., Liao, S., and Li, Q. (2021a). Study on preventive effect of Chinese yam peel polyphenols on intestinal mucosal injury in colitis mice. *J. Food Sci. Technol.* 39 (04), 46–54. doi:10.12301/j.issn.2095-6002.2021.04.005
- Li, S., Hao, X., Gong, Y., Liu, S., Niu, W., Jia, J., et al. (2021b). Effect of shenling baizhu powder on the serum TH1 cytokines of elderly patients with ulcerative colitis complicated by bloody purulent stool. *Am. J. Transl. Res.* 13 (8), 9701–9707.
- Li, Z., Cai, R., and Suan, J. (2021c). Effect of Shenling Baizhu San on expressions of TLR2, MyD88, COX-2 in ulcerative colitis rats with spleen deficiency and dampness stagnation pattern. *J. Beijing Univ. Traditional Chin. Med.* 44 (01), 45–53. doi:10.3969/j.issn.1006-2157.2021.01.008
- Li, D., Zhang, Y., Zhang, Y., Zhou, X., and Guo, S. (2013). Fabrication of bidirectionally doped β -Bi₂O₃/TiO₂-NTs with enhanced photocatalysis under visible light irradiation. *J. Hazard. Mat.* 32 (19), 42–49. doi:10.1016/j.jhazmat.2013.02.058
- Li, Z. (2019). *Effect of shenlingbaizhu powder on pyroapoptosis pathway in C57bl/6J mice induced by DSS in ulcerative colitis*. [master's thesis]. China: South China Agricultural University. doi:10.27152/d.cnki.ghanu.2019.001238
- Liang, T., Liu, Y., and Wang, X. (2020). Study on mechanisms of Poria cocos polysaccharide regulating mast cell activation in rats with ulcerative colitis based on IL-33/ST2 signaling pathway. *Chin. J. Immunol.* 36 (11), 1324–1329+1337. doi:10.3969/j.issn.1000-484X.2020.11.009
- Liu, C., and Zhu, Q. (2018). Study on HPLC characteristic fingerprint of shenlingbaizhu powder and simultaneous determination of its five indicative components. *China Pharm.* 27 (15), 12–16. doi:10.3969/j.issn.1006-4931.2018.15.004
- Liu, Y., Hu, J., and Yi, W. (2015). Effect of shenling baizhu san on regulation of tight junction in DSS-induced IBD mice. *Chin. J. Exp. Traditional Med. Formulae* 21 (03), 130–133. doi:10.13422/j.cnki.syfjx.2015030130
- Liu, X., Tang, Y., Cui, Y., Zhang, H., and Zhang, D. (2016). Autophagy is associated with cell fate in the process of macrophage-derived foam cells formation and progress. *J. Biomed. Sci.* 23 (1), 57. doi:10.1186/s12929-016-0274-z
- Liu, C., Shi, J., and Huang, J. (2018a). Effects of shenling-baizhu-san on the tight junction and MLCK/MLC pathway in mice with ulcerative colitis. *J. Chin. Med. Mater.* 41 (09), 2180–2184. doi:10.13863/j.issn1001-4454.2018.09.036
- Liu, C., Wang, J., Yang, Y., Liu, X., Zhu, Y., Zou, J., et al. (2018b). Ginsenoside Rd ameliorates colitis by inducing p62-driven mitophagy-mediated NLRP3 inflammasome inactivation in mice. *Biochem. Pharmacol.* 155, 366–379. doi:10.1016/j.bcp.2018.07.010
- Liu, D., Huo, X., Gao, L., Zhang, J., Ni, H., and Cao, L. (2018c). NF- κ B and Nrf2 pathways contribute to the protective effect of Licochalcone A on dextran sulphate sodium-induced ulcerative colitis in mice. *Biomed. Pharmacother. = Biomedicine Pharmacother.* 102, 922–929. doi:10.1016/j.biopha.2018.03.130
- Liu, X., Cui, G., and Dong, J. (2018d). Comparative study on mobilization of endogenous MSCs in treatment of ulcerative colitis rats by shenling baizhu powder and tongxie yaofang decoction. *Chin. J. Inf. TCM* 25 (11), 41–45. doi:10.3969/j.issn.1005-5304.2018.11.010
- Liu, X., Yu, X., Xu, X., Zhang, X., and Zhang, X. (2018e). The protective effects of Poria cocos-derived polysaccharide CMP33 against IBD in mice and its molecular mechanism. *Food Funct.* 9 (11), 5936–5949. doi:10.1039/c8fo01604f
- Liu, Y., Ding, Y., Gao, C., Li, L. S., Wang, Y. X., and Xu, J. D. (2018f). Functional macrophages and gastrointestinal disorders. *World J. Gastroenterol.* 24 (11), 1181–1195. doi:10.3748/wjg.v24.i11.1181
- Liu, Y., Xu, W., and Zeng, L. (2019). Shen ling baizhu powder regulates intestinal crypt epithelial cell damage by autophagy. *Traditional Chin. Drug Res. Clin. Pharmacol.* 30 (10), 1165–1171. doi:10.19378/j.issn.1003-9783.2019.10.003
- Liu, Q., Cheng, Z., and Chen, G. (2021a). Progress in TCM treatment of ulcerative colitis. *J. Basic Chin. Med.* 27 (07), 1191–1194. doi:10.19945/j.cnki.issn.1006-3250.2021.07.039
- Liu, R., Zhou, C., and Du, X. (2021b). Stage treatment of ulcerative colitis. *Chin. J. Integr. Traditional West. Med. Dig.* 29 (1), 67–71. doi:10.3969/j.issn.1671-038X.2021.01.15
- Liu, T., Zhu, L., and Wang, L. (2022a). A narrative review of the pharmacology of ginsenoside compound K. *Ann. Transl. Med.* 10 (4), 234. doi:10.21037/atm-22-501
- Liu, Y., Li, B., Su, Y., Zhao, R. X., Song, P., Li, H., et al. (2022b). Potential activity of traditional Chinese medicine against ulcerative colitis: A review. *J. Ethnopharmacol.* 289, 115084. doi:10.1016/j.jep.2022.115084
- Liu, Y., Rui, X., and Li, J. (2022c). Effects of Platycodon grandiflorum polysaccharide on ulcerative colitis. *Chin. Tradit. Pat. Med.* 44 (04), 1093–1099. doi:10.3969/j.issn.1001-1528.2022.04.010
- Long, J., Kang, Z., and Zhong, Y. (2022a). Ginsenoside Rg1 regulates cell balance of Treg/Th9 in mice with DSS-induced colitis. *Traditional Chin. Drug Res. Clin. Pharmacol.* 33 (01), 20–26. doi:10.19378/j.issn.1003-9783.2022.01.004
- Long, J., Liu, X., Kang, Z., Wang, M. X., Zhao, H. M., Huang, J. Q., et al. (2022b). Ginsenoside Rg1 ameliorated experimental colitis by regulating the balance of M1/M2 macrophage polarization and the homeostasis of intestinal flora. *Eur. J. Pharmacol.* 917, 174742. doi:10.1016/j.ejphar.2022.174742
- Lu, Q., Wu, X., Han, W., Zhang, W., Wang, Y., Kong, D., et al. (2021). Effect of Glycyrrhiza uralensis against ulcerative colitis through regulating the signaling pathway of FXR/P-gp. *Am. J. Transl. Res.* 13 (8), 9296–9305.
- Lu, G., Xing, X., Wang, J., et al. (2022). Research progress of Shenling Baizhu San and predictive analysis on quality markers. *China J. Chin. Materia Medica* 04, 1–13. doi:10.19540/j.cnki.cjcm.20220421.201
- Luo, L., Shao, J., and Sun, Y. (2014). Clinical observation on the treatment of ulcerative colitis with Shaoyao decoction and shenling baizhu powder. *Shanxi J. Traditional Chin. Med.* 30 (10), 39–40+60. doi:10.3969/j.issn.1000-7156.2014.10.018
- Lv, Y., Bao, R., and Zhang, L. (2022). Effect of modified shenling baizhusan on gastrointestinal dysfunction and protein-energy wasting in continuous ambulatory peritoneal dialysis patients. *Chin. J. Exp. Traditional Med. Formulae* 28 (03), 116–122. doi:10.13422/j.cnki.syfjx.20220393
- Ma, H., Qin, Y., and Wang, L. (2015). Observation on curative effect of Shenling Baizhu Powder and Aidisha in the treatment of ulcerative colitis and its effect on inflammatory factors. *Guid. J. Traditional Chin. Med. Pharm.* 21 (04), 71–72. doi:10.13862/j.cnki.cn43-1446/r.2015.04.024
- Ma, Q., Ouyang, Y., Meng, F., Noolvi, M. N., Avvaru, S. P., More, U. A., et al. (2019). A review of pharmacological and clinical studies on the application of Shenling Baizhu San in treatment of Ulcerative colitis. *J. Ethnopharmacol.* 244, 112105. doi:10.1016/j.jep.2019.112105
- Ma, Y., Zhang, L., Wu, Y., and Zhou, P. (2019). Changes in milk fat globule membrane proteome after pasteurization in human, bovine and caprine species. *Food Chem.* 32 (02), 209–215. doi:10.1016/j.foodchem.2018.12.015
- Ma, J. (2021). *Effect of Sishen wan combined with Shenling Baizhu san on ulcerative colitis of spleen kidney yang deficiency type*. [master's thesis]. China: Anhui University of Chinese Medicine. doi:10.26922/d.cnki.ganzc.2021.000333
- Mao, M., Lin, P., and Xiong, L. (2021a). Changes in diversity of intestinal butyrate-producing bacteria during treatment with shenling baizhusan and lizhongtang in animal model of AAD. *Chin. J. Exp. Traditional Med. Formulae* 27 (22), 23–30. doi:10.13422/j.cnki.syfjx.20212106
- Mao, Y., Hu, G., Meng, Q., Li, X., Sun, X., Zhou, J., et al. (2021b). Efficacy of shenling baizhu san on stable chronic obstructive pulmonary disease patients: A systematic review and meta-analysis. *J. Ethnopharmacol.* 272, 113927. doi:10.1016/j.jep.2021.113927
- Miao, Z., Yan, J., and Gu, M. (2019). The effects of ginsenoside g3 on the Th1/Th2 imbalance in DSS induced colitis mice. *Pharmacol. Clin. Chin. Materia Medica* 35 (01), 47–51. doi:10.13412/j.cnki.zyyj.2019.01.011
- Mu, L., and Xiao, M. (2016). Long-term efficacy and safety of shenling baizhu powder treating ulcerative colitis. *Liaoning J. Traditional Chin. Med.* 43 (02), 309–311. doi:10.13192/j.issn.1000-1719.2016.02.034
- Murugan, S. K., Bethapudi, B., Raghunandhakumar, S., Purusothaman, D., Nithyanantham, M., Mundkinajeddu, D., et al. (2022). A flavonoid rich standardized extract of Glycyrrhiza glabra protects intestinal epithelial barrier function and regulates the tight-junction proteins expression. *BMC Complement. Med. Ther.* 22 (1), 38. doi:10.1186/s12906-021-03500-1
- Ouyang, Z. (2015). Parallel randomized controlled study of chronic enteritis Shenglingbaizhu powder combined Western medicine. *J. Pract. Traditional Chin. Intern. Med.* 29 (04), 96–97. doi:10.13729/j.issn.1671-7813.2015.04.42
- Pavlick, K. P., Laroux, F. S., Fuseler, J., Wolf, R. E., Gray, L., Hoffman, J., et al. (2002). Role of reactive metabolites of oxygen and nitrogen in inflammatory bowel disease. *Free Radic. Biol. Med.* 33 (3), 311–322. doi:10.1016/s0891-5849(02)00853-5
- Piechota-Polanczyk, A., and Fichna, J. (2014). Review article: The role of oxidative stress in pathogenesis and treatment of inflammatory bowel diseases. *Naunyn. Schmiedeb. Arch. Pharmacol.* 387 (7), 605–620. doi:10.1007/s00210-014-0985-1
- Planell, N., Lozano, J. J., Mora-Buch, R., Masamunt, M. C., Jimeno, M., Ordas, I., et al. (2013). Transcriptional analysis of the intestinal mucosa of patients with

ulcerative colitis in remission reveals lasting epithelial cell alterations. *Gut* 62 (7), 967–976. doi:10.1136/gutjnl-2012-303333

Qi, Y., Niu, M., and Zhang, L. (2022). Effect of Shenling Baizhu Powder on Th17/Treg immune balance in rats with ulcerative colitis. *China's Naturop.* 30 (06), 88–92. doi:10.19621/j.cnki.11-3555/r.2022.0631

Qian, W., and Zhang, W. (2019). Effect of shenlingbaizhu powder combined with mesalamine on inflammatory factors and immune function in children and adolescents with ulcerative colitis. *Her. Med.* 38 (05), 584–588. doi:10.3870/j.issn.1004-0781.2019.05.011

Qin, L. (2012). Clinical observation on treating 75 cases of ulcerative colitis with Shenling Baizhu San. *Clin. J. Chin. Med.* 4 (13), 76–77. doi:10.3969/j.issn.1674-7860.2012.13.042

Qu, H., Ou, H., and Lin, K. (2021). Research progress on chemical constituents and pharmacological activities of Amomum longiligulare. *J. Hainan Medical Univ.* (05), 1–8. doi:10.13210/j.cnki.jhmu.20210524.001

Qu, B., Cao, T., Wang, M., Wang, S., Li, W., and Li, H. (2022a). Ginsenosides Rd monomer inhibits proinflammatory cytokines production and alleviates DSS-colitis by NF- κ B and P38MAPK pathways in mice. *Immunopharmacol. Immunotoxicol.* 44 (1), 110–118. doi:10.1080/08923973.2021.2012482

Qu, L., Shi, K., Xu, J., Liu, C., Ke, C., Zhan, X., et al. (2022b). Atractylenolide-1 targets SPHK1 and B4GALT2 to regulate intestinal metabolism and flora composition to improve inflammation in mice with colitis. *Phytomedicine*. 98, 153945. doi:10.1016/j.phymed.2022.153945

Quan, L., and Tan, J. (2017). Clinical study of shenling baizhu san for ulcerative colitis. *J. new Chin. Med.* 49 (08), 42–44. doi:10.13457/j.cnki.jncm.2017.08.013

Rabe, H., Malmquist, M., Barkman, C., Östman, S., Gertsson, I., Saalman, R., et al. (2019). Distinct patterns of naive, activated and memory T and B cells in blood of patients with ulcerative colitis or Crohn's disease. *Clin. Exp. Immunol.* 197 (1), 111–129. doi:10.1111/cei.13294

Ren, T. (2010). Treating 49 cases of chronic ulcerative colitis with shenlingbaizhu Decoction. *Fujian J. TCM* 41 (02), 39–40. doi:10.13260/j.cnki.jfjtcn.009912

Saba, E., Lee, Y. Y., Rhee, M. H., and Kim, S. D. (2020). Alleviation of ulcerative colitis potentially through th1/th2 cytokine balance by a mixture of rg3-enriched Korean red ginseng extract and persicaria tinctoria. *Mol. (Basel, Switz.* 25 (22), 5230. doi:10.3390/molecules25225230

Shen, L., Liu, J., Qian, Z., et al. (2021). Clinical effect of sishen pills and shenling baizhu powder combined with mesalazine for ulcerative colitis and its effect on intestinal flora and intestinal barrier function. *J. new Chin. Med.* 53 (16), 34–38. doi:10.13457/j.cnki.jncm.2021.16.010

Shi, J., Zhao, Y., Wang, Y., Gao, W., Ding, J., Li, P., et al. (2014). Inflammatory caspases are innate immune receptors for intracellular LPS. *Nature* 514 (7521), 187–192. doi:10.1038/nature13683

Shi, K., Li, Y., and Deng, T. (2018a). Effect of shenling baizhu san on expressions of ICAM-1 and VCAM-1 in colon mucosal tissues of ulcerative colitis rats. *Pharm. J. Chin. People's Liberation Army* 34 (05), 390–393. doi:10.3969/j.issn.1008-9926.2018.05.003

Shi, W., Sun, D., and Hu, Y. (2018b). Effect of shenling baizhu powder on ulcerative colitis patients serum SOD and MDA. *J. Yunnan Univ. Traditional Chin. Med.* 41 (03), 65–68. doi:10.19288/j.cnki.issn.1000-2723.2018.03.015

Shi, J. (2011). Ginsenoside Rd inhibits the activation of NF- κ B signal transduction pathways in colonic tissues of rats with ulcerative colitis in the acute phase.

Shkoda, A., Ruiz, P. A., Daniel, H., Kim, S. C., Rogler, G., Sartor, R. B., et al. (2007). Interleukin-10 blocked endoplasmic reticulum stress in intestinal epithelial cells: Impact on chronic inflammation. *Gastroenterology* 132 (1), 190–207. doi:10.1053/j.gastro.2006.10.030

Sun, X., and Chen, T. (2014). Shenling Baizhu Powder treating 43 cases of diarrhea with spleen deficiency and dampness of irritable bowel syndrome. *Chin. Med. Mod. Distance Educ. China* 12 (03), 23–24. doi:10.3969/j.issn.1672-2779.2014.03.012

Sun, H., and Guo, X. (2022). Clinical effect of modified Shenling Baizhu powder combined with self-made traditional Chinese medicine enema formula in the treatment of ulcerative colitis of spleen deficiency and dampness type and its influence on the levels of inflammatory factors. *Clin. Res. Pract.* 7 (17), 151–154. doi:10.19347/j.cnki.2096-1413.202217041

Sun, J., Ge, Y., and Li, Z. (2020a). Shenling Baizhu San ameliorated murine ulcerative colitis based on TLR4/NF- κ B pathway. *Chin. J. Immunol.* 36 (03), 294–298+304. doi:10.3969/j.issn.1000-484X.2020.03.008

Sun, J., Ge, Y., and Li, Z. (2020b). Shenling Baizhu San ameliorated murine ulcerative colitis based on TLR4/NF- κ B pathway. *Chin. J. Immunol.* 36 (03), 294–298+304. doi:10.3969/j.issn.1000-484X.2020.03.008

Tian, T., and Song, Q. (2015). Therapeutic effect analysis of Shenlingbaizhu Powder in treating chronic enteritis. *Clin. J. Chin. Med.* 7 (36), 111–112. doi:10.3969/j.issn.1647-7860.2015.36.052

Tian, Y., Chen, X., and Zhang, H. (2019). The effect of Shenling Baizhu granule combined with mesalazine on Th17/Treg balance in patients with ulcerative colitis and its clinical efficacy. *Chin. J. Integr. Traditional West. Med. Dig.* 27 (09), 703–706. doi:10.3969/j.issn.1671-038X.2019.09.13

Tian, M., Ma, P., Zhang, Y., Mi, Y., and Fan, D. (2020). Ginsenoside Rk3 alleviated DSS-induced ulcerative colitis by protecting colon barrier and inhibiting NLRP3 inflammasome pathway. *Int. Immunopharmacol.* 85, 106645. doi:10.1016/j.intimp.2020.106645

Tian, L. (2019). Clinical evaluation of Shenling Baizhu powder and lavaging with traditional Chinese medicine in the treatment of chronic nonspecific ulcerative colitis. 14(30), 108–109. DOI: doi:10.14163/j.cnki.11-5547/r.2019.30.064

Tong, J. (2021). Study on the inhibitory effect of Shenling Baizhu powder on inflammation of ulcerative colitis model rats based on Janus kinase 2/signal transduction and transcription activator 3 signaling pathway. *Shaanxi J. Traditional Chin. Med.* 42 (08), 1010–1015. doi:10.3969/j.issn.1000-7369.2021.08.006

Trétou, X., Pédruzzi, E., Cazals-Hatem, D., Grodet, A., Panis, Y., Groyer, A., et al. (2011). Altered endoplasmic reticulum stress affects translation in inactive colon tissue from patients with ulcerative colitis. *Gastroenterology* 141 (3), 1024–1035. doi:10.1053/j.gastro.2011.05.033

Ungaro, R., Mehandru, S., Allen, P. B., Peyrin-Biroulet, L., and Colombel, J. F. (2017). Ulcerative colitis. *Lancet (London, Engl.* 389 (10080), 1756–1770. doi:10.1016/s0140-6736(16)32126-2

Vijay, K. (2018). Toll-like receptors in immunity and inflammatory diseases: Past, present, and future. *Int. Immunopharmacol.* 59, 391–412. doi:10.1016/j.intimp.2018.03.002

Walle, L. V., and Lamkanfi, M. (2016). Pyroptosis. *Current Biol.* 26 (13), R568–R572. doi:10.1016/j.cub.2016.02.019

Wang, C., Xue, L., Wang, Y., Huang, Q., and Zhang, B. (2016). Substituent distribution changes the pasting and emulsion properties of octenylsuccinate starch. *Carbohydr. Polym.* 46 (08), 64–71. doi:10.1016/j.carbpol.2015.08.044

Wang, C. Z., Yao, H., Zhang, C. F., Chen, L., Wan, J. Y., Huang, W. H., et al. (2018a). American ginseng microbial metabolites attenuate DSS-induced colitis and abdominal pain. *Int. Immunopharmacol.* 64, 246–251. doi:10.1016/j.intimp.2018.09.005

Wang, X., Li, Y., and Song, Y. (2018b). Determination of ginsenosides in Shenling Baizhu powder based on HPLC fingerprint. *World Chin. Med.* 13 (11), 2876–2879+2883. doi:10.3969/j.issn.1673-7202.2018.11.052

Wang, M., Hu, R., Wang, Y., Liu, L., You, H., Zhang, J., et al. (2019). Atractylenolide III attenuates muscle wasting in chronic kidney disease via the oxidative stress-mediated PI3K/AKT/mTOR pathway. *Oxid. Med. Cell. Longev.* 1875471. doi:10.1155/2019/1875471

Wang, Z., Li, C., He, X., Xu, K., Xue, Z., Wang, T., et al. (2022). Platycodon grandiflorum root fermentation broth reduces inflammation in a mouse IBD model through the AMPK/NF- κ B/NLRP3 pathway. *Food Funct.* 13 (7), 3946–3956. doi:10.1039/d1fo03969e

Wang, X., Ning, Y., Wang, L., Zhang, J., Wang, Y., and Shen, H. (2016). Treatment of one case with cryoglobulinaemia secondary to connective tissue disease with small doses of rituximab. *West Indian Med. J.* 9 (04), 398–400. doi:10.7727/wimj.2014.384

Wang, X. (2019). Shenling baizhu san modified in the treatment of chronic enteritis :effect observation on 55 cases. *Chin. J. Coloproctology* 39 (01), 29–30. doi:10.3969/j.issn.1000-1174.2019.01.015

Wei, G., Zhen, X., Zhou, Y., et al. (2013). Efficacy of Shenling Baizhu Powder combined with Mesalazine in the treatment of ulcerative colitis with spleen and stomach Qi deficiency and its effect on serum IL-17, TNF- α and IL-23 levels. *Guangdong Med. J.* 34 (01), 143–145. doi:10.13820/j.cnki.gdyx.2013.01.015

Wen, X., Hu, Y., Liao, L., et al. (2017). Meta-analysis on effectiveness and safety of modified shenling baizhu san and western medicines in treating ulcerative colitis. *Chin. J. Exp. Traditional Med. Formulae* 23 (10), 205–210. doi:10.13422/j.cnki.syfx.2017100205

Wu, R., Luo, J., and Wu, J. (2017). Meta- analysis of shenling baizhu powder combined with aminosalicic acid preparation in the treatment of ulcerative colitis. *China Pharm.* 28 (36), 5119–5122. doi:10.6039/j.issn.1001-0408.2017.36.21

Wullaert, A., Bonnet, M. C., and Pasparakis, M. (2011). NF- κ B in the regulation of epithelial homeostasis and inflammation. *Cell Res.* 21 (1), 146–158. doi:10.1038/cr.2010.175

Xiang, W., Liu, J., and Yang, W. (2017). Observation on treating ulcerative colitis with the Shenling Baizhu granules plus lacteol fort and mesalazine. *Clin. J. Chin. Med.* 9 (25), 42–44. doi:10.3969/j.issn.1674-7860.2017.25.021

- Xie, J., Wu, F., and Liu, C. (2015). Efficacy and safety analysis of Shenling Baizhu Powder in treating colitis. *J. Med. Theory Pract.* 28 (06), 760–761. doi:10.19381/j.issn.1001-7585.2015.06.032
- Xin, P., Xu, X., Deng, C., Liu, S., Wang, Y., Zhou, X., et al. (2020). The role of JAK/STAT signaling pathway and its inhibitors in diseases. *Int. Immunopharmacol.* 80, 106210. doi:10.1016/j.intimp.2020.106210
- Xiong, Y., Zhong, Y., Chen, Y., et al. (2021). Anti-inflammatory and antioxidant mechanism of shenling baizhu granules on experimental ulcerative colitis rats with dampness stagnancy due to spleen deficiency. *Traditional Chin. Drug Res. Clin. Pharmacol.* 32 (02), 149–157. doi:10.19378/j.issn.1003-9783.2021.02.001
- Xu, A. T., Lu, J. T., Ran, Z. H., and Zheng, Q. (2016). Exosome in intestinal mucosal immunity. *J. Gastroenterol. Hepatol.* 31 (10), 1694–1699. doi:10.1111/jgh.13413
- Xu, Y., Chen, X., and Huang, H. (2018). Clinical effects of the Shenling Baizhu Jianpi granule on chronic colitis and immune function. *Clin. J. Chin. Med.* 10 (04), 1–3. doi:10.3969/j.issn.1674-7860.2018.04.001
- Xu, Y., Zhu, B., Li, X., Li, Y. F., Ye, X. M., and Hu, J. N. (2022). Glycogen-based pH and redox sensitive nanoparticles with ginsenoside Rh(2) for effective treatment of ulcerative colitis. *Biomaterials* 280, 121077. doi:10.1016/j.biomaterials.2021.121077
- Xu, J., Xue, H. L., Wang, Z., Fan, C., Wu, M., and Xu, L. X. (2021). Estrogen receptor 2 mediates intraspecific aggressive behaviors of the female *Cricetulus barabensis* in the estrous cycle. *J. Integr. Neurosci.* 18 (06), 77–85. doi:10.31083/j.jin.2021.01.302
- Xu, W. (2020). Effect of shenling baizhu powder on the treatment of inflammatory bowel disease by regulating endoplasmic reticulum stress. [master's thesis]. China: Jiangxi University of Traditional Chinese Medicine. doi:10.27180/d.cnki.gjxzc.2020.000175
- Yang, X., Guo, T., Wang, Y., Gao, M. T., Qin, H., and Wu, Y. J. (2012). Therapeutic effect of ginsenoside Rd in rats with TNBS-induced recurrent ulcerative colitis. *Arch. Pharm. Res.* 35 (7), 1231–1239. doi:10.1007/s12272-012-0714-6
- Yang, L., Song, Y., Jin, P., Liu, Y., Wang, Y., Qiao, H., et al. (2018). Shen-Ling-Bai-Zhu-San for ulcerative colitis: Protocol for a systematic review and meta-analysis. *Medicine* 97 (38), e12337. doi:10.1097/md.00000000000012337
- Yang, L., Song, Y., and Niu, J. (2021). The influence of ginseng and Poria and white Atractylodes powder on intestinal flora of patients with ulcerative colitis. *Henan Tradit. Chin. Med.* 41 (09), 1357–1361. doi:10.16367/j.issn.1003-5028.2021.09.0308
- Yang, W. (2012). Clinical effect of Shenlingbaizhu Powder combined with sulfasalazine in chronic colitis. *Guide China Med.* 10 (10), 644–645. doi:10.15912/j.cnki.gocm.2012.10.321
- Yang, H. (2017). Effect evaluation of Shenling Baizhu Powder on ulcerative colitis patients with spleen and stomach Qi deficiency. *World Latest Medicine Inf.* 17 (80), 98. doi:10.19613/j.cnki.1671-3141.2017.80.084
- Yang, F. (2018). Clinical research progress of shenling baizhu powder. *J. New Chin. Med.* 50 (10), 38–42. doi:10.13457/j.cnki.jncm.2018.10.010
- Yao, Z., Chen, W., Yang, Z., et al. (2019). Research progress in Atractylodes macrocephala and predictive analysis on Q-marker. *Traditional Herb. Drugs* 50 (19), 4796–4807. doi:10.7501/j.issn.0253-2670.2019.19.031
- Yap, K. N., Yamada, K., Zikeli, S., Kiaris, H., and Hood, W. R. (2021). Evaluating endoplasmic reticulum stress and unfolded protein response through the lens of ecology and evolution. *Biol. Rev. Camb. Philos. Soc.* 96 (2), 541–556. doi:10.1111/brv.12667
- Ye, H., Chen, C., and Zhu, S. (2014a). Effects of baizhu decoction on ulcerative colitis model rats and the serum IL-6, IL-17. *J. Shaanxi Coll. Traditional Chin. Med.* 37 (1), 69–71. doi:10.13424/j.cnki.jsctcm.2014.01.036
- Ye, H., Wu, Q., Zhu, Y., Guo, C., and Zheng, X. (2014b). Ginsenoside Rh2 alleviates dextran sulfate sodium-induced colitis via augmenting TGFβ signaling. *Mol. Biol. Rep.* 41 (8), 5485–5490. doi:10.1007/s11033-014-3422-0
- Yi, P., Guo, M., and Song, J. (2021). The clinical efficacy of mesalazine combined with Shenlingbaizhu powder in treatment of ulcerative colitis. *Hebei Med. J.* 29 (1), 3741–3744. doi:10.3969/j.issn.1002-7386.2021.24.014
- Yin, Y., Zhan, M., and Hua, D. (2021). Meta-analysis of shenling baizhu powder combined with mesalazine in the treatment of ulcerative colitis. *Guid. J. Traditional Chin. Med. Pharmacol.* 27 (08), 176–181. doi:10.13862/j.cnki.cn43-1446/r.2021.08.037
- You, Y., Liu, Y. H., and Liao, W. D. (2019). Effect of shenling baizhu san on murine model of IBD induced by DSS in mice through regulating of autophagy. *Chin. J. Exp. Traditional Med. Formulae* 25 (5), 43–49. doi:10.13422/j.cnki.syfx.20190504
- Yu, H., Jia, Y., Cheng, Y., et al. (2018). Effect of Shenling Baizhu Powder on expression of IL-6, IL-10 and C-FOS gene in colon tissue of UC rats with spleen deficiency and dampness. *Lishizhen Med. materia medica Res.* 29 (05), 1049–1052. doi:10.3969/j.issn.1008-0805.2018.05.008
- Yu, L., Xing, Z. K., Mi, S. L., and Wu, X. (2019a). Regulatory effect of traditional Chinese medicine on intestinal microbiota. *Zhongguo Zhong yao za zhi = Zhongguo zhongyao zazhi = China J. Chin. materia medica* 44 (1), 34–39. doi:10.19540/j.cnki.cjcmm.20181101.013
- Yu, X., Feng, X., and Zhang, J. (2019b). Research progress on chemical constituents and pharmacological effects of Panax ginseng. *Ginseng Res.* 31 (01), 47–51. doi:10.19403/j.cnki.1671-1521.2019.01.012
- Yu, W., Wang, G., Lu, C., Liu, C., Jiang, L., Jiang, Z., et al. (2022). Pharmacological mechanism of Shenlingbaizhu formula against experimental colitis. *Phytomedicine* 98, 153961. doi:10.1016/j.phymed.2022.153961
- Yu, B. (2017). Clinical observation of Shenlingbaizhu Powder combined with sulfasalazine in the treatment of chronic colitis with spleen and stomach weakness. *J. Pract. Traditional Chin. Med.* 33 (03), 254. doi:10.3969/j.issn.1004-2814.2017.03.022
- Yu, L. C.-H. (2018). Microbiota dysbiosis and barrier dysfunction in inflammatory bowel disease and colorectal cancers: Exploring a common ground hypothesis. *J. Biomed. Sci.* 25 (1), 79. doi:10.1186/s12929-018-0483-8
- Zhang, S., Shen, H., Zheng, K., et al. (2017). Consensus on diagnosis and treatment of ulcerative colitis with integrated Chinese and western medicine (2017). *China J. Traditional Chin. Med. Pharm.* 32 (08), 3585–3589. doi:10.3969/j.issn.1671-038X.2018.02.01
- Zhang, Y., Tang, K., Deng, Y., Chen, R., Liang, S., Xie, H., et al. (2018). Effects of shenling baizhu powder herbal formula on intestinal microbiota in high-fat diet-induced NAFLD rats. *Biomed. Pharmacother.* 102, 1025–1036. doi:10.1016/j.biopha.2018.03.158
- Zhang, J., Xu, X., Li, N., Cao, L., Sun, Y., Wang, J., et al. (2022a). Licoflavone B, an isoprene flavonoid derived from licorice residue, relieves dextran sodium sulfate-induced ulcerative colitis by rebuilding the gut barrier and regulating intestinal microflora. *Eur. J. Pharmacol.* 916, 174730DOI: doi:10.1016/j.ejphar.2021.174730
- Zhang, Y., Gao, H., Zheng, J., et al. (2022b). Shenling baizhu powder combined with gegen qinlian decoction in treating ulcerative colitis for 30 cases. *Chin. Med. Mod. Distance Educ. China* 20 (02), 84–86. doi:10.3969/j.issn.1672-2779.2022.02.031
- Zhang, S. (2010). Consensus on TCM diagnosis and treatment of ulcerative colitis. *China J. Traditional Chin. Med. Pharm.* 30 (05), 527–532.
- Zhang, Z., Liu, H., Shi, Y., Xu, N., Wang, Y., Li, A., et al. (2017). Increased circulating Th22 cells correlated with Th17 cells in patients with severe preeclampsia. *Hypertens. Pregnancy* 9 (16), 100–107. doi:10.1080/10641955.2016.1239737
- Zhao, Y. G., and Zhang, H. (2018). Formation and maturation of autophagosomes in higher eukaryotes: A social network. *Curr. Opin. Cell Biol.* 53, 29–36. doi:10.1016/j.ccb.2018.04.003
- Zhao, C., Wang, F., Xiao, L., et al. (2017). Influence of adjunctive therapy with shenling baizhu powder on the immune function and clinical effect of elderly patients with colitis gravis and bloody purulent stool. *Prog. Mod. Biomed.* 17 (15), 2906+2920–2922. doi:10.13241/j.cnki.pmb.2017.15.031
- Zhao, J. (2009). Effect of volatile from A.longiligulare T.L.Wu on experimental ulcerative colitis and its safety assessment. [dissertation/master's thesis]. China: ChongQing Medical University. doi:10.7666/d.Y1546988
- Zheng, Z., and Wang, J. (2022). Bone marrow mesenchymal stem cells combined with Atractylodes macrocephala polysaccharide attenuate ulcerative colitis. *Bioengineered* 13 (1), 824–833. doi:10.1080/21655979.2021.2012954
- Zhou, T., Yang, S., and Wang, J. (2018). Effects of Shenlingbaizhu powder combined with mesalazine in the treatment of ulcerative colitis and the influence of NLRP3 inflammasome. *Chin. J. Clin. Pharmacol. Ther.* 23 (03), 319–324. doi:10.12092/j.issn.1009-2501.2018.03.013
- Zhou, D., Zhang, H., and Ge, S. (2019). The level changing of serum MCP-1, IL-6, TNF-α from type 2 diabetic nephropathy patients administrated with metformin and shen Qin baizhu powder. *J. Gansu Sci.* 31 (1), 5. doi:10.16468/j.cnki.issn1004-0366.2019.01.014
- Zhou, L., Zeng, L., and Ji, X. (2021a). Effect of warm acupuncture combined with Shenling Baizhu Powder for brain - gut interactions and inflammatory factors in patients with ulcerative colitis of spleen dampness. *Hebei J. Traditional Chin. Med.* 43 (09), 1483–1487+1524. doi:10.3969/j.issn.1002-2619.2021.09.018
- Zhou, Q., Yu, R., Liu, T., Li, Y., Zhong, J., Zhang, T., et al. (2021b). Coix seed diet ameliorates immune function disorders in experimental colitis mice. *Nutrients* 14 (1), 123. doi:10.3390/nu14010123

Zhou, M. (2009). Shenling baizhu powder and tongxie yaofang treat irritable bowel syndrome. *Zhejiang J. Integr. traditional Chin. West. Med.* 19 (06), 359–360. doi:10.3969/j.issn.1005-4561.2009.06.015

Zhu, S., and Li, M. (2012). Treating ulcerative colitis with tongxie yaofang and shenling baizhu powder. *Inn. Mongol J. Traditional Chin. Med.* 03 (11), 36–37. doi:10.16040/j.cnki.cn15-1101.2012.03.018

Zhu, Y., Zhao, J., Chen, G., et al. (2009). Therapeutic effect of volatile oil from *A. longiligulare* T.L.Wu on ulcerative colitis induced by 2, 4-dinitrobenzene-1-chlorobenzene and acetic acid in rats. *Chin. J. Pharmacol. Toxicol.* 23 (05), 388–394. doi:10.3867/j.issn.1000-3002.2009.05.009

Zhu, H., Zhu, H., Chen, W., et al. (2014). Effect of water extract of *Atractylodes macrocephala* on inflammatory factors in rats with ulcerative colitis. *Zhejiang J. Traditional Chin. Med.* 49 (01), 51–53. doi:10.13633/j.cnki.zjtcn.2014.01.043

Zhu, C. (2012). Efficacy observation on treating chronic colitis shenling Baishu San and Bifico. *Clin. J. Chin. Med.* 4 (02), 42–43. doi:10.3969/j.issn.1674-7860.2012.02.027

Zuo, J., Yi, B., and Hu, X. (2019). Research progress in the chemical constituents and modern pharmacology of *Platycodon*. *J. Liaoning Univ. Traditional Chin. Med.* 21 (01), 113–116. doi:10.13194/j.issn.1673-842x.2019.01.031



OPEN ACCESS

EDITED BY

Muhammad Hasnat,
University of Veterinary and Animal
Sciences, Pakistan

REVIEWED BY

Hafiz Ishfaq Ahmad,
University of Veterinary and Animal
Sciences, Pakistan
Tahir Ali Chohan,
University of Veterinary and Animal
Sciences, Pakistan

*CORRESPONDENCE

Xiao-Jian Han,
hanxiaojian@hotmail.com
Cai-Feng Xie,
xiecaifeng@ncu.edu.cn

[†]These authors have contributed equally
to this work

SPECIALTY SECTION

This article was submitted to
Ethnopharmacology,
a section of the journal
Frontiers in Pharmacology

RECEIVED 24 May 2022

ACCEPTED 10 August 2022

PUBLISHED 06 September 2022

CITATION

Wang T, Lu Z, Qu X-H, Xiong Z-Y,
Wu Y-T, Luo Y, Zhang Z-Y, Han X-J and
Xie C-F (2022), Chrysophanol-8-O-
glucoside protects mice against acute
liver injury by inhibiting autophagy in
hepatic stellate cells and inflammatory
response in liver-resident macrophages.
Front. Pharmacol. 13:951521.
doi: 10.3389/fphar.2022.951521

COPYRIGHT

© 2022 Wang, Lu, Qu, Xiong, Wu, Luo,
Zhang, Han and Xie. This is an open-
access article distributed under the
terms of the [Creative Commons
Attribution License \(CC BY\)](https://creativecommons.org/licenses/by/4.0/). The use,
distribution or reproduction in other
forums is permitted, provided the
original author(s) and the copyright
owner(s) are credited and that the
original publication in this journal is
cited, in accordance with accepted
academic practice. No use, distribution
or reproduction is permitted which does
not comply with these terms.

Chrysophanol-8-O-glucoside protects mice against acute liver injury by inhibiting autophagy in hepatic stellate cells and inflammatory response in liver-resident macrophages

Tao Wang^{1†}, Zhuo Lu^{1,2,3†}, Xin-Hui Qu^{1,4}, Zi-Ying Xiong⁵,
Ya-Ting Wu², Yong Luo⁶, Zi-Yu Zhang⁵, Xiao-Jian Han^{1,4,7*} and
Cai-Feng Xie^{2*}

¹Institute of Geriatrics, Jiangxi Provincial People's Hospital, The First Affiliated Hospital of Nanchang Medical College, Nanchang, China, ²School of Basic Medical Sciences, Nanchang University, Nanchang, China, ³Department of Thoracic Surgery, The First Affiliated Hospital of Nanchang University, Nanchang, China, ⁴Department of Neurology, Jiangxi Provincial People's Hospital, The First Affiliated Hospital of Nanchang Medical College, Nanchang, China, ⁵Department of Pathology, Jiangxi Maternal and Child Health Hospital, Nanchang, China, ⁶Key Laboratory of Women's Reproductive Health of Jiangxi, Jiangxi Maternal and Child Health Hospital, Nanchang, China, ⁷Department of Pharmacology, School of Pharmaceutical Science, Nanchang University, Nanchang, China

Acute liver failure (ALF) is an unfavorable condition characterized by the rapid loss of liver function and high mortality. Chrysophanol-8-O-glucoside (CPOG) is an anthraquinone derivative isolated from *rhubarb*. This study aims to evaluate the protective effect of CPOG on lipopolysaccharide (LPS)/D-GalN-induced ALF and its underlying mechanisms. LPS/D-GalN-induced mice ALF model and LPS treatment model in RAW 264.7 and LX2 cells were established. It was found that CPOG ameliorated LPS/D-GalN-induced liver injury and improved mortality as indicated by Hematoxylin-eosin (H&E) staining. Molecularly, qPCR and ELISA results showed that CPOG alleviated LPS/D-GalN-induced release of alanine aminotransferase and aspartate transaminase and the secretion of TNF- α and IL-1 β *in vivo*. LPS/D-GalN-induced intracellular ROS production was also attenuated by CPOG in liver tissue. Further, CPOG attenuated ROS generation and inhibited the expression of p-I κ B and p-p65 as well as the expression of TNF- α and IL-1 β stimulated by LPS in RAW 264.7 cells. In addition, CPOG alleviated LPS-induced up-regulation of LC3B, p62, ATG5 and Beclin1 by attenuating ROS production and inhibiting MAPK signaling in LX2 cells. Taken together, our data indicated that the CPOG protected against LPS/D-GalN-induced ALF by inhibiting oxidative stress, inflammation response and autophagy. These findings suggest that CPOG could be potential drug for the treatment of ALF in clinic.

Abbreviations: ALF, Acute liver failure; ALT, Alanine aminotransferase; AST, Aspartate transaminase; CPOG, Chrysophanol-8-O-glucoside; D-GalN, D-galactosamine; HSC, Hepatic stellate cell; LPS, Lipopolysaccharide; NPC, Non-parenchymal cell; ROS, Reactive oxygen species.

KEYWORDS

acute liver injury, lipopolysaccharide, chrysophanol-8-O-glucoside, autophagy, oxidative stress

1 Introduction

The liver is generally comprised of non-parenchymal cells (NPC) and parenchymal cells (hepatocytes). Non-parenchymal cells include populations of Kupffer cells, hepatic stellate cells (HSCs), liver sinusoidal endothelial cells (LSEC) and intrahepatic lymphocytes (Racanelli and Rehermann, 2006). The crosstalk between hepatocytes and non-parenchymal cells is key to liver homeostasis, while it is commonly believed that non-parenchymal cells can be primary targets for hepatotoxins and mediate physiological response to endocrine and immune signal (Robinson et al., 2016). Acute liver failure (ALF) is characterized by loss of liver function that occurs rapidly in a person who has no pre-existing liver disease (Krawitz et al., 2018). Apart from liver transplantation, there is no effective remedy (Patel et al., 2018). Therefore, the need for efficient drugs for treating acute liver failure is urgent.

Lipopolysaccharides (LPS), also known as endotoxins, could result in systemic inflammatory response syndrome and multiple organ failure (Jirillo et al., 2002). A well-established mice model of macrophage-mediated ALF is gavage administration of LPS and D-galactosamine (GalN) (Nakama et al., 2001; Wan et al., 2008). LPS quickly stimulated reactive oxygen species (ROS) and impart damage to the both parenchymal and non-parenchymal cells (Hsu and Wen, 2002). LPS can also stimulate inflammatory cells especially macrophages to release various inflammatory mediators like TNF- α and IL-1 β by activating NF- κ B signaling pathway, which further escalated the liver damage by feedback mechanism (Muniandy et al., 2018). Autophagic cell deaths mediated by oxidative stress also play important role in the LPS-induced pathogenesis (Yuan et al., 2009; Li et al., 2015).

Chrysophanol is a free anthraquinone compound isolated from *Rheum genus*. Recent studies showed that Chrysophanol may exert anti-cancer effects (Lu et al., 2010; Ni et al., 2014), anti-inflammation activity (Kim et al., 2010) and offer neuroprotection (Chu et al., 2018). Previous study showed that chrysophanol has protective effect on LPS-induced ALF, though the precise mechanism is not clear (Jiang et al., 2016). However, free chrysophanol has potential hepatotoxicity and nephrotoxicity (Yu et al., 2011; Wang et al., 2017). Animals administered of chrysophanol had adverse reactions such as bowel sounds, nausea, vomiting, abdominal pain and diarrhea. Thus, structural modifications of chrysophanol have been utilized to improve therapeutic efficacy and alleviate its side effect (Shrestha et al., 2014; Mondal et al., 2015).

Chrysophanol-8-O-glucoside (CPOG) is glycosylated chrysophanol, whose content is higher than chrysophanol in

Rheum genus (Wang et al., 2013). *In vitro* study showed that CPOG protected against hepatic fibrosis through STAT3 signaling (Park et al., 2020). However, pharmacology activity *in vivo* of CPOG remains largely unknown.

In this study, we aim to investigate the protective effect of CPOG against acute liver failure and to explore the underlying mechanism with respect to oxidative stress, inflammation response and autophagy. It was found that CPOG ameliorated LPS/D-GalN-induced liver damage and improved survival rate. CPOG alleviated LPS-induced oxidative stress both *in vivo* and *in vitro*. Moreover, CPOG showed anti-oxidant effects and inhibited the release of inflammatory cytokines by the inactivation of NF- κ B signaling pathway in RAW264.7 cells. In addition, CPOG blocked LPS-induced activation of MAPK signaling, therefore attenuated the expression of autophagy-related proteins and LC3 puncta formation in LX2 cells. In conclusion, our study indicate that CPOG could protect against ALF by inhibiting oxidative stress, inflammation response and autophagy. We propose that CPOG could be a potential drug for ALF treatment in clinic.

2 Materials and methods

2.1 Reagents

Chrysophanol-8-O-glucoside (PHL84206), N-Acetyl-L-cysteine (A9165), LPS (L4391) and D-GalN (G1639) were purchased from Sigma. Primary antibodies against ATG5 (10181-2-AP), Beclin1 (11306-1-AP), β -actin (66,009-1-Ig), LC3B (18725-1-AP), and ERK (16443-1-AP) were purchased from Proteintech. Antibody against p-ERK (sc-101761) was purchased from Santa Cruz. Antibody against p62 was purchased from OriGene (TA502127). NF- κ B Pathway Sampler Kit (#9936) was purchased from Cell signaling technology.

2.2 Animals

BALB/c mice (6–8 weeks age) were purchased from Hunan SJA Laboratory Animal Co., Ltd. (Changsha, Hunan Province, China), and fed in the Specific Pathogen Free animal facility in the Institute of Life Science at Nanchang University in strict accordance with the recommendations in the Guide for the Care and Use of Laboratory Animals of the Nanchang University in China (IACUC approval No. SYXK 2015-0001).

2.3 LPS-D/GalN-induced acute liver injury

BALB/c mice injected with D-GalN (750 mg/kg) and LPS (0.35 mg/kg, *Salmonella abortus equi*) were treated with CPOG or equal volume of vehicle as previously reported (Nakama et al., 2001). Blood plasma was collected 8 h after administration under isoflurane anesthesia. ELISA assay was used to analyze the levels of serum TNF- α and IL-1 β according to instruction manual (R&D Systems, Minneapolis, Minnesota, United States).

For survival rate calculation, NAC (100 mg/kg), CPOG (20 or 40 mg/kg) were respectively pre-administrated 1 h before LPS/D-GalN injection. Then mice were injected with lethal dose of D-GalN (750 mg/kg) and LPS (1.5 mg/kg) (Tiegs et al., 1994). Every 2 h for 24 h, the number of dead mice was counted.

2.4 Cell culture

Mouse macrophage-like cell line (RAW264.7) were obtained from the Type Culture Collection of the Chinese Academy of Sciences (Shanghai, China). Cells were cultured in DMEM (Gibco) supplemented with 10% heat inactivated FBS (Excel, FCS100) and cultured at 37°C with 5% CO₂. Hepatic cell lines (LO2 and LX2) were cultured in DMEM (Gibco) supplemented with 10% FBS (Excel, FCS100) at 37°C in the presence of 5% CO₂.

2.5 Histological analysis

Under pentobarbital anesthesia (100 mg/kg, intraperitoneal injection), livers were dissected ($n = 8$ per group) from animals. Then, the tissues were fixed and subjected to immunohistochemical staining and Hematoxylin-eosin (H&E) staining conducted by Wuhan Servicebio Technology Co., Ltd. According to Heijnen's technique, extent of liver injury was evaluated (Johnson et al., 1992; Heijnen et al., 2003).

2.6 Immunofluorescence and immunohistochemistry

Mice livers were removed from animals under anesthetic, fixed in 4% paraformaldehyde, and embedded in paraffin. For immunofluorescence assay, paraffin sections were dewaxed in xylene, and rehydrated in ethanol. Then, the sections were washed with PBS, and incubated in boiling antigen retrieval solution for 15 min. The sections were blocked with 1% BSA and 5% serum in PBS at room temperature for 1 h, and then incubated with indicated

primary antibody at 4°C overnight. After washed with PBS for 3 times, the sections were incubated with secondary antibody at room temperature for 1 h. The sections were washed and counterstained with DAPI. The images were analyzed by ImageScope software.

For immunohistochemistry, the sections were dewaxed, rehydrated and treated the same as immunofluorescence assay till the incubation with the second antibody. The sections were then incubated with biotinylated secondary antibody for 1 h at room temperature. Then, the slides were washed with PBS and incubated with ABC Reagent (Vectorlabs) for 30 min. After washed in PBS for 3 times, the sections were incubated with fresh prepared DAB substrate solution. The sections were counterstained with hematoxylin solution, and the images were analyzed by ImageScope software.

2.7 Western blot analysis

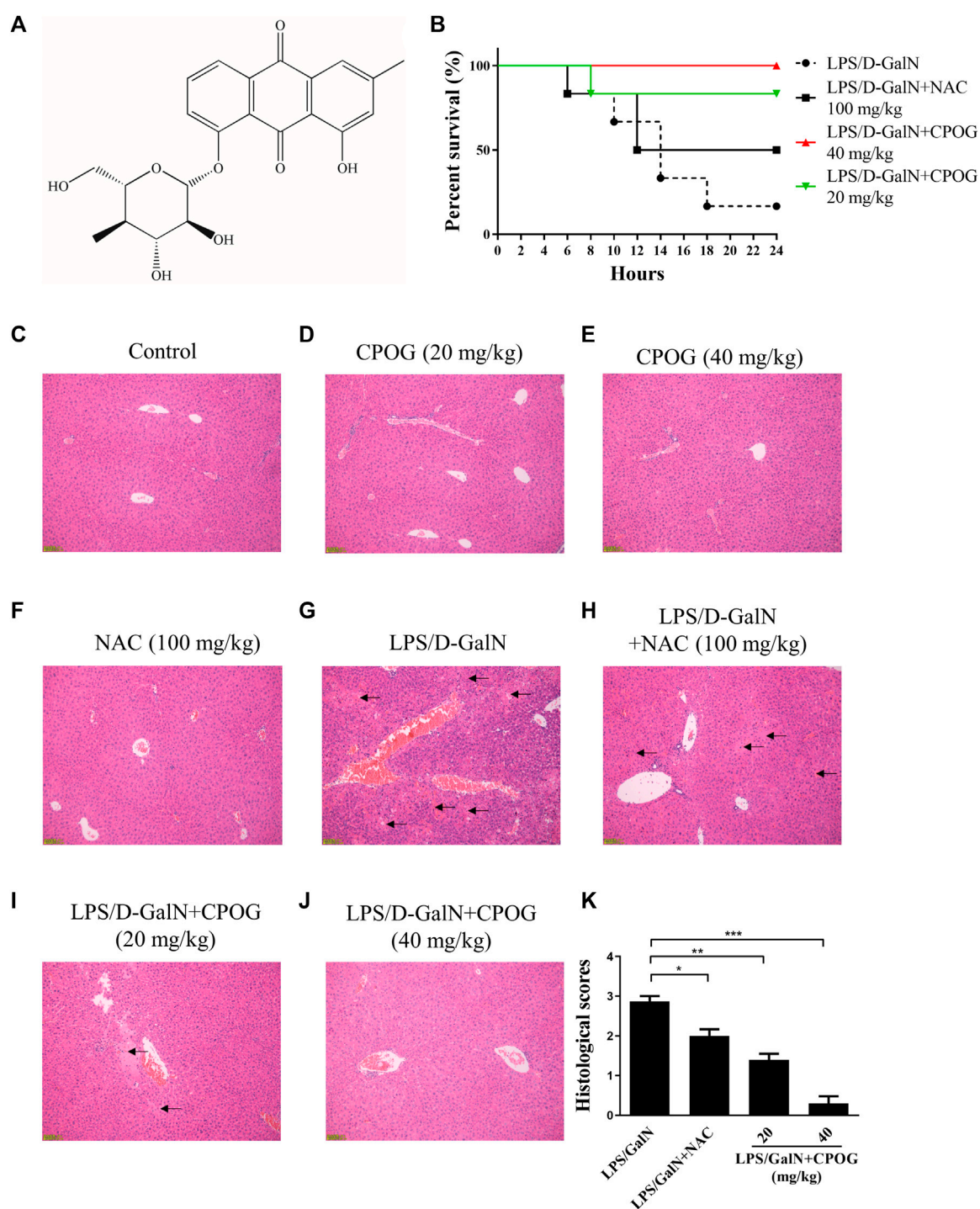
For western blot assay, proteins were separated on gel where appropriate. And then transferred to PVDF membranes (Millipore, IPVH00010), which were blocked with 5% BSA (Genview, FA016). Next, PVDF membranes were incubated with the indicated antibodies. Lastly, PVDF membranes were incubated with anti-rabbit (Thermo Fisher Scientific, 31460) or anti-mouse (Thermo Fisher Scientific, 31430) secondary antibodies. Western blot results were obtained by digital gel image analysis system (TANON 5500) and Pro-Light chemiluminescence detection kit (TIANGEN, PA112-01).

2.8 Quantitative RT-PCR

TRIzol reagent (Invitrogen) were used to extract total RNA of the cells. Then, production of the cDNA was used by the PrimeScript RT reagent kit with gDNA eraser (Takara) according to the instruction manual. The sequences of the probes used to quantify TNF- α (Genbank No. NM_013693.3) mRNA levels were: 5' -CTCCAGGCGGTGCCTATGTCT-3' (sense); 5' -CTCCTCCACTTGGTGGTTTGC-3' (antisense). The sequences of the probes used to quantify IL-1 β (Genbank No. NM_008361.4) mRNA levels were: 5' -GTGTCTTTCCCGTGGACCTTC-3' (sense); 5' -TCATCTCGGAGCCTGTAGTGC-3' (antisense). Quantitative RT-PCR was performed using SYBR Green dye and the expression of GAPDH was used as control.

2.9 Measurement of intracellular ROS level

ROS levels were measured according to the protocol from the CM-H2DCFDA Cellular ROS Detection Assay Kit

**FIGURE 1**

CPOG ameliorates LPS/D-GalN-induced ALF. **(A)** Chemical structure of CPOG. **(B)** Kaplan-Meier method was used to create the survival curves after LPS/D-GalN injection. **(C–G)** Liver sections were subjected to H&E staining. Representative photographs were shown from vehicle mice **(C)**, mice treated with CPOG (20 mg/kg) **(D)**, mice treated with CPOG (40 mg/kg) **(E)**, mice treated with NAC **(F)**, mice treated with LPS/D-GalN **(G)**, mice treated with LPS/D-GalN and NAC **(H)**, mice treated with LPS/D-GalN and CPOG (20 mg/kg) **(I)**, mice treated with LPS/D-GalN and CPOG (40 mg/kg) **(J)**. Arrows represent pathological changes in liver tissue. **(K)** Histological scores of liver sections were determined. Values represent mean \pm S.D. one-way ANOVA test was used to determine the significances. * $p < 0.05$, ** $p < 0.01$, *** $p < 0.001$.

(Invitrogen). Cells or fresh liver tissue were homogenized with NP40 lysis buffer at 4°C for 30 min and centrifuged at 10,000 g for 20 min. The supernatants were incubated in the presence of 10 μ M CM-H2DCFDA at 37°C for 15 min. Fluorescence intensity was measured at an excitation wavelength of 485 nm and an emission wavelength of 535 nm. Supernatant (5 μ L) was used for protein quantification using the Bradford assay. We normalized the fluorescence intensity by dividing the total protein. The total protein was equal to the volume of the supernatant \times the protein concentration.

2.10 Statistical analysis

The data were showed as mean \pm S.D. The results obtained from triplicate-independent experiments. Significance was determined by one-way ANOVA or a two-tailed unpaired Student's *t* test where appropriate. *p* < 0.05 were considered significant.

3 Results

3.1 CPOG protected mice from LPS/D-GalN induced ALF

Chemical structure of CPOG was shown in Figure 1A. To evaluate the effects of CPOG on LPS/D-GalN-induced lethality, mice were gavage administered with LPS and GalN as previously reported (Nakama et al., 2001). As was shown in Figure 1B, the mortality of the LPS/D-GalN treated group was 83.4%. 20 or 40 mg kg⁻¹ CPOG administration significantly decreased the mortality (16.7% and 0%), which was better than that treated with 100 mg/kg N-acetyl-L-cysteine (NAC) (50%). NAC is a thiol antioxidant and employed as positive control (Wang et al., 2007). Mice administered with CPOG or NAC alone showed no mortality (Supplementary Figure S1).

Then, H&E staining was performed to detect the morphology changes in liver tissue. Normal mice or mice administered with CPOG or NAC alone showed no pathological changes in liver tissue (Figures 1C–F). However, massive immigration of inflammatory cells into sinusoids, destruction of hepatic architecture, hepatocyte necrosis and congestion were observed at 8 h after LPS/D-GalN treatment (Figure 1G). Mice co-treated with LPS/D-GalN and NAC or CPOG showed a slight inflammatory cells immigration and mild hepatocytes necrosis (Figures 1H–J). Furthermore, compared with the LPS/D-GalN treated mice, the histological scores of mice treated with CPOG decreased significantly (Figure 1K). These results indicate that CPOG protected against LPS/D-GalN-induced ALF.

3.2 CPOG inhibited aminotransferases and proinflammatory cytokines production in LPS/D-GalN induced ALF model

Alanine aminotransferase (ALT) and aspartate transaminase (AST) are key indicators of liver function (Kim et al., 2020). Our results showed an increased levels of ALT and AST in LPS/D-GalN treated group (5226.9 U/L and 2903.6 U/L), which were 26.8 U/L and 80.6 U/L in control group, indicating that mice administered with LPS/D-GalN had developed serious hepatocytes necrosis. By contrast, the ALT levels in 20 or 40 mg kg⁻¹ of CPOG-treated group decreased to 376.2 U/L (*p* < 0.001) or 223.0 U/L (*p* < 0.001). The AST levels in 20 or 40 mg/kg of CPOG -treated group decreased to 326.8 U/L (*p* < 0.001) or 247.0 U/L (*p* < 0.01) (Figures 2A,B). These results indicated that CPOG administration could ameliorate the increase of ALT and AST induced by D-GalN/LPS. IL-1 β and TNF- α are the most important proinflammatory cytokines that promote the secretion of downstream proinflammatory mediators (Shen et al., 2020). The serum levels of IL-1 β and TNF- α were also increased after LPS/D-GalN injection. However, co-treatment with CPOG or NAC inhibited the release of TNF- α and IL-1 β compared with that in LPS/D-GalN treated group (Figures 2C,D). Furthermore, elevated intracellular ROS level plays an important role in the pathogenesis of LPS-induced ALF (Jiang et al., 2018). CM-H2DCFDA staining results showed that LPS/D-GalN quickly stimulated ROS in liver tissue, which could be attenuated by NAC treatment. Co-treatment with CPOG also inhibited LPS/D-GalN-induced ROS production (Figure 2E), indicating that CPOG antagonized LPS/D-GalN-induced ALF by alleviating ROS generation.

3.3 CPOG inhibited autophagy in LPS/D-GalN-induced ALF model

It was reported that excessive autophagic response contributed to LPS-induced liver injury (Kong et al., 2017). Therefore, immunofluorescence staining was applied to detect the expression of autophagy-related proteins in liver tissue sections. Both the expression of LC3B and p62 were increased after LPS/D-GalN injection, as compared with normal mice and mice treated with NAC or CPOG alone (Figures 3A–E), indicating an increased autophagic activity. The co-treatment with LPS/D-GalN and NAC or CPOG (20 or 40 mg/kg) decreased expression of LC3B and p62 (Figures 3F–H). p65 is an important executor of NF- κ B signaling that regulates the expression of pro-inflammatory cytokines (Li et al., 2021). However, the expression of p65 showed no significant change following the LPS administration.

Then immunohistochemistry was performed to detect the expression of ATG5 and Beclin1 in liver tissue. As shown in

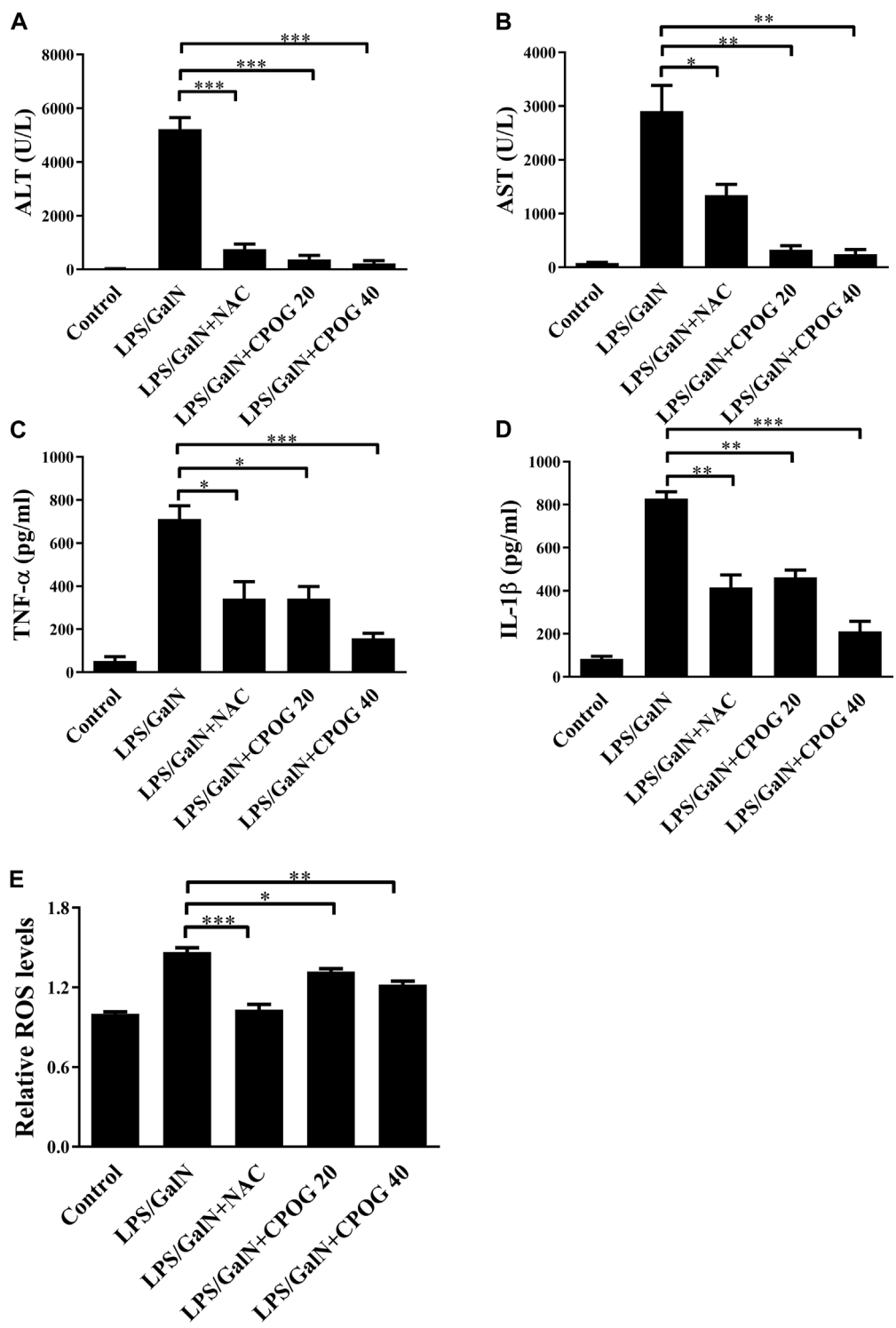


FIGURE 2
CPOG attenuated inflammatory response in LPS/D-GalN-induced ALF model. **(A,B)** 8 h after LPS/D-GalN injection, the serum levels of ALT and AST were detected. **(C,D)** Serum levels of TNF- α and IL-1 β were detected by ELISA at 8 h after LPS/D-GalN injection. **(E)** ROS levels in liver tissue were determined by CM-H2DCFDA at 8 h after LPS/D-GalN injection. Values represent mean \pm S.D. Significance was determined by one-way ANOVA test. Data are representative of three independent experiments. * $p < 0.05$, ** $p < 0.01$, *** $p < 0.001$.

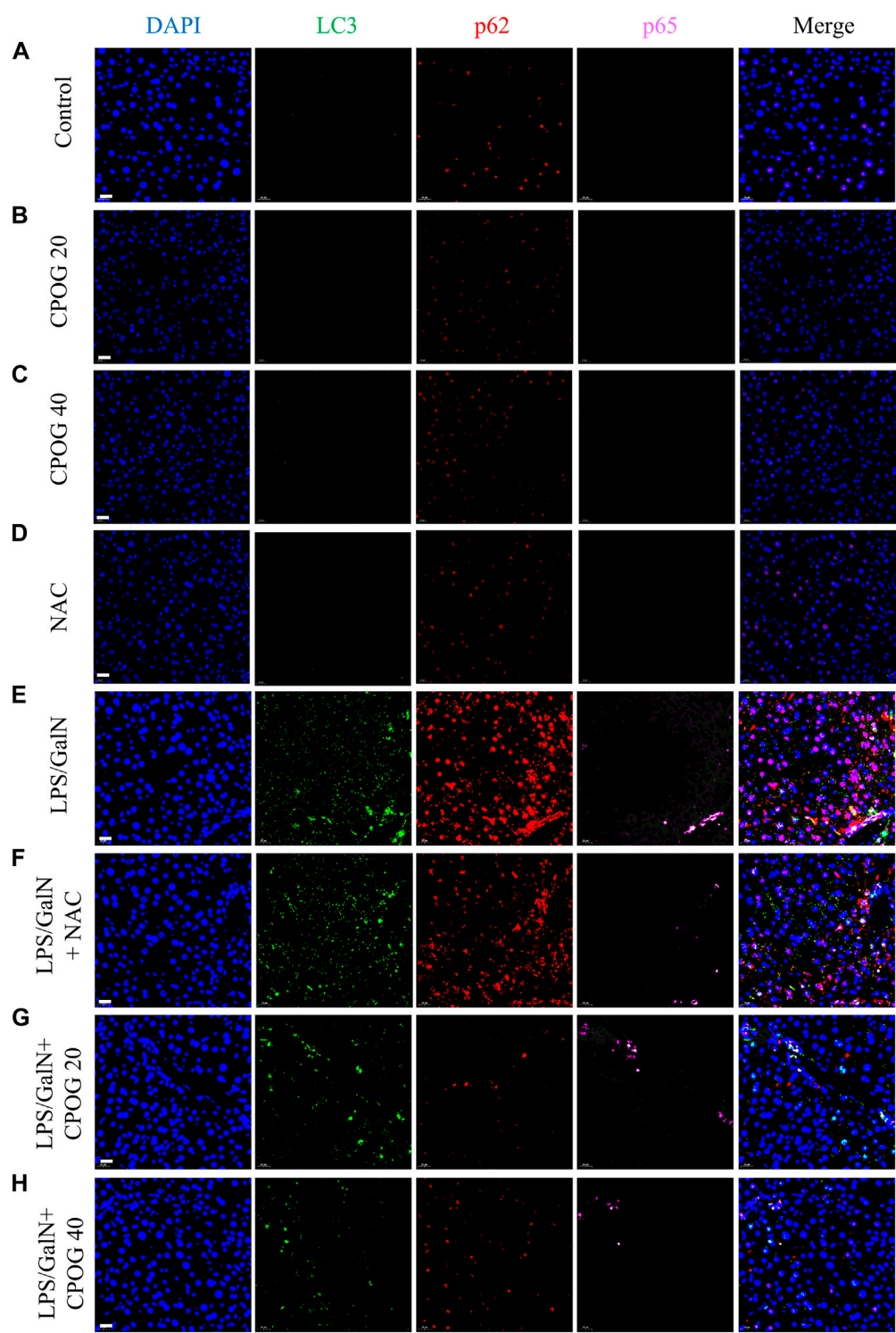
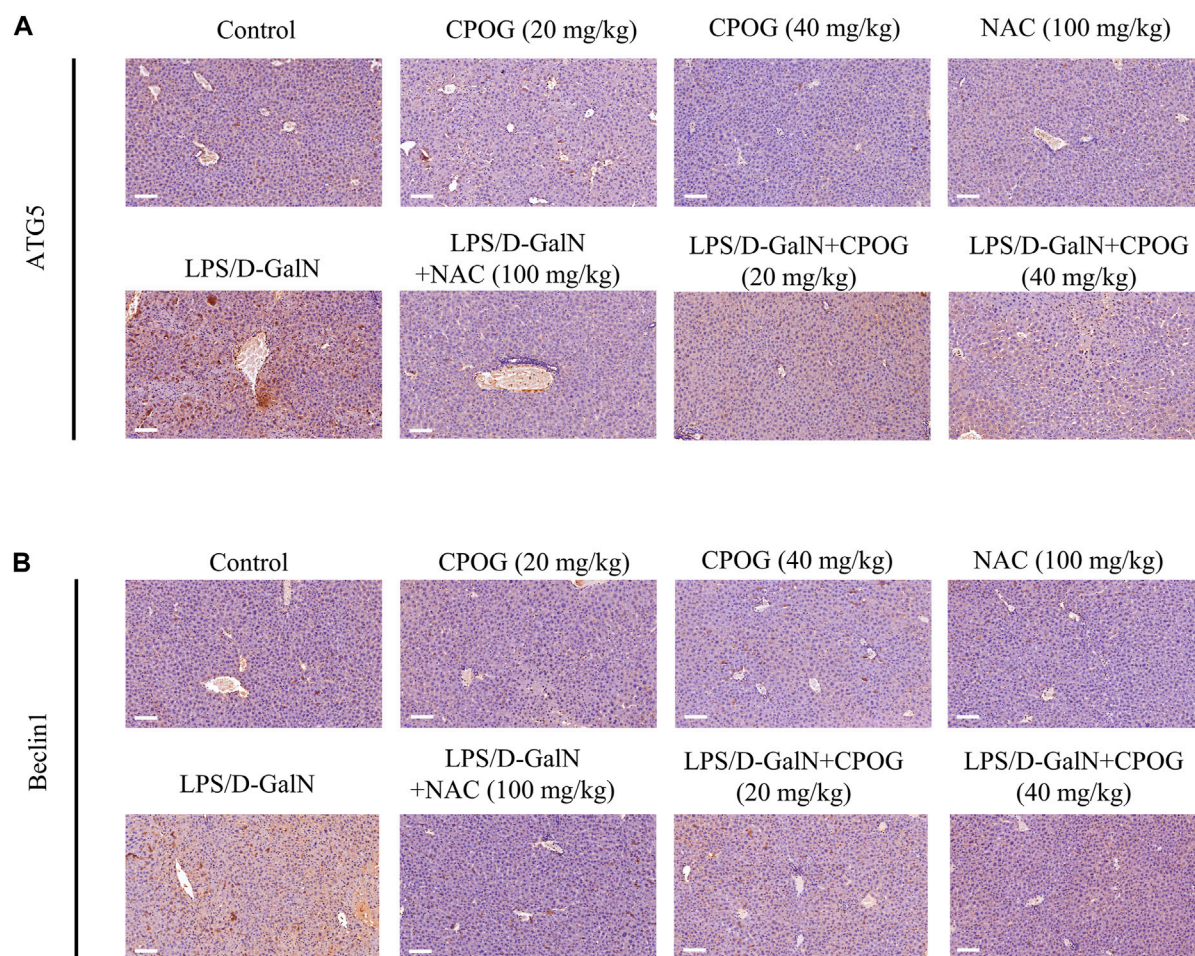


FIGURE 3
CPOG inhibited the expression of LC3B and p62 in LPS/D-GalN-induced ALF model. **(A–H)** Immunofluorescence imaging was performed with the indicated antibodies. The nucleus was stained with DAPI (blue color). Representative photographs were shown from vehicle mice **(A)**, mice treated with CPOG (20 mg/kg) **(B)**, mice treated with CPOG (40 mg/kg) **(C)**, mice treated with NAC **(D)**, mice treated with LPS/D-GalN **(E)**, mice treated with LPS/D-GalN and NAC **(F)**, mice treated with LPS/D-GalN and CPOG (20 mg/kg) **(G)**, mice treated with LPS/D-GalN and CPOG (40 mg/kg) **(H)**. Scale bar = 20 μm.

**FIGURE 4**

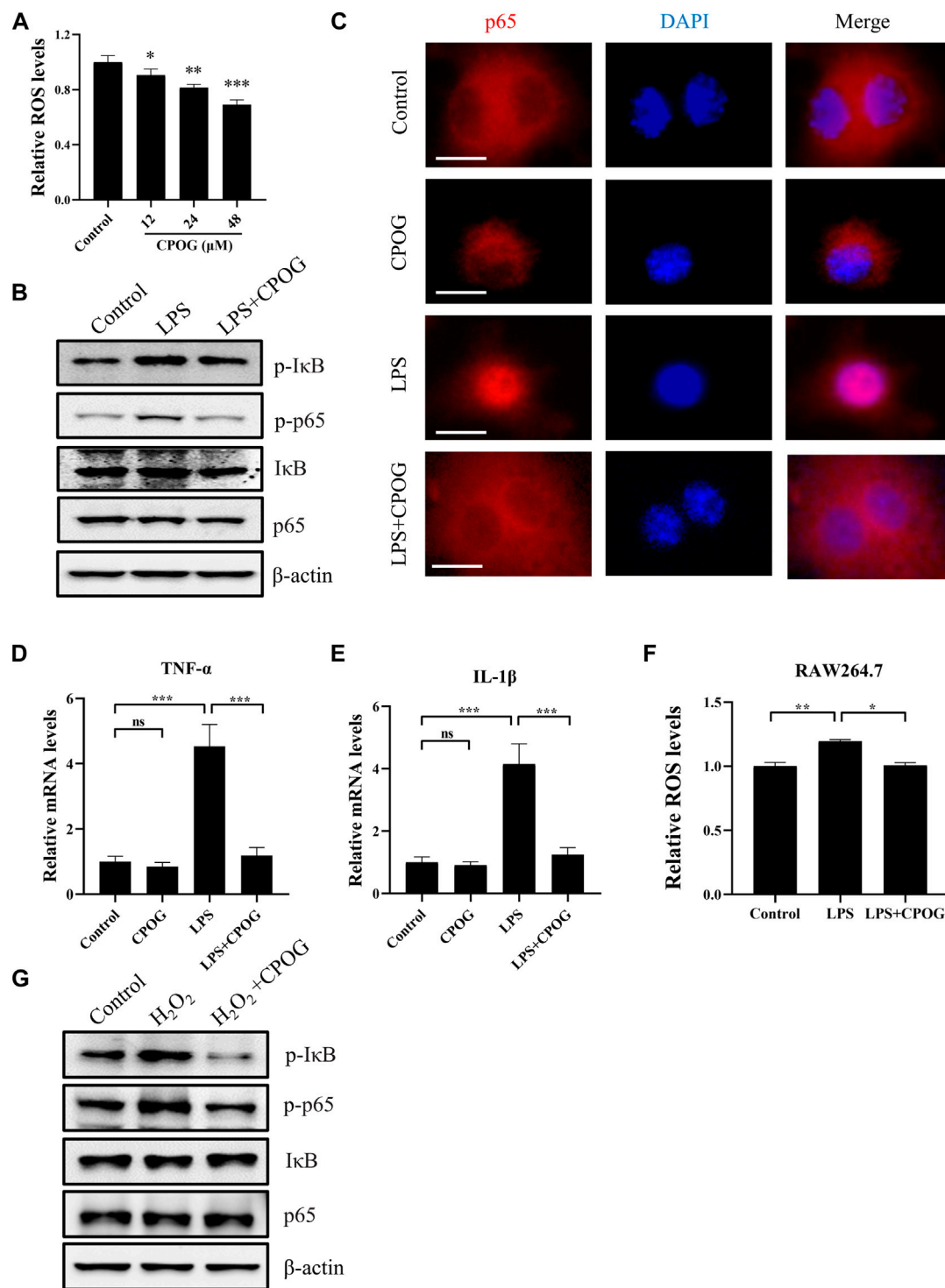
CPOG inhibited the expression of ATG5 and Beclin1 in LPS/D-GalN-induced ALF model. (A,B) Immunohistochemistry assay was performed with the indicated antibodies. The nucleus was stained with DAPI (blue color). Representative photographs were shown from vehicle mice, mice treated with CPOG (20 mg/kg), mice treated with CPOG (40 mg/kg), mice treated with NAC, mice treated with LPS/D-GalN, mice treated with LPS/D-GalN and NAC, mice treated with LPS/D-GalN and CPOG (20 mg/kg), mice treated with LPS/D-GalN and CPOG (40 mg/kg). Scale bar = 100 μ m.

Figures 4A,B, treatment with NAC or CPOG alone had no effect on the expression of ATG5 and Beclin1. LPS/D-GalN injection induced upregulation of ATG5 and Beclin1, which could be alleviated by the treatment with NAC or CPOG. All these results indicate that CPOG alleviated LPS/D-GalN-induced autophagic response in ALF model.

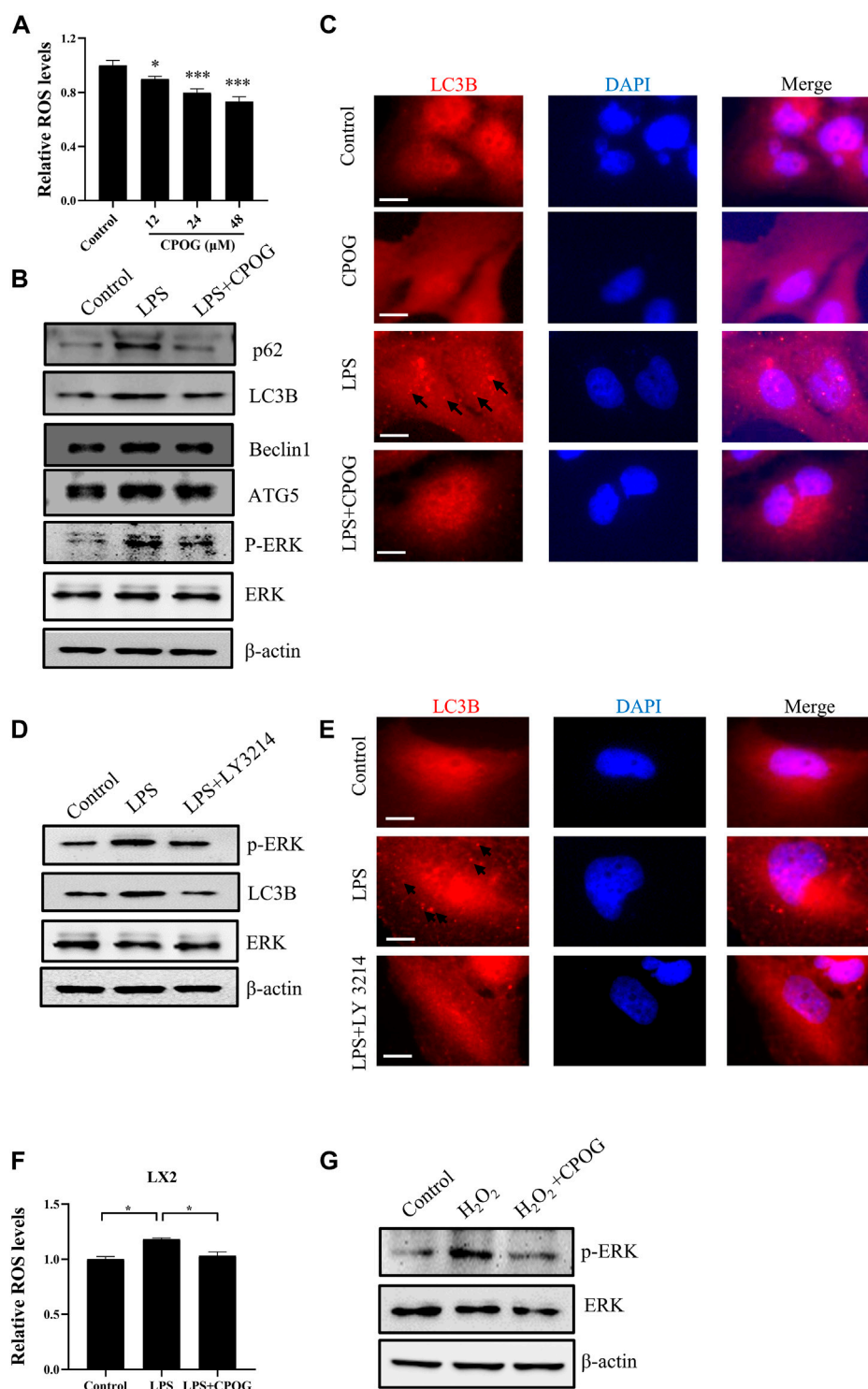
3.4 CPOG alleviated LPS-induced oxidative stress and inflammation response in RAW264.7 cells

CPOG treatment downregulated intracellular ROS level in dose-dependent manner without affecting cell viability in RAW264.7 cells (Figure 5A; Supplementary Figure S2A). In

order to investigate the underlying mechanism of the anti-inflammatory effect of CPOG on LPS/D-GalN-induced ALF, we detected the expression of proteins in NF- κ B signaling pathway in RAW264.7 cells. CPOG treatment alone had no effect on the expression of p-I κ B and p-p65. The expression of p-I κ B and p-p65 were upregulated after LPS treatment. By contrast, CPOG significantly inhibited LPS/D-GalN-induced phosphorylation of I κ B and p65 (Figure 5B; Supplementary Figure S2B). Translocation of the NF- κ B subunit p65 from cytoplasm to the nucleus is key to the activation of the inflammatory signaling pathway. Hence, the location of p65 was detected and the results showed that LPS-induced nuclear translocation of p65 was also reversed by CPOG treatment, which is in accordance with its phosphorylation change (Figure 5C). Next, we examined the effect of CPOG on

**FIGURE 5**

CPOG alleviated LPS-induced oxidative stress and inflammation response in RAW264.7 cells. **(A)** RAW264.7 cells were treated with indicated concentrations of CPOG and intracellular ROS level was detected with CM-H₂DCFDA. **(B–F)** RAW264.7 cells were treated with 1 μ g/ml LPS in the presence or absence of 48 μ M CPOG for 4 h. The expression of indicated proteins was detected by Western blot **(B)**, p65 cell location was detected by immunofluorescence assay **(C)**. Expression of TNF- α **(D)** and IL-1 β **(E)** was detected by RT-PCR. Intracellular ROS level was detected with CM-H₂DCFDA **(F)**. **(G)** RAW264.7 cells were incubated with 48 μ M CPOG for 4 h before treated with 500 μ M H₂O₂ for 30 min. The expression of indicated proteins was detected by Western blot. Values represent mean \pm S.D. Significance was determined by one-way ANOVA test. Data are representative of three independent experiments. * p < 0.05, ** p < 0.01, *** p < 0.001.

**FIGURE 6**

CPOG alleviated LPS-induced oxidative stress and autophagy in LX2 cells. **(A)** LX2 cells were treated with indicated concentrations of CPOG and intracellular ROS level was detected with CM-H₂DCFDA. **(B,C)** LX2 cells were treated with 1 μg/ml LPS in the presence or absence of 48 μM CPOG for 4 h. The expression of indicated proteins was detected by Western blot **(B)**. Formation of LC3B puncta was detected by immunofluorescence assay **(C)**. Scale bar = 10 μm. **(D,E)** LX2 cells were incubated with LY3214 for 12 h before treated with 1 μg/ml LPS for 4 h. The expression of indicated proteins was detected by Western blot **(D)**. Formation of LC3B puncta was detected by immunofluorescence assay **(E)**. Scale bar = 10 μm. **(F)** LX2 cells were treated with 1 μg/ml LPS in the presence or absence of 48 μM CPOG for 4 h. Intracellular ROS level was detected with CM-H₂DCFDA. **(G)** LX2 cells were incubated with 48 μM CPOG for 4 h before treated with 500 μM H₂O₂ for 30 min. The expression of indicated proteins was detected by Western blot. Values represent mean ± S.D. Significance was determined by one-way ANOVA test. Data are representative of three independent experiments. **p* < 0.05, ***p* < 0.01, ****p* < 0.001.

the expression of IL-1 β and TNF- α using q-PCR. LPS treatment increased mRNA levels of IL-1 β and TNF- α , while the application CPOG effectively ameliorated the situation (Figures 5D,E).

LPS exposure may lead to increased reactive oxygen species generation, which is a potential activator of NF- κ B signaling pathway. To determine if the anti-inflammatory effect of CPOG is related to its anti-oxidative property, ROS levels were detected following LPS treatment. Our results showed that LPS-induced oxidative stress was also alleviated by CPOG treatment (Figure 5F). Furthermore, H₂O₂ induced activation of NF- κ B signaling was also blocked by CPOG (Figure 5G). In short, these results suggest that CPOG exhibited remarkably anti-inflammatory effect in association with its anti-oxidative property.

3.5 CPOG alleviated LPS-induced oxidative stress and autophagy in LX2 cells

CPOG treatment downregulated intracellular ROS level in dose-dependent manner without affecting cell viability in RAW264.7 cells (Figure 6A; Supplementary Figure S3A). LPS mediated autophagic cell death induced by oxidative stress is associated with various disease. We tested the autophagy induction effect of LPS in liver cell lines. Our results showed the expression of LC3B and p62 is unaffected by LPS or CPOG treatment in LO2 cells (Supplementary Figure S3B). As shown in Figure 6B and Supplementary Figure S3C, the expression of LC3B, p62, ATG5, and Beclin1 in LX2 cells increased significantly when treated with LPS, which could be alleviated by the application of CPOG. MAPK signaling pathway played an important role in LPS-induced autophagy. Our results showed that ERK phosphorylation was upregulated by LPS, which was attenuated by CPOG treatment. Then, immunofluorescence assay was performed to detect the formation of LC3 puncta in LX2 cells. As shown in Figure 6C, LPS treatment induced the formation of LC3 puncta, which was alleviated by CPOG treatment. To confirm the role of ERK in LPS-induced autophagy, LX2 cells were treated with LY3214, an inhibitor of ERK, and the results showed that LPS-induced up-regulation of LC3B was alleviated by LY3214 treatment (Figure 6D; Supplementary Figure S3D). Immunofluorescence results showed that LY3214 treatment also alleviated LPS-induced formation LC3B puncta (Figure 6E). These observations indicate ERK activity was required for LPS-induced autophagy in LX2 cells. Previous studies indicated that ROS play a role as messengers to activate the mitogen-activated protein kinases (MAPKs) (Traore et al., 2008; Yuan et al., 2021). Therefore, the role of LPS-induced ROS in the activation of ERK was explored. Our results showed that LPS treatment increased ROS production in

LX2 cells, which could be alleviated by CPOG (Figure 6F). Further, CPOG treatment alleviated H₂O₂-induced phosphorylation of ERK (Figure 6G). In conclusion, these results suggest that CPOG alleviated LPS-induced autophagy by inhibiting ROS generation and ERK phosphorylation.

4 Discussion

Mice administrated with LPS/D-GalN is a well-established experimental model that resembles human ALF (Silverstein, 2004; Wilhelm et al., 2009). Cell-to-cell communication within the liver is a rising field to understand the liver pathogenesis, in which non-parenchymal cells may be directly targeted or activated in response to toxic pathogens (Robinson et al., 2016). In this study, we attempted to explore the therapeutic potential of CPOG in the treatment of ALF and its underlying mechanism. We demonstrated that CPOG could ameliorate liver damage induced by LPS/D-GalN and improved survival rates. Importantly, CPOG alleviated LPS/D-GalN-induced oxidative stress in liver tissue. LPS/D-GalN-induced release of AST and ALT as well as secretion of IL-1 β and TNF- α was attenuated by CPOG *in vivo*. Moreover, CPOG alleviated LPS-induced ROS generation *in vitro* and caused significant reduction in IL-1 β and TNF- α production in macrophages and inhibited autophagy as indicated by LC3 puncta formation in hepatic stellate cells.

ROS are by-products of metabolism of oxygen that includes non-radicals like H₂O₂ and ¹O₂ and free radicals like O^{•-2}, OH[•]. Basal ROS production served as signaling molecule in cell survival and proliferation (Forman et al., 2010). However, excessive ROS production induced damage of nucleic acids, proteins, and lipids, and was involved in the pathogenesis of various diseases (Andersen, 2004; Trachootham et al., 2009). It was reported that LPS triggered ROS production by activating NADPH Oxidase four in macrophages and endothelial cells (Hsu and Wen, 2002; Simon and Fernandez, 2009). Here, it was found that LPS induced excessive ROS accumulation in liver tissue as well as in RAW264.7 and LX2 cells. CPOG treatment down-regulated intracellular ROS level and alleviated LPS-induced ROS production both *in vivo* and *in vitro*. These results suggest that CPOG is strong antioxidant that exerts beneficial effect against oxidative stress.

NF- κ B is a family of transcriptional factors including p65, p52, p50, RelB, and c-Rel, which regulates genes involved in inflammatory and immune responses (Oeckinghaus and Ghosh, 2009). Notably, activation of p65 plays vital role in the release of pro-inflammatory mediators in macrophages in response to various stimuli (Giridharan and Srinivasan, 2018). LPS has been reported to induce expressions of many pro-inflammatory mediators like IL-1 β and TNF- α through the activation of NF- κ B signaling (Muniandy et al., 2018). Here, it was found that LPS induced up-regulation of IL-1 β and TNF- α

both *in vivo* and *in vitro*, which could be alleviated by CPOG treatment. IκB is an inhibitor of p65. Phosphorylation of IκB by multi-subunit IκB kinase facilitates its ubiquitin-dependent degradation, resulting in the phosphorylation and nuclear translocation of p65 (Li et al., 2019). Our results showed that CPOG inhibited the up-regulation of p-IκB and p-p65 induced by LPS. Translocation of p65 from cytoplasm to nucleus was also blocked by CPOG treatment. Our results suggested that CPOG inhibited LPS-induced inflammation response through NF-κB signaling pathway by suppressing IκB phosphorylation. Consistent with previous findings that oxidative stress is an activator of NF-κB signaling (Takada et al., 2003), we found that H₂O₂ treatment upregulated the expression of p-IκB and p-p65 in RAW 264.7 cells. CPOG treatment decreased intracellular ROS level and alleviated oxidative stress-induced activation of NF-κB signaling. These data suggest that the anti-inflammatory effect of CPOG was partly due to its antioxidant ability.

LPS-induced dysfunctional autophagy was reported to result in autophagic cell death through oxidative stress in various tissue (Xu et al., 2006; Lin et al., 2016; Liu et al., 2020). p62 and LC3 are two key factors in autophagosomes formation (Klionsky et al., 2010). In this study, we observed upregulated expression of LC3B, p62, ATG5, and Beclin1 followed by LPS treatment in mice liver tissue, which could be alleviated by CPOG treatment. In response to liver damage, hepatic stellate cells play a crucial role in liver fibrosis and scar tissue formation (Krizhanovsky et al., 2008). Our results showed that LPS treatment induced up-regulation of LC3B and P62 in LX2 cells but not in LO2 cells, indicating that LPS had distinct effect on different liver cell types and promoted autophagic activity in LX2 cells. The p38MAPK pathway is involved in a variety of physiological process such as cell proliferation, differentiation, and apoptosis (Zhang and Liu, 2002; Slobodnyuk et al., 2019). Raf/MEK/ERK activation is vital to the expression of LC3B and P62 (Kim et al., 2014). Intriguingly, expression of p-ERK also increased in LX2 cells following LPS stimulation, which was suppressed by CPOG treatment. In particular, pretreatment with ERK inhibitor (LY 3214) blocked LPS-induced LC3B expression and LC3B puncta formation in LX2 cells, suggesting that LPS-induced autophagy was mediated by MAPK signaling pathway. Moreover, it was reported that ERK could be activated in ROS-dependent manner (Deng et al., 2021). Here, it was found that H₂O₂ induced oxidative stress upregulated the expression of p-ERK. Application of CPOG significantly decreased ROS generation in LX2 cells and alleviated H₂O₂-induced ERK phosphorylation. These results indicate that CPOG alleviated LPS-induced autophagy in LX2 cells by inhibiting ROS-mediated ERK phosphorylation.

5 Conclusion

In conclusion, this study first demonstrated that CPOG protected mice from LPS/D-GalN-induced ALF. CPOG showed strong antioxidant ability both *in vivo* and *in vitro*. Molecularly, CPOG inhibited LPS-induced release of IL-1β and TNF-α by the inactivation of NF-κB signaling pathway in RAW264.7 cells. CPOG attenuated LPS-induced activation of MAPK signaling, therefore attenuated the expression of autophagy-related proteins and LC3 puncta formation in LX2 cells. Therefore, CPOG offers a potential therapeutic strategy for the cure of ALF, though further clinical trial is needed.

Data availability statement

The datasets presented in this study can be found in online repositories. The names of the repository/repositories and accession numbers can be found below: <https://figshare.com/s/aa1575aafb9fd25145a2>.

Ethics statement

The animal study was reviewed and approved by The Medical Research Ethics Committee of Nanchang University.

Author contributions

TW, Project administration, writing-original draft, methodology, validation, software. ZL, Project administration, methodology, data curation. X-HQ, Project administration, methodology. Z-YX Project administration. Y-TW, Methodology. YL, Formal analysis. Z-YZ, Formal analysis. X-JH, Conceptualization, resources, writing-review and editing. C-FX, Visualization, conceptualization, resources, writing-review and editing, supervision.

Funding

This study was supported by grants to C-FX from the National Natural Science Foundation of China (81660392, 82002761).

Conflict of interest

The authors declare that the research was conducted in the absence of any commercial or financial relationships that could be construed as a potential conflict of interest.

Publisher's note

All claims expressed in this article are solely those of the authors and do not necessarily represent those of their affiliated

organizations, or those of the publisher, the editors and the reviewers. Any product that may be evaluated in this article, or claim that may be made by its manufacturer, is not guaranteed or endorsed by the publisher.

Supplementary material

The Supplementary Material for this article can be found online at: <https://www.frontiersin.org/articles/10.3389/fphar.2022.951521/full#supplementary-material>

References

- Andersen, J. K. (2004). Oxidative stress in neurodegeneration: Cause or consequence? *Nat. Med.* 10, S18–S25. doi:10.1038/nrn1434
- Chu, X., Zhou, S. H., Sun, R., Wang, L., Xing, C. Y., Liang, R. Q., et al. (2018). Chrysophanol relieves cognition deficits and neuronal loss through inhibition of inflammation in diabetic mice. *Neurochem. Res.* 43 (4), 972–983. doi:10.1007/s11064-018-2503-1
- Deng, J. K., Zhang, X., Wu, H. L., Gan, Y., Ye, L., Zheng, H., et al. (2021). ROS-ERK pathway as dual mediators of cellular injury and autophagy-associated adaptive response in urinary protein-irritated renal tubular epithelial cells. *J. Diabetes Res.* 2021, 6614848. doi:10.1155/2021/6614848
- Forman, H. J., Maiorino, M., and Ursini, F. (2010). Signaling functions of reactive oxygen species. *Biochemistry* 49 (5), 835–842. doi:10.1021/bi9020378
- Giridharan, S., and Srinivasan, M. (2018). Mechanisms of NF- κ B p65 and strategies for therapeutic manipulation. *J. Inflamm. Res.* 11, 407–419. doi:10.2147/JIR.S140188
- Heijnen, B. H., Straatsburg, I. H., Gouma, D. J., and van Gulik, T. M. (2003). Decrease in core liver temperature with 10 degrees C by *in situ* hypothermic perfusion under total hepatic vascular exclusion reduces liver ischemia and reperfusion injury during partial hepatectomy in pigs. *Surgery* 134 (5), 806–817. doi:10.1016/s0039-6060(03)00125-9
- Hsu, H. Y., and Wen, M. H. (2002). Lipopolysaccharide-mediated reactive oxygen species and signal transduction in the regulation of interleukin-1 gene expression. *J. Biol. Chem.* 277 (25), 22131–22139. doi:10.1074/jbc.M111883200
- Jiang, W., Zhou, R., Li, P., Sun, Y., Lu, Q., Qiu, Y., et al. (2016). Protective effect of chrysophanol on LPS/d-GalN-induced hepatic injury through the RIP140/NF- κ B pathway. *RSC Adv.* 6 (44), 38192–38200. doi:10.1039/c5ra19841k
- Jiang, Z., Meng, Y., Bo, L., Wang, C., Bian, J., and Deng, X. (2018). Sophocarpine attenuates LPS-induced liver injury and improves survival of mice through suppressing oxidative stress, inflammation, and apoptosis. *Mediat. Inflamm.* 2018, 5871431. doi:10.1155/2018/5871431
- Jirillo, E., Caccavo, D., Magrone, T., Piccigallo, E., Amati, L., Lembo, A., et al. (2012). The role of the liver in the response to LPS: Experimental and clinical findings. *J. Endotoxin Res.* 8 (5), 319–327. doi:10.1179/096805102125000641
- Johnson, S. J., Hines, J. E., and Burt, A. D. (1992). Phenotypic modulation of perisinusoidal cells following acute liver injury: A quantitative analysis. *Int. J. Exp. Pathol.* 73 (6), 765–772.
- Kim, H. J., Kim, S. Y., Shin, S. P., Yang, Y. J., Bang, C. S., Baik, G. H., et al. (2020). Immunological measurement of aspartate/alanine aminotransferase in predicting liver fibrosis and inflammation. *Korean J. Intern. Med.* 35 (2), 320–330. doi:10.3904/kjim.2018.214
- Kim, J. H., Hong, S. K., Wu, P. K., Richards, A. L., Jackson, W. T., and Park, J. I. (2014). Raf/MEK/ERK can regulate cellular levels of LC3B and SQSTM1/p62 at expression levels. *Exp. Cell Res.* 327 (2), 340–352. doi:10.1016/j.yexcr.2014.08.001
- Kim, S. J., Kim, M. C., Lee, B. J., Park, D. H., Hong, S. H., and Um, J. Y. (2010). Anti-inflammatory activity of chrysophanol through the suppression of NF- κ B/caspase-1 activation *in vitro* and *in vivo*. *Molecules* 15 (9), 6436–6451. doi:10.3390/molecules15096436
- Klionsky, D. J., Codogno, P., Cuervo, A. M., Deretic, V., Elazar, Z., Fueyo-Margareto, J., et al. (2010). A comprehensive glossary of autophagy-related molecules and processes. *Autophagy* 6 (4), 438–448. doi:10.4161/auto.6.4.12244
- Kong, X., Yang, Y., Ren, L., Shao, T., Li, F., Zhao, C., et al. (2017). Activation of autophagy attenuates EtOH-LPS-induced hepatic steatosis and injury through MD2 associated TLR4 signaling. *Sci. Rep.* 7 (1), 9292. doi:10.1038/s41598-017-09045-z
- Krawitz, S., Lingiah, V., and Prysopoulos, N. T. (2018). Acute liver failure: Mechanisms of disease and multisystemic involvement. *Clin. Liver Dis.* 22 (2), 243–256. doi:10.1016/j.cld.2018.01.002
- Krizhanovsky, V., Yon, M., Dickins, R. A., Hearn, S., Simon, J., Miething, C., et al. (2008). Senescence of activated stellate cells limits liver fibrosis. *Cell* 134 (4), 657–667. doi:10.1016/j.cell.2008.06.049
- Li, M., Ye, J., Zhao, G., Hong, G., Hu, X., Cao, K., et al. (2019). Gas6 attenuates lipopolysaccharide-induced TNF- α expression and apoptosis in H9C2 cells through NF- κ B and MAPK inhibition via the Axl/PI3K/Akt pathway. *Int. J. Mol. Med.* 44 (3), 982–994. doi:10.3892/ijmm.2019.4275
- Li, Q., Tan, Y., Chen, S., Xiao, X., Zhang, M., Wu, Q., et al. (2021). Irisin alleviates LPS-induced liver injury and inflammation through inhibition of NLRP3 inflammasome and NF- κ B signaling. *J. Recept. Signal Transduct. Res.* 41 (3), 294–303. doi:10.1080/10799893.2020.1808675
- Li, S., Guo, L., Qian, P., Zhao, Y., Liu, A., Ji, F., et al. (2015). Lipopolysaccharide induces autophagic cell death through the PERK-dependent branch of the unfolded protein response in human alveolar epithelial A549 cells. *Cell. Physiol. Biochem.* 36 (6), 2403–2417. doi:10.1159/000430202
- Lin, L., Zhang, L., Yu, L., Han, L., Ji, W., Shen, H., et al. (2016). Time-dependent changes of autophagy and apoptosis in lipopolysaccharide-induced rat acute lung injury. *Iran. J. Basic Med. Sci.* 19 (6), 632–637.
- Liu, P., Feng, Y., Li, H., Chen, X., Wang, G., Xu, S., et al. (2020). Ferrostatin-1 alleviates lipopolysaccharide-induced acute lung injury via inhibiting ferroptosis. *Cell. Mol. Biol. Lett.* 25, 10. doi:10.1186/s11658-020-00205-0
- Lu, C. C., Yang, J. S., Huang, A. C., Hsia, T. C., Chou, S. T., Kuo, C. L., et al. (2010). Chrysophanol induces necrosis through the production of ROS and alteration of ATP levels in J5 human liver cancer cells. *Mol. Nutr. Food Res.* 54 (7), 967–976. doi:10.1002/mnfr.200900265
- Mondal, P., Roy, S., Loganathan, G., Mandal, B., Dharumadurai, D., Akbarsha, M. A., et al. (2015). 1-Amino-4-hydroxy-9, 10-anthraquinone - an analogue of anthracycline anticancer drugs, interacts with DNA and induces apoptosis in human MDA-MB-231 breast adenocarcinoma cells: Evaluation of structure-activity relationship using computational, spectroscopic and biochemical studies. *Biochem. Biophys. Rep.* 4, 312–323. doi:10.1016/j.bbrep.2015.10.008
- Muniandy, K., Gothai, S., Badran, K. M. H., Suresh Kumar, S., Esa, N. M., and Arulselvan, P. (2018). Suppression of proinflammatory cytokines and mediators in LPS-induced RAW 264.7 macrophages by stem extract of *Alternanthera sessilis* via the inhibition of the NF- κ B pathway. *J. Immunol. Res.* 2018, 3430684. doi:10.1155/2018/3430684
- Nakama, T., Hirono, S., Moriuchi, A., Hasuike, S., Nagata, K., Hori, T., et al. (2001). Etoposide prevents apoptosis in mouse liver with D-galactosamine/lipopolysaccharide-induced fulminant hepatic failure resulting in reduction of lethality. *Hepatology* 33 (6), 1441–1450. doi:10.1053/jhep.2001.24561
- Ni, C. H., Yu, C. S., Lu, H. F., Yang, J. S., Huang, H. Y., Chen, P. Y., et al. (2014). Chrysophanol-induced cell death (necrosis) in human lung cancer A549 cells is mediated through increasing reactive oxygen species and decreasing the level of mitochondrial membrane potential. *Environ. Toxicol.* 29 (7), 740–749. doi:10.1002/tox.21801

- Oeckinghaus, A., and Ghosh, S. (2009). The NF-kappaB family of transcription factors and its regulation. *Cold Spring Harb. Perspect. Biol.* 1 (4), a000034. doi:10.1101/cshperspect.a000034
- Park, Y. J., Lee, K. H., Jeon, M. S., Lee, Y. H., Ko, Y. J., Pang, C., et al. (2020). Hepatoprotective potency of chrysophanol 8-O-glucoside from *Rheum palmatum* L. Against hepatic fibrosis via regulation of the STAT3 signaling pathway. *Int. J. Mol. Sci.* 21 (23), E9044. doi:10.3390/ijms21239044
- Patel, P., Okoronkwo, N., and Pyrsopoulos, N. T. (2018). Future approaches and therapeutic modalities for acute liver failure. *Clin. Liver Dis.* 22 (2), 419–427. doi:10.1016/j.cld.2018.01.011
- Racanelli, V., and Rehmann, B. (2006). The liver as an immunological organ. *Hepatology* 43 (2), S54–S62. doi:10.1002/hep.21060
- Robinson, M. W., Harmon, C., and O'Farrelly, C. (2016). Liver immunology and its role in inflammation and homeostasis. *Cell. Mol. Immunol.* 13 (3), 267–276. doi:10.1038/cmi.2016.3
- Shen, Y., Malik, S. A., Amir, M., Kumar, P., Cingolani, F., Wen, J., et al. (2020). Decreased hepatocyte autophagy leads to synergistic IL-1 β and TNF mouse liver injury and inflammation. *Hepatology* 72 (2), 595–608. doi:10.1002/hep.31209
- Shrestha, J. P., Fosso, M. Y., Bearss, J., and Chang, C. W. (2014). Synthesis and anticancer structure activity relationship investigation of cationic anthraquinone analogs. *Eur. J. Med. Chem.* 77, 96–102. doi:10.1016/j.ejmech.2014.02.060
- Silverstein, R. (2004). D-Galactosamine lethality model: Scope and limitations. *J. Endotoxin Res.* 10 (3), 147–162. doi:10.1179/096805104225004879
- Simon, F., and Fernandez, R. (2009). Early lipopolysaccharide-induced reactive oxygen species production evokes necrotic cell death in human umbilical vein endothelial cells. *J. Hypertens.* 27 (6), 1202–1216. doi:10.1097/HJH.0b013e328329e31c
- Slobodnyuk, K., Radic, N., Ivanova, S., Llado, A., Tremple, N., Zorzano, A., et al. (2019). Autophagy-induced senescence is regulated by p38 α signaling. *Cell Death Dis.* 10 (6), 376. doi:10.1038/s41419-019-1607-0
- Takada, Y., Mukhopadhyay, A., Kundu, G. C., Mahabeshwar, G. H., Singh, S., and Aggarwal, B. B. (2003). Hydrogen peroxide activates NF-kappa B through tyrosine phosphorylation of I kappa B alpha and serine phosphorylation of p65: Evidence for the involvement of I kappa B alpha kinase and syk protein-tyrosine kinase. *J. Biol. Chem.* 278 (26), 24233–24241. doi:10.1074/jbc.M212389200
- Tiegs, G., Barsig, J., Matiba, B., Uhlig, S., and Wendel, A. (1994). Potentiation by granulocyte macrophage colony-stimulating factor of lipopolysaccharide toxicity in mice. *J. Clin. Invest.* 93 (6), 2616–2622. doi:10.1172/JCI117274
- Trachootham, D., Alexandre, J., and Huang, P. (2009). Targeting cancer cells by ROS-mediated mechanisms: A radical therapeutic approach? *Nat. Rev. Drug Discov.* 8 (7), 579–591. doi:10.1038/nrd2803
- Traore, K., Sharma, R., Thimmulappa, R. K., Watson, W. H., Biswal, S., and Trush, M. A. (2008). Redox-regulation of erk1/2-directed phosphatase by reactive oxygen species: Role in signaling TPA-induced growth arrest in ML-1 cells. *J. Cell. Physiol.* 216 (1), 276–285. doi:10.1002/jcp.21403
- Wan, J. Y., Gong, X., Zhang, L., Li, H. Z., Zhou, Y. F., and Zhou, Q. X. (2008). Protective effect of baicalin against lipopolysaccharide/D-galactosamine-induced liver injury in mice by up-regulation of heme oxygenase-1. *Eur. J. Pharmacol.* 587 (1–3), 302–308. doi:10.1016/j.ejphar.2008.02.081
- Wang, H., Xu, D. X., Lu, J. W., Zhao, L., Zhang, C., and Wei, W. (2007). N-acetylcysteine attenuates lipopolysaccharide-induced apoptotic liver damage in D-galactosamine-sensitized mice. *Acta Pharmacol. Sin.* 28 (11), 1803–1809.
- Wang, Y. Y., Li, J., Wu, Z. R., Zhang, B., Yang, H. B., Wang, Q., et al. (2017). Insights into the molecular mechanisms of polygonum multiflorum thunb-induced liver injury: A computational systems toxicology approach. *Acta Pharmacol. Sin.* 38 (5), 719–732. doi:10.1038/aps.2016.147
- Wang, Z., Ma, P., Xu, L. J., He, C. N., Peng, Y., and Xiao, P. G. (2013). Evaluation of the content variation of anthraquinone glycosides in rhubarb by UPLC-PDA. *Chem. Cent. J.* 7 (1), 170. doi:10.1186/1752-153X-7-170
- Wilhelm, E. A., Jesse, C. R., Roman, S. S., Nogueira, C. W., and Savegnago, L. (2009). Hepatoprotective effect of 3-alkynyl selenophene on acute liver injury induced by D-galactosamine and lipopolysaccharide. *Exp. Mol. Pathol.* 87 (1), 20–26. doi:10.1016/j.yexmp.2009.03.004
- Xu, Y., Kim, S. O., Li, Y., and Han, J. (2006). Autophagy contributes to caspase-independent macrophage cell death. *J. Biol. Chem.* 281 (28), 19179–19187. doi:10.1074/jbc.M513372200
- Yu, J., Xie, J., Mao, X. J., Wang, M. J., Li, N., Wang, J., et al. (2011). Hepatotoxicity of major constituents and extractions of radix polygoni multiflori and radix polygoni multiflori praeparata. *J. Ethnopharmacol.* 137 (3), 1291–1299. doi:10.1016/j.jep.2011.07.055
- Yuan, H., Perry, C. N., Huang, C., Iwai-Kanai, E., Carreira, R. S., Glembofski, C. C., et al. (2009). LPS-induced autophagy is mediated by oxidative signaling in cardiomyocytes and is associated with cytoprotection. *Am. J. Physiol. Heart Circ. Physiol.* 296 (2), H470–H479. doi:10.1152/ajpheart.01051.2008
- Yuan, L., Zhu, Y., Huang, S., Lin, L., Jiang, X., and Chen, S. (2021). NF- κ B/ROS and ERK pathways regulate NLRP3 inflammasome activation in *Listeria* monocytogenes infected BV2 microglia cells. *J. Microbiol.* 59 (8), 771–781. doi:10.1007/s12275-021-0692-9
- Zhang, W., and Liu, H. T. (2002). MAPK signal pathways in the regulation of cell proliferation in mammalian cells. *Cell Res.* 12 (1), 9–18. doi:10.1038/sj.cr.7290105



OPEN ACCESS

EDITED BY

Muhammad Hasnat,
University of Veterinary and Animal
Sciences, Pakistan

REVIEWED BY

Hafiz Ishfaq Ahmad,
University of Veterinary and Animal
Sciences, Pakistan
Hamid Saeed Shah,
University of Veterinary and Animal
Sciences, Pakistan

*CORRESPONDENCE

Yongtao Duan,
duanyongtao860409@163.com
Muhammad Abbas,
tanoliabbas7@yahoo.com

[†]These authors have contributed equally
to this work

SPECIALTY SECTION

This article was submitted to
Ethnopharmacology,
a section of the journal
Frontiers in Pharmacology

RECEIVED 05 June 2022

ACCEPTED 05 September 2022

PUBLISHED 05 October 2022

CITATION

Yao Y, Habib M, Bajwa HF, Qureshi A,
Fareed R, Altaf R, Ilyas U, Duan Y and
Abbas M (2022), Herbal therapies in
gastrointestinal and hepatic disorders:
An evidence-based clinical review.
Front. Pharmacol. 13:962095.
doi: 10.3389/fphar.2022.962095

COPYRIGHT

© 2022 Yao, Habib, Bajwa, Qureshi,
Fareed, Altaf, Ilyas, Duan and Abbas. This
is an open-access article distributed
under the terms of the [Creative
Commons Attribution License \(CC BY\)](#).
The use, distribution or reproduction in
other forums is permitted, provided the
original author(s) and the copyright
owner(s) are credited and that the
original publication in this journal is
cited, in accordance with accepted
academic practice. No use, distribution
or reproduction is permitted which does
not comply with these terms.

Herbal therapies in gastrointestinal and hepatic disorders: An evidence-based clinical review

Yongfang Yao^{1,2,3†}, Murad Habib^{4†}, Hajra Fazeelat Bajwa^{5†},
Anina Qureshi^{6†}, Rameesha Fareed^{7†}, Reem Altaf^{8†}, Umair Ilyas^{7†},
Yongtao Duan^{1*} and Muhammad Abbas^{7*}

¹Henan Provincial Key Laboratory of Children's Genetics and Metabolic Diseases, Children's Hospital
Affiliated to Zhengzhou University, Zhengzhou University, Zhengzhou, Henan, China, ²Ministry of
Education of China, Key Laboratory of Advanced Drug Preparation Technologies, Zhengzhou
University, Zhengzhou, Henan, China, ³Medical School, Huanghe Science and Technology University,
Zhengzhou, Henan, China, ⁴Department of Paediatric Surgery, The Children's Hospital, Pakistan
Institute of Medical Sciences, Islamabad, Pakistan, ⁵Islamabad Medical & Dental College, Islamabad,
Pakistan, ⁶Margalla College of Pharmacy, Margalla Institute of Health Sciences, Rawalpindi, Pakistan,
⁷Riphah Institute of Pharmaceutical Sciences, Riphah International University, Islamabad, Pakistan,
⁸Department of Pharmacy, Iqra University Islamabad Campus, Islamabad, Pakistan

The gastrointestinal tract (GIT) and the liver constitute the major organs of the human body. Indeed, the very survival of the human body depends on their proper functioning. Because the GIT is a huge and complex organ system, the maintenance of proper GIT and liver health is an arduous task. GIT disturbances such as diarrhea, stomach ache, flatulence, constipation, nausea, and vomiting are very common, and they contribute to a significant burden on the healthcare system. Pharmacies are full of over-the-counter pharmacological drugs to alleviate its common conditions. However, these drugs do not always prove to be fully effective and patients have to keep on living with these ailments without a proper and long-term solution. The aim of this review article is to present a practical reference guide to the role of herbal medicines in dealing with gastrointestinal and hepatic disorders, which is supported by systematic reviews and evidence-based trials. People have depended on herbal medications for centuries for the treatment of various ailments of the GIT, liver, and other organ system problems. Recently, this trend of incorporating herbal medication for the treatment of various diseases in both developing and developed countries have surged. Many people continue to use herbal medications, even though substantial data about their efficacy, uses, and toxicological effects do not exist. In addition, while herbal medicines have enormous benefits in both the prevention and the treatment of medical ailments, they can also have toxicological effects. It is, therefore, of the utmost importance that appropriate time, energy, and resources are spent on the development of ethnopharmacology. In addition, herbal products should be classified in a pattern similar to pharmacological medications, including their uses, side effects, mechanism of action, efficacy, and so on.

KEYWORDS

ethnopharmacology, herbal medication, GIT, liver, treatment

Introduction

The gastrointestinal tract (GIT) is one of the largest and most functionally vital organ systems of the human body. It consists of many components, including the alimentary canal, salivary glands, the pancreas, and the liver (Hu et al., 2022). All these organ systems within the GIT work in collaboration to bring about the process of digestion, absorption, and excretion after the food is ingested through the mouth (Hornbuckle et al., 2008). GIT discomfort is a very common problem and many people prefer to use herbal ingredients to alleviate these disorders (Campanella et al., 2022). Common GIT disorders such as nausea, vomiting, diarrhea, irritable bowel disease, and so on have all been effectively treated with the use of herbal medicines (Campanella et al., 2022). Functional GIT disorders—namely, gastroesophageal reflux disease, dyspepsia, and functional constipation—have not been completely understood through anatomical and biochemical models, and their complete treatment through allopathic medicines has not proven to be possible (Langmead and Rampton, 2001). Meanwhile, herbal medicines are widely used in many parts of the world to treat these disorders as an alternative (Langmead and Rampton, 2001). The liver is an integral organ of the GIT and herbal medicines are being researched to be used to treat many ailments of the liver, such as hepatitis and clotting problems. However, this research is still in the preliminary stages and several chemicals in these herbal medicines can be hazardous to health (Kim et al., 2020). The objective of this study is to make use the principles of ethnopharmacology to accentuate and understand the advantages of the herbal medicines in the treatment and prevention of GIT and liver diseases. Along with the uses, the toxicological effects of these medicines are also included in this study.

Pre-clinical and clinical studies of herbal products in the management of GIT and liver diseases

GIT disorders contribute a major burden of diseases in the global healthcare system. A GIT disorder as common as diarrhea is one of the leading causes of mortality worldwide (Stickel and Schuppan, 2007). Although there are effective pharmacological drugs to treat most GIT ailments, a surging trend of resorting to more traditional forms of treatment (i.e., through herbal medication) has been noticed recently (Centers for Disease Control and Prevention, 2015).

Because significant pre-clinical and clinical research do not exist when it comes to the scientific effectiveness of herbal medicines, it is important to gather whatever scientific data that is available to substantiate the use of herbal medicines to treat different pathologies. The role of herbal medicines as the major treatment choice is extremely common in developing countries (Balick, 1996). According to research conducted by Tangjitman et al. (2015) in

Thailand on the use of plant products for the treatment of various GIT ailments, various plants species and their different parts are used in Thailand to treat common GIT and liver problems, including diarrhea, flatulence, gastric ulcers, stomach ache, hemorrhoids, jaundice, and so on (Bodeker et al., 1997). Table 1 summarizes the use of different plant species for different GIT problems, along with their informant consensus factor (ICF) in this research (Bodeker et al., 1997; Tangjitman et al., 2015).

It is generally believed that homeopathic or herbal medicines are without any considerable side effects and that they can be consumed without any fear of dangerous consequences on the body. However, this is far from the truth. Only a limited number of studies have been done on herbal products, which are also mostly inconclusive but list several side effects associated with these herbal medications. Table 2 lists a number of side effects of the plant species that are used in the treatment of GIT disorders (Tangjitman et al., 2015).

Many herbal agents have been researched because of their potential use in the treatment of functional GIT disorders. For example, Kim et al. (2020) studied many herbal agents to identify their uses in the treatment of GIT diseases, such as STW-5 (Iberogast, liquid preparation of nine herbs), Mentha x Piperita (Lamiaceae), Rikkunshito (oral dried preparation of eight herbs), DA-9701 (Motilitone, a newer herbal drug from the seeds of *Pharbitis nil* Choisy (Convolvulaceae), and *Corydalis tuber* (Papaveraceae). These herbal medicines have been shown to treat GIT functional disorders such as irritable bowel disease, functional dyspepsia, gastroesophageal reflux disease, and constipation and used as analgesia and anti-spasmodics (Kim et al., 2020).

The liver receives most of its blood supply from the GIT's circulation (Ebrahimi et al., 2020), so abnormalities affecting other areas of the GIT can have a huge implication on liver functionality and anatomy. Nonalcoholic fatty liver disease (NAFLD) is a highly prevalent condition, predominantly in people with obesity, diabetes, and hypertension. This disease has quite a dangerous sequela as it leads to nonalcoholic steatohepatitis (NASH). This eventually results in liver cirrhosis (the end-stage liver disease), which has no other treatment than liver transplant (Kim and Park, 2019; Xiao et al., 2019; Yan et al., 2020).

Various herbal medicines have been tested for use in the treatment of hepatic disorders, such as rhein, from *Rheum palmatum* L. (Polygonaceae), Huanglian Jiedu extract, Shosaiko-to Juzen-taiho-to, and bofutsushosan, which are effective against NAFLD and NASH (Kim and Park, 2019; Xiao et al., 2019; Yan et al., 2020). Other herbal preparations have shown promising results in the treatment of liver ailments, such as like *Phyllanthus* L. (Phyllanthaceae), *Silybum marianum* (Asteraceae, milk thistle), *Glycyrrhiza glabra* (Fabaceae), and Liv 52 (mixture of herbs) (Dočkalová et al., 2018).

TABLE 1 The use of plant species for GIT problems, along with their informant consensus factor (ICF).

GIT disorders	Plant species used	ICF
Diarrhea	<i>Punica granatum</i> Linn (Punicaceae)	0.95
	<i>Psidium guajava</i> (Myrtaceae)	
	<i>Musa sapientum</i> (Musaceae)	
	<i>Leea indica</i> (Vitaceae)	
	<i>Ensete glaucum</i> (Musaceae)	
	<i>Celastrus paniculatus</i> (Celastraceae)	
	<i>Ochna integerrima</i> (Ochnaceae)	
Flatulence	<i>Zingiber montanum</i> (Zingiberaceae)	0.97
	<i>Zingiber ottensii</i> Valetton (Zingiberaceae)	
	<i>Boesenbergia rotunda</i> (L.) (Zingiberaceae)	
	<i>Kaempferia parviflora</i> (Zingiberaceae)	
Gastric ulcers	<i>Dillenia pentagyna</i> (Dilleniaceae)	0.92
	<i>Engelhardtia spicata</i> var. <i>colebrookeana</i> (Juglandaceae)	
	<i>Curcuma longa</i> (Zingiberaceae)	
	<i>Croton kongensis</i> (Euphorbiaceae)	
	<i>Ziziphus cambodiana</i> (Ziziphiaceae)	
Mouth ulcers	<i>Melastoma malabathricum</i> (Melastomataceae)	0.95
Geographical tongue	<i>Melastoma malabathricum</i> (Melastomataceae)	1.00
Tooth ache	<i>Mussaenda sanderiana</i> (Rubiaceae)	0.50
Stomach ache	<i>Acorus calamus</i> (Acoraceae)	1.00
Constipation	<i>Ochna integerrima</i> (Ochnaceae)	1.00
Carminative	<i>Zingiber ottensii</i> (Zingiberaceae)	1.00
Food poisoning	<i>Ensete glaucum</i> (Musaceae)	1.00
Hemorrhoids	<i>Ziziphus cambodiana</i> (Ziziphiaceae)	0.0
Laxative	<i>Senna occidentalis</i> (Fabaceae)	0.97
	<i>Euphorbia heterophylla</i> L. (Euphorbiaceae)	
	<i>Senna alata</i> (Fabaceae)	
	<i>Tamarindus indica</i> L. (Fabaceae)	
Appetite enhancer	<i>Mussaenda sanderiana</i> (Rubiaceae)	1.00
Jaundice	<i>Gymnopetalum integrifolium</i> (Cucurbitaceae)	0.89
	<i>Dendrocalamus strictus</i> (Poaceae)	
	<i>Croton robustus</i> (Euphorbiaceae)	
	<i>Flemingia macrophylla</i> (Fabaceae)	
	<i>Mussaenda sanderiana</i> (Rubiaceae)	

Coon and Ernst conducted a systematic review of the use of herbal medicines in chronic hepatitis C (Xiao et al., 2019). The authors cited 14 randomized clinical trials in view of the combined use of herbal products and interferon-alpha during antiviral treatment. Although there is difficulty in extrapolation and interpretation of results because of different methodological limits of the considered studies, the authors found that several herbal products and supplements (i.e., vitamin E, thymic extract, zinc, traditional Chinese medicine, *Glycyrrhiza glabra*, and oxymatrine) could exert potential virological and biochemical effects in the treatment of chronic hepatitis C

infection because of a greater clearance of HCV-RNA and normalization of liver enzymes.

Novel in vitro assays for the identification of potentially active compounds for the treatment of gastric and hepatic cancer

The cancers of GIT are very common throughout the world (Rasool et al., 2013; Abbas et al., 2017). Gastric and hepatic cancers are the leading causes of death across the

TABLE 2 A number of side effects of the plant species used for different GIT disorders (Tangjitman et al., 2015).

Plant species used for GIT disorders	Family	Toxicological effects
<i>Acorus calamus</i> L.	Acoraceae	Acute toxicity in mice
<i>Cassytha filiformis</i> L.	Lauraceae	Acute toxicity in mice
<i>Zingiber officinale</i> Roscoe	Zingiberaceae	Embryo toxic to pregnant rats
<i>Zingiber montanum</i> (J.König) Link ex A.Dietr	Zingiberaceae	Acute toxicity in mice
<i>Thunbergia laurifolia</i> Lindl	Acanthaceae	Decrease red blood cell in male mice
<i>Senna occidentalis</i> L.	Fabaceae	Intestinal disturbance in long-term used in rats
<i>Senna alata</i> (L.) Roxb	Fabaceae	Decrease hemoglobin and erythrocyte (RBC) count values in rats
<i>Euphorbia hirta</i> L.	Euphorbiaceae	Leukocytosis, dullness, anorexia, starry hair coat, and 20% mortality in rats
<i>Euphorbia heterophylla</i> L.	Euphorbiaceae	Increase leucopenia in rats
<i>Kaempferia parviflora</i>	Zingiberaceae	Hepatotoxic to rats
<i>Flemingia macrophylla</i>	Fabaceae	Severe hypoglycemia followed by death within 24 h after administration to mice
<i>Celastrus paniculatus</i>	Celastraceae	Hyperactivity and loss of righting reflex in rats

world, gastric cancer being the fifth main cause of demise worldwide according to the World Health Organization (Rawla and Barsouk, 2019; Yang et al., 2022).

Gastric cancers are a group of complex cancers that require a multidisciplinary approach to be treated. The conventional mechanism to treat them requires surgical intervention, followed by radiological and chemotherapeutic treatment (Lelisho et al., 2022). Even after all these interventions, end stage cancers lead to death of patients in a very short time period. These interventions also have a toll on the psychological health of the patients, along with physical debility. Recently, attention toward research on herbal medications to treat gastric and other GIT cancers has significantly increased. Various phytochemicals (i.e., the active biochemical compounds present in plants used for health purposes) are being used and researched in GIT oncology (Choudhary et al., 2020). Table 3 lists several phytochemicals, their anticancer characteristics, and their active compounds (Nakoneczna et al., 2020).

Hepatocellular carcinoma has an exponentially increasing incidence with a high mortality rate (Fattovich et al., 2004). The trend of using herbal medications for the treatment of hepatic diseases is not a new concept. The use of herbal products to enhance the pharmacological and surgical treatment of liver cancer is widely studied and experimented upon. Herbal compounds such as *Curcuma longa* (Zingiberaceae), Resveratrol, *Silybum marianum* L. (Asteraceae), and Tanshinone have shown apoptotic and anti-proliferative effects, along with down-regulation of different compounds involved in metastatic cell growth and the arrest of the cell cycle at various stages (Lin et al., 2004).

Beneficial and toxicological effects of herbal drugs in the light of ethnopharmacology

A number of the advantages of herbal medicines in the treatment of different pathologies of GIT and the liver have already been discussed (Carmona and Pereira, 2013). Some of the more general benefits of herbal medicines in enhancing the GIT system include how phytochemicals such as phytohemagglutinin (lectin) are involved in helping the gut to mature by stimulating intestinal growth (Mukonowenzou et al., 2021). The mechanism of action of this herbal drug was understood when administered to a rat's gut, and it was shown to increase the number of crypts in the rat's GIT (Mukonowenzou et al., 2021). Sangild et al. (2013) studied the importance of early-gut maturation and found that it enhances immunity, which protects children against lethal diseases such as necrotizing enterocolitis and post-weaning diarrhea.

Some of the toxicological effects of herbal medicines have been described earlier and it was shown that they can have hazardous effects. One of the common and note-worthy side effects of herbal medicines is their interaction with pharmacological drugs that are concurrently being consumed by the patients. Another important cause of the toxicological effects of herbal medicines is that the patients mostly use them as a self-medication tool. They tend to get them through unqualified practitioners and use them improperly without proper knowledge of their use (Fatima and Nayeem, 2016). A number of herbal medicines are reported to cause major hepatic dysfunctions such as acute hepatitis, hepatic failure, hepatorenal syndrome, and liver toxicity, particularly *Valeriana officinalis* (Valerianaceae),

TABLE 3 A number of phytochemicals with their active compounds and anticancer characteristics (Nakoneczna et al., 2020).

Plant type	Family	Active metabolite	Anticancer characteristics
<i>Cordyceps cicadae</i>	Cordycipitaceae	Cordicepine	Enhances apoptosis Prevents metastasis
<i>Allium sativum</i> L.	Amaryllidaceae	Allicin	Enhances apoptotic Activity of cells
<i>Camellia sinensis</i>	Theaceae	Epigallocatechin gallate	Inhibits proliferation of cells Proapoptotic effect Reduces angiogenesis Anti-metastatic activity
<i>Cardiospermum halicacabum</i>	Sapindaceae	Synthesized gold nanoparticles	Apoptosis enhancing activity
<i>Plumbago zeylanica</i>	Plumbaginaceae	Plumbagin	Proapoptotic activity Anti-metastatic activity Autophagic activity
<i>Chrysosplenium nudicaule</i>	Saxifragaceae	TTF and DTFG	Apoptosis enhancing activity Reduces cell cycle activity
<i>Saussurea lappa</i>	Astreaceae	Costunolide	Inhibits proliferation of cells Proapoptotic effect Anti-metastatic action
<i>Nigella sativa</i> L.	Ranunculaceae	Thymoquinone	Proapoptotic effect Anti-metastatic action Causes sensitization of cells to chemotherapy
<i>Euphorbia lunulata</i>	Euphorbiaceae	Diterpenoids	Proapoptotic effect Anti-metastatic action
<i>Euphorbia esula</i>	Euphorbiaceae	Total extract	Proapoptotic effect
<i>Dioscorea bulbifera</i>	Dioscoreaceae	Diosbulbine B	Inhibits proliferation of cells
<i>Coptis chinensis</i>	Ranunculaceae	Berberine	Proapoptotic effect Anti-metastatic action Increased autophagic activity
<i>Stephania tetrandra</i>	Menispermaceae	Tetrandrine	Increased autophagic activity Proapoptotic effect Causes sensitization of cells to chemotherapy
<i>Piper longum</i>	Piperaceae	Piperlongumine	Inhibits proliferation of cells Proapoptotic effect Anti-metastatic action
<i>Sophora chrysophylla</i>	Fabaceae	Matrine	Inhibits proliferation of cells Proapoptotic effect Increased autophagic activity

Piper methysticum G. (Piperaceae), *Cimicifuga racemosa* (Ranunculaceae), *Scutellaria baicalensis* (Lamiaceae), *Larrea tridentata* (DC) (Zygophyllaceae), and *Stephania sinica* (Menispermaceae) (Licata et al., 2013; Quan et al., 2020).

Conclusion

There is an ever-increasing trend toward the use of herbal medicines in both the developed and developing countries.

Herbal medicines use natural products that are found in herbs and we know that many allopathic drugs contain these natural products in a refined manner. Although herbal medicines do exhibit some toxic effects, they can be very efficacious in treating a number of life-threatening conditions. However, unlike allopathic drugs, there is no authentic data available on their use, efficacy, toxicity, and side effects. Whenever a new pharmacological drug is introduced in the market, a large volume of information is made publicly available. Similarly, the herbal products that are in common use should be properly studied and experimented upon, and

comprehensive data about their pharmacological aspects should be made publicly available.

There is this common myth that herbal medications have no to minimal side effects, so many people tend use them without any proper research and consultation. This can have very dangerous implications.

Future implications

The fact that many herbal medicines have proven to be extremely beneficial against many life-threatening ailments means that it is very important to study them deeply in future. Special emphasis on the advancement of ethnopharmacology can prove to be a vital and excessively advantageous step toward the therapeutic realm of medicine. Future studies should be focused on placebo controlled, randomized, double-blind clinical trials, herbal product quality and standard criteria for diagnosis, treatment, outcome, and assessment of adverse herb reactions. This approach will provide insight into the risk and benefit profiles, which will hopefully be positive for at least some treatment modalities of herbal protagonists of modern herbal therapies. We can best face these promising challenges of pragmatic modern medicine by bridging the gap between the two medicinal cultures. This would be a tremendously prudent decision that will prove to enhance our existing healthcare system in the future.

References

- Abbas, M., Habib, M., Naveed, M., Karthik, K., Dhama, K., Shi, M., et al. (2017). The relevance of gastric cancer biomarkers in prognosis and pre-and post-chemotherapy in clinical practice. *Biomed. Pharmacother.* 95, 1082–1090. doi:10.1016/j.biopha.2017.09.032
- Balick, M. J. (1996). Transforming ethnobotany for the new millennium. *Ann. Mo. Botanical Gard.* 83, 58–66. doi:10.2307/2399968
- Bodeker, G. C., Bhat, K. K. S., Burley, J., and Vantomme, P. (1997). *Medicinal plants for forest conservation and health care*. Rome (Italy): FAO.
- Campanella, A., Sorino, P., Bonfiglio, C., Mirizzi, A., Franco, I., Bianco, A., et al. (2022). Effects of weight change on all causes, digestive system and other causes mortality in southern Italy: A competing risk approach. *Int. J. Obes.* 46 (1), 113–120. doi:10.1038/s41366-021-00954-8
- Carmona, F., and Pereira, A. M. S. (2013). Herbal medicines: Old and new concepts, truths and misunderstandings. *Rev. Bras. Farmacogn.* 23 (2), 379–385. doi:10.1590/s0102-695x2013005000018
- Centers for Disease Control and Prevention (2015). *Diarrhea: Common illness, global Killer*. U.S. Department of Health and Human Services, 2021.
- Choudhari, A. S., Mandave, P. C., Deshpande, M., Ranjekar, P., and Prakash, O. (2020). Phytochemicals in cancer treatment: From preclinical studies to clinical practice. *Front. Pharmacol.* 10, 1614. doi:10.3389/fphar.2019.01614
- Dočkalová, H., Horký, P., Zeman, L., and Skládanka, J. (2018). Influence of milk thistle pressed parts on rats liver histology. *Potravinárstvo* 12 (1). doi:10.5219/864
- Ebrahimi, F., Torbati, M., Mahmoudi, J., and Valizadeh, H. (2020). Medicinal plants as potential hemostatic agents. *J. Pharm. Pharm. Sci.* 23, 10–23. doi:10.18433/jpps30446
- Fatima, N., and Nayeem, N. (2016). “Toxic effects as a result of herbal medicine intake,” in *Toxicology-new aspects to this scientific conundrum* (London, UK: InTech Open), 193–207.
- Fattovich, G., Stroffolini, T., Zagni, I., and Donato, F. (2004). Hepatocellular carcinoma in cirrhosis: Incidence and risk factors. *Gastroenterology* 127 (5), S35–S50. doi:10.1053/j.gastro.2004.09.014
- Hornbuckle, W. E., Simpson, K. W., and Tennant, B. C. (2008). Gastrointestinal function. *Clin. Biochem. Domest. Animals*, 413–457.
- Hu, Q., Liao, W., Zhang, Z., Shi, S., Hou, S., Ji, N., et al. (2022). The hepatoprotective effects of plant-based foods based on the “gut–liver axis”: A prospective review. *Crit. Rev. Food Sci. Nutr.*, 25, 1–27. doi:10.1080/10408398.2022.2064423
- Kim, K., and Park, K.-I. (2019). A review of antiplatelet activity of traditional medicinal herbs on integrative medicine studies. *Evidence-Based Complementary Altern. Med.* 2019, 7125162. doi:10.1155/2019/7125162
- Kim, Y. S., Kim, J. W., Ha, N. Y., Kim, J., and Ryu, H. S. (2020). Herbal therapies in functional gastrointestinal disorders: A Narrative review and clinical implication. *Front. Psychiatry* 11, 601. doi:10.3389/fpsy.2020.00601
- Langmead, L., and Rampton, D. S. (2001). Review article: Herbal treatment in gastrointestinal and liver disease--benefits and dangers. *Aliment. Pharmacol. Ther.* 15 (9), 1239–1252. doi:10.1046/j.1365-2036.2001.01053.x
- Lelisho, M. E., Seid, A. A., and Pandey, D. (2022). A case study on modeling the time to recurrence of gastric cancer patients. *J. Gastrointest. Cancer* 53 (1), 218–228. doi:10.1007/s12029-021-00684-0
- Licata, A., Macaluso, F. S., and Craxi, A. (2013). Herbal hepatotoxicity: A hidden epidemic. *Intern. Emerg. Med.* 8 (1), 13–22. doi:10.1007/s11739-012-0777-x
- Lin, L.-W., Sun, Y., He, Y. M., Gao, S. D., Xue, E. S., Lin, X. D., et al. (2004). Percutaneous intratumoral injection of traditional Chinese herbal compound

Author contributions

MA conceived and designed the study. YY, RF, RA, UI, and YD performed the literature search and data extraction. HB and MH drafted the manuscript. AQ, RF, and UI revised the final manuscript. All authors read and approved the final manuscript.

Funding

This work was supported by the Riphah International University (ORIC-21-22/FPS-51).

Conflict of interest

The authors declare that the research was conducted in the absence of any commercial or financial relationships that could be construed as a potential conflict of interest.

Publisher's note

All claims expressed in this article are solely those of the authors and do not necessarily represent those of their affiliated organizations, or those of the publisher, the editors, and the reviewers. Any product that may be evaluated in this article, or claim that may be made by its manufacturer, is not guaranteed or endorsed by the publisher.

medicine Star-99 in treatment of hepatocellular carcinoma of mice. *Hepatobiliary Pancreat. Dis. Int.* 3 (1), 49–54.

Mukonowenzou, N. C., Adeshina, K. A., Donaldson, J., Ibrahim, K. G., Usman, D., and Erlwanger, K. H. (2021). Medicinal plants, phytochemicals, and their Impacts on the maturation of the gastrointestinal Tract. *Front. Physiol.* 12, 1123. doi:10.3389/fphys.2021.684464

Nakoneczna, S., Grabarska, A., and Kukula-Koch, W. (2020). The potential anticancer activity of Phytoconstituents against gastric cancer—a review on *in vitro*, *in vivo*, and clinical studies. *Int. J. Mol. Sci.* 21 (21), 8307. doi:10.3390/ijms21218307

Quan, N. V., Dang Xuan, T., and Teschke, R. (2020). Potential hepatotoxins found in herbal medicinal products: A systematic review. *Int. J. Mol. Sci.* 21 (14), 5011. doi:10.3390/ijms21145011

Rasool, S., Kadla, S. A., Rasool, V., and Ganai, B. A. (2013). A comparative overview of general risk factors associated with the incidence of colorectal cancer. *Tumour Biol.* 34 (5), 2469–2476. doi:10.1007/s13277-013-0876-y

Rawla, P., and Barsouk, A. (2019). Epidemiology of gastric cancer: Global trends, risk factors and prevention. *Prz. Gastroenterol.* 14 (1), 26–38. doi:10.5114/pg.2018.80001

Sangild, P. T., Thymann, T., SchMidtM.Stoll, B., Burrin, D. G., and Buddington, R. K. (2013). Invited review: The preterm pig as a model in pediatric gastroenterology. *J. Anim. Sci.* 91 (10), 4713–4729. doi:10.2527/jas.2013-6359

Stickel, F., and Schuppan, D. (2007). Herbal medicine in the treatment of liver diseases. *Dig. Liver Dis.* 39 (4), 293–304. doi:10.1016/j.dld.2006.11.004

Tangjitman, K., Wongsawad, C., Kamwong, K., Sukkho, T., and Trisonthi, C. (2015). Ethnomedicinal plants used for digestive system disorders by the Karen of northern Thailand. *J. Ethnobiol. Ethnomed.* 11 (1), 27–33. doi:10.1186/s13002-015-0011-9

Xiao, J., Wang, F., Wong, N. K., He, J., Zhang, R., Sun, R., et al. (2019). Global liver disease burdens and research trends: Analysis from a Chinese perspective. *J. Hepatol.* 71 (1), 212–221. doi:10.1016/j.jhep.2019.03.004

Yan, T., Yan, N., Wang, P., Xia, Y., Hao, H., Wang, G., et al. (2020). Herbal drug discovery for the treatment of nonalcoholic fatty liver disease. *Acta Pharm. Sin. B* 10 (1), 3–18. doi:10.1016/j.apsb.2019.11.017

Yang, Jianqing, Pan, Guangdong, Guan, Linjing, Liu, Zhipeng, Wu, Yongrong, Liu, Zhen, et al. (2022). The burden of primary liver cancer caused by specific etiologies from 1990 to 2019 at the global, regional, and national levels. *Cancer Med.* 11 (5), 1357–1370.



OPEN ACCESS

EDITED BY

Alessandra Durazzo,
Council for Agricultural Research and
Economics, Italy

REVIEWED BY

Hafiz ishfaq Ahmad,
University of Veterinary and Animal
Sciences, Pakistan
Hafiz Muhammad Zubair,
Nanjing Medical University, China

*CORRESPONDENCE

Jiabo Wang,
jiabo_wang@ccmu.edu.cn
Xiaohu Xiao,
pharmacy_302@126.com
Zhaofang Bai,
baizf2008@hotmail.com

SPECIALTY SECTION

This article was submitted to
Ethnopharmacology,
a section of the journal
Frontiers in Pharmacology

RECEIVED 10 August 2022

ACCEPTED 07 October 2022

PUBLISHED 31 October 2022

CITATION

Gao Y, Shi W, Tu C, Li P, Zhao G, Xiao X,
Wang J and Bai Z (2022),
Immunostimulatory activity and
structure-activity relationship of
epimedin B from *Epimedium
brevicornu* Maxim..
Front. Pharmacol. 13:1015846.
doi: 10.3389/fphar.2022.1015846

COPYRIGHT

© 2022 Gao, Shi, Tu, Li, Zhao, Xiao,
Wang and Bai. This is an open-access
article distributed under the terms of the
[Creative Commons Attribution License
\(CC BY\)](#). The use, distribution or
reproduction in other forums is
permitted, provided the original
author(s) and the copyright owner(s) are
credited and that the original
publication in this journal is cited, in
accordance with accepted academic
practice. No use, distribution or
reproduction is permitted which does
not comply with these terms.

Immunostimulatory activity and structure-activity relationship of epimedin B from *Epimedium brevicornu* Maxim.

Yuan Gao¹, Wei Shi^{2,3,4}, Can Tu⁵, Peng Li⁶, Guanyu Zhao¹,
Xiaohu Xiao^{2,3*}, Jiabo Wang^{1*} and Zhaofang Bai^{2,3*}

¹School of Traditional Chinese Medicine, Capital Medical University, Beijing, China, ²Senior Department of Hepatology, The Fifth Medical Center of PLA General Hospital, Beijing, China, ³China Military Institute of Chinese Medicine, The Fifth Medical Center of PLA General Hospital, Beijing, China, ⁴School of Life Sciences, Beijing University of Chinese Medicine, Beijing, China, ⁵Beijing Research Institute of Chinese Medicine, Beijing University of Chinese Medicine, Beijing, China, ⁶State Key Laboratory of Quality Research in Chinese Medicine, Institute of Chinese Medical Sciences, University of Macau, Macau, China

Epimedium Folium (EF, *Epimedium brevicornu* Maxim.), a traditional botanical drug, is famous for treating bone fractures, joint diseases, and several chronic illnesses. However, some studies indicated that EF could induce idiosyncratic drug-induced liver injury (IDILI) in the clinic. The NLRP3 inflammasome plays a crucial role in the pathogenesis of various human diseases, including IDILI. In the present study, we showed that epimedin B could specifically facilitate nigericin- or ATP-induced NLRP3 inflammasome activation under synergistic induction of mitochondrial reactive oxygen species. Moreover, epimedin B resulted in activation of Caspase-1 and IL-1 β secretion in a lipopolysaccharide (LPS)-mediated susceptibility mouse model. MCC950 pretreatment completely abrogated activation of the NLRP3 inflammasome and prevented liver injury. Importantly, several studies have confirmed that some active constituents of EF could enhance activation of the NLRP3 inflammasome and may be involved in the pathogenesis of EF-IDILI. No reports are available on whether the structure-activity relationship associated with the immunostimulatory activity in EF contributes to the pathogenesis of EF-IDILI. These findings have changed our conventional understanding about the more glycogen, the more immunostimulatory activity.

KEYWORDS

epimedin B, idiosyncratic drug-induced liver injury, NLRP3 inflammasome, epimedium folium, mitochondrial ROS

Abbreviations: IDILI, Idiosyncratic Drug-induced Liver Injury; TCM, Traditional Chinese Medicine; NLR, the Nucleotide-binding Domain and Leucine-rich Repeat; PAMPs, Pathogen-associated Molecular Patterns; IL-1 β , Interleukin 1 β ; BMDMs, Bone Marrow-derived Macrophages; DMEM, Dulbecco's Modified Eagle Medium; FBS, Fetal Bovine Serum; ATP, Adenosine Triphosphate; DMSO Dimethyl Sulfoxide; ELISA, Enzyme-linked Immunosorbent Assay; ALT, Alanine Aminotransferase; AST, Aspartate Transaminase; LDH, Lactate Dehydrogenase; ROS: Reactive Oxygen Species.

Introduction

Idiosyncratic drug-induced liver injury (IDILI) is an uncommon but challenging clinical problem with respect to both diagnosis and management (Fontana, 2014; Hoofnagle and Björnsson, 2019; Uetrecht, 2019b; a). IDILI is unpredictable, not dose-dependent, and cannot be easily established in animal models (Benesic et al., 2018). Recently, with the widespread use of herbal and dietary supplements (HDS) worldwide, traditional Chinese medicine (TCM) and dietary supplements have gained prominence as the leading causes of IDILI (Bernal and Wendon, 2013; Shen et al., 2019). Specifically, the incidence of IDILI induced by HDS, such as *Psoraleae Fructus*, *Polygoni Multiflori Radix* and *Epimedii Folium* has increased in recent years (Wang et al., 2014; Lin et al., 2015; Tu et al., 2019; Gao et al., 2020). However, the precise pathogenesis remains elusive.

The NOD-like receptor family, pyrin domain containing 3 (NLRP3) inflammasome is a multiprotein complex that can orchestrate innate immune responses to pathogen-associated molecular patterns (PAMPs) and danger-associated molecular patterns (DAMPs) (Schroder and Tschoop, 2010; Elliott and Sutterwala, 2015). Upon activation, it leads to the cleavage of pro-caspase-1, subsequently resulting in pyroptosis and the production of interleukin 1 β (IL-1 β) and IL-18. Aberrant activation of the NLRP3 inflammasome has been associated with many chronic and degenerative diseases, such as Alzheimer's disease, osteoarthritis, type 2 diabetes, gout, atherosclerosis, and liver disease (Szabo and Csak, 2012; Wen et al., 2012; Wu et al., 2017). Moreover, activation of the NLRP3 inflammasome may be a critical mechanism underlying the development of IDILI (Szabo and Csak, 2012; Wree et al., 2014a; Wu et al., 2017).

As a well-known TCM, *Epimedii Folium* (EF, *Epimedium brevicornu* Maxim.) has a medicinal history of over a thousand years in China and other countries in Asia, HDS containing EF are widely used for treating bone fractures, joint diseases, several chronic illnesses, for delaying aging, etc. Nevertheless, EF and its preparations have garnered significant interest because they can induce liver injury (Wree et al., 2014a; Zhang et al., 2019; Zhong et al., 2019; Gao et al., 2020). In our previous study, we reported that Icariside I and Icariside II can enhance activation of the NLRP3 inflammasome and may be involved in the pathogenesis of EF-IDILI (Wang et al., 2020; Gao et al., 2021). The major active constituents of EF are flavonoids, and over 60 types of flavonoids have been identified, among which epimedin A, B, C, and icariin are considered major bioactive components that constitute more than 52% of the total number of flavonoids in EF. However,

Icariside I and Icariside II, which both contain one glucoside have more immunostimulatory activity. Yet, no reports are available on whether the structure-activity relationship is associated with the immunostimulatory activity in EF and contributes to the pathogenesis of EF-IDILI. In the current study, we demonstrated that epimedin B induced IDILI by promoting activation of the NLRP3 inflammasome both *in vivo* and *in vitro*. These findings have changed our conventional understanding about “the more glycogen, the more immunostimulatory activity”.

Materials and methods

Mice

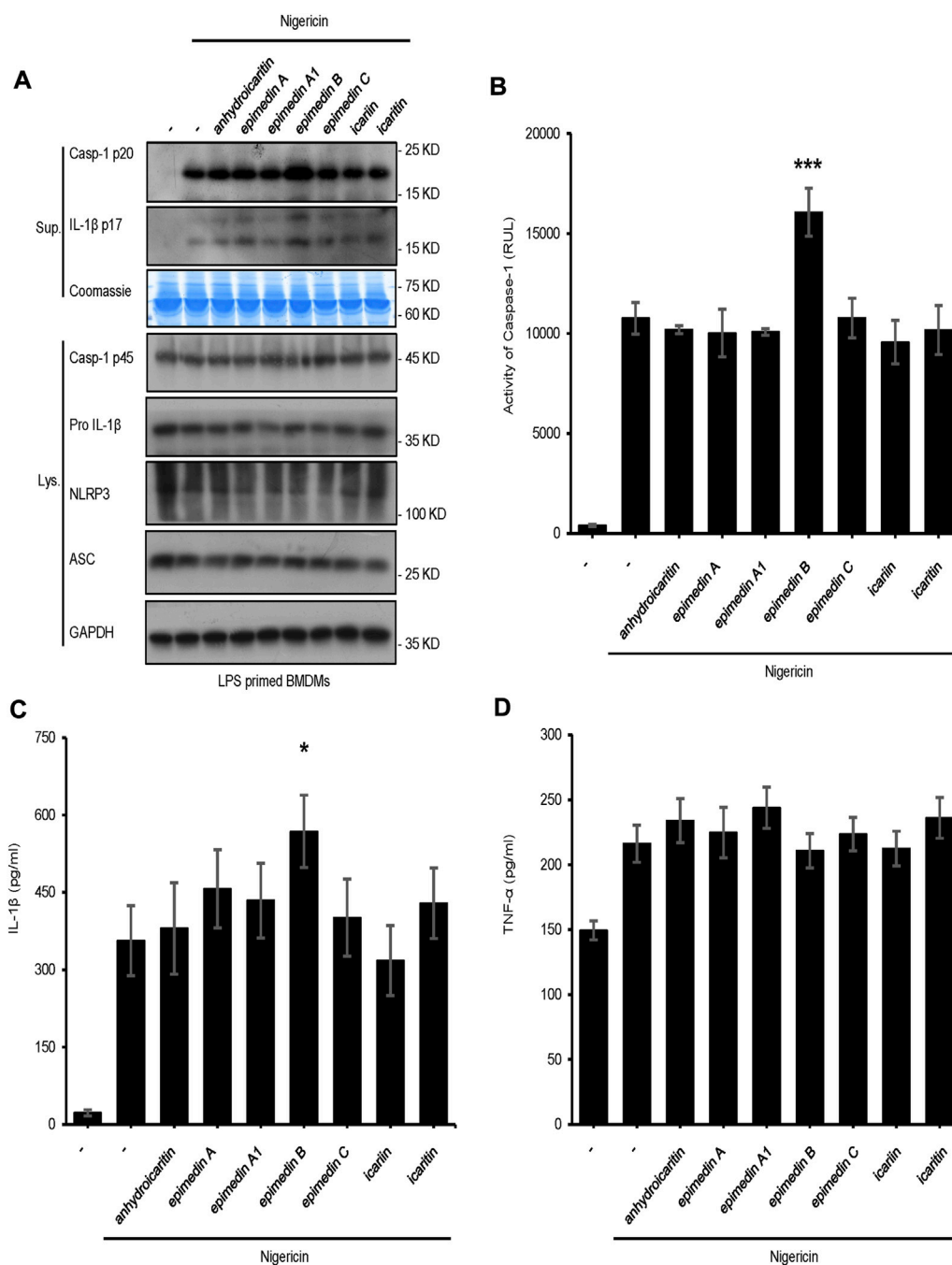
C57BL/6 female wild-type mice (6–8 weeks) were obtained from specific pathogen-free (SPF) Biotechnology Co., Ltd., (Beijing, China). NLRP3 knockout (NLRP3^{-/-}) mice were obtained from the National Center of Biomedical Analysis (NCBA, Beijing, China) and supplied by Dr. Tao Li. All mice were maintained at a temperature of 22–24°C under a 12-h light/dark cycle with *ad libitum* access to food and water. In this study, all animal protocols were performed according to the guidelines for care and use of laboratory animals and approved by the Animal Ethics Committee of the Fifth Medical Centre, Chinese People's Liberation Army General Hospital (animal ethics committee approval No. IACUC-2017-003).

Cell culture

Bone marrow-derived macrophages (BMDMs) were isolated from marrow of the femoral bone of wild type (WT) or NLRP3^{-/-} female C57BL/6 mice (10-week-old). BMDMs were cultured in the Dulbecco's modified Eagle medium (DMEM) supplemented with 10% fetal bovine serum (FBS), 1% penicillin/streptomycin (P/S), and 50 ng/ml murine macrophage colony-stimulating factor (M-CSF). THP-1 cells were cultured in RPMI 1640 medium supplemented with 10% FBS and 1% P/S. Cells were maintained in a humidified 5% (v/v) CO₂ incubator at 37°C.

Antibodies and reagents

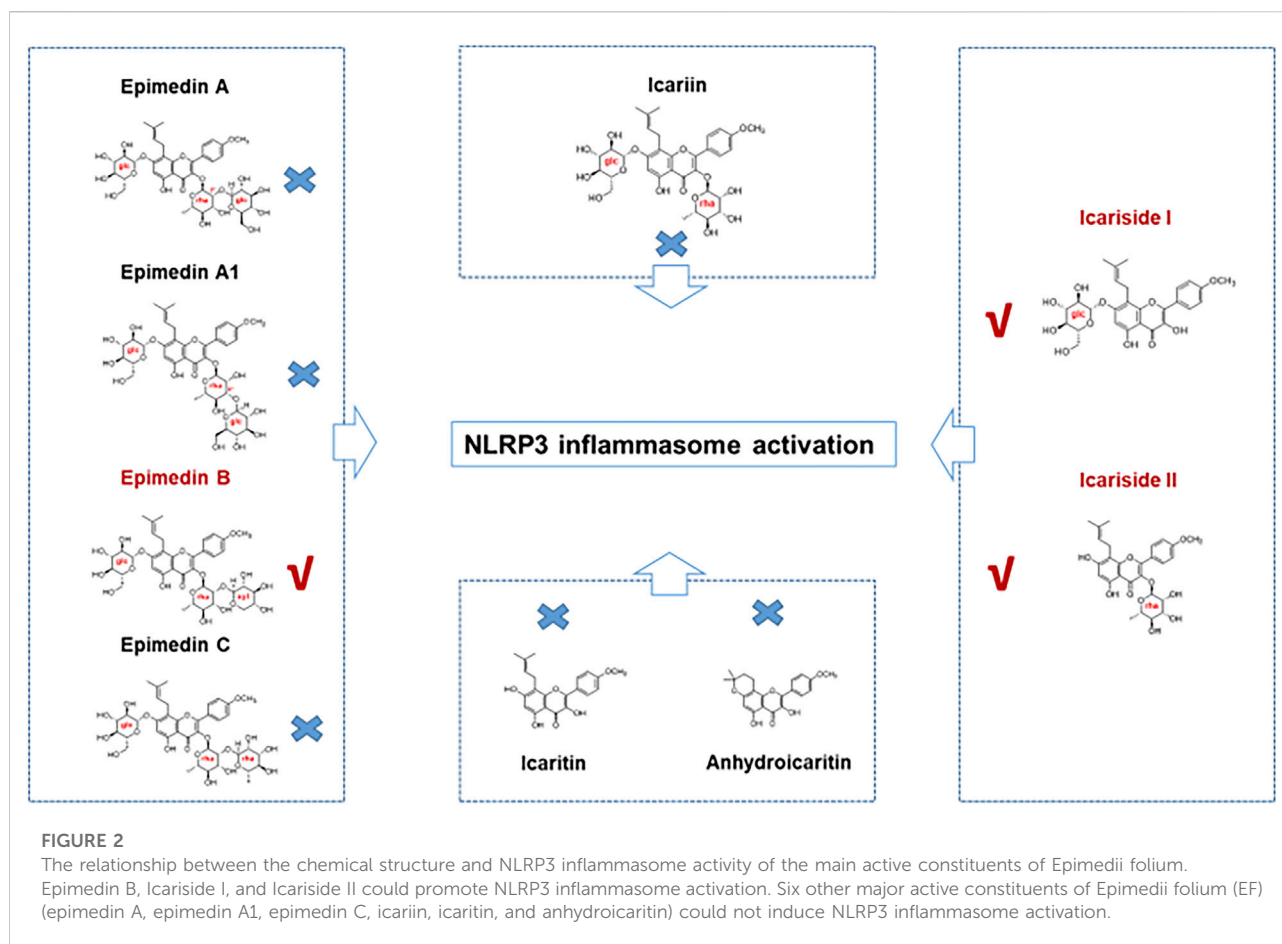
Adenosine triphosphate (ATP), Nigericin, SiO₂, poly (deoxyadenylic-thymidylic) acid sodium salt (poly (dA:dT)), polyinosinic: polycytidylic acid [poly (I:C)], Pam3CSK4, dimethyl sulfoxide (DMSO), and LPS (*Escherichia coli*, 055:B5) were purchased from Sigma-Aldrich (Munich, Germany).

**FIGURE 1**

Effect of the main constituents of *Epimedii folium* on NLRP3 inflammasome activation. (A) Western blot analysis of supernatants (Sup) and whole-cell lysates (Lys) derived from lipopolysaccharide (LPS)-primed bone marrow-derived macrophages (BMDMs) subjected to treatment with the main constituents of EF (40 μ M) and stimulated with nigericin (10 μ mol/L). (B–D) Caspase-1 activity (B) ELISA of IL-1 β (C), and TNF- α (D) in Sup derived from the samples described in (A). Data are expressed as the mean \pm SD from at least three biological samples. The significance of the differences was analyzed using unpaired Student's *t*-test: **p* < 0.05, ***p* < 0.01, ****p* < 0.001, NS; not significant, RLUs; relative light units.

Epimedin A (110623–72–8, purity 99.0%), epimedin A1 (140147–77–9, purity 99.92%), epimedin B (110623–73–9, purity 99.39%), epimedin C (110642–44–9, purity 99.1%),

icaritin (489–32–7, purity 97.64%), caritin (118525–40–9, purity 99%), and anhydroicaritin (38226–86–7, purity 99.51%) were purchased from TargetMol. *Salmonella* strains were kindly



provided by Dr. Tao Li from the National Center of Biomedical Analysis. MCC950 was obtained from TargetMol (Boston, MA, United States). Anti-mouse caspase-1 (1:1000, AG-20B-0042) was purchased from Adipogen (San Diego, CA, United States). Anti-mouse IL-1 β (1:1000, 12,507) and anti-NLRP3 (1:2000, 15101S) antibodies were obtained from Cell Signaling Technology (Boston, MA, United States). Anti-ASC (1:1000, sc-22,514-R) was purchased from Santa Cruz Biotechnology (Dallas, TX, United States). Anti-GAPDH (1:2000, 60,004-1-1 g) was purchased from Proteintech (Chicago, IL, United States). The prestained protein marker (20AB01) was purchased from GenStar (Beijing, China).

Inflammasome activation

To induce activation of the inflammasome, BMDMs were seeded at a density of 5×10^5 cells/well in 0.5 ml of medium in 24-well plates and were incubated overnight. The following day, medium was replaced with fresh medium, and BMDMs were subjected to stimulation with 50 ng/ml lipopolysaccharide (LPS) or 1 μ g/ml Pam3CSK4 for a

duration of 4 h. Next, cells were subjected to treatment with epimedin B for 1 h and were subsequently stimulated as follows: 5 mM ATP for 1 h, 7.5 μ mol/L nigericin for 30 min, or 250 μ g/ml silicon dioxide (SiO₂) for 6 h. Cells were transfected with poly (I:C) (2 μ g/ml), poly (dA:dT) (2 μ g/ml), or LPS (1 μ g/ml) for 6 h using Lipofectamine 2000 according to the manufacturer's instructions.

Caspase-1 activity assay

According to the manufacturer's instructions (Promega, Madison, WI, United States), we used the 1:1 ratio of Caspase-Glo 1 Reagent volume/sample volume to assess caspase-1 activity in cell culture medium.

Enzyme-linked immunosorbent assay

Mouse IL-1 β (R&D Systems, Minneapolis, MN, United States), IL-1 β , TNF- α , and IL-6 (Dakewe, Beijing, China), according to the manufacturer's instructions, were

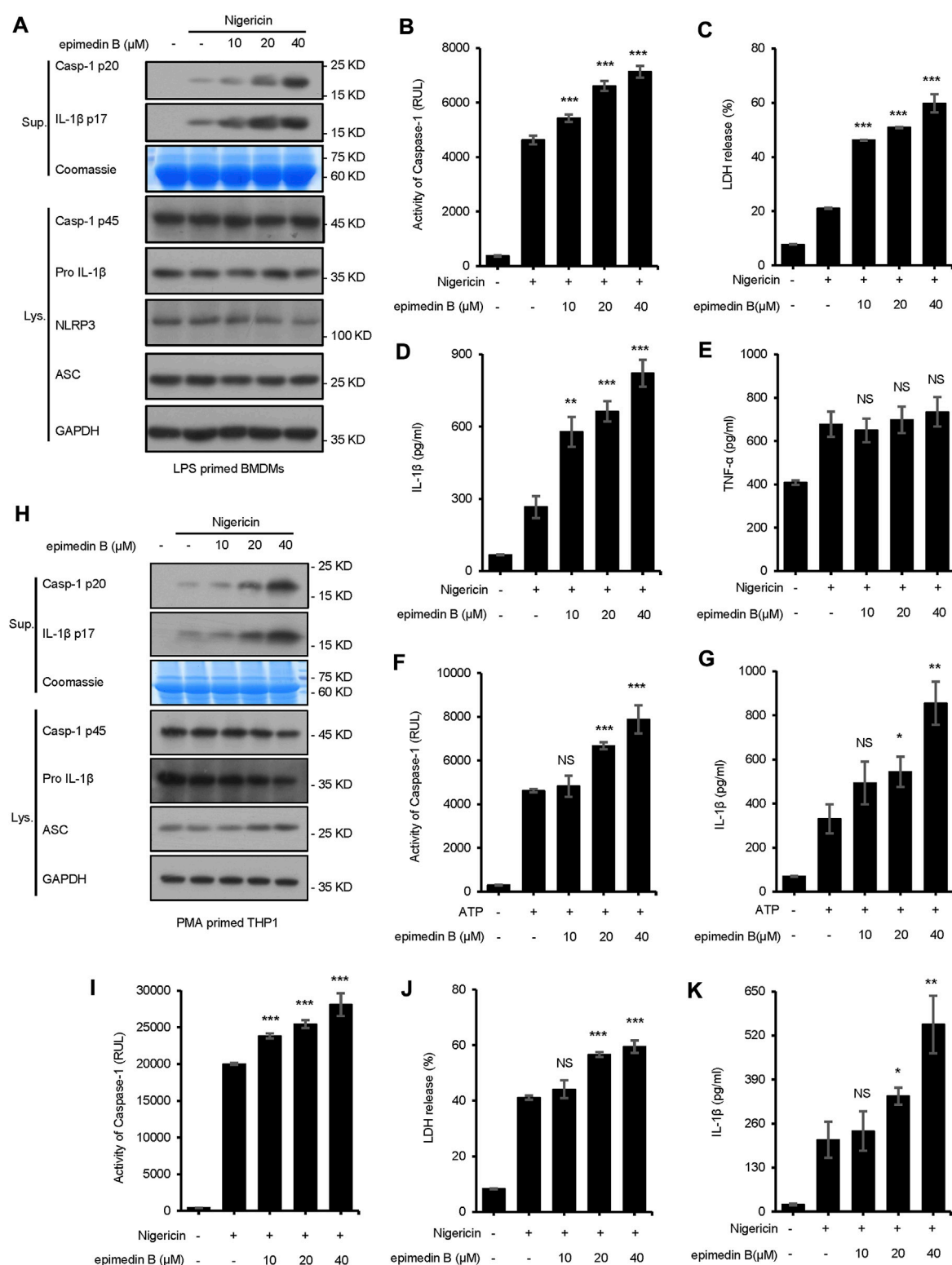


FIGURE 3

Epimedin B promotes NLRP3 inflammasome activation in bone marrow-derived macrophages and THP1 cells stimulated by nigericin or ATP. (A) Western blot analysis of supernatants (Sup) and whole-cell lysates (Lys) derived from lipopolysaccharide (LPS)-primed bone marrow-derived macrophages (BMDMs) subjected to treatment with various doses of epimedin B prior to nigericin stimulation. (B–E) Caspase-1 activity (B), the release of lactate dehydrogenase (LDH) (C), ELISA of IL-1β (D) and TNF-α (E) levels in supernatants (Sup) from samples described in (A) (F,G)

(Continued)

FIGURE 3 (Continued)

Caspase-1 activity (**F**) and ELISA of IL-1 β (**G**) of Sup and Lys derived from LPS-primed BMDMs subjected to treatment with various doses of epimedin B prior to ATP stimulation. (**H**) Western blot analysis of Sup and Lys derived from PMA-primed THP1 cells subjected to treatment with various doses of epimedin B prior to nigericin stimulation. (**I–K**) Caspase-1 activity (**I**), release of LDH (**J**), and ELISA of IL-1 β (**K**) in Sup from samples described in (**H**). Data are presented as the mean \pm SD from at least three biological samples. The significance of the differences was analyzed using unpaired Student's *t*-test: **p* < 0.05, ***p* < 0.01, ****p* < 0.001, NS; not significant, RLUs; the relative light units.

used to measure the cell culture supernatants and mouse serum, respectively.

Alanine aminotransferase and aspartate transaminase

Serum ALT and AST were determined using the commercially available assay kit (Nanjing Jiancheng Bioengineering Institute, Nanjing, China) according to the manufacturer's instructions.

Lactate dehydrogenase assay

The release of LDH into the culture supernatant was assessed using the CytoTox 96® 1 Non-radioactive Cytotoxicity Assay (Promega, Madison, WI, United States) according to the manufacturer's instructions.

ASC oligomerization

Cells were lysed with Triton buffer (50 mM Tris-HCl [pH 7.5], 150 mM NaCl, 0.5% Triton X-100, and EDTA-free protease inhibitor cocktail). The samples were then centrifuged at $6,000 \times g$ at 4°C for 15 min. The supernatant was referred to as Triton X-soluble, and the pellet fractions were referred to as Triton X-insoluble fractions. To enable ASC oligomer cross-linking, the Triton X-100-insoluble fractions were subjected to washing steps and were resuspended in 200 μ l of PBS, followed by the establishment of cross-linking at 37°C with 2 mM disuccinimidyl suberate (DSS) for 30 min. The pellets were centrifuged at $6,000 \times g$ for 15 min, after which they were collected and dissolved in 1 \times SDS loading buffer for immunoblot analysis.

Intracellular K⁺ measurement

BMDMs were seeded in 12-well plates overnight and were primed with 50 ng/ml LPS for 4 h. The cells were subjected to treatment with epimedin B and were then stimulated with nigericin for 30 min. The culture medium was thoroughly aspirated and subjected to washing steps thrice using

potassium-free buffer. Ultrapure HNO₃ was added to perform lysis of the cells. Samples were collected in glass bottles and boiled for 30 min at 100°C. Intracellular K⁺ measurements were performed *via* inductively coupled plasma mass spectrometry.

Measurement of intracellular Ca²⁺ levels

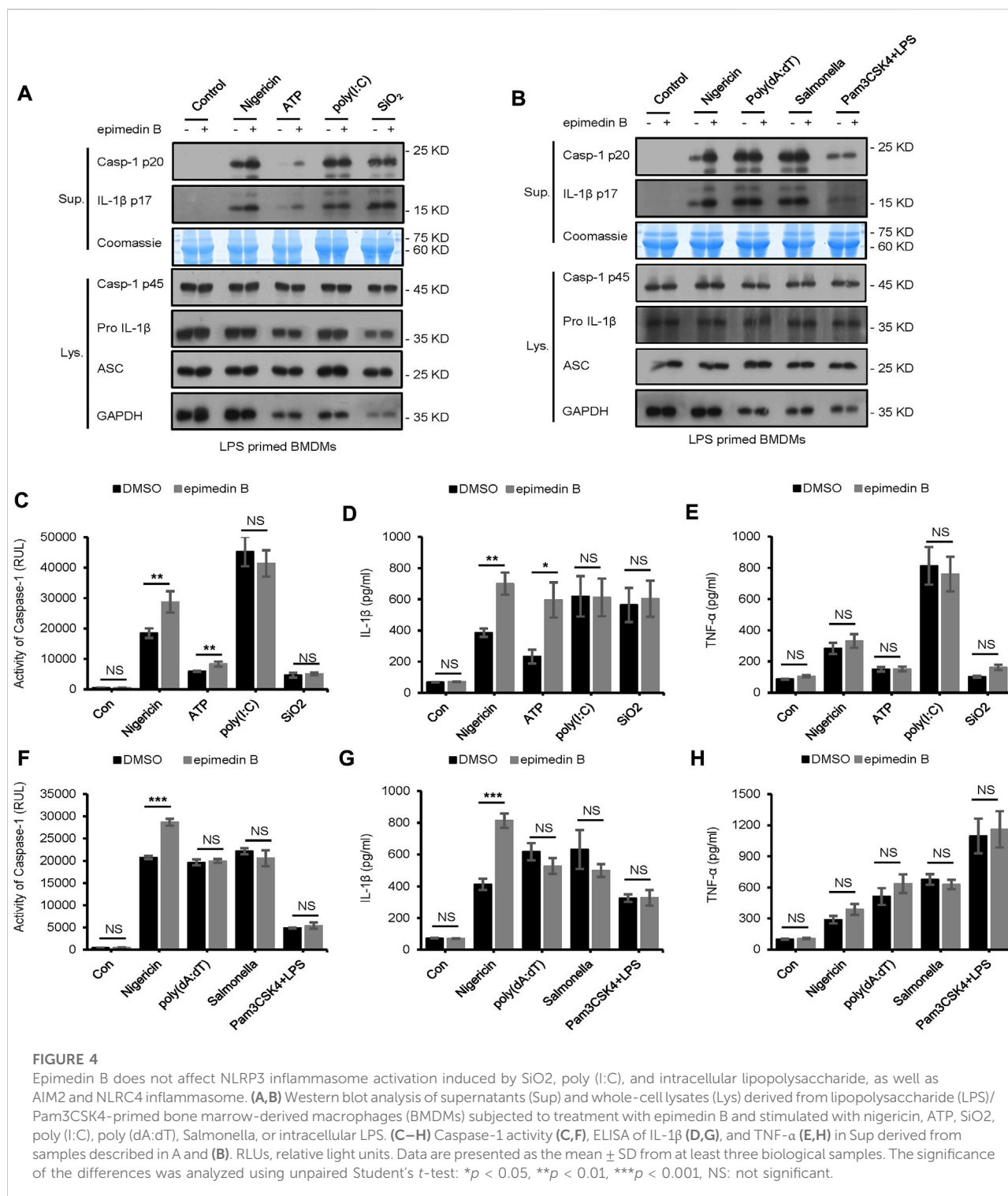
BMDMs were seeded at 2.5×10^4 cells/mL overnight in a 384-well plate. After cells were primed with LPS for 4 h, they were treated with ATP for 45 min with or without epimedin B. Ca²⁺ flux measurements were performed by the FLIPRT Tetra system (Molecular Devices, San Jose, CA, United States).

Mitochondrial reactive oxygen species assay

BMDMs were seeded at a density of 1×10^6 cells/mL in culture dishes with a diameter of 100 mm and primed with LPS (50 ng/ml) for 4 h. Next, cells were transferred to a test tube, subjected to wash steps with Opti-MEM, and were stimulated as per the methods described previously. For measurements the release of mitochondrial reactive oxygen species (ROS), BMDMs were subjected to staining procedures using 4 μ M MitoSOX for 20 min at 37°C, followed by two wash steps with HBSS, and assessment using flow cytometry. After completion of the staining and wash steps, flow cytometry was performed to measure mtROS levels.

Assessment of the effects of LPS/epimedin B cotreatment-induced DILI *in vivo*

C57BL/6 mice (6–8-week-old females) were subjected to starvation for 24 h and were administered LPS (2 mg/kg) or saline vehicle *via* intravenous (i.v.). Tail vein administration. Following an observation period of 2 h, epimedin B (20 mg/kg, 40 mg/kg, and 80 mg/kg) or the vehicle was administered *via* intraperitoneal injection. Serum and a fraction of liver tissues were collected 6 h after epimedin B treatment. Serum ALT, AST, IL-1 β , and TNF- α levels were measured. Histopathological analysis was performed *via* hematoxylin and eosin (H&E) staining. The number of F4/80-positive macrophages in the liver was determined.



In the second experiment, female C57BL/6 mice (6–8 weeks) were administered MCC950 (40 mg/kg) or saline vehicle through intraperitoneal injection. After 1 h,

LPS (2 mg/kg) or saline vehicle was administered i.v. *via* tail vein. After 2 h, epimedin B (40 mg/kg) was administered *via* intraperitoneal injection. Mouse serum

and a fraction of liver tissues were collected after 6 h. H&E staining was performed, and serum levels of IL-1 β , TNF- α , ALT, and AST were determined.

Statistical analyses

For statistical analysis, GraphPad Prism 7 (GraphPad Software) and Microsoft Excel were used. Data are presented as means \pm SD and analyzed using a standard two-tailed unpaired Student's *t*-test for single comparisons and one-way ANOVA for multiple comparisons. Differences with a *p* value <0.05 were considered to be significant. Statistical significance is presented as **p* < 0.05 , ***p* < 0.01 , ****p* < 0.001 vs the control; NS, not significant.

Results

Epimedin B accelerates NLRP3 inflammasome activation

In the present study, seven major active constituents of EF were analyzed for their ability to activate the NLRP3 inflammasome. Figures 1A–C shows that epimedin B significantly promoted the activation of caspase-1 and IL-1 β production induced by nigericin, but did not affect the production of TNF- α (Figure 1D). Therefore, epimedin B enhanced nigericin-induced NLRP3 inflammasome activation. The relationship between chemical structure and NLRP3 inflammasome activity of the main active constituents of EF is summarized. Figure 2 shows that the amount of glycogen contained in the main active constituents of EF is independent on NLRP3 inflammasome activity. These findings have changed our conventional understanding about “the more glycogen, the more immunostimulatory activity.” To determine whether epimedin B could accelerate NLRP3 inflammasome activation, caspase-1 activation and IL-1 β secretion were measured. Epimedin B exhibited dose-dependent active effects on caspase-1 cleavage and IL-1 β secretion (Figures 3A,B,D). In addition, lactate dehydrogenase (LDH) induced by nigericin promoted LPS-primed BMDMs (Figure 3C). We also assessed the effect of epimedin B on ATP-induced NLRP3 inflammasome activation. Our data showed that LPS-induced caspase-1 activation and IL-1 β secretion in BMDMs could be induced by epimedin B. However, no effects were observed on TNF- α production (Figure 3E). Next, we also assessed the impact of epimedin B on ATP-induced NLRP3 inflammasome activation in BMDMs. The results showed that epimedin B treatment increased production of the caspase-1 and IL-1 β and the release of LDH triggered by ATP (Figures 3F,G, Supplementary Figures. S1A–C). Furthermore, THP-1 cells

were selected to measure the effect of epimedin B on nigericin-induced NLRP3 inflammasome activation. The results indicated that epimedin B enhanced caspase-1 maturation, IL-1 β secretion, and LDH release in a dose-dependent manner in response to nigericin in PMA-primed THP-1 cells (Figures 3H–K).

Pretreatment with epimedin B promoted nigericin-induced caspase-1 cleavage and IL-1 β release in WT BMDMs but not in NLRP3^{−/−} BMDMs (Supplementary Figure 3A). MCC950 is a small-molecule inhibitor of the NLRP3 inflammasome (Coll et al., 2019). In this study, it was evaluated whether activation of the NLRP3 inflammasome induced by epimedin B could be inhibited by treatment with MCC950. Our results indicated that epimedin B accelerated NLRP3 inflammasome activation, which could be inhibited by MCC950 (Supplementary Figure S3B).

Moreover, we explored the effect of epimedin B on NLRP3 inflammasome activation initiated in response to other stimuli. Unexpectedly, treatment with epimedin B exerted no effect on caspase-1 cleavage and IL-1 β secretion stimulated by other NLRP3 agonists, including SiO₂ and poly (I:C) (Figures 4A, C–E). Furthermore, epimedin B did not affect cytosolic LPS, NLRC4, or AIM2 inflammasome activation (Figures 4B, F–H). Thus, these results indicate that epimedin B is a specific promoter that increases nigericin- and ATP-induced NLRP3 inflammasome activation.

Next, we examined whether epimedin B affected LPS-induced priming for inflammasome activation. When BMDMs were stimulated with epimedin B before or after LPS treatment, epimedin B did not activate LPS-induced NLRP3 expression, or IL-6 and TNF- α production. The data presented in Figures 5A–C suggest that epimedin B does not enhance LPS-induced priming at the doses that are effective for NLRP3 activation, thereby suggesting that epimedin B exerts a robust effect on NLRP3 inflammasome activation.

Epimedin B promotes nigericin or ATP-induced ASC oligomerization but does not block K⁺ efflux and Ca²⁺ flux

In this study, the mechanism underlying the activation of NLRP3 by epimedin B was investigated. First, our studies showed that epimedin B could activate nigericin-induced ASC oligomerization (Figure 5D), which is an essential step for NLRP3 activation. These findings suggested that epimedin B acts upstream of ASC oligomerization to exacerbate nigericin-induced NLRP3 activation. Second, epimedin B promoted ASC oligomerization induced by ATP (Figure 5E). However, epimedin B had no effect on ASC oligomerization induced by SiO₂, poly (I:C), poly (dA:dT), *Salmonella typhimurium*, or cytosolic LPS (Figure 5E; Supplementary Figure S2). These data also indicated that epimedin B acted upstream of ASC oligomerization, which

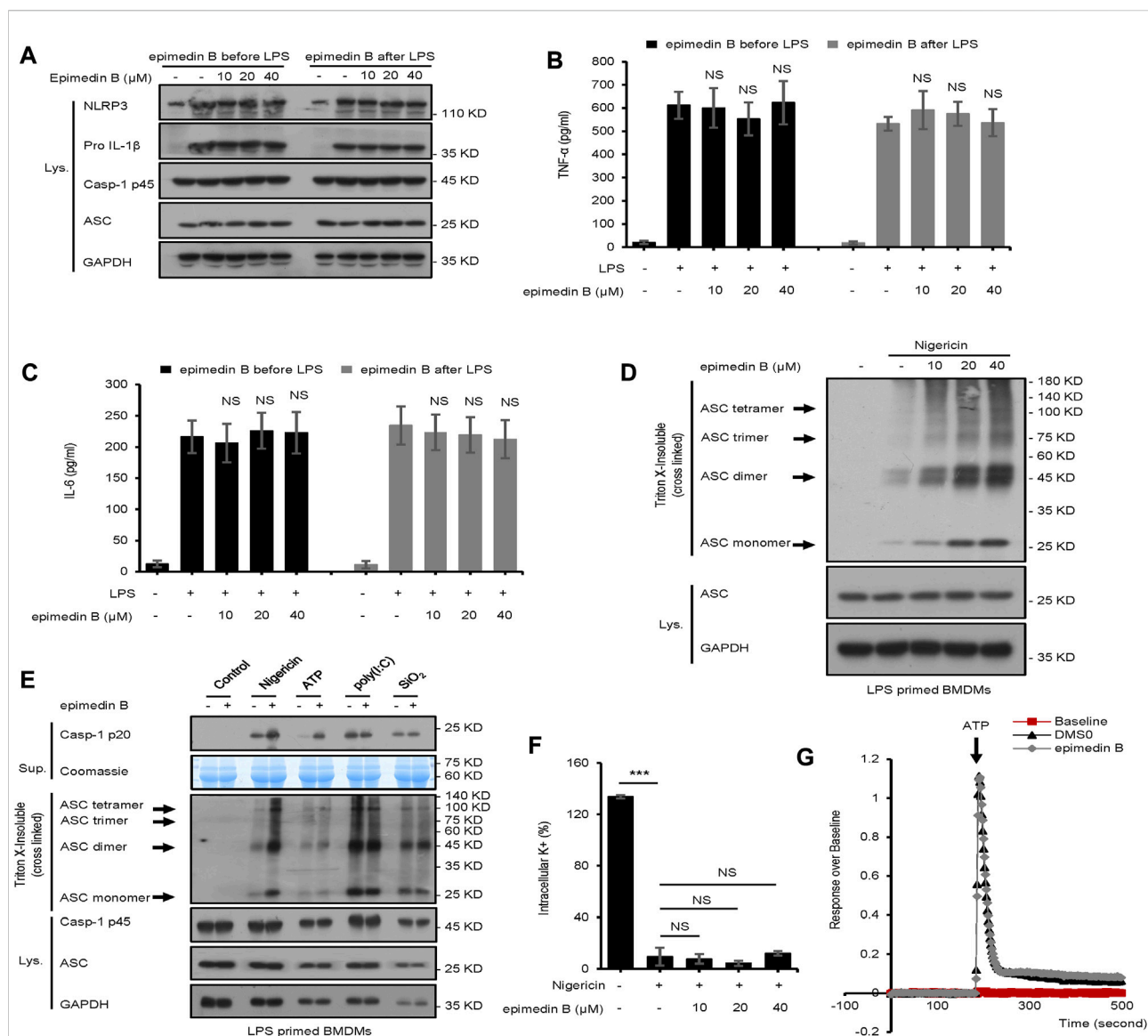


FIGURE 5

Epimedin B promotes ATP or nigericin-induced ASC oligomerization but does not block K⁺ efflux and Ca²⁺ flux. (A) Western blot analysis of whole-cell lysates from bone marrow-derived macrophages (BMDMs) subjected to treatment with epimedin B for 1 h, and stimulated with lipopolysaccharide (LPS) (50 ng/ml) for 3 h or BMDMs were stimulated with LPS (50 ng/ml) for 3 h and then subjected to treatment with epimedin B for 1 h (B,C) ELISA of TNF- α (B) and IL-6 (C) in Sup derived from samples described in (A) (D) Western blot analysis of ASC oligomerization from LPS-primed BMDMs subjected to treatment with various doses of epimedin B prior to nigericin stimulation. (E) Western blot analysis of ASC oligomerization from LPS-primed BMDMs subjected to treatment with epimedin B and stimulated with nigericin, ATP, SiO₂, and poly(I:C). (F) Quantification of potassium efflux in LPS-primed BMDMs subjected to treatment with various doses of epimedin B and stimulated with nigericin. (G) A trace of ATP-induced Ca²⁺ flux was measured using the FLIPRETETRA system in LPS-primed BMDMs subjected to treatment with epimedin B. Data are presented as the mean \pm SD from at least three biological samples. The significance of the differences was analyzed using unpaired Student's *t*-test: **p* < 0.05, ***p* < 0.01, ****p* < 0.001, NS: not significant.

exacerbated activation of ATP- or nigericin-induced NLRP3 inflammasome. We also investigated whether epimedin B affected K⁺ efflux during NLRP3 inflammasome activation. The results showed that

epimedin B exhibited no effect on K⁺ efflux triggered by nigericin (Figure 5F). Moreover, Ca²⁺ flux is an extremely important event in the upstream signaling of NLRP3 inflammasome activation. Epimedin B did not

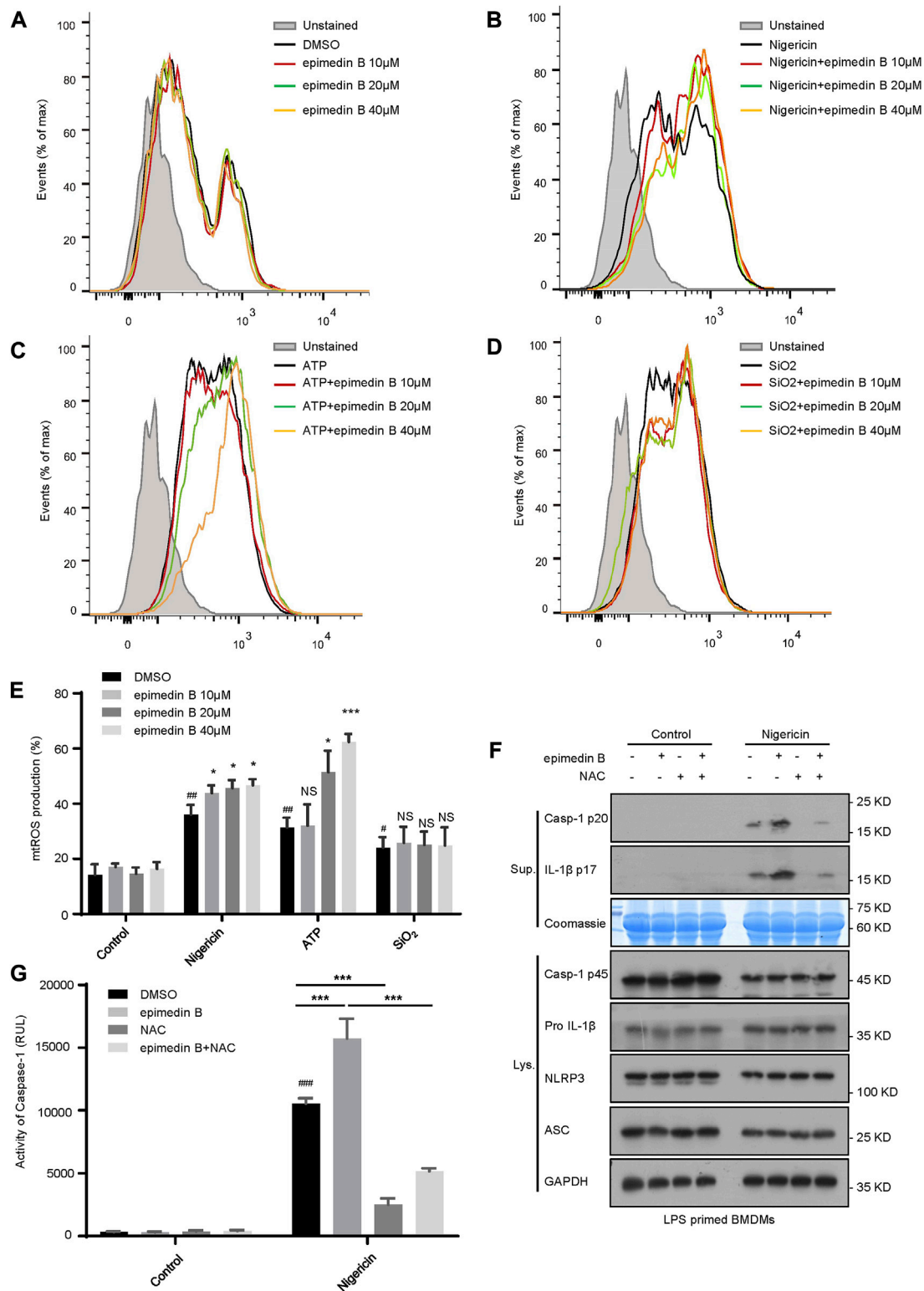


FIGURE 6 Epimedin B facilitates NLRP3 inflammasome activation by increasing mitochondrial reactive oxygen species (mtROS) production. **(A–D)** Percentage of ROS-positive cells in lipopolysaccharide (LPS)-primed bone marrow-derived macrophages (BMDMs) subjected to treatment with epimedin B that were either not stimulated **(A)** or stimulated with nigericin **(B)**, ATP **(C)** or SiO₂ **(D)**, followed by staining with MitoSox. After completion of the staining and washing procedures, flow cytometry was conducted to determine the level of mtROS production. **(E)** (Continued)

FIGURE 6 (Continued)

Percentage of reactive oxygen species (ROS)-positive cells in LPS-primed BMDMs subjected to treatment with epimedin B that were either not stimulated or stimulated with nigericin, ATP, or SiO₂. **(F)** Western blot analysis of supernatants and whole-cell lysates derived from LPS-primed BMDMs subjected to treatment with epimedin B, NAC, or epimedin B plus NAC prior to stimulation with nigericin or without stimulation. **(G)** Caspase-1 activity in samples described in **(F)**. Data are presented as the mean \pm SD derived from at least three biological samples. The significance of the differences was analyzed using unpaired Student's *t*-test: **p* < 0.05, ***p* < 0.01, ****p* < 0.001, **p* < 0.05, ***p* < 0.01, ****p* < 0.001, NS: not significant.

block ATP-induced Ca²⁺ flux (Figure 5G). Thus, Ca²⁺ flux may not be responsible for the enhanced effect of epimedin B on ATP-induced NLRP3 inflammasome activation.

Epimedin B facilitates NLRP3 inflammasome activation by increasing mitochondrial ROS production

Mitochondrial ROS play a crucial role in NLRP3 inflammasome activation (Zhao et al., 2019). In our study, we investigated whether epimedin B-mediated mitochondrial ROS was involved in NLRP3 inflammasome activation. Our data show that epimedin B successfully potentiated mitochondrial ROS production induced by nigericin and ATP but not by SiO₂ (Figures 6A–E). We focused on the ROS scavenger N-acetylcysteine (NAC), which is an inhibitor of mitochondrial ROS production. Mitochondrial ROS production was suppressed by NAC treatment. As expected, when stimulated with nigericin, NAC treatment reversed epimedin B-induced caspase-1 maturation or IL-1 β production (Figures 6F,G). Taken together, these results indicated that epimedin B increased mitochondrial ROS production to facilitate nigericin-induced NLRP3 inflammasome activation.

Epimedin B induces the development of IDILI by promoting NLRP3 inflammasome activation *in vivo*

We next examined whether epimedin B could induce the development of IDILI by promoting NLRP3 inflammasome activation *in vivo*. First, we investigated whether epimedin B, which can activate the NLRP3 inflammasome, could induce liver injury in an LPS-mediated susceptibility mouse model of IDILI. The results showed that treatment with epimedin B alone did not alter plasma levels of ALT and AST. As expected, in the LPS-mediated mouse model, epimedin B increased the levels of ALT and AST, and induced an increase in the production of IL-1 β and TNF- α compared to mice in the LPS group (Figures 7A–D). Similar results were observed for the mRNA expression of the pro-inflammatory genes IL-1 β and IL-18 (Figures 7E,F). Additionally, liver histology analysis showed that the combination of LPS and epimedin B treatment resulted in inflammatory cell infiltration or hepatocyte focal necrosis (Figure 7G). To further explore the effects of epimedin B on the immunological reaction in liver tissue, immunohistochemical (IHC)

analysis of liver samples was performed. IHC staining of liver sections revealed that epimedin B increased the infiltration of F4/80-positive macrophages in the liver (Figure 7H). Furthermore, our results demonstrated that epimedin B could result in liver injury as shown in the LPS-induced mouse model.

MCC950 is a potent selective NLRP3 inhibitor (Coll et al., 2015). To verify the relationship between the NLRP3 inflammasome and epimedin B-induced liver injury, mice treated with MCC950 were selected. Figures 8A–D shows that the combination of LPS and epimedin B resulted in an increase in the levels of ALT, AST, IL-1 β , and TNF- α . These results were not observed in mice co-treated with MCC950. Moreover, the mRNA expression of pro-inflammatory genes IL-1 β , IL-18, and TNF- α was increased in the LPS group as well as in the group subjected to treatment with LPS in combination with epimedin B, but not in the MCC950 cotreatment group (Figures 8E–G). As shown in Figure 7H, MCC950 treatment suppressed caspase-1 activation in liver tissues of mice that were co-treated with epimedin B and LPS. Histology analysis of liver tissue showed that epimedin B treatment resulted in hepatocyte focal necrosis or inflammation in the LPS-mediated mouse model (Figure 8I). Thus, these results confirmed that epimedin B could activate the NLRP3 inflammasome, leading to liver injury *in vivo*.

Discussion

IDILI represents a major global health issue. For instance, in North America, it has already surpassed viral hepatitis as a major factor of acute liver failure (Ostapowicz et al., 2002; Jee et al., 2021). However, in recent years, IDILI caused by TCM has been broadly recognized, especially in traditional non-toxic Chinese medicines. Thus, globally, there is a lack of understanding of possible IDILI mediated by TCM. Few traditional nontoxic Chinese medicines, such as EF, Psoraleae Fructus, and Polygoni Multiflori Radix have been reported to cause IDILI. Our previous studies have demonstrated that EF may induce hepatotoxicity in an LPS-mediated susceptibility mouse model of IDILI. Interestingly, in the present study, we demonstrated that epimedin B, which is one of the constituents of EF, specifically reinforced activation of the NLRP3 inflammasome to induce liver injury.

The NLRP3 inflammasome is one of the major contributors of inflammation and possesses the ability to sense both endogenous and exogenous danger signals through intracellular NLRs (Schroder and Tschopp, 2010; Elliott and Sutterwala, 2015). Several liver-related inflammatory diseases, especially chronic hepatitis C, nonalcoholic

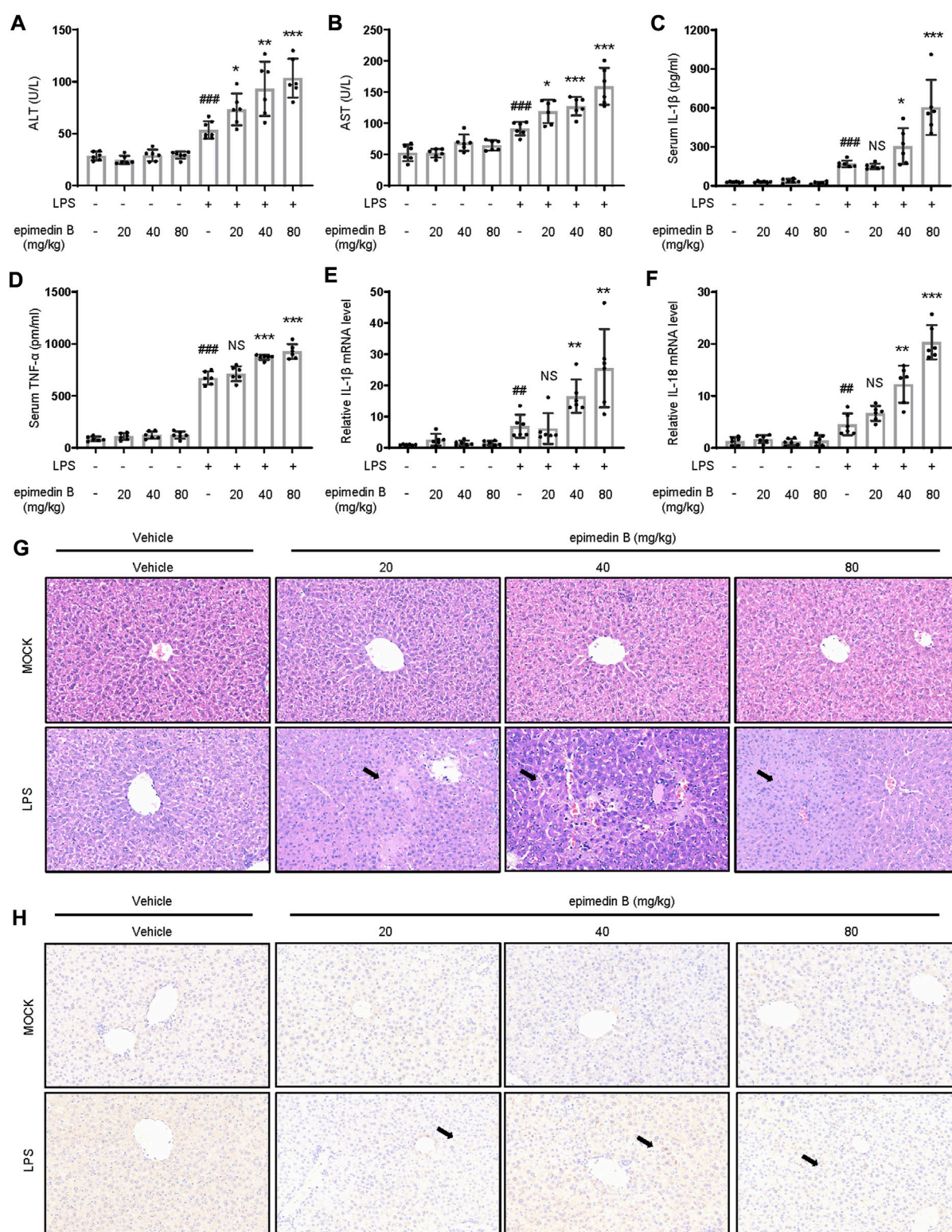


FIGURE 7

Epimedin B promotes early liver injury and inflammatory mediator production *in vivo*. (A–H) Female C57BL/6 mice (age: 6–8 weeks) subjected to starvation for 24 h were administered with 2 mg/kg of lipopolysaccharide (LPS) or its saline vehicle *via* the tail vein (*i.v.*). After an observation period of 2 h, various doses of epimedin B (20 mg/kg, 40 mg/kg, 80 mg/kg) or its vehicle were administered through intraperitoneal injection for 6 h (A,B) Serum levels of ALT (A) and AST (B) and (C,D) Serum levels of IL-1β (C) and TNF-α (D) determined by ELISA. (E,F) PCR of IL-1β (E) and IL-18 (F) mRNA levels. (G,H) Representative micrographs of H&E staining (G) and F4/80 staining (H). Data are presented as the mean ± SD. The significance of the differences was analyzed using unpaired Student's *t*-test: **p* < 0.05, ***p* < 0.01, ****p* < 0.001, **p* < 0.05, ***p* < 0.01, ****p* < 0.001, NS: not significant.

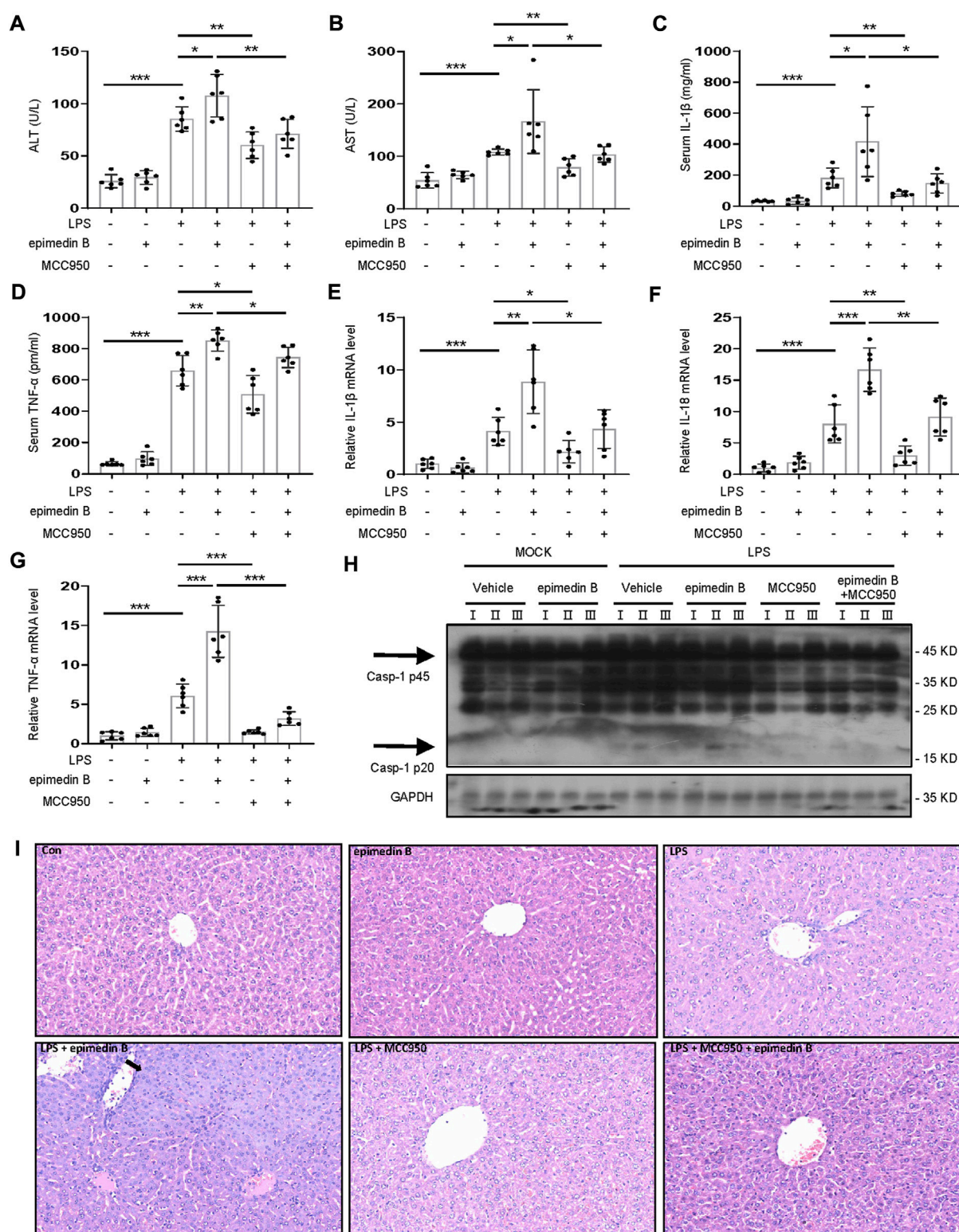


FIGURE 8

Epimedin B induces IDILI by promoting NLRP3 inflammasome activation *in vivo*. (A–I) Female C57BL/6 mice (age: 6–8 weeks) were administered MCC950 (40 mg/kg) or its saline vehicle through intraperitoneal injection. After 1 h, lipopolysaccharide (LPS) (2 mg/kg) or its saline vehicle was administered via the tail vein for 2 h. Subsequently, epimedin B (40 mg/kg) was administered via intraperitoneal injection for 6 h (A,B) Serum levels of ALT (A) and AST (B), and (C,D) Serum levels of IL-1 β (C) and TNF- α (D) determined by ELISA. (E–G) PCR of IL-1 β (E), IL-18 (F), and TNF- α (G) mRNA levels. (H) Western blot analysis of pro-caspase-1 and cleaved caspase-1 expression in liver tissue. (I) Representative micrographs of H&E staining. Data are presented as the mean \pm SD. The significance of the differences was analyzed using unpaired Student's *t*-test: **p* < 0.05, ***p* < 0.01, ****p* < 0.001, NS: not significant.

steatohepatitis, alcoholic liver disease, and IDILI have been reported to be associated with NLRP3 inflammasome activation (Csak et al., 2011; Burdette et al., 2012; Petrasek et al., 2012; Wree et al., 2014a; Wree et al., 2014b; Voican et al., 2015; Kato and Uetrecht, 2017). In the present study, we demonstrated that epimedin B facilitated nigericin- or ATP-induced NLRP3 inflammasome activation, thereby leading to the development of IDILI. Furthermore, epimedin B, *via* enhancement of NLRP3 inflammasome activation, contributes to EF-induced IDILI. In addition, the amount of glycogen contained in the main active constituents of EF is independent on NLRP3 inflammasome activity.

In the present study, epimedin B could only specifically reinforced activation of the NLRP3 inflammasome induced by nigericin or ATP. Additionally, epimedin B exerted no effect on the activation of AIM2 and NLRC4 inflammasomes. We showed that epimedin B specifically enhanced nigericin- or ATP-induced NLRP3 inflammasome activation. We also examined the effects of epimedin B on upstream and downstream signaling, and evaluated the mechanism underlying the enhancement of nigericin- or ATP-induced NLRP3 inflammasome activation by epimedin B treatment. ASC oligomerization is an important event in NLRP3 inflammasome activation. Epimedin B promoted ASC oligomerization triggered by nigericin and ATP. Therefore, we evaluated if epimedin B acted on the upstream signaling events of ASC oligomerization. K^+ efflux or Ca^{2+} flux are deemed upstream mechanisms associated with NLRP3 inflammasome activation. However, our results demonstrated that epimedin B did not alter K^+ efflux or Ca^{2+} flux. Moreover, mitochondrial damage and the release of mitochondrial ROS are key upstream events of NLRP3 inflammasome activation. The findings in this study showed that nigericin and ATP could induce the production of mitochondrial ROS. Notably, epimedin B specifically amplified the production of mitochondrial ROS triggered by nigericin and ATP, but not by SiO_2 , thus suggesting that epimedin B facilitated nigericin- or ATP-induced NLRP3 inflammasome activation dependent on mitochondrial ROS production. Next, we evaluated whether ROS played an important role in the enhanced effect of epimedin B on nigericin- or ATP-induced NLRP3 inflammasome activation. We concluded that the effect of epimedin B was dependent on mitochondrial ROS production for facilitating nigericin-induced NLRP3 inflammasome activation.

We previously reported that EF combined with non-hepatotoxic doses of LPS can induce liver injury. Therefore, we investigated whether epimedin B as an NLRP3 inflammasome activation promoter could cause liver injury. Our results indicated that epimedin B could induce liver injury *in vivo*. MCC950 was used to explore the relationship between epimedin B-induced liver injury

and the NLRP3 inflammasome. The combination of epimedin B and LPS-induced liver injury but not in mice that received MCC950 pretreatment. Together, these data clearly demonstrated that epimedin B induced IDILI by promoting NLRP3 inflammasome activation *in vivo*.

Conclusion

In conclusion, our study demonstrated that epimedin B induced NLRP3 inflammasome activation triggered by nigericin and ATP. Mitochondrial ROS are crucial contributors of the enhancement of the activation of the NLRP3 inflammasome stimulated by epimedin B. Treatment with a combination of nonhepatotoxic doses of LPS and epimedin B increased the production of ALT, AST, IL-1 β , and TNF- α , resulting in hepatocyte necrosis. These results were not observed in mice that were co-treated with LPS and MCC950. Our findings indicated that epimedin B is responsible for EF-induced IDILI, and the amount of glycogen contained in the main active constituents of EF is independent on NLRP3 inflammasome activity.

Data availability statement

The original contributions presented in the study are included in the article/[Supplementary Material](#), further inquiries can be directed to the corresponding authors.

Ethics statement

The animal study was reviewed and approved by the Animal Ethics Committee of the Fifth Medical Centre, Chinese People's Liberation Army General Hospital (animal ethics committee approval No. IACUC-2017-003).

Author contributions

ZB supervised the project. JW designed the experiments. YG and WS performed a considerable portion of the experiments. CT performed mechanistic studies and analyzed the data. GZ analyzed the data derived from mice experiments. XX and PL revised the manuscript. All authors read and approved the final manuscript.

Funding

This work was supported by the National Natural Science Foundation of China (82004057, 81874368, 82104522) and the Beijing Nova Program (Z181100006218001).

Conflict of interest

The authors declare that the research was conducted in the absence of any commercial or financial relationships that could be construed as a potential conflict of interest.

Publisher's note

All claims expressed in this article are solely those of the authors and do not necessarily represent those of their affiliated

organizations, or those of the publisher, the editors and the reviewers. Any product that may be evaluated in this article, or claim that may be made by its manufacturer, is not guaranteed or endorsed by the publisher.

Supplementary material

The Supplementary Material for this article can be found online at: <https://www.frontiersin.org/articles/10.3389/fphar.2022.1015846/full#supplementary-material>

References

- Benesic, A., Rotter, I., Dragoi, D., Weber, S., Leitl, A., Buchholtz, M. L., et al. (2018). Development and validation of a test to identify drugs that cause idiosyncratic drug-induced liver injury. *Clin. Gastroenterol. Hepatol.* 16 (9), 1488–1494. e1485. doi:10.1016/j.cgh.2018.04.049
- Bernal, W., and Wendon, J. (2013). Acute liver failure. *N. Engl. J. Med.* 369 (26), 2525–2534. doi:10.1056/NEJMra1208937
- Burdette, D., Haskett, A., Presser, L., McRae, S., Iqbal, J., and Waris, G. (2012). Hepatitis C virus activates interleukin-1 β via caspase-1-inflammasome complex. *J. Gen. Virol.* 93 (2), 235–246. doi:10.1099/vir.0.034033-0
- Coll, R. C., Hill, J. R., Day, C. J., Zamoshnikova, A., Boucher, D., Massey, N. L., et al. (2019). MCC950 directly targets the NLRP3 ATP-hydrolysis motif for inflammasome inhibition. *Nat. Chem. Biol.* 15 (6), 556–559. doi:10.1038/s41589-019-0277-7
- Coll, R. C., Robertson, A. A., Chae, J. J., Higgins, S. C., Muñoz-Planillo, R., Inserra, M. C., et al. (2015). A small-molecule inhibitor of the NLRP3 inflammasome for the treatment of inflammatory diseases. *Nat. Med.* 21 (3), 248–255. doi:10.1038/nm.3806
- Csak, T., Ganz, M., Pespisa, J., Kodys, K., Dolganiuc, A., and Szabo, G. (2011). Fatty acid and endotoxin activate inflammasomes in mouse hepatocytes that release danger signals to stimulate immune cells. *Hepatology* 54 (1), 133–144. doi:10.1002/hep.24341
- Elliott, E. I., and Sutterwala, F. S. (2015). Initiation and perpetuation of NLRP3 inflammasome activation and assembly. *Immunol. Rev.* 265 (1), 35–52. doi:10.1111/imr.12286
- Fontana, R. J. (2014). Pathogenesis of idiosyncratic drug-induced liver injury and clinical perspectives. *Gastroenterology* 146 (4), 914–928. doi:10.1053/j.gastro.2013.12.032
- Gao, Y., Wang, Z., Tang, J., Liu, X., Shi, W., Qin, N., et al. (2020). New incompatible pair of TCM: Epimedium Folium combined with Psoraleae Fructus induces idiosyncratic hepatotoxicity under immunological stress conditions. *Front. Med.* 14 (1), 68–80. doi:10.1007/s11684-019-0690-z
- Gao, Y., Xu, G., Ma, L., Shi, W., Wang, Z., Zhan, X., et al. (2021). Icariside I specifically facilitates ATP or nigericin-induced NLRP3 inflammasome activation and causes idiosyncratic hepatotoxicity. *Cell Commun. Signal.* 19 (1), 13. doi:10.1186/s12964-020-00647-1
- Hoofnagle, J. H., and Björnsson, E. S. (2019). Drug-induced liver injury - types and phenotypes. *N. Engl. J. Med.* 381 (3), 264–273. doi:10.1056/NEJMra1816149
- Jee, A., Sernoskie, S. C., and Uetrecht, J. (2021). Idiosyncratic drug-induced liver injury: Mechanistic and clinical challenges. *Int. J. Mol. Sci.* 22 (6), 2954. doi:10.3390/ijms22062954
- Kato, R., and Uetrecht, J. (2017). Supernatant from hepatocyte cultures with drugs that cause idiosyncratic liver injury activates macrophage inflammasomes. *Chem. Res. Toxicol.* 30 (6), 1327–1332. doi:10.1021/acs.chemrestox.7b00065
- Lin, L., Ni, B., Lin, H., Zhang, M., Li, X., Yin, X., et al. (2015). Traditional usages, botany, phytochemistry, pharmacology and toxicology of polygonum multiflorum thunb.: A review. *J. Ethnopharmacol.* 159, 158–183. doi:10.1016/j.jep.2014.11.009
- Ostapowicz, G., Fontana, R. J., Schiodt, F. V., Larson, A., Davern, T. J., Han, S. H., et al. (2002). Results of a prospective study of acute liver failure at 17 tertiary care centers in the United States. *Ann. Intern. Med.* 137 (12), 947–954. doi:10.7326/0003-4819-137-12-200212170-00007
- Petrasek, J., Bala, S., Czak, T., Lippai, D., Kodys, K., Menashy, V., et al. (2012). IL-1 receptor antagonist ameliorates inflammasome-dependent alcoholic steatohepatitis in mice. *J. Clin. Invest.* 122 (10), 3476–3489. doi:10.1172/jci60777
- Schroder, K., and Tschopp, J. (2010). The inflammasomes. *Cell* 140 (6), 821–832. doi:10.1016/j.cell.2010.01.040
- Shen, T., Liu, Y., Shang, J., Xie, Q., Li, J., Yan, M., et al. (2019). Incidence and etiology of drug-induced liver injury in mainland China. *Gastroenterology* 156 (8), 22302230–22302241. doi:10.1053/j.gastro.2019.02.002
- Szabo, G., and Czak, T. (2012). Inflammasomes in liver diseases. *J. Hepatol.* 57 (3), 642–654. doi:10.1016/j.jhep.2012.03.035
- Tu, C., He, Q., Li, C. Y., Niu, M., Han, Z. X., Ge, F. L., et al. (2019). Susceptibility-related factor and biomarkers of dietary supplement polygonum multiflorum-induced liver injury in rats. *Front. Pharmacol.* 10, 335. doi:10.3389/fphar.2019.00335
- Uetrecht, J. (2019a). Mechanisms of idiosyncratic drug-induced liver injury. *Adv. Pharmacol.* 85, 133–163. doi:10.1016/bs.apha.2018.12.001
- Uetrecht, J. (2019b). Mechanistic studies of idiosyncratic DILI: Clinical implications. *Front. Pharmacol.* 10, 837. doi:10.3389/fphar.2019.00837
- Voican, C. S., Njiké-Nakseu, M., Boujedidi, H., Barri-Ova, N., Bouchet-Delbos, L., Agostini, H., et al. (2015). Alcohol withdrawal alleviates adipose tissue inflammation in patients with alcoholic liver disease. *Liver Int.* 35 (3), 967–978. doi:10.1111/liv.12575
- Wang, L., Li, Z., Li, L., Li, Y., Yu, M., Zhou, Y., et al. (2014). Acute and sub-chronic oral toxicity profiles of the aqueous extract of Cortex Dictamnii in mice and rats. *J. Ethnopharmacol.* 158, 207–215. doi:10.1016/j.jep.2014.10.027
- Wang, Z., Xu, G., Wang, H., Zhan, X., Gao, Y., Chen, N., et al. (2020). Icariside II, a main compound in Epimedium Folium, induces idiosyncratic hepatotoxicity by enhancing NLRP3 inflammasome activation. *Acta Pharm. Sin. B* 10 (9), 1619–1633. doi:10.1016/j.apsb.2020.03.006
- Wen, H., Ting, J. P., and O'Neill, L. A. (2012). A role for the NLRP3 inflammasome in metabolic diseases—did Warburg miss inflammation? *Nat. Immunol.* 13 (4), 352–357. doi:10.1038/ni.2228
- Wree, A., Eguchi, A., McGeough, M. D., Pena, C. A., Johnson, C. D., Canbay, A., et al. (2014a). NLRP3 inflammasome activation results in hepatocyte pyroptosis, liver inflammation, and fibrosis in mice. *Hepatology* 59 (3), 898–910. doi:10.1002/hep.26592
- Wree, A., McGeough, M. D., Pena, C. A., Schlattjan, M., Li, H., Inzaugarat, M. E., et al. (2014b). NLRP3 inflammasome activation is required for fibrosis development in NAFLD. *J. Mol. Med.* 92 (10), 1069–1082. doi:10.1007/s00109-014-1170-1
- Wu, X., Dong, L., Lin, X., and Li, J. (2017). Relevance of the NLRP3 inflammasome in the pathogenesis of chronic liver disease. *Front. Immunol.* 8, 1728. doi:10.3389/fimmu.2017.01728
- Zhang, L., Wang, T., Zhao, B. S., Zhang, J. X., Yang, S., Fan, C. L., et al. (2019). Effect of 2''-O-rhamnosyl Icariside II, baohuoside I and baohuoside II in herba Epimedium on cytotoxicity indices in HL-7702 and HepG2 cells. *Molecules* 24 (7), E1263. doi:10.3390/molecules24071263
- Zhao, Y., Wang, Z., Feng, D., Zhao, H., Lin, M., Hu, Y., et al. (2019). p66Shc contributes to liver fibrosis through the regulation of mitochondrial reactive oxygen species. *Theranostics* 9 (5), 1510–1522. doi:10.7150/thno.29620
- Zhong, R., Chen, Y., Ling, J., Xia, Z., Zhan, Y., Sun, E., et al. (2019). The toxicity and metabolism properties of herba Epimedium flavonoids on larval and adult zebrafish. *Evid. Based. Complement. Altern. Med.* 2019, 3745051. doi:10.1155/2019/3745051



OPEN ACCESS

EDITED BY

Massimo Lucarini,
Council for Agricultural
Research and Economics, Italy

REVIEWED BY

Tao Yi,
Hong Kong Baptist University,
Hong Kong SAR, China
Ke Ma,
Shandong University of Traditional
Chinese Medicine, China
Junping Wei,
China Academy of Chinese
Medical Sciences, China

*CORRESPONDENCE

Xiyu Zhang,
zhangxiyutcm@yahoo.com

[†]These authors have contributed equally
to this work and share first authorship

SPECIALTY SECTION

This article was submitted to
Ethnopharmacology,
a section of the journal
Frontiers in Pharmacology

RECEIVED 08 June 2022

ACCEPTED 09 November 2022

PUBLISHED 14 December 2022

CITATION

Kang J, Liu Y, Peng S, Tang X, Liu L, Xie Z,
He Y and Zhang X (2022), Efficacy and
safety of traditional Chinese medicine
external washing in the treatment of
postoperative wound of diabetes
complicated with anal fistula: Study
protocol of a randomized, double-blind,
placebo-controlled, multi-center
clinical trial.
Front. Pharmacol. 13:938270.
doi: 10.3389/fphar.2022.938270

COPYRIGHT

© 2022 Kang, Liu, Peng, Tang, Liu, Xie,
He and Zhang. This is an open-access
article distributed under the terms of the
[Creative Commons Attribution License](https://creativecommons.org/licenses/by/4.0/)
(CC BY). The use, distribution or
reproduction in other forums is
permitted, provided the original
author(s) and the copyright owner(s) are
credited and that the original
publication in this journal is cited, in
accordance with accepted academic
practice. No use, distribution or
reproduction is permitted which does
not comply with these terms.

Efficacy and safety of traditional Chinese medicine external washing in the treatment of postoperative wound of diabetes complicated with anal fistula: Study protocol of a randomized, double-blind, placebo-controlled, multi-center clinical trial

Jian Kang^{1†}, Ya Liu^{2†}, Sihan Peng², Xiao Tang³, Lu Liu³, Ziyang Xie³,
Yuchi He³ and Xiyu Zhang^{2*}

¹Department of Anorectal, Hospital of Chengdu University of Traditional Chinese Medicine, Chengdu, China, ²Hospital of Chengdu University of Traditional Chinese Medicine, TCM Regulating Metabolic Diseases Key Laboratory of Sichuan Province, Chengdu, China, ³School of Clinical Medicine, Chengdu University of Traditional Chinese Medicine, Chengdu, China

Introduction: Anal fistula is one of the commonest ailments seen by anorectal surgeons as surgery is currently the preferred treatment for it. Diabetes mellitus is a risk factor that can lead to slow wound healing after anal fistula surgery. Because of the large postoperative wound surface of anal fistula, patients with diabetes can have an increased probability of wound infection, which makes it hard to heal. There is an extensive clinical experience for wound healing in traditional Chinese medicine (TCM). The Jiedu Shengji decoction (JSD) is a widely used external washing decoction in clinical practice. However, the current evidence on it is still insufficient. Therefore, we report this carefully designed clinical trial to assess the efficacy and safety of JSD in the treatment of postoperative wounds in diabetic patients with anal fistula.

Methods and analysis: This study was designed to be a randomized, double-blind, placebo-controlled, multi-center clinical trial. There were 60 eligible participants who were randomized at a 1:1 ratio to the intervention and placebo groups. Both groups received the same standard treatment. The intervention group was given external washing decoction of TCM (JSD), while the placebo group was given the placebo made of excipients and flavoring agents. The main

Abbreviations: AE, adverse event; HDL, high-density lipoprotein; JSD, Jiedu Shengji decoction; LDL, low-density lipoprotein; REC, Research Ethics Committee; SAE, serious adverse event; SF-36, Short-Form Health Survey 36; SPIRIT, Standard Protocol Items: Recommendations for Interventional Trials; TC, total cholesterol; TCM, traditional Chinese medicine; TG, total glyceride.

outcome measures include wound healing, distribution of wound pathogens, levels of inflammatory mediators, and blood glucose. The secondary outcome measures included lipids, the quality of the life evaluation scale (Short-Form Health Survey 36). Assessments were performed before the start of the study, at 1st, 2nd, 3rd, and 4th weeks after the intervention, and at 8th, 12th, and 16th follow-up weeks.

Discussion: The clinical study we proposed will be the first randomized, double-blind, placebo-controlled, multi-center clinical trial study to assess the efficacy and safety of TCM external washing (JSD) in the treatment of postoperative wounds in diabetic patients with anal fistula.

Ethics and dissemination: The Medical Ethics Committee of Hospital of Chengdu University of Traditional Chinese Medicine has reviewed this study protocol and gave its approval and consent on 17 March, 2022 (Ethical Review Number: 2022KL-018).

KEYWORDS

postoperative diabetes with anal fistula, traditional Chinese medicine, external washing, randomized controlled trial, Jiedu Shengji decoction

1 Introduction

Anal fistula is one of the commonest ailments seen by anorectal surgeons. The prevalence of fistula-in-ano is 12.3 cases per 100,000 population in men and 5.6 cases per 100,000 population in women (Mei et al., 2019). Patients with anal fistula usually present with a recurrent abscess or a draining fistula with various severities of symptoms and require surgical interventions (Pigot, 2015; Lu et al., 2019). At present, the preferred treatment on anal fistula is surgery, which is a way to completely cure it, with an unequivocal efficacy and low recurrence rate (Shi et al., 2021). However, the large postoperative wound surface, which can lead to a high probability of wound infection and long healing time, is the reason which causes physical and psychological fear in patients (Kochhar et al., 2014; Farag et al., 2019).

According to the 10th edition of the International Diabetes Federation Diabetes Atlas, it is estimated that the global diabetes prevalence is 10.5% (536.6 million people) in population aged from 20 to 79 in 2021, and this number will rise to 12.2% (783.2 million) in 2045 (Sun et al., 2022). Perianorectal abscess can easily happen on patients with diabetes due to their reduced skin resistance, which might develop into anal fistula. In addition, the high blood glucose level of diabetic patients can provide a favorable nutritional environment for bacteria to grow, which can easily cause postoperative wound infection or even necrosis to slow down wound healing. Studies have shown that diabetes is a risk factor leading to slow wound healing after anal fistula surgery (Wang et al., 2014; Mei et al., 2019; Wang et al., 2021).

Traditional Chinese medicine can exert great clinical effects on wound healing (Mosavat et al., 2015; Yan et al., 2020). In particular, TCM external washing has a long history, extensive experience, and positive efficacy in promoting wound healing

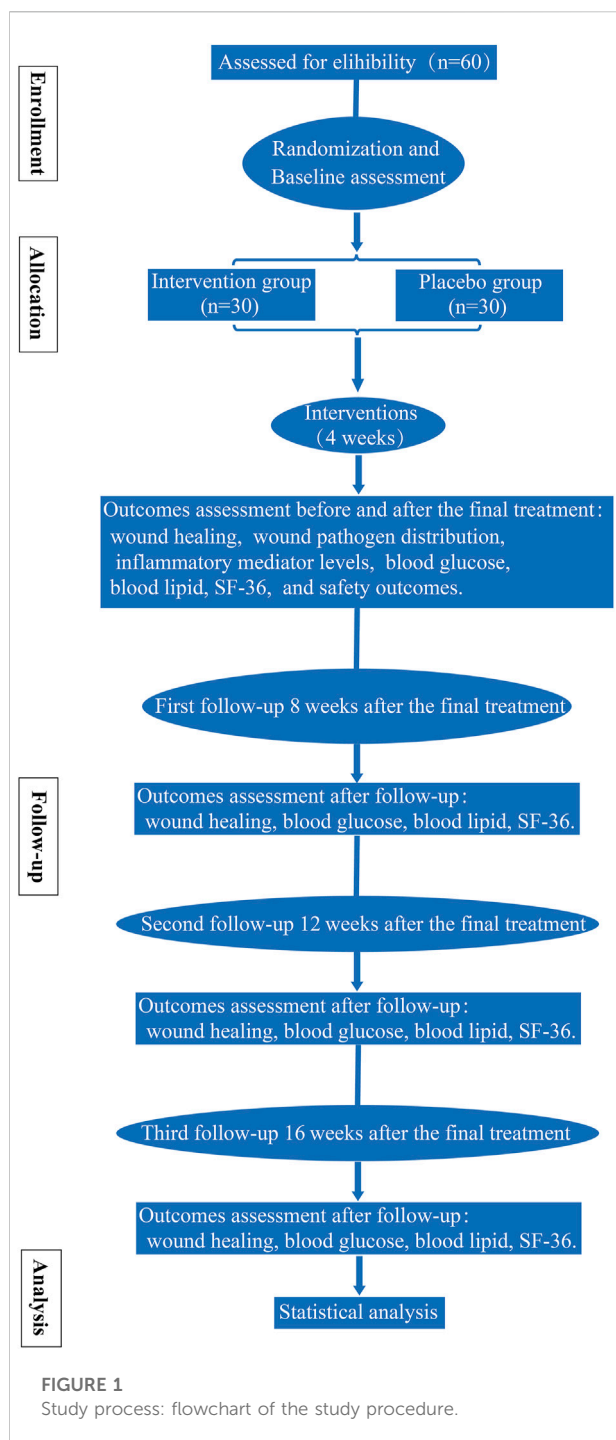
after anal fistula surgery and has been commonly used for postoperative treatment in China. In traditional Chinese medicine, it is believed that dampness, heat, and static blood are the pathological characteristics of postoperative wounds in diabetic patients with anal fistula.

The Jiedu Shengji decoction (JSD) is a widely used external washing decoction in clinical practice, which has the functions of removing toxins for detumescence, discharging pus, and promoting granulation. The main botanical herbs in JSD are Zi Cao (*Arnebia euchroma* (Royle) Johnston.), Dang Gui (*Angelica sinensis* (Oliv.) Diels.), Ru Xiang (*Boswellia carterii* Birdw.), Mo Yao (*Commiphora myrrha* (T.Nees) Engl.), Xue Jie (*Daemonorops draco* (Willd.) Blume), Bing Pian (*Cinnamomum camphora* (L.) J.Presl), Bai Zhi (*Angelica dahurica* (Hoffm.) Benth. Et Hook. f. ex Franch. et Sav), and Er Cha (*Acacia catechu* (L. F.) Willd). Preliminary studies have found that JSD can significantly reduce wound edema after anal fistula surgery, reduce nerve sensitivity, ease the pain in patients, and promote wound healing. However, this study was limited by its single-center and non-double-blind design. Therefore, a multi-center, double-blind, randomized, controlled clinical trial is needed to further determine the efficacy and safety of JSD in the treatment of postoperative wounds in diabetic patients with anal fistula. We proposed that patients treated with JSD will have more positive clinical outcomes than those with placebos.

2 Methods/design

2.1 Trial design

This study incorporates a randomized, double-blind, placebo-controlled, multi-center clinical trial and was



developed according to the Standard Protocol Items: Recommendations for Interventional Trials (SPIRIT) statement (the SPIRIT checklist is shown in [Supplementary Material S1](#)). Every eligible participant was assigned either to the intervention group or the placebo group randomly. All patients received standard treatment. The detailed workflow is shown in [Figure 1](#). The trial is supported by the science and

technology planning project of Sichuan Province [grant no. 2021YFS0275]. The funders have no vote in the study design, data collection and analysis, manuscript preparation, or decision to publish.

2.2 Study population

Patients were recruited from three hospitals: the Affiliated Hospital of Chengdu University of Traditional Chinese Medicine, Yanjiang District Hospital of Traditional Chinese Medicine in Ziyang City, and Chengdu Anorectal Specialized Hospital.

2.3 Recruitment of participants

Three members (ZX, YL, and YHP) were involved in recruiting participants, and the other two members (SP and LL) were responsible for assigning participants to groups. Patients who met the study criteria and volunteered to participate in the study were asked to sign a written informed consent form ([Supplementary Material S2](#)) with a clear understanding of the purpose, procedures, and all potential risks associated with the study. Participants' personal information was kept confidential, and only authorized researchers will have access to them. All paper forms pertaining to this study were kept in a locked and secure office. Participants may obtain dataset from respective authors upon reasonable request.

2.4 Patient and public involvement

Patients or the public were not involved in the design, conduct, reporting, or dissemination plans of our research.

2.5 Inclusion criteria

1. Confirmed diabetes mellitus ([Alberti and Zimmet, 1998](#)) with postoperative anal fistula.

The diagnostic criteria for anal fistula refer to the guidelines for Clinical Diagnosis and Treatment of Anal Fistula (2006 Edition) jointly formulated by the Colorectal and Anal Surgery Group of Chinese Society of Surgery, Anorectal Branch of Chinese Society of Traditional Chinese Medicine, and Specialized Committee of Colorectal and Anal Diseases, Chinese Association of Modern Medicine.

2. Aged 18 to 75.
3. $4\text{cm}^2 \leq \text{postoperative wound area} < 30\text{cm}^2$.

4. TCM syndrome differentiation is dampness–heat blood stasis syndrome, referring to the People's Republic of China Industry Standard for Traditional Chinese Medicine Diagnosis and Efficacy Criteria for Anal Leakage Syndrome.
5. No previous surgery for anorectal disease and no abnormal anal morphology or function.
6. Voluntary participation and signed informed consent.

2.6 Exclusion criteria

1. Patients with severe diseases in important organs, including abnormal liver function, renal failure, heart failure, stroke, and malignant tumors.
2. Participated in other clinical trials within 3 months before enrollment.
3. Allergic to known drugs or experimental drugs.
4. Pregnant and lactating women.
5. Obvious mental disorders.

2.7 Handling of withdrawal and data management

Participants can withdraw from the study at any time. If any participant stops using study medication or takes other medications that may affect the results during the study, the participant will not be a part of the study anymore. Participants failed to follow up and ones withdrawn from the study were recorded and reported. Incomplete data will be cleaned up if less than 5–10% of participants withdraw from the study. Missing data will be processed through data imputation, intention to treat analysis, and sensitivity analysis if greater than 10% participants withdraw from the study.

2.8 Interventions

All participants went through an interview to know more information about this study. After obtaining informed consent and completing baseline assessments, eligible participants were randomized to the intervention and placebo groups. Participants were not allowed to take any other Chinese herbal decoction or Chinese patent medicine during the study.

Both groups received standard treatments, including health knowledge education regarding diabetes and anal fistula, formulations of recipes, and taking hypoglycemic, antihypertensive, hypolipidemic, and anti-infective drugs. A personalized treatment plan was formulated after consultation with an endocrinologist, and the plan was evaluated and adjusted throughout the process. The wound surface was routinely cleaned with povidone-iodine after daily defecation. The intervention group was given TCM external washing

decoction, JSD (Figure 2), and the information of its constituent botanical drugs is shown in Table 1. The JSD decoction was prepared by the Department of Pharmacy, Hospital of Chengdu University of Traditional Chinese Medicine. The specific steps are as follows: (1) Bai Zhi, Zi Cao, and Dang Gui are added to 500 ml of water and soaked for 30 min, and the mixture of water and herbs is transferred to the decoction machine, boiled at high heat to 100°C under standard atmospheric pressure (the boiling time to 100°C should not be more than 5 min), turned to low heat and maintained the temperature constant at 85°C–95°C, then continued to decoct for 30 min, obtained 200 ml of the botanical drug liquid was filtered, and set aside. (2) A measure of 500 ml of water is added again, boiled to 100°C on high heat (boiling time to 100°C should not be more than 5min), turned down the heat and maintained the temperature constant at 85°C–95°C, and decocted for 45 min. (3) The liquid from the previous two steps are mixed to obtain a total of 400 ml of the liquid (liquid 1). (4) Grind Ru Xiang, Mo Yao, and Er Cha, in advance, are filtered through a 2-mm sieve, 400 ml of water is added, boiled in high heat to 100°C (boiling time to 100°C should not be longer than 5 min), turned down the heat and maintained the temperature constant at 85°C–95°C, added pre-ground Xue Jie and Bing Pian (filtered through 2 mm sieve) at the 14th min, continued to boil for 2 min to get 200 ml of the liquid (liquid 2). (5) Liquid 1 and liquid 2 are mixed thoroughly to get 600 ml of liquid. (6) After waiting for its temperature to 35°C–40°C, 200-ml herbal medicine bags are plasticized. The decoction was produced in the same batch as far as possible and quality-checked by the manufacturer. To ensure that the decoction is not contaminated, the decoction vessels and filtration and dispensing equipment were completely cleaned in advance to make sure there were no residuals.

The placebo group was given placebos made of excipients and flavoring agents. Placebo formula: pyrosyrup (edible), apple green (edible), and lactose (medicinal). Placebos were packaged, shaped, and colored to be the same as JSD. Placebos were produced by the Placebo Experimental Center of School of Pharmacy, Chengdu University of Traditional Chinese Medicine, which had no efficacy or side effects. The external washing decoction was placed in a special vessel and air-dried to lukewarm for patients to take sitz bath for 30 min/time. Then, the bases of incisions were packed outward along with a gauze in moderate tightness. The incisions were covered with sterile gauze and fixed with adhesive plaster. The wound dressing was changed once a day for 4 weeks. We followed up the participants at the 8th, 12th, and 16th weeks after the dressing change was finished to record and analyze the recurrence.

2.9 Randomization and allocation concealment

Randomization was performed by an independent statistician (CZQ). Random sequences were generated by BMI



FIGURE 2
Jiedu Shengji decoction (JSD).

SPSS Statistics 24.0 software. Given the number of seeds, 60 participants were randomly assigned to the intervention and placebo groups. The random distribution table was determined in triplicate, with one copy for the project leader (KJ), one for the pharmacist (TX), and another one for the statistician (CZQ).

2.10 Blinding

This study is designed to be a double-blind trial. During the experiment, neither participants nor researchers had group information. The medication number, label, and packaging for each participant were prepared from 001 to 030. Random numbers were sealed in double opaque envelopes, which were kept by CYQ, who was responsible for the blind method management. Every participant received their corresponding emergency letters, which were kept until the end of the trial.

2.11 Outcome measures

Assessments were performed at the baseline (T0), 4 weeks after the final treatment (T1, primary endpoint), 8 weeks after the final treatment (T2, secondary endpoint, first follow-up 8 weeks after the final treatment), 12 weeks after the final treatment (T3, tertiary endpoint, second follow-up 12 weeks after the final treatment), and 16 weeks after the final treatment (T4, final endpoint, third follow-up 16 weeks after the final treatment). The timeframe of data collection and assessments is shown in Figure 3 (the SPIRIT figure).

2.12 Primary outcomes

2.12.1 Wound healing

Assessments were at T0, T1, T2, T3, and T4. At the same time, weekly assessments were conducted during weeks 1–4 of intervention.

- 1) Wound healing rate: The wound area on the first postoperative day was the original area. The maximum length and width of the wound were measured with the calculated area. Formula: Wound healing rate = (original area-current area)/original area \times 100%.
- 2) Wound healing time: From the start of the dressing change to the complete epithelialization and healing of the wound.
- 3) Wound secretion score (Table 2) (Gould et al., 2021): Wound with abundant secretion, two or more pieces of penetrated gauze, dressing change more than twice a day, 3 points; wound with much secretion, one piece of penetrated gauze, dressing change twice a day, 2 points; wound with little secretion, no penetrated gauze, 1 point; and wound with smooth surface and no obvious secretion, 0 point.
- 4) Wound edema score (Table 2) (Gould et al., 2021): Wound with severe edema which is significantly more than the wound edge, surgical resection needed, 3 points; wound with obvious edema which is more than the wound edge, need dressing change to remit, 2 points; wound with mild edema, 1 point; and wound with no edema, 0 point.
- 5) Granulation tissue color score (Table 2) (Gould et al., 2021): Bright red, 1 point; light red, 2 points; and purple, 3 points.
- 6) Anal function evaluation: The Wexner incontinence score was used to evaluate the anal function of participants after wound healing (Zhang et al., 2020a), including the ability of

TABLE 1 Components of JSD.

Name of the drug	Use part	Manufacturer	Dose (g)	Method of use	Dosage form, dosage, frequency, and duration of treatment	Registration or not (Y/N)	Quality control report? (Y/N)	Storage condition
Zi Cao [<i>Arnebia euchroma</i> (Royle) Johnston.]	Whole plants	Sichuan Chinese Herb Preparation Co., Ltd., Sichuan, China	15	Washing and sitz bath for 30 min	Liquid, 200 ml, once a day, last 4 weeks	Y-registered in relevant administration	Y-prepared according to the manufacturer	The drugs are sealed and stored in a Chinese medicine warehouse at 0–30°C and 45–75% humidity
Dang Gui [<i>Angelica sinensis</i> (Oliv.) Diels.]	Roots	Sichuan Chinese Herb Preparation Co., Ltd., Sichuan, China	20	Washing and sitz bath for 30 min	Liquid, 200ml, once a day, last 4 weeks	Y-registered in relevant administration	Y-prepared according to the manufacturer	The drugs are sealed and stored in a Chinese medicine warehouse at 0–30°C and 45–75% humidity
Ru Xiang [<i>Boswellia carterii</i> birdw.]	Resin	Sichuan Chinese Herb Preparation Co., Ltd., Sichuan, China	15	Washing and sitz bath for 30 min	Liquid, 200ml, once a day, last 4 weeks	Y-registered in relevant administration	Y-prepared according to the manufacturer	The drugs are sealed and stored in a Chinese medicine warehouse at 0–30°C and 45–75% humidity
Mo Yao [<i>Commiphora myrrha</i> (T.Nees) Engl.]	Resin	Sichuan Chinese Herb Preparation Co., Ltd., Sichuan, China	15	Washing and sitz bath for 30 min	Liquid, 200 ml, once a day, last 4 weeks	Y-registered in relevant administration	Y-prepared according to the manufacturer	The drugs are sealed and stored in a Chinese medicine warehouse at 0–30°C and 45–75% humidity
Xue Jie [<i>Daemonorops draco</i> (Willd.) Blume]	Resin	Sichuan Chinese Herb Preparation Co., Ltd., Sichuan, China	15	Washing and sitz bath for 30 min	Liquid, 200ml, once a day, last 4 weeks	Y-registered in relevant administration	Y-prepared according to the manufacturer	The drugs are sealed and stored in a Chinese medicine warehouse at 0–30°C and 45–75% humidity
Bing Pian [<i>Cinnamomum camphora</i> (L.) J.Presl]	Extract	Sichuan Chinese Herb Preparation Co., Ltd., Sichuan, China	5	Washing and sitz bath for 30 min	Liquid, 200 ml, once a day, last 4 weeks	Y-registered in relevant administration	Y-prepared according to the manufacturer	The drugs are sealed and stored in a Chinese medicine warehouse at 0–30°C and 45–75% humidity
Bai Zhi [<i>Angelica dahurica</i> (Hoffm.) Benth. Et] Hook. f. ex Franch. et Sav]	Roots	Sichuan Chinese Herb Preparation Co., Ltd., Sichuan, China	20	Washing and sitz bath for 30 min	Liquid, 200ml, once a day, last 4 weeks	Y-registered in relevant administration	Y-prepared according to the manufacturer	The drugs are sealed and stored in a Chinese medicine warehouse at 0–30°C and 45–75% humidity
Ercha [<i>Acacia catechu</i> (L. F.) Willd]	Dry extract of skin, branch, and stem	Sichuan Chinese Herb Preparation Co., Ltd., Sichuan, China	20	Washing and sitz bath for 30 min	Liquid, 200ml, once a day, last 4 weeks	Y-registered in relevant administration	Y-prepared according to the manufacturer	The drugs are sealed and stored in a Chinese medicine warehouse at 0–30°C and 45–75% humidity

the anus to control the intestinal fluid, bowel gas, and loose and formed stools.

- 7) Anal pain score: The pain index tested before the dressing change on the first postoperative day was the baseline pain.

The pain index after the first postoperative day was tested within 2 h after the dressing change. Pain values were tested using the visual analogue scale (Anal pain visual analogue scale, VAS) (Bondi et al., 2017).

TIMEPOINT**	STUDY PERIOD						
	Enrolment	Allocation	Intervention	Primary endpoint	Follow-up		
	-T1	T0	1-4 weeks	4 weeks after the final treatment T1	8 weeks after the final treatment T2	12 weeks after the final treatment T3	16 weeks after the final treatment T4
ENROLMENT:							
Eligibility screen	X						
Informed consent	X						
Medical history	X						
Allocation		X					
INTERVENTIONS:							
Intervention group (standard treatment+JSD)			↔				
placebo group (standard treatment+placebo)			↔				
ASSESSMENTS:							
Wound healing		X	X	X	X	X	X
Wound pathogen distribution		X	X	X			
Inflammatory mediator levels		X	X	X			
Blood glucose		X	X	X	X	X	X
Blood lipid		X	X	X	X	X	X
SF-36		X	X	X	X	X	X
Safety outcomes		X		X			

FIGURE 3

SPIRIT figure showing the time points for enrollment, interventions, and assessment.

TABLE 2 Scale for assessing wound healing.

Wound secretion score (Gould et al., 2021)	Score
Wound with smooth surface and no obvious secretion	0
Wound with little secretion and no penetrated gauze	1
Wound with much secretion, one piece of penetrated gauze, and dressing change twice a day	2
Wound with abundant secretion, two or more pieces of penetrated gauze, and dressing change more than twice a day	3
Wound edema score (Gould et al., 2021)	Score
Wound with no edema	0
Wound with mild edema	1
Wound with obvious edema, which is more than the wound edge and need a dressing change to remit	2
Wound with severe edema, which is significantly more than the wound edge, and surgical resection is needed	3
Granulation tissue color score (Gould et al., 2021)	Score
Bright red	1
Light red	2
Purple	3

2.12.2 Distribution of pathogens on wound

Wound samples of participants were collected for pathogen isolation and cultured to perform identification on the automatic pathogenic microorganism identification instrument (Mark Biotechnology, United States). Weekly assessments were conducted during weeks 1–4 of intervention.

2.12.3 Levels of inflammatory mediators

ELISA was used to measure the levels of IL-6 and TNF- α in related tissues of wound drainage collected from the participants. The streptavidin-peroxidase (S-P) method was used to perform immunohistochemical staining on wound edge tissue samples, which were observed under a 400-fold light microscope and semiquantitatively measured using a medical image analysis system. Weekly assessments were conducted during weeks 1–4 of intervention.

2.12.4 Blood glucose

Blood glucose was measured four times per day by using a glucometer, including fasting and 2-h postprandial blood glucose of breakfast, lunch, and dinner.

2.13 Secondary outcomes

The assessments were at T0, T1, T2, T3, and T4. At the same time, weekly assessments were conducted during weeks 1–4 of intervention.

1. Blood lipids: total cholesterol (TC), total glycerides (TG), high-density lipoprotein (HDL), and low-density lipoprotein (LDL).
2. Quality of the life evaluation scale (Short-Form Health Survey 36, SF-36) (Wang et al., 2021).

2.14 Safety outcomes

The assessments were at T0 and T1.

1. Heart rate, blood pressure, temperature, and respiration.
2. Blood routine, stool routine, and urine routine.
3. Liver function: alanine aminotransferase, aspartate aminotransferase, γ -glutamyl transferase, alkaline phosphatase, and total bilirubin.
4. Renal function: blood urea nitrogen and creatinine.
5. Electrocardiogram.

2.15 Adverse events

Every adverse event (AE) was recorded, including the start date, end date, degree, relationship between the study drug and AE, and whether the participant is still involved in the study. Any serious adverse event (SAE) was reported to the Research Ethics Committee (REC) within 24 h. If any AE happened on any participant, the researcher asked the participant to stop using the washing decoction and determine if the event is related to the study drug formulation. If necessary, researchers took emergency safety measures to protect the participant from direct harm. If AE persisted, we followed it up until it was resolved. The AE in this study does not include complications clearly related to anal fistula, such as necrosis, prolonged healing, discharge, infection, pain, and itching.

2.16 Sample size

According to the sample size estimation method for the comparison of two sample means, we preset the sample size of the placebo group and the intervention group for them to be equal. The calculation formula is as follows:

$$n = 2\sigma^2 \times \frac{f(\alpha, \beta)}{(\mu_1 - \mu_2)^2},$$

where n represents the overall sample size of the study, μ_1 and μ_2 are the mean values of the control group and the test group, respectively, and σ is the standard deviation. We set that the probability of making type I error in this study shall not be greater than 5%, and the probability of making type II error at the same time shall not be greater than 10%, that is, $\alpha = 0.05$ and $\beta = 0.1$. Referring to Chinese literature reports on TCM external washing for the treatment of postoperative wound of anal fistula, the wound healing rate (%) in literatures was set as the clinical efficacy observation, the mean value was 33.35, and the standard deviation was 2.29 in the intervention group, and the mean value was 27.33 and the standard deviation was 2.67 in the placebo group. The estimated loss of the follow-up rate was 20%, so the total study sample size was 60, of which 30 was for the intervention group and 30 was for the placebo group.

2.17 Data and sample collection

Three study members were trained to master the criteria and methods of case collection to minimize the selection bias. During data collection, the medication of participants was recorded in detail, and the interference and contamination factors in the statistical analysis were excluded.

On the consent form, the participants were asked if they agreed with the use of their data or they chose to withdraw from the trial. This trial does involve collecting biological specimens for storage. All samples were destructed after use.

2.18 Data management and monitoring

An independent Data and Safety Monitoring Board has been established to monitor the conduct and safety of the study. Two members of the research group (YH and XZ) entered the collected information into the Chinese Clinical Trial Management Public Platform under a confidential condition. The hard copy records were preserved at a locked office. No one will be able to change or use the hard copy and electronic data without the authorization of our group.

The investigators did their best to avoid missing clinical trial data. In the process of dealing with missing data, we chose different processing methods, according to the judgment of data managers on the mechanism of missing data. At the same time, it is necessary to make a sensitivity analysis of the test results.

2.19 Adherence to study interventions

During the study, we provided clear oral and written instructions to encourage and monitor the interventions. If

necessary, further personalized guidance was provided. All unused medication was returned and recorded.

2.20 Data analysis

All data analyses were conducted by SPSS 24.0 software. Student's *t*-test was performed on continuous normally distributed variables, the Wilcoxon rank-sum test on non-normal variables, and Pearson's χ^2 test on categorical variables. Data were presented as the mean \pm standard deviation for continuous variables or percentage values for categorical variables. The statistical significance level was set at $p < 0.05$, and all the statistical tests were two-sided.

2.21 Frequency and plans for auditing trial conduct

The frequency and plans for the auditing trial conduct are as shown in Table 1. The auditing trial conduct was performed by a team independent from the investigators and the sponsor.

3 Discussion

Anal fistula is one of the common diseases in anorectal department, which is a tube located between the skin and rectum (Zheng et al., 2018; Garg, 2019). It is caused by chronic infection and epithelialization of the drains (Hokkanen et al., 2019; Sahnan et al., 2019). Diabetes mellitus is a risk factor for slow wound healing after anal fistula surgery (Wang et al., 2014; Mei et al., 2019), which can influence the development and outcome of patients with anal fistula (Mei et al., 2019). Surgery is currently the preferred treatment for anal fistula (Andreou et al., 2020; Mei et al., 2020; Wang et al., 2021). However, diabetic patients with large wounds after anal fistula surgery have an increased probability of wound infection, accompanied by pain, itching, swelling, and exudation, which are not easy to heal. Therefore, it is particularly important to shorten the wound healing time (Yang et al., 2017; Zhu et al., 2020).

As is known to all, TCM plays an important role in maintaining the health of Asians (Hao et al., 2017; Dai et al., 2020). TCM external washing has been widely used in clinical practice because of its reliable efficacy and fewer side effects (Guo et al., 2015; Zhang et al., 2020b). Despite the extensive clinical practice, the clinical literature on it for the treatment of postoperative wounds in diabetic patients with anal fistula is still not sufficient (Yang et al., 2017; Zhu et al., 2020). The clinical study we proposed will be the first randomized, double-blind,

placebo-controlled, multi-center clinical trial study to assess the efficacy and safety of TCM external washing (JSD) in the treatment of postoperative wounds in diabetic patients with anal fistula.

However, the study still has some limitations due to the small sample size of the subjects. On the other hand, the action mechanism of JSD is still not clear and needs further investigation.

3.1 Trial status

The recruitment for the trial started in June 2022 and is expected to be completed in December 2022.

3.2 Modification of the protocol

Any changes in the program will be agreed upon by the project leader and supervisor. The sponsor and all members of the research team will be informed after approval by the ethics committee.

Data availability statement

The original contributions presented in the study are included in the article/supplementary material. Further inquiries can be directed to the corresponding author.

Ethics statement

The studies involving human participants were reviewed and approved by The Medical Ethics Committee of Hospital of Chengdu University of Traditional Chinese Medicine, has reviewed this study protocol, and gave its approval and consent on 17 March 2022 (Ethical Review Number: 2022KL-018). The patients/participants provided their written informed consent to participate in this study.

Author contributions

JK was the principal investigator of this study and was involved in the conception and design and critical revision for the important intellectual content. ZX was involved in the conception and design of this manuscript. YL and SP were involved in the conception and design and drafting of the manuscript. LL was involved in the conception and design and statistical advice. XZ was involved in the conception and design and coordination development of the trial. XT and YH were involved in the conception and design. All authors critically revised the protocol for important intellectual content and approved the final manuscript. All named authors adhere to the authorship guidelines of trials.

Funding

This study was supported by the Science and Technology Plan Project of Sichuan Province (grant no. 2021YFS0275) and Science and Technology Plan Project of Sichuan Province (grant no. 23NSFSC2020).

Conflict of interest

The authors declare that the research was conducted in the absence of any commercial or financial relationships that could be construed as a potential conflict of interest.

References

- Alberti, K. G., and Zimmet, P. Z. (1998). Definition, diagnosis and classification of diabetes mellitus and its complications. Part 1: Diagnosis and classification of diabetes mellitus provisional report of a WHO consultation. *Diabet. Med.* 15, 539–553. doi:10.1002/(SICI)1096-9136(199807)15:7<539:AID-DIA668>3.0.CO;2-S
- Andreou, C., Zeindler, J., Oertli, D., and Misteli, H. (2020). Longterm outcome of anal fistula - a retrospective study. *Sci. Rep.* 10, 6483. doi:10.1038/s41598-020-63541-3
- Bondi, J., Avdagic, J., Karlöf, U., Hallböök, O., Kalman, D., Šaltytė Benth, J., et al. (2017). Randomized clinical trial comparing collagen plug and advancement flap for trans-sphincteric anal fistula. *Br. J. Surg.* 104, 1160–1166. doi:10.1002/bjs.10549
- Dai, Y. J., Wan, S. Y., Gong, S. S., Liu, J. C., Li, F., and Kou, J. P. (2020). Recent advances of traditional Chinese medicine on the prevention and treatment of COVID-19. *Chin. J. Nat. Med.* 18, 881–889. doi:10.1016/S1875-5364(20)60031-0
- Farag, A. F. A., Elbarmelgi, M. Y., Mostafa, M., and Mashhour, A. N. (2019). One stage fistulectomy for high anal fistula with reconstruction of anal sphincter without fecal diversion. *Asian J. Surg.* 42, 792–796. doi:10.1016/j.asjsur.2018.12.005
- Garg, P. (2019). Anal fistula and pilonidal sinus disease coexisting simultaneously: An audit in a cohort of 1284 patients. *Int. Wound J.* 16, 1199–1205. doi:10.1111/iwj.13187
- Gould, L. J., Serena, T. E., and Sinha, S. (2021). Development of the BWAT-CUA scale to assess wounds in patients with calciphylaxis. *Diagn. (Basel, Switz.)* 11, 730. doi:10.3390/diagnostics11040730
- Guo, D., Cao, X. W., Liu, J. W., Niu, W., Ma, Z. W., Lin, D. K., et al. (2015). Clinical effectiveness and micro-perfusion alteration of jingui external lotion in patients with knee osteoarthritis: Study protocol for a randomized controlled trial. *Trials* 16, 124. doi:10.1186/s13063-015-0661-x
- Hao, P., Jiang, F., Cheng, J., Ma, L., Zhang, Y., and Zhao, Y. (2017). Traditional Chinese medicine for cardiovascular disease: Evidence and potential mechanisms. *J. Am. Coll. Cardiol.* 69, 2952–2966. doi:10.1016/j.jacc.2017.04.041
- Hokkanen, S. R., Boxall, N., Khalid, J. M., Bennett, D., and Patel, H. (2019). Prevalence of anal fistula in the United Kingdom. *World J. Clin. Cases* 7, 1795–1804. doi:10.12998/wjcc.v7.i14.1795
- Kochhar, G., Saha, S., Andley, M., Kumar, A., Saurabh, G., Pusuluri, R., et al. (2014). Video-assisted anal fistula treatment. *JSL S. Soc. Laparoendosc. Surg.* 18, e2014.00127. doi:10.4293/JSL.2014.00127
- Lu, D., Lu, L., Cao, B., Li, Y., Cao, Y., Li, Z., et al. (2019). Relationship between body mass index and recurrence/anal fistula formation following initial operation for anorectal abscess. *Med. Sci. Monit.* 25, 7942–7950. doi:10.12659/MSM.917836
- Mei, Z., Li, Y., Zhang, Z., Zhou, H., Liu, S., Han, Y., et al. (2020). Development of screening tools to predict the risk of recurrence and related complications following anal fistula surgery: Protocol for a prospective cohort study. *BMJ open* 10, e035134. doi:10.1136/bmjopen-2019-035134
- Mei, Z., Wang, Q., Zhang, Y., Liu, P., Ge, M., Du, P., et al. (2019). Risk factors for recurrence after anal fistula surgery: A meta-analysis. *Int. J. Surg.* 69, 153–164. doi:10.1016/j.ijsu.2019.08.003
- Mosavat, S. H., Ghahramani, L., Haghighi, E. R., Chaijan, M. R., Hashempur, M. H., and Heydari, M. (2015). Anorectal diseases in AVICENNA'S "canon of medicine. *Acta Med. Hist. Adriat.* 13 (2), 103–114.
- Pigot, F. (2015). Treatment of anal fistula and abscess. *J. Visc. Surg.* 152, S23–S29. doi:10.1016/j.jvisurg.2014.07.008
- Sahnian, K., Askari, A., Adegbola, S. O., Warusavitarne, J., Lung, P. F. C., Hart, A., et al. (2019). Persistent fistula after anorectal abscess drainage: Local experience of 11 years. *Dis. Colon Rectum* 62, 327–332. doi:10.1097/DCR.0000000000001271
- Shi, Y., Zhi, C., Cheng, Y., and Zheng, L. (2021). A systematic review and meta-analysis of incision and seton drainage in the treatment of high perianal abscess. *Ann. Palliat. Med.* 10, 9830–9840. doi:10.21037/apm-21-2229
- Sun, H., Saeedi, P., Karuranga, S., Pinkepank, M., Ogurtsova, K., Duncan, B. B., et al. (2022). IDF Diabetes Atlas: Global, regional and country-level diabetes prevalence estimates for 2021 and projections for 2045. *Diabetes Res. Clin. Pract.* 183, 109119. doi:10.1016/j.diabres.2021.109119
- Wang, D., Yang, G., Qiu, J., Song, Y., Wang, L., Gao, J., et al. (2014). Risk factors for anal fistula: A case-control study. *Tech. Coloproctol.* 18, 635–639. doi:10.1007/s10151-013-1111-y
- Wang, F., Li, S., Ma, L., Geng, Y., Shen, Y., and Zeng, J. (2021). Study on the mechanism of *Periplaneta americana* extract to accelerate wound healing after diabetic anal fistula operation based on network Pharmacology. *Evidence-Based Complementary Altern. Med.* 2021, 1–9. doi:10.1155/2021/6659154
- Yan, Y., Liu, X., Zhuang, Y., Zhai, Y., Yang, X., Yang, Y., et al. (2020). Pien Tze Huang accelerated wound healing by inhibition of abnormal fibroblast apoptosis in Streptozotocin induced diabetic mice. *J. Ethnopharmacol.* 261, 113203. doi:10.1016/j.jep.2020.113203
- Yang, D., Xu, J. H., and Shi, R. J. (2017). Root extractive from *Daphne genkwa* benefits in wound healing of anal fistula through up-regulation of collagen genes in human skin fibroblasts. *Biosci. Rep.* 37, BSR20170182. doi:10.1042/BSR20170182
- Zhang, Y., Li, F., Zhao, T., Cao, F., Zheng, Y., and Li, A. (2020). Efficacy of video-assisted anal fistula treatment combined with closure of the internal opening using a stapler for Parks II anal fistula. *Ann. Transl. Med.* 8, 1517. doi:10.21037/atm-20-7154
- Zhang, Y., Yuan, H., Kang, J., Xie, H., Long, X., Qi, L., et al. (2020). Clinical study for external washing by traditional Chinese medicine in the treatment of multiple infectious wounds of diabetic foot: Study protocol clinical trial (SPIRIT compliant). *Medicine* 99, e19841. doi:10.1097/MD.00000000000019841
- Zheng, L. H., Zhang, A. Z., Shi, Y. Y., Li, X., Jia, L. S., Zhi, C. C., et al. (2018). Impact of smoking on anal abscess and anal fistula diseases. *Chin. Med. J.* 131, 1034–1037. doi:10.4103/0366-6999.230738
- Zhu, L., Ma, S., Jia, C., Zhang, B., Ma, Z., and Park, E. (2020). Chinese herbal fumigant and lotion for postoperative complication in surgical wound of anal fistula: A protocol for a systematic review and meta-analysis. *Medicine* 99, e22095. doi:10.1097/MD.00000000000022095

Publisher's note

All claims expressed in this article are solely those of the authors and do not necessarily represent those of their affiliated organizations, or those of the publisher, the editors, and the reviewers. Any product that may be evaluated in this article, or claim that may be made by its manufacturer, is not guaranteed or endorsed by the publisher.

Supplementary material

The Supplementary Material for this article can be found online at: <https://www.frontiersin.org/articles/10.3389/fphar.2022.938270/full#supplementary-material>

Frontiers in Pharmacology

Explores the interactions between chemicals and living beings

The most cited journal in its field, which advances access to pharmacological discoveries to prevent and treat human disease.

Discover the latest Research Topics

[See more →](#)

Frontiers

Avenue du Tribunal-Fédéral 34
1005 Lausanne, Switzerland
frontiersin.org

Contact us

+41 (0)21 510 17 00
frontiersin.org/about/contact



Frontiers in Pharmacology

